PY G345/43
M56

Mineral Resources Report M 56

~~1972~~
1973

Geology and Origin of the Triassic Magnetite Deposit and Diabase at Cornwall, Pennsylvania

Davis M. Lapham and
Carlyle Gray

COMMONWEALTH OF PENNSYLVANIA
DEPARTMENT OF ENVIRONMENTAL RESOURCES
Bureau of
TOPOGRAPHIC AND GEOLOGIC SURVEY
Arthur A. Socolow, State Geologist

DEC 1 1 1974
PENNSYLVANIA STATE LIBRARY
DOCUMENTS SECTION

BULLETIN M 56

Geology and Origin of the Triassic Magnetite Deposit and Diabase at Cornwall, Pennsylvania

by Davis M. Lapham and
Carlyle Gray

PENNSYLVANIA GEOLOGICAL SURVEY
FOURTH SERIES
HARRISBURG

1973

Copyright 1973
by the
Commonwealth of Pennsylvania
Quotations from this book may be published if credit is given to
the Pennsylvania Geological Survey

ADDITIONAL COPIES
OF THIS PUBLICATION MAY BE PURCHASED FROM
BUREAU OF PUBLICATIONS, TENTH AND MARKET STREETS
HARRISBURG, PENNSYLVANIA 17125

FRONTISPIECE

View of Cornwall open pit (1972), looking east toward Miners Village. Diabase on left slopes southward below vertical hanging wall of limestone and ore. Early mining occurred in old open pit (foreground) and culminated in new East End open pit (center to background). Shaft of old western underground ore body is at left foreground. (Courtesy of Bethlehem Steel Corporation.)

PREFACE

This report describes in detail many years of field and laboratory investigations of the magnetite iron ore deposit at Cornwall, Lebanon County, Pennsylvania. The investigation was begun to learn where the magnetite came from and why it was concentrated at this particular location. Ultimately, finding answers to these questions has led to more generally useful information. Because Cornwall is only one magnetite district among several others in Pennsylvania, all with a similar geology, this report was extended to include a comparison with these other districts. Such a comparison, in turn, has led to the discovery of geological and chemical tests that can be made to determine whether or not an area that contains the igneous rock, diabase (locally called "ironstone" or "trap rock"), might have a magnetite ore body near it. This report demonstrates that a locally detailed understanding of rock structure, mineralogy, and chemistry is required to predict the possibility of a new ore body, especially if it lies below the exposed surface rocks. Other, more general studies are shown to be necessary as a first step in selecting sites where detailed examination is most apt to prove useful.

The rock structure (folding and faulting) at Cornwall is very complex. Several different times in the last 500 million years this area has been subjected to mountain-building pressures, to erosion, and to invasion by the sea. These processes have influenced the location of diabase intrusion and ore introduction. Another complex feature at Cornwall, the mineral and chemical nature of the diabase, is of prime importance. The composition of opaque minerals (like magnetite and ilmenite) in diabase and the time when they crystallized are other clues to where and how large a potential ore body might be.

Application of this study can be made to many other occurrences of diabase, to the means by which sedimentary rock are modified by intrusion of diabase and ore, and to the geological history of other Triassic-age basins in the eastern United States. As such, the data and theories discussed in this report should prove useful both to professional geologists and to those concerned with ore exploration and mining technology.

Digitized by the Internet Archive
in 2016 with funding from
This project is made possible by a grant from the Institute of Museum and Library Services as administered by the Pennsylvania Department of Education through the Office of Commonwealth Libraries

https://archive.org/details/geologyoriginoft00laph

CONTENTS

Page

Abstract 1

Part 1. Introduction - D. M. Lapham 5
- General Statement 5
- Theories of origin 6
- Acknowledgments 8
- History 9

Part 2. Stratigraphy and structure in the Cornwall vicinity - Carlyle Gray and D.M. Lapham 10
- Stratigraphy 10
  - Introduction 10
  - The Cambro-Ordovician carbonates 11
  - Pelitic Ordovician (?) formations 14
  - Triassic formations 19
- Structure 20
  - Introduction 20
  - Paleozoic structures 21
  - Triassic structures 25
  - Structure and intrusion of diabase 26
  - Inferred tectonic model for the Cornwall area and the Triassic Basin 29
  - Sequence of depositional and tectonic events 36

Part 3. Contact metamorphism and potassium metasomatism - D.M. Lapham 38
- Contact metamorphism in the Triassic Basin 38
- Metamorphism of limestone at Cornwall 39
- Criteria and terminology of hornfels alteration 42
- Hornfels metamorphism and metasomatism in the Cornwall area 43
  - The Blue Conglomerate 43
    - Introduction 43
    - Mineralogy and petrography 44
    - Chemical composition 49
    - Comparison between metamorphism and metasomatism . 50
    - Facies representations 55
  - The Mill Hill Slate 58
    - Introduction 58
    - Mineralogy and petrography 58
    - Chemical composition and metasomatism 62
    - Facies representations 64
  - Xenoliths in diabase 66

Page
Geochemistry and origin 69
  Introduction 69
  Summary comparison of hornfels units. 69
  Contact metamorphism 71
    Iron oxidation and reduction 71
    Silica and alkali balance 72
    Metamorphic temperature, reactions, and equilibrium. . . 76
  Metasomatism mineralogy and geochemistry 79
    Mineralogical characteristics of metasomatism 79
    Chemical characteristics of metasomatism. 80
    Interdependence with thermal metamorphism 81
    Controls on metasomatism 82
    Mineral chemistry of alkali feldspar and mica (?) metasomatism 83
    Subsidiary metasomatic effects 86
    Temperature and pH of metasomatism 89
  Genesis of potassium metasomatism 90
    The major genetic possibilities 90
    Metasomatism from potassium released during contact metamorphism 90
    Metasomatism from granophyre during diabase differentiation 94
    Metasomatism from hydrothermal ore solutions. 99
  Discussion and summary 101
Part 4. Geology of the Cornwall ores - D.M. Lapham and Carlyle Gray . 103
Mining. 103
  Production and ore grade. 103
  Mining methods 105
Structural description 108
  The ore bodies 108
  Structures of the eastern ore body. 114
Mineralogy and chemistry 120
  Ore textures. 120
  Mineralogy of the eastern ore zone 123
  Chemistry of the eastern ore zone 128
  Mineral paragenesis. 132
Zonation 135
  Mineralogy 135
  Selected chemical constituents 142
  Summary. 154
Ore localization controls. 155

Part 5. Diabase and associated igneous rocks - D.M. Lapham 157
Introduction 157

Page
Petrology 160
  Chilled margin 160
    General description and textures 160
    Mineralogy and alteration 162
    Discussion and summary 168
  Normal holocrystalline diabase 169
    Introduction 169
    Texture 170
    General mineralogical composition 170
    Plagioclase feldspar 171
    Pyroxene 177
    The opaque oxides 182
    A vertical section through the sheet 183
  Diabase pegmatite 188
  Granophyre 191
  Paragenesis of the diabase and differentiates 194
Geochemistry 197
  Analytical accuracy 197
  Composition of the igneous rocks 198
  Normative calculations 202
  Vertical chemical variation 206
  Differentiation 207
    General differentiation trends 207
    Sulfur isotope fractionation 216
    Alkali differentiation trends 217
    Iron differentiation and oxidation trends 220
  Summary of Cornwall magma differentiation environment . . 228
Speculation on the absence of an olivine layer 231
Diabase dikes of Pennsylvania 233
  Introduction 233
  Petrography 235
  Chemistry 235
  Structural deformation 236
Part 6. Genesis of the magnetite ores of Cornwall and of the Pennsylvania Triassic metallogenic province - D.M. Lapham . 241
Introduction 241
Magnetite ore deposit comparisons 242
Hypotheses concerning the origin of magnetite 243
Origin and magmatic history of the Cornwall, Pa. magnetite . . . 245
  Introduction 245
  The country rock as a source of iron 246
  The adjacent diabase as a source of iron 246
  Multiple Diabase Injection as a Source of Iron 252
  A "primary magma" as the source of iron and diabase 252

Page
Early magmatic history of the Cornwall ores 259
Environment of ore transport and deposition 262
Conclusions on the origin of Cornwall ore 264
Summary of post-Paleozoic events at Cornwall, Pennsylvania . . 266
The Triassic metallogenic province 268
Structural environment and diabase sheet terminology 268
Aeromagnetic data 271
Sulfur isotope data 273
Titanium - iron geochemistry and province ore origin 274
Comparison and genesis of Triassic magnetite deposits 280
Comparative data from the Dillsburg, Morgantown, and Boyertown districts 280
Systematic variables 284
Ore genesis generalizations and speculations 288

Part 7. Economic potential of Pennsylvania magnetite - D.M. Lapham . 289
Introduction 289
Exploration in known magnetite districts 291
Exploration for new magnetite deposits 294

References 296

Appendix 306
1. Minerals at Cornwall, Pa 306
2. Garnet X-ray data 307
3. Log of vertical core through diabase (No. 155). 307
4. Chemical analyses at Cornwall 312
A. Diabase and related igneous rocks 312
B. Bulk rock analyses of gangue and hornfels 317
5. Chemical analyses 318
A. Diabase sheets: Triassic of North America 318
B. Diabase sheets: other than North America 320
C. Diabase dikes: Triassic of North America (excluding Cornwall, Pa.) 321
D. Diabase pegmatite 322
E. Diabase granophyre 323
F. Comparative averages of A-E (excluding Cornwall, Pa.) . . 324
6. Reference sources for total Fe and FeO/FeO_2 325

ILLUSTRATIONS

FIGURES

Figure 1. Photomicrograph of a texture transitional between Mill Hill Slate and Blue Conglomerate 16
2. Photomicrograph of late folding in Mill Hill Slate. 24

Page

3. Sketch of bedding laminae in limy Mill Hill Slate from railroad cut west of Rexmont, north of Cornwall 25
4. Sketch from petrographic thin section illustrating metamorphism and metasomatism at the contact between a limestone inclusion and Blue Conglomerate 42
5. ACF diagram for Blue Conglomerate 55
6. AKF diagram for Blue Conglomerate 57
7. ACF diagram for Mill Hill Slate 65
8. AKF diagram for Mill Hill Slate 66
9. Chemical analysis variation trends among granophyre, metamorphosed units, and Martinsburg shale 74
10. ACF diagram illustrating contact metamorphic assemblages 78
11. Wgt. percent ($K_2O + Na_2O$) versus SiO_2 variation in granitic to ultramafic igneous rocks compared with Cornwall rock types 95
12. Wgt. percent ($K_2O + Na_2O$)/Al_2O_3 versus SiO_2 variation in selected rocks compared with Cornwall rock types 97
13. Wgt. percent (Al_2O_3 + CaO) versus ($Na_2O + K_2O$) variation for granitic to ultramafic rocks compared with Cornwall rock types 98
14. Diagramatic sketch of Cornwall mining method 106
15. Modified bell system of mining at Cornwall 107
16. Sections through the East End open pit ore body 110
17. Plan map of the footwall ore body 111
18. Cross sections illustrating the form of the footwall ore body 112
19. Total thickness contours of Blue Conglomerate, eastern ore body 115
20. Total thickness contours of Mill Hill Slate, eastern ore body 116
21. Total hornfels thickness contours (Blue Conglomerate + Mill Hill Slate), eastern ore body 117
22. Simplified north-south cross section of total hornfels illustrating thickness variation along the dip and fold geometry, eastern ore body 118
23. Map of detailed structural feature of the eastern ore body . . 119
24. Sketch of typical ore textures and foliation in replaced host limestone 121
25. Paragenesis of minerals in the ore zone of the eastern ore body 126
26. Mineral distribution in the eastern ore body from footwall to hanging wall 134
27. Contours of magnetite a_0 along the footwall of the central and southern eastern ore body 140

Page

28. Contours of magnetite a_0 along and near the hanging wall of the central and south eastern ore body 141
29. Distribution of total and average percent iron in the eastern ore body 143
30. Distribution of total and average percent copper in chalcopyrite in the eastern ore body 146
31. Distribution of total and average percent pyritic sulfur in the eastern ore body. 149
32-A. Approximate location of sections in Figure 32-B, eastern ore body 152
32-B. Cross sections arranged from north to south (vertically) and down plunge through the eastern ore body illustrating percent nickel distribution 153
33. Idealized block diagram of the eastern Cornwall ore body illustrating zonation 155
34. Generalized MFA diagram of basaltic magma differentiation trends. 159
35. Petrographic sketch of chilled margin of diabase illustrating mineralogy and textures 161
36. Histogram of plagioclase compositions in the top 8 feet of the Cornwall diabase 166
37. Histogram summary of plagioclase compositions in the top 250 feet of the Cornwall diabase 173
38. Average grain size versus average plagioclase composition in the top 300 feet of Cornwall diabase below eastern and western ore bodies 174
39. Plagioclase composition of core-rim pairs in normal Cornwall diabase 175
40. Histogram of plagioclase composition versus average grain size for the Cornwall sheet 176
41. Nomenclature of the clinopyroxenes. 178
42. Orthopyroxene-clinopyroxene phase diagram. 179
43. Histogram of plagioclase compositions from vertical core through the Cornwall sheet 185
44. Average and range of plagioclase compositions of vertical core through the Cornwall sheet. 186
45. Histogram of plagioclase compositions in diabase pegmatite 189
46. Generalized paragenetic diagram for Cornwall diabase minerals 196
47. Comparative vertical chemical variation of Cornwall and Palisades diabase sheets. 200

Page
48. Comparative chemical differentiation trends by igneous rock type for the Cornwall, Dillsburg, Karroo, and Palisades diabase suites 210
49. Solidification Index versus oxide percent for the Cornwall sheet and dike (D) 213
50. MFA differentiation diagram for Skaergaard, Dillsburg, Palisades, Cascades, Cornwall, average tholeiite, and Pennsylvania Triassic dike magmas 214
51. MCA differentiation trend plot of ($Na_2O + K_2O$), CaO, and MgO for Skaergaard, Cascades, Palisades, Dillsburg, and Cornwall magmas 215
52. Silica variation diagram of percent ($Na_2O + K_2O$) versus SiO_2 comparing Cornwall and Dillsburg differentiation trends with the Hawaiian Basalt Line and Japanese basalts. 218
53. Comparison of differentiation trends for percent FeO (total iron) in Skaergaard, Cascades, Cornwall, Dillsburg, and Palisades magmas 222
54. Plot of percent $SiO_2/(Na_2O + K_2O)$ versus percent total Fe comparing differentiation trends for Cornwall, Dillsburg, and Palisades magmas. 223
55. Plot of FeO/Fe_2O_3 versus percent SiO_2 comparing iron oxidation trends during differentiation of mafic magmas . . 226
56. Rose diagram of strike orientations of diabase dikes in Maryland and Pennsylvania. 238
57. Phase diagram of sulfide-oxide stabilities as a function of P_{O_2} and P_{S_2} at one atm. total P and 25C 265
58. Map of diabase-magnetite ore districts in the Pennsylvania Triassic belt. 281

PLATES

To Follow Page 240

1. Metamorphosed Limestone
2. The Blue Conglomerate
3. Mill Hill Slate: Petrographic Composition
4. Mill Hill Slate Texture and Composition
5. Inclusions in Diabase
6. Late Deformation in the Ore Zone
7. Polished Section Petrography: Paragenesis
8. Polished Section Petrography: Paragenesis
9. Ore Replacement of Different Rock Types
10. Magnetite Replacement Textures
11. Magnetite-Gangue Paragenetic Relationships
12. Phenocrysts and Chilled Margin Textures of Diabase

13. Textures and Replacement of Diabase Chilled Margin
14. Plagioclase Paragenesis and Zoning in Diabase
15. Orthopyroxene and Orthopyroxene-Clinopyroxene Relationships in Diabase
16. Clinopyroxene-Clinohypersthene-Hypersthene Relationships in Diabase
17. Exsolution and Alteration Textures of Clinopyroxenes in Diabase
18. Petrography of Diabase Pegmatite and Granophyre
19. Paragenesis and Textures of Diabase Feldspars
20. Paragenesis and Textures of Diabase, Pyroxene and Amphibole

In Box

21. Geologic Map of the Cornwall Area, Pennsylvania
22. Geology of the Top of the Diabase Sheet at Cornwall, Pennsylvania
23. Geologic Sections Across the Cornwall Ore Bodies, Cornwall, Pennsylvania

TABLES

Page

Table 1. Analyses of host limestone from the Open Pit, Cornwall, Pa. . . 13
2. Chemical analyses of Buffalo Springs Formation at and near Cornwall, Pa. 40
3. Percent mineral composition representative of thermally metamorphosed and metasomatized Blue Conglomerate. 45
4. Chemical analyses comparing contact metamorphic and metasomatized Blue Conglomerate (anhydrous) with shale, graywacke, and granophyre. 50
5. Optical and crystallographic data for Fe-orthoclase. 52
6. Comparative X-ray patterns of Fe-orthoclase and orthoclase. . 53
7. Percent mineral composition representative of thermally metamorphosed and metasomatized Mill Hill Slate. 61
8. Chemical analyses comparing metasomatism in Mill Hill Slate hornfels with unmetamorphosed units (anhydrous). 63
9. Mineralogy of a limestone xenolith(?) in diabase (C3-33) from the western ore body. 68
10. Chemical analyses illustrating metamorphic and metasomatic alteration (anhydrous). 72
11. Percent mineral variation during metasomatism. 76
12. Comparative alumina/alkali ratios: alkali feldspar fixation potential. 85
13. Ore production (natural net tons). 104

Page
14. Ore product analyses, 1964 (in %). 104
15. Ore product analyses, 1966 (in %). 105
16. Chemical changes in the ore zone of the eastern ore body. 128
17. Spectrographic trace element analyses of magnetite. 130
18. Spectrographic analysis of pyrite. 131
19. Sulfur isotope abundances in Cornwall ores. 132
20. Comparison of ore textures and magnetite unit-cell dimensions from the eastern ore body 139
21. Comparison of average plagioclase composition in different facies of the Cornwall and Dillsburg sheets. 173
22. Pyroxene paragenesis, reactions, and exsolution. 182
23. Mineralogy of granophyre and transitional rocks from diffractometer and petrographic analyses. 187
24. Mineralogical variation in a vertical core through the Cornwall sheet. 190
25. Average chemical analyses (anhydrous) of Cornwall igneous rocks. 199
26. Comparative chemical composition of diabase and dolerite (anhydrous). 201
27. Comparative chemical analyses of diabase pegmatite (anhydrous). 202
28. Comparative chemical compositions of granophyre (anhydrous). 203
29. Normative calculations from Appendix 4-A. 204
30. Sulfur isotope ranges for S^{34} from Triassic diabase. 217
31. Types of igneous rocks associated with magnetite ore deposits. 243
32. Average percent total iron in diabase and basalt. 248
33. Variation in total iron with depth of Cornwall diabase. 251
34. Summary of observations and conclusions pertinent to ore genesis at Cornwall, Pa. 254
35. Sulfur fractionation in Triassic diabase and ore. 272
36. Total FeO/TiO_2 ratios in diabase. 277
37. Selected significant differences among Triassic ore deposits and diabase sheets in Pennsylvania. 285
38. Average percent total average iron in diabase sheets from Virginia to New Jersey compared with Triassic dikes 295

GEOLOGY AND ORIGIN OF THE TRIASSIC MAGNETITE DEPOSITS AND DIABASE AT CORNWALL, PENNSYLVANIA

by

Davis M. Lapham and Carlyle Gray

ABSTRACT

This report details the stratigraphy, structure, contact metamorphism, metasomatism, petrology, mineralogy, geochemistry, economic geology, and genesis of the sedimentary units, diabase, and magnetite ore bodies of the Cornwall area, Lebanon County, Pennsylvania. Emphasis is placed upon relationships developed from this area as they apply to the Pennsylvania Triassic structural, igneous, and metallogenic province. The data and conclusions are applied to techniques of ore exploration.

The Cornwall magnetite deposit, similar to other Triassic occurrences in Pennsylvania, is essentially a copper-iron sulfide and magnetite replacement of folded and thrust-faulted Paleozoic host limestone (proposed equivalence with the Cambrian Buffalo Springs Formation). Host limestone was rafted above diabase by magmatic intrusion and thermally metamorphosed before metasomatism and ore deposition. The Cornwall diabase is a subophitic tholeiite containing calcium-poor and calcium-rich pyroxenes, approximately equal amounts of pyroxene and plagioclase (averaging about $An_{51.5}$), olivine almost exclusively in the chilled margin, interstitial micropegmatite, and a granophyric residuum. It is somewhat low in total alkalies and total iron. The diabase forms the south-dipping northern limb of a largely concordant, saucer-shaped diabase sheet that is continuous with two other sheets within the closed-form York Haven Diabase Pluton. Three of four such major plutons in Pennsylvania also are arbitrarily divisible into sheets. Four sheets (Dillsburg, Cornwall, Jacksonwald, and Ziegler) and one pluton (Morgantown) are associated with magnetite-sulfide ore. Two deposits, Cornwall and Morgantown, are currently (1972) active. Ore in the Pennsylvania Triassic province is uniquely associated with diabase but not uniquely associated with the presence of late diabase differentiates or with titanium-poor magnetite in the differentiates, leading to the suggestions that not all province ores had the same mode of ingress and that magmatic history prior to sheet injection is of significance, especially at Cornwall where a distant ore source is invoked. At Cornwall, upper Triassic sediments dip northward against south-

dipping diabase and Paleozoic sediments, resulting in a major and characteristic Triassic structural discontinuity. Late fractures and diabase dikes may relate to the initiation of continental rifting.

The following conclusions are discussed:

1. Tholeiite fractionation, initiating at or near 1175°C. ±50° at depth, differed throughout Pennsylvania and was distinctive at Cornwall where there was depletion of total Fe in all diabase stages, a solidification index maximum for TiO_2 that preceded that for Fe, and extreme K_2O late enrichment relative to Na_2O. Tholeiite differentiation probably followed an oxygen depletion scheme rather than a constant P_{O_2} trend. Fractionation at Cornwall somewhat resembles the total Fe and alkali-silica enrichment trends of alkali basalts.

2. Differences in H_2O content of Triassic magmas, oxygen fugacity, and oxidation of iron may have influenced early iron-oxide crystallization, the formation of an ore phase, only moderate diabase iron enrichment trends, a low total iron content in diabase, and to a lesser extent the development of a small volume of granophyre. At Cornwall, initial P_{O_2} may have been as high as $10^{-6.5}$ to 10^{-7} atm. (between 1050°C and 1200°C), but possibly less in the Dillsburg magma.

3. An early magma separation or the later development of a low-temperature fraction rich in K_2O, H_2O, and perhaps Na_2O in conjunction with iron-rich spinel separation tapped together after sheet intrusion are suggested mechanisms for yielding the Cornwall ore.

4. Magmatic activity is proposed for the eastern Pennsylvania Triassic province in the sequence volcanic extrusion, diabase sheet intrusion with cryptic layering (without olivine segregation), hydrothermal ore introduction, and diabase dike intrusion into fractures that fan from a north-northwest strike (to the west) to a northeast strike (to the east). Within the Cornwall sheet, the solidification index does not appear adequate to illustrate successive magma compositions. The chilled margin is believed unrepresentative of *in situ* sheet composition and of parent magma.

5. The amounts of granophyre within diabase, and of ore outside, are believed to be inversely proportional and dependent upon the amount of iron and possibly the mobile constituents excluded from magma before sheet intrusion.

6. A plot of $SiO_2/Na_2O + K_2O$ ("R") vs. total Fe in diabase best illustrates iron differentiation trends and the competition between iron-rich and silica-alkali rich residua.

7. Titanium-iron enrichment after normal diabase crystallization is believed to have occurred at different stages: earlier at Cornwall (in diabase pegmatite), and later at Dillsburg (in transitional diabase pegmatite-granophyre), reflecting two types of diabase-ore districts. Late Ti-poor magnetite in diabase universally resulted from oxidation and is not necessarily related to an ore fluid.

8. Vertical sampling through the Cornwall diabase sheet indicates mixing of magma with consequent chemical and mineralogical cryptic layering, mutual exclusion of pigeonite and clinohypersthene, zoning in plagioclase and pyroxene, a wide range of plagioclase compositions, increased total iron and olivine with hypersthene phenocrysts in the basal 200 feet, and perhaps more than one magma injection.

9. Contact metamorphism attained a maximum temperature of about 600°C; metasomatism (largely potassium) occurred in the range 500°C. to 700°C. The younger metasomatism reduced the number of associated mineral components under conditions of an advancing front of changing chemical composition, chiefly involving Si, Al, Ca, K, Na, H_2O differential mobilities.

10. Silicification was a multi-process sequence of events resulting from thermal remobilization of sedimentary silica (and silicate release), metasomatic and hydrothermal solution redistribution and introduction. Alteration of pre-existing silicates yielded closed-system mobilization.

11. The Cornwall area contains the first reported description of granophyric and metasomatic ferric orthoclase, although the former occurrence probably is common. Optical properties range transitionally from sanidine to microcline.

12. During metasomatism of Mill Hill Slate and Blue Conglomerate, alkali feldspar crystallization was controlled by the alumina/alkali ratio, quartz distribution locally in excess, reaction time, and perhaps stable mineral relics. This bulk rock alumina/alkali ratio is termed the alkali-feldspar fixation potential for pelitic rocks and serves as a measure of the completeness of metasomatism for these hornfels units.

13. The metasomatized hornfels units, Mill Hill Slate and brecciated Blue Conglomerate, originally were a fragmental, calcareous shale above a fragmental sandstone respectively. Both are correlated with the Martinsburg Formation. Primary cross-bedding is preserved in the Mill Hill Slate. They acted as an impermeable cap over the eastern Cornwall ore zone.

14. Ore replaces some diabase, limestone, rarely the hornfels units, early metasomatic minerals, and fills a fault through diabase, illustrating some time lapse between solidification of most of the diabase sheet magma and ore introduction. At both Cornwall and the Carper mine to the west, faulting occurred after diabase sheet injection and before ore introduction.

15. Differences in diabase composition (Au, Fe, K, Mg, Na, Ti), in diabase mineralogy (late, iron-rich pyroxene at Dillsburg; hypersthene - clinohypersthene at Cornwall), in ore composition (e.g., S^{34}), in ore concentration (smaller, scattered deposits at Dillsburg), in granophyre composition (K/Na) and volume (greater at Dillsburg), and in structural location with respect to basin-trend curvature between the Dillsburg and Cornwall areas are suggestive of different modes of ore introduction and/or different original magma compositions. Hydrothermal Cornwall ores are believed to have originated at depth, whereas the Dillsburg ores may represent *in situ* expulsion from diabase if late, titanium-poor magnetite crystallized directly from the magma or was fractionated from ulvöspinel and ilmenite by oxidation and late residual solutions. Neither deposit properly can be termed pyrometasomatic even though both have been considered representative of this type. Most, but not all, ores of the Triassic metallogenic province lie above diabase where carbonate rocks were available for replacement.

16. Ore and metasomatic zonation at Cornwall (actinolite, diopside, mica, chlorite, Cu, Fe, Ni, and S) are focused above a fault between east and west ore bodies and through diabase that contains ore minerals throughout.

17. Modes of deformation in the Cornwall area include nappe folding (Paleozoic), thrust faulting (Paleozoic and possibly late Triassic), normal faulting (late Triassic), extensional fracturing, probable magmatic rafting, and regional rotation with folding and minor northward thrusting (Triassic), some of which were essentially synchronous.

18. The structurally controlled north limb diabase at Cornwall is believed to have intruded as a sole injection along the Mill Hill thrust plane at approximately its present attitude, but the southern limb might have been intruded earlier at a more nearly horizontal attitude.

19. Buried Paleozoic units at Cornwall below Triassic sediments represent a fault scarp or an erosional shelf. At depth, there may be a zone of high-angle faulting (here as at Lemoyne, Highspire, and Boyertown, no Triassic north-border fault is present at the surface) that may have acted as both a diabase and ore channel.

20. Local structures and a pre-Triassic erosion surface probably controlled diabase sheet shape at Cornwall and may have controlled other pluton forms in the province (i.e., a buried border fault, fault zone, or downwarp may extend approximately beneath the centers of major diabase plutons). Magma ascent may have caused progressive collapse faulting.

21. Regional structures and magmatism (including ore deposits) originated by basement tectonics that continued through the time of late Triassic (-Jurassic?) dike intrusion and may be relatable to translation in the basement and tectonic plate separation during continental rifting.

22. Based on the character of the chilled margin, contact alteration, and estimates of other sill intrusion depths and pressure (2000 psi minimum), at least 2000 feet of Triassic lithologies probably have been eroded in the Cornwall area.

23. Exploration techniques and requirements are dependent upon (among lesser factors) a knowledge of the total percent iron in diabase, the total confined granophyre volume, the direction of ore fluid movement as defined by both chemical (Fe, Cu, S, Ni) and mineral (especially actinolite-magnetite paragenetic relationships) zonation, the presence of replaceable limestone, structural channels of access, and perhaps the relative enrichment in S^{34} between diabase and ore.

PART 1. INTRODUCTION

by D. M. Lapham

GENERAL STATEMENT

The magnetite ore deposits of the Cornwall district lie in limestone along the north edge of the Triassic basin above igneous diabase in the central part of eastern Pennsylvania, Lebanon County. Mining of surface exposures of ore became economically important in Revolutionary War days and has continued to the present time. The discovery of other magnetite deposits in Triassic rocks followed the Cornwall discovery and there ensued discussions in the geological literature of the origin of these ores, first for information that might be useful in the exploration for additional deposits, and second for a more fundamental understanding of the processes involved in magnetite crystallization associated with diabase; continued investigations and discussions have been spurred by the economic value of the ore discoveries. As the iron resources of the United States become depleted, particularly in the east, and as more sophisticated methods of geological analysis are developed, detailed geologic knowledge of this area becomes increasingly important. Too often the exploration knowledge that accurate geology can provide has not been available. Until recently, our knowledge of the processes of magnetite origin has not kept pace with the usually fortuitous discovery of economic deposits. But this type of accidental discovery, especially in Pennsylvania, now belongs to the past. The obvious surface ore bodies are known. Henceforth, it is up to the science of geology and the technology of mining engineering to search for the presence of more elusive ore, to determine the most efficient methods of mining the known ore districts, and to re-assess the economic potential of those magnetite occurrences abandoned in the last century. We hope this report on the Cornwall district, by far the most famous of all Pennsylvania's magnetite mines, will help to fulfill these objectives. The data and ideas developed in this report are meant to be applied as working hypotheses, both for fundamental geological knowledge and for ore-mine development, to the entire Triassic magnetite province.

The report raises several basic geologic questions, all of which are noted or discussed, many of which are still largely unanswered. With respect to the origin of this Triassic magnetite, geologists have repeatedly asked why it is always associated with igneous diabase sheets and thereby have implied also the correlative questions, why is ore not associated with diabase dikes or with similar diabase sheets elsewhere in the world? Thus, the problem has been not only how the ore arrived at its present concentration and site, nor even where it came from — diabase, or sediments, or subcrustal magma — but even more fundamentally why the ores are restricted to the younger units of the Triassic basin in the east-west portion of the Pennsylvania Triassic belt, and nowhere else in the many Triassic basins up and down the length of the Appalachian Mountain system. In addition to such problems of locus and process, knowledge of the tangential but equally important question of extent and sequence of Triassic deformation plays a significant role. Indeed, in the last analysis, the answer to all the problems raised by diabase and ore may depend on our understanding of the tectonism that initiated the Triassic basin downwarp and that continued to affect the area after sedimentation ceased. Only through detailed knowledge of such areas as Cornwall can an accurate picture be derived. In many respects, we believe that the structural, magmatic, and ore history at Cornwall elucidates these more general problems of Triassic tectonism, sedimentation, and magmatism.

THEORIES OF ORIGIN

The Cornwall ore body has long been considered to be the representative deposit of its type, termed a pyrometasomatic ore body by Lindgren (1933, p. 696) based on the pioneering work of Spencer (1908). Thus the term "deposits of the Cornwall type" has arisen to describe magnetite replacements of limestone above diabase whose deposition is believed to have originated by expulsion of solutions from the top of the adjacent diabase sheet. Because of the geological significance thus attached to the Cornwall deposit, part of the purpose of this report has been to re-examine the classification of Cornwall as a representative of the class of pyrometasomatic ores.

In spite of this typification, theories concerning the origin of Cornwall have had a more varied history than the above classification might suggest. An historical survey of geological theories concerning the origin of Cornwall type magnetities can be seen to reflect the change in geological thinking from an early emphasis on sedimentary iron to a gradual reliance on a more and more distant magmatic source. All, however, have noted and utilized the spatial significance of magnetite ore adjacent to diabase. Early theories (Rogers, 1858; Lesley and d'Invilliers, 1886) proposed a remobilization of sedimentary limonite caused by the heat of diabase intrusion. Rogers utilized nearby shale as a source of ore, while Lesley and d'Invilliers invoked a residual limestone source. Later, Spencer (1908) proposed, and Hickok (1933) concurred, that iron-bearing solutions originated from within the adjacent diabase sheet. Hotz (1950; 1953), in his study of the Dillsburg deposits, also has essentially concurred, attributing the ore to expulsion during a late pegmatitic - granophyric diabase differentiation stage (1953, p. 703). More recently, Popovich (1964) suggested that silicification and ore mineralization at Cornwall and Morgantown were both related to depletion of the diabase in these constituents. However, he suggested that the silicification was more closely related, spatially and genetically, to the *in situ* diabase sheets than was the ore mineralization. Gray and Lapham (1961, p. 15) and Lapham (1962, p. 37-38; 1968) suggested that both the iron and the diabase at Cornwall came from a common magmatic source rather than requiring an *in situ* derivation of iron from crystallizing diabase. Sims (1968) in a study of the somewhat similar Morgantown magnetite occurrence has concurred in the hypothesis of a distant source. Davidson and Wyllie (1965, 1968) in a general study of the province suggested that a titanium-free late magnetite generated in diabase by alteration of ulvöspinel may have become the low-titanium magnetite of the ore zone, but no mechanisms other than oxidation were discussed.

In the light of the most recent studies, the term pyrometasomatic ore is not strictly applicable to the Cornwall deposit. However, the hypothesis of a distant magmatic source of iron may or may not apply to the Dillsburg deposits, the character of which fits more closely that which would be expected of a pyrometasomatic deposit. Thus, in terms of process of ore introduction, more than one genetic mode may be represented by the Triassic magnetites of Pennsylvania. It is probably misleading to refer to them all as deposits of the Cornwall type. However, the fundamental source seems clearly to be magmatic, and the minor differences seem clearly explainable in terms of the differentiation and fractionation of a once nearly uniform tholeiitic diabase magma.

The present study was preceded by the first detailed study by Spencer (1908) of the Triassic magnetite districts, including Cornwall, and by a study of the western Cornwall ore body by Hickok (1933). The stratigraphy of the Paleozoic rocks is based on, and slightly modified from, the work of Gray and others (1958) and Geyer and others (1958). The stratigraphy of the Triassic sediments is based on unpublished data by D. B. McLaughlin (Pa. Geol. Survey, open file reports) and the work of Glaeser (1963; 1964; 1966). Work on the present project was begun in 1950 with field mapping by Carlyle Gray assisted by Alan Geyer and continued intermittently through 1964 with laboratory and field studies by D. M. Lapham.

ACKNOWLEDGEMENTS

The authors are grateful to many persons too numerous to mention for the contribution of samples, guidance and access to the mine, and discussions. We are especially grateful to the geological and mining staff of Bethlehem Steel Corp. for their cooperation in all phases of the research and report preparation. In particular, we would like to acknowledge G. Adair, D. M. Fraser, G. Hole, and S. Sims from the Bethlehem office and H. Olsen, R. Peets, R. Renfrew, S. Shale, C. Taylor Jr., and R. Wheeler among many at the Cornwall mine. A. C. Spencer, who accompanied C. Gray in the field, revised his published opinion, concurring that the Blue Conglomerate was not of Triassic but of Paleozoic age as described here. He similarly revised his published opinion, to agree that there was no vertical diabase dike at Cornwall. Field mapping and manuscript criticism benefited from the assistance of Alan Geyer, Pennsylvania Geological Survey. Laboratory assistance was kindly provided by M. Woodburn (magnetite X-ray analyses), R. Sponseller (photomicrographic printing), and R. Weiss (notes on metallic mineral petrography), all of the Pennsylvania Geological Survey. Chemical analyses of diabase were kindly provided by R. Smith II, Pennsylvania State University. Trace element analyses of some ore minerals were provided by J. Worthington. Discussion of geophysical interpretations by R. W. Bromery, U.S. Geological Survey, of ore geochemistry by P. Wyllie and A. Davidson, Pennsylvania State University, of diabase chemical composition by A. W. Rose and R. Smith II, Pennsylvania State University, and of structural interpretation by J. D. Glaeser, R Faill, and other staff members of the Pennsylvania Geological Survey have contributed greatly to the report. The project was initiated under the directorship of C. Gray and continued under the direction of A. A. Socolow, State Geologist, both of whom provided stimulation and impetus for the completion of this project.

The manuscript has benefited from review by J. D. Glaeser, David B. MacLachlan, R. T. Faill, J. D. Ridge, S. S. Sims, R. Smith II, and S. A. Morse. The authors, however, accept sole responsibility for all interpretations.

HISTORY

The following historical summary is taken from an article by R. Peets (1937) and an outline provided by H. Olsen, Cornwall Mines Manager.

About 1730, Peter Grubb began prospecting for iron in what is now northern Lancaster County. His father had come from the Cornwall district in England. By 1732, Peter Grubb had extended his prospecting into what is now Lebanon County and had discovered magnetite outcrops on three hills: Big Hill, Middle Hill, and Grassy Hill. In 1734, Peter Grubb purchased 300 acres for 135 pounds sterling from William Allen who had obtained 9669 acres from Joseph Turner who, in turn, had been deeded the land from the three sons of William Penn. In 1737, he was granted an additional 142.5 acres that included the three hills of outcropping ore. He then built two forges on Hammer Creek to smelt the iron ore. By 1742, the transport distance was shortened by the construction of a charcoal furnace adjacent to the present Cornwall ore deposit. This he named the "Cornwall Furnace", the name that eventually gave rise to the town of Cornwall. Charcoal was obtained from nearby forests and kept the furnace in continuous operation for 141 years. It produced shot, cannon, and stoves for the Continental Congress during the Revolutionary War. In 1777, Hessian prisoners were put to work here at the rate of $0.60 per day. In the meantime, ownership had passed to the sons of Peter Grubb after his death in 1754.

From 1783, when Curtis Grubb (son of Peter) granted a 1/6 interest to his eldest son, Peter, until 1926, ownership was split among many interests, attaining a maximum of 96 holdings in 1864. One such holding began with Robert Coleman who received a 1/6 share from the younger Peter Grubb with the stipulation that he could mine enough ore to keep one furnace in operation for as long "as grass grows or water runs". This eventually became the Robesonia Iron Co., the last holding to be bought out by Bethlehem Steel Co. in 1926. Since this time, Bethlehem Steel has been the sole owner and has continued the skein of years of continuous operation begun by the first Peter Grubb.

The original Cornwall Furance of the first Peter Grubb was rebuilt in 1856. In 1883, the last cast was made from this furnace which, now restored, is operated by the Pennsylvania Historical and Museum Commission as a site of historical interest. The nearby Miners Village with its old square stone houses aligned along a narrow street is also worth a visit. The open pit (western mine) where operations first began is now abandoned and inaccessible, but can be viewed from the eastern-mine office at Cornwall.

In 1945, the eastern mine was driven to a final depth of 1225 feet. From here, exploratory drilling outlined the confines of the ore body down dip. In 1950, the first commercial pelletizing furnace in the United States was placed in operation at the Lebanon concentrator. In 1962, this pelletizing plant was moved to Cornwall near the eastern mine. From 1960 to 1964, a small open pit, the Elizabeth mine, was operated near the eastern ore body. In 1964, plans were made to mine a pocket of open pit ore at the eastern end of the open pit (western ore body) and operations are now (1972) underway here. At present, the somewhat leaner ore of a footwall ore body enclosed by diabase in not planned to be mined. Mining at Cornwall is now nearly completed unless a significant, new deposit is discovered at depth. In all, a total of more than 230 years of continuous operation will mark the Cornwall district as one of the most famous and interesting mines in the United States, an important part of our history, and a colorful record of our economic growth.

PART 2. STRATIGRAPHY AND STRUCTURE IN THE CORNWALL VICINITY

by Carlyle Gray and D. M. Lapham

STRATIGRAPHY

Introduction

The Cornwall ore deposits lie between two totally different stratigraphic and tectonic provinces: highly deformed, lower Paleozoic carbonates and pelites to the north, and relatively undeformed upper Triassic clastics and intrusive diabase to the south. The ore is a replacement of carbonate which is referred to the lower Paleozoic sequence (Spencer, 1908; Hickok, 1933).

In order to determine the extent of stratigraphic control on ore deposition, one of the authors (Gray) undertook a program of detailed mapping of the previously undifferentiated carbonates of the Great Valley in the vicinity of Cornwall. The results of this study have been published (Gray and others, 1958; Geyer and others, 1958) and need not be repeated in detail here. The sequence established has been extended to other areas with only minor modification, (McLaughlin and Gerhard, 1953; Geyer and others, 1963; Glaeser, 1963 and 1966; McLachlan, 1967; and Geyer, 1970).

The carbonate sequence, from the oldest exposed beds to the youngest is: Buffalo Springs Formation, Snitz Creek Formation, Shaefferstown Formation, Millbach Formation and Richland Formation, all presumed to be of Cambrian age. These are overlain by lower and middle Ordovician carbonates which are not exposed in this area.

No diagnostic fossils have been found in the Cambrian units listed above, and they are differentiated on the basis of gross lithology, i.e., abundance of dolomite versus limestone, abundance of shaly laminae or sandy beds, and the presence of algal structures. Limestone predominates over dolomite. Calcareous, dolomitic, shaly, and sandy interbeds are common in all units.

Recrystallization by dynamic metamorphism has modified the limestones and transformed two pelitic units (the Mill Hill Slate and the Blue Conglomerate) into hornfels. However, some original sedimentary structures remain. Generally, Triassic units have not been modified except by thermal alteration adjacent to plutons.

The Triassic clastics are largely composed of coarse red beds of laterally varying facies (Glaeser, 1963). Triassic sediment textures and mineralogy differ widely, but have not been tectonically modified except adjacent to diabase plutons. Some volcanic flows are interbedded with the younger Triassic sediments (Hammer Creek equivalents) 30 miles east of Cornwall, near Reading.

The Cambro-Ordovician Carbonates

Of the several carbonate formations in the area (Plate 21), only three are possible correlatives of the host limestone above the diabase sheet. Thus, they are of particular interest to this study. The characteristics of the host limestone, which must be sought in the Great Valley carbonates, are 1) tight isoclinal folds, 2) laminae of alternating calcium-rich and magnesium-rich composition, the latter occasionally shaly, 3) lack of algal structure, 4) approximate chemical equivalence, and 5) a structural position reasonably relatable to known tectonics. The three lithologic units which might fulfill these requirements are the Millbach, the Snitz Creek, and the Buffalo Springs Formations.

Of the three, the Snitz Creek Formation in the Conococheague Group in the Great Valley province is least likely to be the host limestone. This formation stratigraphically overlies the Buffalo Springs Formation to the north but is structurally below it because of overturning. The Buffalo Springs Formation at the surface separates the Snitz Creek Formation from the Triassic border (Plate 21). The Snitz Creek Formation consists essentially of massive, medium-gray, crystalline dolomite, commonly oolitic, with some light gray limestone or dark gray shaly limestone interbeds. Shaly partings in the dolomite are commonly stylolitic. Some quartzose sandstone with dolomite cement is present. The preponderance of dolomite, the presence of stylolites and sandstone interbeds, and in the host limestone, the absence of fine laminae and a high calcium content are probably sufficient criteria to eliminate the Snitz Creek Formation from consideration as correlative to the host rock. In addition, it is somewhat difficult to provide a mechanism for Snitz Creek emplacement above diabase without also including emplacement of the subjacent Buffalo Springs Formation (Plates 21 and 23).

The Millbach Formation in the Conococheague Group, also in the Great Valley, presents a more difficult correlation problem because it is more similar than is the Snitz Creek Formation to both the Buffalo Springs Formation and to the host limestone. The Millbach Formation, largely interbedded limestone and dolomite appears to differ somewhat from the Buffalo Springs Formation by having a greater proportion of light gray to bluish gray limestone interbeds. A few thin quartzose and sandy limestones or dolomites also are present. Cryptozoans are only rarely present in this area, so that their absence from the host limestone is not diagnostic. Elimination from consideration is more easily made upon structural grounds. Structurally and stratigraphically the Millbach Formation is the most distant of the three from the Triassic contact (Plate 21). More extensive faulting than is believed present would be required to displace it above diabase as the host limestone. Furthermore, this faulting would have had to eliminate the intervening Buffalo Springs Formation, and perhaps also the Snitz Creek and Schaefferstown Formations since only one unit is recognizable in the host limestone.

The Buffalo Springs Formation is the oldest mappable unit in the area, lies immediately north of the Triassic border (Plate 21), is overturned, and dips south. It consists of light-gray to pinkish-gray, crystalline limestone alternating with buff-weathering, light-gray, dense dolomite and shaly limestone (Geyer and others, 1963, p. 69). Light-gray limestone often grades laterally into medium-gray, finely crystalline limestone; locally both types are oolitic. Light-gray limestone is most common near the top of the formation, whereas medium to medium-dark gray limestone occurs throughout the lower parts. Algal structure (cryptozoan) is present near the top of the formation. Thin (2-6 inches) sandy to silty limestone beds also occur and can be traced for short distances. Flow cleavage commonly is well developed in the limestone and shaly limestone beds and may obliterate bedding planes. Extreme drag folding and flowage are common. One of the best exposures of the Buffalo Springs Formation is in a railroad cut one-fourth mile north of Cornwall Center (Gray and Lapham, 1961, Figure 4). The beds exposed here are in a complex anticline with a double crest and are typical of the upper beds of the Buffalo Springs Formation. There is an abundance of pinkish-gray and light-gray, crystalline limestone with buff-weathering, dolomitic and shaly interbeds. Near the center of the cut a few sandy carbonate beds are exposed.

The host limestone above the main open pit and the "East End" open pit is characterized by fine laminae that are intensely folded and usually recrystallized. The laminations are dolomitic and limy. The dolomitic portions usually are more shaly or silty than the limy portions (Tables 1 and 2). These are also the characteristics of the limestone beds in the Buffalo Springs Formation. Chemical analyses of the Buffalo Springs Formation (O'Neill, 1964) fall within the range of analyses of the host limestone (Tables 1 and 2). However, the range of composition, recrystallization, and secondary alteration of the host limestone is too broad for these analyses to serve as diagnostic criteria. Above the ore where the host beds were sampled, they were traced directly into banded, replacement magnetite. Replaced and unreplaced host limestone rests upon the chilled margin of the top of the

Table 1. *Analyses of Host Limestone Taken from the Open Pit, Cornwall, Pa.*

Sample	Fe_2O_3 (total)	$CaCO_3$	$MgCO_3$	Al_2O_3	SiO_2
50	.7	78.0	8.6	2.4	10.6
51	.7	72.1	15.6	2.4	12.6
52	.6	71.0	18.0	1.6	9.6
53	2.5	49.0	25.2	3.8	23.0
54	1.0	69.7	10.5	2.4	17.0
55	.7	84.8	7.6	.8	7.0
56	2.0	58.8	22.9	3.1	13.4
57	.5	86.8	6.8	.9	5.0
58	1.1	76.6	6.7	2.8	13.8
59	.6	86.0	4.0	1.5	6.1
60	.9	80.8	5.8	2.4	10.7
61	.8	77.6	4.2	3.0	13.3
62	.5	88.4	3.6	1.5	6.7
63	1.0	71.7	13.2	3.1	12.0
64	.9	72.8	9.3	2.7	14.9
65	.3	92.8	3.7	.4	2.5
66	.4	82.2	11.8	1.2	4.7
67	.5	86.7	6.5	1.4	5.7
68	.7	79.6	4.0	2.3	11.6
69	1.2	66.9	.1.6	2.8	18.4
70	1.1	75.5	11.0	1.7	17.7
71	1.0	80.7	6.0	2.1	10.4
72	.8	77.7	10.5	2.0	10.0
73	3.0	52.0	22.0	3.0	20.8
74	.6	82.7	5.0	1.7	10.0
75	.7	82.5	5.1	2.2	9.7
76	.9	74.3	7.3	2.2	13.4
77	.8	72.7	10.5	1.4	9.6
78	1.2	71.7	14.0	2.0	12.0
79	1.0	75.3	10.5	2.2	9.6
80	.6	73.4	16.4	1.5	9.0
Avg.	0.95	75.83	10.25	2.08	11.32
Range	0.3-3.0	49.0-92.8	3.6-25.2	0.4-3.8	2.5-23.0

gently undulating diabase sheet below Blue Conglomerate or Mill Hill Slate (Figure 16 and Plates 22 and 23). At some places, this contact is an observable low angle reverse fault (Figure 16-A). The top of the host limestone is in fault contact with Blue Conglomerate (Figure 16) and Mill Hill Slate (Plates 21 and 23), with the former to the east and down-dip and with the latter to the west and up-dip. Mill Hill Slate also occurs below diabase where it is believed to be in thrust contact with the Buffalo Springs Formation of the Great Valley sequence (Plate 21). It is this structural proximity of the Buffalo Springs Formation below Mill Hill Slate that is believed to be the strongest indication that the host limestone is a detached segment of the Buffalo Springs Formation (Plates 21 and 23).

Pelitic Ordovician (?) Formations

The Mill Hill Slate and the overlying Blue Conglomerate, frequently referred to together as hornfels units in succeeding discussions, are two units local to the Cornwall area. They are believed to be of middle or upper Ordovician age correlative with the Martinsburg Formation, although the evidence is largely conjectural. The Mill Hill Slate, named for nearby Mill Hill, is not a slate, but a laminated, calcareous, shaly hornfels. The term was adopted by miners at Cornwall and has been retained to avoid confusion. Similarly, the Blue Conglomerate is probably not a conglomerate, but a quartz-and shale-fragment breccia. Its name is derived from large, blue-gray masses of quartz with carbonaceous rims that characterize the unit underground in the eastern ore body. Originally it also was a miner's term. Both of these units are metamorphosed and metasomatized. In this report the names are capitalized for clarity of discussion. They are not formally named stratigraphic units.

The present Mill Hill Slate is a dense, dark brown to gray-black, laminated hornfels (Plate 4), frequently rich in carbonate or calc-silicate minerals. Alternating bands are silica-poor and silica-rich, or calcium-poor and calcium-rich (Plate 4). These thin, remarkably persistent laminae are the relics of an originally variable bedding composition. Primary cross-bedding structures have been preserved. Small scale folding is often evident, especially in surface exposures (Figures 2 and 3). Samples of the Mill Hill Slate from underground are typically composed of pinkish-gray or pinkish-brown bands with some greenish-gray bands. Gray and dark-gray colors are less common. The banding of the rock is evident, but it tends to be shattered or microfaulted and rehealed by later mineralization (Plates 3 and 4). Pyrite crystals are common. Pelitic and quartzitic fragments are less common than in the Blue Conglomerate (Plate 2).

The Blue Conglomerate is a breccia, at least in part of tectonic origin. It contains sub-angular to sub-rounded quartzitic, and less commonly pelitic, fragments (replaced by pink orthoclase in the eastern ore body) from a few millimeters to a meter in diameter in a hornfels matrix of mica, chlorite, actinolite, and feldspar (Plate 2). The quartzitic fragments commonly have a carbonaceous (graphitic) coating and evidence a weak lineation (Figure 16) that is probably tectonic in origin. Bedding plane surfaces are rarely evident. The matrix contains little or no quartz. The true nature and origin of the Blue Conglomerate is uncertain but the most likely explanation is that it is a metamorphosed and metasomatized tectonic breccia, composed of brecciated Mill Hill Slate quartzose and pelitic beds with inclusions of Cambrian (?) limestone. For the purpose of subsequent correlation discussions, the Blue Conglomerate is considered to be a lithologic variant or facies of the more extensive Mill Hill Slate; some compositions and textures have characteristics both of Blue Conglomerate and Mill Hill Slate (Figure 1). One such transitional sample from a railroad cut through laminated Mill Hill Slate (Figures 1 and 3) contains quartz aggregates more characteristic of the Blue Conglomerate (Plate 2, B-D). However, these aggregates are smaller, less brecciated, and in a quartz-bearing matrix that is characteristic of Mill Hill Slate. Pelitic and quartzitic fragments also may be found in the Mill Hill Slate (Plate 3-A), but they are atypical. Similar transitional lithologies occur above the open pit and further west in Mill Hill Slate south of Quentin and south of Mount Pleasant (Geyer, 1970). For this reason, the contact between Mill Hill Slate and Blue Conglomerate is uncertain (geologic map, Plate 21), but can be illustrated on locally detailed maps and sections (Plates 21, 22, 23 and Figure 22) where the two often are distinguishable. We wish to emphasize that at many localities, particularly surface exposures and at the eastern and western terminations of Blue Conglomerate, this differentiation is arbitrary. In succeeding discussions of these two units, their typically representative character has been studied rather than transitional lithologies.

Blue Conglomerate has not been found below diabase, although it may be present down dip (Plate 21). It crops out east of Miners Village, and to the west lies between overlying Triassic sediments and unreplaced limestone above the ore body (Plate 21, 22, and 23). At the "East End" open pit its contact with underlying host limestone is a low angle normal fault (Figure 16). South of Quentin (west of the ore-bodies), the Mill Hill Slate contains thin, folded quartz-rich interbeds that resemble the Blue Conglomerate in the eastern ore body. Because of this, the two lithologies are believed to belong to a single formation that has been disrupted by faulting in the eastern ore zone (see Part 4, "Structures of the Eastern Ore Body"). If the Blue Conglomerate were originally a basal, sandy facies of the Mill Hill Slate, the units are now inverted (see "Paleozoic Structures" for structural evidence for overturning).

The Mill Hill Slate, the more extensive of the two hornfels, crops out both above and below diabase. To the east, it extends to a fault near the Doner mine (Plate 21); to the west, it extends several miles and is partially enveloped by diabase (Geyer and others, 1958; Plate 21). Underground in the eastern ore body, it is overlain by Blue Conglomerate down dip to the south (Plates 21 and 23; Figure 22).

Both of the hornfels lithologies recognized on the surface (the quartz-rich interbeds of Blue Conglomerate and the limy, laminated Mill Hill Slate) are difficult to recognize underground. Identification is based primarily on physical continuity proved by drilling and secondarily by the laminations of the Mill Hill Slate (where it is not replaced by ore and therefore distinguishable from laminated host limestone). Neither unit is interbedded with the Triassic sediments and this contact is sharp, frequently angular. Logs of individual drill cores seem to indicate interbedding of Blue

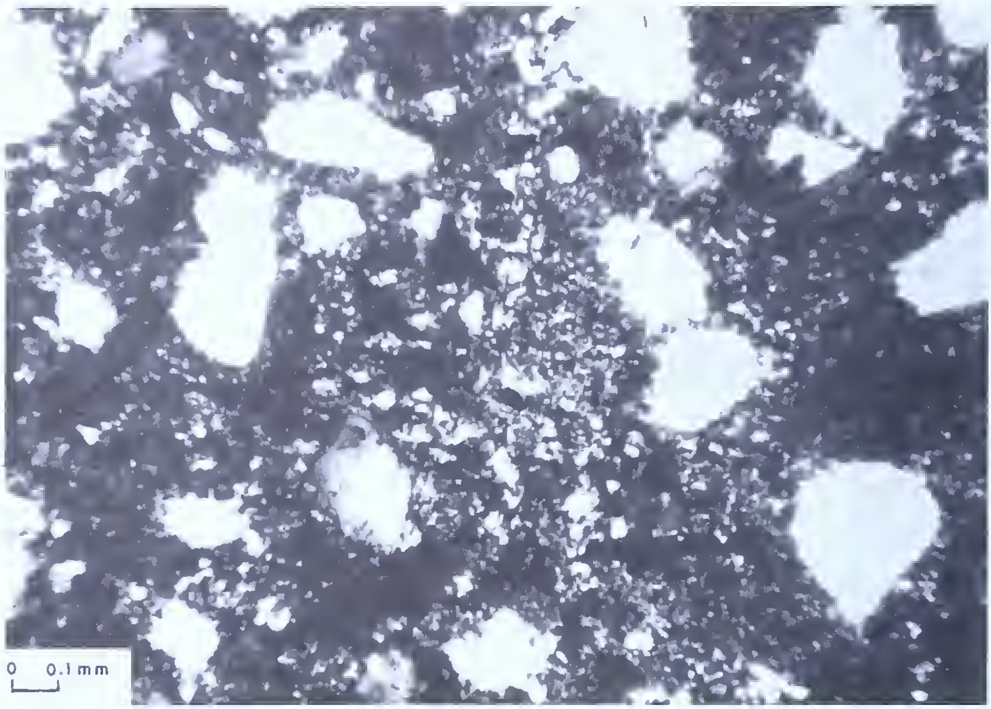

Figure 1. Photomicrograph of a texture transitional between Mill Hill Slate and Blue Conglomerate. Angular quartz fragments are set in a matrix of fine-grained plagioclase (dark) and some quartz (light); plane light.

Conglomerate and Mill Hill Slate with limestone, but where a series of cores from 10° angled holes were drilled at the same station, the results could not be correlated. Therefore, presumably this alternation results from faulting. However, no faults are observable in the east end open pit. These, therefore, may be penecontemporaneous slump blocks (wildflysch) within the Mill Hill Slate hornfels.

In an underground exposure above the western edge of the eastern orebody, the full thickness of the Blue Conglomerate was seen (also see Figure 19). Here, the unit overlies the host Buffalo Springs Limestone. The contact shows evidence of movement, shearing, and slickensiding. A few inclusions of limestone occur in the Blue Conglomerate immediately above the contact, confirming the presence of the included breccia blocks deduced from drill core examination. There is no clear indication of bedding. The only fabric is a faint indication of parting that has a dip roughly parallel to the contacts of the unit and a suggestion that the stretched quartz clasts are partially oriented (see Figure 16). The upper contact, with Triassic beds, ocasionally shows a small one to two inch, fine-grained zone that may be a mylonite. The Triassic beds dip north into the south-dipping contact of pre-Triassic rocks.

Any movement along this contact appears to have been small (see "Triassic Structures" and Part 4: "Structure of the Eastern Ore Body"). Logs of drill cores in the down dip part of the western ore body show alternation of Blue Conglomerate and limestone similar to that reported in the lower part of the eastern ore body.

The Mill Hill Slate generally has been considered to be an outlier of Ordovician Martinsburg shale although it occurs eight miles south of the main outcrop belt (Lesley and d'Invilliers, 1886, p. 541; Spencer, 1908, p. 26). Rogers (1850) considered the "slate" to be "Primal", that is, Cambrian. Lesley's identification, which was accepted by Spencer and later writers, was based on limited understanding of the stratigraphy and structure of the Lebanon Valley. Lesley and d'Invilliers tried to show that the valley probably had an anticlinal structure and that the Mill Hill Slate lay conformably above the Great Valley limestone north of Cornwall. Mapping (Gray and others, 1958) has shown that this interpretation is oversimplified. The Cambrian and Ordovician sediments of the Great Valley are now considered to be involved in a complex pattern of recumbent folds broken by thrusts. The mapping of these structures has made it clear that the Mill Hill Slate north of the diabase (below it) lies directly on the Buffalo Springs Formation, the oldest unit exposed in the immediate area. It is over 2000 feet lower in the stratigraphic section than the beds on which the Martinsburg Formation generally lies. It is, therefore, necessary to reexamine all evidence concerning the correlation of the Mill Hill Slate.

Three possibilities must be considered: 1) the Mill Hill Slate was originally a shale of Cambrian age in conformable contact with the Buffalo Slprings Formation, 2) it is younger than the Buffalo Springs Formation and lies unconformably on it, 3) it is in fault contact with the Buffalo Springs Formation and is either younger or older in age. The evidence for any correlation has to be based both on lithology and on structural and stratigraphic position because no fossils have been reported from the unit.

Structural evidence indicates that the Mill Hill Slate is in thrust contact with the Buffalo Springs Formation on the north. If the sequence were conformable, the Mill Hill Slate should be folded with the Buffalo Springs Formation. The map pattern of the contact (Plate 21) is more regular, however, and drill holes indicate that the contact has a uniformly southward dip. There are no abrupt changes in strike, offsets, or anomalies that would indicate that the Mill Hill Slate-limestone contact reflects any of the second-order folds seen elsewhere at contacts within the limestone belt of the Great Valley (Plate 21; Geyer and others, 1958). The same reasoning applies to an unconformable contact; it also should be folded. Furthermore, the Mill Hill Slate cannot be an unconformable Cambrian or Ordovician shale lying on the Buffalo Springs Formation because the structural evidence indicates that the Buffalo Springs Formation on the north side of the diabase sheet is overturned (Geyer and others, 1958) such that Mill Hill Slate lies on the base of the underlying Buffalo Springs Formation. It is exceedingly unlikely that there was sufficient deformation and erosion before the end of Ordovician time for an Ordovician shale to have been deposited on overturned, recumbent beds: the major overturning (the Taconic orogeny?) would have to have occurred in pre-Martinsburg time. However, thrusting to such a position could have occurred later.

If the possibilities of conformable or unconformable stratigraphic sequence are eliminated, correlation must be based on lithology alone. However, direct lithologic correlation is difficult because of the extensive metamorphism and metasomatism which has altered the Mill Hill Slate (Plates 3 and 4; Tables 7 and 8). Nevertheless, some evidence permits a possible correlation. About eight miles east of Cornwall, near Schaefferstown, an outlier of dark-gray, greenish-gray, and purple shale lies on Cambrian carbonate formations, including the Buffalo Springs Formation. Although it is not continuous with the Cornwall hornfels, it appears likely that the Mill Hill Slate is a metamorphosed equivalent of the shale at Schaefferstown because it occupies a very similar structural position; that is, both shales lie in fault contact with an overturned Cambrian formation. The same structure and a similar lithology occur farther east near Kleinfeltersville (Geyer and others, 1963) at the north contact of Triassic units and Great Valley Cambrian carbonate rocks. Although the unit here is termed Martinsburg, it does not differ greatly from Mill Hill Slate. A similar shale also occurs to the west at Highspire between the Epler Formation and Triassic sediments. The shales at Schaefferstown and Highspire are not well exposed. Lithologies only approximately correspond to the Mill Hill Slate lithology. However, the Schaefferstown shale does include purple and greenish shales very much like those to the south in the probably correlative Cocalico Formation of Lancaster County.

The Cocalico Formation is described by Jonas and Stose (1930, p. 39) as a "bluish-black to dark-gray fissile shale" with purple and green shales near the base. Not mentioned in the original description are limy shale beds that occur within the gray shales. These are exposed in a road cut south of Brickerville. Therefore, the Cocalico Formation is very likely the correlative of the shale at Schafferstown, and furthermore contains limy banded shale similar to that in the Mill Hill Slate. The Cocalico Formation occupies the same stratigraphic position as the Martinsburg Formation and its lithology is very similar (Jonas and Stose, 1930). The name Cocalico was originally proposed (Stose and Jonas, 1927) because of a supposed difference in age limits for the two units. The name has since been perpetuated in the areas southeast of the Triassic basin even though significant differences do not now appear to exist.

On this rather circuitous basis, a correlation of the Mill Hill Slate with the Martinsburg Formation is used as the best present working hypothesis. Primarily, it should be emphasized that it is not in normal stratigraphic contact with the adjacent Buffalo Springs Formation, neither below nor above the diabase sheet (Plate 21).

Triassic Formations

Triassic sediments lie on a buried basement of largely unknown stratigraphic and structural character. Where drilling evidence is available near basin edges, these basement rocks have the same lithology as rock units adjacent to the Triassic border, although no Precambrian "basement" below the Triassic basin has been proved to exist, and therefore the concept of a pull-apart structure in the middle of the Great Valley is untested. However, because structures and lithologies both north (or northwest) and south (or southeast) of the Triassic province are very similar, the Triassic units at the north margin are believed to rest on an erosional surface (lower Paleozoic limestone and shale at Cornwall, to the west at Highspire, and to the east at Boyertown) now deformed to encompass the volume of Triassic sediments. Drill data at Cornwall confirm the presence of limestone below diabase as represented in Plate 21. Such an erosional surface presumably would have been a depressed valley by the beginning of Triassic time because it lies between the more resistant Reading Prong (or Valley and Ridge Province) to the north and Piedmont to the south. It is upon this valley depression that Triassic deposition began with or without any additional relief in the valley resulting from structural depression (Faill, 1969).

The Triassic sediments in the Cornwall area belong to the Hammer Creek Formation of the Newark Group (Glaeser, 1963). This formation has been described in detail by Glaeser (1963; 1966). It is a facies, and in part a time equivalent of the Gettysburg (to the west) and the Brunswick (to the east) Formations. It has been geographically and lithologically restricted to the central Triassic basin area where older Triassic sediments are relatively thin or absent (Gray, Shepps and others, 1960; Glaeser, 1963 and 1966). The type section is along Hammer Creek (Glaeser, 1963) just east of Cornwall in the Richland quadrangle (Gray and others, 1958).

The eastern arbitrary cut-off (Schuylkill River) and western arbitrary cut-off (Susquehanna River) are the defined lateral limits of the Hammer Creek Formation. They bound an area in which the clastics are coarser than elsewhere in its facies equivalents. The unit is laterally and vertically heterogeneous. Coarse red sandstone and red conglomerate dominate, but lesser amounts of siltstone, shale, and finer-grained sandstone are present (Glaeser, 1963, p. 184). At Cornwall, thin red shale, bleached near diabase, is interbedded with conglomerate and coarse sandstone. The source of Hammer Creek detritus is believed to have been from the north side of the basin with a sediment distribution east-west parallel to the long axis of the basin (Glaeser, 1966).

The younger Triassic sediments are interbedded with vesicular, basaltic flows and intruded by tholeiitic diabase sheets. The sheets are either penecontemporaneous with, or younger than, the flows (see Part 5, "Diabase Dikes of Pennsylvania: Introduction"). According to the summary by Frankel (1967, p. 96), in many areas, particularly South Africa and Brazil, sheets consistently are younger than the associated flows. Ore following diabase intrusion at Cornwall has been dated at about 190 my. by the helium method (Fanale and Kulp, 1962) and by the K-Ar method (Erickson and Kulp, 1961), fixing a minimal age for the intrusives. The similar intrusives in the Connecticut Triassic basin are considered by DeBoer (1968) to be time equivalents of the Holyoke volcanics. DeBoer also suggests (1968) that the time span of flow and sheet activity was short in the Gettysburg-Newark basin. Diabase dikes, apparently cross-cutting, (see Pa. State Geologic Map, Gray, Shepps and others, 1960 and Part 5., Diabase Dikes of Pennsylvania) may be post-Triassic in age, although clear-cut age relationships with the sheets have not been described. These igneous formations are discussed in detail in succeeding sections of this report.

Erosion subsequent to Triassic time has removed Triassic sediments, diabase, some ore, and adjacent Precambrian and Paleozoic units. If the data assembled by Mudge (1968) on depth of intrusion of concordant plutons apply here (see "Structure and Intrusion of Diabase"), then somewhat more than 2000 feet of sediments have been stripped by erosion. Frankel (1967, p.96) also notes that most basaltic sills and cone sheets were intruded under a sedimentary overload of 5000 to 15,000 feet. At Cornwall, if the hydration of chilled margin olivine to amphibole and chlorite were the result of high H_2O concentration, then a rather high hydrostatic (hence lithostatic) pressure may have been required to maintain dissolved H_2O in the melt. The thickness of the diabase chilled margin, the width of the contact alteration aureole around sheet plutons, and the amount of sheet diabase that must have been removed (note particularly the Coffman Hill diabase in extreme eastern Pennsylvania where only the basal center of a sheet remains), all support the removal of several thousand feet of upper Triassic sediments. For this to have occurred, either sedimentation was completed at a rather high elevation (2500 feet above sea level, or higher), or uplift and erosion occurred after completion of sedimentation at a lower elevation.

STRUCTURE

Introduction

The structural geology of the Cornwall area includes two very different depositional and tectonic groups: to the north, lower Paleozoic carbonates that are intensely folded and faulted and, to the south, upper Triassic redbeds that are intruded by diabase and monoclinally tilted to the north. The carbonates are part of a large folded and thrust-faulted nappe sequence in the Great Valley structural province that lies between the more intensely deformed Piedmont to the south and the less intensely deformed Valley and Ridge province to the north. Comprehensive details of the Paleozoic Great Valley province have been discussed elsewhere (e.g., Geyer and others, 1958; Gray and others, 1958; MacLachlan, 1966 and 1967; Root, 1970; Gwinn, personal communication).

The Triassic basin separates two groups of Great Valley lithologies and structures in an east-west arc across Pennsylvania sub-parallel to the arc of Appalachian curvature (Gray, Shepps and others, Geologic Map of Pennsylvania, 1960). The Cornwall area (Plate 21) lies along the northern Triassic basin margin on an east-west striking portion of the Triassic outcrop belt and near its western arcuate bend (Figure 58). Here there is no visible major north-border fault (Plate 21) although locally minor basin-margin faults have been proposed to the east (between the Reading Prong and Triassic sediments) and west (between the Blue Ridge and Triassic sediments). The Cornwall diabase sheet is one of several similar Triassic plutons, in part concordant and in part discordant, that are tabular, saucer-shaped intrusives near the northern Triassic border. Diabase dikes transect Triassic sediments and probably diabase sheets.

Paleozoic Structures

The Paleozoic carbonate rocks in the vicinity of Cornwall have been intensely folded and faulted. It was necessary to map these rocks in considerable detail to unravel the structural and stratigraphic relations (Geyer and others, 1958; Gray and others, 1958). The structure of the rocks is characterized by recumbent folds that have been refolded, so that axial planes also are folded. Folding and tectonic transport have produced a strong tectonic fabric. Flow features, such as axial-plane cleavage, plication of shaly laminae (drag folding), stretching of oolites, stromatolites or of other primary features, and boudinage are seen in nearly every outcrop (Gray and Lapham, 1961, Figure 4 and Plate 1). Dolomite interbeds have behaved somewhat less plastically than limy interbeds (Gray and Lapham, 1961, Plate 1).

The over-all structure of the valley north of Cornwall is particularly important with regard to the stratigraphic relations of the host Buffalo Springs Limestone that is believed to have been replaced by ore. It also bears upon the extent of deformation assigned to Triassic, or post-Triassic, time. The entire carbonate sequence north of Cornwall is overturned to the north and belongs to the lower limb of a major recumbent anticlinal nappe (Plate 21). The axis of this anticline has not been located and may be buried beneath Triassic sediments. Secondary anticlinal axes seen in the cuts on the Cornwall and Lebanon Railroad line north of Cornwall Station are interpreted as axes of second-order folds; i.e., digitations on a major fold (Figure 3) and are generalized in Plate 21. This interpretation is based on the fact that there is no mappable reversal of sequence; that is, the Snitz Creek Formation does not reappear south of the axis, which it probably would if this were a major axis. Therefore, the root zone of the major fold lies to the south, either beneath the Triassic cover or south of the Triassic basin in the limestones of the Lancaster Valley.

The cross sections in Plate 21 contain a generalized representation of the carbonate structure north of Cornwall, partly determined from the railroad cut mentioned above (illustrated in detail in Gray and Lapham, 1961, Plate 1). It shows the recumbent nature of the secondary folds well, but does not fully represent their isoclinal nature. Flow cleavage is more or less parallel to the axial planes of the major recumbent fold and to the axial planes of the secondary folds (digitations) on the flanks of the major fold. The axial planes of these recumbent folds are themselves broad and gently folded. Their axes, for the most part, strike generally east-west, parallel to the dominant regional strike of Great Valley folds. This gentle folding is sufficient to cause local reversal of cleavage dip; that is, in some outcrops the cleavage dips north more steeply than the beds so that individual outcrops appear to represent the normal limb of a fold overturned to the south (dip data, Plate 21). A later folding of the cleavage, with fold axes trending a few degrees east of north, was observed a few miles north and east of the mine but not in the immediate Cornwall vicinity.

In exposures of host limestone above ore in the open pit, the beds also are isoclinally folded. An unreplaced tongue projecting into ore is the crest of an isocline of dolomitic limestone (Plate 23). In mapping the beds on the bench above the ore, it was found that right-side-up beds alternated with upside-down beds without any evidence of fold crests. It should also be noted that the axial planes of these folds dip rather steeply north, 30° to 40°. This represents a secondary rotation or more intense folding of the cleavage (axial planes) than was observed in the Lebanon Valley carbonates. This anomalous dip may be the result of thrust displacement from the Buffalo Springs Formation at depth (Plate 21, cross sections) during emplacement of the limestone - Mill Hill Slate - Blue Conglomerate sequence or the result of displacement by diabase intrusion (Figure 16A).

Underground exposures of ore and limestone are so limited that it has not been possible to arrive at a unified pattern of the Paleozoic structures in the vicinity of the mines. Flow features such as drag folding and boudinage commonly are seen in banded ore (Figure 24). Brecciation of host limestone, particularly down dip in the southern end of the eastern ore body, also is present. At least in part, this brecciation is contemporaneous with, or later than, the ore stage (see Part 4, "Structures of the Eastern Ore Body" and "Ore Textures").

The formation of nappe structures, probably initiated during Taconic deformation, resulted in overturning and eventual rupture into northward-moving thrust slices (Plate 21). A major slice, the Yellow Breeches thrust (MacLachlan, 1966 and 1967; Geyer, 1970) lies north of the Cambro-Ordovician carbonates of Lebanon Valley at the Martinsburg shale contact, or within the shale, and is continuous westward to Harrisburg. Just south of Lebanon, another and probably subsidiary slice, the South Lebanon thrust (Geyer and others, 1958; Gray and others, 1958; MacLachlan, 1966 and 1967), displaces the carbonates, cutting slightly down section eastward from within the Stonehenge Formation to the Richland-Millbach and Richland-Schaefferstown (Plate 21) formational contacts (north of Cornwall). There is a third, apparently more local, slice northeast of Cornwall (Gray and others, 1958) and south of the South Lebanon thrust (Plate 21). This thrust lies structurally above the Snitz Creek Formation (i.e., at the base of the overturned unit). It is stratigraphically the lowest thrust in the area and is a subsidiary of the South Lebanon thrust. The above mentioned three slices all have cut successively lower in the section southward through the overturned carbonates. A fourth slice must also exist still further southward, but higher up in the section. This thrust plane lies below Mill Hill Slate at its contact with the overturned Buffalo Springs Formation at the north Triassic margin (Plate 21; also Plate 1 of Geyer, 1970). It apparently has not been folded (Plate 21). At least locally, a fault also is present at the same stratigraphic horizon above diabase at the Blue Conglomerate-host limestone contact, but present attitudes indicate a low-angle normal fault rather than a thrust fault (Figure 16-A and 16-B). If this is the same fault plane as the one at the base of Mill Hill Slate below the diabase, the sequence has been overturned subsequent to thrusting. The rotation of axial planes in the host limestone and the presence of a possibly basal unit (Blue Conglomerate) above a shaly facies (Mill Hill Slate) also may be indications of overturning. Based on the stratigraphic equivalency of Mill Hill Slate and a limy portion of the Martinsburg Formation (Middle to Upper Ordovician) the slice at the base of the Mill Hill Slate represents considerable apparent displacement. Conceivably it could be a remnant of the Yellow Breeches thrust (MacLachlan, 1966 and 1967) that also involves the Martinsburg Formation and separates it from the Lebanon Valley carbonates. Its unfolded nature indicates that it is younger than the folded thrusts in the Cambro-Ordovician limestones. Thus, it may be Acadian or younger. As such it may have rotated Buffalo Springs Limestone axial planes from nearly horizontal and south-dipping in the Great Valley (to the north) to north-dipping in host limestone above the diabase (an underthrust rotation). A similar axial plane disorientation may have resulted from the rafting apart of the Mill Hill Slate—host limestone sequence by diabase intrusion (Plate 21). Some movement at the base of the Mill Hill Slate or in the hornfels wedge also may have occurred during Triassic time resulting from basin tilting (rotation) and northward thrusting against Paleozoic rocks; however, a thrusting mechanism may not be required (Faill, 1969), even though evident to the west at Highspire. Top-bottom criteria have not been satisfactorily determined for the Mill Hill Slate so that its relation to nappe structure, except by analogy, is unknown, although some local overturning is evident south of Quentin. Other more local thrusts probably exist.

Structures within the Mill Hill Slate also are complex, although some primary laminations and cross-bedding are still visible, particularly in the road cut on Route 72, south of Quentin. Here, brecciated, quartz-rich beds (Blue Conglomerate facies?) outline folds asymmetrical to the north with beds dipping south 40° to 60°. Overturning could not be determined. Small faults with small displacement are present and commonly have been healed by secondary mineralization (Plate 4, B and D). West of Rexmont in a railroad cut, Mill Hill Slate attitudes range from steeply north dipping to the south to nearly horizontal and south dipping to the north (Figure 3). Tight, small, chevron folds, probably faulted on the steep, overturned north limb and a more gentle syncline are visible (Figure 3). The syncline plunges gently west with small-scale subsidiary folds (Figure 2), and the small chevron folds

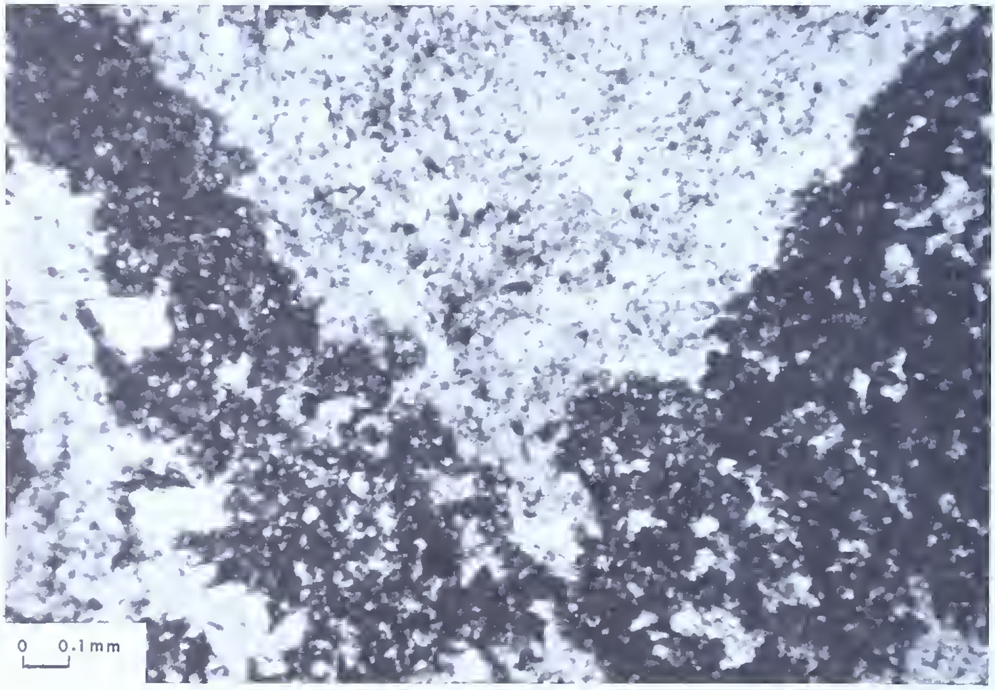

Figure 2. **Photomicrograph of late folding in Mill Hill Slate; taken from outcrop folds illustrated in Figure 3; fine-grained dark bands chiefly feldspar (less competent) and light bands (more competent) chiefly calcite and diopside; plane light.**

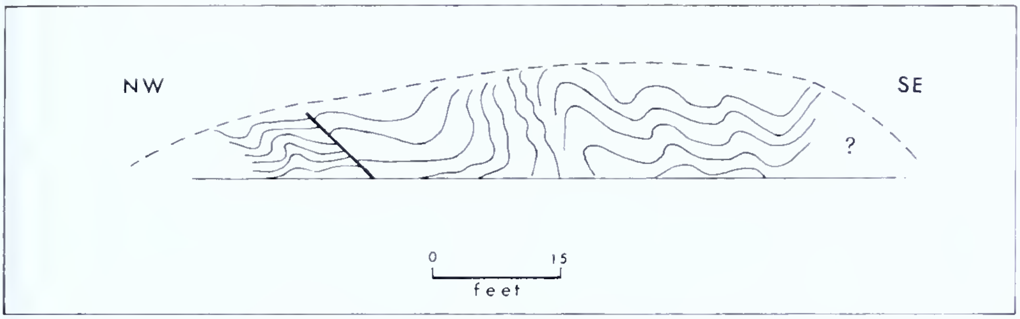

Figure 3. Sketch of bedding laminae in limy Mill Hill Slate from railroad cut west of Rexmont, north of Cornwall.

appear to plunge to the east. Faulting also is evident. Lamination textures and mineralogy of the Mill Hill Slate at these two localities are similar. Also at both localities the rock outcrops exhibit a mineralogical composition that is transitional between typical Mill Hill Slate and typical Blue Conglomerate (Figure 1). East of Cornwall, Mill Hill Slate terminates at a fault that also offsets diabase (Gray and others, 1958) near the Doner Mine (Plate 21).

Triassic Structures

Folding in Triassic sediments is far from conspicuous anywhere in the belt and, except for domains of differing strike and dip (Faill, 1969), is not evident at all in the Cornwall area. To the east (see Gray, Shepps and others, 1960), arcuate diabase sheets are paralleled by arcuate sediment patterns in a series of synclines and anticlines associated with the Quakertown Pluton (McLaughlin, 1959). Dips across the Triassic basin, however, are highly diverse, ranging from a few degrees to more than 50° north, often differing considerably over a small area. In addition, the strike in any one small area may change considerably so that rotation back to a common strike tends to emphasize dip variations. Folding is implied, especially since there are domains of rather constant strikes, the boundaries of which can be considered as fold axes. Primary and secondary folds certainly exist, whether due to deposition on lenses of different lithologies with resultant differential compaction, to diabase magma movement, to draping over an irregular basement (McLaughlin, 1964), or to deformation during (or after?) basin rotation.

In the Triassic belt south of Cornwall, as throughout much of the Triassic province, the known structural data are few. South of Cornwall, north dips on the lower Hammer Creek Formation range from about 30° to 50° (Plate 21; D. B. McLaughlin, unpublished data). To the north, toward the Cornwall mine, the upper Hammer Creek Formation dips north 20° to 30° on the surface (Plate 21), but in drift exposures underground in the eastern ore body, dips may be as low as 10° to 15° north. Rather gentle northward dips of approximately this magnitude also are present at the surface along the base of the New Oxford Formation (lower Newark Group) (Glaeser, 1964, Appendix I) but are steeper to the north toward the Hammer Creek contact, ranging from 30° to 60° for the most part (op. cit.). The high dips in the lower Hammer Creek and in the underlying New Oxford Formations are steeper south of Cornwall than at these same horizons elsewhere in the basin. Consequently, the upper Hammer Creek Formation at Cornwall dips somewhat less steeply than older Triassic sediments. Although these dip data are rather scanty and the measurements made were unevenly distributed, this irregular but rather abrupt northward decrease in dip may be more extreme than the usual trend elsewhere across the basin.

Strikes of lithofacies elements throughout the basin are similarly diverse. They may be attributed to drape folds, to minor late compression resulting from tilting (rotational) deformation, or to faulting. South, west, and east of Cornwall the strike of lithofacies laminations changes noticeably (Plate 21; Gray, Shepps and others, 1960). To postulate rigid rotation of this block, bounded by faults on the east and the south, would create a volume problem even if the southern fault were considered a hinge line with vertical displacement dying out westward. Such a movement would, however, displace the north-dipping units toward the north (after erosion), yielding the present map pattern. Some mobile or plastic behavior (e.g., interlaminar slip) combined with the movement of a bounded block could create a fracture sufficiently open to act as a terminus, both on the south and east, for the intrusion of diabase. Hence the site of the diabase might have been controlled by rotational, non-rigid fault-block movement.

The contact of the Hammer Creek Formation with the Blue Conglomerate seen underground is sharp, somewhat irregular, but without major brecciation of the Hammer Creek Formation. Several late, or post, Triassic faults offset Triassic lithologies oblique to the basin trend (Plate 21), but no border fault has been observed or intersected by drilling; although D. B. McLaughlin (unpublished manuscript, Pa. Geological Survey) has estimated a 7000 foot displacement near the Triassic north border in the Sinking Spring 7 ½' quadrangle. Elsewhere, some high angle faulting is believed present at the northern Triassic margin (Gray, Shepps and others, 1960; Geyer, 1970). Near Boyertown to the east, the Paleozoic units dip 35° to 45° beneath the Triassic sediments (Hotz, 1952, p. 384) and at Highspire about 15-20°. At neither locality is there a high-angle fault.

Structure and Intrusion of Diabase

The Cornwall deposits are located on the north side of a roughly oval outcrop of diabase that is in large part concordant to the enclosing sediments. The Buffalo Springs Formation lies directly beneath diabase (Plate 21 and Appendix 3, Drill Hole Location #155) south of the northern Triassic border in the area of the western ore body. The south dipping diabase sheet is parallel or sub-parallel to the contact of the Mill Hill Slate, to the Blue Conglomerate contact down dip, and to the overturned contact of the Buffalo Springs Limestone that outcrops immediately north of the Triassic- (Mill Hill Slate) border (Plates 21 and 23, cross sections). The southern part of the saucer-shaped sheet is, for the most part, parallel to north-dipping beds in the Hammer Creek Formation (Plate 21). Earlier interpretation of the intrusive as a combination of a vertical dike on the north and a sill on the south (Spencer, 1908) has been disproved by recent diamond drilling. In the vicinity of the mine, there is no surface evidence of a dike which is of sufficient size to have acted as a feeder for the sheet. West of Cornwall, the sheet diabase completely envelops Mill Hill Slate (Geyer and others, 1958).

The top of the south-dipping diabase sheet, mapped by plane table and from drill hole data, is irregular, exhibiting rolls, valleys, and apophyses or tongues extending into country rock (Plates 22 and 23). The average dip of the diabase in the mine area is about 25° south, but it dips less steeply down dip to the south, before steepening again at the toe of the ore body (Plates 21 and 23). The steepest dips (up to 60°) are over a roll between the eastern and western mines, at Middle Hill near the open pit (western mine), and at the north outcrop edge. The ore deposits tend to be located above valleys in the upper surface of the sheet (Plates 22 and 23). Surficial map data west of Cornwall (Plate 21) show that the base of the sheet also may be somewhat irregular.

The deepest point of the basin is not precisely known. Diamond drilling south of the mine has penetrated the top of the diabase in several places. The deepest penetration is about 2000 feet south of the open pit, where the top of the diabase is 2140 feet below the surface, at an elevation of 1320 feet below sea level. Here, diabase is probably close to the bottom of the present Triassic basin.

Only a few drill holes have penetrated to the underside of the York Haven Diabase Pluton, and these are all on the northern side of the basin in the vicinity of the mines. Just west of the western ore body, three diamond drill holes show that the dip of the underside is 35° south near the outcrop. Two holes, one drilled in the open pit and the other north of the open pit, give a dip of 25° to 30° south for the underside of the sheet (Plate 21, Section B-B'; Plate 23). At the east end of the open pit, a hole drilled through the sheet gives an average dip of 25° south, as does the hole drilled below the lowest workings of the eastern mine. This last hole indicates that the general southward dip of the underside of the sheet continues at least one-third of the distance between the northern and southern outcrop edges of the sheet.

Several holes drilled to explore for ore beneath the diabase at the Doner Mine near Rexmont indicated a dip of 50° to 55°. This may indicate a general steepening of the sheet toward the north Triassic margin, or perhaps only a local steepening of the contact in this vicinity. The data from these holes all support the conclusion that, in the vicinity of Cornwall, the underside of the diabase sheet dips south, nearly parallel to the top. On the south, the near parallelism of the outcrop to the strike of the enclosing sediments indicates that the dip of the sheet here is conformable with the enclosing beds (the so-called "York Haven Sill").

Drill core and outcrop information indicate that the diabase sheet is 1000 to 1200 feet thick in the vicinity of the ore bodies and for at least 1500 feet down dip. Based on width of outcrop and dip of the top of the sheet, the thickness is the same directly south of the western ore body but lessens eastward. Around the east end of the Cornwall sheet outcrop closure and on the northern side east of Rexmont, the thickness is apparently less than 1000 feet.

Several small faults and one major fault offset diabase (Plates 21 and 22). The major fault is located between the western and eastern ore bodies and continues through Triassic sediments for a total length of about 2 miles (Plate 21). Near the Elizabeth mine, its position is slightly displaced from that previously reported (Gray and Lapham, 1961). A fault near the Doner Mine also offsets diabase. Most of these younger faults have a NE or ENE orientation and are related to late Triassic or younger deformation of the Triassic basin (see Part 4, Structures of the Eastern Ore Body and Part 5, Diabase Dikes in Pennsylvania). A smaller fault offsets diabase in the subsurface near the western edge of the eastern ore body and is referred to in discussions of ore zoning (Plates 21 and 22). It is believed to be subsidiary to the major surface fault. As noted previously, the boundaries of the sheet, particularly on the east and west ends, may be controlled by buried or obscured faults striking essentially perpendicular to the basin and now filled by diabase.

The location of a "feeder" for the diabase sheet is problematical. Hotz (1952) has shown that the form of the sheet at Cornwall is typical of all Pennsylvania Triassic diabase intrusives, but makes no suggestion as to location of the feeders for these sheets other than that "steep fractures, formed during the tilting of the Pennsylvania Triassic basin, probably served as conduits through which the diabase magma rose" (op. cit., p. 385-7). Whether or not such steep fractures exist is unknown. Drilling has clearly shown that there is no large vertical dike directly below the ore bodies. The feeder must be located deeper in the basin, at the base of the saucer, or at one of the sheet extremities. The aeromagnetic maps of the region (Bromery and others, 1961) do not give any unequivocal indication of a feeder location, but the presence of a rather strong group of anomalies directly over diabase (rather than along the contact) in the vicinity of Governor Dick Hill would appear to favor the presence of a feeder there, if it is present anywhere in the area (Socolow, 1961).

It seems likely, therefore, that the sheet was emplaced by magma spreading laterally from a stock or dike, possibly at Governor Dick Hill. As Hotz (1952, p. 387) says, "Probably no actual fractures were necessary for the magma to assume a sheet-like form. It may have been easier for the magma to spread laterally than to rise to higher levels. Under these circumstances, the magma could probably make its own way by starting with initial irregularities in the conduit walls or by following potential planes of weakness. . . .". Details of the top surface of the diabase in the open pit favor this mode of emplacement. Pitches and flats in the top of the sheet when examined in the field appear to be the result of alternate cross cutting and concordant relationships on a small scale. Remnants of ore from the western ore body on some of the flats show banding parallel to the flats, while the pitches are cross cutting. The effect is clearly that of both magma and ore seeking the lines of easiest penetration, cutting across bedding on major joints or at structural discontinuities but paralleling bedding elsewhere.

From a study of sills intrusive into undeformed sediments, Mudge (1968) estimated that depth of burial ranged between 3000 and 7500 feet. Assuming that one foot of overburden is equivalent to about one psi, he concluded that the magmatic force of sill intrusion (i.e., lifting of the overburden) ranged from 3000 to 7500 psi. However, parts of the Cornwall sheet and parts of other Triassic plutons in Pennsylvania are not sills and have intruded inclined sediments. In addition, the mechanism of intrusion has not been simply to lift an overlying sedimentary load, but in part (e. g., north diabase limb at Cornwall) to utilize pre-existing structural planes. Hence the force of magmatic intrusion for north limb diabase may have been somewhat less than for the examples cited by Mudge (op. cit.), perhaps with a minimum force in the neighborhood of 2000 psi.

Inferred Tectonic Model for the Cornwall Area and the Triassic Basin

Evidence of thrusting at the host limestone-hornfels horizon may be inferred from the alternation of units encountered in drilling and from brecciation, particularly of the Blue Conglomerate (Plates 2 and 21). A low-angle north fault also has been observed in the "East End" open pit at this contact (Figure 16). Therefore, it probably is valid to assume that this contact is faulted throughout the Cornwall area. The existence of a *buried* high-angle reverse fault near the north border is problematic, but has been inferred in the cross-sections (Plate 21). The presence of Blue Conglomerate or Mill Hill Slate below diabase along a fault scarp (Plate 21) is also a structural inference for which there is no direct evidence. The reasons behind these inferences will become clear from ensuing discussions. They are posed as possible solutions to tectonic problems rather than as necessary requirements of the data.

The simplest mode of emplacement of the host limestone (correlated as the Buffalo Springs Formation) to a position above Triassic diabase is to invoke displacement by a magmatic intrusion, rafting the Buffalo Springs Formation and hornfels units up from below (Plate 21). If true, part of the Mill

Hill thrust now lies above diabase at the Mill Hill Slate — host limestone contact. Thus, intrusion is envisioned as in part following the plane of the Mill Hill thrust (a sole injection), and in part engulfing blocks of the Buffalo Springs Formation along with overlying Mill Hill Slate and Blue Conglomerate. One such block formed the "footwall ore body" enclosed in diabase, and another the limestone and hornfels units above diabase. A more complex and unsupported alternative is that the south-dipping portion of the diabase sheet followed an unrecognized, pre-existing, Paleozoic fault that cut across the Cambrian Buffalo Springs Formation and across the previously thrust Middle-to-Upper Ordovician hornfels units above the Buffalo Springs Formation. To us, displacement by Triassic magma seems more likely because there is no other evidence for such a locally significant thrust.

At Cornwall and elsewhere in this province, the saucer shape of the diabase sheet (Plate 21 and Figure 58) probably was governed by two factors: 1) the attitudes of the Paleozoic and Triassic sediments and of structural-stratigraphic contacts such that subparallel (concordant) intrusion presented the easiest intrusion path, and 2) the presence of a buried fault scarp and/or erosional shelf that provided a junction of the two structural attitudes (north-dipping Triassic sediments and south-dipping Paleozoic shelf) at the center of the diabase saucer and also provided a possible magma feeder channel. It does not seem likely that the shape of this sheet is accidental, particularly since there are numerous, similarly shaped sheets along the north Triassic border (Figure 58). Control of sheet shape by a buried north scarp raises the interesting possibility that buried faults exist at depth approximately beneath the center of each of the diabase plutons in other areas of the Pennsylvania Triassic basin. Certainly such an explanation would account for the lack of a visibly continuous north border fault at the presently exposed surface. The scattered occurrences of faults at the north Triassic margin as now mapped would then be minor features related to deformation during or after youngest Triassic sedimentation. In fact, similar small-scale adjustments may have prevailed throughout the sedimentational history. Another consequence of this suggestion may be that the northern part of the Triassic basin actually contains a series of steep, south-dipping, normal faults in a wide fault zone, most of them buried with only a few of the more recent ones visible at the present limit of exposure. However, interpretations other than that of a buried fault zone are possible (Faill, 1969).

Some restrictions also can be placed upon the attitude of the diabase at Cornwall at the time of intrusion that in turn can help to define the time of northward rotational tilting of the Triassic sediments. The Paleozoic formations beneath the north (south-dipping) limb of the Cornwall pluton contain thrust fault and fold attitudes that coincide with adjacent and regional Great Valley structures. This means that the Paleozoic formations cannot have been rotated significantly from their present position unless Great

Valley attitudes also have been rotated as much as 40° — 50°. This is considered unlikely, although some rotation has been suggested (e.g., Drake, 1969, p. 113-114; MacLachlan, personal communication). Thus, either the diabase is essentially in the same original attitude as at the time of intrusion or only the Triassic sedimentary cover (with or without diabase, host limestone, and hornfels units) has been rotated (underground observation showed that there is no significant and consistently present fault at the Hammer Creek—hornfels contact).

Several lines of evidence suggest that the diabase at Cornwall has not suffered a major change in attitude since emplacement. Less-dense, late differentiates have concentrated near the top of the diabase; olivine and MgO are slightly more abundant near the base. The sheet is thick, about 1000 feet, in comparison with the narrow, vertical, diabase dikes and Frankel (1967, p. 95) in a summary discussion notes that the greater the angle of intrusion into sediments, the narrower the width of the pluton. Rotation of the Triassic sediments (plus diabase) back to approximate sediment horizontality would result in a 65° to 85° dip for this part of the sheet, which is probably too steep for its thickness and for the ascent and concentration of differentiates. If the diabase here were once nearly vertical, erosion should have contributed diabase minerals to the north basin; but there does not seem to be any evidence of diabase minerals or rock fragments in the coarser sediments (Glaeser, 1966) unless they all have been removed by subsequent erosion. Although cryptic layering indicates a significant horizontal component for the sheet attitude (see Part 5, "Petrology"), significant gravitational layering is not present, as it is in the nearly flat-lying Palisades sheet. Together these observations would seem to confirm a moderate original dip, between 20° and 50° for this part of the sheet (i.e., emplacement after basinal tilting).

The character of the chilled facies, coarse-grained interior textures, width of contact aureole, evident erosional stripping, and, by analogy, the depths of intrusion noted by Mudge (1968) and Frankel (1967) indicate that intrusion probably occurred under at least 2000 feet of sedimentary cover. Bleaching and metamorphism indicate that these sediments were at least partly lithified, or pore water would have rapidly dissipated heat transfer and greatly reduced contact metamorphic effects. Together, these observations also imply that intrusion occurred after Triassic sedimentation (the last preserved Triassic sediments are fanglomerates (Glaeser, 1966), some of which are cut by diabase.

The lines of evidence that might be construed to suggest horizontal diabase intrusion before major tilting (Stose, 1932) are less convincing. There are a few north margin normal faults cutting both Triassic sediments and diabase which could indicate that tilting occurred after sedimentation. However, they are of small extent, of irregular distribution, and probably are related to late

Triassic or post (?) Triassic deformation (see Part 5, "Diabase Dikes of Pennsylvania," Figure 56, and Sanders, 1963). In addition, some late tilting by major fault reactivation at depth could have produced these observed fault relationships and seems a more likely, perhaps a necessary event to explain the magnitude of observed variation in the dip of late Triassic sediments. Another feature that might suggest horizontal intrusion before tilting is the system of thermal contraction cracks in the top of the sheet that are oriented approximately perpendicular to the upper surface. However, the present diabase sheet dips only 15° to 30° (Plate 23) and this attitude probably would not preclude their development. In addition, the best contraction cracks observed are where the diabase sheet dips more gently, below the eastern ore body (sections L—N, Plate 23).

Another source of support for late basinal tilting comes from Beck (1965) who collected diabase samples from Pennsylvania sheets for paleomagnetic pole measurements. He believed that the rather small scatter of magnetic pole alignments before dip correction could be encompassed by a small circle whose pole represents a rotational axis approximately parallel to the strike of the Triassic basin. He concluded that basinal tilting occurred after sill intrusion, that both diabase and sediments have since been rotated along a basinal axis, and that initial diabase intrusion occurred along a plane within 5° of horizontal. The significance of these data we believe, however, to be open to question, particularly in the Cornwall area. The paleomagnetic sampling did not include the Cornwall mine area of the sheet; in fact, there is almost no representation of samples from the south-dipping, northern portions of any of the sheets. The data are largely based on samples from the southern sills. Furthermore, the data for the York Haven Pluton (including Cornwall, but from the south sheet edge) he notes as anomalous, in that the pole plots do not exhibit a uniform distribution for sight-mean pole directions of magnetization. Thus, Beck's interpretation of the paleomagnetic data can, *in sensu strictu,* be applied only to the Gettysburg and Morgantown ("Birdsboro") Plutons (Figure 58). As a final comment, it should be noted that the scatter of all points is large and is not greatly improved after dip corrections as should be the case for late rotation of the basin (viscuous remanent magnetization probably is not the cause of this scatter; see DeBoer, 1968). In view of these objections, we do not feel that there is any justification in applying the hypothesis of horizontal magma intrusion to the diabase at Cornwall, whether or not it does apply to the south diabase limb of the York Haven Pluton.

If then, Cornwall diabase emplacement occurred at approximately its present attitude, major basinal tilting occurred somewhat before diabase emplacement, or diabase was not noticeably involved in the tilting rotation of the upper Triassic sediments. There is not a great deal of inferential evidence from which to make a choice between these hypotheses. The first model requires that a buried fault scarp or erosional shelf edge be covered by Hammer Creek sedimentation without a major amount of thrusting along the Paleozoic — Triassic contact but leaves unexplained the steep north dips of the Triassic sediments unless the Paleozoic prism below and adjacent to the north margin has been tilted considerably. Data are not available to show whether the Triassic beds flatten out somewhat at depth, which they would have to do if no faulting were involved. The second model requires a compression against the scarp, thrusting Hammer Creek sediments northward to cover the earlier basin edge, but without significant reorientation of diabase. It seems likely that thrusting of this magnitude would involve more brecciation at the Triassic — hornfels contact than has been observed at Cornwall, especially within the Triassic sediments (although the contact is only rarely observable). It also seems likely that any major thrusting would have involved the diabase to a greater extent than the evidence supports.

However, the lack of major faulting and brecciation at the Triassic-Paleozoic boundary here (according to Hawkes and others (1953), a core near Boyertown did show evidence of faulting at the Triassic contact with Paleozoic carbonates and small thrust faults were observed by the author at this horizon near Highspire) suggests an alternative deformational mechanism for tilting the Triassic beds northward (R. Faill, personal communication). If this contact acted as a mechanical boundary, then initially, approximately horizontal Triassic beds may have been rotated by flexural bedding-plane slip in response to an assumed subhorizontal maximum principal stress, much as beds are rotated in kink-band deformation. The low friction on the Triassic beds, because of their initial low angle to the maximum stress direction, would facilitate this process, whereas the less favorable orientation of mechanical anisotrophy in the Paleozoic rocks would inhibit the mechanism. Therefore, the Triassic-Paleozoic contact was a mechanical boundary surface which parallels, and approximates the position of, the unconformable contact. In this manner, deformation could proceed within the Triassic beds with little or no deformation in the Paleozoic units. As the rotation of the Triassic beds proceeded, friction between the beds increased because of the increasing angle of bedding to the maximum stress direction. This process could then "lock" when the friction became great enough and, if relief of stress were still necessary, faulting adjacent and parallel to the mechanical boundary (uncomformable) contact could occur as a late stage of deformation. Because some disruption of the rocks would accompany such deformation, diabasic magma intrusion could occur either during rotation of the Triassic beds (at some depth below presently exposed levels) or later accompanied by minor thrusting against the Paleozoic-Triassic shelf after the locking mechanism had essentially caused the cessation of tilting. Utilization of this mechanism of tilting, which can be referred to as interlaminar ("flexural") slip, is rather like compression against a deck of cards locked against a dipping surface.

Two premises are implicit in the foregoing discussion: 1) that discontinuites acted as a control on the shape of the diabase sheet at Cornwall as previously discussed and 2) that magma will rise into the highest crustal level permitted by overlying lithologic pressure, magmatic and tectonic forces, and rock unit densities within the crustal column. If, then, diabase magma rose into the Hammer Creek Formation because this was the highest level that it could attain, its restrictive locus near the north border is at least partly explained. Magma conduits may have been along an erosional fault scarp at the Paleozoic-Triassic discontinuity, along a series of scarps within the Paleozoic or lower Triassic formations below the presently exposed Hammer Creek level, along a steepened thrust contact (such as a nappe root zone) similar to , or part of, the Yellow Breeches and Mill Hill thrusts.

As the magma moved at depth, deformational stress intiated the mechanism of interlaminar tilting within Triassic lithofacies. At the same time, and possibly as a consequence of subcrustal tholeiite generation, cross faults may have formed, dividing the basement of the Triassic basin into blocks at different depths. These block edges and lesser cross faults then would control the eastern and western terminations of major plutons. Initial magma intrusion may have occured, on the south limb only, at a nearly horizontal attitude. Magma that continued to intrude (north limb) would have had to remain essentially fluid until tilting was nearly completed. Magma ingress on the north limb was facilitated by an erosional discontinuity and the Mill Hill fault plane. Completion of tilting may have been related to a locking of interlaminar slip caused in part by the thick, competent, crystallized north limb plate of diabase. By this mechanism, only the Triassic sediments are required to have participated in the major part of the northward basin rotation. The chief advantages of such a mechanism are that: 1) it allows tilting of Triassic sediments with only a slight disturbance of the earlier Paleozoic attitudes (minor late thrusting occurred at Cornwall within the Mill Hill Slate and Blue Conglomerate and also at Highspire and Boyertown) and 2) it explains the shape of the Cornwall sheet in terms of structural discontinuities and does not require breaking or bending of largely solid diabase (e.g., at the saucer center) during rotation.

This model has several consequences capable of testing with presently available data. During the intrusion of the diabase south limb, the diabase is hypothesized as having been more nearly horizontal than diabase intruded later at the north limb. Small thicknesses of olivine concentrations have been noted in the Gettysburg and York Haven Plutons that have not been observed along the north limb. Thus, in the more nearly horizontal position of the south limb, gravitational settling has played the role expected from such a model. In addition, the data of Beck (1965) taken from south limbs are now in better agreement: the scatter of south limb pole plots can be attributed to rotation of diabase (and sediments); the north limb magma still retained some mobility while sediment and crystallized south-limb diabase were changing attitude.

A uniform structural control along the east-west bending axis (linking the saucer centers) also is required. Possible surficial discontinuities meeting this requirement already have been noted. However, the deep-seated origin of tholeiite requires, in addition, a more fundamental structural control at the subcrustal level. A major tectonism is required for the formation and deformation of the surficial Triassic basin, such a contemporaneous tectonic and magmatic coincidence as is implied by this hypothetical model need not be accidental but can be considered to be a result of magma formation and movement at depth caused by major subcrustal instability. The Triassic basin thus becomes a kinematically induced magmatic and tectonic feature that began with the basement and concluded, after magma solidification, with late surficial readjustment and basement uplift (see Part 5, "Diabase Dikes of Pennsylvania").

The problem of the mode of Triassic basin downwarp and the exact nature of basement involvement is still unknown. Geophysical interpretation of aeromagnetic data (Bromery and Griscom, 1967) for some areas of the Triassic basin indicates a rather shallow basin on the order of, and not exceeding, about two miles of sediments. Projection of dips from the south basin edge northward, on the other hand, requires a basin several times this depth. Drilling in the southern Triassic basin in York County encountered almost 9000 feet of sediments, an amount very close to a thickness predicted on the basis of dip projection. Thus, for at least moderate distances from the southern margin, dip projection may provide an accurate thickness. Another consideration is the large number of transverse and oblique faults that offset sedimentary lithologies. These also might be faults parallel to arcuate lithologic outcrop patterns and eastern or western fault terminations of major diabase plutons, but these would be extremely difficult, if not impossible, to observe in the field. These data — the variations in sedimentary dip, numerous small faults with minor displacement, the possibility of small, unrecognized drape folds, interpretations of the geophysical data that permit the interpretation of different depths to basement (R. W. Bromery, personal communication), and the possibility of faults as the causal factor in confining major plutons — all point to the possibility that the depth of the basin is not uniform, but may be broken into a series of east-west blocks with various vertical displacements. Supporting this is the belief that some crustal instability is required to explain sedimentary petrographic data that show a source direction that changed from south (older Stockton — New Oxford time) to north (younger Hammer Creek time) with different distribution patterns for each (Glaeser, 1966) without major uplift of the Piedmont during Triassic time (for which there presently is no independent sedimentational, structural, or radiogenic evidence).

One hypothesis to cover these somewhat disparate facts regarding basin geometry is a basin step-faulted on the north (similar to the section at Buckingham Mountain proposed by Zietz and Gray, 1960), thereby considerably reducing and varying basin depth from a single, uniform, maximal thickness calculated by dip projection. Such a model requires a series of transversely faulted blocks at various depths from the present surface. Progressive northward faulting of the Triassic basement with time would have the additional advantage of reducing basin depth without yielding conspicuously large drape folds, while maintaining a steep north dip throughout the sedimentary column. It also permits the existence of different depths to basement at different locations, helping to reconcile the view of the various geologists who have studied the Triassic basin (e.g., Stose, 1932; McLaughlin and Gerhard, 1953; Sanders, 1963; Glaeser, 1963, 1964, 1966; Bromery and Griscom, 1967). How great a role ascent from depth of a tholeiitic magma may have played in a progressive basinal subsidence to initiate basement fault movement remains unknown. Another possibility, presently under investigation (Faill, 1969) is of basin down-warp with rotational axes marginal to and parallel to the Triassic outcrop belt. Since most of the basin-margin faults (north-border faults) are younger than the initial basin (i.e., post sedimentation and post diabase emplacement) and since in many areas only an overlap relationship can be demonstrated, this hypothesis deserves some consideration.

Sequence of Depositional and Tectonic Events

The following summary presents a generalized sequence of sedimentational and tectonic events derived from study of the Cornwall area. Details of the events have been discussed in this report or can be obtained by reference to the cited literature.

1) Cambro-Ordovician carbonates and shales were deposited under miogeosynclinal conditions.

2) Paleozoic sediments were deformed. Beginning in middle or upper Ordovician time, deformation alternated with periods of more quiescent sedimentation throughout the Paleozoic era. Ultimately, extensive recumbent folds, satellite isoclinal folds with south-dipping axial planes, and thrusts were formed. At Cornwall, one thrust (among several) placed an Ordovician limy shale (Mill Hill Slate), originally deposited at a considerable distance (probably miles) to the south, on top of the Cambrian Buffalo Springs Formation. This thrust is considered to be a late phase of nappe deformation. Earlier thrust planes are folded, and thus folding and thrusting probably are both Taconic and Acadian or Alleghanian (MacLachlan, 1966 and 1967). Plastic flowage in the limestones indicates that the folds were formed under a thick cover of Paleozoic sediments. During the episodes of deformation and erosion, and before Triassic time, much of the post-Ordovician cover probably was removed.

3) Deposition of Triassic sediments occurred first from a south source and then from a north source (Hammer Creek Formation). Initial deposition may have begun in an erosional Paleozoic limestone valley. Subsidence, perhaps resulting from a zone of step-faulting in the basement, may have been more rapid toward the north progressively with time.

4) Rotation tectonics and probably magma movement occurred at depth essentially contemporaneously. Volcanism occurred before the completion of Hammer Creek time sedimentation. Rotation probably was accomplished either by down-warping or successive down-faulting of the Paleozoic formations, or by upwarp of the adjacent basement, and by interlaminar slip within the Triassic sediments along lithologic boundaries.

5) Tholeiitic diabase magma was intruded. The magma rose to the highest attainable level, the Hammer Creek Formation. It either remained mobile along the north limb at Cornwall until rotation was nearly concluded, or it intruded after rotational tilting. Readjustment faulting as sediments were compressed over an uneven, perhaps faulted, pre-Triassic basement is believed to have continued after Hammer Creek lithification (small intra-basinal and basin-margin faults). Intrusion was localized by the Mill Hill thrust plane, by an erosional shelf, and engulfed and rafted upward blocks of pre-Triassic sediments.

Tilting occurred with attendant compressional force. A possibly earlier diabase injection on the south limb followed nearly horizontal boundaries but was subjected to tilting. Terminations of major plutons may have followed faults transverse to the basin strike.

6) Further tilting by laminar slip became difficult, if not impossible, at a critical stress angle, perhaps abetted by diabase crystallization. The emplaced diabase sheets are concordant to Triassic sediments and to overturned, south-dipping Paleozoic nappe limestones; thus, they followed major lithologic or structural discontinuities. The mechanisms of tectonic deformation all are believed to have been localized by a zone of subcrustal instability (basement tectonics).

7) Fractures formed in solidified diabase. Steeply dipping faults and joints developed cutting through the entire sheet at Cornwall. These movements may belong to the final stage of basin rotation. Potassium metasomatism, followed by ore solutions, passed through these fractures into adjacent rocks (see Part 3, "Contact Metamorphism and Potassium Metasomatism"). A buried fault scarp may have been utilized as an ore solution channel. Movement of this ore fluid was in part controlled by previous fracturing, fold laminae, pitches and rolls in the top of the diabase, and sediment permeability (see Part 4, "Geology of Cornwall Area").

8) Later fractures throughout the Triassic province, formed by broad regional arching, are radially distributed and were influenced by a locally variable stress field (see Part 5, "Diabase and Associated Igneous Rocks").

These fractures were intruded by diabase dikes. Throughout this final stage in Triassic basin development, small scale faulting may have been a continuing, although not a spatially or temporally uniform, process.

9) Erosion of probably at least 2000 feet of Triassic sediments to the present topography occurred. Epicenters of minor earthquakes have been recorded here up to the present time (Bromery, 1967, Map 1) as part of an eastern Appalachian belt of foci with depths near, or below, the Mohorovicic Discontinuity (Woolard, 1969), indicating continued structural readjustment.

PART 3. CONTACT METAMORPHISM AND POSTASSIUM METASOMATISM

by D. M. Lapham

CONTACT METAMORPHISM IN THE TRIASSIC BASIN

Throughout the Triassic province of Pennsylvania, widespread mineralogical and textural changes accompanied the Triassic intrusion of diabase into the surrounding sediments. The contact aureole characteristic of narrow, vertical diabase dikes is small (or absent) and mineralogically distinct from that of the larger sheets and plutons with which magnetite ores are occasionally associated. Characteristics of alteration adjacent to sheets due solely to thermal metamorphism are somewhat obscured by metasomatism and hydrothermal alteration in the vicinity of ore bodies (e.g., Dillsburg, Cornwall, Morgantown, French Creek, and Wheatfield), so that the best estimate of these effects is obtained from contacts where no appreciable magnetite is present. Unfortunately, these have not been studied systematically. However, a few effects appear to be characteristic, based on data from a few areas lacking metasomatic alteration and on mineral assemblages replaced by metasomatism and ore-stage deposition at Cornwall.

At the contact of sheet diabase with red Triassic sediments (arkose, quartzose sandstone, shale, and limy or quartzose conglomerate), the sediments are bleached from a light pink to dark gray, becoming darker and denser ("hornstone") nearer the contact (Spencer, 1908; Montogomery, 1956). Frequently, specular hematite has developed by the mobilization of iron under oxidizing conditions, commonly at some distance from diabase and especially along fracture planes in the adjacent sediments. Less commonly, epidote (Spencer, 1908, p. 14), serpentine, garnet, and chlorite are present associated with the hematite, especially in limy hornfels or metamorphosed carbonates. Locally, muscovite, feldspar, hornblende, and less commonly pyroxene or cordierite, may be developed quite near the diabase intrusive (Montgomery, 1956, p. 179-180; Hotz, 1950, p. 4-5), although cordierite has not been detected at Cornwall in the present study. Normally, red Triassic shale in contact with diabase is typically a dark gray to black, fine-grained hornfels, often difficult to distinguish from the diabase chilled margin. The widths of this bleached aureole differ (summary by Frankel, 1967, gives a range of about 200 to 1000 feet), but extends at least 300 feet from Cornwall diabase (also see Hickok, 1933, p. 210). Secondary zeolite mineralization (veinlets and vugs), in addition to secondary quartz (rims on older quartz cores and veins) and calcite, is common, yielding many notable mineral localities both at Cornwall and elsewhere (Lapham and Geyer, 1969).

Less is known about bulk-rock chemical changes, if any, adjacent to diabase. Simpson (1969) reports a hornfels deficient in silica with no evidence of secondary deposition of quartz within the sediments. Therefore, he suggests that silica either moved from the sediments into the diabase or that there was an addition of other major elements such as aluminum, calcium and sodium to the hornfels. Although analyses of diabase are not presented, there is no evidence elsewhere of silica enrichment of diabase magma; hence, the latter process (addition) seems more reasonable. In the Cornwall area, thermal metamorphism of hornfels units is believed to have occurred essentially in a closed chemical system.

METAMORPHISM OF LIMESTONE AT CORNWALL

At a few localities such as Cornwall, Paleozoic limestone formations (at Cornwall, carbonaceous near the Blue Conglomerate contact) are in contact with, or only a short distance from, diabase. However, their proximity to ore renders difficult any assessment of purely thermal metamorphic effects. Throughout the Triassic belt, tremolite is the most ubiquitous mineral, but it is more abundant in dolomitic horizons; mica (frequently phlogopite), diopside (Plate 1-A), feldspar, garnet, epidote, pyrite, and hematite also are commonly present. Veins of datolite and prehnite occur rarely within limestone adjacent to diabase contacts, notably at Cornwall and near Dillsburg (Hotz, 1950, p. 6). At least some of these minerals are believed to be metasomatic in origin, closely associated with ore-bearing hydrothermal solutions (see Part 4).

At Cornwall, euhedrally recrystallized metamorphic quartz (strain-free) and chlorite are present in shaly laminae. Also at Cornwall, pyrite and, to a lesser extent, quartz and feldspar (most commonly microcline) are concentrated in carbonaceous stringers in otherwise pure marble, probably as reconstituted or recrystallized minerals and relics of an original banding. These contact limestones generally are recrystallized to marble and may contain secondary quartz or calcite in solution cavities.

It is interesting to note that despite the metamorphic silicates developed in the Cornwall host limestone, chemical analyses of limestone from above the ore in the open pit (Table 2, column 3) do not show any significant chemical addition when compared with Buffalo Springs Limestone north of the Triassic belt (Table 2, columns 1 and 2). However, the individual oxide

Table 2. *Chemical Analyses of Buffalo Springs Formation at and near Cornwall, Pa.*

	(1)	(2)	(3)
SiO_2	8.21	12.61	11.27
Al_2O_3	6.91	2.24	2.07
Fe_2O_3		0.95	0.94
CaO	41.25	32.24	42.51
MgO	5.56	12.88	4.88
CO_2	38.08	39.09	38.33
	100.01	100.01	100.00

(1) Average of 4 Buffalo Springs Formation samples, ½ mile northwest of Cornwall (O'Neill, 1964, p. 30).

(2) Average of 11 Buffalo Springs Formation samples, northeast of Cornwall mine (by Bethlehem Steel, 1952).

(3) Average of 31 host limestone samples, Cornwall, open pit western ore body (by Bethlehem Steel, 1952); presumed Buffalo Springs Formation.

ranges for each sample that comprise each average are very broad (Table 1 and O'Neill, 1964). To determine addition or subtraction of oxides, a comparison would have to be made within the same lamina of Buffalo Springs Limestone and host limestone. Since the two limestones are not continuous, such a comparison cannot be accomplished. However, there probably is sufficient SiO_2 in the Buffalo Springs Formation to make unnecessary the postulation by Popovich (1964) of silica metasomatism in the hanging wall of the western ore body.

Silica addition within the ore zone, below the hanging wall, presents a different problem. In both the eastern and western ore bodies, and especially near the footwall, there is considerable silication of limestone. Diopside, actinolite, and mica make up as much as 90 percent of the gangue (non-ore) rock, exhibit major concentrations throughout the ore zones (Plate 1, A-C and Figure 26), and represent at least a local concentration of silica. Popovich (1964) on the basis of calibrated X-ray fluorescence analyses presented evidence for considerable SiO_2 introduction at Cornwall and an even greater amount at Morgantown. Simplifying the rock types into limestone, actinolite-rich rock, diopside-rich rock, magnetite-rich rock, and diabase, he obtained the silica amount (by planimetry) and the density of each altered rock type. From these data, he calculated that there was significant silica addition, a maximum in the diopside-rich rock and a minimum in the limestone. Magnetite-rich rock, the distribution of which is inverse to that of the silicate minerals, is also low in silica (see Part 4, "Geology of the Cornwall ores") as noted by Popovich (1964). Popovich concluded that silica was introduced from adjacent diabase because his analyses of a core through diabase showed decreasing SiO_2 toward the top of the sheet and because SiO_2 in host rock also decreases upward from the diabase upper surface into limestone (western ore body only). However, as discussed subsequently, there is more than one possible origin for the silicate minerals. Earliest silicates, such as coarse diopside and coarse actinolite, are uniformly present as contact metamorphic minerals in limestone whether or not ore is present. Their silica content easily could have been supplied from siliceous laminae in the host Buffalo Springs Limestone (Table 1 and column 3, Table 2). Later, metasomatism and hydrothermal ore deposition will be shown to have introduced additional silica yielding finer-grained actinolite, chlorite, and perhaps diopside (the minerals that replace those of the contact metamorphic suite). There is no necessary connection between silication in the ore zone and silica distribution in the diabase sheet. In fact, the top of the diabase most probably is not depleted in silica if diabase pegmatite and granophyre compositions are considered.

Within these contact-metamorphosed limestones, there is a fairly consistent paragenetic sequence, although not all the minerals listed below are the result of thermal metamorphism. Remnants of the original sediment, which are rarely present, include quartz (usually rounded grains or cores), muscovite (small shreds that are in contrast with coarsely crystalline metamorphic minerals), potassium feldspar (rounded, detrital grains), calcite, and dolomite, the latter two commonly recrystallized. Following lithification, the first new crystallization is represented by contact-metamorphic minerals: first diopside and then tremolite with phlogopite, both of which were observed to enclose diopside. Biotite, which is rare in limestone, may be of metamorphic origin. Transecting veins of cloudy orthoclase and coarsely crystalline tremolite cut this fabric and are in turn replaced by actinolite, magnetite, and pyrite (ore-stage mineralization). The waning stage of mineralization was characterized by veinlets of calcite, serpentine, chlorite, and zeolites. Some of this sequence is illustrated in Plate 1 and Figure 4.

An example of typical metamorphic and metasomatic relationships is illustrated by the textures and minerals at the host limestone-Blue Conglomerate contact from underground drifts in the eastern ore body (Figure 4). The Blue Conglomerate contains breccia fragments of quartz and feldspar in a fine-grained matrix of mica (biotite and muscovite) and plagioclase feldspar (also see Plate 2). The limestone largely has been recrystallized to calcite. Hematite occurs on the limestone side of the contact and grossular garnet at the contact, or just within the Blue Conglomerate facies. Metallics (pyrite and magnetite) occur preferentially in calcite, but replace all minerals, including a vein of cloudy orthoclase and actinolite. The effects of compositional control are clearly illustrated by these spatial relationships: available silica in Blue Conglomerate localized silicate mineralization; both calcium from limestone and SiO_2 from Blue Conglomerate localized garnet near the contact; and hematite preferentially replaced limestone (especially at this formational contact).

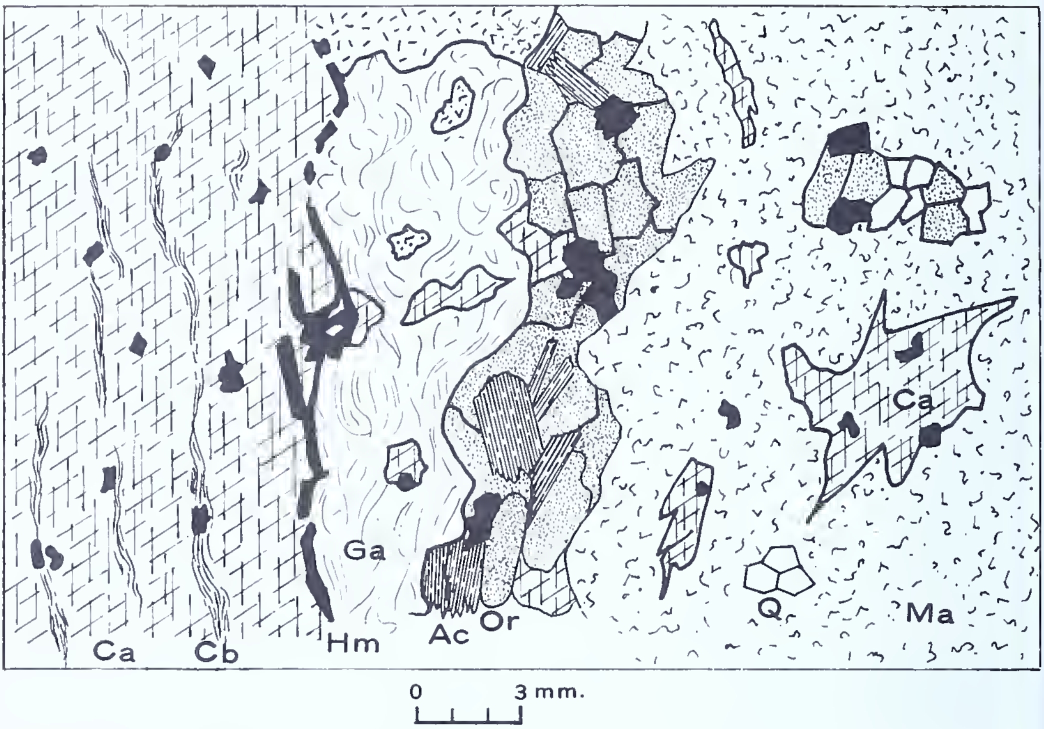

Figure 4. Sketch from petrographic thin section illustrating metamorphism and metasomatism at the contact between a limestone inclusion and Blue Conglomerate. Inclusion is carbonaceous (Cb) calcite (Ca) with pyrite and magnetite. Hematite (Hm) formed on limestone side and grossular (Ga) at the Blue Conglomerate contact. Blue Conglomerate matrix (Ma) with some secondary quartz (Q) is transected by a vein of cloudy orthoclase (Or) and actinolite (Ac).

CRITERIA AND TERMINOLOGY OF HORNFELS ALTERATION

Recognition of thermal metamorphism (as distinct from metasomatism and hydrothermal alteration) has been made largely on the basis of mineral associations common to non-ore and ore-bearing diabase contacts. However, other criteria also have been used. From paragenetic observations(see Plates 1-4 and 8-11) metasomatic minerals such as potassium and sodium feldspar and hydrothermal minerals such as actinolite and chlorite associated with magnetite-pyrite ore mineralization are consistently younger than a group of contact thermal minerals (diopside, tremolite, garnet, phlogopite) which they replace or whose fabric they transect in cross-cutting pods and veinlets. In addition, the chemistry of hornfels units in the vicinity of ore indicates chemical reorganization and addition superimposed upon an amphibolite and (hornblende) hornfels facies (see Part 3, "Hornfels Metamorphism and Metasomatism in the Cornwall Area"). Nevertheless, in spite of chemical and mineral-replacement criteria, the time boundary between these processes is indistinct and is more a convenience for discussion than an indication of any large time separation.

The term metasomatism is used in this report for the process of chemical addition typified by the crystallization of potassic feldspar in the eastern ore zone that originated from a potassium source outside the immediate hornfels system as defined by Goldschmidt (1922). It does *not* include a possibly earlier hornfels enrichment in Na_2O of uncertain origin that may be widespread at diabase contacts (adinole development) and that also could be a metasomatic addition to the system. In so doing, Goldschmidt's usage has been modified to include wall-rock alteration. Metasomatism is usually nonexistent, or of very limited extent, where there has been no development of magnetite-sulfide ore (cf. Montgomery, 1956, p. 180-181). Hornfels, as used here, refers to the combined Blue Conglomerate and Mill Hill Slate units but not to altered limestone (referred to as tactite by Hotz, 1950, p. 5).

The term "Fe-orthoclase" is used for orthoclase in which some amount of Fe^3 is believed to have substituted for Al^3 in the feldspar lattice. Hematitic orthoclase refers to hematite clouding of orthoclase.

In the vicinity of the Cornwall ore body, metasomatism and hydrothermal alteration have produced widespread changes in Mill Hill Slate and Blue Conglomerate. Because these changes are an important link in the chain of events between diabase crystallization and the formation of ore and because they yield pertinent geochemical data on the conditions affecting ore formation, these units are discussed in detail below. Mineral and chemical facies assemblages, mineral reactions, and rock textures are utilized to help differentiate contact metamorphism from metasomatism. In these units, alternation during ore-stage mineralization is at a minimum because these hornfels units have been impermeable to ore replacement except over the central part of the eastern ore body.

HORNFELS METAMORPHISM AND METASOMATISM IN THE CORNWALL AREA

The Blue Conglomerate

Introduction

The Blue Conglomerate has been described as a metamorphosed breccia (Part 2), probably of Ordovician age (Martinsburg equivalent), intimately associated with, and overlying, the Mill Hill Slate. It was originally defined from underground workings and is a major unit above the eastern ore body. Here, on down-dip portions, it forms the ore hanging wall (Plates 21 and 23). The original unit from which this fault breccia was derived may have been a quartz (shale) pebble conglomerate, a coarse sandy facies within a shale unit, or a shale containing vein quartz. Petrographic and stratigraphic observations favor the interpretation of a local conglomerate interbedded with sandy and limy shale, but brecciation, metamorphism, and metasomatism have obscured most clues to its original nature except that it was a clastic rock, as noted by Spencer (1908, p. 18). Very little has been written about this unit other than to note its presence in the hanging wall above host limestone (or above Mill Hill Slate), partly because it was not a major rock type over the western ore body where open pit operations, underground mining, and geological studies began. Since the initiation of mining in the eastern ore body, the Blue Conglomerate has taken on added significance both as a "cap rock" above ore and as a unit typifying silicate alteration.

Mineralogy and Petrography

Normal blue-gray Blue Conglomerate (as opposed to altered pink Blue Conglomerate) is composed largely of plagioclase feldspar, quartz, and mica (representative sample analyses given in Table 3). Kaolinite, calcite, chlorite, orthoclase, microcline, and actinolite are present in minor amounts (each less than 3 percent).

This mineralogy differs from that of metasomatized, pink Blue Conglomerate (Table 3). Ferriferous orthoclase is present only in the metasomatized unit. Kaolinite and chlorite are present only in the normal contact metamorphic Blue Conglomerate. The average An content of plagioclase in the metamorphic unit is higher (An_{25} or greater) than in the metasomatic unit (average about An_{15}). Normal Blue Conglomerate contains more quartz, about 25 percent compared to an average of about 12 percent in metasomatized Blue Conglomerate. The X-ray reflections for muscovite are broad in the contact metamorphic facies, indicating the presence of "illite" that is not present in the metasomatized unit. These mineralogical data, together with chemical data presented subsequently, serve to distinguish metasomatism from contact thermal metamorphism. Rock color reflects these differences. The metasomatic unit is pink (ferriferous orthoclase) and black (less quartz), whereas the contact facies is gray-black (chlorite, actinolite, muscovite) to blue-gray and white (calc-silicates).

The texture of normal, contact metamorphic Blue Conglomerate ranges widely. Breccia fragments and metamorphic pods of calc-silicates (chiefly diopside, tremolite, plagioclase) are coarse grained. However, the majority of the unit is a matrix of very fine grain size. Because of this, optical properties and the paragenesis of the minerals usually are indeterminate. For the same reasons, and also because of the paucity of outcrop, the geographic distribution of minerals within this facies largely is unknown.

In the samples of normal Blue Conglomerate examined, plagioclase content ranges widely, from about 6 to 35 percent. Estimates are based on petrographic counts (100 points minium) of coarse-grained areas and on X-ray diffractometer patterns of fine-grained matrix. Separation of (131) — (131) X-ray reflections indicates that the matrix plagioclase is nearly all at

Table 3. *Percent Mineral Composition Representative of Thermally Metamorphosed and Metasomatized Blue Conglomerate*

	Metamorphosed				Metasomatized			
	C4-306	C4-304^T	C4-93B^T	C4-301	C4-114	C4-307	C4-170	C-A
Plagioclase	15-25*P	25-35*	5-10*P	20-30*	15-25	15-25	8-12	5-15P
An content	20-30	30-50	20	30-60		10-15	10-15	20-30
Orthoclase	12-18(?)	6-10(?)	2-5P	0-5	2-5	6-10(?)	4-8(?)	3-7
Obliquity °2θ	0.65	0.69	0.66	0.63(?)	0.74	0.67		0.62
%Ab in Or	0-10	?	0-10	?	4-24(?)	10-15(?)		10-20(?)
Fe-Orthoclase	?				1-5	12-18	15-20	6-10
Microcline	1-5	1-5(?)	3-8(?)	?	?	?	?	1-3P
Quartz	25-35	0-15	15-25	55-60	0-5	0-5	15-20	10-15
Calcite				0-3			20-25	
Diopside	?	?		?			0-3	
Garnet		0-2						
Amphibole	3-7	3-7		3-7	3-7	5	12-18	
Mica	12-18*B	35-50*B,M	55-65M		50-60M	40-50M	8-10B,M	50-60M
Chlorite	3-7	3-7						
Kaolinite	3-7	3-5	3-5	8-12				
Prehnite							0-2	
Tourmaline							2-3	
Pyrite							0-2	
Magnetite	0-2	0-2	0-2	0-2	1-3	1-3	2-4	0-2

* Broad (001) mica or (200) feldspar reflection

? Indicates doubtfully present or unknown quantity

Obiquity = for Cu K_α radiation for $2\theta_{(111)} - 2\theta_{(1\bar{1}1)}$

°2θ Angular separation, Cu K_α

B = Biotite

M = Muscovite

P = Perthitic

T = Analysis excludes large breccia fragments of quartz least as calcic as An_{30} (from Smith and Yoder, 1956; Smith and Gay, 1958). Measurements of polysynthetic twin extinction angles on coarse-grained plagioclase show that the majority of compositions range between An_{35} and An_{65}. In a few instances it was observed that a more sodic (about An_{35-40}) plagioclase was younger than (rimmed) the more calcic member (about An_{55-60}). A minor amount of even more sodic plagioclase, An_{20} (oligoclase), occurs in pods associated with potassic feldspar and transects the weak fabric of the Blue Conglomerate. Sericitization and epidotization of andesine-labradorite is common. Oligoclase is only rarely, and much less extensively, sericitized. Twinning by albite and pericline laws is regular and well-developed. No zoning of plagioclase was observed.

Alkali feldspar is present in coarse-grained fragments or pods and less commonly in fine-grained matrix. Obliquity (triclinicty) is rather large, estimated from the $CuK_{\alpha}2\theta_{(111)} - 2\theta_{(1\bar{1}1)}$ (Table 3) and the $2\theta_{(131)} - 2\theta_{(1\bar{3}1)}$ contrasting with lower values in Mill Hill Slate (cf. Table 7). Orthoclase is the major alkali feldspar present (1-18 percent), identified by a large 2V (greater than 60°), lack of twinning, and by X-ray diffraction patterns showing monoclinic symmetry (a general absence of the (111) — $(1\bar{1}1)$ and (131) — $(1\bar{3}1)$ pairs of reflections). Microcline, identified by presence of the paired X-ray reflections and by the occasional observance of grid twinning, ranges from about 1 to 8 percent. Twinning of orthoclase has not been observed. Microcline is present in discrete grains in the matrix and in breccia fragments, but not in the transecting pods where only orthoclase has been found. Solid solution of the albite molecule in alkali feldspar (chiefly orthoclase) is small, ranging from 0 — 10 percent based on the feldspar $(\bar{2}01)$ — quartz $(10\bar{1}0)$ separation (not accurate for amounts less than 10 percent, Tuttle and Bowen, 1958). This use of the $(\bar{2}01)$ reflection is valid only if the alkali feldspar is Ca-poor, homogeneous, and if there is little variation in the structural state (Laves, 1952). In many cases, the $(\bar{2}01)$ X-ray reflection is broad but two distinct peaks are not present. Patch microperthite is present, but rare. Consequently, the $(\bar{2}01)$ determination of albite solid solution is only approximate.

Adularia, based on the presence of euhedral crystals, occasionally is present. Its optical properties (large 2V, untwinned) are the same as for orthoclase. The adularia occurs as rare, late veinlets transecting the plagioclase-orthoclase matrix fabric.

Anorthoclase is believed to have been identified in one sample (C4-306, Table 3). Two feldspar grains were observed having a 2V between 40° and 55° with almost indistinguishable fine polysynthetic twin lamellae. Both grains contained patch exsolution of albite or albite-oligoclase. Because of the uncertainty of the identification and the rarity of the occurrence, no conclusions can safely be drawn regarding the presence of this high-temperature feldspar.

Quartz grains in aggregate breccia fragments (0-60 percent) (Plate 2) in normal Blue Conglomerate hornfels from the ore-zone hanging wall are occasionally highly strained, yielding a biaxial interference figure with a 2V as great as 8°. However, non-brecciated Blue Conglomerate (gradational with Mill Hill Slate) not adjacent to the ore zone contains strain-free, recrystallized quartz (C4-306 in Table 3, and Figure 1). Thus, either recrystallization (or annealing) did not affect the hanging-wall quartz (it is farther from diabase than the strain-free quartz because of the intervening host-limestone wedge), or brecciation and straining of quartz occurred after hornfelsing (see Part 4, "Structures of the Eastern Ore Body").

The quantity of fine-grained mica, estimated from X-ray diffractometer patterns, comprises from 0 to 60 percent of normal, contact metamorphic Blue Conglomerate (Table 3). The 5.04Å reflection is usually weak or absent; there commonly are pairs of reflections at 3.00Å and 3.13Å, at 2.88Å and 2.19Å, and at 2.59Å and 2.64Å, all of which indicate the presence of both biotite and muscovite. Where only muscovite reflections were observed (C4-93B, Table 3), the second and third order basal reflections are weak suggesting that it may have a high-iron content.

Chlorite estimated from X-ray diffractometer patterns and thin section observation, ranges between 0 and 7 percent, appearing in about half the hornfels Blue Conglomerate samples examined. The intensity of the (003) X-ray reflection if low (less than ½ the (001) intensity), indicating a high-iron variety. From the d(004) spacing (3.545Å) and the c_0 (about 14.15Å), the amount of tetrahedral aluminum is estimated to be 1.1 ions per unit cell (Brindley and Gillery, 1956; Shirozu, 1958). Using the nomenclature of Hey (1954), this chlorite probably is either ripidolite or pycnochlorite.

Texturally, the normal, unmetasomatized, Blue Conglomerate is characterized by large angular, brecciated fragments of aggregated quartz grains and, more rarely, by large orthoclase crystals in aggregates accompanied by quartz (Plate 2). Mortar structure is common. These aggregates are set in a fine-grained matrix (Plate 2-A and B). Under crossed nicols the fragmented, brecciated texture may disappear almost completely as a result of metamorphic superposition (Plate 2, C and D). The matrix mica is commonly clay-sized but, where coarse enough to be identified, is usually brown biotite. Twinned calcic plagioclase in the matrix is only rarely visible at a magnification of 450X. Oligoclase is usually coarser grained and its albite-twin extinction angle can be measured. The matrix frequently shows a flow texture around floating grain aggregates (usually quartz, Plate 2) and rarely small-scale flow folds. In hand specimen, a faint foliation of the aggregates resulting from stretched quartz grains is visible, especially where the aggregates are an inch or more in diameter (see also Figure 16 for a sketch of Blue Conglomerate foliation in outcrop). Occasional rounded to sub-angular shale fragments of clay-shale particles partially kaolinized are present but are much less common than in Mill Hill Slate (Plate 2-B). The two types of clastic fragments, quartzose sandstone and shale, are about evenly mixed in samples that are gradational between typical Mill Hill Slate and typical Blue Conglomerate lithologies. Along the borders of large quartz aggregates, the normally strained quartz has been recrystallized into euhedral, unstrained, metamorphic quartz. Fine-grained matrix frequently has invaded aggregate rim boundaries, apparently replacing the inner core of strained quartz. At contacts of orthoclase aggregates and ground mass, fine-grained mica (biotite?) has been recrystallized to muscovite with a much coarser grain size and is associated with some chlorite. Late vein material transecting foliation is composed of quartz, chlorite, or calcite with specular hematite inclusions along calcite cleavages.

Samples taken near the Blue Conglomerate-Triassic conglomerate contact, but within the Blue Conglomerate, appear to represent a fault gouge. Here, there are no large, floating fragments and the quartz has been granulated to the same grain size as the normal, quartz-free matrix. However, there is no observable fault gouge within the Triassic sediments, no slickensiding, and the contact is tight and angular.

Because of the fine grain size and the several processes (shearing and metamorphism) that have modified the Blue Conglomerate, the determination of paragenetic relationships is difficult, but somewhat more reliable than for the even finer-grained Mill Hill Slate. The earliest minerals are those enclosed within breccia fragments and are the only possible remnants of the original rock previous to shearing and metamorphism. Quartz predominates among them, but detrital muscovite, albite-oligoclase, and potassium feldspar are occasionally present in aggregates with quartz; in the silty and clayey shale fragments, some "sericite" and kaolinite also are present. However, the kaolinite may be a post-lithification weathering product not associated with the original rock mineralogy. The absence of quartz in the matrix may reflect an original absence in the parent rock, in which case the parent rock was probably a quartz pebble conglomerate with a shaly matrix, or, as discussed subsequently, it may reflect a loss of silica by metasomatic leaching and/or recombination into silicate minerals such as mica and feldspar.

The first recognizable event is brecciation that resulted in highly strained quartz, followed by re-solution and secondary re-deposition of silica in conjunction with recrystallization (and consequent strain-free quartz).

Following this, diopside, tremolite-actinolite, and andesine-labradorite formed under conditions of moderately rapid crystallization resulting in almost submicroscopic crystals. These minerals were in turn replaced by orthoclase, albite-oligoclase, quartz, biotite, and possibly muscovite and magnetite. An orthoclase porphyroblastic texture resulted. Ore-stage mineralizaton followed: magnetite, chlorite, actinolite, and pyrite (some pyrite also may have been an original constituent). The final group of minerals to crystallize either in transecting veinlets or as alteration products or preexisting minerals, includes "sericite," chlorite, zeolites (in the ore area), adularia feldspar, secondary quartz, calcite, kaolinite, and hematite. All of the magnetite in the Blue Conglomerate is present as fine-grained particles dusting the matrix and normally does not exceed 2 percent (Table 3, columns 1-4); commonly, it is much less abundant than this except where some massive replacement magnetite forms hanging-wall ore in hornfels.

Chemical Composition

Chemical analyses of representative normal Blue Conglomerate from the eastern underground mine and of representative altered, pink Blue Conglomerate from the ore-zone hanging wall are presented in Table 4. In the selection of each sample for analysis, care was taken to select material typical of each of the two rock types. The average shale of Clarke (1924), the average graywacke of Pettijohn (1949), average Martinsburg shales from Lebanon County (O'Neill and others, 1965), and granophyre from Cornwall are shown for comparison. A normal Blue Conglomerate analysis (column 1) is used to represent the original sedimentary rock, whereas metasomatically altered Blue Conglomerate (Table 4, column 2) represents an addition imposed only in the hanging wall of the eastern ore body. The analyzed normal Blue Conglomerate sample is noticeably low in silica and high in alumina, total iron, and ferrous iron when compared either with an average shale or an average graywacke. However, its quartz content ranges widely (Table 3) so that the silica analysis in Table 4 propably is not representative of the average silica content of the entire unit. Normal Blue Conglomerate resembles most closely the chemical composition of an average of eight oxidized Lebanon County Martinsburg shales from the leached zone of weathering. Furthermore, it lies within the range of Martinsburg compositions (see O'Neill and others, 1965; Hoover and others, 1972). The resemblance would be expected if the Blue Conglomerate were originally part of the Martinsburg Formation (cf. Table 4, columns 1 and 4).

The Fe^3/Fe^2 ratio and total iron both decrease from normal to altered Blue Conglomerate, which compares with a decrease in biotite and an increase in magnetite nearer the ore zone. Also noteworthy are the differences in K_2O: Blue Conglomerate hornfels contains much less K_2O than average Martinsburg shale, whereas metasomatized Blue Conglomerate contains much more, an amount exceeded only by that in granophyre (Table 4, column 3). The CaO content of metasomatized Blue Conglomerate is highly varied because of irregular distribution of vugs containing secondary calcite, none of which was present in the sample analyzed. Distribution of calcic plagioclase also is varied (Table 3), affecting CaO, Al_2O_3, and SiO_2 content.

Table 4. *Chemical Analyses (anhydrous) Comparing Contact Metamorphic and Metasomatized Blue Conglomerate with Shale, Graywacke and Granophyre*

	C4-304*	C-A*	G*t	M*	1.	2.
SiO_2	53.65	55.86	65.62	59.72	62.2	65.8
TiO_2	N.A.	N.A.	0.36	1.05	0.7	0.5
Al_2O_3	23.85	24.24	16.05	20.63	16.5	14.4
Fe_2O_3	3.77	3.63	1.79	7.96	4.3	1.0
FeO	6.08	3.34	0.53	1.56	2.6	4.3
MnO	N.A.	N.A.	0.04	N.A.	Tr	0.1
MgO	2.80	2.09	1.25	2.04	2.6	3.0
CaO	2.62	0.49	3.15	0.41	3.3	3.6
Na_2O	4.09	3.78	2.18	0.74	1.4	3.5
K_2O	2.47	6.18	8.44	5.29	3.5	2.1
PO_4	N.A.	N.A.	0.19	N.A.	0.2	0.1
CO_2	0.68	0.30	0.16	0.62	2.7	1.6
F	N.A.	0.09	0.22	N.A.	N.A.	N.A.
S_{tot}	N.A.	N.A.	0.03	N.A.	N.A.	N.A.
Total (recalc.)	100.01	100.00	100.01	100.02	100.0	100.0
Fe_{total}	7.35	5.13	1.67	6.80	5.03	3.04

N.A. = No analysis determined Tr = Trace

* Wet chemical analysis by Spectrochemical Laboratories, Pittsburgh, Pa.

t Wet chemical analysis by A. S. McCreath and Son, Harrisburg, Pa.

C4-304	Metamorphosed Blue Conglomerate (Appendix 4-B)
C-A	Metasomatized Blue Conglomerate from hanging wall (Appendix 4-B)
G	Avg. granophyre (C4-150 and 11-38G: Appendix 4-A)
M	Avg. of 8 Martinsburg shales, Lebanon Co., (O'Neill and others, 1965)
1.	Avg. shale (Clarke, 1924, p. 30)
2.	Avg. graywacke (Pettijohn, 1949, p.250)

Comparison between Metamorphism and Metasomatism

Assuming that normal Blue Conglomerate is a brecciated contact metamorphic facies of average Lebanon County Martinsburg shale, aluminum, ferrous iron, total iron, magnesium, calcium, and sodium apparently have been added; ferric iron, potassium, and perhaps silica apparently removed. Actually, removal of elements may have caused an apparent but unreal increase in the "added" constituents. The chemical analyses do not specify process. In the alteration from normal to metasomatized Blue Conglomerate (Table 4), potassium increased; ferrous iron, total iron, and perhaps magnesium and calcium decreased, and the other elements remained unchanged. Regardless of the actual processes of introduction and removal (discussed subsequently), it is only important here to note that chemical differences exist between an average Martinsburg Shale composition and representative Blue Conglomerate hornfels composition, and between the latter and pink, metasomatized Blue Conglomerate. A similar change is apparent in the Mill Hill Slate (considered subsequently).

The chemical analyses (Table 4) confirm the composition and quantity of the feldspars determined by X-ray analysis (Table 3): plagioclase in normal Blue Conglomerate is more calcic than plagioclase in metasomatized pink Blue Conglomerate paralleling the metasomatic decrease in CaO. Similarly, the increase in K_2O in the metasomatized samples largely is a result of an increase in potassium feldspar, the mica content remaining essentially constant. In part, however, there may be a decrease in the K_2O content of the mica (a broad basal reflection indicating degraded mica) in normal Blue Conglomerate. This contrasts with better crystallized muscovite in the metasomatized rock type that may contain more K_2O. The slight increase in SiO_2 in the metasomatized Blue Conglomerate correlates with an increase in quartz content between the two units (cf. C4-304 and C-A, Table 4). At least part of the ferrous iron in normal Blue Conglomerate is present in biotite. Both ferrous iron and biotite are much less abundant in the metasomatized portions, indicating agreement between the chemical and mineral analyses.

The distribution of Na_2O and K_2O also is interesting. Na_2O in both hornfelsed and metasomatized Blue Conglomerate shows considerable enrichment relative to the Lebanon County and Clarke's average shales (Table 4). However, K_2O is enriched only in the metasomatized unit (Table 4). Thus, a case can be made for separate sodium and potassium introduction, the former having occurred earlier associated with contact metamorphism (see "Silica and Alkali Balance").

A few other mineralogical and textural comparisons can be made between normal metamorphic and metasomatic Blue Conglomerate. Plagioclase X-ray reflections from metasomatized Blue Conglomerate tend to be sharper with more limited sodium-calcium solid solution (i.e., separate calcic and sodic feldspars coexisting metastably) than in Blue Conglomerate subjected only to contact metamorphism. Potassium feldspar obliquity (rather large (111) — $(\bar{1}\bar{1}1)$ separation) remains about the same and indicates a low-temperature structure. Such obliquity is characteristic of a high orthoclase content in the potassic phase (Wright, 1964).

Cloudy, pink ferriferous orthoclase is the most distinctive mineral in pink, metasomatized Blue Conglomerate in the vicinity of the eastern ore zone. It also occurs sparingly in normal Blue Conglomerate where the two facies merge, in metasomatized Mill Hill Slate above the eastern ore zone, and in granophyre. Optical (Table 5) and X-ray (Table 6) properties for this Fe^3-rich orthoclase match the data given by Coombs (1954). The 2V angle ranges from

Table 5. *Optical and X-ray Crystallographic (CuK$_\alpha$ Radiation) Data for Fe-Orthoclase*

	Cornwall, Pa.*	Coombs, 1954, Madagascar
Optic Angle	approx. 0° to>40° ~ ⊥(010); variable	40° ⊥ (010) to 60° ∥ (010); variable
Refractive Indices:	variable:	
n_α	1.518 - 1.524 ± .002	1.520 - 1.5285
n_γ	1.523 - 1.530 ± .002	1.524 - 1.533
$2\Theta_{(002)(040)} - 2\Theta_{(220)}$	0.62 - 0.68	0.62 - 0.77
$2\Theta_{(11\bar{2})} - 2\Theta_{(130)}$	2.06 - 2.13	2.115 - 2.185

* Range of values for pink orthoclase from granophyre, metasomatized Blue Conglomerate, and metasomatized Mill Hill Slate.

sensibly uniaxial to greater than 40°. Indices of refraction also have a wide range, tending to increase with increasing cloudiness of the grain and therefore presumably with Fe_2O_3 content (either structural Fe or exsolved iron as hematite). According to Coombs' refractive index data for Madagascar material (1954, p. 414), the indices of the Cornwall feldspar indicate a range in structurally substituted Fe_2O_3 from 0 to about 3 percent. Although these X-ray data are very similar to his Madagascar material, several weak reflections are present in the Cornwall samples that Coombs did not record. However, they usually are present as significantly stronger reflections in normal orthoclase (Table 6) and in synthetic $KFeSi_3O_8$ (Wones and Appleman, 1961 and 1963a). There are three possible explanations for these reflections: intergrowths of normal and ferriferous orthoclase; varied intensity for certain reflections from ferriferous orthoclase resulting from differences in amount of iron substitution, or the metastable presence of the two polymorphs, iron-sanidine and iron-microcline (Wones and Appleman, 1961, 1963a, and 1963b). Both stable forms of Fe-feldspar may be present in addition to metastable ferriferous-orthoclase if there is a partial (incomplete) transition from the high- to the low-temperature form. The frequent presence of 4.01Å and 3.95Å reflections suggests the possibility of (111) and $(\bar{1}11)$ planes both of which are present in synthetic iron-microcline (Wones and Appleman, 1963a) and hence some low temperature form (Fe-microcline) is probably present at Cornwall (column 1, Table 6). However, those grains with a 2V approaching zero as some do in the Cornwall samples (Table 5), or with an optic axial plane parallel to (010) (Coombs, 1954, p. 410), or with only one (111) reflection (columns 2-4, Table 6) are probably monoclinic and may be,

Table 6. *Comparative X-ray Patterns of Fe-Orthoclase and Orthoclase*

1.		2.		3.		4.		5.		6.	
dÅ	I/I$_o$	dÅ	I/I$_o$	dÅ	I/I*$_o$	dÅ	I/I*$_o$	dÅ	I/I*$_o$	dÅ	I/I*$_o$
6.45 - 6.51	5-14	6.45	15	6.49	2	6.49	5			6.44	60
5.86 - 5.87	0-5	5.95	2	5.88	1	5.96	3			5.86	20
4.22 - 4.23	7-19	4.22	20	4.24	10	4.23	30	4.22-4.23	40	4.25	30
4.01 - 4.03	0-5	4.03	30	4.01	8					4.02	90
3.93 - 3.95	3-10					3.96	10	3.939-3.945	25		
3.767-3.775	13-27	3.81	30	3.80	20	3.79	35	3.773-3.785	70	3.80	80
3.620-3.631	0-5	3.68	30	3.70	10	3.63	8	3.616-3.621	20		
3.453-3.470	5-15	3.50	15	3.49	20	3.48	30	3.458-3.467	30	3.49	20
3.310-3.322	8-25	3.33	12	3.34	35	3.31	70	3.313-3.321	70	3.33	70
								3.283-3.286	4		
3.232-3.240	100	3.21+	100$_B$	3.22	100	3.24	100	3.234-3.237	100	3.18	100
3.989-2.995	8-17	2.96	25$_B$	3.00	35	3.01	40	2.989-2.994	50	3.00	70
2.920-2.934	0-3			2.92	10	2.90	20			2.93	70
2.820-2.830	0-2	2.79	5$_B$	2.80	3	2.77	15	2.764-2.767	<10	2.83	60
						2.61	20	2.605	10	2.65	60
2.574-2.590	0-10	2.56	20$_B$	2.55	60	2.55	20	2.573-2.580	20		
		2.44						2.547	<10	2.53	70
		2.41	6$_B$	2.41	2	2.43	3$_B$			2.47	60
										2.39	60
		2.32	7			2.33	3			2.29	70
		2.165	10	2.17	5	2.17	18	2.162-2.170	<30		
										2.13	40
		2.12	10	2.10	5	2.13	4			2.10	70
		1.99	4	1.98	?	1.992	6			1.99	60
		1.937	3	1.94	?	1.938	7			1.91	60

* Intensities estimated visually. B = Broad Reflection

1. Range of values for 5 diffractometer runs of Fe-orthoclase from granophyre, metasomatized Mill Hill Slate, and metasomatized Blue Conglomerate
2. C3-5 light pink single crystals in vuggy granophyre
3. C-A metasomatic aggregates in Blue Conglomerate
4. C4-250 pinkish-orange vein in Blue Conglomerate
5. Coombs, 1954, p. 421 Madagascar Fe-Orthoclase
6. ASTM orthoclase; Cole, Sorum, and Kennard, 1949, p. 280

in part, the high-temperature iron-sanidine. This suggestion is supported by the small angular separation of (11$\bar{2}$) and (130) (Table 5). If the alkali feldspar curves of Wright (1968, Figures 1 and 2) are applicable to Fe-orthoclase, the CuK$_\alpha$ 2θ measurements for ($\bar{2}$04) and (060) can be used to distinguish among the maximum microcline, orthoclase, and high sanidine series. Using the approximate spacings in Table 6, Cornwall samples 2 and 3 (granophyre and Blue Conglomerate Fe-orthoclase), agree with Wright's curve for the high sanidine-high albite series, and sample 4 (Blue Conglomerate Fe-orthoclase) agrees with his curve for orthoclases. From these data, it seems probable that the Cornwall Fe-orthoclase is a metastable phase structurally between iron-sanidine and iron-microcline, but that some of the feldspar has approached or attained the low-temperature equilibrium iron-microcline form. The same conclusion was reached by Coombs (1954 p. 410), although Wones and Appleman (1963a) did not find the transitional form of iron-orthoclase in their synthesis experiments. Presumably the transition to iron-microcline at Cornwall was inhibited by short-duration crystallization at the required energy levels or by slow reaction rates within the stability field of iron-microcline. Lack of available water may have contributed to the sluggish transition (note the low H_2O of metasomatized Blue Conglomerate, Appendix 4-B).

There appears to be slightly more microcline and microperthite in the metasomatized unit and more of the normal Al^3 -rich orthoclase. Kaolinite is conspicuous by its absence in the strongly metasomatized portions (Table 3). Rarely, tourmaline and fluorite are present as trace minerals in pods or veinlets with Fe-orthoclase where metasomatized Blue Conglomerate is rich in calcite and late feldspar (albite and Fe-orthoclase). To date, fluorite and tourmaline in the Blue Conglomerate have been found only near the diabase.

The paragenetic sequence in metasomatized Blue Conglomerate is very nearly the same as in the contact-metamorphic phase. A matrix of actinolite, biotite, quartz, magnetite dust, and rarely diopside is earliest and corresponds to the sequence in metamorphosed, or normal, Blue Conglomerate. Pods or veins containing Fe-orthoclase, with or without biotite, tourmaline, calcite and fluorite, crystallized after more calcic plagioclase, but before or simultaneous with a more calcic plagioclase. Adularia, calcite, chlorite and zeolites closed the mineralization. Massive, crystalline magnetite occasionally replaces Fe-orthoclase but more commonly merely surrounds it. However, ore-replacement magnetite in Blue Conglomerate is uncommon and is found only where metasomatized Blue Conglomerate forms the hanging wall of the ore zone (central part of eastern ore body). Very fine grains of magnetite dust are found only in matrix, not in metasomatic pods and veinlets. Metasomatic crystallization thus separates two periods of magnetite crystallization.

Except for metasomatic aggregates of potassic feldspar and minor muscovite, textures in the two Blue Conglomerate facies are very similar. Matrix foliation is less pronounced in areas of intense metasomatism that produced a miarolitic texture, especially near the diabase-Blue Conglomerate contact where structural rafting of hornfels by diabase and mineral replacement have been most effective. Sodic plagioclase frequently is present in metasomatic aggregates in recognizable crystal grains, as opposed to submicroscopic and more calcic plagioclase present in the fine-grained matrix of normal, unmetasomatized Blue Conglomerate. In addition to recrystallized metamorphic quartz (common to both types), some secondary quartz, usually in transecting veinlets, is present in the matrix of metasomatized Blue Conglomerate.

Facies Representations

Because of the complex history of the Blue Conglomerate, representation of its chemical composition in terms of mineral components on triangular diagrams can be misleading. The mineral phases present, especially in metasomatized portions, are most certainly not in local equilibrium. Initial thermal metamorphism from cooling diabase produced very rapid crystallization with consequent submicroscopic to microscopic crystal grains. Mineral composition changes from place to place, in part reflecting the inhomogeneities of the pre-metamorphic breccia, although this effect is less pronounced than in laminated Mill Hill Slate. Reduction of the Blue Conglomerate mineralogy to representation by three components, or groups of components, gives a gross graphical demonstration of the possible extent of local mineral equilibrium; only analyzed minerals from several sets of assemblages can yield accurate facies representations (see Thompson, 1957, p. 849-855). Such a representation also serves to distinguish contact-thermal from metasomatic compositions.

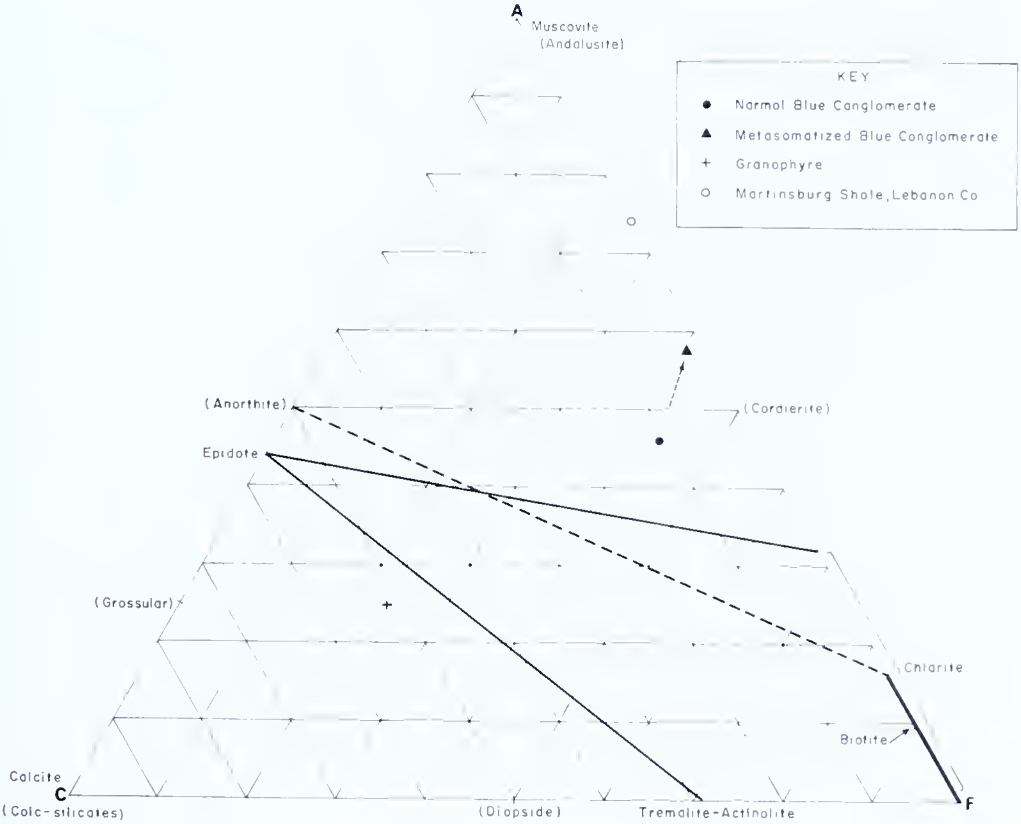

Figure 5. ACF diagram for Blue Conglomerate, illustrating albite-epidote hornfels facies for excess silica.

In Figure 5, chemical compositions of metamorphosed and metasomatized Blue Conglomerate have been recalculated for an ACF diagram according to the method of Eskola (1939). The minerals in parentheses are aluminous minerals stable only in a potassium-deficient environment and hence do not strictly apply to Blue Conglomerate, Martinsburg shale, or Cornwall granophyre. The diagram most nearly representing the observed metamorphic assemblage (Table 3) is the albite-epidote-hornfels facies, assuming excess silica. However, the positions of diopside, grossular, and anorthite from the hornblende-hornfels facies also are shown because most of the feldspar present is rather calcic and other minerals from this facies frequently are present. An average of eight Martinsburg shale analyses (O'Neill and others, 1965) from Lebanon County is shown for comparison based on the correlation between the Martinsburg Formation and the Blue Conglomerate (although the actual correlation probably is not with analyzed Martinsburg rocks immediately to the north). An analysis of Cornwall granophyre (see Appendix 4-B), which does not belong on a hornfels diagram, is shown because of a possible genetic connection between it and the metasomatized Blue Conglomerate. Figure 5 illustrates a changing "C" (CaO) component at nearly a constant "A" and "F" reflecting the decrease in plagioclase-anorthite component from normal to metasomatized Blue Conglomerate; that is, an approach to local mineral-chemical equilibrium. Biotite, actinolite, and perhaps kaolinite and chlorite present in the Blue-Conglomerate indicate a metastable, inequilibrium assemblage. Lack of hornfels equilibrium is emphasized by comparing the Blue Conglomerate (Figure 5) with Mill Hill Slate (Figure 7). Although their mineral assemblages are similar, their facies representations are not.

A slightly different representation (Figure 6) is an AKF diagram (Turner and Verhoogen, 1960, p. 514) that assumes MgO and FeO act as one component and that better illustrates the varied potassium content ("K" apex, Figure 6) of these units. Cordierite, stable in the hornblende-hornfels facies, has not been verified in this study although Hickok (1933) reported it in Mill Hill Slate. It is absent because of an excess of potassium (in feldspar) and a deficiency in MgO/MgO+FeO at the time of metamorphism, and because at most locations the samples plotted represent a lower grade than the maximum grade attained adjacent to diabase where hornblende is present. From Figure 6, it is clear that any cordierite present locally in the hornfels would not be expected to survive metasomatism. This is even more strikingly illustrated for Mill Hill Slate (Figure 8). Plagioclase and quartz (where there is an excess of silica) may be present in all fields and are present throughout the Blue Conglomerate.

During metasomatism, biotite became unstable (decreased in abundance as MgO and FeO decreased) and was partially replaced. Ferriferous orthoclase and hematite (± magnetite) became a significant iron-bearing assemblage. This change probably represents an increase in oxygen fugacity, and possibly decreasing water pressure, with or without a temperature change. Above approximately 470°C at 1035 bars total gas pressure and above approximately 510°C at 2070 bars, ferriannite + gas is not stable in association with iron-feldspar + hematite + gas. Iron-feldspar + magnetite + gas is a stable association with either of the other two assemblages (Wones, 1963, p. 594, Figure 3). The iron-microcline to Fe-sanidine transition (without ferriannite) occurs at about 700°C (Wones and Appleman, 1963-A). This is more than 100° C higher than the normal sanidine-microcline transition temperature.

The absence of kaolinite in the microcline - muscovite - biotite (- plagioclase, quartz) field suggests that it is not stable in this potassium-rich environment, similar to the instability of the higher-temperature aluminum silicates, andalusite, and cordierite, where there is excess potassium.

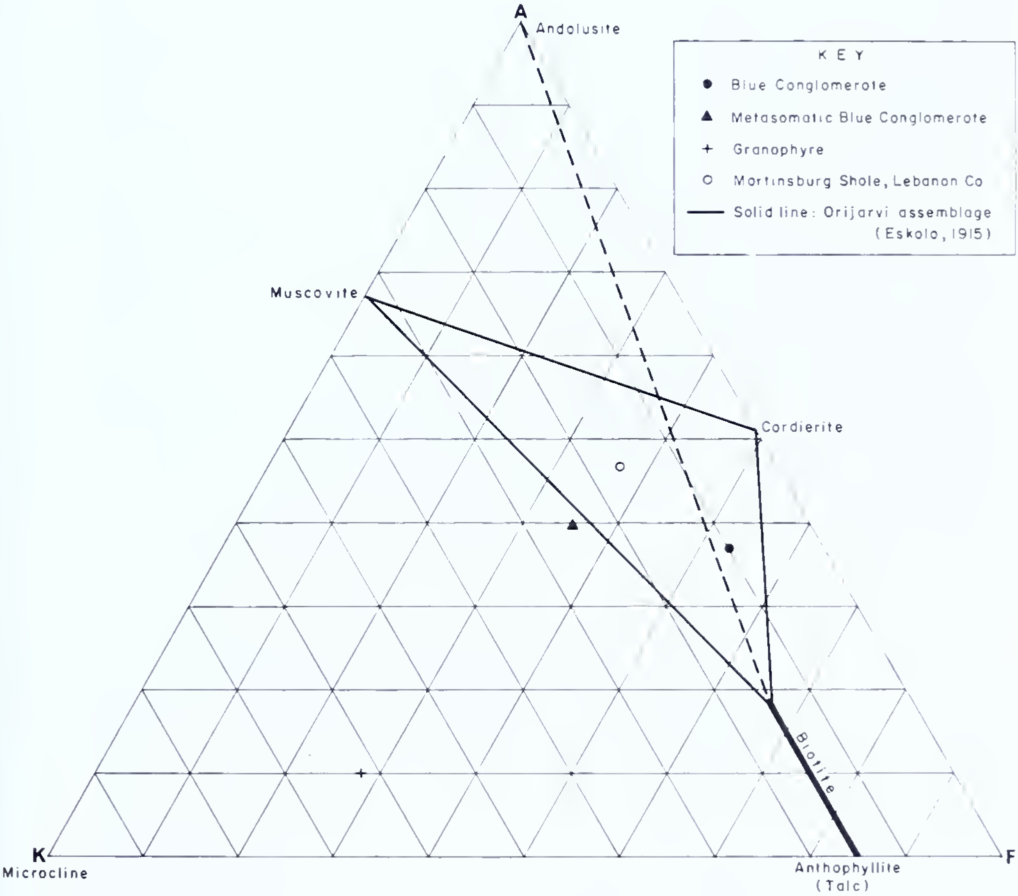
A
Andalusite
KEY
● Blue Conglomerate
▲ Metasomatic Blue Conglomerate
+ Granophyre
○ Martinsburg Shale, Lebanon Co
Solid line: Orijarvi assemblage (Eskola, 1915)
Muscovite
Cordierite
Biotite
K
Microcline
Anthophyllite (Talc)
F

Figure 6. AKF diagram for Blue Conglomerate, illustrating hornblende-hornfels facies for excess silica and alumina.

The Mill Hill Slate

Introduction

The Mill Hill Slate, named for Mill Hill north of the Elizabeth open pit near the eastern ore body, is a miners' term for a shaly, limy hornfels that crops out near the headframe of the eastern mine shaft. The Mill Hill Slate (believed to be an Ordovician Martinsburg equivalent) is the major unit in contact with diabase and ore in the vicinity of Cornwall, except where host limestone separates it from diabase. Its occurrence is more widespread than that of the Blue Conglomerate (Plates 21 and 22), although in Mill Hill Slate just south of Quentin thin quartzitic layers may be an interbedded Blue Conglomerate facies that was less extensively brecciated than in the mine area. The majority of the Mill Hill Slate outcrop belt lies below the north limb of the Cornwall diabase sheet; some lies above diabase in the vicinity of the ore bodies (Plates 21 and 23). As was the case with the Blue Conglomerate, there is both a normal contact-metasomatized facies outside the mine area and a superposed metasomatized facies in the ore zones.

Both Spencer (1908) and Hickok (1933) recognized the Mill Hill Slate (the slate no. III of Lesley and d'Invilliers, 1886) as a hornfels. Hickok (1933, p. 211), largely from a study of the western ore body area, stated that it is dominantly a quartz-cordierite hornfels with minor andalusite, biotite, and sericite but does not mention plagioclase. No cordierite or andalusite were recognized in this study of the Mill Hill Slate above the eastern ore body. Hickok noted that potassic feldspar and some plagioclase are present at limestone-diabase contacts acting as an "impermeable barrier, thus protecting the areas of unaltered limestone from the exhalations that elsewhere formed the ore bodies" (Hickok, 1933, p. 237). He also mentioned that metasomatism resulted in the addition to limestone of potassium without introducing alumina (Hickok, 1933, p. 238-240). The entire Mill Hill Slate unit has received relatively little attention although it is of prime importance in understanding the geologic events at Cornwall.

Mineralogy and Petrography

The most striking characteristic of metamorphosed Mill Hill Slate is the relic primary laminations of grayish white, gray, and black ranging from less than ½ inch to several inches thick (Plate 4). These laminae persist to within a few tens of feet of the diabase contact. The laminae near diabase, although frequently somewhat brecciated and with less color contrast, still can be discerned, particularly on a polished surface, even in some areas previously noted by Hickok (1933) as showing a uniform hornfels texture. Throughout, the texture is so uniformly fine-grained that individual grains cannot be distinguished in hand specimen and frequently are too small for identification with a petrographic microscope (Plate 3). Metamorphosed pelitic fragments may be present (Plate 3, B and C). Occasionally mimetic crystallization and foliation of the bands (or cross-bedding laminae) are cut by veinlets and ellipsoidal pods of coarser-grained, subhedral crystals of potassic feldspar, actinolite, muscovite, and calcite (Plate 4, B-D). In addition to these minerals, epidote, zeolites, and less commonly chlorite and sodic plagioclase are present.

The mineral composition of normal contact metamorphic Mill Hill Slate is extremely varied (Table 7) as determined by petrographic and X-ray analyses. Samples C-1, C-51, C-46 and C4-295 probably are most representative of Mill Hill Slate lithology. Plagioclase, orthoclase, microcline, small euhedral pyrite cubes, and fine-grained magnetite dust are consistently present. Occurring with somewhat less consistency but frequently as a major component are, calcite, diopside, or actinolite. Diopside occurs mostly in the fine-grained matrix and calcite and actinolite in veins or pods. Quartz and mica (biotite was identified optically; muscovite by X-ray diffraction) exhibit a very irregular distribution. Rarely chlorite-vermiculite (undifferentiated), montmorillonite(?), epidote, garnet(?), and prehnite are present, the latter being a major component in a few samples (Table 7). The banding in Mill Hill Slate is in part a textural and in part a compositional variation (Table 7, columns 1, 2, and 4 and Plate 4). The lighter bands are consistently coarser grained and contain noticeably less magnetite dust. They also are richer in calcium-rich minerals such as calcite, calcic plagioclase, and diopside. The darker and finer-grained bands, on the other hand, contain more mica, quartz, and potassic feldspar. These two types of bands probably correspond respectively to limy and shaly bands of an original sedimentary lamination. *In situ* crystallization, rather than penetrative metamorphic mobilization, has been the rule; the rare pods and veins are exceptions (Plates 3 and 4).

Although individual grains of plagioclase commonly are too small to utilize twinning to determine composition (most are unrecognizable as plagioclase grains), separation of the $(1\bar{3}1)$ — (131) planes on X-ray diffraction patterns (Smith and Yoder, 1956; Smith and Gay, 1958) indicate that matrix plagioclase is more calcic than An_{30}. The few optically determined compositions (Michel-Levy method) ranged from An_{40} to An_{75} (Table 7). Coarser plagioclase in pods measured optically by the Michel-Levy extinction method range from about An_{10} to about An_{25}.

As in the case for Blue Conglomerate, the X-ray patterns indicate both a monoclinic (orthoclase) and a triclinic (maximum microcline) form of alkali feldspar (Tables 3 and 7). Probably because of fine grain size, no grid twinning was observed. The alkali feldspars usually are clear and present in ellipsoidal pods in the hornfels, but are much more abundant in the pink metasomatized lithology (Table 7). The amount of albite in solid solution in potassium feldspar, determined by the Cu $K_a 2\theta$ separation of the (201) feldspar reflection from the $(10\bar{1}0)$ quartz reflection (Tuttle and Bowen, 1958), ranges from about 7 to 28 percent in normal metamorphic Mill Hill Slate lithology (less in metasomatized portions), although this may be more apparent than real because of inhomogeneity, structural strain, and the presence of both monoclinic and triclinic alkali feldspar in most samples. Perthite was not observed in any of the thin sections, although it may be present in fine-grained matrix as X-ray- or cryptoperthite.

The obliquity (triclinicity) in Mill Hill Slate alkali feldspar determined from the (111) - $(1\overline{1}\overline{1})$ separation is more varied than in samples from Blue Conglomerate (Tables 3 and 7). The separation in degrees 2θ (Cu K_a radiation) ranges from 0.40° 2θ to 0.65° 2θ in contact metamorphic Mill Hill Slate and on the average seems to be slightly less in pink, metasomatized Mill Hill lithology. These values suggest a more monoclinic character for the Mill Hill alkali feldspar than for that in Blue Conglomerate. Because the samples upon which these obliquity measurements in the Mill Hill Slate were made are considerably closer to diabase than those samples analyzed from Blue Conglomerate, this indication of a high-temperature, more monoclinic form is reasonable. However, conclusions based on these data are subject to the same homogenization and structural order limitations as for alkali feldspar in Blue Conglomerate.

Quartz, which is not a characteristic mineral of normal, metamorphic Mill Hill Slate lithology, cannot be seen in thin section (except in transecting veins as in Plate 4-B) but was detected in a few samples by X-ray analysis.

Muscovite basal spacings from X-ray patterns of normal, metamorphic Mill Hill Slate lithology indicate that it is a muscovite low in iron, especially when compared with micas in normal metamorphic Blue Conglomerate lithology (Table 3). All, or nearly all, of the muscovite occurs in the very fine-grained ground mass (Plates 3 and 4). Some biotite was identified optically.

No kaolinite was observed from the X-ray data, although a minor amount could be concealed in X-ray reflections for undifferentiated chlorite-vermiculite. A 15.3Å montmorillonite-like reflection was present in one sample (Table 7).

Pink, metasomatized Mill Hill Slate lithology differs from its contact metamorphic counterpart by the presence of a typical hematitic pink color and by mineralogy. Laminae are either absent or less conspicuous. The chief mineralogical difference is the presence of very fine-grained ferriferous orthoclase with the same X-ray properties as that from metasomatized Blue Conglomerate (Table 6). The grains in Mill Hill Slate, however, are much too fine for optical data to be obtained from them, and secondary potassic feldspar vugs were not formed in this lithology as they were in the more permeable Blue Conglomerate. The fine-grained hornfels of contact metamorphic Mill Hill Slate was less susceptible to replacement and to the growth of large crystals during later metasomatism than was Blue Conglomerate, which usually is farther from the diabase contact (Plates 21 and 23). Other mineralogical changes in the metasomatic facies are uncertain (Table 7): a decrease in the anorthite molecule in plagioclase feldspar, and a

Table 7. *Percent Mineral Composition Representative of Thermally Metamorphosed and Metasomatized Mill Hill Slate*

	Metamorphosed Mill Hill Slate											Transitional sample	Metasomatized Mill Hill Slate	
	C-1 Light Band	C-1 Dark Band	C-42	C-43 Light Band	C-45	C-46	C-47	C-48	C-49	C-50	C-51	C4-295	C4-10	C4-251
Plagioclase	40-50	25-35	12-18	—	10-15	25-30	5-10	12-18	50-60	20-30	45-55	30-40	10-15	12-18
An Content	20,60-80	10,55-75	15-20	—	35-50	?	Intermed.	10-20	25	?	Variable	20,55-75	10-15	10-20
Potassic Feldspar														
% Ab in K-feldspar	~ 18	~ 13	—	~ 13	~ 9	~12	~ 9	~ 28	~ 14	~ 12	0-10	0-10	0-10	12
Orthoclase	12-18	8-12	—	15-25	5-10	?	4-8	8-12	3-7	5-10	10-15	10-15	3-7	5-10
Fe-Orthoclase	—	—	—	—	6-10	—	—	—	—	—	—	3-7	40-50	25-30
Microcline	12-18	15-25	1-5	?	3-8	15-25	3-7	5-10	10-15	10-15	20-30	15-20	10-15	8-12
Obliquity CuK_{α}, 2θ	0.56	0.51	0.58	0.40-0.60	0.65	0.6(?)	?	0.58	0.59	0.51	0.55	0.57	0.40	0.45
Quartz	0-5	0-5	1-3	0-5	30-40	10-15	40-50	0.5	—	0-5	5-10	8-12	0-5	0-10
Calcite	—	—	40-50	8-12	?	—	0-10	25-35	—	30-40	—	0-3	0-5	0-5
Diopside	—	—	20-30	35-45	6-10	16-20	?	5-10	5-10	12-18	5-10	2-6	10-20	5-10
Epidote	?	—	—	—	—	—	—	8-12	?	3-7	—	?	?	3-7
Amphibole	—	—	3-5	2-4	5-10	8-12	8-14	5-10	—	—	—	—	3-7	3-7
Mica	0-5	25-35*	—	—	6-10	5-10*	8-12	—	—	—	—	10-15*	—	—
Chlorite- Vermiculite	—	—	—	2-4	3-7	—	7-10	—	—	—	0-5	—	3-5	3-5
Montmorillonite	—	—	—	—	—	—	3-8	—	—	—	?	—	—	—
Prehnite	—	—	8-12	15-20	—	—	—	—	—	—	—	—	—	—
Pyrite	—	0-1	0-1	—	0-1	1-3	—	0-1	0-1	—	0-2	?	1-2	2-3
Magnetite	0-1	1-2	1-2	1-2	1-2	1-2	1-2	0-1	0-1	0-1	0-2	0-1	2-5	1-3

*Broad basal mica reflection at 10A°

decrease in the amounts of plagioclase, quartz and mica. These mineralogical variations are paralleled by chemical changes (Table 8 and Figures 5-10) and are similar to variations in metasomatically altered Blue Conglomerate.

The paragenetic sequence of mineral crystallization is very difficult to determine because of a nearly sub-microscopic grain size. However, wherever paragenetic relationships could be discerned they were the same as observed in the Blue Conglomerate. Three broad time subdivisions can be made. The first is composed of the contact metamorphic minerals, with or without any relic minerals from the original sediment. These include calcic plagioclase, quartz, muscovite, and possibly epidote, diopside, pyrite and magnetite. The second group is associated more closely in time with metasomatism and includes orthoclase or ferriferous orthoclase, tremolite-actinolite, sodic plagioclase, and possibly pyrite, magnetite and epidote. The third group, occurring in transection veins, includes calcite, zeolites, and chlorite-vermiculite (undifferentiated). The time separation at any one place between these groups probably was not very great, although a pattern to the veining and pod orientation suggests crystallization in a set of shear fractures after the initation of contact metamorphism.

Chemical Composition and Metasomatism

Two samples of laminated Mill Hill Slate were selected for chemical analysis, one of the normal and one of the pink, metasomatized type. Although these laminated types comprise the majority of Mill Hill Slate outcrops, the mineralogy of this unit is extremely varied (Table 7) and these two analyses may not be representative of the unit as a whole. The mineral analyses, largely estimated from X-ray diffractometer patterns (Table 7), indicate that the chemically analyzed Mill Hill Slate samples may be higher than average Mill Hill Slate in plagioclase and microcline content and somewhat lower in amphibole and mica content. The metasomatized part of this unit is more uniform in composition, and hence the sample analyzed is more representative.

In general, although the composition of Mill Hill Slate differs from that of Blue Conglomerate, the chemical changes accompanying metasomatism are the same (cf. Tables 4 and 8). Normal Mill Hill Slate differs only slightly from the composition of Clark's (1924) average shale. The higher CaO in the Mill Hill Slate results from original limy laminae; the higher Na_2O results from a probable sodium introduction into the hornfels. An average of eight Martinsburg shale samples from Lebanon County (Table 8) corresponds less closely to average shale, partly because of the loss of CaO and Na_2O during weathering of the Martinsburg samples. The normal metamorphic lithology contains more CaO, FeO, and Na_2O and less Al_2O_3 than metasomatized

Mill Hill Slate, Clark's averge shale, and Martinsburg shale. The high calcium and sodium are concentrated in metamorphic plagioclase and recrystallized calcite. The low alumina is a consequence of a lack of mica and kaolinite. The difference in oxidation ratio (Fe^3/Fe^2) is at least in part a consequence of the weathered state of the Martinsburg Shale samples (O'Neill and others, 1965) and perhaps also a consequence of contact metamorphism in a locally reducing environment. It is interesting to note that metasomatized Mill Hill Slate also resembles Cornwall granophyre (Table 8).

Table 8. *Chemical Analyses Comparing Metasomatism in Mill Hill Slate Hornfels with Unmetamorphosed Units (anhydrous)*

	c-51*	c4-10*	G*t	M*	1.*
SiO_2	60.54	60.27	65.62	59.72	62.2
TiO_2	0.93	0.89	0.36	1.05	0.7
Al_2O_3	15.17	16.61	16.05	20.63	16.5
Fe_2O_3	3.59	2.48	1.79	7.96	4.3
FeO	3.57	1.47	0.53	1.56	2.6
MnO	0.21	0.15	0.04	N.A.	Tr
MgO	1.91	0.91	1.25	2.04	2.6
CaO	6.00	5.02	3.15	0.41	3.3
Na_2O	3.76	2.92	2.18	0.74	1.4
K_2O	3.77	8.07	8.44	5.29	3.5
PO_4	N.A.	N.A.	0.19	N.A.	0.2
CO_2	0.16	0.75	0.16	0.62	0.7
F	0.33	0.23	0.22	N.A.	
S_{tot}	N.A.	N.A.	0.03	N.A.	
ZnO	0.001	0.10	N.A.	N.A.	
CuO	0.01	0.05	N.A.	N.A.	
NiO	0.05	0.01	N.A.	N.A.	
CoO	0.002	0.01	N.A.	N.A.	
BaO	0.01	0.03	N.A.	N.A.	
Total	100.013	99.97	100.01	100.02	100.0
$Fe_{tot.}$	5.29	2.88	1.67	6.80	5.03

N.A. = no analysis determined Tr = trace

* Analysis by Spectrochemical Laboratories, Pittsburgh, Pennsylvania.

t Analysis by A. S. McCreath and Son, Harrisburg, Pennsylvania.

C-51 Banded, normal metamorphic Mill Hill Slate
C4-10 Metasomatized, banded Mill Hill Slate from ore hanging wall
G Avg. granophyre (C4-150 and 11-38G, see Appendix)
M Avg. 8 Martinsburg shales, Lebanon Co. (O'Neill and others, 1965)
1. Avg. shale (Clarke, 1924, p. 30)

Metasomatism resulted in addition of aluminum and potassium among the major elements, and of zinc, copper, cobalt, and barium among the minor and trace elements (Table 8 and Appendix 4-B). There was a noticeable loss of iron, calcium, sodium, and nickel. Differences in silica, titanium, and magnesium probably are not significant. CaO is not representative because of highly varied amounts of secondary calcite. However, the apparent loss of calcium during metasomatism probably is real because it is accompanied by an increase in CO_2 and therefore the change in calcium is a reflection of the calcium content of silicates, chiefly calcic plagioclase. A similar decrease in the calcium content in plagioclase was noted in the metasomatism of Blue Conglomerate where replacement by more sodic plagioclase occurred. After subtracting the calcite content, there is a similar decrease in the CaO/Na_2O ratio (1.29) from hornfels to metasomatized Mill Hill Slate. Part of the calcium decrease also can be attributed to an overall decrease in total plagioclase feldspar content (Table 7). The apparent addition of aluminum is less easily accounted for. Replacement of calcic plagioclase by more sodic plagioclase or by orthoclase releases aluminum, which is the reverse of the observed change. Addition of chlorite or aluminous amphibole may account for some of the increase. The source of the aluminum probably was the replacement of muscovite by microcline during thermal metamorphism. The addition of potassium, the major characteristic of metasomatism, resulted in metasomatic crystallization of ferriferous orthoclase. The apparent introduction of cobalt during this alteration is interesting in the light of the high cobalt content of much of the pyrite in the ore zone. Nickel however, which also is concentrated in the ore zone, does not appear to be spatially related to metasomatism.

Facies Representations

The representation of normal and metasomatized Mill Hill Slate on ACF or AKF diagrams (Figures 7 and 8) illustrates chemical changes in terms of mineral components, particularly from contact metamorphism to metasomatism, emphasizes differences between Mill Hill Slate and Martinsburg shales from Lebanon County, and can be used to estimate equilibrium attained locally when compared with the actual mineral phases present. Because of its chemical similarity, an analysis of Cornwall granophyre is also presented for comparison. On the ACF diagram (Figure 7), the normal metamorphic hornfels lithology lies within the epidote-chlorite (biotite)-actinolite field whereas the metasomatized lithology and granophyre lie within the epidote-actinolite-calcite field. This representation could be misleading because of extreme differences in the mineral composition, especially in the contact metamorphic lithology. However, this representation does conform to the observed mineralogy. Biotite is present in normal metamorphic Mill Hill Slate but was not identified (thin section and X-ray analysis) in metasomatized portions. Chlorite is present in both the hornfels

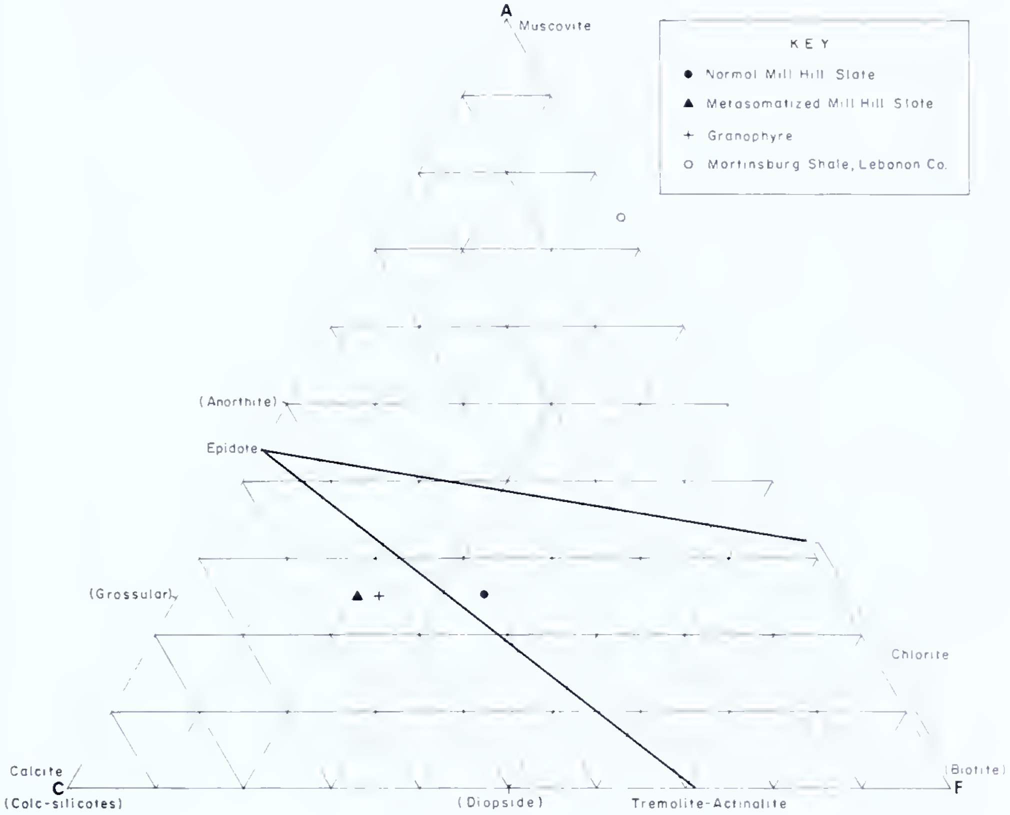

Figure 7. **ACF diagram for Mill Hill Slate, illustrating epidote-hornfels facies.**

and the metasomatized hornfels lithology. Such rather meager data suggest that locally biotite became unstable although cholorite persisted (metastably or with a different composition?) in the metasomatized unit despite a decrease in FeO/MgO from 1.87 to 1.61.

The AKF diagram (Figure 8) illustrates the high potassium content of metasomatically altered Mill Hill Slate and its chemical similarity to Cornwall granophyre. The mineral assemblage for the five rock types represented (Figure 8) is somewhat different from that of the ACF diagram: both biotite and muscovite are theoretically stable in all assemblages but, in actuality, commonly are not present (Table 7). In general, the composition points representing Martinsburg shale, hornfels, and metasomatized hornfels do not lie along a single tie line as might be expected of a continuous alteration sequence. There is, however, a consistent, albeit irregular, increase in K_2O content from Martinsburg shale to thermally metamorphosed Mill Hill Slate to metasomatized Mill Hill Slate and granophyre (3.77 to 8.07 to 8.44 percent respectively). For the same sequence, Na_2O decreases from 3.76 to 2.92 to 2.18 percent. Because of a closer similarity in composition between average shales and Mill Hill Slate than between average shales and Blue

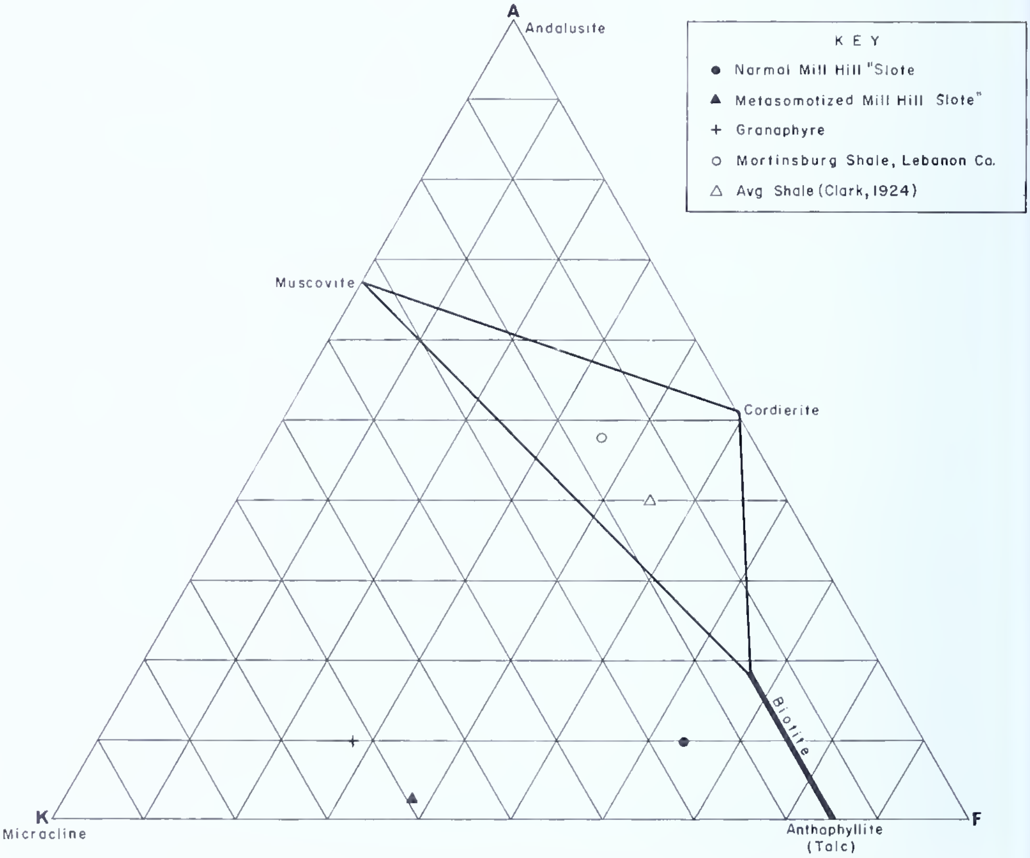

Figure 8. AKF diagram for Mill Hill Slate, illustrating hornblende-hornfels facies for excess silica and alumina.

Conglomerate, Figure 8 illustrates particularly well the alteration both in thermal metamorphic (addition of Na_2O) and metasomatic (addition of K_2O) rock types from an originally shaly unit.

Xenoliths in Diabase

A 1-foot by 3-foot xenolith of Blue Conglomerate was encountered in drilling approximately three feet below the top of the diabase in the eastern ore body. Quartz aggregates characteristic of Blue Conglomerate lithology have been recrystallized, particularly along their perimeter, such that quartz crystals are euhedral toward diabase and anhedral toward aggregate centers (Plate 5 B and C). There is very little inter-aggregate matrix remaining, only a few shreds of muscovite and some actinolite and epidote. Large perthitic feldspars occur as porphyroblasts at the diabase—Blue Conglomerate contact (Plate 5-C). Plagioclase in perthite is sodic, and albite twinning occurs as domains in untwinned potassic feldspar host. There is no sericitization of the calcic plagioclase in the fine-grained diabase near the inclusion although sericitized plagioclase commonly occurs in diabase pegmatite and granophyre near their contact with normal diabase within the top of the sheet. Veins of chlorite (very low birefringence) transect both the diabase and the Blue Conglomerate inclusion.

Xenoliths of limestone within diabase are not infrequent, but no systematic study has been made of them. A few are replaced by magnetite (see "Geology of the Cornwall Ores"); others are not (Plate 5-A). Tremolite, serpentine, and brucite are present, with or without magnetite. Samuel J. Sims, Bethehem Steel Corporation, (personal communication) noted the following associations in limestone inclusions in diabase from the 880-foot level of the eastern ore body: 1) diopside-calcite-magnetite-tremolite, 2) garnet-blue-green hornblende-phlogopite-calcite-diopside (minor)-apatite (minor), 3) diopside-apatite-magnetite-calcite, and 4) zeolite-serpentine-calcite-magnetite-garnet-diopside. Because these minerals are representative of environments of different Si/Al and Ca/Mg ratios, as well as different temperatures and/or P_{H_2O} conditions, it is probable that they are not equilibrium assemblages but crystallized sequentially under the influence of different thermal and chemical gradients. Sims also noted small xenoliths of calc-silicates found on the 1140-foot level of the eastern mine. Very little is known about the ore-body within diabase, but it may be a replacement of a large limestone xenolith (see Part 4).

An X-ray analysis was made of a xenolith at the top of the diabase as a result of misidentification in the field. The pink color of this sample led to a field identification of aplite. However, the texture is much coarser-grained than typical Cornwall granophyre (or aplitic granophyre) and it contains about 35 percent coarsely crystalline calcite with hematite inclusion. Its mineralogy, derived from both petrographic and X-ray analysis, is presented in Table 9. Despite the apparently large amounts of calcium available (now in calcite, diopside, and fluorite), no plagioclase is present. However, much of the muscovite (5-10 percent) is in lath-shaped aggregates and may, in part, have pseudomorphically replaced plagioclase. Ferriferous, or hematitic orthoclase comprises nearly a third of the sample and has the same optical properties as described previously, except that the 2V is less than 30° approximately ⊥ to (010) in all the grains examined. Orthoclase is pink, cloudy, crystalloblastic, untwinned, and occasionally sericitized. Microcline, optically unidentifiable, occurs in a fine-grained ground mass (identified by X-ray analysis). Neither the microcline nor the orthoclase appear to contain more than 10 percent albite molecules in solid solution (the method, described previously, is not reliable below 10 percent). The presence of the volatiles, fluorine and boron, in fluorite and tourmaline is unusual at Cornwall and has been found only in granophyre and metasomatized Blue Conglomerate near the diabase. Therefore, the xenolith is believed to be a metasomatized limy hornfels.

Because of the coarse-grained, and nearly equant, crystallization of most major mineral components in this xenolith, there is almost no consistent paragenetic relationship. Small relics of muscovite are the earliest recognizable mineral grains. Calcite, chlorite, and "sericite" have followed the crystallization of hematitic orthoclase, fluorite, and tourmaline. The position of microcline, diopside, and phlogopite in this sequence is not clear, although orthoclase appears to be younger than microcline and forms metasomatic porphyroblasts. The metasomatic and contact metamorphic minerals in this pink, limy sample comprise the same mineral associations as in metasomatized Mill Hill Slate and Blue Conglomerate.

Table 9. *Mineralogy of a Limestone Xenolith (?) in Diabase (C3-33) from the Western Ore Body*

	%
% Ab in K-feldspar	0-10
Fe-Orthoclase	25-35
Microcline	5-15
Calcite	30-40
Diopside	5-10
Epidote	?
Garnet	5-10
Muscovite	5-10
Chlorite	5
Fluorite	1-2
Tourmaline	1
Pyrite	0-1
Magnetite	0-1

As discussed subsequently in sections concerning the origin of potassium metasomatism and the characteristics of diabase differentiation, the hematitic or ferriferous orthoclase may have had several possible origins. However, regardless of the source of this feldspar, its presence in a carbonate-rich matrix without plagioclase requires one of the following: a separation of more mobile K from less mobile Si and Al constituents in a magmatic fluid, proximity to granophyre, or potassium metasomatism of a contact unit in addition to contact metamorphism. In any case, the high carbonate content and sharp lithologic boundaries require the presence of a discrete limy shale block. If the potassium came from a tholeiitic residuum, this residuum would have to have been active within the sheet after engulfment and after the crystallization of contact metamorphic diopside and phlogopite. Both conditions are possible since the sample was at or within the top of the sheet where late residual fluids are known to have concentrated. There is no magnetite ore present.

With the possible exception of a large block of limestone, now a magnetite — actinolite ore body deep within the sheet, there is very little concrete evidence of roof stoping and no noticeable evidence of the formation of rheomorphic veins of sedimentary material. Rheomorphism of the Karroo type (Walker and Poldervaart, 1949) has not been observed. The only evidence of *in situ* diabase magmatic activity toward the sediments is the introduction of fluorine, boron, possibly of sodium and potassium all of which occur only above the eastern ore body at Cornwall.

GEOCHEMISTRY AND ORIGIN

Introduction

In previous discussions, the Blue Conglomerate and Mill Hill Slate have been treated as separate entities and their alteration, either by thermal metamorphism or by potassium metasomatism, has been treated as the result of two distinct processes. Actually, the two units are very similar: both were probably derived from facies of the Martinsburg Formation and both reacted in a similar fashion to a sequence of alteration events in which thermal recrystallization and mobilization within an essentially closed system were related temporally, genetically, and spatially. For both units, chemical addition and crystallization occurred during metasomatism. The resultant geologic units evolved from a complex interaction in a continually changing environment (e.g., temperature and concentration gradients) such that the metamorphic and metasomatic processes varied locally. Commonly, these processes cannot be clearly delineated. For the most part, chemical reactions among minerals will not be of a simple binary or ternary type, except locally; hence, a specific replacement reaction will not represent the exact conditions that existed during alteration. However, from a gross aspect a single equation can represent a resultant direction of change even though intermediary or subsidiary steps are omitted. Utilizing this approach, a comparison of simple binary and ternary reaction systems (derived from laboratory synthesis studies) yields useful information regarding the geochemistry of alteration. Many of the variables measured here do show that there was a significant difference between the conditions of thermal metamorphism and metasomatism, that time-space played a significant role in progressive mineralization, and that original rock character (e.g. composition and texture) was important in controlling the formation of alteration products.

Summary Comparison of Hornfels Units

Somewhat hidden among previously presented data are the differences between the Mill Hill Slate and the Blue Conglomerate, differences that are important in revealing the character of metamorphism and that controlled, in part, the ensuing metasomatism. Foremost among these differences probably was the character of the original sedimentary units previous to diabase intrusion. Unfortunately, the complexity of post-lithification events has obscured much of this evidence. Thin laminations, cross-bedding, and overall composition of Mill Hill Slate strongly suggest an originally fine-grained shale irregularly interbedded with calcarenities, some perhaps dolomitic, and a few pelitic fragments. The Blue Conglomerate apparently was composed of a shale or silty shale matrix with clastic, pelitic, and quartzose fragments. Interbedded were small sandstone lenses. Considerable brecciation and faulting occurred after lithification but before metasomatism and ore deposition. As a consequence of its greater range in grain size, lack of thin laminations, and extensive brecciation, the Blue Conglomerate was a more permeable unit for solution or ion migration than was the Mill Hill Slate at the time of contact metamorphism. Another important factor in the different behavior of the two units has been their spatial position relative to diabase and limestone (Plates 21 and 23 and Figure 22). On the east, the Mill Hill Slate predominates at the diabase contact and where overlying Blue Conglomerate also is present, both cap the eastern ore zone (Plates 21, 22 and 23). To the west, ore and diabase are capped by unreplaced metamorphosed limestone. West of the ore bodies, metamorphosed but not metasomatized Mill Hill Slate comes in direct contact with diabase (Plate 21). This spatial association helps to relate thermal metamorphism to diabase intrusion and metasomatism to ore mineralization.

Considering the Mill Hill Slate and Blue Conglomerate as contact metamorphic lithologies (hornfels), a few significant chemical and mineralogical differences serve best to differentiate the two. The Mill Hill Slate has a significantly higher Si/Al ratio, although containing much less quartz. In Mill Hill Slate, a greater calcium content is a consequence of limy intercalations and the greater potassium content, although there is less muscovite, is a consequence of a greater microcline content. The Blue Conglomerate, on the other hand, contains somewhat more total iron (for the samples studied this in part is a consequence of sample location immediately above areas of ore) and a higher Al/alkali ratio. Mineralogically, the Mill Hill Slate is distinguished by the presence of microcline, diopside, calcite, and solid solution of sodium in potassium feldspar, whereas the Blue Conglomerate is distinguished chiefly by abundant mica (ferriferous) and by sparse matrix quartz that contrasts with a high quartz content in breccia fragments (Plate 2). Both contain considerable calcic plagioclase feldspar. These distinguishing characteristics are, in part, a function of the original sedimentary facies composition but are also, in part, a result of a different thermal metamorphic history. For example, the higher temperature facies of Mill Hill Slate, where it is in direct contact with diabase, is represented by lower obliquity (triclinicity) of feldspar, greater sodium solid solution in potassic feldspar, finer grain size, and a more heterogeneous mixture of several superimposed metamorphic facies (hornblende-hornfels, albite-epidote-hornfels etc.). Because the Blue Conglomerate was not subjected to this degree of thermal metamorphism (in the areas sampled) and because of its structural position, its lack of impermeable laminae, its extreme variation in grain and fragment sizes, its brecciation, and its higher Al/alkali ratio after metamorphism, its potential for subsequent metasomatism was much greater than was the potential for the Mill Hill Slate.

Contact Metamorphism

Iron Oxidation and Reduction

The role of oxidation during thermal metamorphism is interesting, especially in view of the presence of both magnetite and hematite. In the Triassic sediments at some distance from diabase, hematitic sediments have been bleached from reddish to grayish color, especially the finer-grained silts and shales. Specular hematite occurs quite commonly throughout the diabase magmatic province in conglomerates, in fractures, in siltstones, and at formational contacts with other sediments. There probably has been some migration of iron near diabase and subsequent recrystallization of hematite locally where the oxidation potential was high as it would be at contacts or in fractures under near-surface conditions. Thus fine-grained matrix hematite (causing red sediments) may have formed specularite at these loci, yielding 'bleached' sediments; reduction of hematite to magnetite has not necessarily occurred.

In the Blue Conglomerate and Mill Hill Slate, nearer the diabase sheet, the situation seems to be quite different. Even though the Fe^3/Fe^2 ratio in the analyzed Martinsburg shale samples in abnormally high as a result of recent weathering (Table 10), the ratio in the hornfels with which it is compared is abnormally low; in fact, the ratio is less than that of normative magnetite (Table 10). Thus, although total iron has not changed at all from average Martinsburg shales to the weighted hornfels average (Table 10), a considerable reduction in the oxidation state did occur. This is further supported by the crystallization of dust-sized particles of magnetite in both the Blue Conglomerate and the Mill Hill Slate previous to metasomatism and magnetite ore introduction. Such reduction during thermal metamorphism is common and could be expected in these dense and fine-grained units during dehydration (cf. H_2O analyses, Appendix 4-B).

Oxidation and recrystallization potential, however, were not the only controls upon the formation of oxidized minerals. At shale-limestone contacts, hematite preferentially replaced the limestone side and garnet crystallized at the shale contact or within it (Figure 4), illustrating a compositional control in addition to that of increased available oxygen at a formational contact at shallow depth. There is a similar development of garnet at other such contacts and within conglomeratic facies of the Triassic sediments where silica and alumina are available.

Thus, the oxidation potential has varied locally depending on texture and location of the units undergoing metamorphism and in addition the resultant mineralogy has been controlled by the composition of the rock units in the immediate vicinity of the alteration. Migration of iron in the contact

Table 10. *Chemical Analyses Illustrating Metamorphic and Metasomatic Alteration (Anhydrous)*

	1.	2.	3.	4.
SiO_2	62.3	59.7	58.8	57.3
TiO_2	0.7	1.1	N.A.	N.A.
Al_2O_3	16.5	20.6	18.3	22.0
Fe_2O_3	4.3	8.0	3.7	3.3
FeO	2.6	1.6	4.5	3.0
MgO	2.6	2.0	2.2	1.7
CaO	3.3	0.4	4.9	2.0
Na_2O	1.4	0.7	3.9	3.5
K_2O	3.5	5.3	3.4	6.8
CO_2	2.7	0.6	0.3	0.5
Total	99.9	100.0	100.0	100.1
Fe_{tot}	5.0	6.8	6.0	4.4
Ca/Na ratio*	0.4	0.0	1.1	0.4

* Excluding calcite N.A. = No analysis determined

1. Avg. shale (Clarke, 1924, p. 30)
2. Avg. of 8 Martinsburg shales, Lebanon Co. (O'Neill and others, 1965)
3. Weighted avg. : 1 metamorphosed Mill Hill Slate hornfels (times 2) and 1 metamorphosed Blue Conglomerate hornfels
4. Weighted avg. : 1 metasomatized Mill Hill Slate and 1 metasomatized Blue Conglomerate (times 2)

sediments on a large scale does not appear to have been significant at this early stage of compositional reorganization; rather, there has been an outward migration of an irregular zone of oxidation, more or less coincident with a loss of water, silica, and mobile constituents toward the fringes of thermal metamorphism leaving behind a reduced assemblage approximately parallel to isotherms of a declining thermal gradient.

Silica and Alkali Balance

By definition, contact thermal metamorphism does not result in any addition of chemical elements to the units metamorphosed, although some may be lost from the system or undergo a change in oxidation state. This is undoubtedly the case with the Mill Hill Slate and Blue Conglomerate at Cornwall, but it is difficult to prove because there is no unmetamorphosed parent sediment available for comparison. However, an approximation can be made by a comparison of the metamorphosed units with an average of eight Martinsburg shale samples from the vicinity of Cornwall in Lebanon County (Figure 9), and by comparing a weighted average of one average Blue Conglomerate hornfels composition (Table 10). This weighted average is based upon the observation that the areal extent of Mill Hill Slate hornfels is *at least* twice that of the Blue Conglomerate (Plates 21 and 23). From these weighted compositions it can readily be seen that differences among most major elements are small. Arrows in Figure 9 indicate probable directions of change between average Martinsburg shale and the weighted hornfels composition. With the exceptions of sodium and calcium, no significant addition of constituents is indicated (total iron is approximately constant even though the Fe^3/Fe^2 ratio differs because of weathering). Average percent CaO in the Martinsburg shale is low as a result of leaching so that there has been no significant addition of calcium to the hornfels.

An increase in Na_2O presents more of a problem. Some, of course, may have been lost from the Martinsburg shale during weathering; however, an initial content of nearly 4 percent Na_2O (the amount in the weighted hornfels) is more than twice that of average shales (column 1, Table 10). Either this facies of the Martinsburg Formation was initially unusually rich in Na_2O or some addition occurred associated with diabase intrusion, metasomatism, or hydrothermal ore mineralization. Even increasing the Mill Hill Slate to Blue Conglomerate ratio will not appreciably lower the Na_2O content of average hornfels (see Tables 4, 8, and 10). The addition of sodium from crystallizing diabase is not uncommon especially of albitic diabase, and may result in the formation of adinoles composed largely of albite and quartz (Turner and Verhoogen, 1960, p. 571). Such may be the case to a much more limited extent here. Adinoles have not been observed, but more data are needed on Na_2O content away from ore zones and on unmetamorphosed parent rock. If sodium has been introduced into the sedimentary system, mineral parageneses show it to have been earlier than potassium metasomatism and unrelated to both this metasomatism and to ore introduction in areal distribution. Enrichment of Na_2O in hornfels before K_2O enrichment is evident in a sample from west of the ore zone (Table 3, column 1). Thus, K_2O enrichment is localized above the eastern ore zone, whereas Na_2O enrichment appears to be more ubiquitous. The only elements that may have been lost from the hornfels system are silicon and potassium.

Petrographic observations and chemical inferences concerning the silica balance are similarly complex, involving reactions among quartz, mica, plagioclase, pyroxene, amphibole, chlorite, kaolinite, zeolites, and calcite. Popovich (1964) concluded that silica in host limestone decreases away from the diabase contact and that silica (total) was added to the limestone. A small amount of this silica may have migrated from overlying hornfels units. However, contact metamorphism of existing silicates in the siliceous laminae of the host rock, introduction during potassium metasomatism, and hydrothermal ore fluid migration probably were largely responsible for its introduction. The decrease in silica in limestone away from the diabase (Popovich, 1964) is also in large part a consequence of thermal gradients, the sequence of ore zone mineralization, and the difficulty of ore in replacing earlier silicates relative to carbonates (see Part 4, "Mineral Paragenesis" and "Zonation").

As noted, both Mill Hill Slate and Blue Conglomerate evidence only a slight, perhaps insignificant, loss in total SiO_2 (Figure 9). However, the mineralogical form of this silica differs in the two units. The Mill Hill Slate,

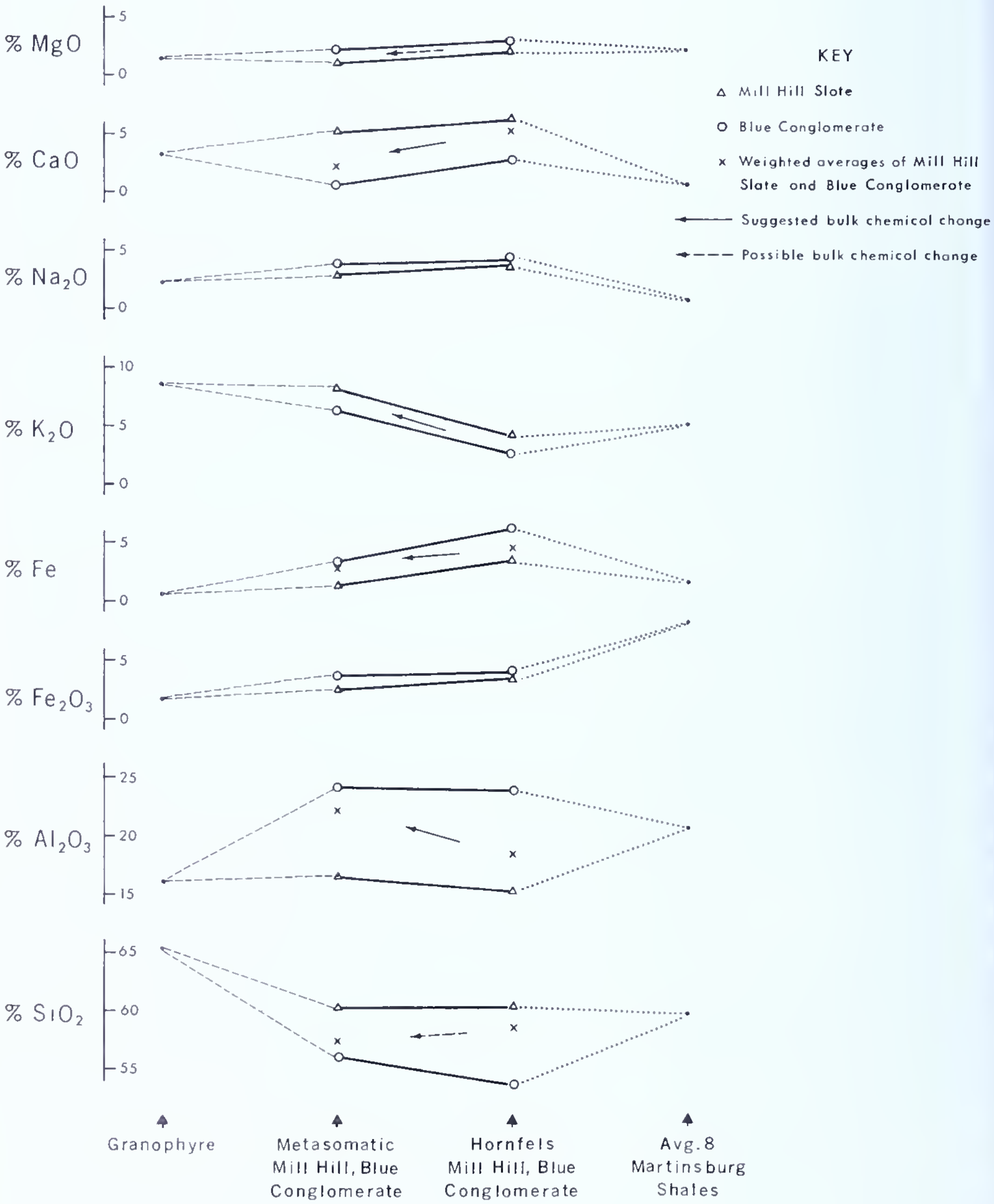

Figure 9. Chemical analysis variation trends among granophyre, metamorphosed units, and Martinsburg shale; arrows indicate possible alteration trends.

which contains more total SiO_2, contains very little free quartz (Table 7). The Blue Conglomerate, although it has little or no matrix quartz, contains considerable amounts of coarse-grained brecciated aggregates of quartz. The absence of quartz in the fine-grained phases of both units indicates that any loss of silica from the fine-grained portions has been largely consumed by essentially *in situ* metamorphic reaction. Such quartz would have a higher reactive potential than quartz in the coarse-grained aggregates. That silica mobility did occur is shown by: 1) a slight decrease in total silica from that of average shale compositions, 2) the presence of veins and overgrowths of secondary quartz, 3) vugs of secondary quartz in Blue Conglomerate, and 4) perhaps also by the metamorphic silication of limestone. From these observations, it appears that silica in hornfels units has reacted and moved largely within a closed hornfels system.

Another way of looking at the silica migration process is to consider the conversion of shale (or siltstone) to hornfels before the introduction of alkalies or alumina. The available reactants would have been quartz, muscovite, calcite, some detrital clay mineral, and minor feldspar. In both hornfels units, calcic plagioclase is a major metamorphic product. The simplest procedure for feldspathization would involve the recombination of free quartz with calcite and mica (or chlorite) with the consequent release of some potassium and/or magnesium, carbon dioxide, and water. Any excess silica from siliceous laminae could have migrated into host limestone lying farther above diabase. This type of reaction represents changes that may have occurred in hornfels units, although the actual reaction steps must have been much more complex. In some cases, especially where mica and clay minerals were in excess and free quartz was minimal, the original minerals remained essentially unchanged because the metamorphic potential (or chemical potential under a thermal gradient) was insufficient to initiate reaction. Such original remnants have been observed: some chlorite (notably within the Blue Conglomerate breccia fragments), clay, and detrital illitic mica that yield broad basal X-ray reflections. Both the chemical and mineral compositions indicate that a summation reaction for calcic plagioclase such as noted above was probably the major recombination involved during hornfels metamorphism.

Utilizing the average hornfels CaO content (Table 10), after subtracting for calcite and for diopside (about 3 percent), the average hornfels is composed of approximately 25 percent calcic plagioclase of An_{50} average composition, agreeing well with semi-quantitative X-ray estimates (Table 11). The limy intercalations of Mill Hill Slate may well have been the source of calcium for plagioclase in both hornfels units, and therefore there is somewhat less calcic plagioclase in the Blue Conglomerate than in the Mill Hill Slate (Tables 3, 7, and 11).

Another important reaction in Mill Hill Slate involved the formation of microcline from muscovite and quartz with the consequent release of alumina and water. From Table 11, it can be seen that quartz and

Table 11. *Percent Mineral Variation During Metasomatism*

	Avg. Mill Hill Slate (10)	Avg. Blue Conglomerate (4)	Avg. altered Mill Hill Slate (2)	Avg. altered Blue Conglomerate (4)
Plagioclase	24	20	13	16
An content	20, 55	20-30, 35-60	15	10-15, 30
Alkali feldspar				
Orthoclase	8	6	6	5
% Na in Or	14	0-10	12	12
Fe-orthoclase	3		34	13
Microcline	9	1	11	?
Obliquity $^\circ 2\theta$	0.56	0.66	0.42	0.68
Quartz	10	27*	4	9*
Calcite	11		3	5
Diopside	11		11	1
Epidote	0-3		0-5	
Amphibole	5	4	5	6
Mica	7	31		41
Fe in mica	Low	High		High
Chlorite	0-5		2-4	
Kaolinite		6	?	
Prehnite	0-20			?
Tourmaline				1
Pyrite	1	0-1	1-3	0-1
Magnetite	1	0-1	2-4	1-2

* Excludes quartz breccia fragments

microcline, and to a lesser degree mica and microcline, appear to be antithetic. This reaction was even more pronounced in Blue Conglomerate where less quartz was available for combination with mica. Thus, quartz (or available silica) did not exceed the solubility product constant for the formation of microcline, and hence it is essentially absent in the matrix of metamorphosed Blue Conglomerate (Table 11).

Undoubtedly other reactions played a role in desilication, but the fixation by available aluminum, calcium, or potassium determined the rather slight extent to which silica migrated from the shaly hornfels outward toward limestone (in part to yield diopside, tremolite, and phlogopite) or toward Triassic sediments to form garnet or epidote.

Metamorphic Temperature, Reactions, and Equilibrium

The question of the establishment of metamorphic equilibrium is rather arbitrary and academic: both the Blue Conglomerate and the Mill Hill Slate exhibit several metamorphic facies and relict minerals as a result of incomplete reaction. However, some local stabilization of equilibrium mineral assemblages in Mill Hill Slate seems to have occurred during temperature gradient migration. Because the Mill Hill Slate does not have a large excess of alumina beyond that which could combine with calcium, sodium, and potassium, it can be represented in terms of four "components": (Si,Ti) O_2, K_2O-Al_2O_3, CaO-Na_2O-Al_2O_3, and MgO-FeO. In the Blue Conglomerate, which does have an excess of alumina, Al_2O-Fe_2O_3 should be added to the above component list for a total of five components. Restriction to these components assumes that both H_2O and CO_2 are mobile components as appears to have been the case in these units. The associated mineral phases in Mill Hill Slate hornfels are calcic plagioclase, orthoclase, microcline, calcite, diopside, and some quartz, mica, and rarely actinolitic amphibole and younger prehnite, yielding a total of five to eight. The mineral phases in Blue Conglomerate hornfels are calcic plagioclase, quartz, mica, and some actinolitic amphibole, microcline, and kaolinite, yielding a total of three to six. For the purposes of this discussion, orthoclase and microcline are treated as a single phase. Assuming the applicability of the mineralogical phase rule as a minimal requirement for an equilibrium assemblage (see discussions by Thompson, 1959 and Zen, 1963), the number of theoretical components should equal, or not be exceeded by, the number of minerals observed. On this basis, the Blue Conglomerate hornfels samples examined contain approximately the predicted number of mineral phases, whereas Mill Hill Slate hornfels assemblages commonly exceed the predicted number. This is expectable because the Mill Hill Slate hornfels samples were collected much closer to the diabase contact than those of the Blue Conglomerate hornfels, and therefore it was subjected to steeper temperature gradients. Total internal equilibrium could not be obtained under this gradient and some minerals exist metastably. On the scale of a thin section, bimineralic or polymineralic aggregates occur in Mill Hill Slate; for example, bands composed essentially of diopside and calcic plagioclase adjacent to an orthoclase-microcline-calcic plagioclase assemblage. The existence of polymineralic, rather than monomineralic, zones may have resulted in part because such original components as calcite and quartz were consumed in reaction before total equilibrium could be established. In part, reaction, nucleation, and diffusion rates may have been insufficient. The situation, both for contact metamorphism and potassium metasomatism, undoubtedly is more complex than has been considered here (see Thompson, 1959) so that attainment of equilibrium cannot be rigorously specified without a minutely detailed program of sampling and analysis. However, total rock equilibrium did not result, and this is particularly obvious where hornblende (Table 7 and 11) of the hornblende-hornfels facies (Figure 10) is present along with later minerals that formed at lower temperatures. In fact, the existence of a crude paragenesis of groups of associated minerals in both hornfels units is indicative of broad facies inhomogeneities such that it was possible to attain only a very local equilibrium.

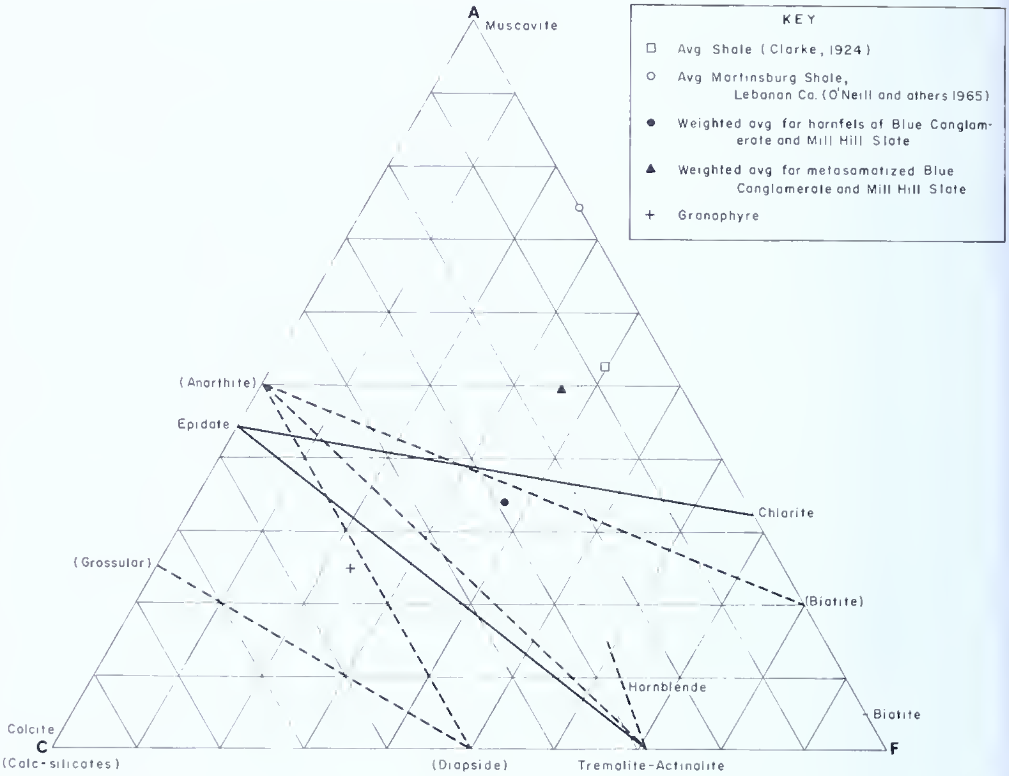
A
Muscovite
KEY
□ Avg Shale (Clarke, 1924)
○ Avg Martinsburg Shale, Lebanon Co. (O'Neill and others 1965)
● Weighted avg for hornfels of Blue Conglomerate and Mill Hill Slate
▲ Weighted avg for metasomatized Blue Conglomerate and Mill Hill Slate
+ Granophyre
(Anorthite)
Epidote
Chlorite
(Grossular)
(Biotite)
Hornblende
Biotite
Calcite
C
(Calc-silicates)
(Diopside)
Tremolite-Actinolite
F

Figure 10. **ACF diagram illustrating contact metamorphic assemblages; albite-epidote hornfels facies (solid line) and hornblende-hornfels facies (dashed line), both with excess silica and the latter with excess alumina.**

According to the estimate by Turner and Verhoogan (1960, p. 520), the hornblende-hornfels facies corresponds to a temperature range of 550-700°C. In addition to rare hornblende, diopside is present in the lime-rich portions of Mill Hill Slate, although it does not appear as a stable mineral from calculations based on the weighted average hornfels plot (Figure 10) because the Mill Hill Slate samples, when chemically analyzed, were not particularly lime-rich. Other co-existing minerals such as hornblende-actinolite, muscovite-actinolite, oligoclase-labradorite, diopside-epidote, or muscovite-biotite-chlorite suggest an incomplete transition to the lower temperature albite-epidote hornfels facies (Figure 10) in the temperature range of 400-550°C, and in even lower retrograde temperatures. Another temperature estimate utilizing the mineral phases present can be obtained from the previously discussed alteration of mica and quartz to microcline feldspar:

Muscovite + Biotite + Quartz → Cordierite + K-Feldspar (3-1)

at 660-670C. (Winkler, 1957). This is approximately the temperature for the destruction of muscovite (Yoder and Eugster, 1955; Crowley and Roy, 1964). In the absence of sufficient magnesia or alumina, as in the Mill Hill Slate, or without an excess of potassium, as in both Mill Hill Slate and Blue Conglomerate, cordierite will not form. A more accurate summation representation is:

Muscovite + Quartz ± Biotite → Potassium Feldspar + Water ± Amphibole (3-2)

Jaeger's (1957) method of contact temperature estimation yields similar temperatures. For a sheet of this thickness, about 1000 feet, the temperature at the contact (T) is estimated to be 60 percent of the intrusion temperature (T_i) plus the temperature of the country rocks (T_c):

$$\begin{aligned} T &= .6T + T_c \qquad (3\text{-}3)\\ &= .6\,(1100 \pm 50^\circ) + 40^\circ \pm 20^\circ \\ &= 700^\circ C \pm 60^\circ C. \end{aligned}$$

This serves as a maximum temperature, slightly above, but very close to the hornblende-pyroxene facies boundary. As a result, the maximum temperature reached during contact metamorphism was probably near, or somewhat greater than, 600°C, but below the stability temperature of sanidine (microcline is the major K-feldspar and most orthoclase is paragenetically later). This is compatible with a range of 900 - 1100°C. for diabase crystallization, the difference being accounted for by thermal insulation of the rapidly crystallized chilled margin and by initially rapid thermal diffusion at the time of intrusion into the relatively cold, hydrous country rock reservoir.

Metasomatism Mineralogy and Geochemistry

Mineralogical Characteristics of Metasomatism

The mineralogical characteristics that differentiate thermal metamorphism and metasomatism are summarized in Table 11, based on data from Tables 3 and 7. The major minerals affected by metasomatism are alkali-feldspar, plagioclase, quartz, and mica. Calcite increases slightly in Blue Conglomerate and decreases in Mill Hill Slate, but the samples are not representative because of the vagaries of secondary calcite veins. Diopside does not change appreciably in either unit.

The metasomatized portions of both units are characterized by new crystallization of pink, ferriferous and/or hematitic orthoclase (Table 11). Total average alkali feldspar increases from 20 percent to 51 percent in the Mill Hill Slate, and from about 7 percent to 17 percent in the Blue Conglomerate. Both the microcline and the unclouded orthoclase of the hornfels remain in the metasomatized units. (Table 11).

Plagioclase feldspar content decreases in the metasomatized portions of both units (Table 11). Where an optical estimate of composition could be made (most grains are too small), there appears to be less of the more calcic plagioclase relative to sodic plagioclase.

Quartz content decreased in both units during metasomatism (Table 11), excluding the unaffected, large (greater than 1 inch diameter) quartz-breccia fragments in the Blue Conglomerate.

Mica (muscovite plus biotite) decreases in the metasomatized Mill Hill Slate, but increases in the metasomatized Blue Conglomerate. Almost all of the mica is too fine-grained for optical quantification and hence was estimated by X-ray diffractometer traces. The error limits may be greater than the apparent increase and decrease. Biotite and muscovite are present in both the contact metamorphic and the metasomatic facies (Table 3). Sharper X-ray reflections in the metasomatized parts of both units are characteristic and are believed to represent metasomatic recrystallization from illite (2M) or new mica formation. Where less silica was available for reaction with introduced potassium, metasomatic muscovite (or biotite) may have crystallized rather than orthoclase (or Fe-orthoclase) (see "Mineral Chemistry of Alkali Feldspar and Mica (?) Metasomatism").

It is interesting to note that the range of plagioclase and quartz percentages is wide in the hornfels units but narrow in the metasomatic units (Tables 3 and 7). Plagioclase plus quartz in the contact metamorphosed Blue Conglomerate and Mill Hill Slate averages 47 percent and 17 percent respectively (Table 11).

These approximate quantitative data together with the crystalloblastic texture of the metasomatic units clearly distinguish them from their contact metamorphic equivalents.

Chemical Characteristics of Metasomatism

The chemical changes believed to have occurred during metasomatism are compared for anhydrous weighted averages of contact metamorphic and metasomatic units in Table 10 and have been discussed under "Silica and Alkali Balance".

Major changes occurred in Al_2O_3, K_2O, total iron, and CaO. There also may have been a light loss in SiO_2, MgO, and Na_2O. Of these, the most striking change is an increase in K_2O (3.4 to 6.8 percent) corresponding to the increase in orthoclase feldspar. This is accompanied by an increase in Al_2O_3 (18.3 to 22.0 percent) and decreases in total iron and CaO. The latter agrees with the suggestion above that less calcic plagioclase is present (diopside and calcite do not change noticeably). Among the trace elements, flourine and boron also may have been introduced.

Because the element most conspicuously added to the hornfels is potassium and because orthoclase is the major crystalloblastic mineral replacing the hornfels minerals, the metasomatism subsequently will be referred to as potassium metasomatism; nevertheless, it should be remembered that some loss and gain of other constituents has occurred.

Interdependence with Thermal Metamorphism

At this point in the discussion of metamorphism and metasomatism, the possible or probable interdependence of metamorphic and metasomatic processes should be emphasized. Perhaps the most obvious connection is the formation of albite with consequent sodium enrichment in the hornfels country rocks. Adinoles have not been observed; however, chemical addition of sodium can be considered either as contact metamorphism because of a direct connection with thermal fronts emanating from the injected diabase sheet or as metasomatism resulting from magmatic addition into adjacent sediments.

In a diabase sheet to the east, Montgomery (1956, p. 180) believed there had been no metasomatic addition, although there is no quantitative data on sodium. In similarly negative fashion, Hotz (1953) does not note any addition of sodium into the country rock sediments. Soda metasomatism connected with an early stage of hydrothermal ore deposition should also be considered. For this process to have occurred, there would have had to have been considerable sodium mobility extending well beyond the ore zone on the order of a mile or more from Cornwall to Quentin (Plate 21). This seems unlikely. The simplest explanation might be a sodium redistribution within pre-existing sediments under a thermal gradient, if it were not for the large volume of average shale required (also see Table 10 and Figure 9):

(5.3) (Avg. Martinsburg shale) = 1 Avg. Hornfels, (3-4)
(2.8)(Avg. shale of Clarke) = 1 Avg. Hornfels, (3-5)

where the parenthetical numbers are the required volume multipliers to attain sodium balance. A sodium source associated either directly with *in situ* diabase or with, but earlier than, potassium metasomatism is preferred. Sufficient data are not available to determine whether or not sodium introduction is unique in the Cornwall ore district. (The data of Simpson, 1969, permit but do not prove, addition of sodium; see "Contact Metamorphism in the Triassic Basin.")

Interdependence of metamorphism and metasomatism also is illustrated by migration of silica, potassium, and perhaps aluminum (Figure 9) during thermal metamorphism, although largely within the hornfels system. Other evidence for interdependence is the overlap in the crystallization sequence of contact metamorphic minerals (such as calcic plagioclase, diopside, muscovite, and phlogopite) with younger and more sodic plagioclase, with the decrease in amount and/or iron content of ferriferous mica, with chlorite, and with K-feldspars (microline and orthoclase). Migration of silica already has been discussed. That most silica remained within the zone of metasomatism (essentially those areas proximal to the ore zones) seems probable in the light of the crystallization of secondary quartz in vugs associated with metasomatic ferriferous orthoclase (in spotted pink and white

Blue Conglomerate). A similar migration of alumina within the present zone of contact metamorphic facies into the present zone of metasomatism or into limestone may have occurred. Aluminum migration from Mill Hill Slate into overlying Blue Conglomerate might have occurred during metasomatism: the alteration of muscovite to microcline and the formation of calcic plagioclase from mica (or chlorite) would liberate some alumina to participate in metasomatism; indeed, a small increase in alumina in the metasomatized units is suggested by the bulk chemical analyses (Figure 9).

The migration of potassium may be considered as an additive during metasomatism, rather than as the result of thermal migration within the hornfels system. On the other hand, if average Martinsburg shale analyses from Lebanon County are an accurate measure of hornfels K_20 content previous to thermal metamorphism, then K_20 loss during this contact metamorphism (Figure 9) in part may be accounted for by gain within the metasomatized zone surrounding the eastern and western ore bodies. This hypothesis will be considered later in greater detail ("Genesis of Potassium Metasomatism").

Finally, it should be noted that, with the exception of silica, the direction of all chemical changes from average Lebanon County Martinsburg shale to hornfels is opposite to that from hornfels to metasomatized units. This in itself suggests genetic interdependence within the Blue Conglomerate and Mill Hill Slate system, an approach to chemical equilibrium, and essentially a contained, perhaps closed, system for most major components.

What remains unexplained is why any chemical migration should occur toward the very confined area of metasomatic alteration from the much more vast areal extent of the two hornfels facies. Such a migration through hornfels units, approximately parallel to diabase, would have had to occur over a distance on the order of a mile or more since some of the hornfels samples used to characterize metamorphic loss were collected at Quentin (Plate 21), 2.0 miles west of Cornwall. Detailed geochemical characteristics and observed paragenetic mineralogy provide some clues concerning the likelihood of such a migration.

Controls on Metasomatism

A delineation of the environment of metasomatism is more important to an understanding of the origin of both ore and diabase than is an understanding of thermal metamorphism because metasomatism may be genetically connected with ore, or diabase, or both. Part of the complexity in understanding Cornwall metasomatism is derived from the varied character of the hornfels units that are both a cap and a host rock for ore, and in part is derived from the complexity of a continually changing chemical front of unknown mobility rate, concentration, and, to some degree, of unknown composition. Temperature, pH, and perhaps oxidation influenced the formation of the present metasomatic mineral suites. Diffusion rates, permeability-porosity, chemical potential, concentration gradients, and leaching potentials of pre-existing minerals are a few of the more important variables considered essential to a complete understanding of the metasomatic process that operated in the Cornwall area.

Mineral Chemistry of Alkali Feldspar and Mica (?) Metasomatism

The chief characteristic of the metasomatized portions of Mill Hill Slate and Blue Conglomerate is the crystallization of pink, ferriferous orthoclase (either Fe-sanidine or Fe-microcline) replacing earlier hornfels minerals, in crystalloblastic growths, or in transecting veins. These textures in turn are replaced by magnetite ore, chlorite, actinolite, and zeolites. Some hematite, microcline, albite, fluorite, and tourmaline crystallized essentially contemporaneously.

The formation of Fe-orthoclase, more abundant in Blue Conglomerate than in Mill Hill Slate, is the result of a combination of factors. Although both units are dense, fine-grained hornfelsic rocks, the brecciated texture and extreme range in grain size of the Blue Conglomerate (Figure 1 and Plate 2) have rendered it more permeable to metasomatizing solutions. The Mill Hill Slate, on the other hand, acts as a more impermeable cap to both metasomatism and to later ore solutions. Thus, intergranular diffusion was more rapid through the Blue Conglomerate. Furthermore, desilication and probably solution-migration of calcite resulted in a vuggy texture throughout the Blue Conglomerate immediately above ore (eastern ore body). Both factors facilitated the concentration and preciptiation of Fe-orthoclase and resulted in the present crystalline cavities lined with pink orthoclase and later zeolites, magnetite, and actinolite. Visually, this Blue Conglomerate texture is distinctive at Cornwall but is not characteristic for Fe-orthoclase-rich, laminated, pink Mill Hill Slate where megascopic crystalloblastic growth is not evident and vugs are absent. The reaction rate with regard to alkali feldspar equilibrium in these now rather anhydrous units (Appendix 4-B) after contact metamorphism was probably sluggish as evidenced by the presence of both hematitic and ferriferous orthoclase and of hematite and microcline far from the diabase contact. The presence of aggregates of ferriferous potassic feldspar exhibiting characteristics of both Fe-sanidine and Fe-microcline as well as the presence of lesser amounts of non-ferriferous potassium feldspar, frequently within the same grain or grain aggregate, is further evidence of a sluggish transition or of a short annealing time. The optical and X-ray data for Fe-orthoclase (Tables 5 and 6) support a sluggish transition.

The initial potassium metasomatic alteration can be summed as follows (not to be construed as an actual reaction):

$K_2O + CO_2 +$ (Ca, Na) Plagioclase + Quartz + Mica ($\pm$ Chlorite) $\rightarrow$ Fe-Orthoclase + (Ca, Na Plagioclase – exsolved Na, Ca Plagioclase) + H_2O + Calcite

(3-6)

the silica and alumina balance depending on whether the altering unit was the Mill Hill Slate (lower in mica and alumina) or the Blue Conglomerate (higher in quartz but lower in total silica). The exsolving of a Ca-Na plagioclase into a more sodic end-member with the release of calcium (forming secondary calcite rather than the higher temperature, more aluminium-rich, calcic plagioclase end-member) was apparently a subsidiary reaction. The formation of orthoclase from quartz and muscovite (Goldschmidt, 1922, p. 118) should be considered as a possible reaction with the addition of ferric iron to yield Fe-orthoclase:

$$H_4K_2Al_6Si_8O_{24} + 2K_2O + 12SiO_2 + xFe_2O_3 \rightarrow 3K_2(Al, Fe_{2x})_2Si_6O_{16} + H_2O + xAl_2O_3 \qquad (3\text{-}7)$$

where x is very small and Al_2O_3 is not present as a separate phase. In this "reaction," the amount of Al^3 replaced by Fe^3 may be taken up in the crystallization of a more aluminous chlorite, an amphibole, or cordierite (reported by Hickok, 1933). This equation could be interpreted as the fixation of potassium feldspar by excess quartz or as the fixation of alkali by excess alumina as noted by Goldschmidt (1922) and Turner and Verhoogen (1960) for alkali metasomatism.

However, the evidence for reaction (3-7) is questionable and the actual process probably was more complex. The scarcity of free quartz in the present metasomatized Mill Hill Slate and Blue Conglomerate suggests that quartz may have "fixed" potassium and ferric iron in orthoclase, the reaction proceeding until nearly all the fine-grained silica was consumed. From Table 11, it can be seen that quartz content decreases markedly from hornfels to metasomatized hornfels. However, there is very little evidence that mica was involved; only a sharpening of basal X-ray reflections that could have resulted from recrystallization. The quantity of mica does not appear to have decreased; in fact, it is greater in metasomatized Blue Conglomerate than in hornfelsed Blue Conglomerate (Table 11). Total plagioclase, on the other hand, does decrease (Table 11). Therefore, equation (3-6) may be more representative; that is, the replacement of Na-Ca feldspar by K-feldspar. Unfortunately, the grain size is too fine to observe definitive replacement textures.

Another way to determine potassium feldspar fixation is to calculate the total rock alumina-to-alkali ratio in both hornfels and metasomatized hornfels and to compare these ratios with that of the introduced feldspar. If it can be assumed that all minerals in the rocks under consideration were subject to alteration processes in the new environment, then this bulk rock chemical ratio will yield a good measure of the potential for metasomatic alkali feldspathization. Even if some aluminous and alkali minerals remained stable, as long as their volume was not large, this ratio will preserve some usefulness in determining the potential for alkali feldspathization, or, alternatively, for determining the extent to which this metasomatism proceeded to completion. Here such a ratio is termed the alkali feldspar fixation potential for pelitic rocks. This potential becomes zero as the ratio approaches 1.65 for albite and 1.09 for orthoclase, the ratios in their normative compositions (Table 12).

The Blue Conglomerate hornfels, the average shale of Clarke (1924), and the average of 8 Martinsburg Formation shale samples from Lebanon County (O'Neill and others, 1965) all illustrate a high feldspathization potential (Table 12). The analyzed sample of metasomatized Blue Conglomerate shows that it is not saturated with respect to alkali but that the crystallization of such a feldspar was limited by some other factor. In part this limitation results from the increased volume of muscovite in the metasomatized Blue Conglomerate over that in the hornfels (Table 11). The normative Al_2O_3/K_2O ratio for muscovite is 2.09, and thus, it and orthoclase are in competition for available K_2O, Al_2O_3 and SiO_2. In this case, *availability* of SiO_2 for reaction would have been a limiting factor because orthoclase requires more SiO_2 than muscovite. In the Blue Conglomerate, the matrix of which contains little or no quartz, muscovite may have been able to crystallize locally after the silica supply necessary for orthoclase had been exhausted (providing that sufficient alumina was available from such sources as kaolinite, illite, chlorite, or the replacement of Al^3 by Fe^3 in orthoclase). A decrease in the supply of K_2O also must have been a limiting factor, particularly away from the central portion of the eastern ore-zone hornfels where hematitic and Fe-orthoclase feldspar gradually decrease and the unit becomes a typical, unmetasomatized hornfels.

Table 12. *Comparative alumina/alkali ratios: alkali feldspar fixation potential*

Unit or Feldspar	Total $Al_2O_3/K_2O + Na_2O$ (by wgt.)
Normal Blue Conglomerate hornfels	3.64
Avg. 8 Martinsburg shales, Lebanon Co. (O'Neill and others, 1965)	3.42
Avg. shale (Clarke, 1924)	3.37
Metasomatized Blue Conglomerate	2.44
Normal Mill Hill Slate hornfels	2.01
Theoretical albite	1.65
Metasomatized Mill Hill Slate	1.51
Theoretical orthoclase	1.09

The feldspathization ratio for Mill Hill Slate hornfels (thermal metamorphism) illustrates its low potential for additional alkali feldspar crystallization by any later metasomatism and an even lower potential for albitization as shown by the composition of theoretical albite (Table 12). This low fixation potential is largely a consequence of the high microcline content of Mill Hill Slate hornfels previous to metasomatism. Metasomatized Mill Hill Slate is essentially saturated with respect to alkali feldspar and thus, even where Mill Hill Slate is closer to diabase or to the ore zone than Blue Conglomerate, extensive replacement did not occur; that is, metasomatizing solutions would not yield further alkali feldspathization until encountering Blue Conglomerate. The change between the metamorphic and metasomatic ratios in Blue Conglomerate and Mill Hill Slate illustrates the greater potential of hornfelsed Blue Conglomerate for feldspathization — approximately twice that of the Mill Hill Slate. The rather high ratio in metasomatized Blue Conglomerate indicates either lack of potassium saturation or insufficient reaction time and perhaps the presence of stable alkali-aluminous mineral relics.

Subsidiary Metasomatic Effects

Other chemical and mineralogical changes are of considerably lesser magnitude. Fluorine-boron metasomatism is evident only near diabase, either in inclusions within the top of the sheet or near the base of altered Mill Hill Slate and Blue Conglomerate above the eastern ore body. Goldschmidt (1922, p. 114) notes that fluorine- and boron-bearing minerals are fixed by excess alumina, yielding tourmaline (present here) and topaz (not detected), and that chlorine and fluorine are fixed by feldspars often yielding scapolite (not detected). Excess aluminum would be expected only within the Blue Conglomerate (Figure 9 and Table 10) and then only during initial potassium metasomatism before significant incorporation in orthoclase and/or mica. The concentration of these mobile components early in the metasomatic mineral sequence (with Fe-orthoclase), near the base of the metasomatized zone (near the top of the diabase sheet), may indicate a genetic connection (the chemically analyzed metasomatized Blue Conglomerate (Table 4) is not from this lower zone). Chemical analyses (Appendix 4) illustrate a high fluorine content in both hornfelsic and metasomatic Mill Hill Slate comparable to amounts in diabase at Cornwall.

Trace elements that show a significant increase from Mill Hill Slate hornfels to the metasomatic facies are zinc, copper, cobalt, and barium (Appendix 4). With the exception of barium, these also are concentrated in the ore zone. However, it should be noted that this hornfels unit caps the ore zone and is only slightly replaced by ore. Sodium, iron, and calcium decrease appreciably in metasomatic rocks, although the varied content of secondary calcite in these units may account for some or all of the calcium differences. Sodium has migrated or been lost during the alteration of hornfels plagioclase with the subsequent release of both calcium and sodium (equation 3-6). Sodium was in competition with potassium for the formation of alumino-silicates and did not attain sufficient concentration (or was not in environmental equilibrium) to crystallize significant amounts of albite-oligoclase. Some, however, was apparently taken up in the potassium feldspar structure (Tables 3 and 7) rather than lost to the system.

Within and beyond the zone of metasomatism, calcium and sodium zeolites formed after the main stage of orthoclase crystallization. The water released during metamorphism and metasomatism (see equations 3-6 and 3-7) also may have contributed to zeolite formation; however, most zeolitization postdates both metasomatism and ore introduction. Prehnite formed principally in Mill Hill Slate after the crystallization of earlier silicates (e.g., tremolite, diopside, muscovite, feldspars) when much of the free silica had been consumed. In the more quartz-rich environment of the Blue Conglomerate quartz breccia, quartz was still available to form more silica-rich zeolites, notably calcium-rich apophyllite, the four calcium-sodium zeolites, heulandite, stilbite, chabazite, thomsonite, and the two sodium-bearing zeolites, analcime and natrolite. A generalized alteration equation for this mineralization can be summarized as:

$$x\mathrm{CaO} + y\mathrm{Na_2O} + \mathrm{H_2O} \pm \text{quartz} \pm \text{mica} \pm \text{calcite} \rightarrow \text{Ca-Na zeolites} + \text{paragonite} \pm \mathrm{CO_2} \qquad (3\text{-}8)$$

The relative abundance of calcium and sodium in zeolites was controlled, in part, by the changing composition of the advancing metasomatic front in which the replacement of early, more calcic plagioclase released calcium and some sodium. Both elements were in competition for the available silica during decreasing concentrations of potassium in the areas of metasomatism (for outward moving metasomatic alteration) forming potassic feldspar. The lower temperature zeolites also suggest that temperature zoning was a factor in controlling the zeolite-feldspar competition. For example, a high temperature and high-calcium environment will yield calcic plagiolcase; any later, lower temperature environment will yield only calcium-poor zeolites. Because of primary and later secondary zeolitization, distinct zones of these minerals do not occur at Cornwall. The relative mobilities of potassium, sodium, and calcium dominated the competition of calcium for $\mathrm{CO_2}$, except in limestone, and thus the more mobile sodium (in analcime, natrolite, and stilbite) was dominant during later zeolite formation (they are the most prevalent zeolites). The crystallization of datolite is restricted by the availability of boron near the top of the diabase and by calcium near limestone (limestone replaced by magnetite also contains a notable amount of boron (Table 17)).

Another important reaction subsidiary to the major direction of metasomatism (addition of potassium) involves a decrease in total iron from hornfels to metasomatic units (Tables 10) and a slight increase in the $\mathrm{Fe_2O_3/FeO}$ ratio. Using weighted averages for the hornfels units (Table 10), this ratio changes as follows:

	Fe_2O_3/FeO
Avg. of 8 Martinsburg shales	5.10
Avg. hornfels	0.82
Avg. metasomatized rock	1.07

The metasomatic alteration thus may represent a slightly more oxidized environment and a higher potential for the formation of hematite during metasomatism than existed previously during metamorphic hornfelsing (excluding rock boundary discontinuities). Hematite associated with Fe-orthoclase has been noted previously. However, hematite is particularly noticeable in the Blue Conglomerate as well as at its formational contacts (also see Figure 4). Although occurring at Mill Hill Slate lithologic contacts, hematite is not usually present within the unit. Both units are considerably depleted in total iron. Using the Blue Conglomerate as an example, the following unbalanced reaction summarizes this alteration:

Blue Conglomerate hornfels + $K_2O \rightarrow$ metasomatized Blue Conglomerate + approx. 2% Fe_2O_3. (3-9)

This then is a source for hematite formed above the ore body. Hematite is almost universally absent at contacts of lime-rich lithologies, emphasizing the importance of an iron source from Mill Hill Slate and Blue Conglomerate hornfels during metasomatism. This hematite has, in turn, been replaced by ore magnetite, representing a local change in the activity of oxygen within the ore zones. That the Fe^{3}/Fe^{2} ratio did not change more radically during metasomatism is the result of buffering action established by the previously formed magnetite "dust" and hematite during hornfels metamorphism. This illustrates the common observation that, once established, a mineral assemblage subjected to an alteration fluid tends to remain at the same oxidation state except under prolonged or drastic environmental change. H_2O, which is not in excess in these units, is a prime factor in promoting such an oxidation change.

In summation of the chemical changes produced by metasomatism, it is interesting to note that in the Mill Hill Slate, and perhaps in the Blue Conglomerate, there has been a reduction of the number of major associated mineral components: in Mill Hill Slate from 5-8 to 3, and in the Blue Conglomerate from 3-6 to 3-4. This reduction is in agreement with the usual tendency of metasomatic reactions to proceed toward monomineralic zonation. Notable also is the greater reduction in the number of minerals (component phases) in that part of the Mill Hill Slate that was saturated with alkali feldspar during potassium introduction. This reduction in mineral phases is most pronounced above the eastern ore zone and to a lesser extent westward. Had alumina and silica been important components of addition to the hornfels, additional reaction would have occurred; actually, mobilization-migration and introduction resulted in an excess of potassium, sodium, and calcium away from ore areas. Thus, they were not fixed by excess silica and alumina; the excess was of alkalies instead. That there was insufficient potassium available locally for complete equilibrium facies transformation above and east-west from the ore zone is evident from the mineralogy, the aluminum-alkali ratio, and probably the number of component phases remaining in the Blue Conglomerate. An infinite reservoir did not exist, as might have been the case if the source of potassium were an extensive mobilization resulting solely from thermal metamorphism of the quantitively large Mill Hill Slate lithology.

Temperature and pH of Metasomatism

Temperatures of metasomatism are as elusive to determine for these metasomatized units as they are for thermal metamorphism, but, as in that discussion, there are good indicators of the general temperature range attained. The same equations relating the conversion of mica into potassic feldspar (equations 3-1 and 3-2) are applicable to metasomatism and yield a minimum temperature of about 600° C. However, at Cornwall, the potassium feldspar is not microcline but hematitic or ferriferous orthoclase that, especially in the Mill Hill Slate, has the optical characteristics both of Fe-sanidine and Fe-microcline. Fe-orthoclase probably is a metastable form and may represent an incomplete transition from the higher to the lower temperature state, although the pre-existence of a completely disordered form is not required. This means that the maximum temperature attained was within the stability field of Fe-sanidine, however briefly this temperature may have been maintained. The transition temperature for sanidine to microcline is about 525°C.; however, the experimental data of Wones and Appleman (1963a, p. 134) indicate that the Fe-sanidine to Fe-microcline transition temperature is 698° C. at 2000 bars for 3330 hours, a rather surprising increase in transition temperature as a result of the incorporation of Fe^3 into the system. Apparently Fe^3 lattice substitution inhibits the initiation of this phase transformation. Similar temperatures are given (op. cit; p. 134) for hematite mixes and for glass-magnetite mixes at 1000 and 2000 bars for the two ferriferous polymorphs. A lower temperature for the formation of Fe-sanidine was obtained in the reaction,

$$\text{Ferriannite} \rightleftharpoons \text{Fe-sanidine} + \text{magnetite} + \text{hematite} \qquad (3\text{-}10)$$

that went to the right above 470°. Since biotite is present in both the Mill Hill Slate and the Blue Conglomerate and probably took part in the formation of Fe-orthoclase, some reduction in temperature below 698° C. is probable; that is, a small component of the ferriannite end-member is present to lower the transformation temperature. However, as Wones (1963, p. 595) states, the amount of the ferriannite end-member in most natural biotites is small because of the presence of Al_2O_3. Thus, the transition at Cornwall probably initiated in the 600°-650°C. range but may have extended to considerably lower temperatures depending upon the sluggishness of the sanidine to microcline inversion rate. The predominance of Fe-orthoclase here and at the Madagascar occurence (Coombs, 1954) leads to such a conclusion, unless there is a minimum in the microcline-sanidine loop in the system $KAlSi_3O_8$-$KFeSi_3O_8$ (Wones and Appleman, 1963a, p. 135). A third temperature estimate can be obtained by comparison with that of the hornblende-hornfels facies of metamorphism that generally is considered to be similar to that of alkali metasomatism (Turner and Verhoogen, 1960, p. 514, Figure 71 and p. 571) and that also lies within the range, at 550°-700°C. Taken together, these data suggest that the maximum temperature attained for metasomatism was at least 600°C. and quite possibly higher.

At these high temperatures, and perhaps moderate pressures, very little can be determined about the pH of the metasomatizing fluids. As temperature increases, the pH of neutrality decreases slightly so that the fixation of halogens becomes difficult. However, pH may not be an important factor at elevated temperatures (Helgeson, 1964, p. 106). Nevertheless, the presence of some of the boron- and fluorine-bearing minerals near the diabase suggest that acid conditions may have existed locally. On the other hand, the bulk of the alteration is an alkali metasomatism that culminated in a late low temperature crystallization stage represented by chlorite and zeolites. Thus pH (at the site of crystallization) may have increased as temperature decreased. The pH during transport is unknown.

Genesis of Potassium Metasomatism

The Major Genetic Possibilities

A mechanism for potassium metasomatism can be postulated from the foregoing data and theoretical considerations. Each of three possible sources will be considered: 1) the release of potassium from contact metamorphism of Martinsburg shale, 2) the release of potassium from granophyric residue of *in situ* differentiated diabase, and 3) hydrothermal introduction of potassium immediately preceeding, and genetically related to, magnetite ore deposition.

Metasomatism From Potassium Released During Contact Metamorphism

Considerable addition of potassium to the hornfels units (metasomatism) contrasts with a loss of potassium during the formation of the contact metamorphic hornfels from the pre-metamorphic sediments. As previously discussed, this antithetic relationship assumes a normal initial K_2O content for Mill Hill Slate comparable to that of average Martinsburg shale from Lebanon County (O'Neill and others, 1965) or from the average shale of Clarke (1924). Furthermore, the direction of change in many other chemical elements also is opposite for the two processes (Figure 9). This general antithetic relationship requires consideration as a possible source for potassium metasomatism. A contact metamorphic source would imply the existence of an essentially closed system with respect to potassium and the crystallization of potassium-bearing minerals would be regarded as a product of differential chemical migration resulting from thermally induced chemical gradients. Another observation in support of this hypothesis is an apparently continuous loss of water from earlier thermal metamorphism through later metasomatism as if driven by a continuous thermal energy front. The crystallization period of minerals that are considered to be wholly contact metamorphic in origin overlaps the time of earliest crystallization of potassic feldspar. Thus, such a process also could be interpreted as genetically continuous. The temperatures previously derived for both types of mineralization lie within approximately the same maximum temperature range; i.e. they do not represent drastically different temperature environments but are instead, consistent with temperatures that have been estimated for rocks in contact with the cooling Cornwall diabase sheet. And finally, the previous discussion of sodium addition during metamorphism may be used as negative support. If sodium were derived by subsequent escape from late-stage diabase differentiates, then its widespread occurrence throughout the hornfels facies should be paralleled by the addition of potassium if it also emanated from a diabase differentiate. Since this parallel does not exist; i.e., the potassium distribution is spatially localized and sodium addition is not localized (with respect to the distribution of hornfels lithologies), the potassium source probably differed from that of sodium. Therefore, K_2O might have been derived from the sediments.

The bulk equations for K_2O balance, if the source were originally a facies of Lebanon County Martinsburg shale, would have been approximately:

$$\begin{gathered}\%K_2O \text{ Metamorphic Loss} = \%K_2O \text{ Metasomatic Gain} \\ (5.3) - (3.4) = (6.8) - (5.3) \\ 1.9\% \neq 1.5\%\end{gathered} \tag{3-11}$$

where 5.3 percent is the average K_2O content in Lebanon County Martinsburg shale, and the other K_2O percentages are the weighted hornfels and metasomatic anhydrous averages (Table 10). If hydrous analyses are used, the balance swings into equality (after rounding off percentages to the nearest tenth):

$$\begin{gathered}(5.0) - (3.3) = (6.7) - (5.0) \\ 1.7\% = 1.7\%\end{gathered} \tag{3-12}$$

The difference between the two equations, 3-11, and 3-12, is a consequence of H_2O decrease from average Martinsburg shale to hornfels to metasomatic units (Appendix 4-B and Lapham, 1968, Table 6). If the two processes (migration of K_2O and H_2O) are separate, or nearly so, equation (3-11) more nearly applies; if they are related, equation (3-12) must be considered. Both equations assume a volume-for-volume replacement. They also assume an original shale that had considerably more K_2O than the average shale of Clarke (1924, p. 30) (Table 10). Thus, from an empirical viewpoint the potassium of metasomatic potassium feldspar might have originated during metamorphism of Martinsburg shale. Such potassium metasomatism would be even more likely if associated with some H_2O migration at this stage.

However, the validity of either of these reactions involves several unlikely assumptions. First, the original shale would have to be at least as high in K_2O as this average Lebanon County Martinsburg shale, which is itself unusually high in K_2O. In actual fact, it is unlikely that the Lebanon County Martinsburg shale average can be used accurately for such geochemical comparisons. A major thrust plane below the hornfels units (Plate 21 and see also Figure 16 and discussions in Part 2) indicates that they are allochthonous from the south (such as the Cocalico Formation) and are not part of the Martinsburg lithology to the north from which the average was calculated. Thus, any K_2O percentages from this formation to the north may be completely irrelevant for use in K_2O balance equations. As shown in O'Neill and others (1965), and Hoover and others (1972), K_2O differs notably in the Martinsburg Formation throughout Pennsylvania. Secondly there would have to be no significant loss of K_2O from the hornfels system in the area of the ore bodies. This excludes any introduction into, or fixation in the host limestone. Because the mobility of potassium in a water-rich fluid once the potassium has been released from a mineral (mica) lattice is rather high, such spatial confinement of potassium without regard to redistribution along thermal gradients seems unlikely. The movement of H_2O out of the total hornfels system could have provided a potassium migration medium, but all, or nearly all, of the potassium would have been fixed by silica-alumina within the ore zone-hornfels system (Table 8), while H_2O was lost to the system (except for minor, local zeolitization). The above balance also assumes that the volume of Mill Hill Slate in the potassium-rich portions does not exceed half that of the metasomatized Blue Conglomerate nor twice that of the Blue Conglomerate in the contact thermal facies (because of the weighted averages used in equations (3-11) and (3-12). If the volume of Mill Hill Slate in the total hornfels system were greater, significant addition of potassium would be required beyond that available from contact metamorphism. At least in the contact metamorphic facies, a greater ratio of Mill Hill Slate to Blue Conglomerate is probable (Plates 21 and 23).

In addition to these necessary assumptions, there are several cogent theoretical reasons why such a migration of potassium during contact metamorphism is unlikely. The potassium-rich mineralization is concentrated in the Mill Hill Slate and Blue Conglomerate only immediately adjacent to the ore zone. This means that potassium would have had to migrate laterally through a large volume of Mill Hill Slate toward this zone. There is no good reason why thermal metamorphism would cause lateral migration along what would have been essentially an isothermal direction.

In fact, the greatest concentration of potassium feldspar is at the base of the altered hornfels units, above limestone, whereas there is essentially no potassium enrichment where Mill Hill Slate is in direct contact with diabase to the west. At other locations, potassium would have had to migrate into a higher temperature environment. Together, these observations do not exhibit the characteristics of a contact thermal gradient. Furthermore, the K_2O content in unmetamorphosed Martinsburg shale would already have been in a silica- and alumina-rich environment such that the formation of potassium feldspar should have occurred *in situ* without potassium migration (see Table 12). Therefore, because the environment of the Martinsburg shale had a high feldspar fixation potential before metamorphism (i.e., was undersaturated with respect to potassium feldspar), no chemical potential existed for extensive leaching and re-precipitation of potassium-rich minerals elsewhere. Furthermore, not only is the potassium migration direction improbable, but it would have had to migrate from Mill Hill Slate at least as far away as Quentin, and below diabase, to the very localized area of potassium metasomatism at Cornwall above diabase. This is very nearly a structural impossibility.

The paragenetic sequence, although evidencing overlapping crystallization, shows that the formation of potassium feldspar followed that of the contact minerals as probably would not everywhere have been the case if the two types of crystallization were the consequence of a single process. The metastable form of the feldspar is considered to be evidence of rather high temperatures and appears to be unique to the eastern Cornwall ore zone above diabase. Its occurrence does not agree well with a continuous metamorphic-metasomatic process where ferriferous potassium feldspar should be homogeneously distributed without regard to the distribution of ore minerals.

The migration of other elements during thermal metamorphism, which might support the single process theory, is more apparent than real, as previously discussed. Potassium and perhaps sodium are the only elements added to the hornfels units in any significant amount. Other changes represent a loss to the system or a change in oxidation state. The opposite directions of potassium and sodium migration during metasomatic feldspar formation cannot be accounted for by any single process because such a process should have similarly fixed both ions, particularly in the feldspar lattice and should have resulted in an Na_2O concentration from original Martinsburg shale into the K_2O-rich zone, but it did not.

The adduced temperatures of these alterations are also inconsistent with a single process. Both contact-metamorphic and metasomatic minerals attained the same range of maximum temperature, but the metasomatic potassium feldspar crystallized after the maximum temperature of thermal metamorphism at a time when a lower contact-temperature environment existed. Finally, this single-process hypothesis does not explain the fluorine and boron content of minerals spatially associated with potassium introduction (even though limestone and illite may have contributed boron) to ore stage mineralization (see Part 4, "Chemistry of the eastern Ore Zone"). The spatial relationship with the ore and the chemical and mineralogical similarities with the granophyre also are unexplained. Thus, although some migration of potassium probably occurred on a very local scale during contact metamorphism, it was largely either lost to the hornfels units or yielded *in situ* microcline development (Tables 3 and 7) and was not responsible for the younger, spatially unique, Fe-orthoclase metasomatism.

Metasomatism From Granophyre During Diabase Differentiation

The metasomatic introduction of Na_2O, CaO, and Al_2O_3 into country rocks adjacent to rocks of basaltic composition (Simpson, 1969 and summary by Frankel, 1967, p. 91), the formation of adinoles, and spilitization all attest to the activity of certain chemical components associated with basaltic rocks. Osborne (1929) and Hotz (1953) have attempted to explain the presence of magnetite-diabase associations on the basis of late magma-residua emanations rich in alkalies. Introduction of Na_20 at Cornwall is believed to have occurred as a result of diabase magma intrusion. Although K_20 introduction from diabase residua has not previously been specified (although it apparently has been noted near Palisades diabase by Walker, 1969, p. 29), in view of the above, it deserves careful consideration as the source for potassium metasomatism.

The most obvious reason for this hypothesis at Cornwall is the presence of the unusual ferriferous (and hematitic) orthoclase in granophyre and in altered Mill Hill Slate and Blue Conglomerate above the eastern ore body. Observations of its occurrence appear to show more Fe-orthoclase in Blue Conglomerate where it is the ore hanging wall than where Mill Hill Slate forms the hanging wall. Another approach to a possible granophyre-metasomatism relationship arises from the close chemical similarity, already mentioned, between metasomatic and granophyric rock types. Their similar bulk rock chemistry and mineral content could be an indication of a common origin. The following rock alteration equation is an approximate representation of this hypothesis:

$$\text{Martinsburg shale} + \text{``Granophyre''} = \text{Hornfels} + \text{Metasomatized Hornfels} + H_20 \pm SiO_2 \qquad (3\text{-}13)$$

Although the introduction of granophyre, *in toto*, into shale (through intervening limestone?) could not have been an actual process, the observed chemical changes from shale to hornfels to metasomatized hornfels form a chemical series that approaches granophyre in composition and therefore a genetic connection is possible. This approach is illustrated by several types of differentiation diagrams (Figures 11-13) that compare the units at Cornwall

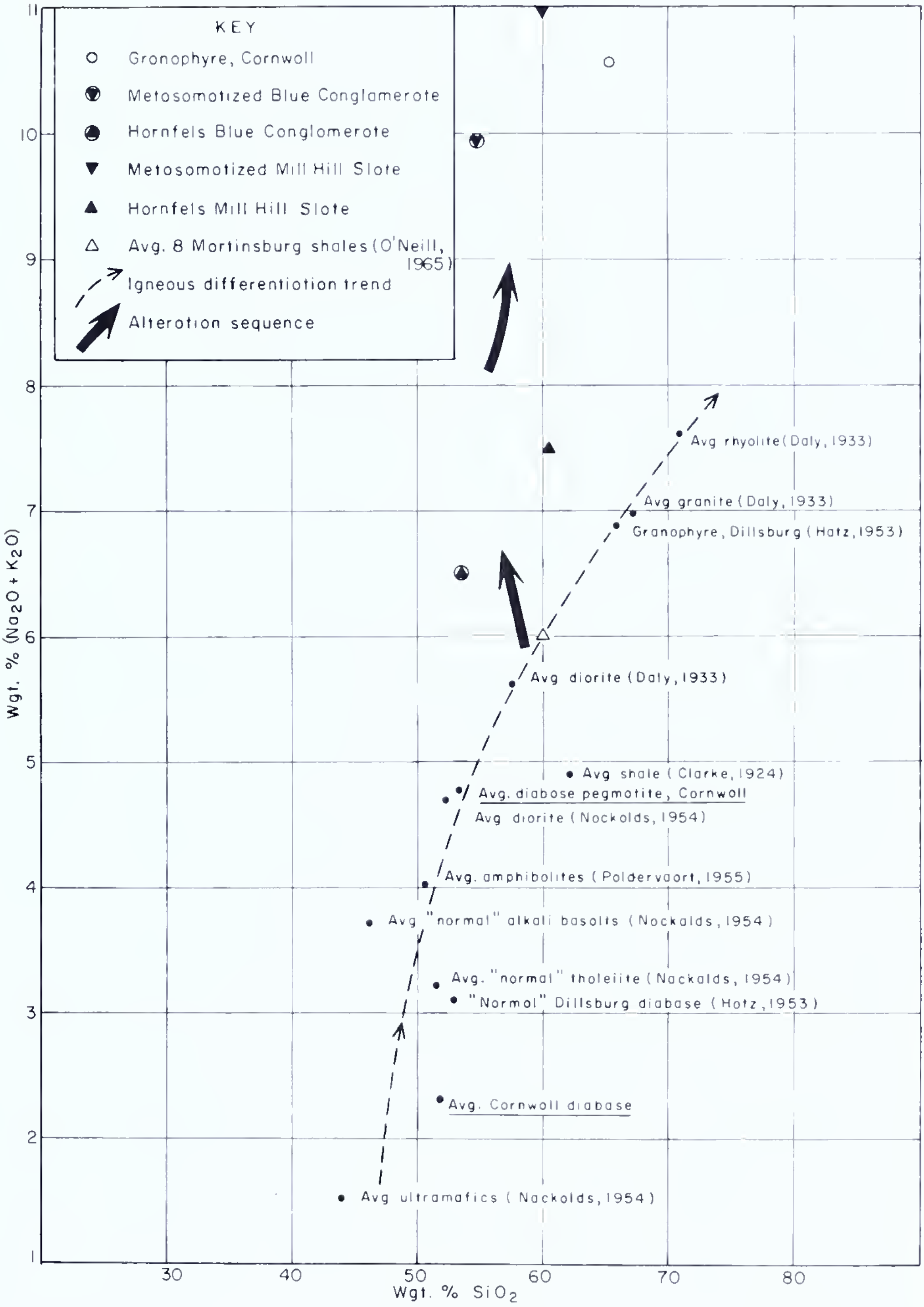

Figure 11. Weight percent $(K_2O + Na_2O)$ versus SiO_2 variation in granitic to ultramafic rocks compared with Cornwall rock types and possible Cornwall alteration trend (large arrows).

(anhydrous) with the nearby Dillsburg granophyre (Hotz, 1953) and with a series of average igneous rock compositions ranging from ultramafic to granitic. Three observations are particularly interesting: 1) in each diagram the compositional rock alteration sequence including Cornwall granophyre, is consistently away from the normal differentiation trend, 2) in each diagram, the analyzed samples form a crudely linear sequence from average shale to Cornwall hornfels to Cornwall metasomatic rocks and Cornwall granophyre, and 3) the direction of change from contact metamorphic to metasomatized hornfels, although crudely linear toward Cornwall granophyre as a possible "end-point" composition, is not sequentially linear with respect to Dillsburg granophyre composition. The Dillsburg granophyre composition lies along a normal differentiation trend, and there is no reported potassium metasomatism associated with the Dillsburg magnetite ore district. This latter point could be used as evidence that potassium metasomatism does not depend on the presence of granophyre or that only granophyres of a special composition are associated with potassium metasomatism. The two granophyres are of considerably different mineral and chemical composition. The Cornwall differentiate is much richer in total K_20 and potassic feldspar (see Part 5, "Geochemistry"). It could be argued either that the granophyre richest in K_20 (Cornwall) is least likely to have been depleted in any K_20 that might lead to potassium introduction into the hornfels or that K_20 enrichment in granophyre did not occur at Dillsburg and hence no potassium metasomatism occurred. For potassium metasomatism to have occurred by this process, the present difference in the K_20/Na_20 ratio at Cornwall and at Dillsburg (see Figures 48, 52, 54) would be enhanced, and the contrast in original composition of the two differentiates would be further exaggerated. On the other hand, the presence of ore at both localities, but apparently only potassium metasomatism at Cornwall (Hotz, 1950 and 1953, did not specifically examine host or hornfels units for addition of K_20), could be presumed to support a separation in mode of origin of the ore from the K_20 introduction process.

Figures 11, 12 and 13 illustrate changes in alkali vs. silica, alkali/alumina vs. silica, and alumina-calcium oxide vs. alkali content. Each shows a rather consistent differentiation trend for the whole range of igneous rock average compositions (anhydrous recalculation). The granophyric differentiate at Cornwall does not lie along these trends. This variance is discussed elsewhere as a possible function of alkali-silica-alumina balance during diabase differentiation (see Part 5, "Alkali Differentiation Trends"). In order to calculate original magma composition for these oxides such that their total can be compared with that in the other diabase sheets within this province (and with diabase plutons elsewhere), it is necessary to include not only the granophyre composition but also any elements introduced into the hornfels from the magma (see Part 5, "Geochemistry"). Such a summation of introduced ore-zone and diabase constituents is less important for the otherwise similar Dillsburg occurrence where granophyre is of a larger areal extent and where there is an apparent lack of potassium metasomatism outside the confines of the sheet.

These two occurrences thus could represent excellent examples of Lodochnikow's (1936) principle of polarity, which states that those elements in which an igenous rock is deficient are in abundance in the contact rocks (e.g., Cornwall where diabase may be K_2O-deficient) or, if not found beyond the contact, are in abundance within the igneous rock (e.g., Dillsburg diabase). However, this principle does not necessarily specify the mode of this depletion, whether from direct expulsion from the main pluton or from the source magma. From the available geochemical evidence, it is not possible definitely to ascertain the precise mode of potassium introduction at

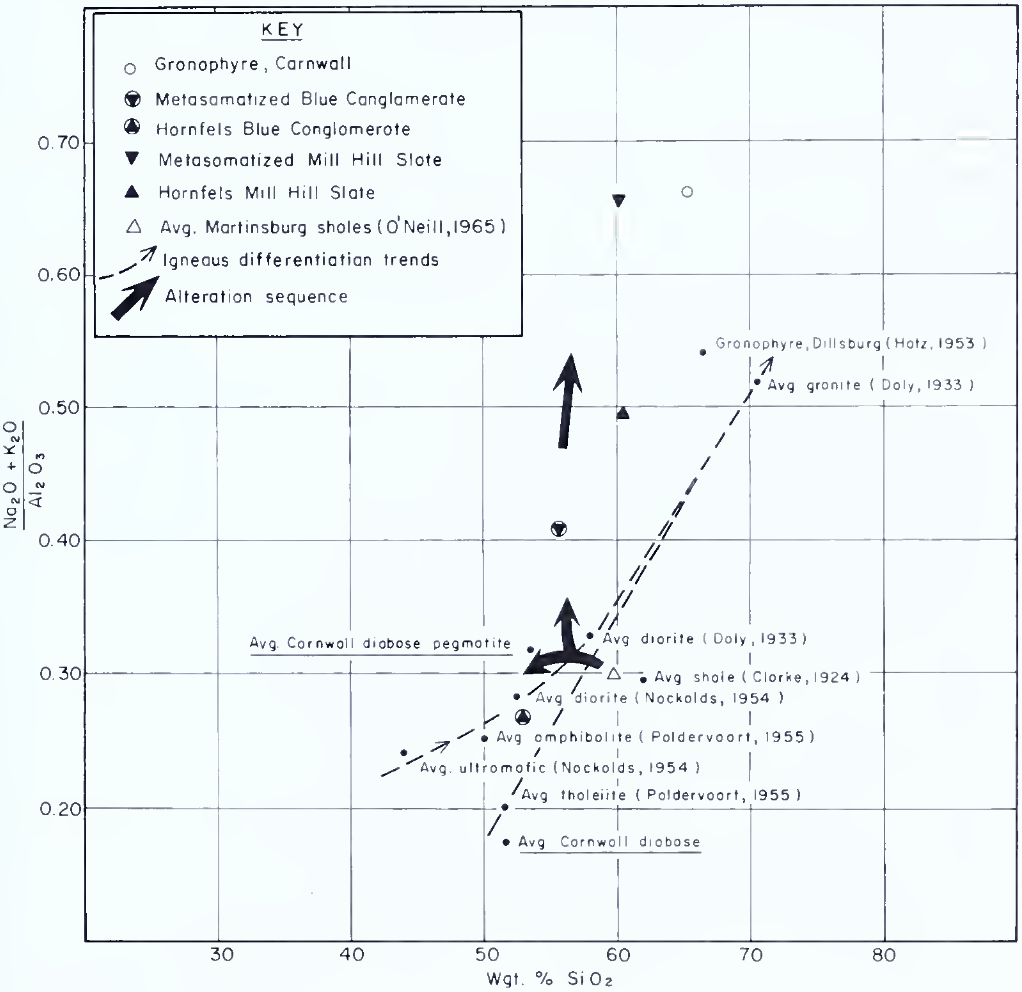

Figure 12. Weight percent (K_2O + Na_2O)/Al_2O_3 versus SiO_2 variation in granitic to ultramafic rocks compared with Cornwall rock types and possible Cornwall alteration trend (large arrows). Note divergence of basalt and ultramafic trends.

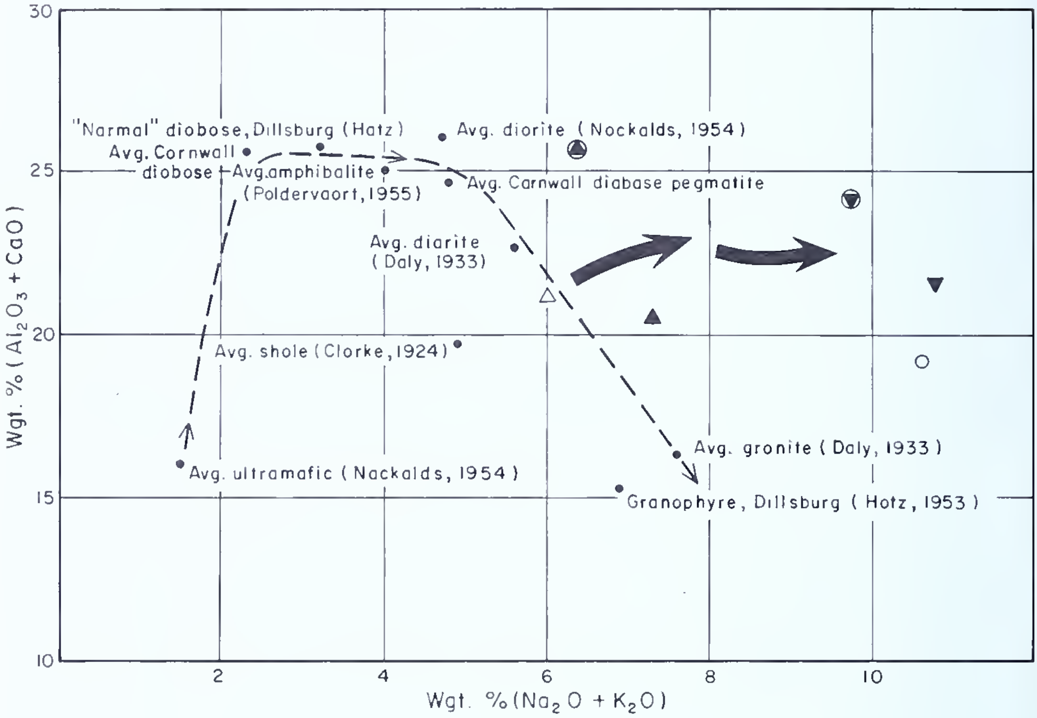

Figure 13. Weight percent (Al_2O_3 + CaO) versus (Na_2O + K_2O) variation for granitic to ultramafic rocks compared with Cornwall rock types and possible alteration trend (large arrows); for key, see Figures 11 and 12.

Cornwall. Nevertheless, there are several reasons for suspecting that the Cornwall granophyre may not have been the source for potassium metasomatism:

1. Neither at Cornwall nor elsewhere in the Triassic diabase province has there been any documentation of any spatial association between granophyre and potassium introduction. For example, at Dillsburg where granophyre is common, no associated metasomatism has been observed.

2. The volume of granophyre at Cornwall is quite small, and there is no textural evidence (see Part 5, "Petrology") that any significant volume of fluid residuum has escaped what was an already largely solidified diabase sheet. The Cornwall differentiates are not depleted in K_2O.

3. Mapping of the upper surface of the diabase over the western ore body has not revealed any penetration of the chilled margin by granophyre. A "granophyre" is reported to be in direct contact with Blue Conglomerate at one location in the southeastern part of the eastern ore body (Samuel Sims, written communication). At the same location, pink, orthoclase-bearing veins ("aplite") occur in Blue Conglomerate ("Metasomatic Vein", Figure 23). A granophyre-like sample collected by C. Gray from this area was studied

petrographically. In spite of a holocrystalline appearance, the sample is metasomatized Blue Conglomerate rather than granophyre. Although identification of granophyre is often difficult, and although much of the diabase surface in the eastern mine could not be observed (the critical area for potassium metasomatism), there is no evidence here of penetration of the diabase chilled margin by granophyric veins.

4. There is no evidence of sodic plagioclase introduction in the area of potassium introduction, even though it also is a major constituent of the granophyre. Sodium could, perhaps, have been lost to the system, but such a K-Na partition by a single metasomatizing fluid seems unlikely. The fixation potential for feldspar indicates that sodium-rich feldspar should have crystallized together with potassic feldspar in the hornfels units.

Other reasons that chiefly favor a mode of K_2O origin associated with hydrothermal ore are discussed subsequently.

Metasomatism From Hydrothermal Ore Solutions

The third consideration for the origin of potassium introduction is that the same solutions responsible for ore formation were also potassium-rich. The brief discussion here will be centered on the hypothesis of both potassium and iron introduction from a common magmatic source other than from the *in situ* diabase. The possibility that both ore and potassium introduction are diabase differentiation products is further considered in detail in subsequent discussions of ore genesis. Because of the nature of the hypothesis, which is in essence a reliance upon a distant, non-observable source, direct evidence is lacking. Therefore, the support presented here cannot be conclusive. The objections and difficulties of this hypothesis are presented so that independent evaluation of the probability of either a granophyre or magma-at-depth origin can be made.

One of the major observations in favor of a magmatic origin is, as noted above, the restriction of the zone of potassium metasomatism to the rocks immediately surrounding the eastern ore body; that is, the pink Blue Conglomerate and pink Mill Hill Slate appear as if they were an ore zone alteration similar to the chloritization, silicification, or dolomitization often associated with other types of ore deposits. In this respect, potassium can be said to be zoned in the same way as the ore-stage minerals (see Part 4, "Zonation"); that is, the distribution of potassium is not uniform, but is spatially related to the directional migration of ore-stage minerals from a focus within the eastern Cornwall ore zone.

Within diabase, K_2O (in feldspar) is a common major constituent of granophyre throughout the southwestern part of the Pennsylvania diabase province regardless of the presence of ore. On the other hand, potassium introduction beyond diabase in the form of hematitic orthoclase has been noted only at Cornwall, and there only in the vicinity of the eastern ore body.

Thus, in the metallogenic province as a whole, K_2O introduction is neither common to the presence of granophyre in diabase nor to magnetite ore concentrations. Other than the previously cited objections, there are many theories for and against a granophyric source. If potassium escaped from a late diabase-residua system, it should have done so along the entire dip and strike length of the Cornwall sheet. There is no evidence for this. It is unlikely that K_2O was locally concentrated coincidentally where ore solutions happened also to be introduced and where a limestone slice also happened to be available above the diabase sheet. If potassium escaped at different places through the top of the entire Cornwall sheet, it would have had to migrate through hornfels toward the eastern ore zone. The arguments previously adduced against such a metamorphic migration from Mill Hill Slate also would apply here.

Another such kind of evidence is the sequence of pH change from halogen-rich to alkali-rich in a gradually changing ore and alteration fluid leading to eventual alkaline iron ore migration (see Part 6, "Environment of Ore Transport and Deposition") and culminating in zeolitization at a rather high pH. The potassium feldspar (— halogen?) metasomatism would then correspond to an early stage in this alteration sequence, before the buffering action from limestone leaching was effectively overcome. Silicification in the ore zone after contact metamorphism and before magnetite crystallization would then become part of a continuously changing pH sequence, modified by the presence in the host carbonates of calcium and magnesium ions. Such a magmatic fluid also corresponds to an early tholeiitic fractionation based upon data concerning diabase differentiation and crystallization trends (see Parts 5 and 6). Particularly significant in this regard is the slight, but apparently real, deficiency in K_2O in the normal diabase of the *in situ* sheet. The residual enrichment of both iron and alkalies frequently has been noted in association with tholeiitic magma (Edwards, 1942; Walker and Poldervaart, 1940; Hotz, 1950 and 1953; McDougall, 1961; and Osborn 1962).

Yet another line of reasoning may provide a genetic link between potassium and iron enrichment. The paragenetic proximity of Fe-orthoclase and magnetite appears to be so close that a sequence of crystallization is often indeterminable, although occasional clear relationships indicate that Fe-orthoclase preceded magnetite ore. This relationship also may indicate a continuously decreasing temperature characteristic of metasomatic and hydrothermal migration. The formation of magnetite and associated minerals probably occurred at temperatures somewhat lower (see Part 6, "Origin and Magmatic History of Cornwall Magnetite") than that of the maximum for potassium feldspar, reflecting a gradual trend from 600-650° C. to about 500° C. during magnetite crystallization.

A single process for potassium introduction and ore deposition also is indicated from a study of titanium distribution (see Part 6., "Titanium-Iron

Geochemistry and Province Ore Origin"). The ore minerals are almost completely deficient in titanium and no titaniferous minerals have been noted in the metasomatized units (Tables 3, 4, 7 and 8). On the other hand, titanium and iron-rich minerals in the potassic diabase differentiates are distinctively and closely associated (Plate 20). Thus, a potassium introduction might be viewed as genetically related to iron mineralization by the absence of titanium in the ore and its concentration in granophyre.

Most of the above considerations do not specify the actual source of potassium; but instead indicate that potassium and iron are spatially and probably genetically related. Other observations do not clearly link potassium and iron introduction, nor discriminate their source, even though upon first glance they may appear to do so. The introduction of trace metals, such as cobalt and zinc (Tables 16 and 17 and Appendix 4), into metasomatized units where ore is lean or nearly absent might have occurred either during potassium metasomatism or during a separate hydrothermal ore stage.

In similar fashion, the apparent slight K_2O deficiency of normal diabase at Cornwall does not specify at what point potassium escaped during the history of magmatic crystallization (assuming an originally normal K_2O content for the Cornwall tholeiitic parent). This fact only becomes meaningful in the light of a lack of evidence for escape from the *in situ* sheet. A more thorough study of K_2O distribution throughout the Triassic diabase province in connection with the geometric distribution of granophyre could prove enlightening in this respect.

Discussion and Summary

Several major difficulties in accepting the genetic continuity of K-Fe alteration have been somewhat obscured by the above arguments. The first is that two separate modes, times, and sources of Fe- or hematitic- orthoclase crystallization at Cornwall are called for: one in granophyre and one in the overlying ore zone. The second is that considerable concentrations of ore are present elsewhere with little or no recognized potassium metasomatism (deposits such as at Morgantown, Dillsburg, and French Creek). Thus, it might seem that they are not related to each other. However, to the extent of present knowledge, potassium introduction apparently is unique to Cornwall and thus requires a unique explanation.

Another serious problem is the continuity of the chilled margin, because if it were observed to be unbroken everywhere potassium (and an ore fluid) could not have escaped during granophyre segregation. Hickok (1933, p. 206) reports that a vein termed "aplite" in the western ore body terminated at the diabase-ore contact. Possibly others exist that were not observed or have not been uncovered by more recent mining. The mapped upper diabase surface (Plate 22) over the western ore body shows no visible breakthrough of "aplite" or granophyre, but potassium introduction here also is negligible. There also is no evidence that fractures in diabase, later filled by ore, had been utilized earlier as channels for escape; in fact, there is no spatial relationship between known fractures and late residuum differentiates. As a consequence of the extensive surface and underground mapping, these field data are considered reliable, and the discussion of potassium origin has utilized these prime observations. We felt that the only presently justifiable origin for potassium introduction is as a genetically, ore-associated phase that preceded metallization. Whether this is called metasomatism, resulting from the tapping of a fractionated source or hydrothermal alteration is mostly a matter of semantics. The process envisioned here partakes of some of both concepts depending on the exclusiveness or inclusiveness of the rock-magma system. Metasomatism, as used here, serves to separate the discussion of alkali feldspathization from that of ore deposition.

In summary, the following observations and conclusions are submitted as favoring a mechanism of potassium metasomatism related to hydrothermal ore introduction rather than one related to either sediment remobilization during thermal metamorphism or escape from diabase during late residuum (granophyric) differentiation:

1. The chilled margin of the upper surface of the diabase sheet is essentially unbroken; however, a critical area below the eastern ore body was observable at only a few locations.

2. There is no known spatial relationship between faults or joints transecting diabase and the distribution of granophyre or diabase pegmatite within diabase.

3. There is no known spatial relationship between diabase, granophyre, and the distribution of K_2O (as feldspar) in the ore zone.

4. Areas of known granophyre in the diabase province (usually containing less K_2O than at Cornwall) are common but are not associated with known potassium metasomatism in the surrounding country rock, except in the Cornwall ore district.

5. The addition of potassium and sodium to hornfels units (Blue Conglomerate and Mill Hill Slate) is not spatially the same, as might be expected if both were directly related to expulsion from diabase and as might be expected from the feldspar fixation potential of the hornfels. The sodium addition is more widespread.

6. Extensive potassium introduction is unique to the eastern ore zone at Cornwall where ore zonation is most conspicuous.

7. Movement of a potassium-rich fluid through large volumes of Mill Hill Slate into the eastern ore zone is improbable. Such a migration is nearly impossible because of structural location and unlikely because such movement would cross thermal gradients. The argument applies equally to a granophyric fluid and a migrating metamorphic front.

8. The observations of 1) mineralization sequence, 2) composition sequence, 3) changing crystallization temperatures, and 4) changing pH, show that potassium and ore introduction form a likely continuous sequence in the slowly changing character of a single altering fluid. This sequence supports a genetic linkage of the two processes.

9. Because of this genetic link, an apparent deficiency in the Cornwall diabase sheet in K_2O indicates the high probability of a potassium-rich source fluid related to an original tholeiitic magma (assuming an original magma of normal K_2O composition: see Part 5, "Geochemistry"). Combined with lack of evidence for *in situ* escape of K_2O an earlier tapping of a magma is believed to be required.

10. Direct comparison of Cornwall with the Dillsburg diabase and ore is not valid because of differences in diabase composition, in different magnitudes of ore, and in different country rock compositions of contact lithologies. A lack of potassium metasomatism associated with magnetite at Dillsburg is not necessarily genetically applicable to the origin of either potassium or iron in the Cornwall area.

Controlling factors in contact thermal metamorphism at Cornwall were the composition, both mineralogical and chemical, of the host rocks, their spatial distribution with respect to the upper diabase contact, and the temperature gradient resulting from cooling diabase. The most important controlling factors in potassium metasomatism were the composition and texture of the pre-existing hornfels units, the feldspar fixation potential of these hornfels lithologies, the permeability of the hornfels units, a changing concentration gradient in an advancing metasomatic front, the presence of only a small quantity of potassium-rich granophyre in an otherwise slightly potassium-deficient diabase, and the history of diabase magma generation and crystallization.

PART 4: GEOLOGY OF THE CORNWALL ORES

by D.M. Lapham and Carlyle Gray

MINING

Production and Ore Grade

Except for the recovery of supergene enriched copper in the early days of mining, iron was the only metal recovered until 1920. At this time, magnetic separation and froth flotation were initiated to remove sulfides from the iron ore. Now, chalcopyrite is separated from pyrite and cobalt is recovered from the pyrite (Table 15). Some gold (1700 oz. in 1953) and silver have been recovered from chalcopyrite during refining. Limestone overburden removed

Table 13. *Ore Production (Natural Net Tons)*

Year	Open Pit*	No. 3 Mine*	No. 4 Mine +	Total
1740-1926	31,185,518	110,671		31,296,189
1927-1940	12,349,595	1,977,854	928,968	15,256,417
1941-1950	10,492,356	138,485	8,714,816	19,345.657
1951-1960	2,155,874	3,380,025	10,717,458	16,253,357
1961-1965		2,446,020	5,018,521	7,464,541
	56,183,343	8,053,055	25,379,763	89,616,161

* Western ore body

+ Eastern ore body

from the open pit was crushed and sold for aggregate until the cessation of open pit mining in 1953.

The record of mining in natural net tons of iron ore from 1740 through 1965 is shown in Table 13 (revised from Lapham, 1968, Table1). The present production of ore averages about 1.4 million tons per year. About 90 million tons have been removed to date (1966). Typical recovery analyses are shown in Tables 14 and 15 for 1964 and 1966 respectively. The ore grade averages about 40 percent iron. Ore from the western open pit averaged 42 percent iron and was even higher in the early days of mining. Pelletized magnetic

Table 14. *Ore Product Analyses, 1964 (in %)*

	Fe	S	Cu	Ni	Co	Mn	P
Ore (mill feed)	39.4	1.29	0.29				
Fe concentrate	64.8	0.06	0.05				
Final tailing	7.7	0.61	0.04				
Pellets	63.6	0.02	0.05			0.06	0.006
Cu concentrate	28.7	33.1	26.68	0.046			
Pyrite concentrate	41.5	49.4	0.09	0.15	1.37		

Recovery: Magnetic iron – 99%
Copper – 94%
Pyrite – 73%

Table 15. *Ore Product Analyses, 1966 (in %)*

Component	Ore	Mag.Conc.	Pellets	Tails	Copper Conc.	Pyrite Conc.
Fe	39.6	65.5	64.1	7.7	30.1	42.7
Magnetic Fe	35.2	64.1	0.8	0.7	–	–
Cu	0.27	0.019	0.021	0.080	28.40	0.08
S	1.29	0.05	0.013	0.37	31.6	49.1’
SiO_2	21.2	3.9	3.9	43.5	3.6	2.7
P	–	0.005	0.006	–	–	–
Co	–	–	0.004	–	0.12	1.35
Al_2O_3	–	1.6	1.5	–	–	0.3
Ca	–	1.0	1.0	–	–	0.8
MgO	–	1.9	1.8	–	–	1.4

concentrates average about 64 percent iron. Cobalt in pyrite concentrate ranges widely but averages between 1.2 and 1.4 percent averaging about 1.7 percent in the East End open pit. Phosphorous and titanium are not present in any significant amounts. Electron microprobe studies (Davidson and Wyllie, 1965) show a small variation in iron, magnesium, and aluminum in magnetite ore, depending upon its geologic history, but they are insignificant in terms of any effect upon ore grade.

Mining Methods

A detailed description of mining methods used at Cornwall, both in the open pit and underground, has been given by Shale (1953). Since this publication, a few modifications have been made to keep pace with modern mining technology. A recent summary of mining methods was kindly provided through the courtesy of Bethlehem Steel Corporation by H. Olsen, Manager of the Bethlehem-Cornwall Division, from which the following is taken.

Underground mining at Cornwall began in 1921 with a shaft into footwall diabase at the western end of the western ore body, below the open pit. Early mining was by sublevel stoping and later changed to a shrink stope and pillar method. After discovery of the eastern ore body 150 feet below the surface, a shaft was sunk in 1924 and mining began here following the shrinkage stope

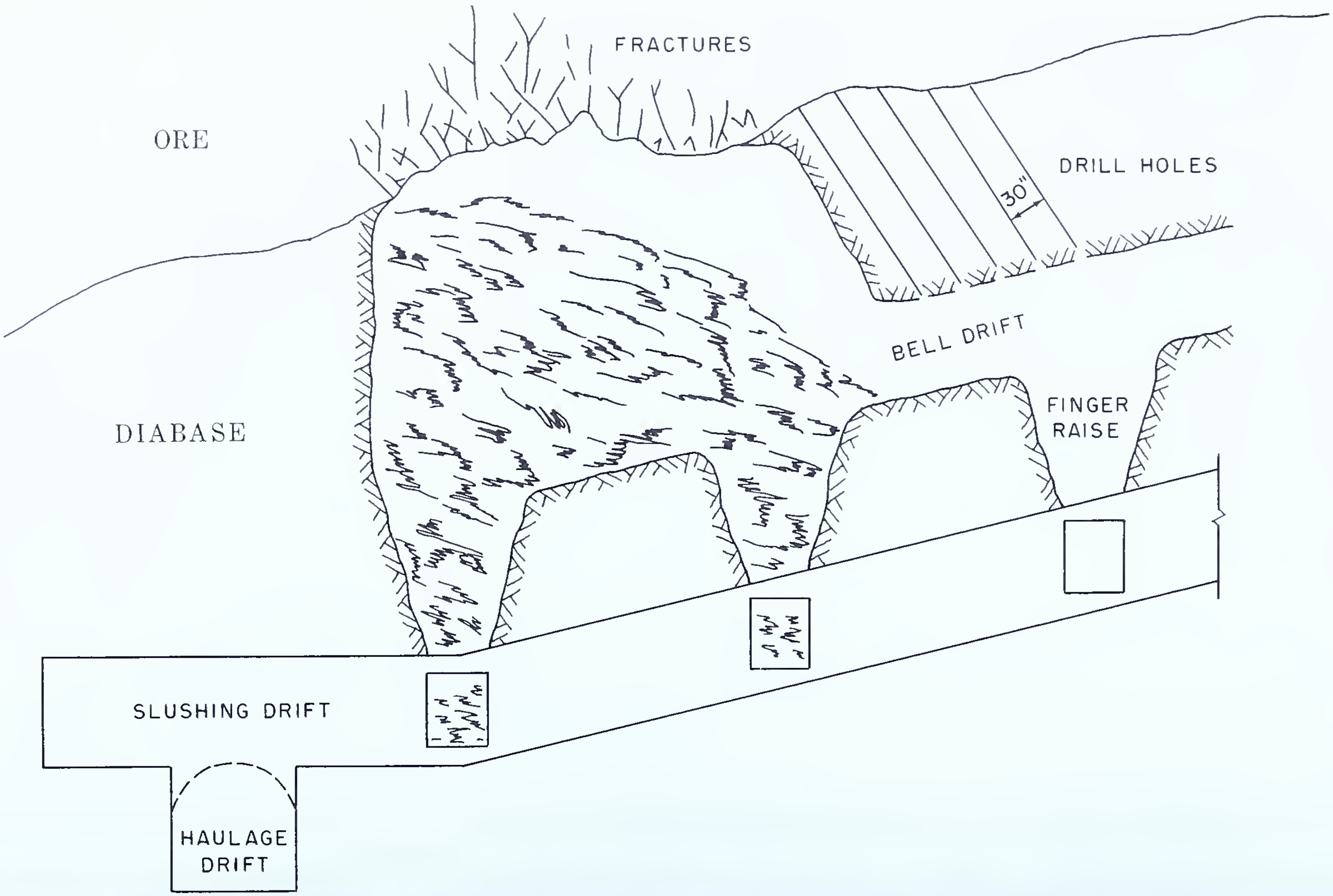

Figure 14. Diagramatic sketch of Cornwall mining method (courtesy of Bethlehem Steel Corp.).

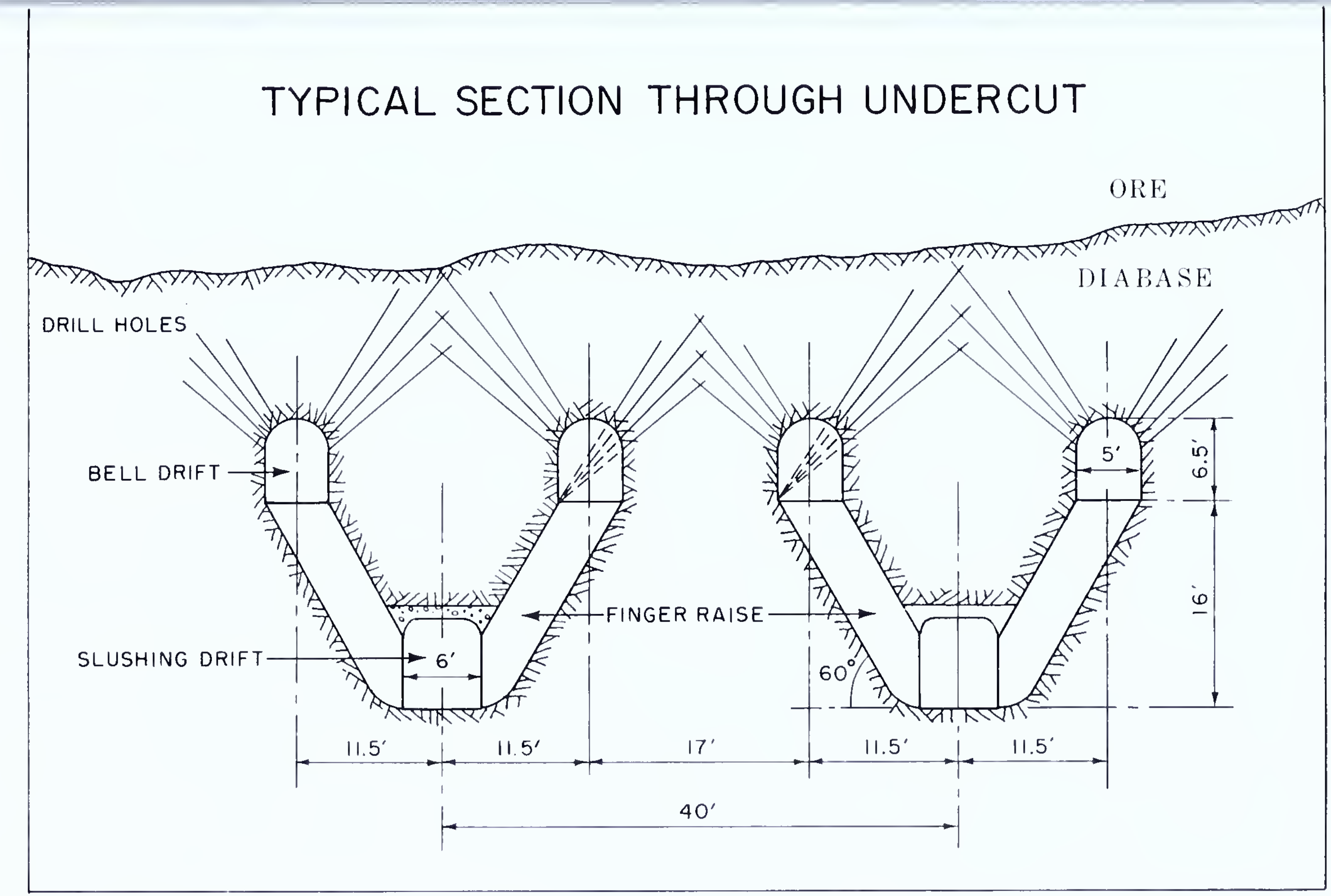

Figure 15. Modified bell system of mining at Cornwall (courtesy of Bethlehem Steel Corp.).

method of the western ore body. Ore was drawn through a system of breaking subs, grizzlies, and transfer raises. In 1937, block caving was utilized and was later modified by the use of slushing drifts through which ore was drawn directly from ore bells at finger raises into transport cars (Figures 14 and 15). Haulage drifts along the east-west strike of the deposit and perpendicular to the shaft, and slushing drifts parallel to the shaft, are supported by concrete arches through the jointed diabase. In 1962, the procedure of driving raises into ore and enlarging them into a cone-shaped bell was eliminated. Instead, from each finger opening a 60° inclined raise was driven above the slushing drift and undercutting of the ore was accomplished by blasting inclined holes drilled perpendicular to the drift. Caved ore was then scraped into slushing drifts for transport by cars and skip haulage to the surface.

Preliminary treatment of ore consists of two crushing stages, screening, and cobbing before concentration and agglomeration. Pelletizing of magnetic concentrates is performed at the mine.

STRUCTURAL DESCRIPTION

The Ore Bodies

The Cornwall mine area comprises two major ore bodies (an eastern and a western mine) two minor ore pockets (the Elizabeth mine which is a small open pit at the eastern end of the main open pit and the East End open pit, part of the western ore body), and an undeveloped concentration of ore within diabase (the "footwall" ore body) between the two major ore bodies (see Plate 23 and Figures 17 and 18). In addition, there are occasional occurrences of ore veins in diabase and a small ore concentration to the north below diabase (the Doner mine).

The western ore body, the site of the original open pit operations and now largely mined out, was a wedge-shaped mass that lay directly on diabase except for small, intervening blocks of limestone. It originally cropped out up dip, and hence its upper limit was the present erosion surface (Plate 23). The strike length of this ore body before mining was nearly 4000 feet. At its western limit it had a dip length of about 1600 feet, decreasing eastward. Maximum ore thickness exceeded 150 feet. At its eastern end the ore was divided by a roll, or ridge, in the diabase sheet. The northern part of the bifurcation formed the "Big Hill" ore in a depression in the top of the diabase. If the bifurcated areas were once continuous, considerable ore has been eroded since ore deposition. A rise in the diabase at the western end terminates both limestone and ore. Near the eastern end of the open pit, hanging wall ore in line with the southern bifurcation fingered out into isoclinally folded limestone. Preferential replacement of non-dolomitic laminae was visible during open pit operations. At the extreme eastern end and down dip, Blue Conglomerate cuts out host limestone and forms a somewhat irregular ore boundary (Plates 22 and 23).

The eastern ore body is lenticular with a lima-bean shape (Plates 21 and 22). It extends 2000 feet along strike and more than 2400 feet down dip. Ore thicknesses average about 100 feet, but attain a maximum of 240 feet just south of the center of the ore body (Plate 23 and Figure 29). Along the extreme northwestern edge, ore tongues cut into limestone both in the hanging wall and the footwall. Elsewhere, either Mill Hill Slate (up dip) or Blue Conglomerate (down dip) forms the ore hanging wall (Plates 21 and 23). Near the center of the ore body an apophysis of diabase protrudes into ore. In this apophysis, the diabase shows more extensive bleaching and chloritization than elsewhere, with deposition of magnetite and actinolite within fractures in the diabase. The hanging-wall contact is generally sharp. There is, however, some mineralization of actinolite, pyrite, and chalcopyrite in the overlying Mill Hill Slate. The Blue Conglomerate, where it is the hanging wall, commonly contains lenses or masses of magnetite and diopside or garnet. These are interpreted as replaced, discontinuous fragments of limestone that formed during the brecciation of the Blue Conglomerate along its contact with limestone (also see "Structure of the Eastern Ore Body").

Both major ore bodies are pod-shaped, for the most part lying directly on diabase. The average ore thickness of each was about 100 feet, except at the extremities of the ore bodies where the ore thinned. Both are spatially related to the strike and dip of tabular masses of ore (veins?) that penetrate deeply into the diabase east of the western ore body (see "Structures of the Eastern Ore Body"). The mineralogy and texture of the limestone replacement ore is similar in both bodies. In neither ore body are the Triassic sediments in direct contact with ore. In the eastern ore body, a rather thick mass of Blue Conglomerate, as well as the limestone of the hanging wall, separates Triassic sediments from ore. In the eastern ore body, there is always either Blue Conglomerate or Mill Hill Slate between Triassic sediments and ore.

There is a decided contrast between the limestone hanging wall of the western ore body, which shows rather extensive intertonguing of ore into barren limestone, and the more even hanging wall of the eastern ore body. There, Mill Hill Slate and Blue Conglomerate in the hanging wall form a distinct impermeable cap, except in the lower extremity down dip where there is some apparent tonguing of ore into Blue Conglomerate (Plate 23). At the updip end of the ore body, Mill Hill Slate thickens as ore thins; that is, the distance between Triassic sediments and diabase remains approximately constant and the ore pinches out while the Mill Hill Slate thickens (Figures 19-22). However, in one area, there is unreplaced limestone at the up-dip extremity of the ore (Plate 23, section K).

The two smaller ore concentrations at Cornwall replaced limestone where there was a small trough in the upper surface of the diabase sheet. For the most part, the hanging wall has been eroded. At the Elizabeth open pit, almost in line with the north bifurcation of the western ore zone, ore rested

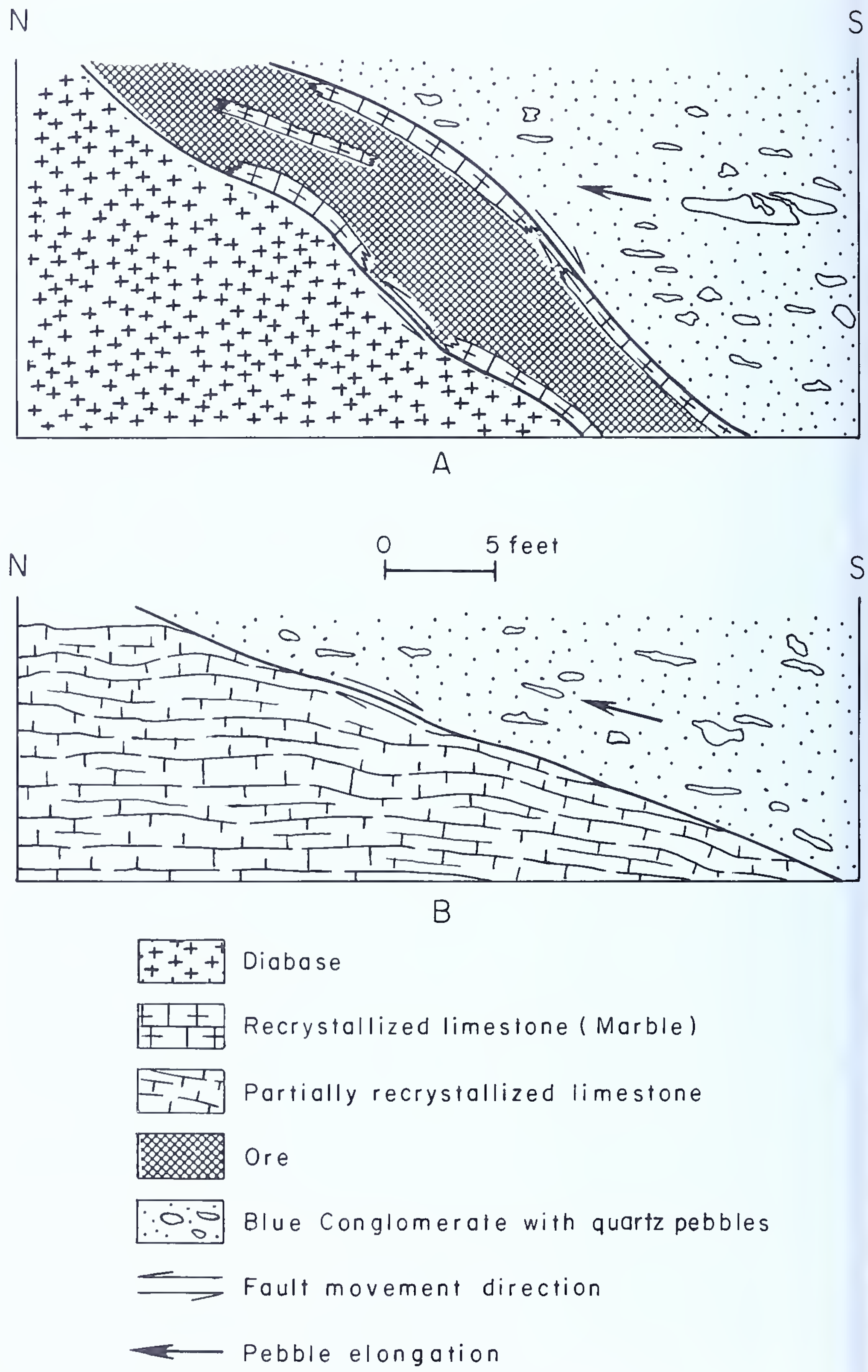
N
S
A
0
5 feet
N
S
B
Diabase
Recrystallized limestone (Marble)
Partially recrystallized limestone
Ore
Blue Conglomerate with quartz pebbles
Fault movement direction
Pebble elongation

Figure 16. **Sections through the East End open-pit ore body; A at extreme east end, and B at west end adjacent to main open pit. Fault at base of Blue Conglomerate extends from A on the east to B on the west (courtesy of A. Geyer, Pa. Geol. Survey). Some fragments in Blue Conglomerate are limestone and do not resemble the Buffalo Springs Formation or the host limestone.**

on diabase that was frequently of pegmatitic texture. Granophyre was not observed here. The East End open pit ore body is expected to be reached late in 1970, to remain active for a few years, and then to cease operation coincident with the closing of all Cornwall operations. Ore here replaces limestone between diabase and Blue Conglomerate (Figure 16-A). Unreplaced limestone exists at both the footwall and the hanging wall (Figure 16-A). The limestone is recrystallized and serpentinized. Both the upper and lower limestone contacts are faulted, with relative movement such

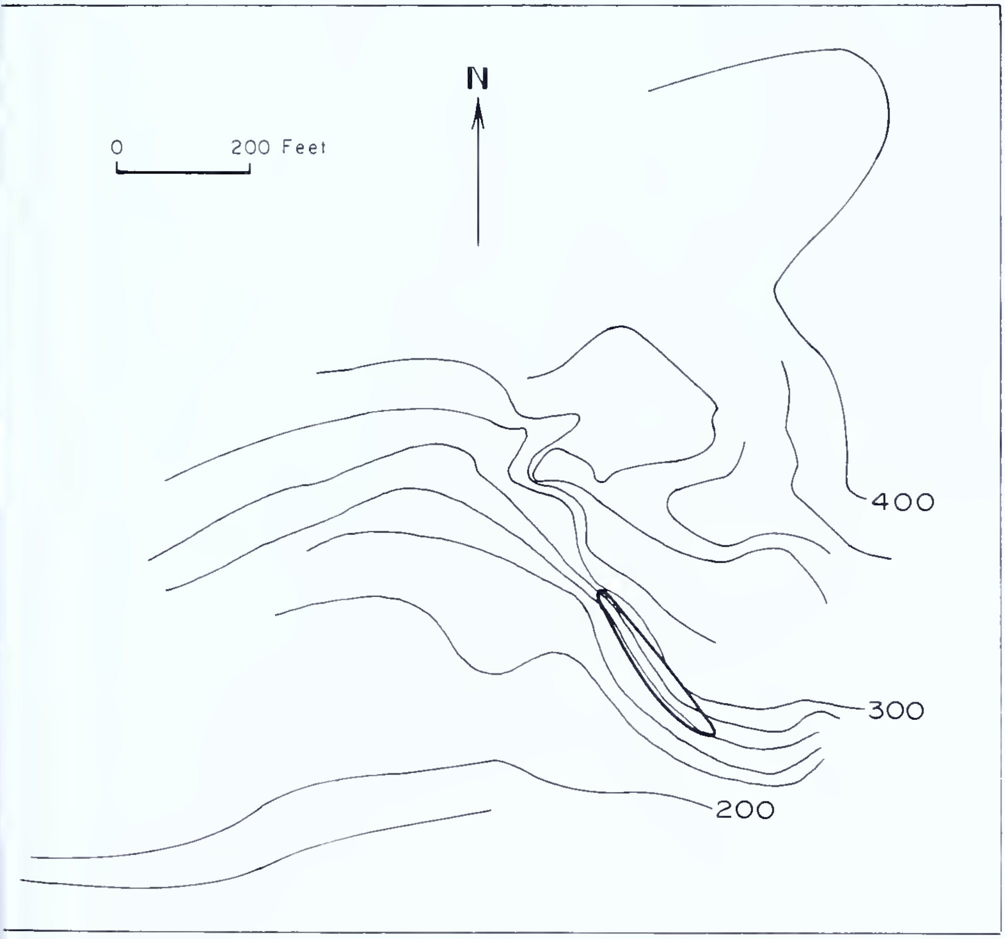

Figure 17. **Plan map of the Footwall ore body between eastern and western mines (see Plate 22, Footwall Ore for location); diabase contours at 20′.**

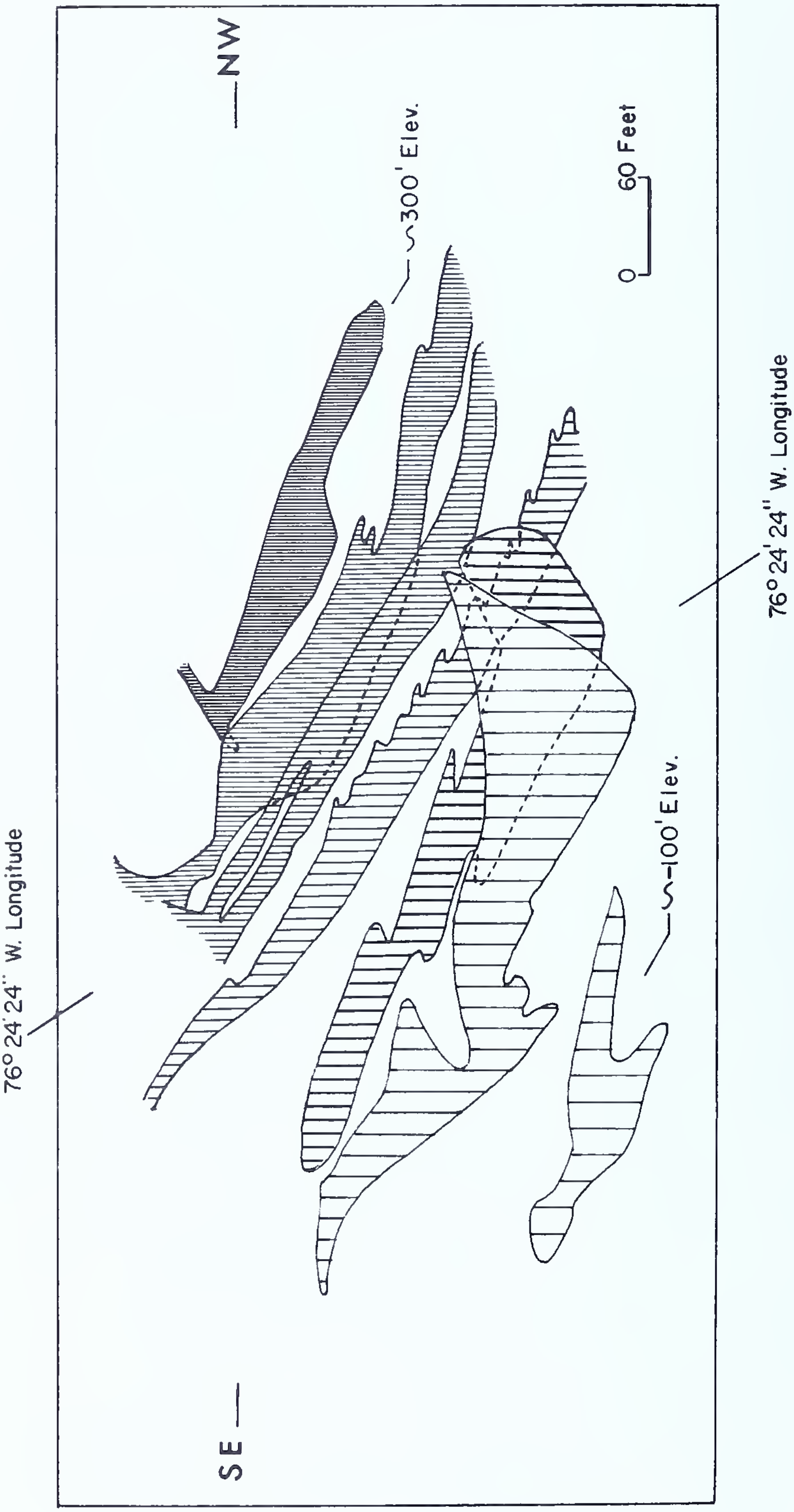

Figure 18. Cross sections illustrating the form of the "Footwall" ore body, from southwest to northeast (down plunge). Note strike of ore body is northeast, parallel to strike of major fault (see Figure 17 and Plates 22 and 23).

that the limestone appears to have been thrust up-dip between diabase and Blue Conglomerate. Ore here is rich in chalcopyrite.

Very little information is available about the Doner mine (Spencer, 1908, p. 26-27). The ore body was a small magnetite concentration that replaced limestone, extended east-west, and lay below the now eroded diabase. The Carper mine (Spencer, 1908, p. 28), 8 miles west of Cornwall, also probably lay below diabase.

A mass of lean ore (footwall ore body), not mined at present, lies beneath the eastern end of the western ore body, almost wholly enclosed by diabase (Figures 17 and 18; Plates 22 and 23-G). This ore is oviod and intersects the main ore above through a narrow ore bridge. The ore mass strikes about N35° W (Figure 17) and plunges about 40° NE (Figure 18). At the intersection with the main ore body, banded and brecciated limestone replacement textures are common. Some banding in diamond drill cores is present below this intersection. Within the footwall ore, frequent blocks of normal, barren diabase have been intersected by diamond drill cores; however, some blocks are noticeably amphibolitized and chloritized. One footwall ore-body sample containing ore-grade magnetite also contained replaced, herringbone-twinned, and inverted pyroxene, augite, and serpentinized primary orthopyroxene (Samuel Sims, personal communication). In this instance, the ore is a replacement of diabase rather than of limestone. Shearing and brecciation in diabase are present down dip and below this footwall ore. Strike projections of ore veins in diabase observed in the eastern end of the open pit also are on strike with the footwall ore body. This ore occurrence is believed to be a replacement of limestone at its intersection with the overlying main ore body, but below this intersection, at least in part, is a replacement of diabase along a major ore channel through the sheet. Engulfment of limestone blocks by diabase and ore-fluid along this channel also is probable, but unknown.

Near the lowest part of the eastern ore body on the south and southwest several veins bearing ore minerals were discovered in the driving of the drifts to be used as sumps on the 1225-foot level (Figure 23). A vein in diabase having a maximum width of six feet was intersected, as well as a number of parallel veinlets one-half inch to more than an inch wide. The thick vein was explored further by means of diamond drilling, and traced downward to nearly 300 feet below the footwall (top of the diabase). The vein narrowed downward but still was present at that depth with a width of more than two feet. Other drilling indicates that the vein is traceable for a strike length of nearly 1000 feet. The thick vein was reported to be massive magnetite, with actinolite, chalcopyrite, and pyrite. This vein is referred to subsequently in discussions of ore channels and their origin. Thinner veinlets seen here (and elsewhere) show no uniform crustification but the most common arrangement is a thick layer of magnetite on the walls, usually mixed with actinolite, and actinolite in the center with grains or masses of magnetite embedded in the actinolite. Chalcopyrite and pyrite also occur in the central parts of the veins. In some veinlets, the magnetite on the wall is missing, and magnetite occurs only in the vein center.

Structure of the Eastern Ore Body

Mapping (Plates 21 and 23) has shown that the ore-limestone horizon of the eastern body is oval in plan and lens or wedge-shaped in section, overlain by a thin plate of metasomatic and contact metamorphic Mill Hill Slate and Blue Conglomerate. The eastern ore body now is separated from the western ore body by a ridge of diabase, which presumably once was capped by limestone and ore, that forms a bridge between the two bodies. The outcrops at Big Hill and the Elizabeth open pit mine are remnants. The bridge of ore has since been eroded. Near the western edge of the eastern ore body, a major fault transects diabase (Plate 22) and is structurally in line with ore veins, brecciation, and a footwall ore body within diabase. Diamond drill cores and underground mine mapping of the eastern mine have revealed complex ore, vein, and hanging wall structures that bear on the tectonic history of the area and on ore fluid movement.

Where observed, the contact between hornfels (Blue Conglomerate or Mill Hill Slate) and the Triassic sediments is always sharp. This contact was well-exposed in the 820-foot level water drift of the eastern mine. The contact here between Blue Conglomerate and Triassic siltstone dips southward about 30-35° and the Triassic sediments dip northward into it about 40°. Pebbles in the Blue Conglomerate show a faint elongation subparallel to the dip of the contact; that is, the Paleozoic units dip approximately conformably to the contact, a situation found elsewhere at Cornwall and at Boyertown by Spencer (1908). The contact is sharp, angular, and tight. Blue Conglomerate boulders "protrude" into the Triassic sediments. No slickenside is present at the contact and the Triassic rocks are not brecciated (although the microscopic texture of the Blue Conglomerate here, as elsewhere, is mylonitized and brecciated). Thus, here there is no basin-margin fault and no Triassic conglomerate that could be construed as a fanglomerate resulting from faulting.

Diamond drill cores from the surface intersected Blue Conglomerate, Mill Hill Slate, host limestone, and ore. In Plates 21 and 23 and in Figure 22, the hornfels units are shown as a wedge of nearly constant thickness with Blue Conglomerate structurally overlying Mill Hill Slate and both capping the limestone-ore horizon. However, the drill data reveal that the picture is more complex. Contour maps of unit thicknesses for the eastern ore body based on 24 holes show the general relationships of these units (Figures 19-21). In the northern part of the ore body, Blue Conglomerate is absent. In the southern part of the body, Mill Hill Slate is absent. Across the central part of the ore zone, both units usually are encountered. The strike trend of this overlap is east-northeast. In many of the drill cores, limestone is encountered before the last of the hornfels units so that slices of limestone, or alternatively, slices of either Mill Hill Slate or Blue Conglomerate, are present. Further indication of tectonic brecciation is evident from the character of the Mill Hill Slate-Blue Conglomerate contact. Here also, alternate slices of the two units are encountered in the cores. However, whereas the alteration with limestone is present throughout the dip length of the ore body, alternations of the two

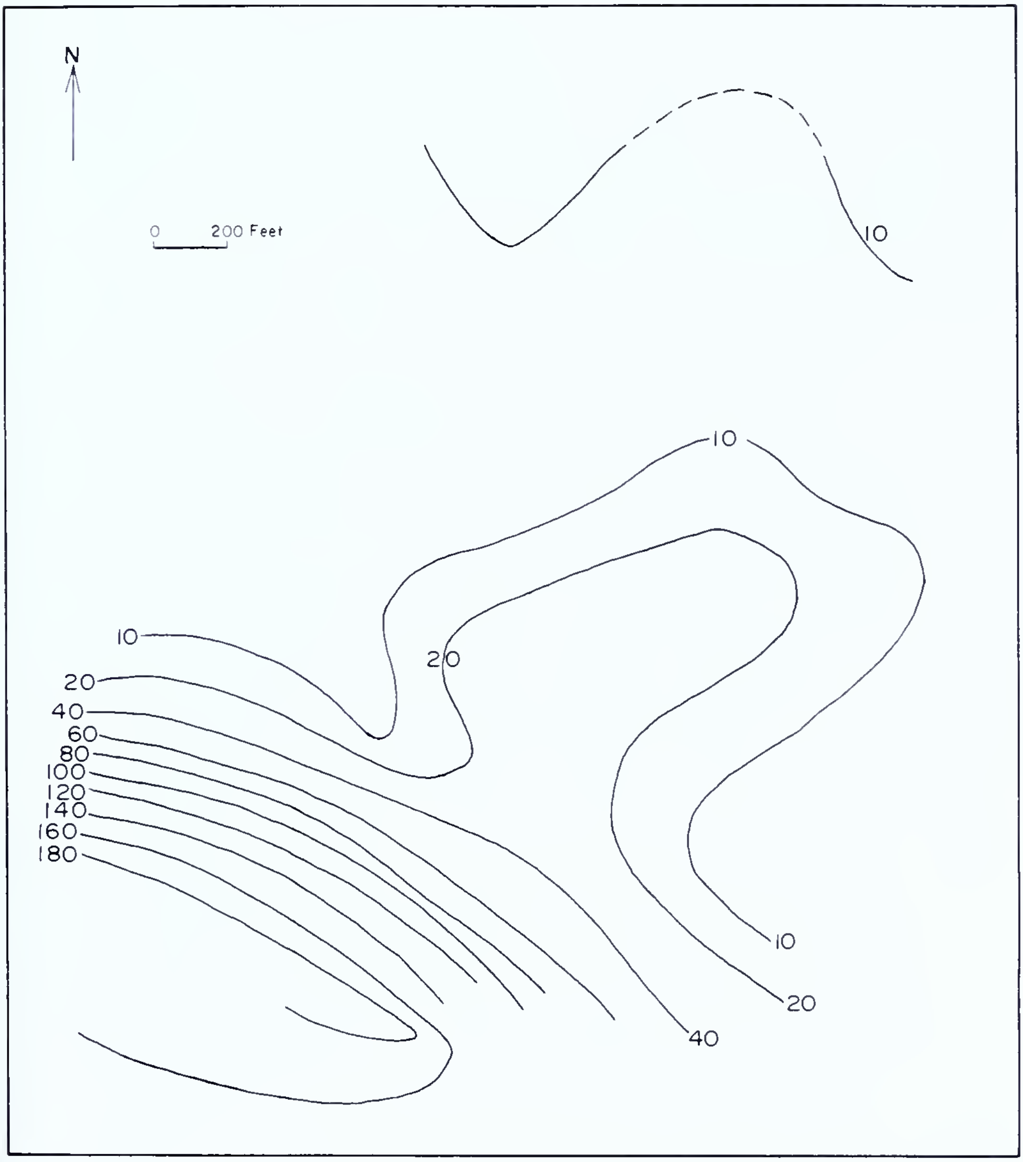

Figure 19. Total thickness contours of Blue Conglomerate, eastern ore body, from sections K to N in Plate 23. Note variable contour interval.

hornfels units are restricted to the central part of the ore body where the total thickness of these units is least (Figures 21, 22). In part, the contact between Mill Hill Slate and Blue Conglomerate (see Parts 2 and 3) and limestone at the base of both units indicate that this contact, as well as that between them and limestone, is a faulted contact. The arched geometry of the two hornfels units, and their extreme thinness over the ore body (Figure 22), probably contributed greatly to rupture. Since the two hornfels units are believed to be time-correlatives with the Martinsburg Formation, initial brecciation probably occurred during emplacement of a thrust sheet over Cambrian carbonates, perhaps as part of the Yellow Breeches thrust system (MacLachlan, 1967). Folding and subsequent erosion of this thrust plate resulted in the present thin arch (note the vertical exaggeration in Figure 22) of metasediments that presently confine the ore. It is also possible that the intrusion of diabase was in part responsible for the arching of this overlying plate, although the thickness of the diabase sheet may be too uniform to have caused such a small, local effect.

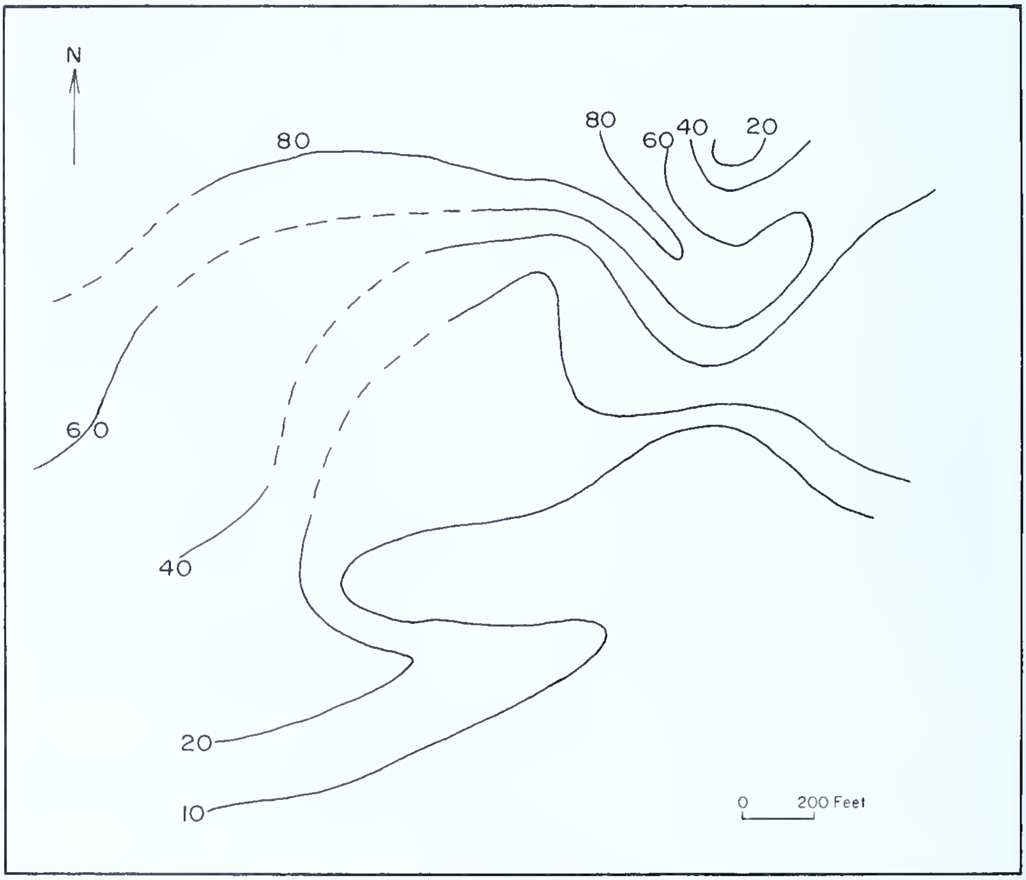

Figure 20. Total thickness contours of Mill Hill Slate, eastern ore body, from sections K to N in Plate 23. Note variable contour interval.

Joints, small faults, folds (Plate 6 and Figure 24), and breccia zones are common throughout the eastern underground ore body but are too small and too numerous to be mapped. However, several of the larger features have been recorded (Figure 23) from different mine levels for the southern half of the ore zone. The more persistent of these have been projected to the footwall (top of the diabase). There are essentially two distinct sets of fractures: a northeast-striking group and an east-northeast-striking group. Northwest-striking features are quite rare both at this map scale and also in thin section at the micro-fracture scale. Along the west boundary, a major fault offsets diabase (see also Plate 21) and strikes northeast. To the east, a smaller strike-slip fault parallels it and offsets a more easterly striking fault. The more easterly striking faults frequently are ore veins in diabase, and one major system in the southern part of the ore zone is extensive (Figure 23 and Plate 22). It is paralleled by a smaller ore vein up dip that continues to the east as a breccia zone. Still further up dip to the north, there are a series of smaller faults and joints striking northeast in a zone that strikes east-northeast.

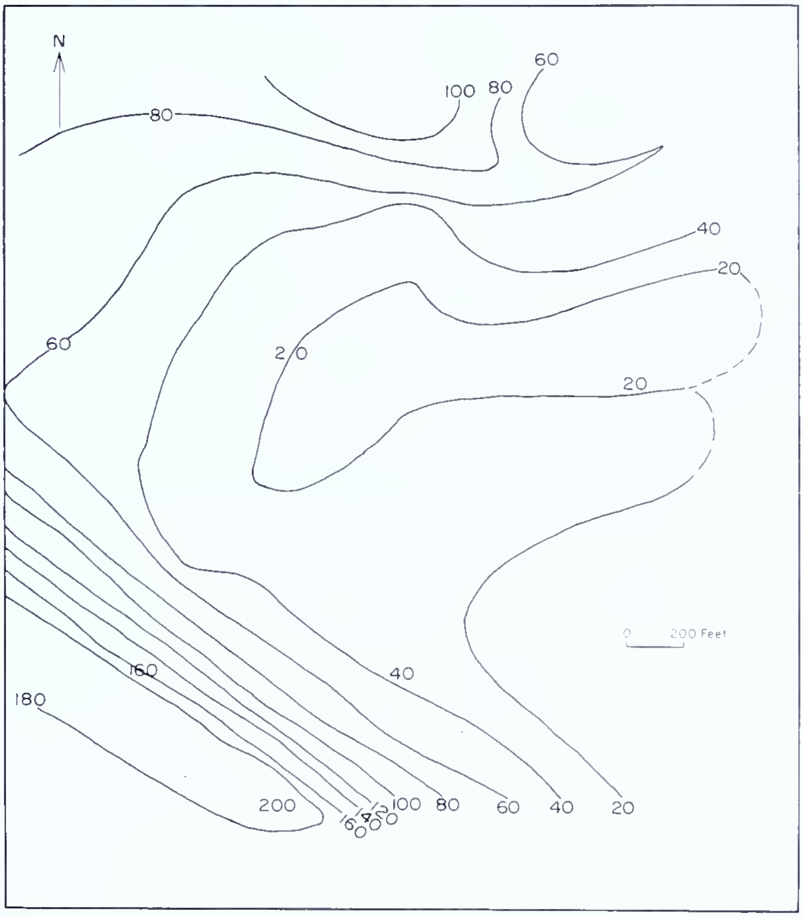

Figure 21. Total hornfels thickness contours (Blue Conglomerate + Mill Hill Slate), eastern ore body, from sections K to N in Plate 23.

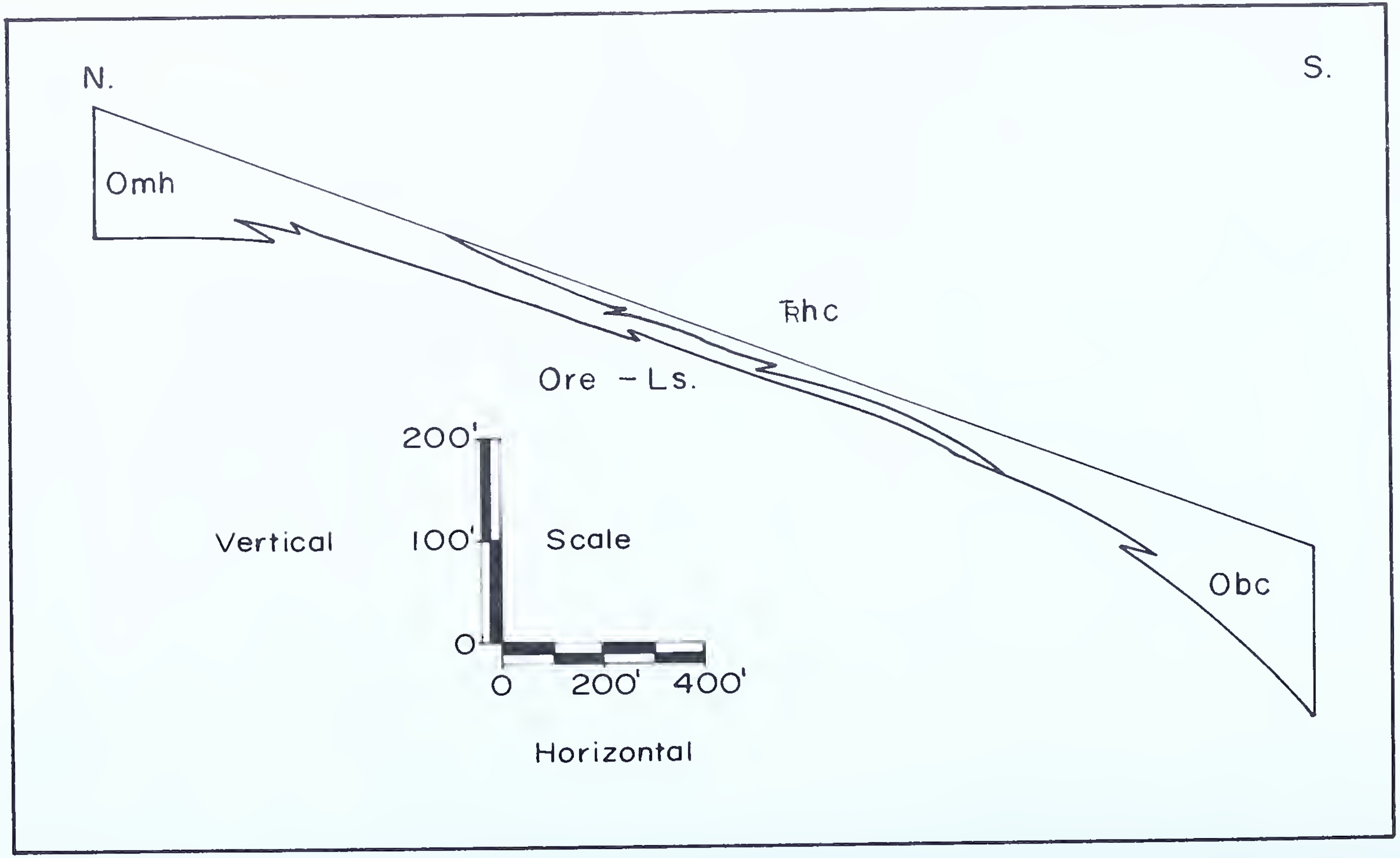

Figure 22. Simplified north-south cross section of total hornfels illustrating thickness variation along the dip and fold geometry above the central portion of the eastern ore body.

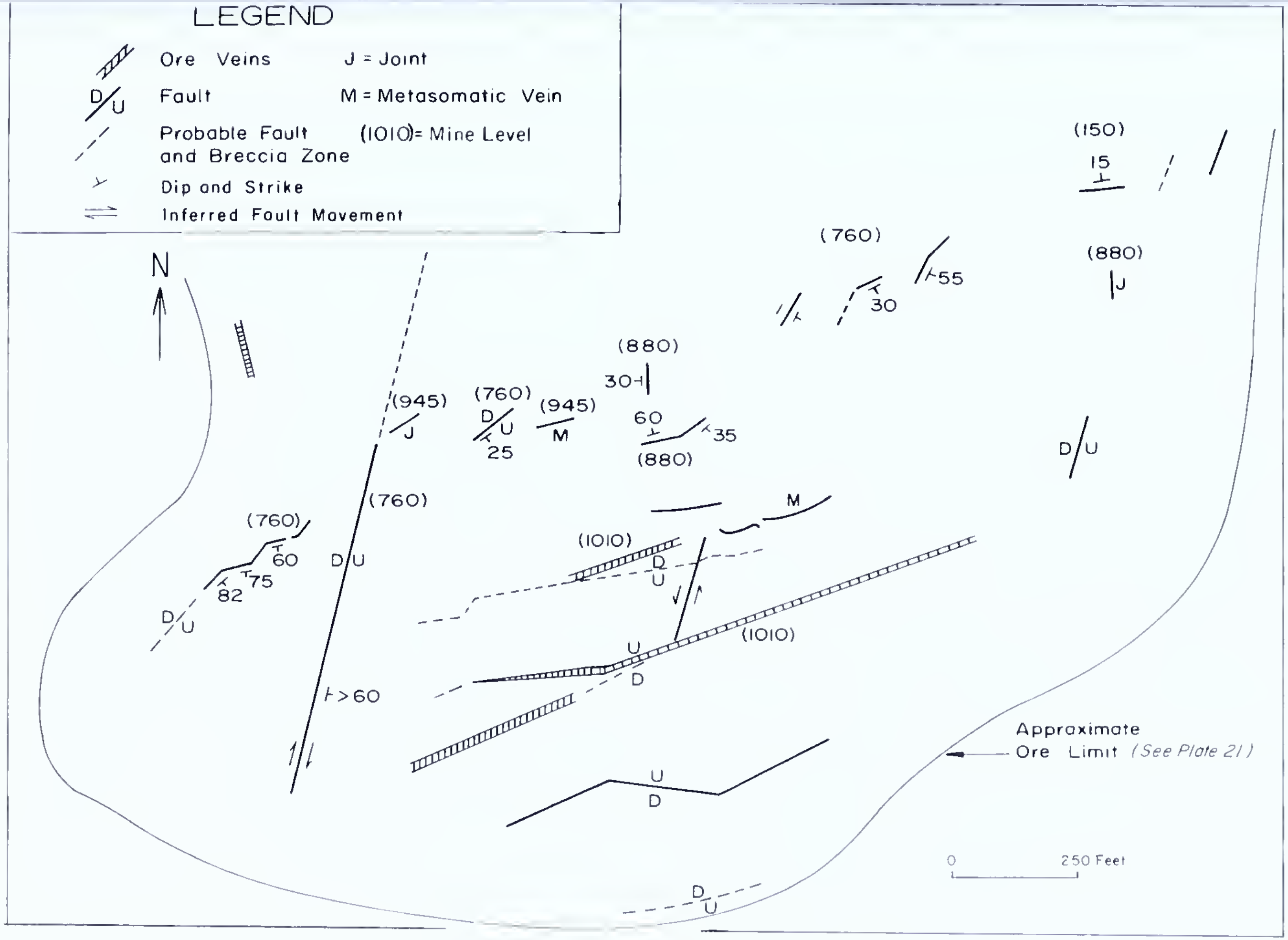

Figure 23. Map of detailed structural features of the eastern ore body, illustrating general northeast trend of ore veins and of major fault zone; where mine levels (in parentheses) are noted, they have been projected down to the top of the diabase.

If projected, the ore veins would intersect the major northeast fault that offsets diabase in the southwest corner of the eastern ore body. There is evidence that the distribution of ore in the eastern ore zone may be related to these ore veins (see magnetite unit-cell data in "Mineralogical Zonation"). In addition, there is considerable other evidence that this area was the focus of ore fluid movement. If this is accepted and if the major fault was an ore channel through diabase, then the following sequence occurred: first, northeast faulting with diabase offset, then east-northeast fracturing with the introduction of ore minerals, and finally repeated movement on the northeast fracture set. This latter tectonism is largely responsible for late deformation textures in the ore zone (Plate 6). It also is interesting to note that the northeast set is parallel to a more regional northeast set into which late diabase dikes intruded (see Figure 56).

Petrographic examination also reveals more than one deformational episode, although a time separation is not always clear (Plate 6). The earliest recognizable deformation is associated with, or is slightly later than, ore stage introduction (Plate 6-C). Any earlier tectonic fabrics have been obliterated by succeeding folding, faulting, and solution flow. Deformation of contact metamorphic phlogopite, muscovite, and tremolite is clear (Plate 6A, B, C). Flow of actinolite matrix (fine-grained and associated with ore-stage mineralization) is common (Plate 6-D) and may have occurred during or later than magnetite crystallization. Deformation continued after magnetite introduction ceased (Plate 6-A and D; also Plate 11-B), while lower temperature and later minerals were remobilized and recrystallized. Apparently much of the late stress applied to the ore zone is taken up by movement within the least competent lithology, the fine-grained actinolite matrix which generally post-dates magnetite-pyrite crystallization (Plate 6-C).

MINERALOGY AND CHEMISTRY

Ore Textures

Megascopic ore textures at Cornwall reflect very well the textural and compositional variation of the units that they replaced (Figure 24). However, except for a few minor exceptions, typically folded and banded textures occur throughout both mine areas (Figure 24). Mapping of textures has not yielded observable large scale textural zonation. It has, however, yielded much information about the conditions governing relative ease of replacement and some information about ore-fluid movement.

Of the many ore textures (see Plate 10), the most striking is banded green and black ore, found throughout the eastern and western ore bodies. Magnetite-rich laminae alternate with green, gangue-rich laminae (Figure 24), or in gangue, more siliceous and calcium-poor laminae alternate with less siliceous and more calcium-rich laminae. They commonly range in width from tenths of inches (Plate 9-C) to several inches, are discontinuous beyond a few feet (commonly, a few inches), are offset by small microfaults, and exhibit numerous small-scale drag folds (Plates 7-B, 9-A). In every respect, they resemble the laminae in unreplaced limestone or less commonly in Mill Hill Slate. Bedding and axial plane attitudes, however, are oriented with remarkable irregularity, a consequence of brecciation and small-scale faulting largely restricted to the ore zone. Particularly in the lower part of the eastern ore body, bands of essentially gangue-free magnetite are separated by planar vugs into which dodecahedral or octahedral magnetite terminations project, touching the crystal projections of an adjacent band. In places, all banding has been destroyed by a brecciation previous to ore introduction that probably was Paleozoic and associated with the thrust between Mill Hill Slate (-Blue Conglomerate) and Cambro-Ordovician carbonates. Sulfides commonly are cross-cutting (Figure 24, Plates 7-C and 8-C), although in lean ore, usually near the hanging wall, veins of magnetite also transect banded gangue.

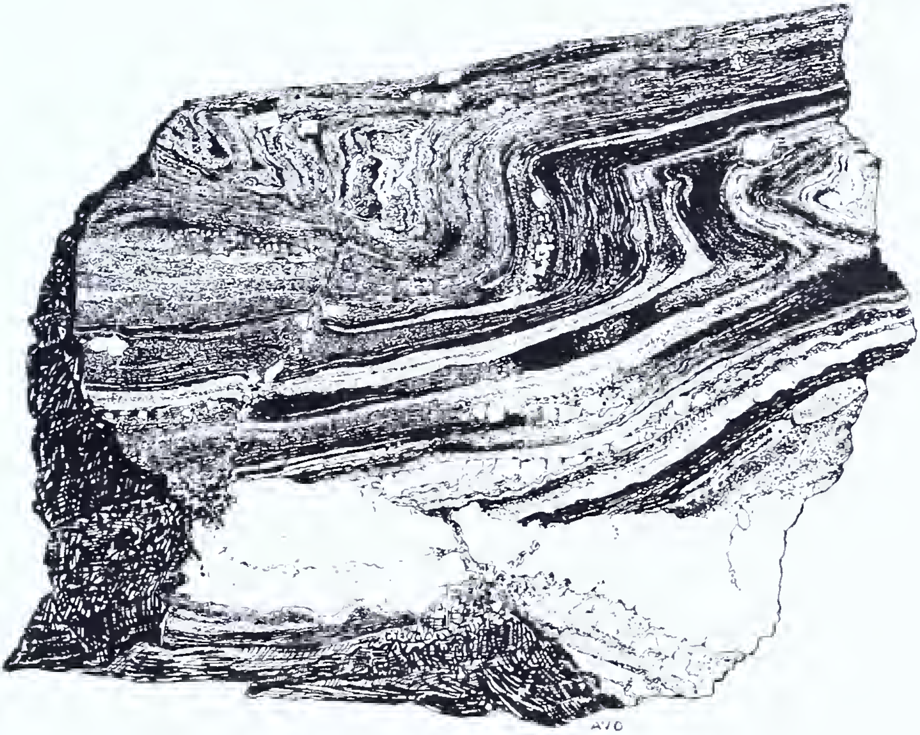

Figure 24. Sketch of typical ore textures and foliation in replaced, laminated, host limestone. Dark bands contain actinolite and magnetite; light bands contain actinolite, chlorite, and traces of magnetite. Pyrite cubes (disseminated) and veins (transecting) are typical; natural size.

In some of the ore, there is no clearly banded texture. This massive ore consists of scattered magnetite grains (disseminated ore) in a non-foliated matrix of gangue minerals. The only texture here is imparted by masses or veinlets of magnetite and/or sulfides. Where rich, the massive ore consists of magnetite with scattered grains or veinlets of sulfides and silicate gangue.

In the eastern ore body, textures are present that are characteristic of replacement of Blue Conglomerate, or more rarely of Mill Hill Slate. Blue Conglomerate replacement has resulted in a spotted ore that frequently resembles phenocrystic texture. Especially where limestone has pinched out and Blue Conglomerate approaches diabase, this spotted ore commonly is a mottled pink color resulting from the presence of ferriferous or hematitic orthoclase. This usually lean ore has acquired the misnomer of aplitic ore. Frequently, it is brecciated as in the east-northeast ore veins of the south-central part of the ore body (Figure 23). Here only gangue, usually actinolite or mica, has been replaced by magnetite; feldspar and quartz breccia fragments remain unreplaced. Replaced laminae of Mill Hill Slate are difficult to distinguish from replaced limestone laminae. Usually, however, in Mill Hill Slate there is much less magnetite, the laminae are less contorted than in limestone, and calcic feldspar is present.

Another characteristic texture is that of platy magnetite. It is most common at the footwall and hanging wall of both ore bodies where it has pseudomorphically replaced pre-existing specular hematite (Plate 7-B). Minor compositional variation and optical zoning in this magnetite (Plate 8-A) are common and have been discussed by Davidson and Wyllie (1965). In part, the zoning may result from sequential replacement of calcite along its cleavages by hematite, and finally by magnetite. Interrupted magnetite crystallization is indicated by the zonal growth of bluish cores rimmed by brownish, more impure magnetite (Davidson and Wyllie, 1966, Plate 8-A).

Vein magnetite, massive or vuggy, occurs in diabase and more rarely transects banded gangue-ore textures. Such veins are usually down dip along the footwall, and the magnetite commonly is more euhedral than up dip or toward the hanging wall. Vug ore in the eastern mine appears to be restricted to the south-central footwall area.

Contraction cracks in the top of the diabase commonly are filled with magnetite and diopside (Plate 13-C); only rarely is the chilled margin actually replaced (i.e., along the southwestern and south-central footwall of the eastern ore body). The diabase - ore contact is visually sharp except where replaced and the fine-grained Blue Conglomerate or Mill Hill Slate hornfels in contact with diabase is nearly indistinguishable from chilled diabase. In the south-central part of the eastern ore body, a tongue of diabase extending into ore (Plate 23) has been bleached and chloritized by ore-zone mineralization. Small magnetite-actinolite fractures extend into the diabase tongue. These relationships help to date ore mineralization as having occurred after the main stage of diabase crystallization.

Although mylonitic, brecciated, and sheared ore textures are found throughout the mine, they are especially prominent in the southwest and south-central parts of the eastern ore body (Figure 23). On a microscopic scale, shear flowage postdates the crystallization of metamorphic mica, tremolite-actinolite, and at least some of the magnetite (Plates 7-B and C; Plate 8-C). Sericitization of clinopyroxene and plagioclase at the top of the diabase sheet (Plates 9-B and Plate 13) is especially noticeable in this area (although present throughout the chilled margin).

Slickensided joints and fractures, post-magnetite shear flowage, and offset bands of ore and gangue, show that there has been considerable post-ore movement. These fractures are small, rarely traceable for more than a few tens of feet, and could not be traced to a major fault. The thin plate of host and ore between Cambro-Ordovician carbonates and diabase below and the Triassic sediments above should probably be considered as a zone of tectonic weakness subject to repeated readjustment by brecciation and microfracturing, perhaps during final basinal tilting (earlier, Paleozoic brecciation also occurred; see Part 2, "Structure)."

In general, both metallic and gangue minerals are finer-grained toward the hanging wall and are mixed coarse- and fine-grained at the footwall (Plates 10-B and D and 11-A and B). This is particularly true for diopside and actinolite. Grain size also crudely follows laminated texture of the replaced units, alternating coarser- with finer-grained laminae (Plates 9-A, B, and C). This textural lamination is less pronounced for magnetite replacement than for gangue silicates. Grain size is also dependent upon the kinds of minerals and their sequence of crystallization. This is particularly true for minerals of the ore stage, the grain size of which depends on the amount and type of previously crystallized metamorphic silicates. For example, large amounts of diopside, which is more difficult to replace, (Plate 10-D) limit the amount of later magnetite (see "Mineral Paragenesis") and tend to result in finer-grained ore minerals. Maximum grain size of ore minerals is attained by direct replacement of limestone or secondary calcite (Plate 10-B). To a minor extent, particularly along the southwestern footwall of the eastern ore body, flow textures resulting from late shearing have modified the metamorphic silicate gangue by imposing a foliation and brecciation (Plate 6).

Mineralogy of the Eastern Ore Zone

The composition of the ore zone is the result of several, crudely consecutive, processes: thermal metamorphic reconstitution, metasomatic permeation, ore-stage mineralization, and secondary alteration.

The major metallic minerals present, listed in approximate order of decreasing abundance, are magnetite, pyrite, chalcopyrite, and hematite. Minor metallic minerals include bornite, chalcocite, covellite, native copper, galena, marcasite, millerite, pyrrhotite, sphalerite, and wurtzite. The major gangue minerals associated with the main stage of ore deposition are actinolite and chlorite. Other minerals found within the ore zone are listed in Appendix 1. The most common ore mineral associations are magnetite-chalcopyrite-pyrite (-sphalerite), magnetite-pyrite-actinolite (-phlogopite), magnetite-chlorite-orthoclase or magnetite-chlorite-zeolite (-pyrite), magnetite-hematite-calcite (-zeolite), and magnetite alone (Plates 7 and 8). Pyrite may be present in any of the above associations but is frequently of more than one generation (relative both to magnetite and to gangue). Details of individual mineral occurrences given below are taken from studies of the eastern ore body, which has a more complex mineralogy, particularly with respect to gangue minerals, than the western ore body studied by Hickok (1933). Among the metallic minerals, wurtzite (4H and/or 6H polymorphs) and pyrrhotite were not positively identified from the western ore body, although they may have been present. Pyrrhotite has been identified from the East End open pit. Native copper was found near the surface at the eastern end of the open pit (western ore body) and some was found on the dump in the underground samples taken from the western ore body. Pink, spotted ore (the so-called "aplitic ore" containing hematitic or ferriferous orthoclase) has been reported only from the eastern ore body.

Cornwall magnetite ranges in morphology from anhedral-granular to euhedral (Plates 6-11) in octahedrons and dodecahedrons modified by octahedral faces. Where both are present in composite grains (Plate 10-B), massive and granular ore has been replaced or capped by crystalline vug ore. As illustrated in Plate 8-A, the former is light gray in reflected light (the blue magnetite of Callahan and Newhouse, 1929) and the latter euhedral replacement is darker gray (the brown magnetite of Callahan and Newhouse, 1919). Two similar types of magnetite occur at Morgantown (Sims, 1929). Davidson and Wyllie (1965, p. 770) note that many cores of platy magnetite have a lighter, bluish cast and tend to be richer in iron and poorer in magnesium, aluminum, titanium, vanadium, silicon, and calcium than the brownish rims. Cores also frequently contain oriented inclusions richer in magnesium and/or aluminum than matrix magnetite (Davidson and Wyllie, 1965, p. 760-769). Most magnetite crystals near the footwall or magnetite replacing hematite crystals are zoned or contain patches of different reflectivity. Magnetite elsewhere in the ore body is not noticeably zoned (Plates 7 and 8), especially for non-equant, granular or massive, and anhedral ore. Where the magnetite is not zoned, it is not possible to distinguish "blue" and "brown" types; hence, composition of unzoned ores cannot be estimated by petrographic observation. However, the data of Davidson and Wyllie (1965) show that early, "blue," platy magnetite is richer in iron than later magnetite, possibly as a result of contamination of the later ore fluid during transport. Another possibility is that the early cores represent a reduction of essentially pure hematite to magnetite before the main stage of multi-cation introduction.

Platy magnetite after hematite (Plate 10-A) is primarily concentrated at the ore hanging wall, secondarily at the footwall, and rarely between these extremes. At the hanging wall, where both calcite cleavages (secondarily recrystallized) and hematite are present, magnetite frequently has capped hematite but is not otherwise present in the calcite. The hematite crystals are located along the principal calcite cleavage directions and hence both calcite and hematite existed before magnetite formation. Such occurrences at the hanging wall favor hematite reduction rather than preferential replacement. Micro-faulting and folding followed (Plates 6 and 7-B).

The replacement of magnetite by later metallics, either sulfides or later magnetite, took place along planes parallel to the (111) face of magnetite (Plates 7-C and 8-A and B). Oriented overgrowths of chlorite are common. Inclusions of gangue within magnetite grains illustrate interrupted growth. Octahedral faces are occasionally cavernous, probably indicating differential growth rates rather than crystal etching. Large euhedral crystals and grains occur near the footwall but are not present at the hanging wall where magnetite "dust" is common.

Pyrite is ubiquitously present in simple and exceedingly complex crystals. Simple cubes, frequently as limonite pseudomorphs, have been found in the surrounding area. The Mill Hill Slate west of Cornwall is pyritized. In the ore zone, pyrite crystallization has spanned the period of ore mineralization (Figures 24 and 25; Plates 7-A and 8-C) through that of zeolite crystallization (colloidal pyrite "dust" on stilbite). Late pyrite veins transecting magnetite-actinolite foliation frequently show crystal terminations (Plate 8-C and Figure 24). Pyrite extends beyond the magnetite-ore hanging wall and into hornfels. Crystals of pyrite are notable for their cobalt content (as in French Creek pyrite) which, based on semi-quantitative X-ray fluorescence analyses, may exceed two percent. The possibility of spatial or morphological control on the cobalt content of pyrite is not known. Other spectrographically determined trace elements include arsenic, bismuth, copper, lead, silver, zinc, and nickel (Table 18).

Pyrrhotite in crystals of hexagonal outline has been found associated with calcite and minor magnetite in serpentinized and steatitized portions of the ore body. Its distribution is not known. Several X-ray patterns indicate that its symmetry is actually monoclinic.

Chalcopyrite occurs as massive pods or veins replacing pyrite and magnetite (Plate 7-C) along preferred crystallographic planes and in veins transecting the laminae of magnetite and gangue silicates. Sphalerite occurs sparsely during the end of chalcopyrite crystallization, replacing both chalcopyrite and pyrite (Plate 8-B and Figure 25). Some of the late sphalerite is a pale-yellow, iron-poor variety.

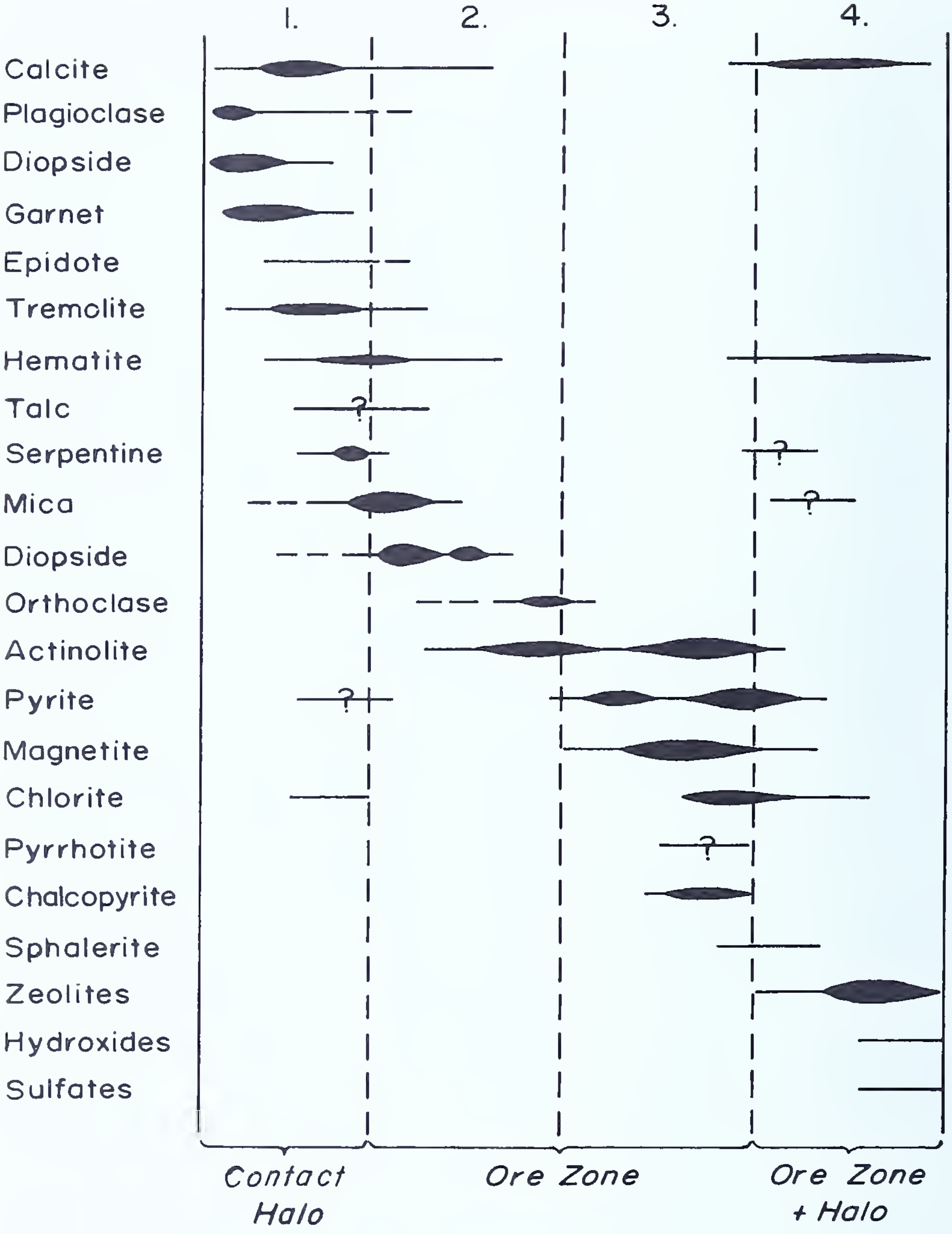

after Lapham (1968)

Figure 25. Paragenesis of minerals in the ore zone of the eastern ore body. Width of line indicates approximate quantity of mineral development. A "?" indicates uncertain paragenetic position. Arbitrary divisions (see text) are: 1. contact metamorphic mineralization, 2. metasomatic and hydrothermal silication, 3. hydrothermal ore deposition, 4. low temperature - secondary mineralization.

Except for the previously noted hematite, the other metallics are of minor importance and occur as fracture fillings or interstitially among the major metallic and gangue components. Millerite, marcasite, wurtzite, cuprite, malachite, azurite, some pyrite, and probably bornite and covellite are secondary minerals most frequently found at the present erosion surface.

Actinolite and, to a lesser extent, chlorite are almost universally associated with magnetite ore. Together, they impart the banded, green color so characteristic throughout the ore body (Figure 24). The actinolite associated with magnetite occurs in slender prisms or needles with nearly parallel extinction (i.e., a high-iron variety) and is the youngest of two types of actinolitic amphibole. The older, lower-iron actinolite has a greater extinction angle (up to 28°), is coarser-grained, occurs only near the footwall (see "Zonation"), and is replaced by magnetite parallel to the actinolite (100) cleavage. Both varieties are colorless to pale green in thin section. Byssolite is characteristic of vug ore associated with zeolites.

Chlorite associated with magnetite has anomalous blue interference colors and is iron-rich. Earlier chlorite associated with alteration of early actinolite and later chlorite associated with zeolitization are less iron-rich. Chlorite associated with serpentinization and steatitization is magnesium-rich. It is more abundant in the more aluminum-rich Blue Conglomerate matrix than in the Mill Hill Slate. Cross-cutting magnetite veins usually are zoned with actinolite walls and chlorite-magnetite cores in exactly the same way as the ore veins in diabase. The extent of amphibole chloritization increases as the amount of magnetite increases.

Several varieties of mica occur at Cornwall. The majority of it is a dark-green, iron-rich mica with low 2V similar to the phlogopite of Hickok (1932). Rarely, it is interleaved with chlorite in veins (a more common occurrence at Morgantown, Pennsylvania). Zircon inclusions are sometimes present. Pink muscovite (coating) was found on the Big Hill dump, apparently a late crystallization. Although no shift in spacings from normal 2M-muscovite was found, a semi-quantitative spectrographic analysis showed 0.1 to 0.5 percent Na_2O (and a trace of MnO) corresponding to about 2.5 percent paragonite by weight.

Garnet is present in the hanging wall of the ore body, commonly associated with hematite, and in Triassic sediments. In the ore zone, they are almost wholly restricted to the north, or upper, part of the eastern ore body where Mill Hill Slate hornfels predominates in the hanging wall and where sufficient calcium and silica were available. X-ray data (Appendix 2) indicate that all occurrences are chemically similar and are composed largely of the andradite end-member.

Serpentine with minor talc occurs sporadically throughout both major ore bodies and the East End ore body. In the eastern mine, it occurs most notably in the west-central part of the ore body and in recrystallized limestone above the ore hanging wall with brucite. According to Faust (1963), the Cornwall serpentine contains less nickel, calcium, cobalt, and selenium than serpentine associated with ultramafic rocks.

Plagioclase occasionally is present throughout the ore zone but particularly on the northeast (up dip) in Mill Hill Slate. The plagioclase is calcic (oligoclase to labradorite). It is associated with potassic feldspar that exhibits both microcline grid and Carlsbad twinning.

Numerous zeolites occur throughout both major ore bodies (Appendix 1). Particularly fine specimens of heulandite, apophyllite, and analcime came from the western ore body. Large scalenohedral calcite crystals, with stilbite and pyrite coatings and tufted natrolite with byssolite, have come from the eastern ore body. Veins of prehnite and datolite have been found in the upper part of the diabase and in overlying hornfels units.

Chemistry of the Eastern Ore Zone

Chemical changes in the ore zone reflect the mineralogical alterations consequent upon both metamorphism and ore mineralization (Table 16). Comparison of the Buffalo Springs Formation (assuming it to be the host limestone), the Blue Conglomerate, which forms much of the ore hanging wall and down dip is in contact with diabase, and gangue from the ore

Table 16. *Chemical Changes in the Ore Zone of the Eastern Ore Body*

	(1)	(2)	(3)
SiO_2	12.61	52.11	42.76
TiO_2	N.A.	N.A.	0.64
Al_2O_3	2.24	23.75	10.78
Fe_2O_3	0.95	3.66	5.82
FeO	N.A.	5.90	4.02
MnO	N.A.	N.A.	0.133
MgO	12.88	2.72	20.13
CaO	32.24	2.54	6.83
Na_2O	N.A.	3.98	0.27
K_2O	N.A.	2.41	5.43
PO_2	N.A.	N.A.	0.190
CO_2	39.09	0.66	0.37
F	N.A.	N.A.	0.163
S	N.A.	N.A.	0.013
H_2O comb.	N.A.	2.27	2.45
	100.00	100.00	99.999

N.A. = No analysis determined

1. Avg. of 8 samples of Buffalo Springs Formation (O'Neill, 1964).

2. Blue Conglomerate (Appendix 4-B).

3; Avg. of 2 gangue samples, footwall and hanging wall (Appendix 4-B).

footwall and hanging wall are representative only of gross chemical changes. Most such changes occurred before ore stage mineralization (see Part 3). Footwall and hanging-wall gangue samples have been averaged (Table 16, column 3) to yield gross chemical trends. Neither alone would be representative because of the varied effects of alteration of these ore zone units.

There is very little chemical evidence of the original host-limestone composition (also see Part 3). Laminations preferentially replaced by gangue rather than ore were richer in SiO_2 and MgO, and perhaps also in Al_2O_3. It is possible that silicon and aluminum migrated up dip by ore-fluid leaching of the Blue Conglomerate hornfels from down dip where it is in contact with diabase. Lack of ground-mass quartz in the Blue Conglomerate might be explained in this manner. CaO and CO_2 have been removed from the system. If leaching of the Blue Conglomerate occurred, sodium also has left the hornfels-host limestone system. K_2O in mica and in minor feldspar has been added to the limestone during metasomatism. There is no necessity for migration of magnesium from the host rock since ore replaced lime-rich portions of the Buffalo Springs Formation and gangue replaced magnesium-rich portions. The Fe^3/Fe^2 ratio in the ore zone is approximately that of magnetite so that, except for areas rich in relict hematite, an approximately uniform oxidation has been attained. Comparative chemical analyses of the hornfels and limestone units show that in the ore area iron has been added rather than subtracted, although there is no petrographic evidence of massive magnetite ore in these samples.

Spectrographic analyses of several different occurrences of magnetite ore and vug crystals from Cornwall are compared with magnetite from Sterling Lake and Mineville, New York in Table 17. The New York occurrences are not contact metasomatic limestone deposits and the ores contain considerably more apatite than the Cornwall ores. Unit-cell dimensions for some of the magnetite samples also are given for comparison. Two of the sample separates (samples 3 and 4, Table 17) contained visible sulfides; the remainder of the samples did not appear to have any impurities. However, some silicate gangue apparently was present in samples 3 and 6 (Table 17). Elements other than those listed were below detection limits.

The Cornwall ores contain noticeable amounts of boron, cobalt, manganese; nickel, titanium and vanadium. The nickel, titanium and vanadium contents at Cornwall are low in comparison with the New York magnetite samples. The low titanium content of magnetite in ores from Cornwall, and in ores in Pennsylvania magnetite ores in general, is a notable feature that distinguishes these deposits from most other magnetite ores. A high boron content may be characteristic of metasomatic magnetites that have replaced limestone (personal communication, Joseph Worthington). Boron is somewhat higher in magnetite that has replaced a pre-existing gangue silicate (sample 5). Boron also tends to be higher nearer the footwall than the hanging wall. Sodium maxima follow boron and also may indicate a sediment source. Copper in magnetite increases away from the footwall of the southwestern side of the eastern ore body toward the hanging wall and northward. This is the same pattern followed by total copper in the ore body (see "Zonation-Selected Chemical Constituents"). In part, this may be due to included sulfide impurities in the separated magnetite from one of the two hanging wall samples. Since the high nickel values are in samples high in sulfide impurities, it is probable that most of the nickel is not in the magnetite lattice.

Table 17. *Spectrographic Trace Element Analyses of Magnetite (wt. %)*

	1.	2.	3.*	4.*	5.	6.	7.
B	.008	.03	.009	.006	.002	—	—
Be	.0001	.00005	.00005	—	—	.0002	—
Ca	3.	1.	.8	.8	.08	—	<.2
Co	.006	.02	.004*	.04*	.03	.002	.015-.03
Cr	.004	—	—	—	.005	.004	.02-.22
Cu	.0006	.0008	.004*	.05*	.04	.0005	0.0-.004
Ga	.002	.002	.0015	.0015	.001	<.001	—
Mg	1.	.9	.4	.5	.9	—	—
Mn	.08	.03	.03	.05	.08	.05	—
Na	.09	.15	.15	.02	.03	—	<0.2
Ni	.02	.007	.01*	.03*	.003	<.002	.02-.072
Si	—	—	3.	—	—	<.1	—
Ti	.06	.05	.03	<.01	.04	.4	1.1-2.0
V	.04	.003	.04	.009	.006	.0075	.19-.2
Zn	—	—	—	.005	.005	.002	—

*Contains some unseparated sulfide

1. Southwest footwall, Cornwall
2. South-central footwall, Cornwall; $a_o = 8.407 \pm .002$Å
3. Southeast footwall, Cornwall; $a_o = 8.411 \pm .002$Å
4. East-central hanging wall, Cornwall; $a_o = 8.391 \pm .002$Å
5. North-central hanging wall, Cornwall
6. Avg. of 3 samples from Mineville, N.Y. (Samples courtesy of Republic Steel Co. Inc.) avg. $a_o = 8.397 \pm .002$Å
7. Range of 3, Sterling Lake, N.Y. (analyses expressed as oxide) (Hanger, Collins, and Clemency, 1963)

None of the above elements alone appears able to explain the differences in unit cell a_o. Changes in cobalt, nickel, and titanium are all approximately in the correct direction of unit-cell change (Table 17), but their variation is not strictly parallel to a_o variation. Although increasing titanium would be expected to increase the cell edge, the high-titanium New York magnetites have a low cell edge compared with some Cornwall magnetites. Both cobalt and nickel have cationic radii very close to that of Fe^2 and would not alone be expected to cause this magnitude of change. In addition, they probably are present largely in sulfide impurities. It is suggested that in addition to a possible combination of the above element substitutions, differences in Fe^3 Fe^2 may be a principal cause of cell size. The possibility of excess Fe^3 in Cornwall magnetites remains to be investigated. Several analyses of Cornwall magnetites were made that suggest considerable excess Fe_2O_3, but the amount of excess was so great that the analyses are considered suspect and are not presented. Either of these causes, element substitution or oxidation variation, may be a consequence of zoned magnetite grains (Davidson and Wyllie, 1965); in particular, brown magnetite may correspond to the more Ti- and V-rich analyses (Davidson and Wyllie, 1965). However, zoned (or "blue" versus "brown" magnetite) compositional differences should be evident from spectrographic and major element analyses. Such a correspondence is not evident from these analyses. Data are insufficient at this time to make any definite correlation.

Spectrographic analysis of a single sample of pyrite from ore is given below (Table 18):

Table 18. *Spectrographic Analysis of Pyrite (Wgt. %)*

Ag	0.00005
As	0.02
Bi	0.00006
Ca	0.05
Co	2. (est.)
Mg	0.09
Ni	0.1
Pb	0.005
Zn	0.0015

The presence of noticable calcium and magnesium probably indicates some carbonate impurity in the pyrite separate. Cobalt, nickel, and arsenic are present in significant amounts. Other elements are quite low or were below the limit of detection (not reported in Table 18).

A summary of sulfur isotope data from Cornwall, Dillsburg, and French Creek ore samples is given in Table 19. The δS^{34} (0/00) values for Cornwall are noticeably higher than in diabase (cf. Table 30), whereas the values for Dillsburg and French Creek ore samples more closely approaches the δS^{34} (0/00) of late diabase differentiates. The cause of the great range in Cornwall values remains to be investigated. However, it is clear that greater enrichment in S^{34} has occurred at Cornwall than at the other magnetite deposits. Although Smitheringale and Jensen (1963) have shown that there is enrichment in S^{34} as differentiation proceeds, it seems doubtful that the extent of enrichment shown at Cornwall could have been produced by this method, especially since there is a greater volume of differentiates at Dillsburg, yet the S^{34} enrichment there is less. Therefore, it seems likely that enrichment at Cornwall represents greater crustal contamination of S^{34} such as might accrue from a longer crustal transport path for the ore solutions (also see Part 6, "The Triassic Metallogenic Province").

Table 19. *Sulfur Isotope Abundance In Cornwall Ores*

	δS^{34}o/oo)
*Pyrite, Middle Hill	+ 0.9
*Pyrite with hematite (Mill Hill Slate?)	+10.4
*Chalcopyrite	+ 8.6
*Pyrite with magnetite (Big Hill)	+10.0
**Pyrite	+10.3
**Pyrite	+17.0
**Pyrite	+ 9.9
**Avg. of 7 Cornwall	+ 9.6
**Avg. of 3 Dillsburg	+ 5.2
**Avg. of 3 French Creek	+ 5.4

* Ault and Kulp (1959)
** Smitheringale and Jensen (1963)

Mineral Paragenesis

A generalized paragenetic diagram for the eastern ore body (Figure 25) is similar in broad outline to that derived by Hickok (1933, p. 232) for the western ore body. Maximum amounts of mineral crystallization are indicated crudely by line thickness. Mineral associations (Figure 25) have been divided, somewhat arbitrarily, into four groups: 1) an outer halo chiefly representing contact thermal metamorphic minerals; 2) the development of metamorphic and metasomatic silicates in the ore zone before the onset of metallic mineralization; 3) the main ore stage with continued silicate mineral crystallization; and 4) final low temperature mineralization and weathering products. Only the major minerals are illustrated; many trace minerals, especially of secondary origin, are present (Appendix 1). However, such a generalized diagram obscures significant details. Notably erroneous is the impression of a consistent time sequence throughout the ore zone, whereas in actuality mineralization proceeded by the migration of chemical and thermal fronts such that in the eastern ore zone the development of minerals near the hanging wall postdates the formation of the same minerals nearer the footwall. In addition, the migrating crystallization fronts of some minerals moved more rapidly than those of others. The extent to which differential migration has occurred is largely unknown, but it also probably is sufficient to make time sequence comparisons from one part of the mine to another unreliable. Paragentic zoning is discussed under "Zonation."

Predominant among the significant paragenetic relationships is the consistent replacement of contact metamorphic minerals by metasomatic silicates and their replacement, in turn, by ore minerals (Plates 9-11). Near the footwall, early phlogopite, diopside (coarser-grained), zoisite, and garnet (replacements of recrystallized calcite or Blue Conglomerate) are mantled by later metasomatic diopside (finer-grained), muscovite, and actinolite (coarser-grained). The early diopside fills contraction cracks in the top of the diabase. These metasomatic minerals are in turn replaced or mantled by pyrite, magnetite, fine-grained actinolite, and chlorite. The sequence of these groups is consistent at any one level above the footwall and across the dip, illustrating a time separation between cooling of the emplaced diabase sheet and ore deposition. Silicate metasomatism in the host limestone indicates local introduction of silica, aluminum, potassium, sodium, and possibly some iron.

The two periods of diopside formation within the ore zone (Figure 25) are largely spatial phenomena. Coarser-grained diopside predominates along the footwall, and finer-grained diopside attains a maximum about midway between the footwall and the hanging wall (Figure 26). Actinolite, on the other hand, is present along the footwall in both coarse blades (extinction angle up to 28°) and fine felted needles (extinction angle usually 0° to 10°) associated with magnetite (Plate 11-A). The latter pair replace coarse actinolite along the principal "c"-axis cleavage, resulting in a ragged, feathered termination (Plate 11-A). Away from the footwall, only fine-grained actinolite is present (Plates 10-D and 11-B), except for late byssolite fibers in zeolitic vugs.

Magnetite and chalcopyrite replace early pyrite along the principal cleavage directions and also embay it (Plate 7-A), resulting in highly corroded pyrite anhedra. Chalcopyrite and a later generation of pyrite fill interstices between magnetite grains or fill fractures or, more rarely, replace the preexisting magnetite (Plates 7-C and 8-C). Where magnetite replaces coarse-grained footwall amphibole (Plate 11-A), the amphibole has been protected from chloritization and fine-grained amphibole replacement. Magnetite only rarely replaces diopside and then only the coarser-grained crystals. More commonly, isolated diopside grains have acted as a nucleation growth center for magnetite crystallization (Plate 10-D). Where hematitic or ferriferous orthoclase is present, it may be mantled or cut by magnetite along pre-ore fractures. Where calcite is present with specular hematite, magnetite appears

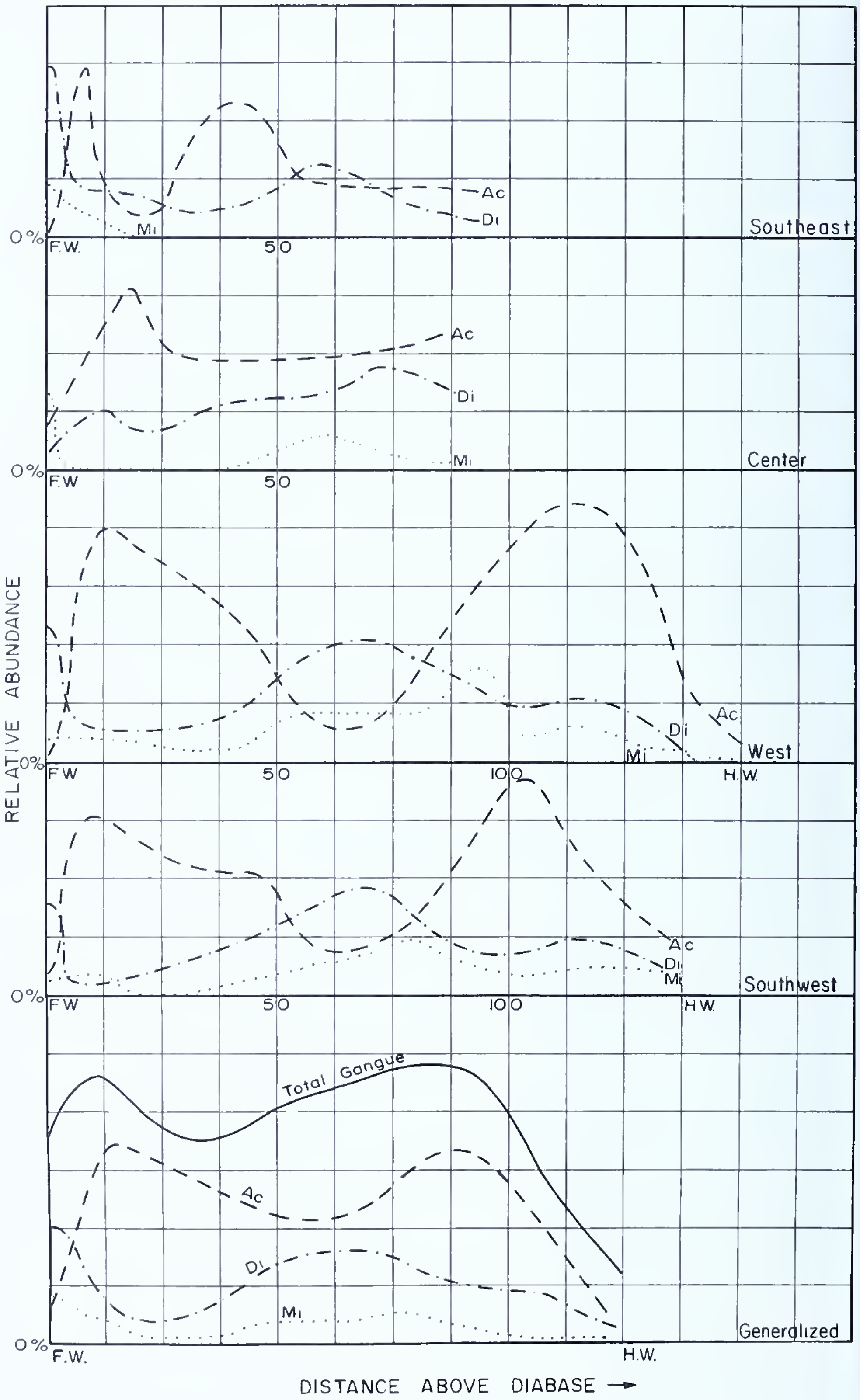

Figure 26. Mineral distribution in the eastern ore body from footwall to hanging wall; smoothed curves for actinolite (Ac), diopside (Di), and mica (Mi). Generalized section represents idealized distribution.

to have replaced hematite preferentially, although the relationship may be one of oxide reduction rather than replacement. Where calcite is present with amphibole, magnetite has selectively replaced calcite or, if replacing both, is euhedral toward calcite and anhedral toward amphibole (Plate 10-B). Where the pre-ore gangue is largely phlogopite (or muscovite) and fine-grained actinolite, magnetite preferentially replaces the finer-grained actinolite, only penetrating mica along its cleavage (Plate 10-C).

To summarize the paragenetic relationships of magnetite, it crystallized 1) after the solidification of the diabase chilled margin, 2) after hematite formation, 3) after amphibolitization of olivine phenocrysts in the chilled margin (see Part 5, "Petrology - Chilled Margin"), and 4) after the contact metamorphic crystallization of phlogopite, tremolite, coarser-grained diopside, and garnet in the host limestone. Magnetite is approximately contemporaneous with 1) sulfide mineralization, 2) a fine-grained amphibolitization, and 3) some alteration of the chilled diabase margin (sericitization and iron introduction). The formation of magnetite preceeded the formation of late pyrite, quartz, chlorite, byssolite, calcite, zeolites, and local shear foliation development.

These observations lead to the following generalized selective replacement series in which magnetite exhibits increasing difficulty of replacement: hematite - calcite - fine grained actinolite - pyrite - mica - coarse-grained amphibole - feldspar - pyroxene - quartz.

Secondary, or at least very late, magnetite is present. Occasionally, vugs of zeolite crystals, particularly analcime, are lightly dusted with magnetite in association with pyrite. Such vugs are usually rich in byssolite. In zeolite vugs, some of the sequences observed are 1) magnetite - calcite - stilbite - pyrite, 2) magnetite - apophyllite, analcime - natrolite and byssolite, 3) orthoclase - magnetite and chlorite - actinolite - prehnite.

ZONATION

Mineralogy

Mineral zonation is not a conspicuous feature of the Cornwall ore body. However, subtle variations do exist and are genetically as well as spatially significant. If a larger area of the ore bodies had been available for study (before drift cementing and mining out of upper levels), possibly more definite relationships would have become clear.

The only previous studies of zonation have been concerned with diopside-actinolite and metallic - silicate mineral distribution from the western ore body. Hickok (1933, p. 230-231) noted a concentration of diopside near the diabase which gradually gave way to a zone of actinolite near the hanging wall. He also noted platy magnetite along the hanging wall and garnet along the footwall. Earlier, Callahan and Newhouse (1929, p. 409) had noted a similar distribution and had stated "toward the upper part of the ore body the pyrite and chalcopyrite increase in amount...." They also noted (p. 409) that "the silicate minerals are most concentrated toward the diabase" and "magnetite, pyrite, and chalcopyrite are all most abundant in that part of the ore body which is farthest from the diabase." As has been shown, much of the concentration of silicates near the diabase is a consequence of the formation of contact-metamorphic silicates. Later metasomatic silicates, previous to formation of the ore, reinforced this concentration and penetrated beyond the contact mineralization limits. In part, because these silicates are replaced by magnetite only with difficulty, and in part because there was less available carbonate for emplacement by the time of ore introduction, the maximum concentration of ore minerals lies above (toward the hanging wall) both types of silicate mineralization.

Data for the following discussion were all taken from diamond drill cores and hand-specimen sampling of the eastern ore body, largely from the southern (down-dip) portions. The mineral distributions are not strictly in accordance with those cited by Hickok (1933) for the western ore body. Because of the presence of Mill Hill Slate and Blue Conglomerate above this eastern ore body, composition of host rocks has exerted a greater control than to the west where the ore zone hanging wall generally terminates in limestone.

Grain size and textural distributions have already been noted. In general, contact-metamorphic minerals form a tabular aureole approximately paralleling the upper surface of the diabase sheet. The later silicate and metallic mineralization that extends farther above the sheet is more conical (see Figure 33) but is less extensive up dip and is essentially absent outside the mine area. Other controls on grain size and textural distribution include mylonitization and brecciation (Plates 6 and 9), composition of the host rocks (Plate 9), texture of the host rocks (Plate 10), and the time migration of thermal and chemical fronts (Plate 11 and Figure 25). Many of these variables appear to be related to the southwestern and south-central part of the eastern ore body (Figures 26-33). For example, in this area of the mine, both the diabase (especially plagioclase and olivine) and the ore zone are more extensively altered and sheared than is apparent elsewhere. In the hanging wall of this area, diopside (on the southwest) and actinolite (west and south-central) extend beyond the limits of magnetite ore (Figure 33), and magnetite, in turn, extends beyond specular hematite. Elsewhere, the silicate aureole is less extensive and magnetite extends to, or beyond, silicate metasomatism and terminates against hornfels in association with specular hematite. In part, these relationships may represent ore-zone telescoping against a less permeable barrier, but ore termination is also evident in limestone (particularly to the northwest and west), and beyond the limestone - hornfels contact into Mill Hill Slate and Blue Conglomerate. This extension into hornfels units is also in the area of maximum potassium metasomatism ("aplitic" ore), ore veins in diabase, and vug ore at the footwall-diabase contact.

In the eastern ore body, garnet is confined almost exclusively to the northern half where there was sufficient calcium available in the Mill Hill Slate hanging wall. In the hanging wall above the southern part of the eastern edge of the western ore body, a four-inch vein of massive datolite fills a fracture in both diabase and ore. Sparse fluorite is associated with orthoclase in granophyric diabase on the western edge of the eastern ore body and was detected in one sample of orthoclase-rich ore collected on the Big Hill dump.

These data indicate that a single metasomatic aureole is an over simplification. Different minerals, or mineral associations, exhibit different distribution patterns so that each may be said to have its own aureole, or limits. Exceptions to these generalizations exist but do not obscure the essential validity of zonation. Of particular interest is the distribution of the three major gangue minerals, diopside, actinolite, and mica, above the ore footwall (Figure 26). Four sections from diamond drill cores illustrate differences from footwall to hanging wall from east to west and to the southwest across the eastern ore body. A generalized distribution diagram of the spatial distributions is also included. Diopside (and to a lesser degree mica) shows two maxima: one, at the footwall, of coarser grain size, and a second, near the center of the ore zone (at 60 feet to 90 feet above the footwall), of finer grain size. Actinolite shows a similar bimodal distribution (at 10 to 20 feet and 40 to 120 feet), but with maxima displaced beyond diopside maxima toward the hanging wall. These resemble shells or envelopes of lower temperature metasomatism toward the hanging wall. Distribution of diopside and actinolite is not spatially inverse except on the west but is inverse when together they are compared with metallic mineral concentration (not illustrated). This is a consequence of the difficulty of replacement of these earlier minerals by magnetite rather than a function of ore solution source or temperature-gradient distribution. An exception to this replacement rule may be the concentration of magnetite at the footwall along the western and southwestern portions of the ore body. Here silicates, particularly actinolite, have been noticeably replaced by ore. Magnetite, although more varied, generally has two maxima: one near the footwall and a second at least 40 to 60 feet above the footwall. A third occasionally is present near the hanging wall.

In Figure 26, a crude zonal arrangement can be discerned extending outward from the southwest and south-central footwall. To the north, up dip, diopside maxima are of greater amplitude farther from the footwall (see center and west sections, Figure 26). Actinolite is similarly displaced beyond diopside toward the north and toward the hanging wall. Chlorite (not illustrated) appears to parallel the actinolite distribution except where there is a hanging wall magnetite concentration. Here chlorite is also abundant.

Although these gangue distributions appear to be generally correct, it must be cautioned that the data are drawn from only four complete sections and several partial sections comprising about 275 ore-zone thin sections. Overlap of spatial distribution and local irregularities are most certainly present so that zonation is not always obvious. No one part of the eastern ore body follows all of these generalizations; they emerged only from analysis of the entire ore zone.

One of the most interesting types of zoning is the paragenetic relationship between the finer-grained (younger) actinolite of the ore stage and magnetite. At the footwall in the central to southwestern part of the eastern ore body, magnetite replaces fine-grained actinolite which in turn has replaced coarse-grained actinolite and/or diopside (Plate 11). Up dip and north along the footwall, and also near the hanging wall, magnetite preceded the finer-grained actinolite (Plates 10 and 11). In areas between these extremes, the two minerals are essentially contemporaneous. Thus, magnetite-depositing ore solutions eventually overtook the migrating front of fine-grained actinolite crystallization.

Zoning of metallics is less pronounced. Chalcopyrite appears to have penetrated the least distance outward, magnetite is next, and pyrite is commonly outside the ore zone. However, pyrite is ubiquitous and chalcopyrite is much less abundant than the other two, so that this distribution may be more apparent than real. It is supported, however, by the distribution of total iron and copper (Figures 29 and 30).

In summary, the above paragenetic zonation illustrates early coarser-grained crystallization near the footwall and later finer-grained crystallization toward the hanging wall for both diopside and actinolite. For each grain-size pair, the actinolite is younger and farther from the southwest and south-central footwall than the corresponding diopside grain size. Only the youngest, the fine-grained actinolite, is closely associated in time with magnetite ore, and this relationship changes from earlier actinolite at the southwest footwall to earlier magnetite at the hanging wall. These mineral distributions indicate 1) migration away from the southwestern and south-central footwall, 2) different rates of migration by iron (-sulfur) and silicon-aluminum fronts, and 3) decreasing temperature of crystallization outward from the footwall focus.

Magnetite from the eastern ore body was magnetically separated from gangue minerals until it was pure under binocular microscope examination. Thirty-three different samples, including massive footwall ore, massive hanging wall ore, vug ore, banded ore, platy magnetite, diabase ore veins, and pink feldspathic ore, were ground and X-rayed with Cu K_α radiation to determine unit cell variation. Corrections were made for film shrinkage. For comparison, samples from the Fisher Hill Mine, Harmony Mine, and Old Bed Mine, Mineville, New York were also analysed. Two types of plots were averaged for unit cell values: 1) a_o vs. $\cos^2 \theta$ and 2) a_o vs. 2θ from high angle reflections (440) to (10. 2.2). No attempt was made to separate, or take into account, zoned magnetite. Thus the results discussed are bulk, average dimensions. Differences in re-runs and re-measurements generally are within ±.002 Å of the stated cell size.

As the cell sizes listed below (Table 20) show, there is no noticeable correspondence between texture and a_o (in Å):

Table 20. *Comparison of Ore Textures and Magnetite Unit Cell Dimensions for the Eastern Ore Body (± .002 Å)*

	Range	Avg.	No. Samples
Vug Ore	8.396 - 8.408	8.404	3
Feldspathic Ore	8.398 - 8.403	8.400	8
Platy Ore	8.393 - 8.403	8.398	3
Banded Ore	8.391 - 8.407	8.400	8
Vein Ore	8.395 - 8.411	8.399	4
Massive Ore	8.391 - 8.407	8.400	6

Most measurements of a_o at the footwall and hanging wall for vertical sections through the eastern ore zone show a larger unit-cell edge at the footwall than toward, or at, the hanging wall (Figure 27 and 28). Samples from intermediate depths usually show intermediate cell edges (within the ±.002 Å limits of error), but are occasionally somewhat greater than at either extreme (dashed contours, Figure 28). Including the vertical sections, a total of 10 footwall and 13 hanging wall unit-cell measurements (from replicate analyses) have been plotted and contoured (Figure 27 and 28). Both show a "ridge" of maximum a_o trending northeast-southwest. This ridge near the hanging wall is displaced to the northwest relative to the footwall ridge. The lowest dimensions are at the southwest footwall and the northeast hanging wall. From the southwest, the unit cell edge increases northeastward along the footwall. These a_o zonal distributions trend similarly to a prominent zone of faults, joints, and ore veins (Figure 23), to the previously described mineral distributions, and to metallic element zonation (see "Selected Chemical Constituents"). It is also interesting to note that the high a_o "ridge" at the hanging wall bends westward at the north end of the ore body toward the western ore body. A similar chemical trend is discussed subsequently. Whatever is the cause of the cell variation (substitution, defect structure, oxidation, mixed crystals), its distribution is relatable to iron-ore solution migration through the eastern ore body.

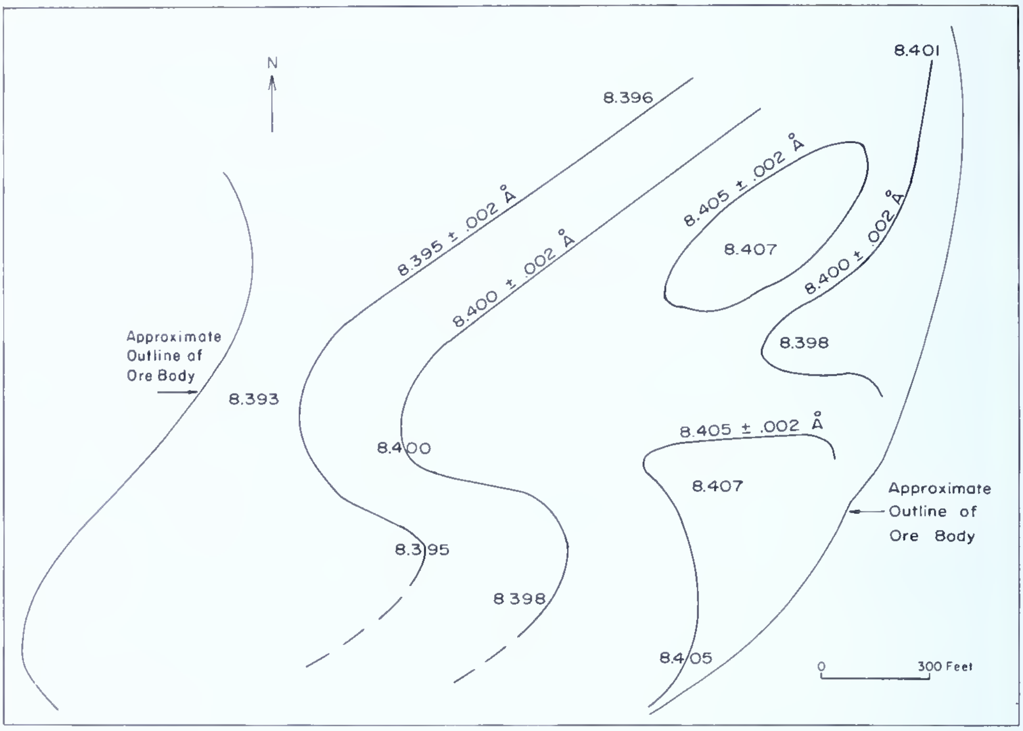

Figure 27. **Contours of magnetite a_o, in Angstroms, along the footwall of the central and southern parts of the eastern ore body, illustrating a northeast distributional trend (cf. Figures 23 and 28).**

Some speculations can be made with regard to the cause of cell-edge differences. Recently published a_o measurements of pure magnetite range from 8.391 Å (Turnock and Eugster, 1962) to 8.396 Å (Wones and Eugster, 1965, p. 1233). Other published cell dimensions range from 8.379 Å to 8.434 Å (Donnay and Donnay, 1963). The southwest footwall magnetites of Cornwall fall within the range of the most recent cell dimensions for pure magnetite. Although this suggests that substitution at Cornwall is not great, it does not prove it. The trace element composition of magnetites (Table 17) gives further evidence that substitution is quite limited. The up-dip and hanging-wall magnetites, on the other hand, might be suspected to exhibit greater substitution as a result of such factors as a longer migration path and changing ore solution composition. In the light of the few trace element analyses available for hanging wall magnetite (Table 17), this does not seem probable (see discussion under "Chemistry of the Eastern Ore Zone"). If, then, chemical substitution does not seem to be the major cause of a zonal distribution at Cornwall, compositionally mixed crystals would also be an unlikely cause. In view of this, it is suggested that excess Fe^3 may be present. If, for example, δ Fe_2O_3 (spinel structure) were present, the a_o of magnetite

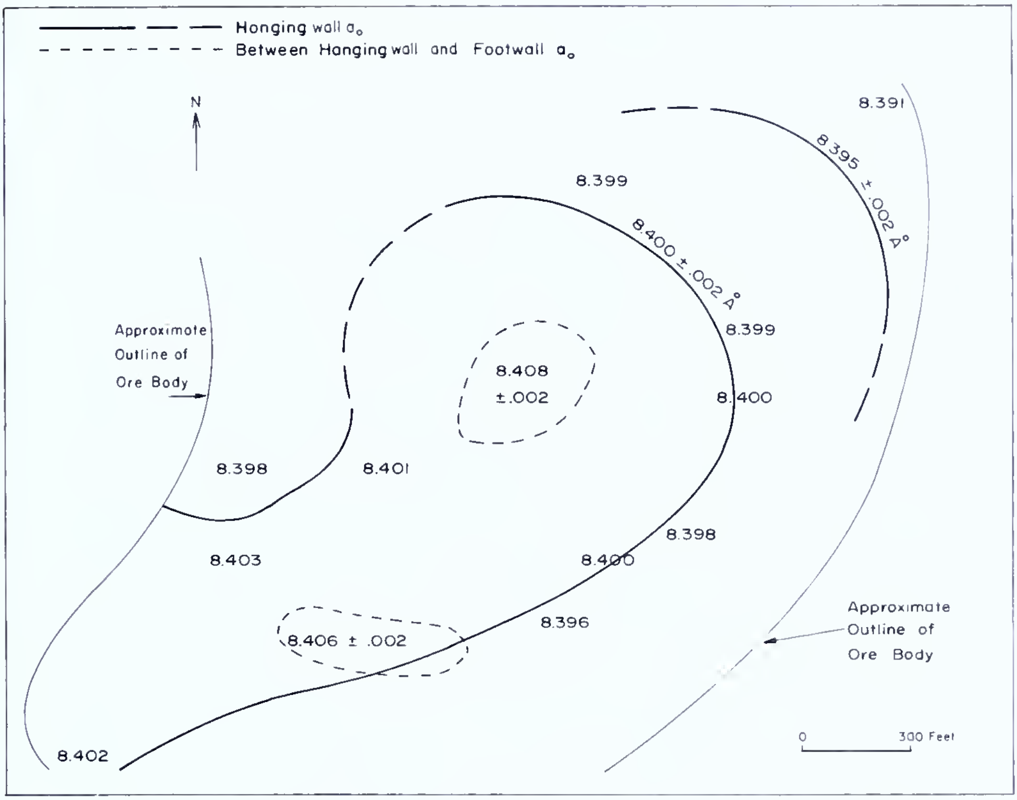

Figure 28. **Contours of magnetite a_0, in Angstroms, along and near the hanging wall of the central and southern eastern ore body, illustrating a northeast distributional trend (cf. Figures 23 and 27). Note shift in the trend of maxima between footwall (Figure 27) and hanging wall.**

would be decreased (a_0 of δFe_2O_3 ranges from 8.33Å to 8.35Å). This, in turn, could be interpreted to mean that for vertical sections through the ore zone, as a_0 decreases upward, Fe^3 increases proportionately. This is a reasonable expectation because oxidation (and replacement of hematite) might very well have increased as the ore solutions migrated upward through the sedimentary column.

Kullerud and Donnay (1967, p. 357) suggest another possible mechanism for the formation of an oxidized magnetite. They found that reaction between magnetite and pyrite in ores is common and that such a reaction can result in a ferrous-deficient magnetite. In addition, the superstructure diffraction lines characteristic of magnetite-oxygen reactions are not present in their experimental magnetite-sulfide reactions. Resultant magnetite compositions in magnetite-sulfide ore reactions are given as $Fe_{3-z}O_4$, where $0 < z < 1/3$. Depending on the length of reaction time and the temperature, a_0 values of 8.3945 Å and 8.3990 Å were experimentally produced. As a consequence, increasing sulfur-magnetite reaction increases the Fe^3/Fe^2 ratio and may increase the unit cell size. Because of the Cornwall zonal distribution of sulfur (Figure 31), increased reaction may be a prime cause of a magnetite variation at Cornwall. In view of the work of Kullerud and Donnay (op. cit.), Fe^2 tetrahedral vacancies should be sought in Cornwall magnetites.

Selected Chemical Constituents

Zoning of chemical constituents in the ore zone is more easily illustrated than mineralogical zonation. Numerous drill cores through the eastern ore body were analyzed for iron, copper, sulfur, and nickel by Bethlehem Steel Corporation as controls on the grade of the ore body. As a résult, there is good sample distribution for elements associated with ore stage mineralization. Trace element and gangue analyses have not been carried out, and their distribution is unknown. In general, the major cation distributions follow the same zonation trends as major-mineral distributions and reinforce the previously noted migration pattern. All data discussed below refer to the eastern ore body, although some inferences are made with regard to the western ore body.

The occurrence of iron at the footwall (Figure 29-A), at the hanging wall (Figure 29-B), and in an ore-body, average (Figure 29-C) contoured at five percent (total iron) intervals, illustrates the iron distribution, chiefly of magnetite. Along the footwall, the major maximum is in the south-central part of the ore body, with a secondary maximum to the north and northwest. At the hanging wall, this major maximum has shifted up dip to the north and northwest. This upward, northwestward migration is best illustrated in the pattern for average iron (Figure 29-C). Particulary interesting is the open contoured maximum leading toward the western ore body (upper left, Figure 29-C).

The distribution of copper in chalcopyrite, contoured at .05 percent copper and 0.10 percent copper intervals, also shows a zonation pattern. Here, however, the major footwall maximum is to the north and the major hanging wall maximum is to the south (Figures 30-A and B). Total average percent copper for the whole ore body (Figure 30-C) shows that the major concentration is to the north. Because magnetite preceded chalcopyrite, there was less replaceable host limestone available at the southern footwall for chalcopyrite deposition; hence, its distribution pattern is displaced toward the hanging wall and toward the north from that of iron. Once again, as with iron, there is a distinct hanging wall extension of copper concentration toward the western ore body at the northwestern edge (Figure 30-B). This concentration is near the observed occurence maximum of chalcopyrite in the East End open pit between the major western and eastern ore bodies.

Total percent sulfur at the footwall and hanging wall and average sulfur percent for the eastern ore body contoured at .02 percent intervals illustrate a more varied pattern but have essential characteristics in common

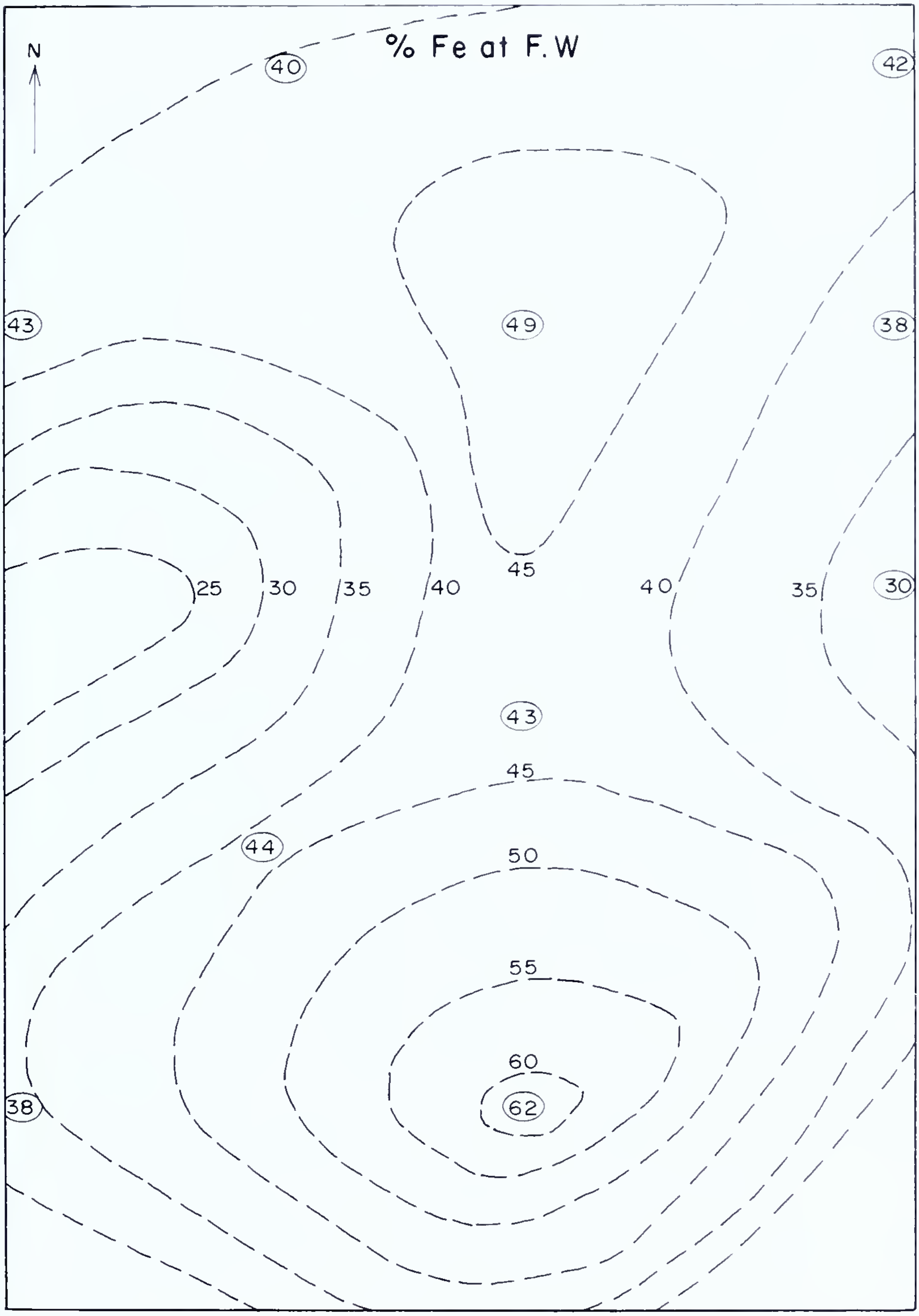

Figure 29A- Footwall. Distribution of total and average percent Fe in the eastern ore body; borders of diagrams are approximately at ore-body limits. Contour interval - 5% Fe. From drill core analyses, courtesy of Bethlehem Steel Corp.

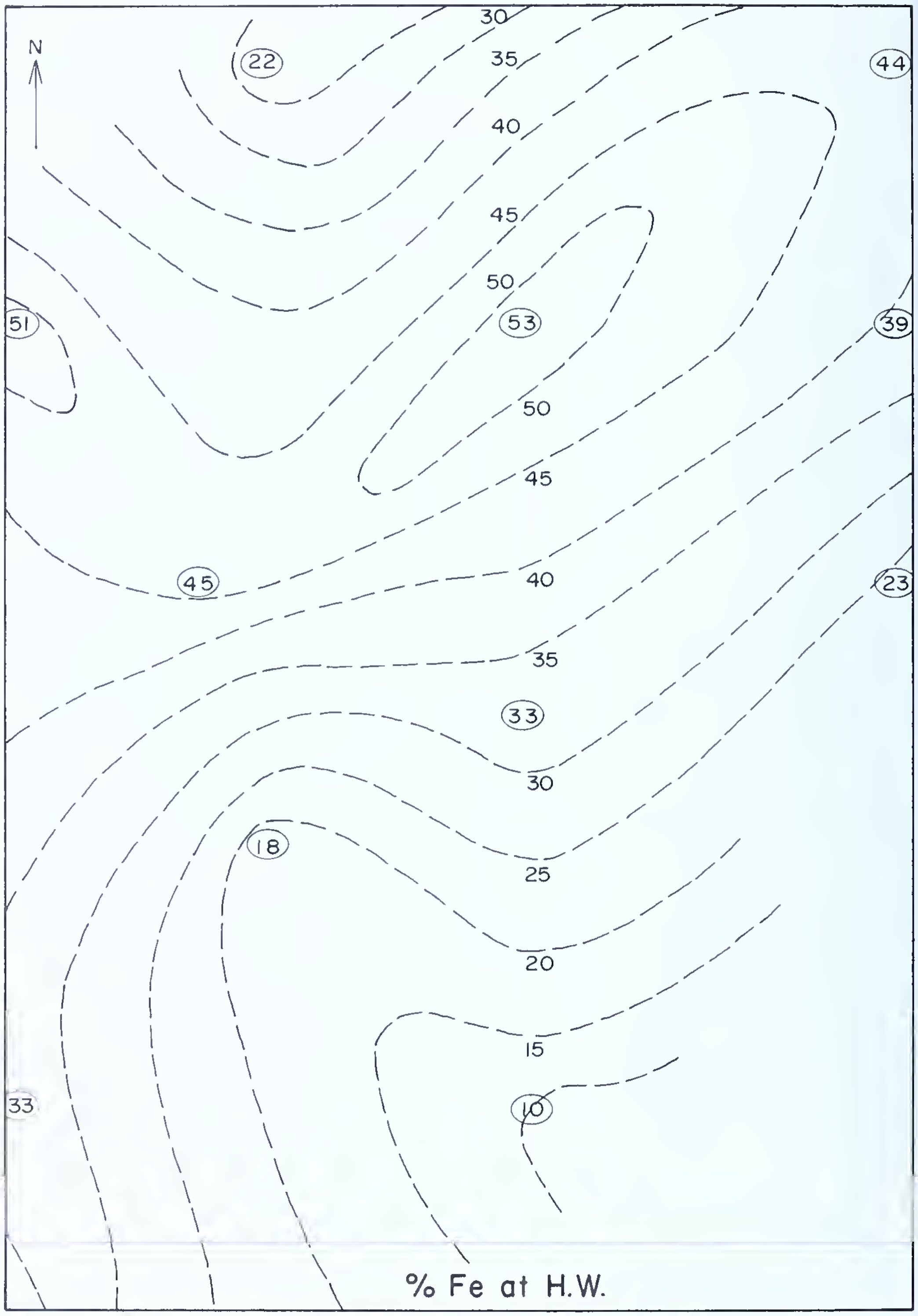

Figure 29B- Hanging wall. Distribution of total and average percent Fe in the eastern ore body; borders of diagrams are approximately at ore-body limits. Contour interval - 5% Fe. From drill core analyses, courtesy of Bethlehem Steel Corp.

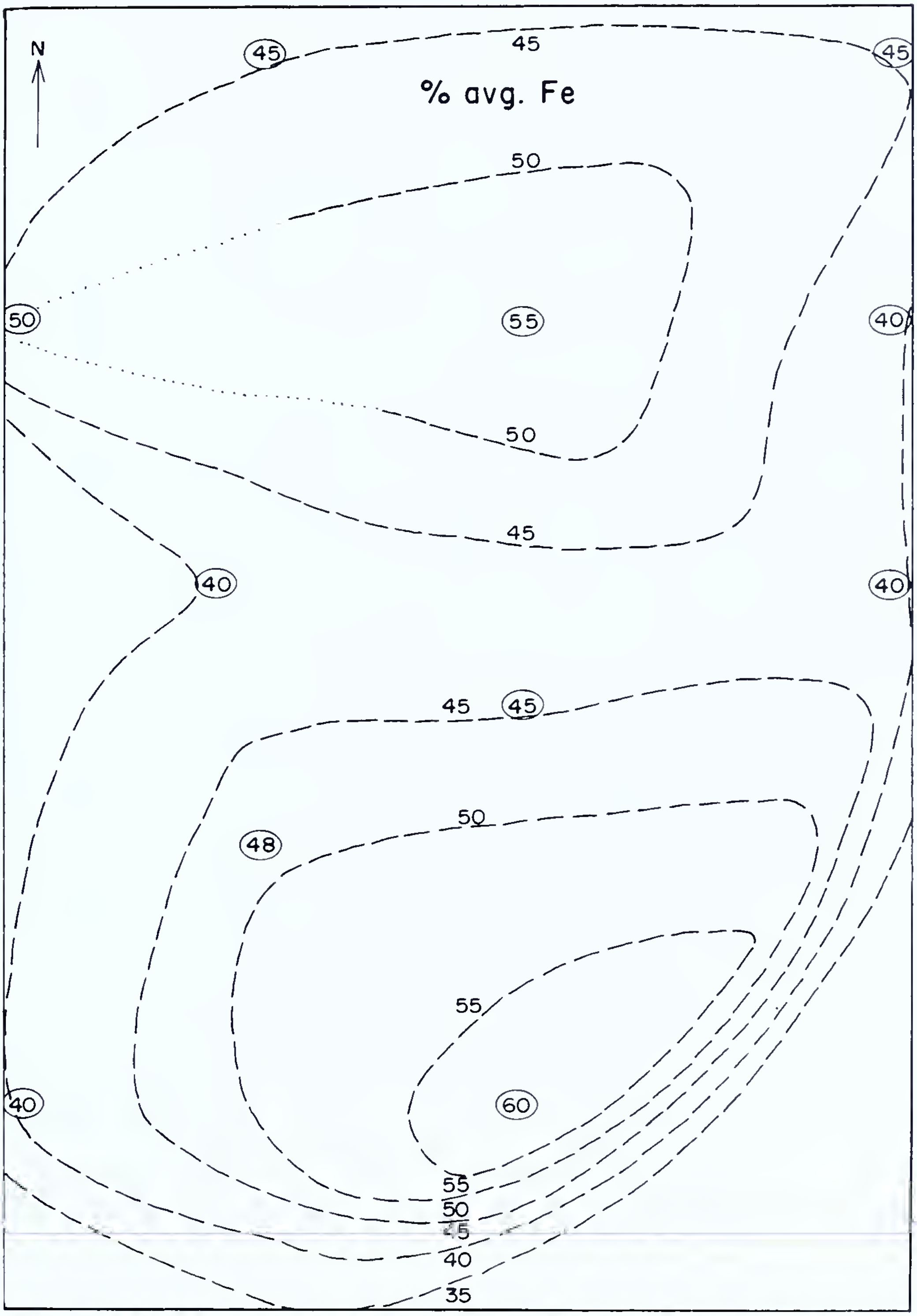

Figure 29C- Average distribution. Distribution of total and average percent Fe in the eastern ore body; borders of diagrams are approximately at ore-body limits. Contour interval – 5% Fe. From drill core analyses, courtesy of Bethlehem Steel Corp.

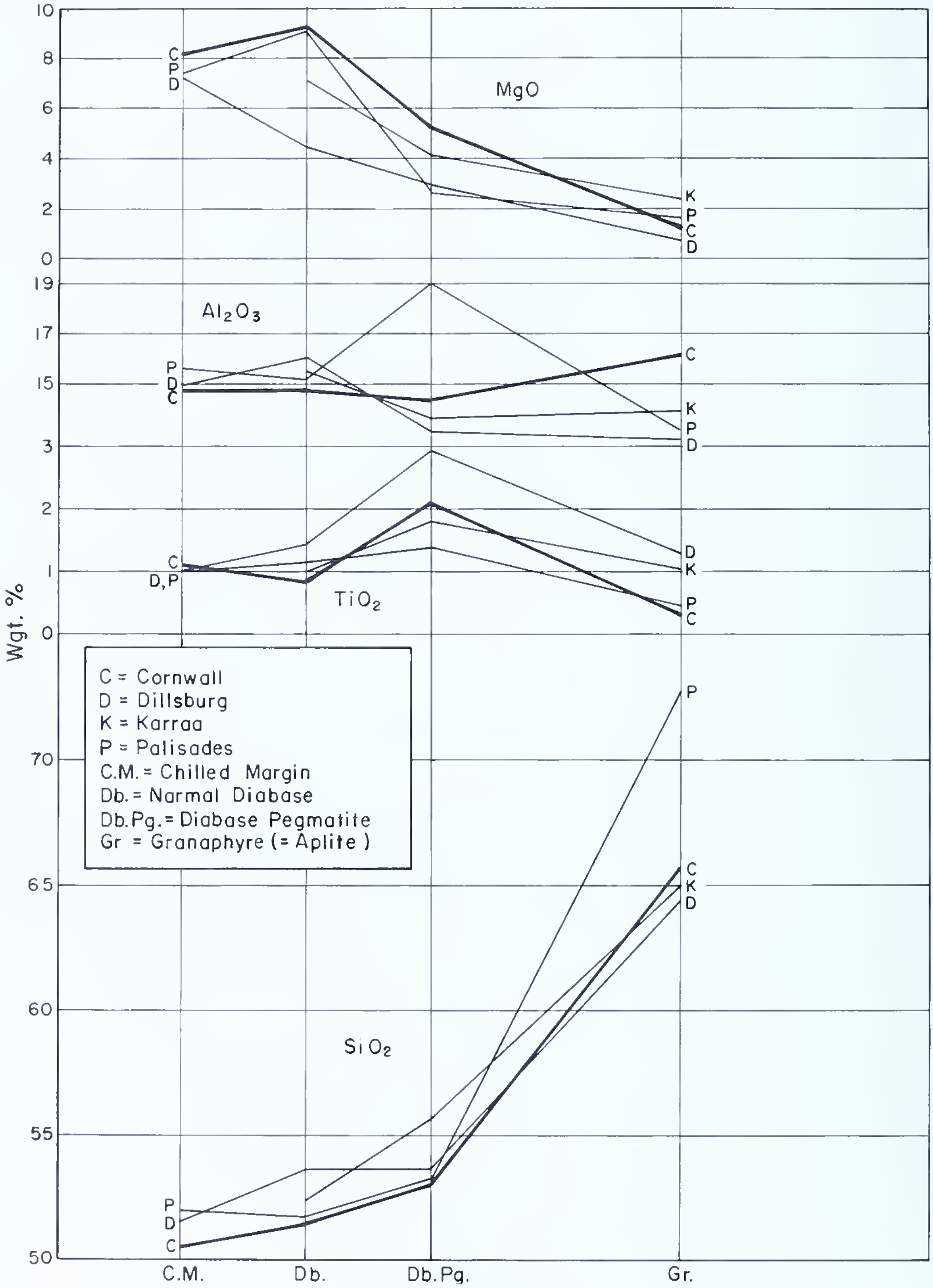

Figure 30A- Footwall. Distribution of total and average percent Cu in the eastern ore body; borders of diagrams are approximately at ore-body limits. From drill core analyses, courtesy of Bethlehem Steel Corp. Note variable contour intervals.

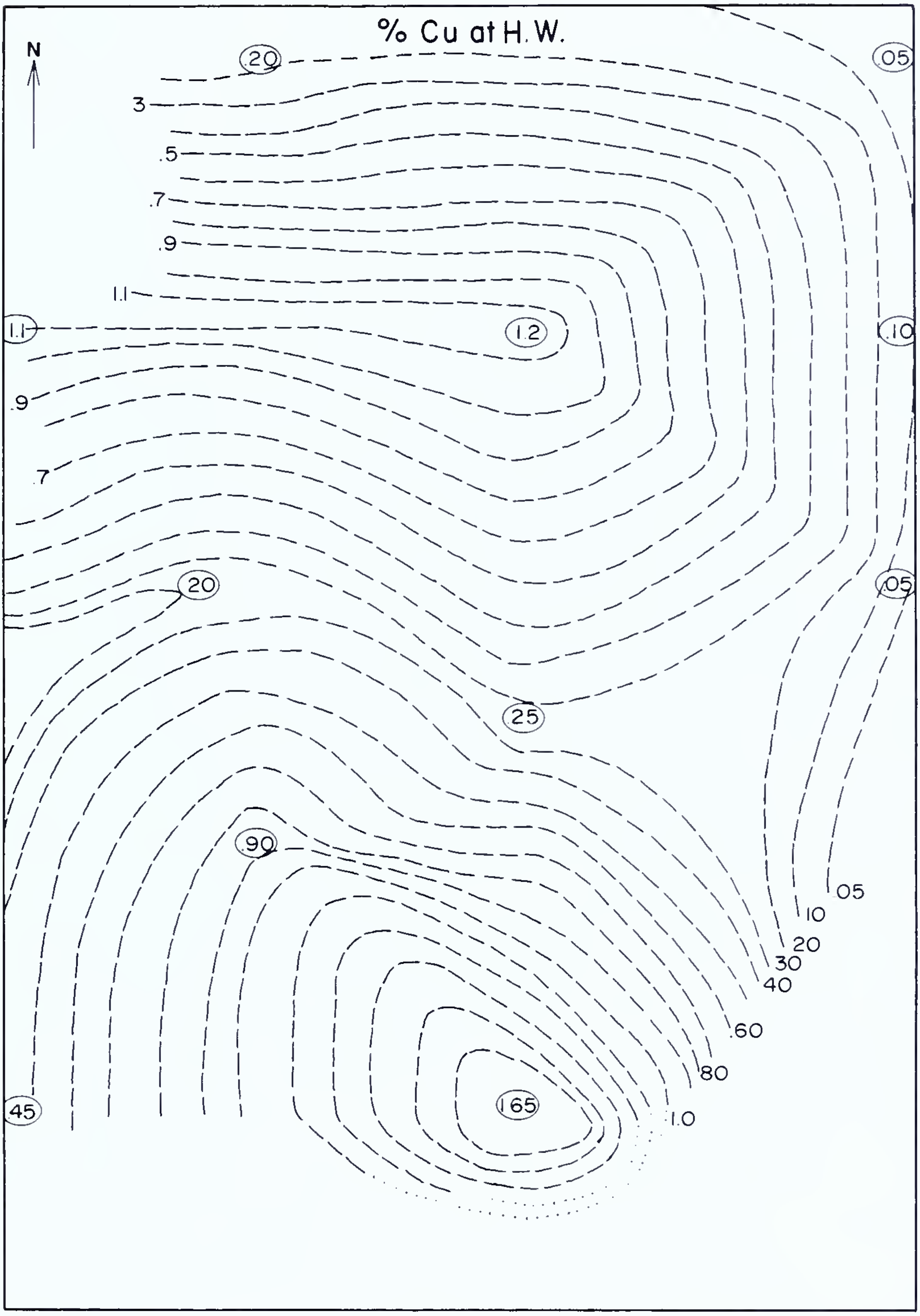

Figure 30B- Hanging wall. Distribution of total and average percent Cu in the eastern ore body; borders of diagrams are approximately at ore-body limits. From drill core analyses, courtesy of Bethlehem Steel Corp. Note variable contour intervals.

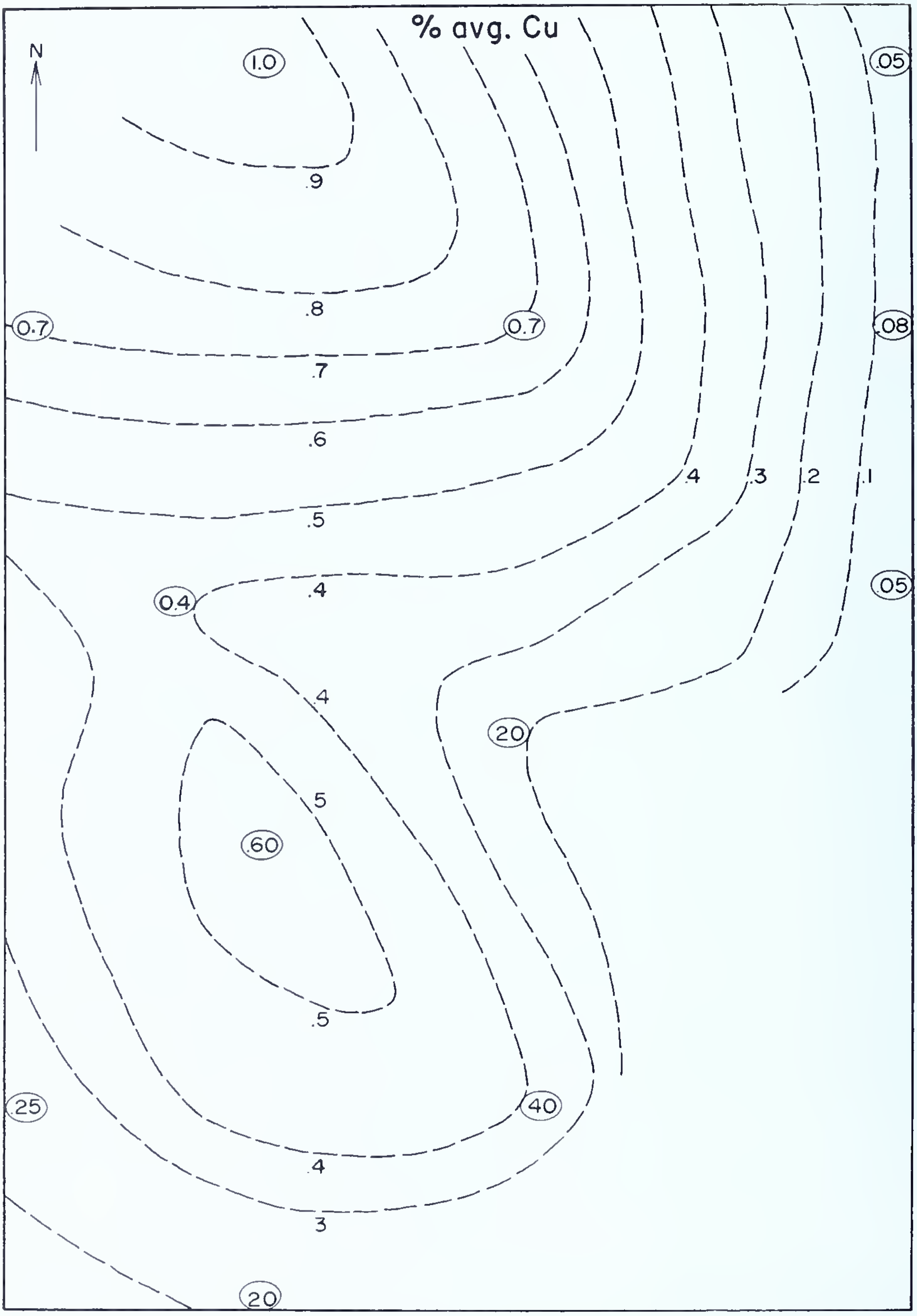

Figure 30C- Average Distribution. Distribution of total and average percent Cu in the eastern ore body; borders of diagrams are approximately at ore-body limits. From drill core analyses, courtesy of Bethlehem Steel Corp. Note variable contour intervals.

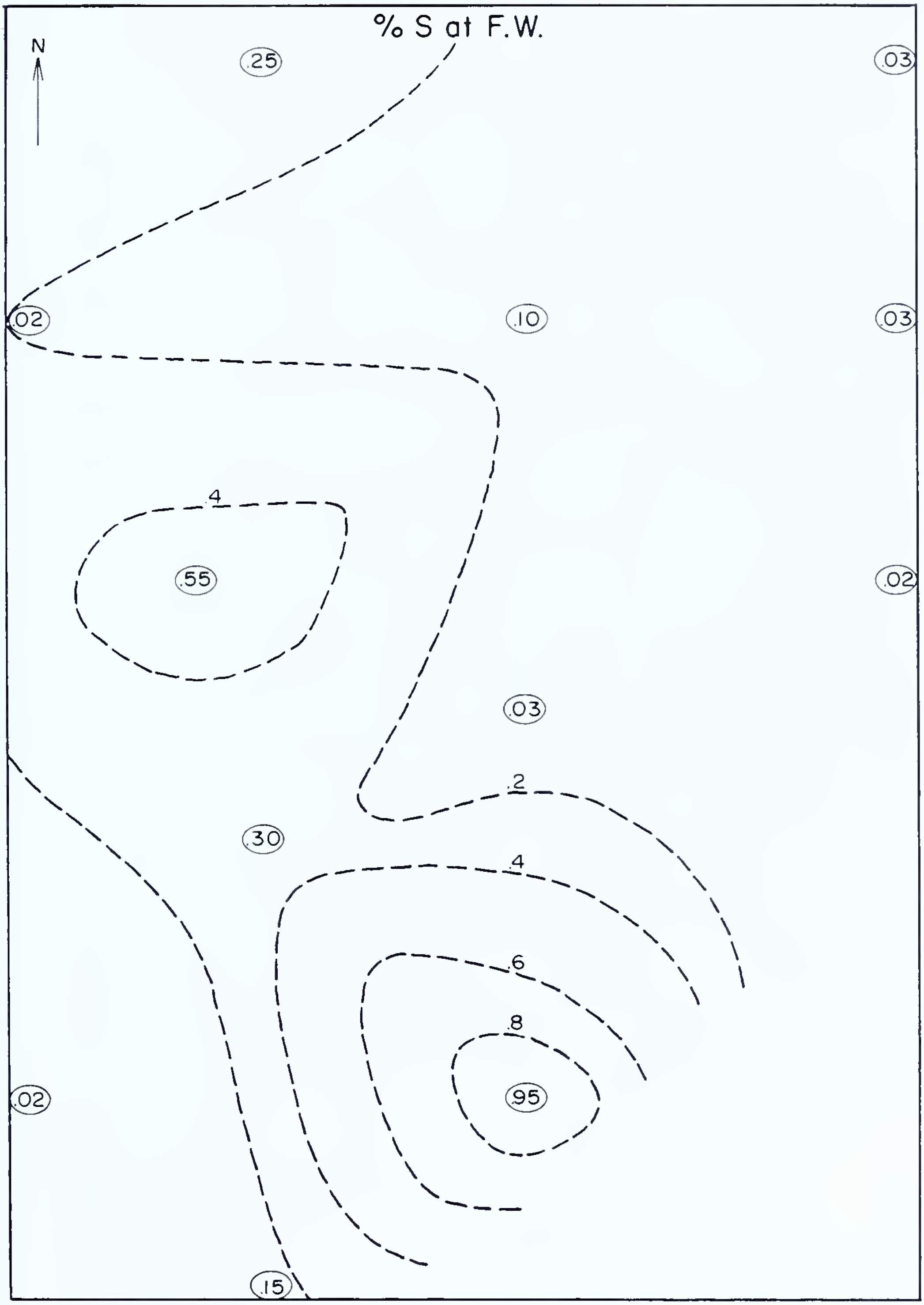

Figure 31A- Footwall. Distribution of total and average percent pyritic sulfur in the eastern ore body; borders of diagrams are approximately at ore-body limits. Contour interval = 0.2% S. From drill core analyses, courtesy of Bethlehem Steel Corp.

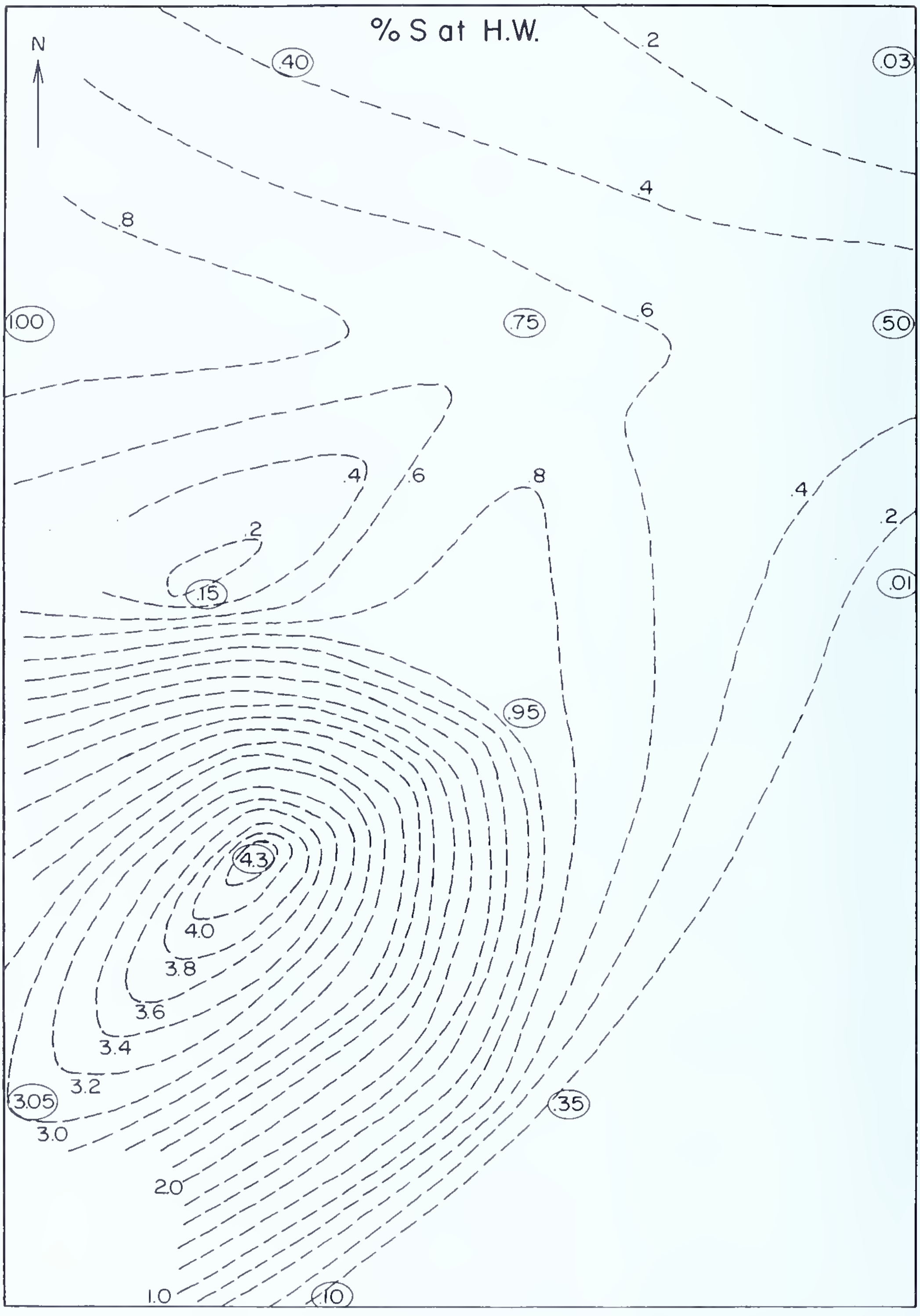

Figure 31B- Hanging wall. Distribution of total and average percent pyritic sulfur in the eastern ore body; borders of diagrams are approximately at ore-body limits. Contour interval = 0.2% S. From drill core analyses, courtesy of Bethlehem Steel Corp.

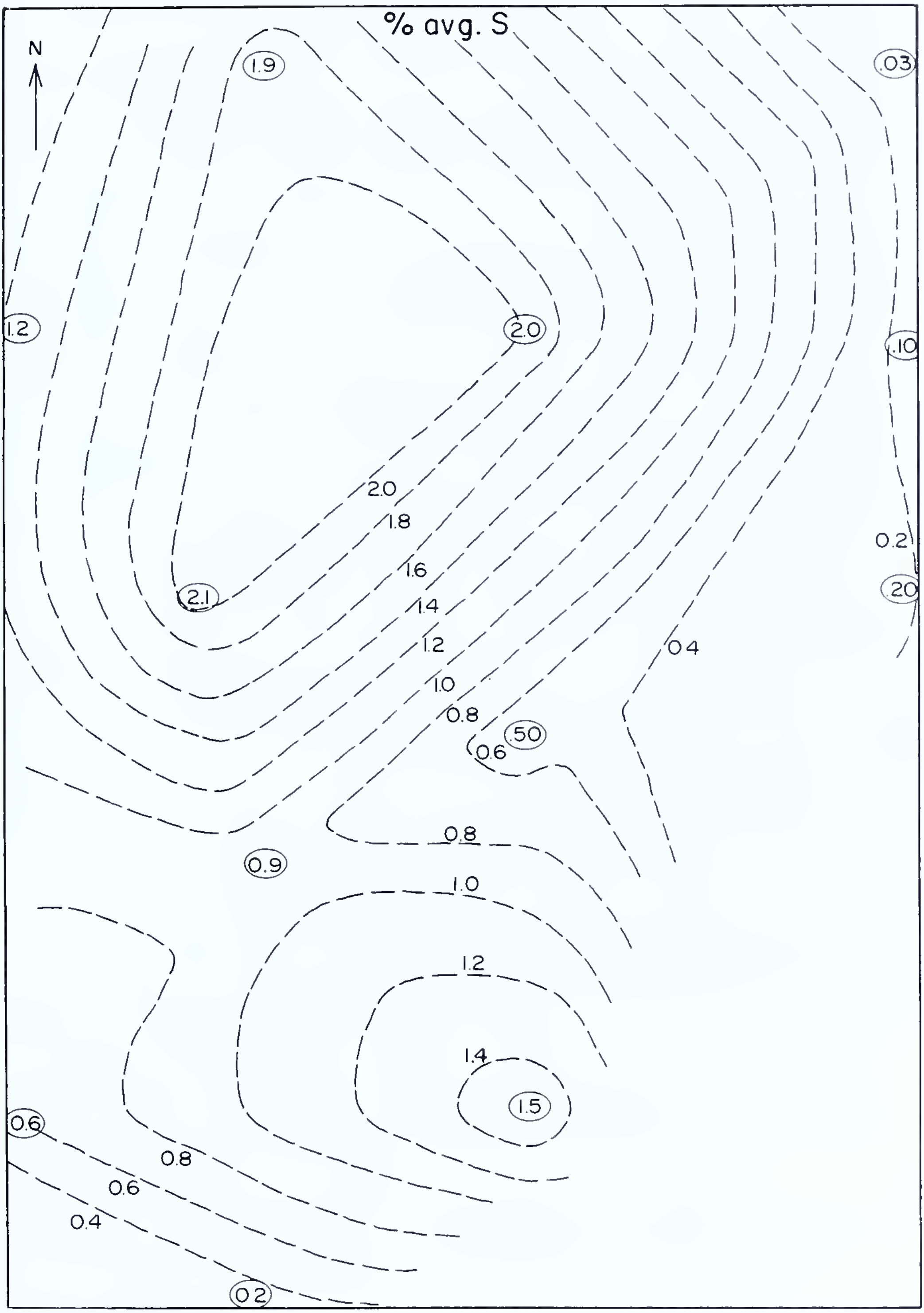

Figure 31C- Average Distribution. Distribution of total average percent pyritic sulfur in the eastern ore body; borders of diagrams are approximately at ore-body limits. Contour interval = 0.2% S. From drill core analyses, courtesy of Bethlehem Steel Corp.

with iron distribution. The major sulfur footwall maximum is in the south-central part of the ore body, as it is for iron distribution, but the secondary footwall maximum is not as far to the north (Figure 31-A). This is a consequence of the paragenetic sequence; much of the pyrite preceded both magnetite and chalcopyrite and hence its ability to replace host carbonates was less restricted by previous metallic mineralization. As with other ore stage minerals, the maximum concentration of sulfur is toward the hanging wall (Figure 31-B) along the southwestern side of the ore body. Total average pyritic sulfur illustrates well the bimodality of concentration maximum (Figure 31-C). Although sulfur percentages are high at the northwestern edge of the ore body, there is no indication of an extension toward the western ore body.

The distribution of nickel in the eastern ore body (Figure 32) is shown by a series of footwall to hanging wall cross sections from north, on the up-dip

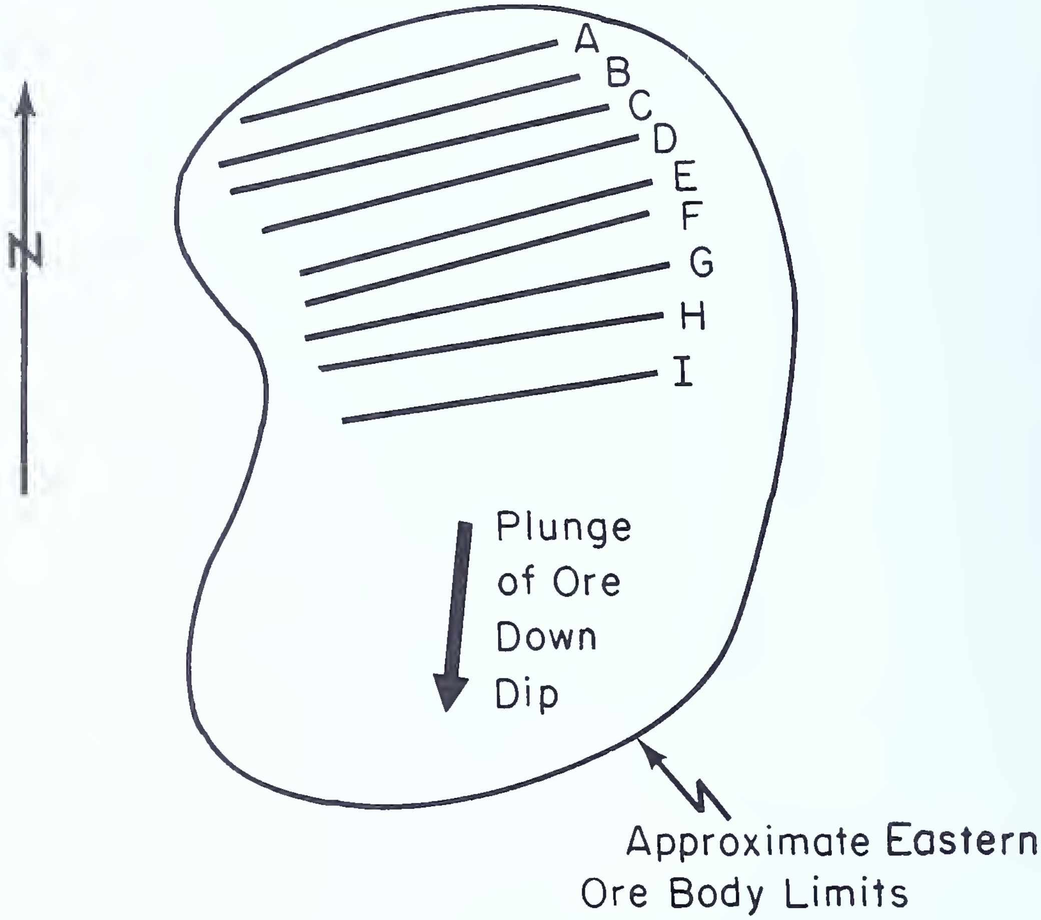

Figure 32-A. Approximate location of sections A-I in Figure 32-B, eastern ore body; plan view.

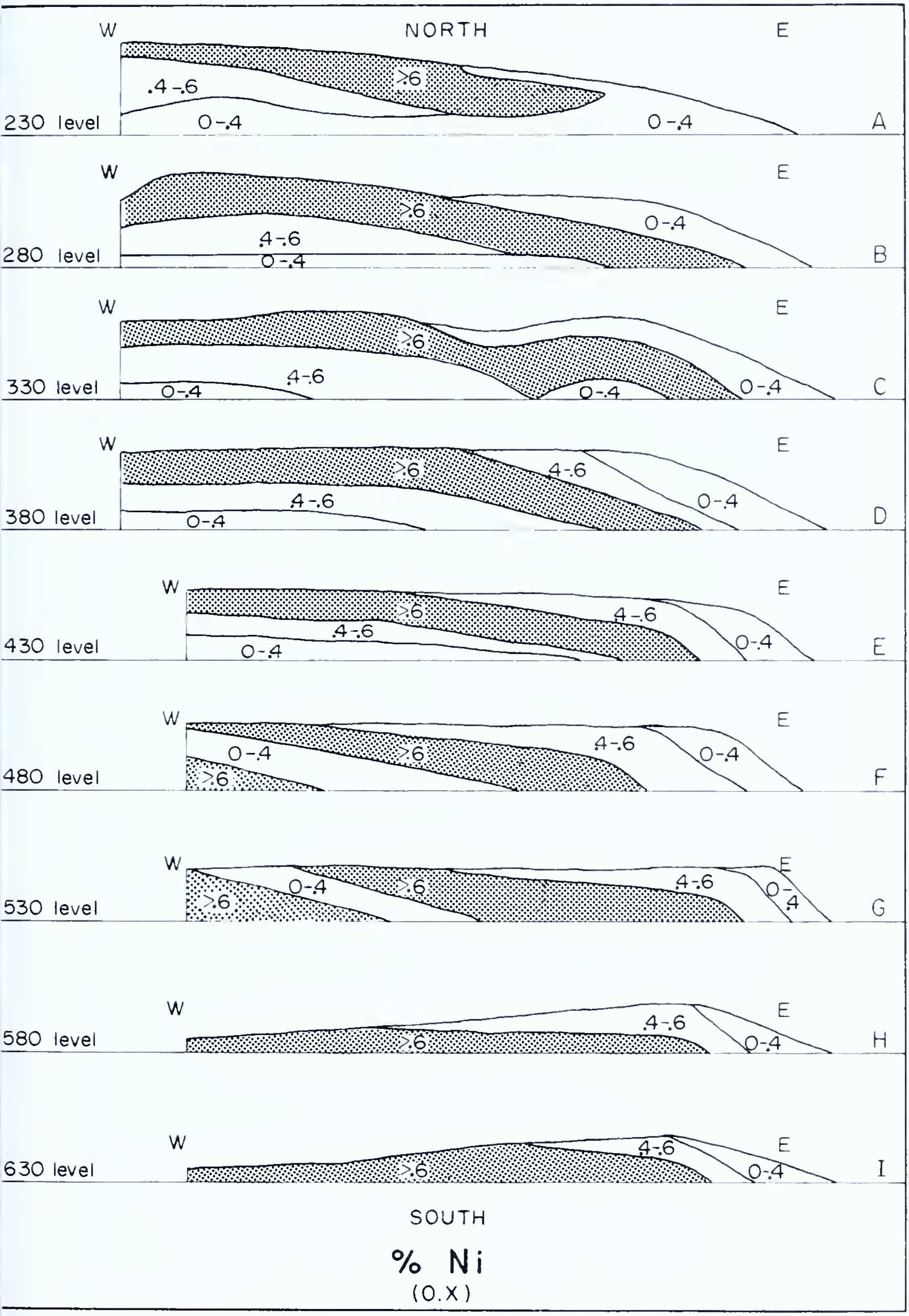

Figure 32-B. Cross sections arranged from north to south (vertically) and down plunge through the eastern ore body, illustrating percent Ni distribution in ores; quantities in tenths of a percent; scale approximately 1" = 200' (see Figure 32-A).

mine levels, to south, on the down-dip mine levels. The same pattern is evident: maximum nickel concentration occurs at the southern to southwestern footwall and migrates toward the hanging wall and toward the northwest, up dip. These sections show more clearly than the contour diagrams the migration outward and upward from a focal source in the south-central to southwestern part of the ore zone, a migration common to all elements for which analyses were available.

Summary

Zonal distribution has been documented for the eastern ore body for the major metasomatic gangue minerals, for metallic mineralization (both mineralogically and chemically), for unit cell magnetite variation, for some ore textures, and for some local structural elements. Each of these variables shows the same pattern: ore solution and associated gangue mineralization migrating from a focus at the south-central to southwestern footwall up toward the hanging wall and also northward and northwestward up the dip of the diabase. Maximum concentrations were controlled partly by this directionalization and partly by an ease of replacement and migration that was dependent upon the previously-formed minerals. The chemical element distributions and magnetite unit-cell differences also suggest that an ore bridge once existed between the northwestern edge of the eastern ore body and the western ore body. Although observational evidence for a bridge has been removed by erosion, it seems probable that a part, or all, of the western ore body was "poured" in from the top and east side, rather than introduced through a separate footwall ore channel. The presence of small ore bodies such as the Elizabeth open pit and East End open pit mines, both of which lie between the two major bodies, may be remnants of this bridge. Ore banding in the western ore body parallel to flats and transecting pitches on the upper surface of diabase is believed to be a direct indicator of ore flow into the western ore body.

A simplified, greatly idealized sketch of the metamorphic, metasomatic, and ore relations for the eastern ore body which is derived from the foregoing zonation is presented in Figure 33. The diagram is an attempt to show several generalized cones of metasomatic and hydrothermal mineral penetration from a footwall focal source. Both processes are superimposed on a footwall contact metamorphism that dips south parallel to the diabase dip (dashed line, Figure 33). Of the three metasomatic-hydrothermal mineral cones, the diopside limit of migration (the second paragenetic maximum of Figures 25 and 26) is usually closest to the footwall, the magnetite limit next, extending approximately to the upper limit of the hornfels roof, and the actinolite and chlorite limits (second actinolite paragenetic maximum) extending into the hornfels units. To the west, the cones are shown as incomplete in accordance with the hypothesis that ore moved into the western ore body from the east over a diabase roll now at the level of erosion.

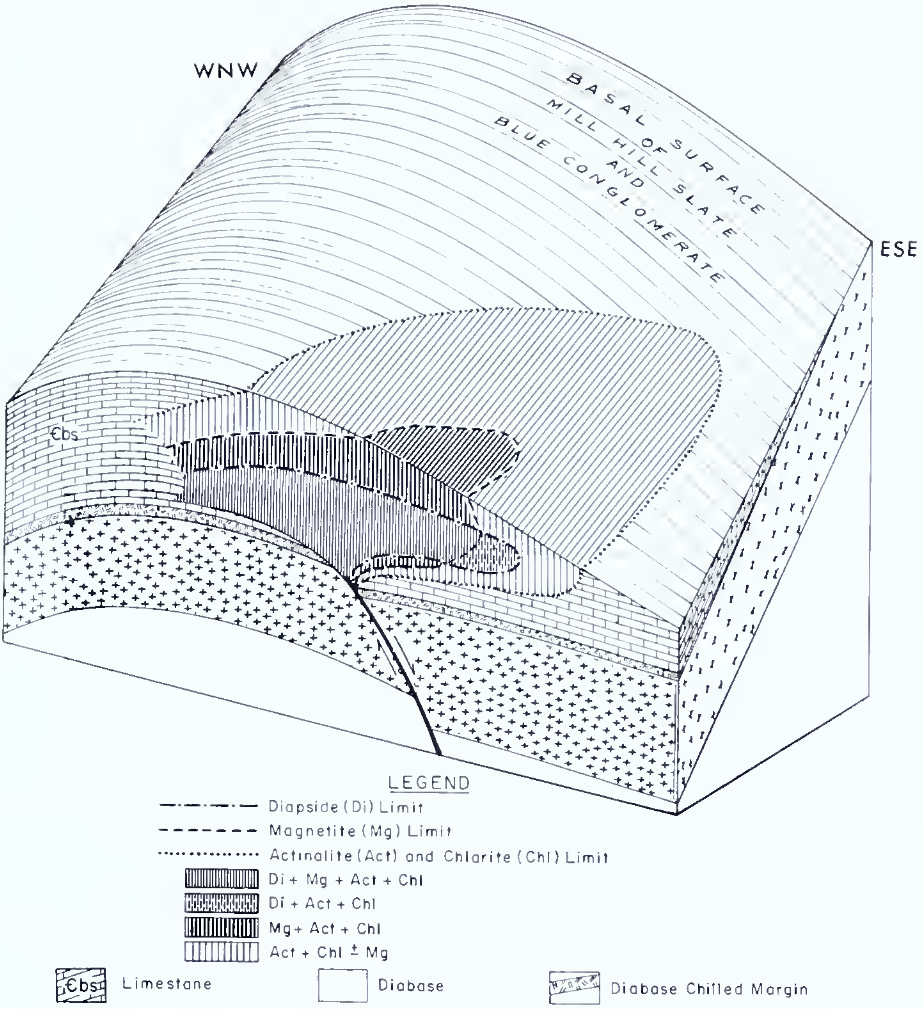

Figure 33. Idealized block diagram of the eastern Cornwall ore body illustrating zonation. Roof of diagram is hornfels basal contact with limestone. Arrow indicates postulated direction of ore movement from eastern ore body into western ore area. Cones indicate idealized shape of limits of metasomatic diopside (inner cone) and actinolite - chlorite - muscovite (outer cone) and of hydrothermal ore and sulfides.

ORE LOCALIZATION CONTROLS

As the previous discussions illustrate, many factors have combined to control the locus of ore deposition at Cornwall. The two most obvious, because they are uniformly present throughout the Triassic metallogenic province, are the presence of a diabase sheet (as contrasted to later, barren dikes) and the presence of replaceable carbonate beds above diabase. Others of varied importance, which have been discussed previously or are discussed subsequently, are briefly noted below. The most fundamental control of all may have been structural: some basement dislocation that affected the course of magma fractionation and/or generation and eventual intrusion of diabase composition in two stages (sheets and dikes) separated by a hydrothermal ore solution.

1. Compositional stratigraphy: Limestone or dolomitic limestone was more easily replaced than the hornfels and breccia units (Mill Hill Slate or Blue Conglomerate). Compositional laminae in host limestone have yielded typical laminae of ore alternating with Na-Ca-Mg-K alumino-silicate gangue.

2. Structure: Thrust faulting emplaced Cambrian and Ordovician(?) units. The present form of the thrust sheets and of the textures of the laminated ore are, in part, the result of the dips and small scale folds, respectively, of the associated sedimentary and hornfels rock types. Faulting also has cut off limestone and resulted in a damming effect on the ore by the overlying rafting of hornfels above the eastern ore zone. Faulting occurred after sheet emplacement, both before and after ore introduction (also the case at the Carper mine to the west). A major fault offset of the diabase between the eastern and western ore bodies is believed to be genetically related to a mineralized shear zone that extends at least 660 feet below the top of the diabase, to the plunge of an ore body within diabase, and to chemical and mineralogical zonation within the eastern ore body. A roll in the top of the diabase separates two major ore bodies, but was probably once a continuous ore bridge. Ore flow-banding that is parallel to flats and cross-cuts over pitches on the upper surface of diabase (western ore body) indicates an ore movement control exerted by diabase topography.

3. Mineralogy: Magnetite has selectively replaced earlier minerals, and their quantitative distribution has in part controlled the quantity and loci of ore deposition. Diopside and actinolite bear an inverse relationship to magnetite abundance. For contact metamorphic minerals, the distribution is temperature dependent with respect to distance from the cooling diabase sheet; metasomatic and hydrothermal ore minerals are crudely conically zoned. Magnetite also has preferentially replaced grains of medium grain size rather than the very coarse-grained or the very fine-grained metasilicates. It also has replaced diabase and filled contraction cracks on the upper surface of the sheet.

4. Geochemical environment of the ore fluid: Changes in oxidation environment are reflected in the distribution of hematite at formational contacts; a decrease in this oxidation state resulted from the replacement of hematite and hornfels units by sulfides and magnetite. Presumably pH, by solution of the $CO_3{}^{=}$ radical, has played a significant role both in migration and precipitation of the invading metasomatic and ore solutions. For the magnetite - pyrite - pyrrhotite association, alkaline ore fluids may be

required. The crystallization of halogen-bearing minerals (datolite, fluorite, idocrase) somewhat earlier may indicate a more acid pH and a supercritical or rather dense gaseous phase. However, as a consequence of the ore fluid salt content, the critical temperature of such an ore fluid probably would have exceeded the ore deposition temperature at Cornwall (personal communication, John D. Ridge).

5. Finally, the composition and differentiation history of the diabasic magma played a primary role. Certain limiting conditions are believed to have proscribed the particular chemical fractionation required to yield both diabase and ore as discrete entities.

PART 5. DIABASE AND ASSOCIATED IGNEOUS ROCKS

by D. M. Lapham

INTRODUCTION

In this report, the term diabase is used for an intrusive, mafic, igneous rock with subophitic texture containing calcium-poor ortho- and clinopyroxenes, calcium-rich clinopyroxene, plagioclase, opaque oxides, interstitial micropegmatitic quartz, and late, less mafic, differentiates. Olivine is present only sparsely in the chilled margins and near the base of the sheet. Although the term dolerite is preferred by many authors, the term diabase for these Pennsylvania rocks is so entrenched in the literature that it is retained here. At some localities, quartz content exceeds five percent, and the rock may be called quartz diabase, but normal Cornwall diabase contains less than five percent quartz (excluding granophyric differentiates).

Throughout Pennsylvania, Triassic diabase is essentially unaltered. Flow textures are generally absent and layering, except for some occurrences of cumulate bronzite bands (e.g., Gifford Pinchot State Park), is restricted to differences in mineral and chemical composition ("cryptic layering"). Pennsylvania diabase is a competent rock that is consistently a ridge former. It weathers with a characteristic limonitic rind. Locally, diabase often is referred to as traprock when fresh and ironstone when weathered. Deep weathering along fractures and plow marks have given rise to grooves that have been misinterpreted as "Phoenician Writing" by several popular writers (see Witthoft, 1964).

Diabase is coarser-grained than basalt but mineralogically and chemically very similar (the Triassic flows in Pennsylvania and New Jersey are basaltic). Because the origin and crystallization history of diabase is directly related to the petrogenesis of basalt magmas, data and interpretations for the Cornwall diabase will be compared with those for basalts.

Wilkinson (1967) lists three primary basalt magma series that have characteristic fractionation and differentiation sequences: alkali olivine basalt usually containing normative olivine and nepheline but which may or may not contain normative hypersthene (Kuno, 1968), tholeiite basalt containing normative hypersthene but which may or may not contain normative olivine or quartz, and the calc-alkali basalt series that shows continuous alkali enrichment and contains more Al_2O_3 than tholeiite (Kuno, 1968). To this list, high-alumina basalt may be added as a possible primary magma (Kuno, 1968; Engel and others, 1965). TiO_2 content might be used to classify basalts (discriminant function analysis of Chayes and Velde, 1965), but the geological significance of a TiO_2 partition is not clear. A further subdivision of tholeiite and high-alumina basalt series can be made by considering high and moderate (or low) iron-concentration subtypes (Kuno, 1968). The Karroo, Palisades, and Dillsburg sheets are grouped with the high-iron tholeiites and the Skaergaard with the high-iron, high-alumina basalts (Kuno, 1968, p. 633). As will be shown, the Cornwall sheet probaby should be classified as a variant of the high-iron tholeiite suite even though FeO and Fe_2O_3 (as FeO) are less than the 15 percent boundary limit of Kuno (1968, p. 632). With regard to the differentiation trend, the low total iron of the Cornwall sheet resembles the iron content of some alkali-olivine basalts, but in all other respects it conforms to the tholeiite group.

Basalt magma types can be characterized by differentiation trends represented by the composition of their associated rock suites. Graphical representations of indices of differentiation (Thornton and Tuttle, 1960), indices of crystallization (Poldervaart and Parker, 1964), and ternary trend diagrams are among those commonly used. A generalized trend diagram such as in Figure 34, a reduction of approximately 15 oxides to Na_2O+K_2O ("A"), $FeO+Fe_2O_3$ as total FeO ("F"), and MgO ("M"), can only crudely represent differentiation trends or magma types and should be used with caution. However, the iron-enrichment trend and strong fractionation of the Skaergaard tholeiite (according to the trend of Osborne, 1959; also see Yoder and Tilley, 1963) or high-alumina basalt suite (Kuno, 1968) and the Cascades calc-alkali continuous alkali enrichment trend are well contrasted by such a generalized representation (Figure 34). The alkali end of the Skaergaard curve is dashed because of uncertainty regarding crustal contamination of one of the two granophyric rock types (Hamilton, 1963; Taylor and Epstein, 1963; Wager, 1960). Similar granophyres are present in the Pennsylvania Triassic diabase sheets.

Other compositional features can be useful in tracing basalt origin and history relative to that of the tholeiitic Pennsylvania diabase. The high-alumina basalt of Yoder and Tilley (1962) has a higher Na/K ratio than most other basalts, including the high-alumina basalt of Kuno (1960). As will be shown, the residuum of Pennsylvania diabases has a highly variable Na/K

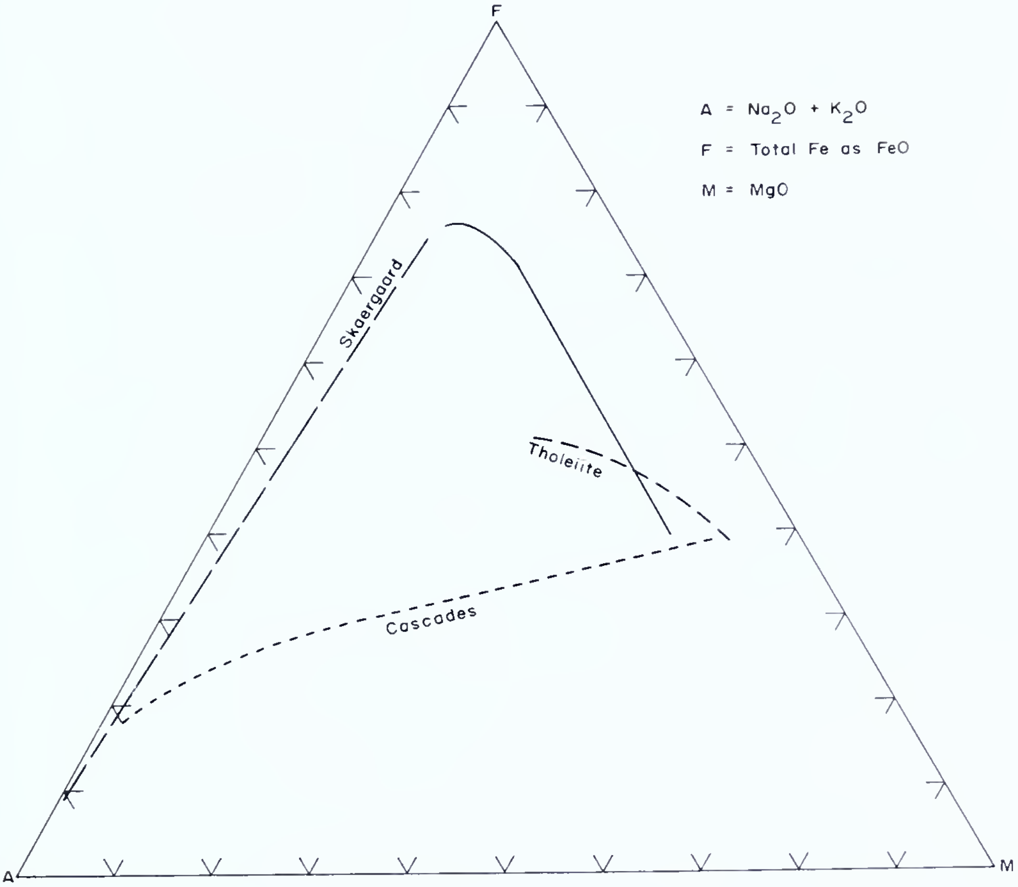

Figure 34. **Generalized MFA diagram of basaltic magma differentiation trends; Skaergaard (Wager and Deer, 1939), average tholeiite (Nockholds, 1954), and Cascades suite (Turner and Verhoogen, 1960).**

ratio that may, in part, reflect original magma differences. Most of the tholeiites of Engel, Engel, and Havens (1965) have low FeO/Fe_2O_3 ratios and a high Al_2O_3 content when compared with other tholeiites (cf. Yoder and Tilley, 1962; Poldervaart, 1955; Kuno and others 1957; Kuno, 1959 and 1960). The Pennsylvania diabases resemble more closely the latter type of tholeiite. Increasing Al_2O_3 and/or increasing Fe_2O_3 (relative to FeO) commonly are evident in basalt types in the progression from tholeiite to olivine tholeitte to alkali basalt to andesite. A slight increase in Al_2O_3 and perhaps in Fe_2O_3 relative to FeO occurs in the Cornwall diabase differentiation suite (see Table 25).

Of the several mechanisms for differentiation such as sulfide immiscibility, thermodiffusion, gaseous transfer, and fractional crystallization, only the latter is considered to have played a significant role in the Cornwall area. Fractional crystallization of the *in situ* sheet magma proceeded by successive compositional changes. Crystal accumulation and segregation is discussed as a possible fractionation mechanism with regard to an ore source and in connection with the absence of an olivine layer.

Assuming that the ultimate source of the Pennsylvania basaltic magma was the upper mantle, at least 30 km below the surface in this area, and given a tholeiitic parent affinity, the fundamental questions to be discussed related to the general problem of basalt-diabase origin are: 1) the physico-chemical environment of diabasic magma and the extent to which the Cornwall sheet is typical of tholeiites, 2) comparison between the Cornwall diabase and other differentiated diabase sheets, 3) the extent to which the trend of Cornwall diabase differentiation is normal and the factors controlling this trend, 4) the effects of fractional crystallization, and 5) any relationships unique to the association of magnetite ore and diabase that might genetically relate the two.

PETROLOGY

Chilled Margin

General Description and Textures

The chilled margin data reported here are all from the top of the diabase sheet at Cornwall. Although a chilled facies also exists at the base, it could not be studied because of a lack of outcrops and diamond drill hole data. Diamond drill hole #155 through the diabase sheet (Appendix 3 and Plate 21) reveals a decrease in grain size to a very fine-grained diabase at the base, but the actual texture at the contact is usually obscured by brecciation, replacement, and metamorphism. The zone of decreasing grain size appears to be narrower at the base than at the top of the sheet. The width of the upper chilled margin ranges from about two to eight feet, the first two feet distinctly aphanitic and the next three to six feet transitional between aphanitic and fine-grained diabase (grains about 0.01 to 0.09 mm. in diameter). Phenocrystic texture ("porphyritic diabase") exists throughout the first six to eight feet and near the base, but shows an irregular distribution both in amount and mineral composition. In some places, the chilled contact with overlying sediments or magnetite ore is sharp. Only rarely has ore replaced the top six to eighteen inches so that the chilled margin resembles massive ore more than it does diabase. As noted previously, the top of the sheet contains rolls, step faults, mineralized joints, and polygonal contraction cracks (Plates 9 and 13; Figure 35). Because the chilled margin is in direct contact with ore above and with normal diabase below, study of the margin is important in determining genetic relationships between diabase and ore.

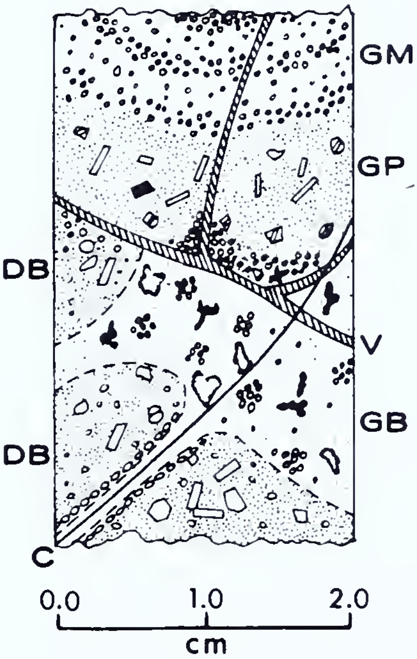

Figure 35. Petrographic sketch of chilled margin of diabase illustrating mineralogy and textures. GM = 60% banded, isotropic glass matrix with small clinopyroxene, olivine, and magnetite grains; GP = 90% isotropic glass as matrix and as pseudomorphs with "idding site" after pyroxene and feldspar with some serpentinized and amphibolitized olivine and with magnetite dust; V = veins of serpentine or zeolite; GB = 15% glass matrix 10% glass blebs, and patches of small olivine and clinopyroxene grains; Db = fine-grained diabase with up to 10% glass matrix, large altered olivine crystals in a groundmass of small olivine, clinopyroxene, and plagioclase grains with considerable magnetite dust; C = polygonal contraction crack with a center line of glass blebs replaced by magnetite and with coarsely crystalline clinopyroxene along crack boundary.

Although the chilled margin is aphanitic, the microscopic texture is varied, ranging from an isotropic glass to fine-grained (0.01 to 0.09 mm) or normal (0.1 to 1.0 mm) diabasic texture. The chilled margin as used here refers to that portion of the diabase that is porphyritic (phenocrystic and/or porphyroblastic) regardless of the grain size of the matrix (Plate 12). Hickok (1933, p. 200) noted the presence of a narrow zone of glass about 5 mm thick. However, re-examination of his thin sections labeled "glass" failed to reveal any true isotropic glass, but rather an extremely fine-grained matrix of crystalline aggregates. Glass does exist (Figure 35), but does not seem to be a universal characteristic near the contact. Textures within the top two centimeters are varied, but some glass is nearly always present. Nearest the contact are flow bands of glassy material blebs and small olivine, clinopyroxene (?), and magnetite grains. This part of the chilled phase is not porphyritic. Immediately below this lies a thin zone of isotropic glass matrix containing pseudomorphs of glass after olivine and plagioclase phenocrysts. These glassy phenocrysts are outlined by fine magnetite dust that occurs only in the matrix glass (Figure 35). Below this is an irregular zone of fine-grained glass matrix with larger blebs of patchy glass similar in optical character to opaline silica. Olivine and clinopyroxene occur in clusters of small grains, but no phenocrysts were observed. This zone contains much less magnetite dust than the zones above and below. At the base of the glass zone, normal, although fine-grained, diabase mineralogy begins to appear. The overall appearance is a web structure, the strands having the geometry of polygonal contraction cracks separating the several textures of the chilled margin. After the first two feet of chilled facies, the porphyritic texture gradually gives way to sub-ophitic diabasic texture for a distance of six to eight feet below the upper contact. These zones differ from each other principally in amount and grain size of magnetite, amount and type of glass, amount and kind of phenocrysts (or metacrysts), and in the grain size of the crystalline matrix. The size of the blebs and grains in Figure 35 is slightly exaggerated for purposes of illustration. Rarely present in the chilled facies are coarsely crystalline vein minerals, intergranular diabase pegmatite, and intergranular granophyre. The latter two types have not been found in the top two feet of the diabase although Hickok (1933) reports their presence in an area of the western ore body that is now inaccessible.

Mineralogy and Alteration

Minerals in the matrix are commonly entirely unidentifiable, or only their group (for example, of plagioclase or pyroxene) are identifiable. The identification of porphyritic minerals presents a similar problem because most of them are amphibolitized, chloritized, or serpentinized. Unaltered phenocrysts comprise less than one percent of an original two to five percent. Because of this, it can be assumed that large altered aggregates were phenocrysts from the original basaltic magma, but there is very little positive evidence to support this. Perhaps the best evidence is the replacement of feldspar and olivine phenocrysts by chilled glass (Figure 35). The composition of the feldspars in the top two feet is unknown. Polysynthetic twinning characteristically is lacking. Olivine (altered), orthopyroxene (enstatite), and clinopyroxene are present but rare. Aggregates of porphyritic amphibole, chlorite, and serpentine usually have a varied rim of massive (Ti-?) magnetite (Plate 12). The matrix immediately surrounding these aggregates frequently has been cleared of magnetite dust-sized particles (Plate 12-B), and matrix pyroxene grains frequently are coarser here than elsewhere in the matrix. Diffusion of iron toward coarse-grained aggregates is characteristic of the margin and probably occurred during hydrous alteration of olivine and pyroxene phenocrysts to amphibole (Plate 12-B), serpentine, and chlorite minerals. Some metamorphic growth also may be indicated by the presence of occasional large untwinned crystals of diopside that lack exsolution lamellae. These, however, occur in a matrix of fine-grained diopside rather than in a typical chilled matrix, except near the top of the diabase where the matrix of the chilled margin has been metamorphosed to a diopside-rich mineral assemblage. In the absence of other evidence, the most probable explanation for the observed alteration is that original phenocrysts present were altered by magmatic metasomatism (deuteric alteration) from a rather hydrous magma and by later metasomatism associated with ore-zone processes.

The ratio of amphibole to magnetite in altered olivine phenocrysts ranges from 10:1 to 1:10 (Plate 12). Some sections exhibit a quite uniform ratio, whereas others exhibit the complete range (Lapham, 1960). Thus, it is not possible to derive even approximate olivine compositions from magnetite rim volumes, nor is there a constant relation between the amphibole to magnetite ratio and the amount of clearing of opaques from the matrix. In some instances, all of the rimming magnetite easily could be accounted for by matrix clearing (of an early crystallized spinel?) and subsequent nucleation (Plate 12). For some of these areas, alteration of a fayalitic olivine could have yielded the requisite amount of magnetite, followed by particle nucleation from clearing of the magnetite-dusted matrix induced by ore-stage metasomatism. However, typical tholeiitic diabase olivines from chilled margins are magnesium rich, Fa_{15}-$_{25}$(Wilkinson, 1967, p. 183). Fayalite would not be expected in the early, high-temperature phase represented by the chilled margin and none has been reported from the Palisades or Dillsburg sheets. In some areas at Cornwall, there is no dust clearing (Plate 12-C) and the altered phenocrysts are nearly wholly magnetite. Some of this magnetite was clearly introduced (see Plates 12 and 13) and is particularly abundant where the top of the diabase is near ore, highly fractured, and commonly veined. Here again, nucleation of magnetite accounts for its concentration around altered phenocrysts.

In summary, the rim magnetite associated with altered olivine, and to a lesser extent altered orthopyroxene (Plate 12-A), could have originated in several ways: 1) by alteration of olivine to amphibole and minor magnetite, 2) by induced clearing of previously crystallized ground mass magnetite "dust" and preferential nucleation on phenocrysts (before, during, or after amphibolitization), and 3) by introduction of magnetite with preferential nucleation around phenocrysts (during or after amphibolitization). Introduction of magnetite is inferred to have occurred because there is more magnetite than could have come from the alteration of olivine (even if highly fayalitic) or from the clouded ground mass, and because of observed magnetite replacement of the chilled margin. The second process, clearing, was active in some areas but not in others, suggesting a local internal or external control; the metamorphism noted above could have triggered small-scale diffusion of iron during phenocryst amphibolitization and chloritization. Any additional amount of magnetite released by olivine amphibolitization is unknown. Probably this amount was somewhat varied, resulting from originally different olivine compositions (see Evans, 1967; Wright and Weiblen, 1967), but total contribution of magnetite to the chilled margin by the mechanism must have been small.

Contraction cracks and small, oblique fractures in the top few feet of the diabase, some originally containing isotropic glass, have in part been replaced by sulfides or magnetite, by diopside in turn replaced by magnetite or sulfides, by serpentine, or by zeolites (Plate 13). This replacement by magnetite and sulfides, mostly pyrite (as in C2-1, Appendix 4-A), along fractures was also responsible for coarse-grained recrystallization of metamorphic diopside along vein walls. A slight granulation on one clinopyroxene phenocryst adjacent to such a vein may indicate slight volume expansion during replacement but little shearing because the phenocryst fragments are still essentially optically continuous. Other than this, there is no evidence in the chilled margin of fragmentation or textural disruption that might have been caused by a transfer of constituents out of diabase. The pyrite and magnetite filled in the contraction cracks from above, decrease in amount as the joints narrow with depth, and disappear within a few feet of the top.

Alteration is varied throughout the chilled margin. Only two generalizations have been noted: intensity of alteration increases toward the top of the sheet, and phenocrysts of olivine and clinopyroxene are more commonly altered than those of plagioclase. A few olivine phenocrysts are completely altered to a greenish, translucent, isotropic material, serpentine (usually a typical chrysotile mesh pattern), or pleochroic pale green amphibole. In some cases, the amphibole has further altered to chlorite. Pyroxene phenocrysts have altered to uralite and subsequently to chlorite. Plagioclase is saussuritized or rarely sericitized. Plagioclase is heavily clouded just below the zone containing matrix glass, but is largely clear of dust-sized particles above, within the glass zones, and below in fine-grained diabase (Plate 12). The portions of the top of the chilled zone that contain diopside are essentially free of magnetite dust but do contain some massive magnetite ore (Plate 13-C and D). Scattered opaque grains have a hematite core and a magnetite rim within the two feet of the top. The matrix below the glass zone usually is thoroughly uralitized, serpentinized, or saussuritized for the first three or four feet from the top. Identification among these types of alteration is often uncertain because of the fine grain size and because of clouding. Toward the base of the chilled margin where phenocrysts are less common, although still present as altered relics, the matrix exhibits less alteration and individual grains of pyroxene and feldspar are recognizable.

The major minerals of the chilled facies are clinopyroxene and plagioclase. Clinopyroxene may comprise as much as 60 percent of the matrix but usually is not identifiable as to subspecies except for younger diopside that has replaced matrix minerals (Plate 13-C). Irregularly distributed phenocrysts of clinopyroxene have a 2V of less than 40° an extinction angle of $c \wedge z$ of 35° to 44°. Clinopyroxene appears to be more completely altered to chlorite or amphibole than orthopyroxene, but the extensive alteration makes identification, and hence quantitiative determination, impossible. Twinning on (100) is rare and no exsolution lamellae have been observed in ortho-or clinopyroxene. One grain of clinopyroxene (subcalcic augite?) was observed mantled by orthopyroxene, and another by a thin rim of second generation clinopyroxene, perhaps metamorphic diopside. Other than this, no paragenetic relationships were observed among the porphyritic pyroxenes. Just below the matrix glass zone (Figure 35), clinopyroxene (pigeonite at least in part) occurs without plagioclase; elsewhere, the two are always found together. Diopside, irregularly distributed and only within the top two feet, is not altered. It has a large 2V and its identity has been confirmed by X-ray diffractometer patterns. Diopside occurs as mantles around plagioclase, rarely around pigeonite, in contraction joints replaced by magnetite (Plate 13-C), and in an aphanitic matrix, especially near the glass zone. Basal twinning is almost nonexistent in these metamorphic diopside crystals. The extinction angles have a considerable range but generally are rather low (38° to 40°), which may indicate that very little of the hedenbergite molecule is present.

Locally, plagioclase comprises up to 50 percent of the chilled margin, but usually is less abundant. From about four to six feet from the top to the base of the sheet it is generally constant at 40 to 50 percent. Near the top of the diabase below the matrix glass zone (Figure 36), plagioclase crystals occur as very thin laths with a high elongation ratio and usually are smaller toward the middle and base of the zone. Only simple Manebach twins were observed. Toward the upper chilled margin base, combination Manebach, albite, and

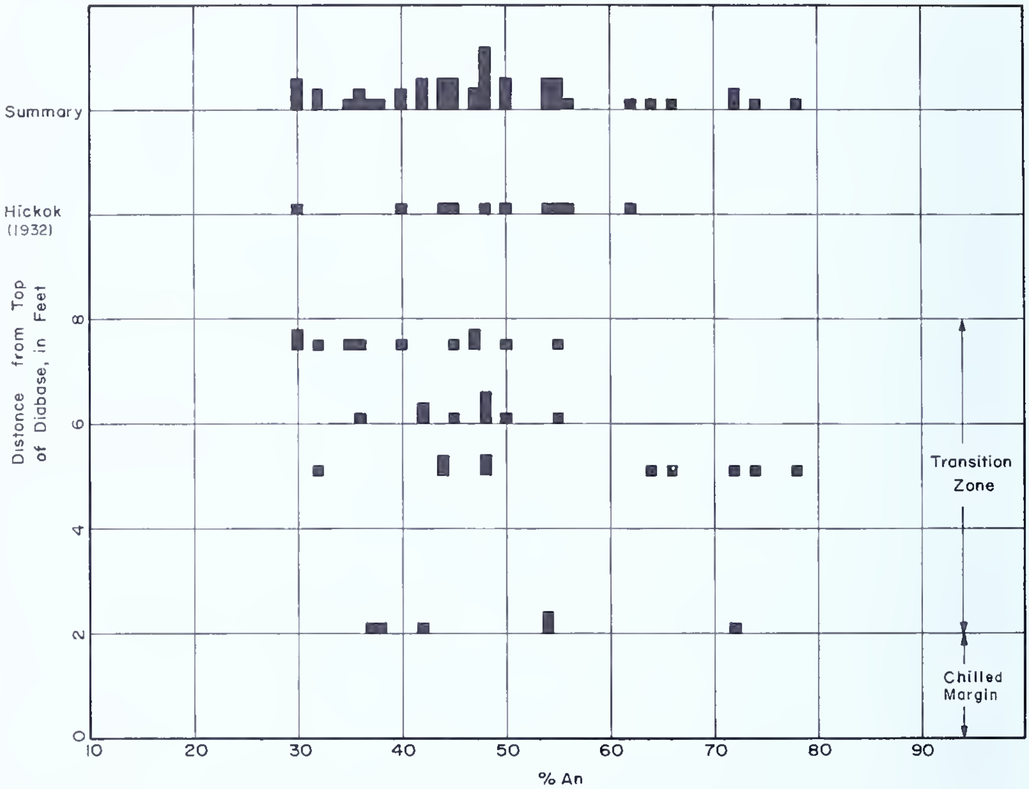

Figure 36. **Histogram of approximate plagioclase compositions in the top 8′ of the Cornwall diabase. Compositions were determined from average Michel-Levy extinction angles.**

rarely pericline twins become more common and the elongation ratio decreases. This distribution is in line with the suggestions that Manebach simple twins represent magmatic crystal growth during initial stages of crystallization when supersaturation is most apt to prevail (Seifert, 1964) and perhaps also under conditions of rather slow crystallization (Sarbadhikari, 1965, p. 1468). Composition of the feldspars is difficult to determine for several reasons. In the first two feet, the feldspars are highly altered (in some cases to an isotropic material), are very small, and exhibit only Manebach twinning. Toward the base of the zone, some approximate determinations were made based largely on the Michel-Levy extinction method for sections with albite twins normal to (010). However, many of the unaltered feldspars do not belong to this stage of early crystallization but crystallized instead in or near the chilled margin from later pegmatitic or granophyric intercumulus liquid. Those determinations of anorthite content for the first 7.5 feet which are considered reliable are shown in the histogram of Figure 36, representing 46 determinations. Structural state may affect these determinations slightly and some of the measurements may not represent a maximum extinction angle; and hence the compositional range may be narrower than reported and the reported An content may be too low by several percent. Most plagioclase in chilled basaltic magmas has the normative range An_{65}-$_{70}$ (Brown, 1967). Optical determinations at two inches below the top suggest a modal range of An_{37} to An_{72}, the more sodic being within micropegmatite. Therefore, assuming the more calcic to be typcial of the chilled top (phenocrysts are typically bytownite or anorthite, and groundmass plagioclase is about An_{65}; see normative calculations in Table 29 and Wilkinson, 1967, p. 182), plagioclase occurs in the first two feet in the range An_{55}-An_{75} (cf. Palisades at An_{66} according to Walker, 1969) and from two feet to eight feet it ranges An_{45}-$_{56}$ at which compositions the histogram shows a maximum frequency. Later, interprecipitate plagioclase (uncommon) is of the composition An_{30} - An_{40} and very rarely An_{10}-An_{20}, the latter occurring in transecting veinlets.

The more sodic plagioclases are frequently associated with actinolite needles as are the infrequent potassium feldspar and quartz. Clouding (hematite or magnetite) is characteristic of the chilled margin and saussuritization is noticeable, especially of the matrix and smaller plagioclase crystals (i.e., the earlier, more calcic plagioclase). At about two feet below the top, several plagioclase laths show re-solution and corrosion effects that may indicate that they grew in a metastable region ranging between saturation and unsaturation (Seifert, 1964, p. 313) after an initial super-saturation at the top of the chilled zone. Zoned plagioclase grains (uncommon) contain cores of about An_{58} and mantles of about An_{32} (based on albite twin extinctions), representing the precipitation of a small amount of interstitial late feldspar (also see Figure 39).

Other minerals present are in minor or trace amounts. Assuming that about 90 percent of the completely altered phenocrysts were originally olivine (relict pyroxene grain outlines are rare), olivine originally comprised one to four percent of the chilled margin. The original composition of the olivine has not been determined, but several lines of evidence suggest that it was not rich in fayalite but was an intermediate olivine. Wilkinson (1967), in a summary of olivine compositions from diabase, notes that magnesian olivines are the general rule (Fa_{15} - Fa_{25}), even though more ferrous olivines have been reported. The alteration of olivine phenocrysts to amphibole, chlorite, or serpentine has, in some instances, taken place with no accompanying *in situ* iron oxide. In other cases where iron-oxide rims are present, they can best be accounted for by migration and nucleation of matrix iron-oxide dust or by introduction of iron (Plates 12, 13). Lapham (1960, p. 1913) has noted that the amount of iron around these altered phenocrysts occassionally far exceeds that which could have been released even by the pure fayalite.

Orthopyroxene, largely enstatite as adduced from the few relicts, shows little exsolution, twinning, or Schiller structure. Originally, it comprised between zero and three percent of the phenocrysts. It could not be identified in the very fine-grained matrix.

A large number of minerals are present in trace amounts, most of them associated with trapped intercumulus liquid (see Wager and others, 1960) or in late transecting veinlets. Included in the former type are untwinned potassic feldspar, quartz, apatite, and microcline microperthite. Included in the latter category are actinolite, zeolites (chiefly datolite and prehnite), sphene, calcite, serpentine (chiefly chrysotile), magnetite, chalcopyrite, chlorite, and pyrite. Associated with ilmenite and/or titaniferous magnetite is a red-brown hornblende and a red-brown biotite, the latter occasionally constituting up to four percent of the chilled margin. This consistent association suggests that both minerals may be titaniferous. Garnet, associated with diopside, rarely is present at the top of the chilled margin. Clinozoisite (or epidote) and sericite are present as alteration products of feldspar.

Discussion and Summary

Because of rapid nucleation and crystallization in the chilled margin, paragenetic relationships among most minerals have little meaning. Essentially two separate processes have resulted in the present assemblage. The first involved the early cyrstallization of phenocrysts of olivine and orthopyroxene followed by rapid crystallization of glass or small (clino-) pyroxene and plagioclase crystals. Early amphibolitization of olivine and pyroxene phenocrysts may have occurred penecontemporaneously with their crystallization if the H_20 concentration was sufficiently great, resulting in deuteric alteration. Alteration of phenocrysts, and to a lesser extent of the more stable and younger minerals in the matrix, also occurred after sheet emplacement and resulted in amphibole, serpentine, and chlorite. Approximately coincident with this later alteration was the metamorphic growth and replacement of the chilled matrix by diopside and, less frequently, by actinolite, phlogopite, and garnet. These are in turn replaced by magnetite, chlorite, actinolite, and minor pyrite. Final stages of mineralization, not separable into distinct episodes, include veins of albite-oligoclase, potassic feldspar with some microperthite, calcite, hematite, quartz, and zeolites. These interstitial minerals are essentially unaltered. However, they were probably stable under the conditions of alteration and metamorphism that affected the upper portions of the diabase and thus could have slightly preceded metamorphism. A silica-rich fraction (micropegmatite and granophyre) crystallized near the base of the chilled margin after the chilled margin matrix and contemporaneously with, or after, the alteration of the phenocrysts.

The chilled margin at the top of the diabase sheet at Cornwall is fairly typical of chilled borders with the exception of the later replacement by diopside and magnetite. Typical textures include some glass at the top contact and a phenocrystic texture below grading into normal diabase as the crystalline grain size of the matrix increases. Phenocrysts of olivine and pyroxene have been hydrated to secondary Fe-Mg-Al silicates (amphibole, serpentine, chlorite). This extensive alteration of phenocrysts may be the result of deuteric alteration reflecting a locally hydrous magma or the result of metasomatic activity above the diabase sheet. Pyroxene does not exhibit exsolution lamellae or noticeable twinning. Plagioclase of An_{65} is generally unzoned, has a high elongation ratio, and exhibits only simple twins, predominantly Manebach. The rapid crystallization that these characteristics reveal also has resulted in the trapping of an intercumulus, or interprecipitate, liquid that has yielded a more sodic plagioclase with some potassic feldspar, quartz, and microperthite. Small grains of iron oxide dust, probably magnetite, occur throughout the chilled matrix but not through the intercumulates, a result of the rapid nucleation of magnetite and its inability to form recognizable crystal grains.

Normal Holocrystalline Diabase

Introduction

Holocrystalline and subophitic diabase with a grain size diameter of 0.1 to 1.0 mm, hereafter referred to as "normal" diabase, extends to within a few feet of the top of the sheet and is gradational in texture and composition with the chilled margin above. Below the first fifty to seventy-five feet, the diabase is uniform in texture with the exception of small pockets of micropegmatite, segregates of coarsely crystalline diabase pegmatite (grains 0.3 to 5.0 mm in diameter), somewhat finer-grained granophyre either in segregates or veins, and sub-porphyritic diabase near the base of the sheet. No banding or layering has been noted, although only one drill core that penetrated through the diabase has been studied. With the exception of this one core, all of the petrographic and chemical information concerning the Cornwall sheet has been compiled from the top three hundred feet. Data from the western mine were obtained from a re-study of Hickok's thin sections plus a few new sections. The area studied by Hickok (1933) is now largely mined out and inaccessible. Unfortunately, his key to the locations of samples from which his sections were made is lost so that depth information was not directly available. However, texture and grain size yield a crude approximation of depth within the first fifty to one hundred feet (see Figures 38 and 40). Samples studied from the eastern mine were collected by the authors.

In all, 67 thin sections were studied in detail (excluding the granophyre) and approximately 30 additional sections were examined more briefly. X-ray diffractometer patterns were analyzed for a few samples, chiefly those containing feldspars and "exotic" vein minerals such as datolite and apophyllite. Mineral percentages were estimated visually and spot checked by point counts.

Texture

The texture ranges from hypocrystalline and subophitic in the finer-grained portions near the top to typically holocrystalline-ophitic ("diabasic") in the coarser-grained portions where plagioclase is consistently intergrown with pyroxene. Only rarely at the base and at the top of the sheet is there a suggestion of glomeroporphyritic character. Especially in the more coarsely crystalline portions, hypidiomorphic to idiomorphic-granular textures predominate, indicative of essentially simultaneous crystallization. Resorption embayments and poikilitic grains are noticeably characteristic of pyroxenes in addition to zoned and mantled crystals of both plagioclase and pyroxene. Both ocillatory and simple progressive zoning are present, the former noted only in the plagioclase series. Near the base, where the texture becomes sub-porphyritic, cataclastic mortar textures, shear foliation, and veining are present. Small pockets of graphic granite, called micropegmatite, are present throughout the sheet. In the top third of the sheet, segregations of coarse diabase pegmatite occur and locally, but not commonly, are gradational into finer-grained granophyre. With these exceptions, the texture of the diabase sheet is remarkably consistent both laterally and vertically.

Differences in grain size with depth and with mineral composition are similar to those noted by Walker (1940, p. 1069, 1070, and 1075) for the Triassic Palisades diabase, except that the increase in length of plagioclase laths near the base is not so pronounced at Cornwall. Frequency of twinned plagioclase and clinopyroxene and extent of pyroxene exsolution tend to increase, although not uniformly, with increasing grain size.

General Mineralogical Composition

Mineralogical composition conforms to that of most diabases and dolerites or, more properly, quartz-bearing diabase according to the classification of Johannsen (1937, p. 318), since quartz normally comprises less than five percent of the rock. It is a universal constituent of the York Haven Pluton in both the mode and the norm. The two major constituents of diabase, plagioclase and pyroxene, are dealt with later to emphasize subtle differences between the Cornwall sheet and other diabases. The remaining minerals fall into the following four genetic groups: (1) accessory minerals (5 percent or less) that are primary, universal constituents; (2) late-stage differentiates mostly concentrated near the top of the sheet (see Appendix 3); (3) alteration products of the early-formed minerals; and (4) secondary minerals that usually occur in veins transecting characteristic diabase textures.

The accessory minerals are: zircon, usually enclosed within biotite; biotite that probably is titaniferous (brown to purple-brown) in diabase pegmatite and that is always closely associated with iron-titanium oxides; ilmenite and magnetite (or titaniferous magnetite); apatite, quartz, and rarely potassic feldspar in interstitial micropegmatite; pyrite; chalcopyrite; olivine, especially in the chilled margin and rarely toward the base of the sheet; enstatite, also restricted to or near the chilled margin; and possibly stilpnomelane. In a study of the opaque minerals in Pennsylvania diabase (not restricted to the Cornwall area) Davidson and Wyllie (1968) report ulvöspinel intergrown with magnetite and trace amounts of chalcopyrite in addition to those mentioned above. They also identified an earlier titaniferous magnetite associated with ilmenite and ulvöspinel and a later, titanium-poor magnetite. The greatest concentration of opaque oxides occurs in diabase pegmatite or transitional granophyre, rather than in normal diabase.

Minerals that are characteristically alteration products of earlier minerals are: sericitic muscovite (from plagioclase); chlorite (from biotite or pyroxene and uncommonly from hornblende); hornblende (from clinopyroxene); leucoxene and sphene (from ilmenite or ulvöspinel); hematite (from the opaque oxides); and chrysotile (from orthopyroxene or, less commonly, pigeonite). Below the upper chilled margin, chrysotile was noted only within the basal third of the sheet. Sericitization of plagioclase is particularly well developed near contacts with diabase pegmatite, granophyre, and ore veins in the diabase. Chloritic alteration of pyroxene is distinguished from later, secondary chlorite by its anomalous brown birefringence and contiguity with pyroxene.

The secondary minerals, largely introduced into diabase during metasomatism and ore-stage mineralization, are: carbonates associated with quartz in veins; muscovite; chlorite with anomalous blue birefringence (a high-iron variety typical of the ore zone) and associated with magnetite; actinolite or tremolite-actinolite associated with muscovite and rarely with calcite, magnetite, and chlorite or with epidote, garnet, and quartz; and the zeolites, chiefly datolite (rarely containing sphalerite), apophyllite, natrolite, stilbite, analcime, and heulandite (for a complete listing see Appendix 1). Veins of massive datolite up to several inches thick have been found near the top of the sheet and veins of apophyllite were observed as much as 700 feet below the top of the sheet.

Plagioclase Feldspar

Differences in plagioclase composition with both depth and time yield significant information about the crystallization history of the Cornwall diabase, and this in turn can be contrasted with other ore-associated and non-ore-associated types of diabase. The plagioclase compositions presented here are only approximate and could well profit from more sophisticated and accurate analytical methods.

The majority of plagioclase compositions were determined by a modification of the Michel-Levy method; that is, the angular measurement of twin extinction angles at equal twin illuminations. These measurements were averaged for each thin section, or for each texture and composition within a section. Compositions reported in all figures and tables utilized this modification. Consequently, maximum An composition may be several percent too low (e.g., Table 21), however, the method does enable rapid estimation for compositions more sodic than the most calcic plagioclase present. In a few cases, composition curves for combined Carlsbad-albite twins were used (after F.E. Wright, in Kerr, 1959, p. 261). An attempt was made to select grains that did not show internal optical-crystallographic scatter (Vogel, 1964), that were normal to (010), and that yielded maximum extinction angles; but some variation in the compositional determinations probably resulted, especially in the coarser-grained textures where optical scatter is almost universally present and where several compositions are present in one thin section. Structural disorder, not determined in this study, also affects the twinning orientations and hence also affects the composition determined from the published curves. Thus, not all compositions plotted on the illustrations (Figures 36-40 and 43-45) are real; compositional maxima are more accurate reflections of true compositions. However, complete homogeneity would not be expected in most magmas (see Brown, 1967). To arrive at an average, bulk plagioclase composition, determinations were made on all properly oriented grains within the field of view at 100X magnification around the perimeter of each thin section. For the majority of thin sections, this averaging method resulted in at least 25 determinations for each section. If this method did not yield a minimum of 15 determinations, additional grains from the center of the slide were sought at random and measured. A total of 1700 measurements were made.

The average Michel-Levy extinction angle yields a composition of all plagioclase in the Cornwall sheet is $An_{51.5}$, excluding granophyre. Preliminary results (Gray, 1956, p. 184-185) suggested a more calcic composition, but this study was later expanded to include a wider sampling of normal diabase, units transitional between diabase and diabase pegmatite, diabase pegmatite, and some plagioclase at contacts between micropegmatite and normal diabase (Lapham 1962, p. 38) which lowered the average composition. The top 250 feet (Figure 37) yields about An_{48}, as does the basal 135 feet. The center of the sheet averages about An_{55}(see Figure 44), which is only a few mol. percent less anorthitic than Walker (1940) reported for the Palisades diabase. Plagioclase analyses of two other Triassic diabase sheets, at Dillsburg, Pennsylvania (Hotz, 1953) and at Deep River Basin, North Carolina (Hermes, 1964), are noticeably more calcic, although the entire sheet thickness at Dillsburg was not studied. However, the average composition of typical tholeiite, about An_{50}(Yoder and Tilley, 1962), is very near that of the Cornwall sheet, and the range, excluding interstitial micropegmatitic plagioclase, is An_{40-65}(Figure 37), similar to that of most tholeiitic diabase (An_{50-70}, Wilkinson, 1967). Shannon (1924, p. 10) notes compositions of An_{53} and An_{58} as typical of the Goose Creek, Virginia, Triassic diabase sill.

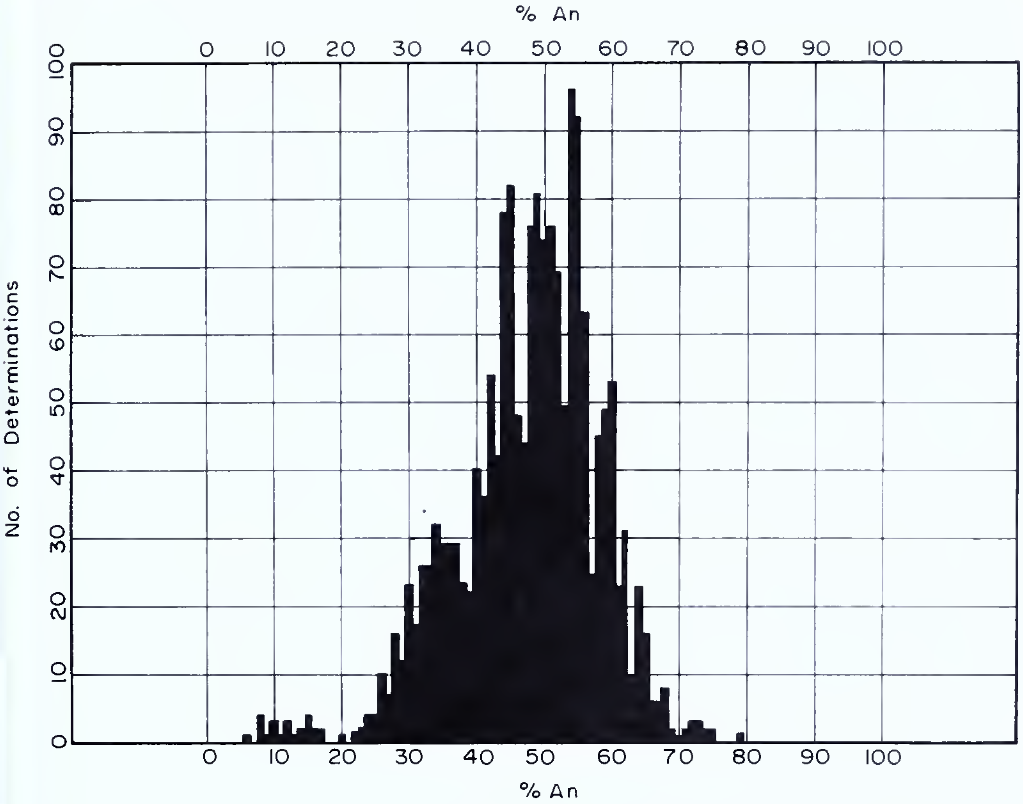

Figure 37. Histogram summary of approximate plagioclase compositions in the top 250′ of the Cornwall diabase. Compositions are note as gradational as illustrated. Compositions An_{5-17} are in late veinlets and An_{20-38} are interstitial or micropegmatitic plagioclase. Compositions determined from average Michel-Levy extinction angles.

A better comparison of the Triassic sheets is obtained by textural subdivisions (Table 21):

Table 21. *Comparison of Average Plagioclase Compositions in Different Facies of the Cornwall and Dillsburg Sheets*

	An Content at Cornwall *	An Content at Dillsburg (Hotz, 1953, p. 685)
Chilled facies	60+	65
Normal diabase	58	62
Transitional to diabase pegmatite	54	—
Diabase pegmatite	50	55
Transitional to granophyre	38	47
Micropegmatite	35	—

* Compositions from Michel - Levy average rather than maximum extinction angles.

With the exception of occasional sharp contacts between micropegmatite or diabase pegmatite and normal diabase, there is a continuous textural and compositional gradation among these subfacies. Even where contacts appear to be sharp, a compositional transition zone may be present. Generally, however, there is a consistent increase in anorthite content as grain size increases throughout the first 250 to 300 feet (Figure 38). Below this depth, anorthite content tends to change independent of grain size, increasing slightly toward the base (Figure 44).

Changes in composition in the Cornwall diabase can be recognized in several ways: 1) near the top very small crystals are more calcic; 2) simple Manebach and Carlsbad twins are characteristic of early, usually more

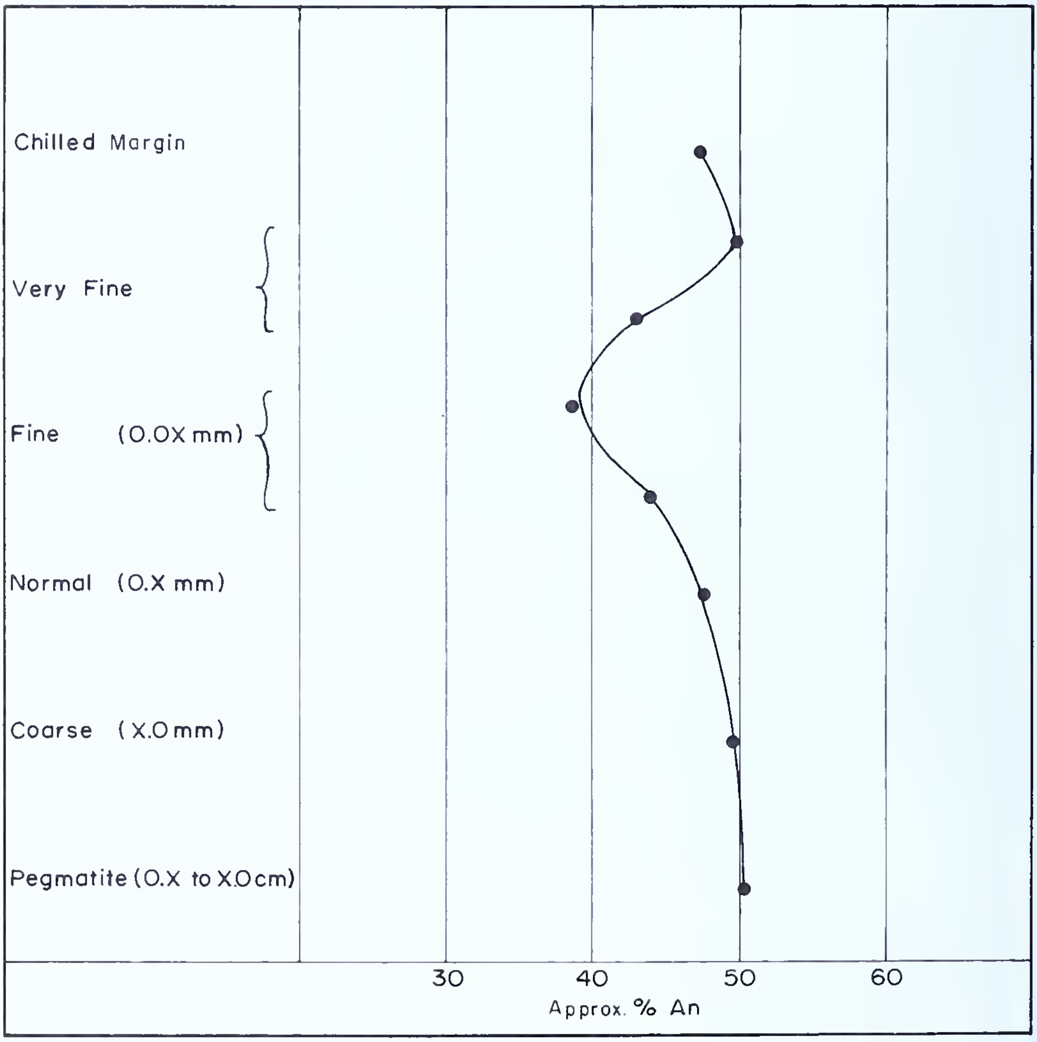

Figure 38. Average grain size versus average plagioclase composition (approximate) in the top 300′ of Cornwall diabase below eastern and western ore bodies.

calcic, plagioclase; 3) pericline and complex albite twins with optical-crystallographic scatter are characteristic of the intermediate (An_{48-58}) plagioclases; 4) zoned crystals with a core 10 mol. percent to 20 mol. percent richer in anorthite than the rim (Figure 39 and Plate 14-C); 5) oscillation zoning with as many as 14 zones (Plate 14-D); and 6) sericitization of early-formed, more calcic plagioclase where it is in contact with younger, more sodic, plagioclase in micropegmatite and granophyre (Plate 14-A).

Although there appears to be a complete gradation in composition and grain size throughout the range An_6 to An_{79} (Figures 37 and 40), the gradation is at least partly the result of the optical method used and in reality the compositions are more discrete than illustrated. Where compositions could be determined on mantled plagioclase, some of the maxima in Figures 37 and 40 coincide with core and rim compositions (Figure 39). These maxima tend to smooth out as more thin sections are averaged together. Furthermore, compositional range narrows and maxima sharpen as the grain size increases (Figure 40). This suggests that some compositional scatter is real and may be a function of the rate of crystallization (see Brown, 1967, p. 111 and Plate 14-B). In the finer-grained portions, the earlier crystals formed too rapidly to be re-equilibrated with later magma compositions. Where plagioclase in diabase pegmatite has the same composition as in adjacent normal diabase, the compositional range is narrower and the maxima are sharper in the pegmatitic facies (compare Figures 37, 44, and 45). Plagioclases in normal diabase between the extremes of rapid chilled margin crystallization and rather slow, pegmatitic crystallization were con-

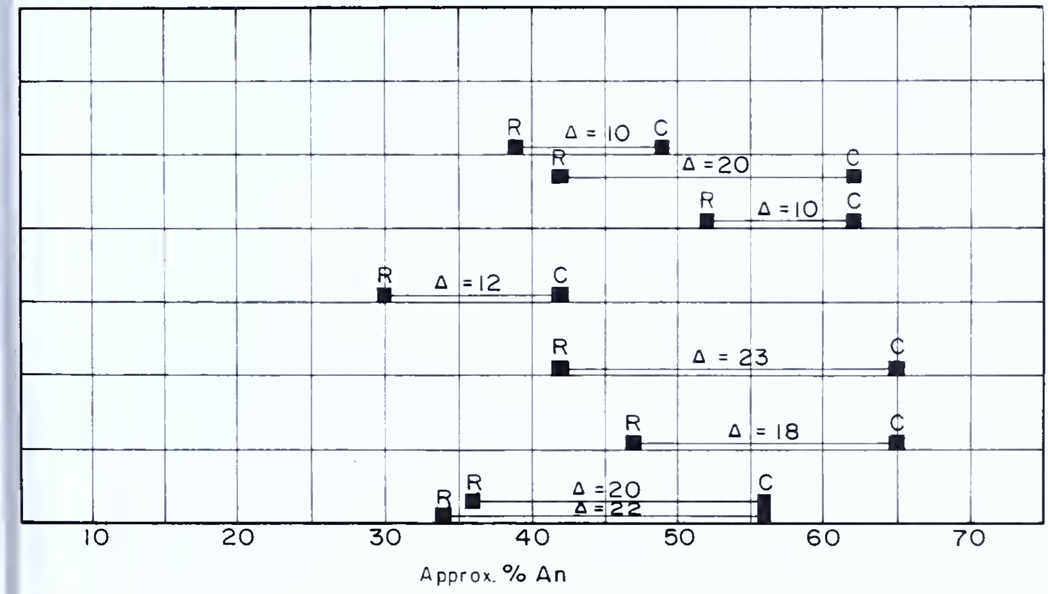

Figure 39. **Approximate plagioclase composition of core-rim pairs in normal Cornwall diabase.**

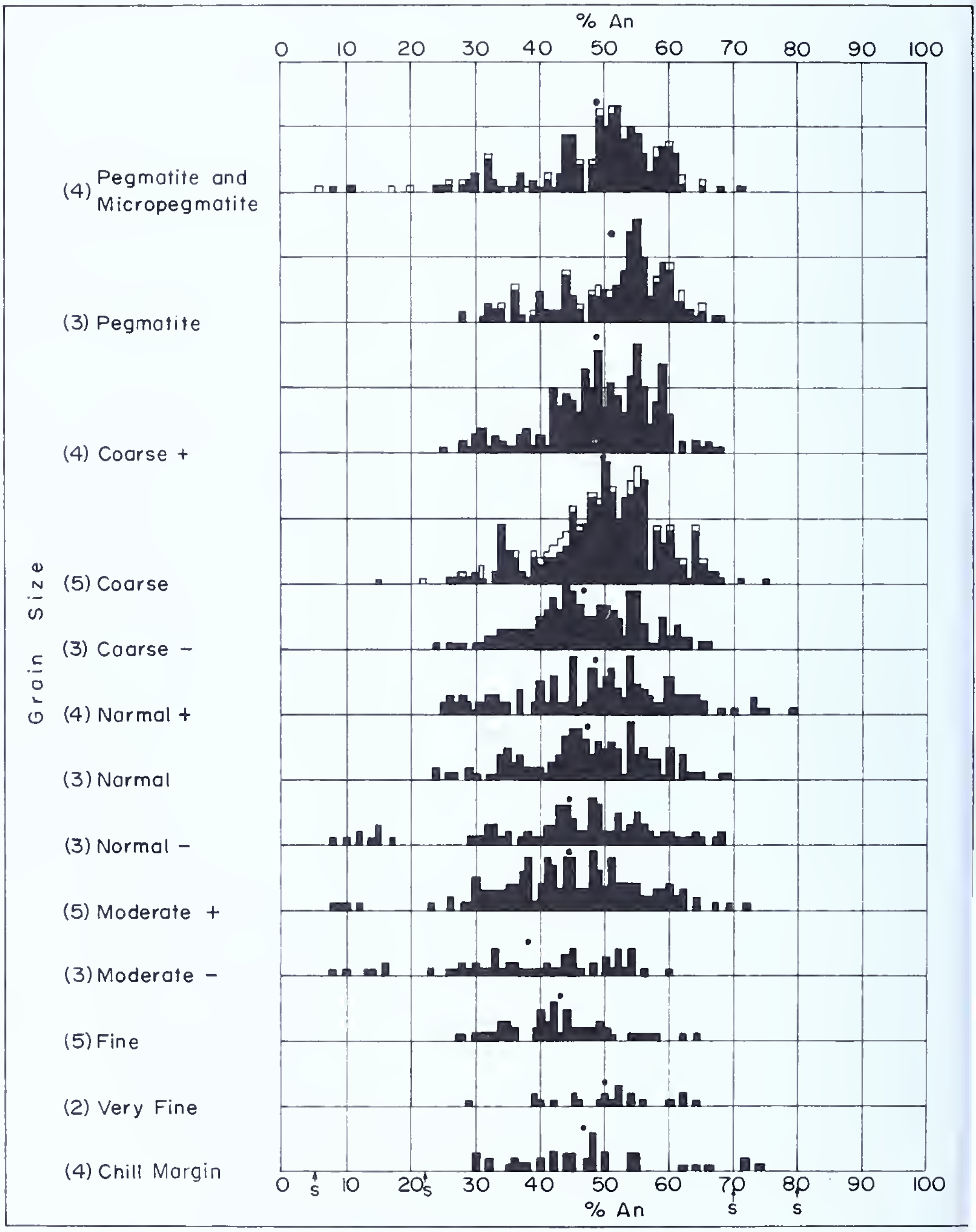

Figure 40. Histogram of approximate plagioclase compositions versus average grain sizes for Cornwall diabase; parentheses indicate number of samples analyzed; dots indicate average compositions; ranges between arrows (S) indicate chilled margin (high An) and micropegmatite (low An) limits; open boxes are from altered diabase samples. Compositions determined from average Michel-Levy extinction angles.

trolled by the fractionating liquid as it became more enriched in sodium relative to calcium. Here, individual thin sections, or textural groups of thin sections, exhibit three to five compositional maxima (Figures 40 and 43) representing different time-temperature-composition environments of crystallization without any textural evidence of re-equilibration reaction between magma and earlier crystals. In general, the wide range of plagioclase compositions indicates crystallization under new conditions. The presence of lamellar-twinned plagioclase may indicate rather rapid plagioclase crystallization (Sarbadhikari, 1965, p. 146). Zoning, which is common near the top and the base of the sheet (Table 23), indicates a lack of reaction and a weak response to the new conditions. The continuous compositional range of plagioclase is indicative of weak fractionation, and the zoned type of locally stronger fractionation (Bowen, 1928, p. 96-124).

Pyroxene

As is true of the plagioclase series, the ortho- and clinopyroxene series are major components of the Cornwall diabase sheet. Their varieties and differences yield important information about diabase crystallization. For example, pairs of pyroxenes within the Ca-poor and Ca-rich varieties should not coexist (see Brown, 1967).

Where sufficient data have been obtained, the nomenclature of Poldervaart (1947) for the orthopyroxenes and that of Poldervaart and Hess (1951) for the clinopyroxenes has been used (Figure 41). For the orthopyroxenes, usually only a two-fold division was possible: enstatite for optically positive grains and hypersthene for optically negative gains. For the clinopyroxenes, precise 2V measurements with a universal stage were not made, so diopside was not further subdivided (Figure 41). Undifferentiated pyroxenes are termed Ca-rich pyroxene or augite. The identification and designation of a particular pyroxene in the Cornwall diabase has been simplified to certain optical criteria and is valid only within these limits.

Orthopyroxene, whether early or late in the crystallization sequence, has been identified by its parallel extinction, optic sign (usually negative and therefore hypersthene), large 2V and, if late in the sequence, by its rather coarse exsolution. Orthopyroxene inverted from pigeonite has been identified by negative optic sign, large 2V (if not altered), frequent alteration to chlorite or less commonly to serpentine, frequent herringbone structure, the presence of both coarse and fine exsolution lamellae parallel to (001) and (100) respectively, and rarely by relict pigeonite cleavage (Plates 15, 16, and 20).

Pigeonite is easily recognized by its small, positive 2V, inclined extinction, and fine exsolution lamellae (Plate 17).

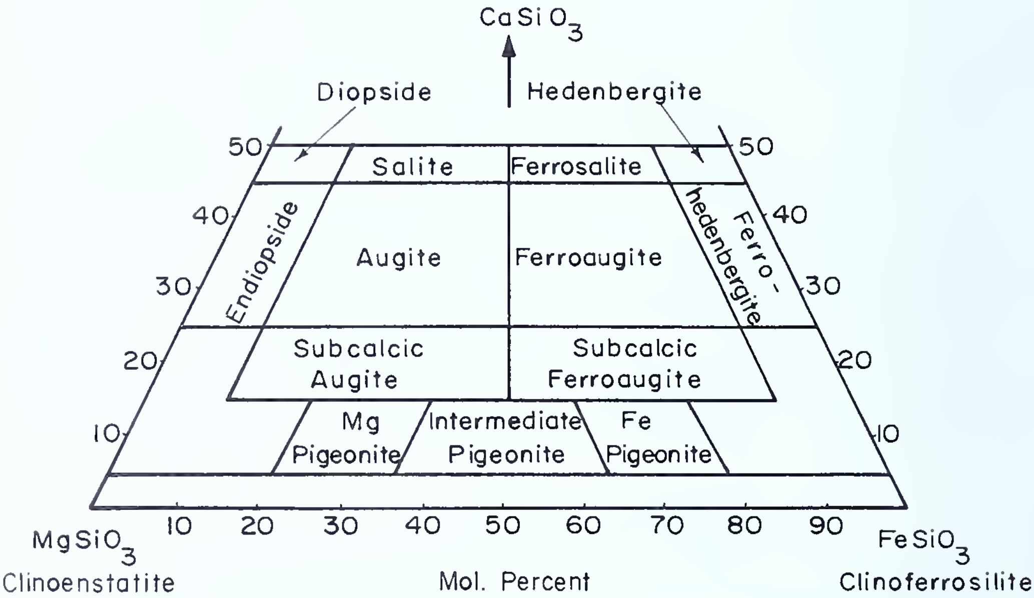

Figure 41. Nomenclature of the clinopyroxenes (after Poldervaart and Hess, 1951).

Clinohypersthene is a name given to grains with optical properties characteristic of both hypersthene and clinopyroxene. It has a large, negative 2V as in normal hypersthene, possesses inclined extinction usually between 6° and 15° but up to 30°, and is distinguished from inverted pigeonite by a lack of augite exsolution lamellae parallel to (001) (Plates 16 and 20). It is apparently similar to the Palisades clinohypersthene of Walker (1949). Boyd and Brown (1969) have noted a clinohypersthene in Bushveld pyroxene that results from augite exsolution from pigeonite that remained uninverted as lamellae because of inhibition by energy relations along the host-lamellae interface.

Augite is distinguished by a moderately large, positive 2V (usually 40° to 55°), inclined extinction, resistance to secondary alteration (Plate 15-B, D), faint pleochroism, especially in the ferriferous and titaniferous varieties, and a very fine vermicular exsolution visible under high magnification (Plates 15, 17, and 20). Hedenbergite, or ferrohedenbergite, is distinguished chiefly by its green pleochroism and large, positive optic angle. Similarly, ferroaugite (possibly titaniferous) was identified by its purplish brown to green pleochroism. Both of the latter two clinopyroxenes are only rarely present.

The three pyroxenes most abundant in the Cornwall diabase are hypersthene and pigeonite in the calcium-poor series and augite in the calcium-rich series. As differentiation proceeded, pyroxene composition changed in each series. Ferroaugite and probably ferrohypersthene with some ferrohedenbergite are present in diabase pegmatite and rocks transitional with diabase pegmatite and with granophyre. Where ilmenite is abundant, as in pegmatitic diabase, clinopyroxene may be titaniferous. Very early enstatite and very late aegirine-augite are quite rare, the former near the borders of the sheet where the Mg/Fe ratio is high and the latter in transition zones between diabase pegmatite and the alkali-rich granophyre.

Hypersthene crystallized early, presumably at or above 1050° C (Figure 42), below the temperature of clinopyroxene inversion (see Karroo and pigeonitic rock series curves, Kuno, 1968, p. 637). Use of this inversion curve presupposes a separation between stable phases (see discussion by Yoder, Tilley, and Schairer, 1963, p. 89-90). Most of this hyperthene was followed by the crystallization of pigeonite that has since inverted to hypersthene (Figure 42, Table 22; also Kuno, 1968, Figure 7; Poldervaart, 1944). Most of the hypersthene present is an inversion product of pigeonite that crystallized above the inversion temperature (Plate 20-A). This later hypersthene should be richer in the ferrosilite molecule than the earlier hypersthene. As temperature dropped and the fractionating magma became enriched in iron, hypersthene crystallized simultaneously with pigeonite along the inversion-curve boundary, followed by some ferrohypersthene in diabase pegmatite. Exsolution lamellae are not as characteristic of this later hypersthene as of the earlier types. Hypersthene, present throughout the entire sheet, is optically zoned near the base. Such grains consist of a core and rim for which extinction positions differ by 5° to 10° while maintaining a cleavage-parallel extinction.

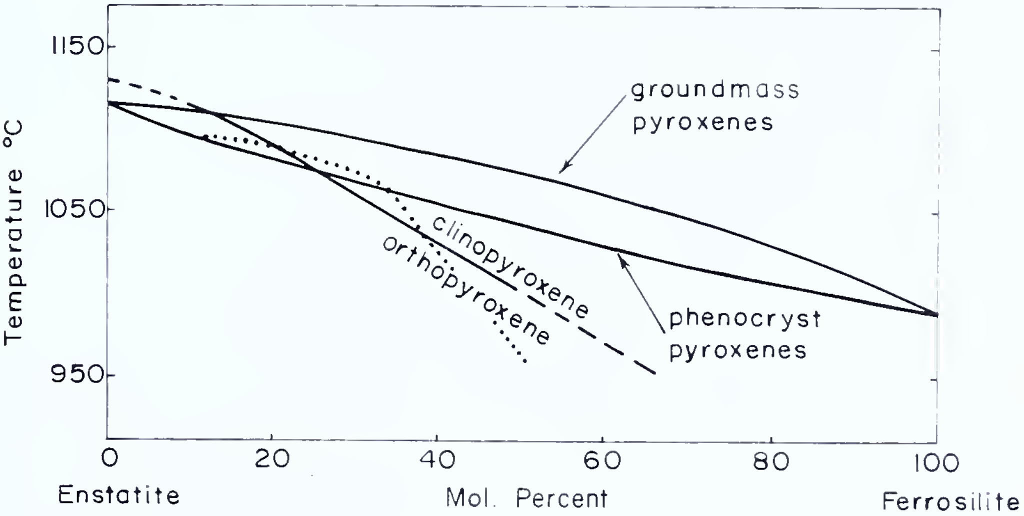

Figure 42. Orthopyroxene - clinopyroxene phase diagram (after Brown, 1957). Inversion curve neglects pressure effects (see Yoder and Tilly, 1962, p. 390-391). Dotted curve = hypothetical course of Cornwall magma.

Clinohypersthene, probably a metastable form similar to clinoenstatite but the exact nature of which is unknown, is a calcium-poor clinopyroxene that has not inverted to orthorhombic symmetry (see Boyd and Brown, 1969). It is a minor but universal constituent near the base, and to a lesser extent near the top of the sheet (Plate 16 and Table 23). Optically, it resembles hypersthene except for its inclined extinction. Walker (1940, p. 1073) ascribed the anomalous extinction in clinohypersthene from the Palisades diabase to either rod-like graphic intergrowths of two pyroxenes or to strain. In bronzites from the Karroo dolerite, Walker and Poldervaart (1949, p. 636) suggested that the separation of a calcium-rich clinopyroxene caused the inclined extinction. Boyd and Brown (1969) note that clinohypersthene is an intermediate stage in the inversion of pigeonite to hypersthene. Coarse, graphic types of exsolution commonly are present in Cornwall clinohypersthene (as well as in pigeonite), but lamellar exsolution usually is absent.

The optically positive orthopyroxene, enstatite, occurs only sparingly in or near the base of the chilled margin. Some phenocrysts in the chilled margin, now completely altered to an isotropic material, may have been enstatite. Fine exsolution lamellae rarely are present.

The determination of relative abundance of the various clinopyroxenes depends largely on the determination of optic angle (2V); hence, in practicality, because the 2V of every grain cannot be measured, the abundances noted are approximate. Based on approximate optic angle, three arbitrary divisions of clinopyroxene can be used to represent major abundance groupings in the Cornwall sheet: 1) pigeonite with 2V between 0°and 10°; 2) pigeonite with 2V between 10°and 30°; and 3) calcium-rich pyroxene with 2V between 40°and 60°. Clinopyroxenes with 2V between about 30°and 40°have not been observed. For pigeonites, 2V decreases with progressing differentiation (optic axial plane perpendicular to (010)). Throughout most of the sheet, augite and pigeonite are the dominant pyroxenes, but orthopyroxene is nearly always present and dominates in the basal third of the sheet (Table 23). The major episode of diabase crystallization appears to have been within the two pyroxene field (i.e., two clinopyroxenes) when both a calcium-rich and a calcium-poor pyroxene were stable, presumably in the element ratio composition range within the magma of $Mg_{70} Fe_{30}$ to $Mg_{35} Fe_{65}$. Some augite continued to crystallize beyond this composition but not to the extent noted by Hotz (1950, 1953) in the Dillsburg sheet where more ferriferous augites are more common.

Exsolution is a common feature of all pyroxene in the Cornwall sheet (Plates 15-17 and 20). Microscopically visible exsolution of a calcium-rich phase in a Mg(Fe)-rich host is more common than the reverse. Primary orthopyroxene, both early and late, frequently contains coarse lamellae or graphic-textured exsolution of augite (Plates 15 and 20), the latter frequently restricted to a core area of the hypersthene grain (Plate 15-A). It is suggested that coarse, continuous lamellae result from a slower, more complete exsolution parallel to (100) of the calcium-rich member than the less regular graphic exsolution and finer lamellae (see Boyd and Brown, 1969, p. 215).

In contrast to the coarse lamellae in orthopyroxene, lamellae in pigeonite and augite are finer, more uniform, and more closely spaced (Plate 17). Birefringence of the exsolution phase rarely is visible. Most lamellae are parallel to (001) of the clinopyroxene host. In pigeonite, the lamellae are presumed to be augite; in augite they are presumed to be either pigeonite or hypersthene. Composition of vermicular exsolution, characteristic of relatively late augite, was not identifiable. Lamellae present in augite that crystallized at a temperature and composition for which orthopyroxene is the stable phase probably are hypersthene. Lamellae of pigeonite in augite host probably have not inverted to hypersthene (Brown, 1967, p. 127); some may be clinohypersthene as noted in Bushveld augite (Boyd and Brown, 1969). Herringbone twins (Plate 16-D) parallel to (100) are common in pigeonites that have inverted to hypersthene, indicating not only exsolution of calcium-rich clinopyroxene (presumably before inversion, Brown, 1967, p. 125) parallel to (001) in an original pigeonite host, but also additional exsolution of calcium-rich clinopyroxene parallel to (100), possibly during inversion to hypersthene. Exsolution in early, primary hypersthene also may have occurred during pigeonite inversion. Exsolution lamellae tend to be somewhat thicker in inverted than in uninverted pigeonite, perhaps resulting from additional exsolution upon inversion.

The extensive exsolution in the Cornwall diabase represents an attempt to maintain chemico-structural equilibrium. Some of the forms that this exsolution takes (graphic, lamellar, etc.; see Plates 15, 17 and 20) are not clearly understood; for example, the blebs restricted to the rim of a single pyroxene grain (Plates 15-C and 20-C). This exsolution is especially noticeable where pyroxene is in contact with large pockets of micropegmatite. Microprobe analyses of the host and exsolved phases would aid in determining whether or not the exsolution distribution is the result of a compositionally zoned host or of incomplete exsolution. In this regard, it is interesting to note the presence of partially inverted and mantled pigeonites (pigeonite cores and hypersthene rims) closely associated with both uninverted pigeonite and with hypersthene (Plates 15-A, B and 17-C, D).

Exsolution is more common and more coarsely developed in the coarse facies of normal diabase than in the fine-grained facies, suggesting that perhaps crystallization of the finer-grained facies was too rapid for microscopically visible exsolution. Exsolution is especially noticeable near the base of the diabase sheet where its condition of formation may be related to that which resulted in abundant clinohypersthene. Diabase pegmatite, on the other hand, contains less fine lamellae and more coarse exsolution than normal diabase, perhaps because the cooling rate usually was sufficiently slow for the pyroxene phase to separate more completely. Graphic exsolution (rapid?) is almost universally absent in diabase pegmatite. As Brown (1967, p. 127) notes, graphic exsolution in pigeonite is characteristic of small intrusions where cooling is rather rapid.

The paragenetic relationships among the pyroxenes are summarized schematically in Table 22 and illustrated in Plates 15-17 and 20. In reaction (1), Table 22, the inversion commonly is incomplete and pigeonite with a rim of hypersthene is associated with the pigeonite of reaction (2). Crystallization at the inversion curve probably occurred during slight fluctuations in temperature or fluid composition, resulting in both ortho-and clinopyroxene forms. Simultaneous crystallization of pigeonite and hypersthene may, in part, result from a partition of iron and magnesium between the two phases as the Fe/Mg ratio increases such that the pigeonite-hypersthene pair does not have the same ratio. However, most "pigeonite" associated with hypersthene has inverted.

Table 22. *Pyroxene Paragenesis, Reactions, and Exsolution*

1)	Hypersthene └Augite exsol. ∥ (100)	→	Pigeonite └Augite exsol. fine lamellae ∥ (100)	Inversion →	Hypersthene └Augite exsol. coarse lamellae ∥ (100)
2)	(Mg) Hypersthene └Fe-Ti oxide exsol.	followed by →	Pigeonite └Augite patch exsol.	followed by →	Augite (Fe, Ti) └Vermicular exsol. (pigeonite ?)
3)	Inverted pigeonite (hypersthene) ± herringbone exsole.	followed by →	Augite, Hedenbergite, (Fe-) Hypersthene		
4)	Pigeonite ($2V \doteq 10$)	replaced by →	Pigeonite ($2V \doteq 0$)		
5)	Pigeonite ($2V \doteq 0$)	replaced by →	Ca-rich clinopyroxene		

The Opaque Oxides

The opaque oxides in the differentiation stages of Pennsylvania diabase have been summarized by Davidson and Wyllie (1968). Most of the relationships discussed by them have been observed in the Cornwall diabase: a mixed spinel intergrowth that corresponds to their description of approximately equal proportions of magnetite and ulvöspinel intergrowths, mixed spinel with ilmenite, and late magnetite with no apparent ulvöspinel (the titanium-free magnetite of Davidson and Wyllie) in discrete grains or rimming mixed spinel grains. Skeletal ilmenite after spinel and bladed ilmenite crystals are common in diabase pegmatite, but also occur in transitional pegmatite-granophyre. Hematite, present only in granophyre, occurs as small flecks usually within orthoclase.

All of the iron-titanium oxides are assumed originally to have been a member of the magnetite-ulvöspinel solid solution series that has since undergone exsolution and partial oxidation (see summary by Brown, 1967; Davidson and Wyllie, 1968; Buddington and Lindsley, 1964) to the present assemblage. Oxidation of ulvöspinel to ilmenite in diabase pegmatite is believed to have occurred, but has not gone to completion in any sample examined from Cornwall.

A Vertical Section Through the Sheet

In 1952, the Bethlehem Steel Corp. drilled a vertical core through the diabase sheet to explore for magnetite beneath the diabase. None was found. The hole is located between the eastern and western ore bodies near the south outcrop margin of the north diabase limb, beginning in the chilled facies at the top of the sheet (D.D.H.#155, Plate 21) and continuing into recrystallized, serpentinized, and brecciated limestone below the diabase. Assuming an average dip of 25° south for the sheet at this location, the sheet is 1130 feet thick. Depths given in the text, tables and figures to follow all refer to vertical depth below the sheet surface without the dip correction and are taken directly from the core log (Appendix 3).

The detailed description of this core (Appendix 3) reveals several interesting features. Normal diabase textures prevail throughout most of the sheet except for the basal 70 feet, the upper 90 feet, and where there are coarser differentiates. Diabase pegmatite schlieren and pods (which frequently, but not always, grade into normal diabase) are more common than granophyre and are irregularly distributed throughout the upper 370 feet of the sheet. A very small amount of pegmatitic diabase occurs between depths of 1130 feet and 1140 feet and at 565 feet. Granophyre and transitional granophyre (usually associated with pegmatitic diabase) occur between depths of 270 feet and 335 feet, similar to the depth of much of the granophyre in the Dillsburg sheet (Hotz, 1950 and 1953), and at 1130 feet. Rocks transitional between diabase pegmatite and granophyre have a transition zone narrower than that between normal and pegmatitic diabase. Zeolite and magnetite-actinolite veins occur sporadically throughout the sheet. Both have sharp contacts with the diabase wall rock and have usually caused considerable alteration of the adjacent diabase (sericitization of plagioclase, amphibolitization of pyroxene, and chloritization). Magnetite veins at a depth of 690 feet occur approximately along the strike and down dip from the underground (footwall) ore body enclosed within diabase (see Part 4). Near the base of the sheet, beginning at a depth of about 950 feet, large phenocrysts of pyroxene appear and the diabase becomes porphyritic downward. From about 1065 feet to 1120 feet, just above pegmatitic to coarse-grained diabase, there is considerable shearing, brecciation, an apparent increase in the iron content of augite (105 feet above the base and similar to augite 100-300 feet below the top), a slight decrease in plagioclase An content, and bent plagioclase crystals indicative of stress during crystallization. These observations together with a decrease in grain size at 1065 feet, a somewhat higher TiO_2 content in the lower part of the sheet, the occurrence of transitional granophyre and diabase pegmatite (characteristic of the upper parts of sheets), serpentinization, and the presence of olivine relics, lead to the conjecture that approximately the basal 200 to 260 feet may have been a separate injection with a sheared and internal chilled contact. A similar suggestion by Poldervaart and Walker (1962) and by Walker (in Pearce, 1970, p. 32) has been made for the Palisades diabase. At Goose Creek, Virginia, Shannon (1924, p.37-39) noted silica-rich differentiates near the base of a diabase sill. Although he was unable to adequately explain their position (since light, acid differentiates would be expected at the top rather than at the base of the sill), he suggested that water may have migrated from adjacent shales into the diabase magma. The hydrous minerals, serpentine and chlorite are more abundant at this level (1065 feet) at Cornwall; on the other hand, the zone is well above the base of the sheet.

From 270 to 1227 feet below the top, samples were selected for petrographic examination and chemical analysis (see "Geochemistry-Vertical Chemical Variation"). As might be expected from the textural differences, there are considerable mineralogical changes also. In many ways, these differences are similar to those of the Palisades (Walker, 1969) and Karroo (Walker and Poldervaart, 1949) sheets, but there are significant dissimilarities. Notable is the lack of an olivine layer near the base of the Cornwall sheet, a feature that is prominent in the Palisades intrusion and to a lesser extent in the Karroo province (Walker and Poldervaart, 1949, p. 651). Other comparisons will be considered subsequently in greater detail.

A histogram summary of approximate plagioclase compositions as determined by the Michel-Levy extinction angle method is presented in Figure 43. Solid boxes represent normal diabase; open boxes are less useful because of diabase alteration (hydrothermal magnetite veins, zeolitization, chloritization), shearing, or the presence of late diabasic fractions (micropegmatite, diabase pegmatite) that contain more sodic plagioclase than normal diabase. Average plagioclase compositions and ranges of compositions for the vertical core are summarized in Figure 44. There is considerable apparent plagioclase compositional scatter throughout the sheet, particularly between 10 and 250 feet below the top and near the base of the sheet.

From the curve trend (Figure 44), average plagioclase composition 0 to 40 feet above the base probably exceeds An_{50}, but samples were not available

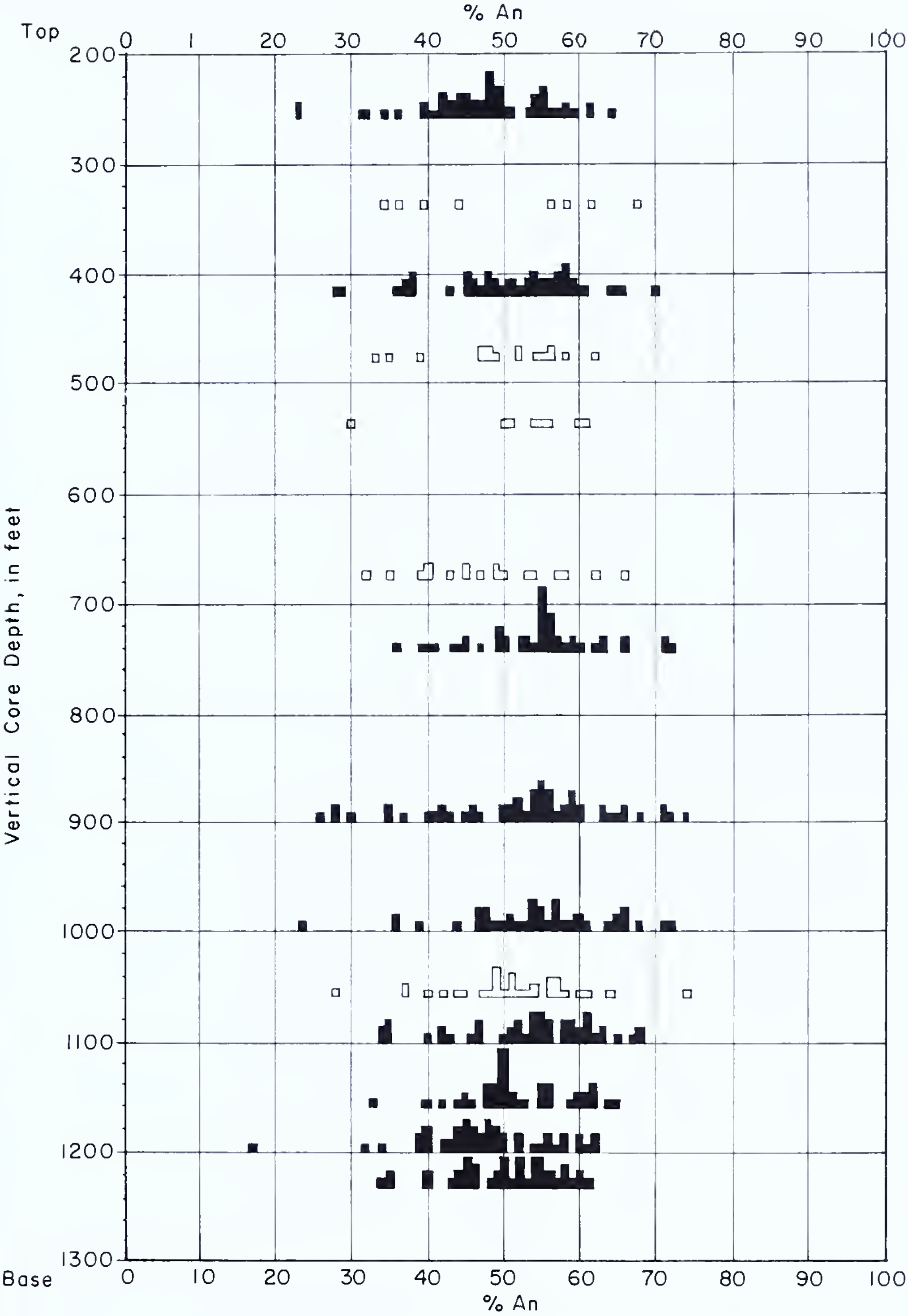

Figure 43. Histogram of number of samples and approximate plagioclase compositions from vertical core through Cornwall diabase sheet beginning at 200′ depth. Open boxes are highly altered plagioclase or less accurate determinations (see text); smallest box represents a single determination. Compositions determined from average Michel-Levy extinction angles.

for determination. Average composition reaches a minimum of about An_{48} about 60 feet above the base; after that, both the An average and maximum content (an approximation to the liquidus composition) steadily increase to about An_{73} about 190 feet above the base. Both average and maximum An content then remain nearly constant to about 450 feet above the base, after which a trend of gradually decreasing An content occurs to a minimum average composition of An_{40} 1160 feet above the base (90 feet from the top), where roof effects dominate and An content again increases.

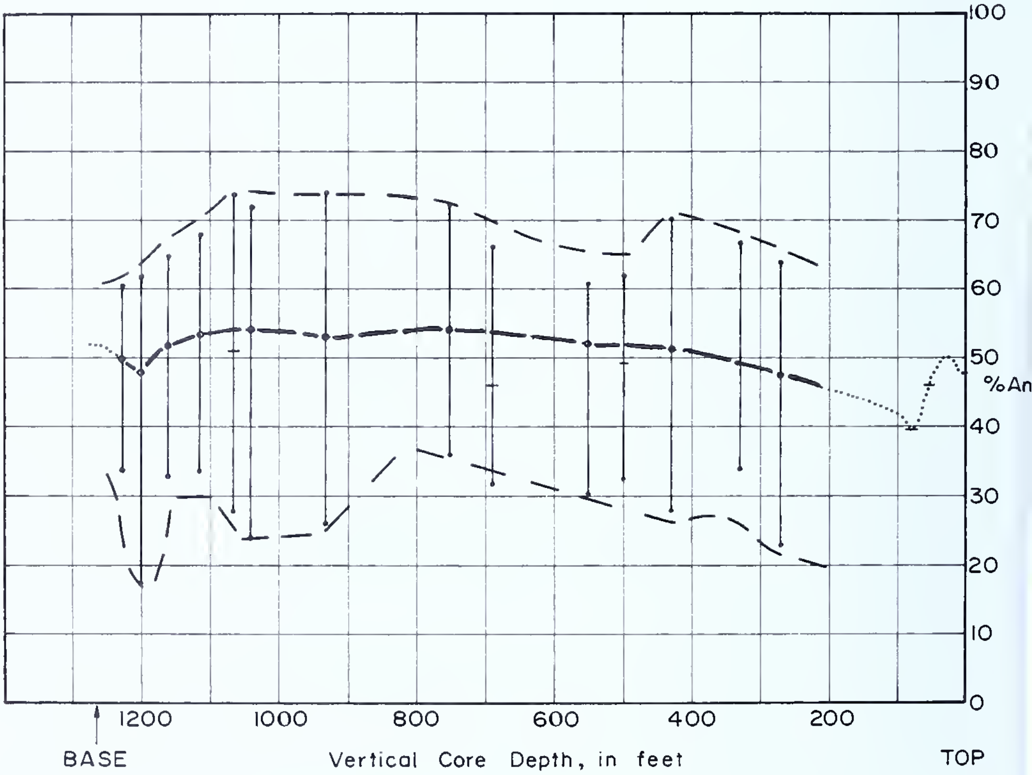

Figure 44. **Average and range of plagioclase compositions of vertical core through Cornwall diabase sheet. Dash = generalized curves; dotted line = determination largely by grain size comparison (see Figure 36-38). Compositions determined from average Michel-Levy extinction angles.**

The Cornwall average composition may be five to seven An mol. percent more sodic than the Palisades curve (Walker, 1940, p. 1070), but the Cornwall distribution from about 250 feet above the base to the top of the shee parallels that for Palisades plagioclase compositions (Walker, 1940, p. 1020) The decrease in An content near the base and the top probably are typical o compositional changes near contacts. Some crystal settling is evident in th top 400 feet, where maximum and average An content increase with depth

Below about 700 feet, there is no evidence of plagioclase accumulation. The large range of plagioclase compositions throughout the sheet is indicative of intercumulus crystallization of entrapped liquid. There is no evidence from plagioclase compositional distribution of more than one magma pulse, even though there is a slight minimum in average composition (An_{51}) at 1065 feet (Figure 44).

The mineralogical variation from 270 feet below the top to within 36 feet of the base (Table 23) illustrates trends that are common to other sills which have undergone some differentiation. Zones of mutual exclusion of pigeonite

Table 23. *Mineralogical Variation in a Vertical Core Through the Cornwall Sheet*

Depth (ft.)	Texture	Pigeonite 2V 0-10°	Pigeonite 2V 15-30°	Augite	Hypersthene Primary	Hypersthene Inverted from Pigeonite	Herringbone Pyroxene	Clino-Hypersthene	Plagioclase avg. An (approx.)	Zoned Plagioclase	Zoned Pyroxene	% Biotite	% Micropeg.	Notes
270	Coarse	X	X	X		X	Rare	?	47	Rare		1-2	3-4	Carbonate, Hornblende, Augite>Pigeonite>Hyp., Fe- Augite
330	Peg-matitic			X	X	X	X		49				7-10	Granophyre: transitional Fe-Ti Aug.; Fe-Or, Ilmenite, Actinolite
433	Coarse	X	Rare	X	X	X	X		51	Rare		1-2	2-3	Fe-hyp., Aug.≥Hyp.>>Pig.
493	Coarse-	?	Rare	X	X	X	X		49			1	1	Granophyre: transitional; Actinolite, Fe- Or, Aug.> Hyp.>>Pig.
550	Normal+	?	X	Rare		X	X		52			1-2	1-2	Qtz.-Actinol.-Muscov. vein, Pig.≥Hyp.> Aug.
688	Normal		X	?		X	X		46			1	1	Apophyllite vein, Fe-chlorite
750	Coarse-		X	X		X	Rare		54	X		1	1	
937	Normal	X	X	?	?	X			53	X	X	1	1	Zoned Pigeonite, Pig.> Hyp.>> Aug.
1040	Normal+	X	X	X	X	X	Rare	X	54	X	X	1-2	1-2	
1066	Normal-			?	X	X			51	X		1	1	Muscovite, Actinolite, Sheared, Serpentinized, Olivine (?)
1114	Normal+		X	X	X	?	Rare	X	53	X	?	1	2-3	Clhyp.>Pig.≥ Aug.> Hyp.
1159	Normal+		?	X	X	?	X	X	52	X	X	1-2	3- 4	Subophitic to granulated, Hyp.> Aug., Ilmenite
1202	Fine+		?	X	X			Rare	48	Rare		2	1	Phenocrysts of Hyp., Brecciated, Serpentine, Olivine (?)
1227	Fine+			X	X			Rare	50		X	2-3	3-4	Brecciated, Phenocrystic, Zoned Hyp., Enstatite, Serpentine

and hypersthene are not as distinct as those by Walker (1940) in the Palisades diabase, but nevertheless are noticeable. These have been termed the Downes Mountain type of dolerite (Walker and Poldervarrt, 1940) and are similar to pyroxene relationships in the Whin sill (Holmes and Harwood, 1928) and the Tasmanian dolerites (Edwards, 1942). The more magnesium-rich pigeonite (larger 2V, column 4) is concentrated in the central two-thirds of the sheet. Inverted pigeonite (hypersthene), usually with herringbone structure, disappears about 1000 feet to 1100 feet below the top. Below this depth hypersthene is the dominant calcium-poor form (along with the calcium-rich augite). Hypersthene, however, is present throughout the sheet, with the exception of the chilled margin. Clinohypersthene is associated with hypersthene, inverted pigeonite, and augite, but almost never with uninverted pigeonite (Table 23). Augite is ubiquitous in distribution. Late Ca-Fe augite (ferroaugite, hedenbergite) occurs in diabase pegmatite in the top half of the sheet and in coarse to pegmatitic diabase about 125 feet above the base. Zoned plagioclase, both progressive and oscillatory, is most common throughout the basal half of the sheet, but occurs sparingly elsewhere (Table 23, column 11). In the Palisades sheet, zoned plagioclase is present throughout, but zoned hypersthene was not mentioned (Walker, 1940). Bent plagioclase crystals are especially common about 150 feet above the base, but locally are present throughout the sheet, frequently adjacent to micropegmatite or diabase pegmatite pockets. Micropegmatite increases slightly toward the base and the top of the sheet. Biotite is present throughout. Actinolite, on joints or in veins, is present throughout the sheet, usually associated with magnetite, rarely with sulfides (Appendix 3). Pyrite and chalcopyrite occur almost exclusively within the top 330 feet, associated with coarse-grained and pegmatitic diabase near and in spinels (Appendix 3).

Diabase Pegmatite

Most of the characteristics of diabase pegmatite have been noted in the previous section on normal diabase and will be summarized only briefly here. Included in the term "diabase pegmatite" is a frequently miarolitic, aplitic pegmatite, distinguished from normal diabase pegmatite by an abundance of white sodic plagioclase, frequent cavities with secondary minerals (epidote, sphene, actinolite, zeolites), and the absence of pink orthoclase feldspar. Aplitic pegmatite, described more fully by Shannon (1924, p. 15-29) at Goose Creek, Virginia, is gradational both with diabase pegmatite and with granophyre. Diabase pegmatite (Plate 18-A and B) is slightly later and of simpler mineralogy than normal diabase, and occurs as schlieren or small pods most commonly in the top third of the sheet, but also near the base. It has a higher Ca/Mg ratio, more TiO_2, more K_2O, more Cl (personal communication, R. Smith II) and more total iron than normal diabase. Here, there is maximum development of the iron titanium oxides, magnetite and ilmenite. Such iron enrichment is typical of differentiated diabase sills;

for example, the Palisades (Walker, 1940), the Karroo (Walker and Poldervaart, 1949) and the Dillsburg, Pennsylvania (Hotz, 1953) sheets. Typical plagioclase compositions (approximate) for 353 determinations range from An_{48} to An_{63} (Figure 45), but include more sodic feldspar where granophyre, micropegmatite (Plate 18 A-C), or transitional rocks are present. Zoned plagioclase has not been observed. As noted by Walker (1940, p. 1092-1093) for Palisades diabase pegmatite and by Wilkinson (1967) in a general summary, the average plagioclase composition is not greatly different from that of normal diabase. Perthite and micropegmatite are somewhat more common, especially where the pegmatite is transitional with granophyre.

The major difference between normal and pegmatitic diabase is in the ferromagnesian minerals, rather than in plagioclase. Pigeonite is not present (except rarely as inverted pigeonite) and hypersthene (probably ferriferous) is less common. In the Karroo dolerite pegmatites, hypersthene is not present (Walker and Poldervaart, 1949, p. 616). Augite is common in large, twinned crystals. Ferroaugites are present in at least two overlapping generations, but probably not with the compositional extremes noted by Hotz (1950; 1953) at Dillsburg. Exsolution in clinopyroxene is somewhat less abundant than in normal or coarse-grained diabase, and in orthopyroxene the lamellae are coarse. Iron, magnesium, and calcium contents in the diabase pegmatite magma probably were more restricted and volatiles somewhat more

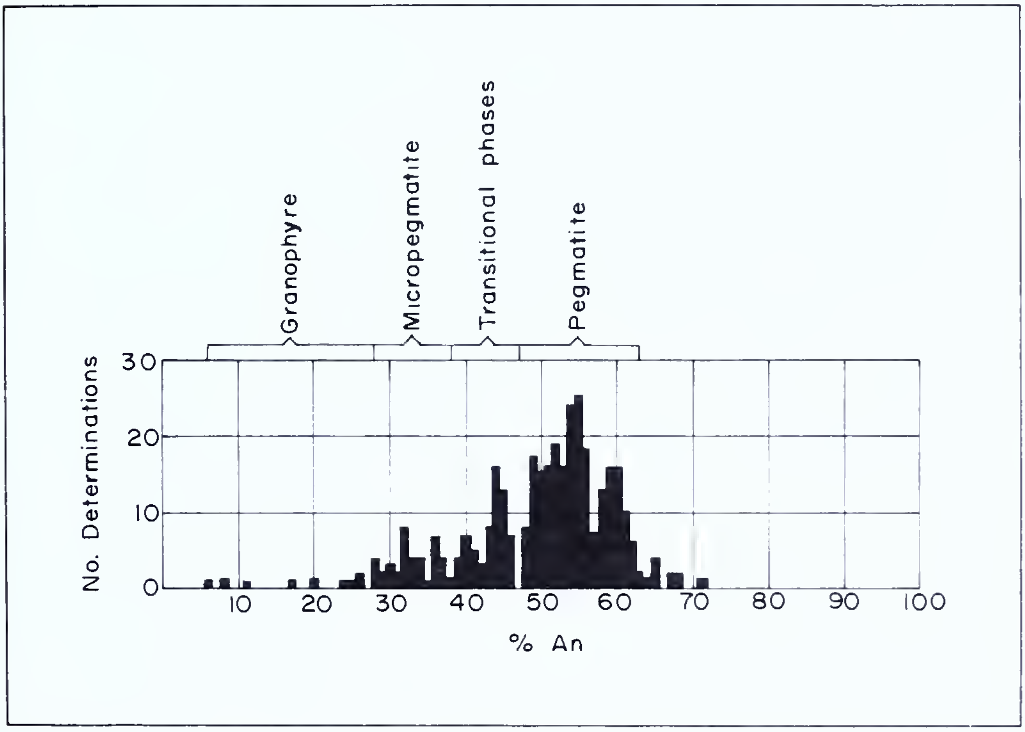

Figure 45. Histogram of approximate plagioclase compositions in diabase pegmatite. Range is of textural types approximate (see text); from average Michel-Levy extinction angles.

Table 24. *Mineralogy of Granophyre and Transitional Rocks from Diffractometer and Petrographic Analyses (in %)*

	1.	2.	3.	4.	5.
Plagioclase	$\sim 40 \begin{cases} \sim 30\ \mathrm{An}_{20\text{-}30} \\ \sim 10\ \mathrm{An}_{40\text{-}60} \end{cases}$	$\sim 25 \begin{cases} \sim 15\text{-}20\ \mathrm{An}_{20\text{-}30} \\ \sim 5\text{-}10\ \mathrm{An}_{40\text{-}60} \end{cases}$	$\sim 15 \begin{cases} \sim 10\text{-}15\ \mathrm{An}_{10\text{-}20} \\ \sim 0\text{-}5\ \mathrm{An}_{30\text{-}40} \end{cases}$	$\sim 35 \begin{cases} \sim 30\text{-}35\ \mathrm{An}_{18\text{-}25} \\ \sim 0\text{-}5\ \mathrm{An}_{10\text{-}15} \end{cases}$	$\sim 40\text{-}50\ \mathrm{An}_{5\text{-}20}$
Microcline	1-5	2-5	5-10	–	5-10
Orthoclase (ferriferous)	–	30-40	50-60	40-50	–
Quartz	15-20	5-10	0-2	1-5	12-18
Amphibole	5-10	3-7	5-10	5-10	25-35
Pyroxene	15-20	1-3	–	–	1-5
Chlorite	5-10	10-15	0-1	1-2	0-2
Mica (biotite ± sericite)	4-8	1-3	0-1	1-2	0-1
Magnetite-Ilmenite	2-5	1	0-2	2-5	0-2
Apatite	–	–	0-1	–	0-1
Zeolites	–	–	5-10	–	–

1. Cornwall: Transitional rock between diabase pegmatite and granophyre (C4-164)
2. Cornwall: Transitional rock between diabase pegmatite and granophyre (C3-5)
3. Cornwall: Typical granophyre (C4-112)
4. Cornwall: Very fine-grained granophyre (C4-112)
5. Dillsburg: Coarse-grained granophyre from Nell's Hill (see Hotz, 1950 and 1953)

abundant than during earlier diabase crystallization, contributing to less subsolidus exsolution. Zoned pyroxenes have not been observed. Biotite associated with the opaque oxides and rarely apatite are present as accessory minerals.

Normal diabase is somewhat altered (sericitization of plagioclase, some amphibolitization of pyroxene, and rarely chloritization of biotite) where it is in contact with diabase pegmatite; the pegmatite is, in turn, somewhat altered (plagioclase to uralite or potassic feldspar) where it is in contact with granophyre (Plate 17). Areas of diabase pegmatite commonly grade over a few millimeters into granophyre (Table 24, columns 1 and 2) as a result of a rapid change in the composition of the residual liquid during the crystallization of the last few percent of the magma. A similar transition into granophyre from diabase pegmatite has been described by Walker and Poldervaart (1949, p. 663) for the Hangnest type of dolerite (which the Cornwall sill most closely resembles among the several Karroo dolerite types). In one Cornwall sample of transitional diabase pegmatite-granophyre, aegirine-augite was identified, but it is not common.

Most of the opaque-oxide characteristics noted by Davidson and Wyllie (1968) in Pennsylvania diabase sheets appear to be present at Cornwall (Plate 18-A), but quantitative differences among the sheets are not known. Such a distribution study is important and ought to be undertaken. Patch exsolution textures and lamellae along (111) spinel planes are intergrowths of magnetite, probably titaniferous, and ulvöspinel. In addition, skeletal ilmenite is present. The matrix of the skeletal ilmenite usually is one or more of the silicates in addition to an oxidized phase such as rutile or leucoxene. Some hematite is commonly present. These later, oxidized phases are more abundant in pegmatitic diabase than in normal diabase. At Cornwall, the quantity of late, titanium-free magnetite cannot be determined until electron probe analyses are available. The textures and associates of ilmenite and late magnetite with quartz-feldspar intergrowths indicate that at least these opaque oxides postdate most pyroxene and calcic feldspar crystallization. An earlier, unmixed parent spinel is presumed but cannot be established on the available textural evidence that consists largely of separate oxide minerals.

Granophyre

Granophyre at Cornwall is a pink, holocrystalline, occasionally miarolitic, fine to medium-grained rock, composed largely of potassic feldspar, some quartz, and minor sodic plagioclase (Table 24). It occurs only within the diabase sheet. The major constituent of Cornwall granophyre is pink, hematitic or ferriferous orthoclase. Because the granophyre is commonly fine-grained, it has locally been called "aplite," but this term is inappropriate in view of the common usage of granophyre for this late differentiate. Granophyre at Cornwall occurs as small schlieren, veinlets, or pockets within the top 350 feet of the sheet (Appendix 3). Veinlets usually have sharp contacts with adjacent diabase, but in many cases the larger pockets are transitional with pegmatitic diabase. Granophyre does not exceed a few percent of the Cornwall diabase and there are no large bodies such as are associated with the Dillsburg sheet (Hotz, 1953). Texturally, the Cornwall granophyre is finer grained than that at Dillsburg and is presumed to result from rapid crystallization (see Barker, 1970, p. 3343).

The final potassium-rich stage of the Hangnest type of Karroo dolerite (Walker and Poldervaart, 1949, p. 681) is directly comparable to the Cornwall granophyre. Lacking in both occurrences is any notable sodium enrichment, although some enrichment did immediately precede the crystallization of Karroo granophyre. The slight trend of sodium enrichment previously noted in Cornwall rocks transitional between diabase pegmatite and granophyre (Table 24) does yield the normal enrichment sequence of iron to sodium to potassium.

The Cornwall granophyre is an important rock for many reasons. It is the last differentiate of the diabase magma and as such contains clues to magma crystallization history; in a time sense, it is the unit that may separate diabase crystallization from magnetite-ore introduction and thus may have a bearing upon ore origin. Granophyre from similar sheets has been interpreted as both an igneous and a metasomatic rock resulting from the transfusion of, or contamination by, sedimentary rocks (Taylor and Epstein, 1963; Hamilton, 1963; Walker and Poldervaart, 1949). The mineralogical resemblance of Cornwall granophyre to metasomatic alteration in the area of the Cornwall ore bodies yields genetic information unique to the Cornwall area.

Approximate quantification of mineralogical components for transitional diabase pegmatite-granophyre, typical Cornwall granophyre, and granophyre from Dillsburg are compared in Table 24. The Cornwall granophyre is characterized by an almost total lack of any pyroxene, a trace to minor amount of quartz, considerable ferriferous and hematitic orthoclase (Tables 5 and 6), and less than 40 percent plagioclase (largely approximately An_{10-20}). These characteristics serve to distinguish the Cornwall granophyre from that at Dillsburg (Hotz, 1953 and Table 24). Myrmekite and graphic granite textures are common; perthite is absent.

Ferriferous orthoclase is usually untwinned, cloudy, presumably with minute hematite inclusions indicating excess Fe^3 in addition to any substituting for Al^3, and is responsible for the pink color of the rock. Optically, it is intermediate between a high-temperature and a low-temperature potassium feldspar (see "Hornfels Metamorphism and Metasomatism" where the same Fe-orthoclase is described from the siliceous country rocks of the eastern Cornwall ore zone). Potassium feldspar (Fe-orthoclase, orthoclase, and microcline) content ranges from 20 to 90 percent of the rock. Plagioclase of about An_{10-20} makes up from 0 to 25 percent of the rock; plagioclase more calcic than this occurs in units transitional with diabase pegmatite or normal diabase (thus the two populations in Table 24). Two micas are present: biotite from 0 to 5 percent and muscovite from 0 to 2 percent. Both actinolitic and blue-green hornblende are always present but seldom exceed 10 percent. Pyroxene is not present in normal granophyre, but in transitional rocks a brown to pink (titaniferous?) hypersthene occurs sparingly. Quartz is present in graphic, or less commonly myrmekitic, intergrowths with potassic and sodic feldspar and only rarely as separate quartz grains. It is not common and appears only as a very minor constituent in the normative calculation (Table 29). Chlorite, usually of a moderately high iron content (X-ray data and indices of refraction suggest on the order of 25 percent total iron), may comprise as much as 15 percent of transitional granophyre and of areas where there has been intense alteration of diabase pegmatite adjacent to granophyre or adjacent to late actinolite-chlorite veins transecting granophyre. Other minor and trace minerals are sphene, rutile, ilmenite, pyrite, hematite, magnetite, apatite, and zeolites. The opaque iron-titanium oxides are much less abundant than in diabase pegmatite; in fact, they are commonly absent in individual thin sections. Spinel minerals are rare in Cornwall granophyre. Skeletal ilmenite is uncommon and has been oxidized to sphere and rutile and the spinels have been oxidized to hematite. In addition, hematite is present in clouded orthoclase.

The change from diabase pegmatite to granophyre commonly is abrupt and marks a rapid increase in alkalies, particularly potassium, and silica (also see Figures 10-13, 47, 48, and Tables 24-25 and 27-28). Alteration effects at granophyre contacts indicate that several reactions between earlier-formed diabase or diabase pegmatite and the residual liquid occurred. Hematite, Fe-orthoclase, chlorite, and possibly "sericite" are the resultant products. One such possible reaction is that described by Wones and Appleman (1961) for biotite, which is a characteristic mineral in diabase but which may be absent in granophyre (also see equations 3-7 and 3-10):

$$2KFe_3FeSi_3O_{10}(OH)_2 + 5/4\ O_2 \rightarrow 2KFeSi_3O_8 + Fe_3O_4 + 3/2\ Fe_2O_3 + 2H_2O. \tag{5-1}$$

(Ferriannite) (Fe-orthoclase) (Magnetite) (Hematite)

Another similar reaction which may have yielded orthoclase is that of Chayes (1955):

$$2KFe_3AlSi_3O_{10}(OH)_2 + 2H_2O \rightarrow Fe_5FeAlSi_3O_{10}(OH)_8 + KAlSi_3O_8 + K^+ \tag{5-2}$$

(Annite) (Chlorite) (Orthoclase)

However, there is such an excess of potassium feldspar, and such a relative deficiency of sodic plagioclase, that residual concentration of a potassium-rich liquid is required at Cornwall. Reactions of the above types cannot account for more than a small fraction of the total potassium feldspar in Cornwall granophyre; for example, orthoclase-chlorite and orthoclase-iron oxide associations in a thin zone between typical granophyre and earlier crystallized diabase. However, the chlorite is more magnesian than indicated in (5-2).

The alteration of (Na, Ca) plagioclase to sodium and calcium zeolites with secondary calcite as a by-product probably occurred where there was excess calcium (equation 3-8). This type of alteration represents the last stage of crystallization within the igneous rocks, including granophyre. Zeolitic products have been found throughout the diabase sheet as well as in metasomatized country rocks near the top of, or included in, the sheet.

There is no evidence that the Cornwall granophyre resulted from the transfusion of sedimentary rocks by a process of metasomatically active fluids or from contamination by sedimentary rock inclusions. All available underground exposures of granophyre show that even the veins with a rather large proportion of mobile constituents terminate beneath the upper chilled facies and do not extend into country rock. The area of exposed diabase is, however, limited. The data do not exclude an origin, at least in part, by contamination. Hotz (1953, p. 701-702) advocated an igneous origin for the more extensive granophyres within the Dillsburg sheet. Pearce (1970) rejects the hypothesis of arkose assimilation for the Palisades sill. Granophyres in the Skaergaard are believed to have been somewhat affected by crustal contamination based on O^{18}/O^{16} (Taylor and Epstein, 1963) and Sr^{87}/Sr^{86} (Hamilton, 1963) ratios. Johns and others (1969) raised the possibility of aqueous vapor transport in their experimental production of granophyre from basalt. Nevertheless, there is no doubt that the Cornwall granophyre is at least in part a result of igneous fractionation during differentiation.

Paragenesis of the Diabase and Differentiates

The sequential mineral crystallization in the Cornwall diabase sheet follows the normal trends of large diabase (or dolerite) sills that have progressed from early ferromagnesian minerals to alkali feldspar. The stages, which have been treated separately, can be summarized in order from oldest to youngest, based on the expected decrease in cooling rate, from sheet margins to the interior: the chilled border facies; normal diabase in the top third of the sheet; the central portions of the sheet either coincident with the basal third or slightly after the basal third; pegmatitic diabase; and finally, granophyre. The solidification index (Figure 49) indicates that the bulk diabase composition at 1066 feet below the top represents that magmatic liquid richest in MgO and poorest in SiO_2, the solidification index decreasing uniformly toward the chilled margins at the top and the base. In contrast to the Skaergaard solidification sequence (see Kuno, 1968, p. 634), this index for Cornwall rocks apparently cannot represent an undisturbed sequence of successive liquids (the chilled margin should be the earliest crystallizing liquid). Chemical fractionation, perhaps by convective settling, may have yielded this cryptic layering effect, although no olivine layer is present in the samples, and indeed would not be expected since the samples with an SI (Solidification Index) greater than at the chilled margins (Figure 49) constitute at least 700 feet of the 1200- foot thick sheet.

The sequence of mineral crystallization (Plates 19-20) parallels that given by Walker and Poldervaart (1949, p. 624-625) for the Karroo dolerites. The first mineral to crystallize probably was phenocrystic olivine in the chilled margin (plagioclase crystals are quite small by comparison and pyroxene is uncommon). As crystallization proceeded, nearly all of the sparse olivine was resorbed, settled or altered. Nearly coincident with olivine was the crystallization of calcic plagioclase (An_{65}), followed closely by primary, magnesium-rich orthopyroxene, largely hypersthene. The early appearance in the chilled margin of hypersthene (Plate 20) suggests that this magma may have been more magnesian than $En_{64}Fs_{36}$ (Yoder and others, 1963, p. 90). The appearance of clinohypersthene and/or pigeonite in the central to basal portions suggests either a less magnesium-rich contemporary magma or a higher Fe/Mg ratio, in addition to differential ion diffusion rates. The two major series, plagioclase and pyroxene, then continued to crystallize with gradually changing compositions (Plates 18-A, C, and D, 20 A-C) through the pegmatitic and subsequent transitional stages. Of the two, only plagioclase (approx. An_{10-20}) continued on into the final granophyre stage. After the first orthopyroxene, pigeonite continued to crystallize, gradually becoming richer in iron. These pigeonites are now associated with inverted pigeonite (Plate 20, A and B) and late hypersthene. Near the base of the sheet clinohypersthene crystallized instead of magnesiam pigeonite. Somewhat earlier than, or coincident with, intermediate pigeonite, augite began crystallizing, becoming progressively poorer in calcium and richer in iron until the last stages of pegmatitic diabase (Plate 19-A) when enrichment in calcium reversed the chemical partition trend. The majority of the plagioclase (An_{45-60}) crystallized with intermediate pigeonite and with augite. Late hypersthene crystallization and inversion of pigeonite to hypersthene occurred subsequently. The more sodic plagioclases tended to aggregate into late interstitial micropegmatite that is prevalent throughout the sheet. Diabase pegmatite, perhaps crystallizing near the top of the sheet about the time that the center of the sheet was crystallizating, concluded pyroxene crystallization. At this stage, plagioclase slightly more sodic than in normal diabase crystallized and the maximum concentration of iron and iron-titanium oxides occurred. The last few percent of the magma to crystallize was granophyre. It represents a sharp compositional break (Table 25) as the residual fluids became enriched in silica and alkalies, yielding sodic plagioclase, orthoclase, Fe-orthoclase, and a minor amount of quartz. Throughout the crystallization history, there was some alteration of earlier stages by succeeding magmatic liquids (Plates 20-A and C). This crystallization sequence is summarized in Figure 46, approximately grouped according to the major stage to which the minerals belong. Because different

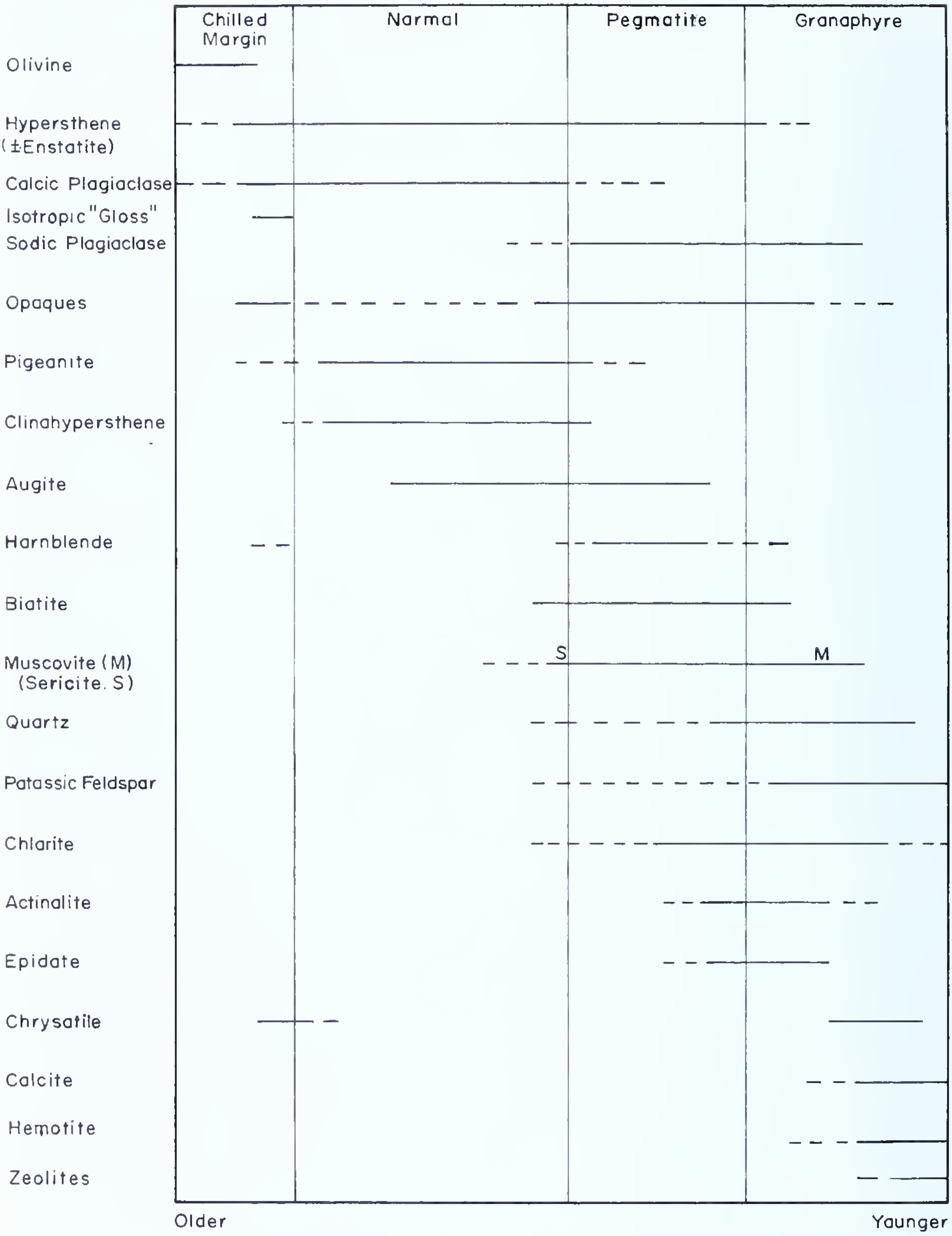

Figure 46. **Generalized paragenetic diagram for Cornwall diabase minerals. Textural limits are approximate (see text).**

differentiation trends are believed to have been proceeding simultaneously in different parts of the sheet, this diagram is not strictly accurate in a time sense. Also, according to Evans (1967), slow diffusion rates in pyroxene and more rapid diffusion rates in plagioclase (particularly when the liquid is rich in sodic plagioclase composition) affect the relative rates of crystallization of these two series.

The present opaque mineral assemblage is interstitial to pyroxene and feldspar, is frequently associated with interstitial micropegmatite, and hence is a late crystallization product. The textural evidence, however, is permissive of an early, mixed magnetite-ulvöspinel. The present mineralogy is that of a later, oxidized suite, perhaps now remobilized. Most original textures are now largely obliterated. In general, oxidized phases increase in amount relative to magnetite-ulvöspinel assemblages from normal diabase to diabase pegmatite to granophyre. The presence of low-Ti magnetite, especially prevalent in the differentiates, has been noted at Cornwall and in the extreme eastern and western ends of the Pennsylvania Triassic diabase province (A. Davidson, personal communication).

GEOCHEMISTRY

Analytical Accuracy

Samples of diabase and associated igneous rocks were analyzed by two commercial laboratories, submitted under a lowest-bid proposal system, and by R. Smith II at the Pennsylvania State University. One crushed diabase sample was split and analyzed by the two commercial laboratories and several different rock-chip splits from the same samples were analyzed at the Pennsylvania State University (Appendix 4-A). One sample was analyzed for Fe_2O_3 and FeO by a third commercial laboratory, in addition to analyses by the other three laboratories (C-19, Appendix 4-A). Analyses of splits of G-1 and W-1 for Fe_2O_3 and FeO and of BCR-1 for all major elements and trace elements were reported by the commercial laboratories and found to be acceptable (Appendix 4-A; Lapham and Saylor, 1970). Analyses of FeO and Fe_2O_3 by Spectrochemical Laboratories were calculated from total iron reported as Fe_2O_3 and from the FeO/Fe_2O_3 ratio taken from an earlier analysis of the same sample which had been inaccurate with regard to Al_2O_3, Na_2O, and K_2O. All major elements were analyzed by quantitative wet chemistry by the commercial laboratories. Analyses by Robert Smith II for SiO_2, Al_2O_3, TiO_2, MnO, Fe_2O_3, MgO, CaO, K_2O, and Na_2O were determined by atomic absorption of $LiBO_2$ fused samples; for FeO and Fe_2O_3 by $KMnO_4$ titration and by the pyrophosphate methods. Elements reported by Smith were analyzed by X-ray spectrometry (P_2O_5, Cl, S) and by atomic absorption (TiO_2, MnO, SrO, Cr, Co, Ni, Cu, Zn, Rb).

In utilizing diabase chemical analyses for succeeding tables and illustrations, several procedures were followed to maximize their reliability. The FeO and Fe_2O_3 results used are those of Smith and Conwell; all other results reported show Fe_2O_3>FeO and are considered to be incorrect (analytical oxidation). The only exceptions may be the Fe_2O_3 and FeO commercial analyses for granophyre in which hematite has been observed, and that for the dike (C2-1) which has been metasomatized. Because total iron is more accurate, it can be utilized from all analytical sources. Where there are complete analyses for more than one sample, the results have been averaged (Appendix 4-A), and these average compositions have been treated as representative of that sample. Analyses by Smith commonly total less than 100 percent because H_2O and CO_2 were not reported. A few analyses by Smith exceed 100 percent and may result from excess Al_2O_3 (samples C-17 and C-34, Appendix 4-A) or excess SiO_2 (samples C-19 and C-28, Appendix 4-A). In two of these samples (C-17 and C-34), the apparent excess in Al_2O_3 is partially offset by apparently low MgO. Two other samples (C-20 and C-31, Appendix 4-A) also appear to show excess Al_2O_3 (Smith notes that some variability in Al_2O_3 results from contamination during grinding). Sample analyses for Al_2O_3 marked by an asterisk in Appendix 4-A are considered unreliable and are not used in succeeding illustrations. In general, the total iron content is lower in analyses reported by Smith than in those reported by commercial analysts. NiO and CoO in analyses by Spectrochemical Laboratories probably are of poor quality. All trace element analyses are semi-quantitative.

Composition of the Igneous Rocks

The average chemical composition of each major rock type in the diabase sheet is presented in Table 25. The younger diabase dike differs considerably from that of the sheet (more Al_2O_3 and K_2O content and less CaO and Na_2O) and probably is not representative of most Triassic dikes (Appendix 5-C; Lapham and Saylor, 1970). The remaining analyses are from the main Cornwall sheet and are mineralogically representative of their respective rock types. The analysis of the upper chilled margin sample is slightly higher in TiO_2 and K_2O and slightly lower in CaO and MgO than normal Cornwall diabase (Table 25, column 3). However, small contraction joints in the top of the sheet have been filled with metasomatic mica that in part may explain the compositional difference in K_2O.

The statement often is made that the composition of the non-volatiles in the chilled margin represents most closely the composition of the undifferentiated magma (e.g., Hotz, 1953, p. 691). However, this statement implies several assumptions that require examination. First, all chilled margin crystallization must have occurred *in situ;* that is, there must not have been any early chemical fractionation or physical separation of differentiates. Second, the strong thermal gradient between diabase magma and country rock could not have resulted in any corresponding effective chemical (or convective) gradient. Third, there cannot have been any physical sorting of crystals; that is, movement of crystals out of or into the margin. In addition, changing composition of minerals in mineral series must be

Table 25. *Average Chemical Analyses of Cornwall Igneous Rocks (Anhydrous)*

	(1)	(2)	(3)	(4)	(5)
SiO_2	50.64	51.68	51.69	53.21	66.10
TiO_2	0.95	1.12	0.86	2.04	0.36
Al_2O_3	15.61	14.65	14.90	14.41	16.15
Fe_2O_3	5.54*	6.70*	1.80	3.58	1.80*
FeO	6.45*	3.74*	7.79	6.89	0.53*
MnO	0.28	0.25	0.17	0.188	0.04
MgO	9.00	8.15	9.16	4.95	1.26
CaO	4.28	10.23	11.33	9.95	3.17
Na_2O	0.18	1.70	1.75	2.64	2.19
K_2O	7.07	1.77	0.54	2.11	8.49
Totals	100.00	99.99	99.99	99.968	100.00
Fe_{total}	8.888	7.59	7.31	7.85	1.67

(1) Diabase dike in western ore zone (Laphan and Saylor, 1970): C2-1, Appendix 4-A, metasomatized.

(2) Top chilled margin of sheet: C4-308, Appendix 4-A.

(3) Average normal diabase from samples C-19, C-20, C-22, C-24, C-26, C-27, C-31, C-32, C-33, and C-34, Appendix 4-A.

(4) Average diabase pegmatite: 38-P and C-18, Appendix 4-A.

(5) Average granophyre; C4-150 and 38-G, Appendix 4-A.

*Fe_2O_3 may be too high and FeO correspondingly too low; see discussion in text.

considered. For example, the upper chilled margin of a normal olivine tholeiite from Hawaii resembles alkali basalt (Evans, 1967). For an intrusion with a significant horizontal component (as at Cornwall), complete mixing also would be required for a short time until the chilled margin had crystallized. Finally, multiple magma injection may yield a non-representative chilled margin (see Walker, 1969, p. 83 concerning the Palisades sheet).

In part, the analyses from the vertical core (Table 25 column 3; Appendix 4-A; Figure 47) lead to the suggestion that these assumptions are not wholly justified. The bulk of the *in situ* diabase is represented by a vertical core analysis whose bulk chemical composition differs somewhat from that of the chilled margin. When the differentiation of diabase magma is discussed, it will be shown that this *in situ* diabase probably does not represent the entire magma composition, neither by bulk compositional, normative, nor modal types of measurement. However, to a large extent, the chilled margin may be representative of the magma. For example, addition of diabase pegmatite and granophyre compositions to normal diabase would yield a total average composition more nearly like the chilled margin anaysis than is the average normal diabase composition, with the exception of K_2O content.

Analyses (recalculated anhydrous) comparing the composition of the Cornwall sheet with other diabases and dolerites (Table 26) show that the

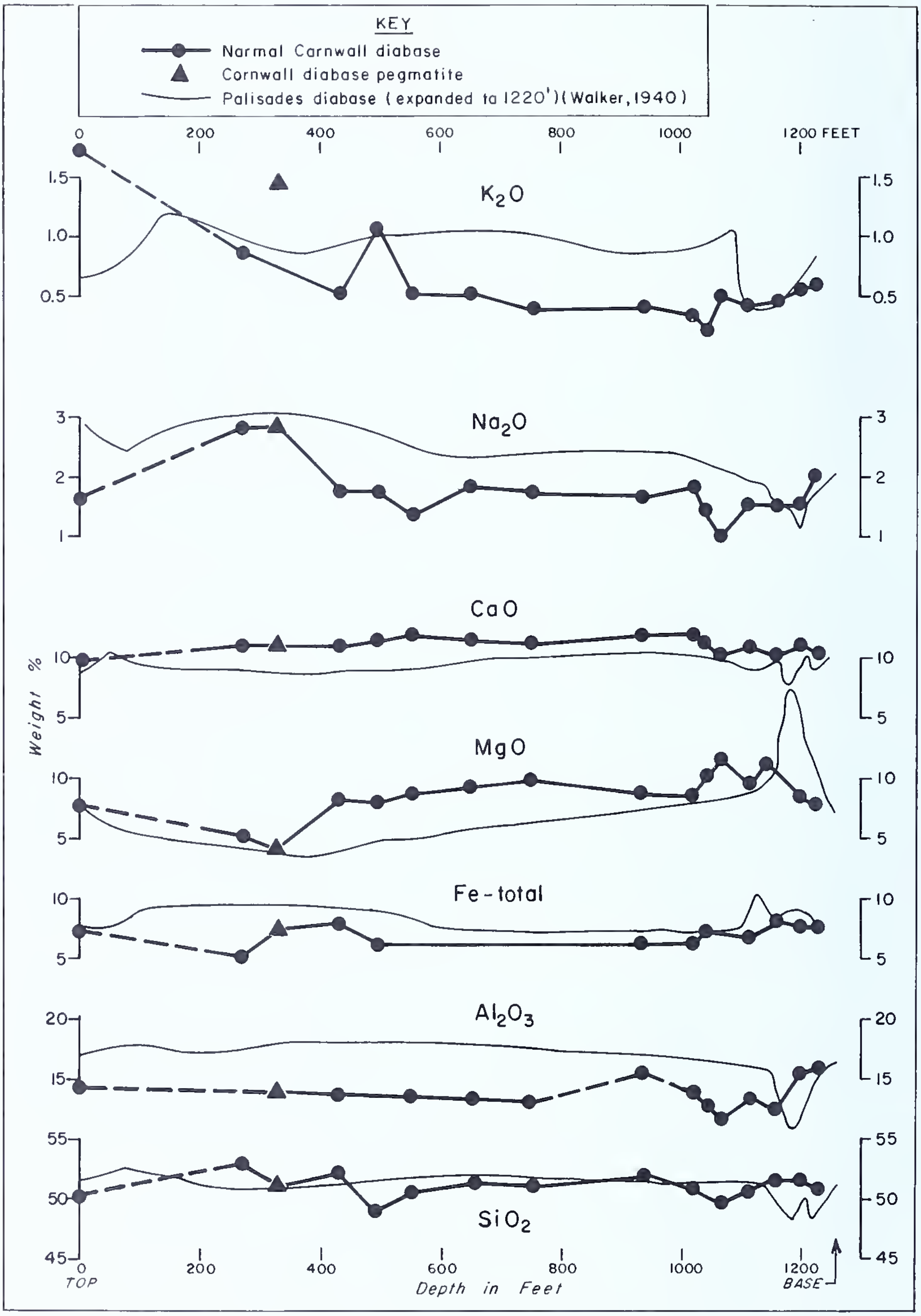

Figure 47. Comparative vertical chemical variation of Cornwall (heavy line, points) and Palisades diabase sheets; the Palisades sheet has been expanded from its 1000′ thickness to about 1230′ for easier comparison with Cornwall analyses (Appendix 4A); dashed curve = region of roof effects and granophyre occurrence.

Cornwall sheet conforms to the general composition for this rock type. It is lower in TiO_2, FeO, total Fe, Na_2O, and K_2O, and somewhat higher in MgO and CaO than most analyses (cf. Appendices 4 and 5). If late enrichment and fractional depletion are considered, this deviation would be even less, since the Cornwall diabase is low in those elements that show late enrichment and high in those that show late depletion. Direct comparison with the Dillsburg sheet (Hotz, 1953) cannot be made *in sensu strictu* because the "normal" Dillsburg composition was taken only from near the top of the sheet and some vertical chemical differences are likely. Thus, from these comparisons (Table 26 and Appendix 5-B), it can be seen that the Palisades sill (Walker, 1940; Walker, 1969) and the Hangnest type of Karroo dolerite (Walker and Poldervaart, 1949) are very similar to the Cornwall sheet, perhaps more similar than the Dillsburg sheet is to Cornwall.

Table 26. *Comparative Chemical Compositions of Diabase and Dolerite (Anhydrous)**

	(1)	(2)	(3)	(4)	(5)
SiO_2	51.69	53.73	51.82	52.77	51.1
TiO_2	0.86	1.46	1.16	1.58	1.4
Al_2O_3	14.90	16.04	14.28	15.04	15.6
Fe_2O_3	1.80	1.74	1.82	1.84	1.1
FeO	7.79	9.34	9.31	8.68	9.8
MnO	0.17	0.18	0.09	0.17	0.2
MgO	0.16	4.40	9.06	6.51	7.0
CaO	11.33	9.93	9.51	10.37	10.5
Na_2O	1.75	2.53	2.17	2.11	2.2
K_2O	0.54	0.65	0.78	0.94	1.0
Totals	100.00	100.00	100.00	100.01	99.9
Fe_{total}	7.31	8.57	8.60	8.03	8.38

(1) Average of 10 normal diabase analyses, Cornwall, Pa. from Table 25.
(2) "Normal" diabase, Dillsburg, Pa. (Hotz, 1953, p. 690).
(3) Average of 12 diabase analyses, Palisades, N.J. (Walker, 1940, p. 1080).
(4) Average of 6 diabases and dolerites (Whin Sill, Holmes and Harwood, 1928, p. 529; Karroo and Downes Mountain, Walker and Poldervaart, 1949, p. 649; Tasmania, Edwards, 1942, p. 465; Victoria Falls and Antarctica, DuToit, 1939, p. 516).
(5) Average tholeiite (Poldervaart, 1955, p. 134).
*Excluding P_2O_5 and CO_2; for complete data see Appendices 4 and 5.

Analyses (recalculated anhydrous) comparing an average of two Cornwall diabase pegmatites with other similar occurrences illustrate a general uniformity but with the greater divergence expectable in an early stage of fractionation (Table 27). The Cornwall average composition is low in total Fe and FeO, and high in K_2O and CaO. However, alkalies and total iron differ widely among all the analyses. All (except the Palisades sample) exhibit high TiO_2, K_2O, Na_2O, SiO_2, and total iron, and low MgO and CaO, relative to normal diabase. Transitional, or aplitic, diabase (not analyzed) also may be high in Na_2O (Shannon, 1924, p. 28). The higher TiO_2, alkalies, and total iron percentages are particularly characteristic of diabase pegmatite. In general, the contrast between pegmatitic and normal diabase is not great.

Table 27. *Comparative Chemical Analyses of Diabase Pegmatite (Anhydrous)*

	(1)	(2)	(3)	(4)	(5)	(6)
SiO_2	53.21	50.68	53.64	53.28	54.05	55.82
TiO_2	2.04	2.66	2.97	1.38	2.37	1.81
Al_2O_3	14.41	13.38	13.03	18.55	15.12	13.51
Fe_2O_3	3.58	6.69	4.88	2.00	0.16	2.02
FeO	6.89	11.25	10.39	7.72	12.25	10.75
MnO	0.19	0.30	0.20	0.09	—	0.28
MgO	4.95	6.33	2.75	2.62	5.53	4.20
CaO	9.95	5.02	7.36	9.48	8.49	8.07
Na_2O	2.64	2.84	3.73	3.84	2.02	2.28
K_2O	2.11	0.85	1.05	0.05	—	1.26
Totals	99.97	100.00	100.00	100.01	99.99	100.00
Fe_{total}	7.85	13.42	11.48	7.40	9.63	9.76

(1) Average of 2, Cornwall, Pa.; Table 25.
(2) "Coarse Syenite" in diabase, Dillsburg, Pa. (Frazer, 1880, p. 266).
(3) Dillsburg, Pa. (Hotz, 1953, p. 690).
(4) Palisades, N. J. (Walker, 1940, p. 1080).
(5) Goose Creek, Va. (Shannon, 1924, p. 19).
(6) Average of 6, Karroo (Walker and Poldervaart, 1949, Table 15).

Chemical analyses comparing an average of two Cornwall granophyres with similar rock types (Table 28) show that the Cornwall granophyre contains the same major components: silica, alumina, and alkalies. Characteristically, granophyre from all localities is low in TiO_2 and MgO. The analyses *per se* do not distinguish transfused sediments from magmatic differentiates. The Cornwall samples are slightly lower in TiO_2, FeO, CaO, Na_2O, and total iron, and slightly higher in Al_2O_3 and K_2O, than the other granophyres. However, such variance among the final residua is expectable; indeed, it is characteristic of all the granophyre analyses. Notable are the low total iron and the low Na_2O/K_2O ratio at Cornwall.

Normative Calculations

Standard CIPW normative calculations are presented for five rock types: diabase dike, chilled margin, normal diabase, diabase pegmatite, and granophyre (Table 29). Calculations for normal and pegmatitic diabase are the most accurate because the chemical analyses for these rocks are the most reliable. In general terms, normative mineralogy and observed mineralogy are in agreement. However, the norm does not take into consideration the changing compositions in the plagioclase and pyroxene mineral series. For example, the total amounts of pyroxene and plagioclase are accurate even though the normative compositions may not represent actual compositions; that is, in normal diabase plagioclase is approximately equal to, or only slightly greater in amount than, pyroxene. In diabase pegmatite, normative plagioclase greatly exceeds pyroxene and this is true of the mode as well.

Table 28. *Comparative Chemical Compositions of Granophyre (Anhydrous)*

	(1)	(2)	(3)	(4)	(5)
SiO_2	66.01	64.49	73.56	64.96	58.69
TiO_2	0.36	1.26	0.43	1.04	1.26
Al_2O_3	16.15	12.78	12.01	13.97	11.99
Fe_2O_3	1.80*	2.76	1.25	1.65	5.76
FeO	0.53*	7.51	0.88	5.91	9.36
MnO	0.04	0.13	0.06	0.10	0.21
MgO	1.26	0.67	1.50	2.40	0.72
CaO	3.17	3.38	2.58	4.11	5.02
Na_2O	2.19	5.22	7.22	3.13	3.90
K_2O	8.49	1.43	0.36	2.58	2.38
P_2O_5	—	0.36	0.14	0.15	0.71
Totals	100.00	99.99	99.99	100.00	100.00
Fe_{total}	1.67	7.84	1.56	5.80	11.40

(1) Avg. of 2, Cornwall, Pa., Table 25.
(2) Avg. of 2, Dillsburg, Pa. (Hotz, 1953, p. 690).
(3) Diabase aplite, Palisades, N. J. (Walker, 1940, p. 1080).
(4) Avg. of 7 "metasomatic granophyres" (Walker and Poldervaart, 1949, Table 15).
(5) Hedenbergite granophyre, Skaergaard (Wager and Deer, 1939, p. 210).

*Fe_2O_3 may be high and FeO may be low; see discussion in text.

Certain differences between mode and norm require brief comment. Because Fe_2O_3 exceeds FeO in the chilled margin and in granophyre, all of the Fe^2 is used up in the calculation of magnetite and there is none left for clinopyroxene, hypersthene, or olivine. In actuality, Fe^2 is present in these minerals and the chemical analyses may be in error.

Utilizing all available aluminum (with the necessary amount of calcium) to make anorthite before calculating pyroxene content is misleading because some calcium enters the pyroxene structure. An excess of anorthite results, and the normative plagioclase composition becomes excessively calcic.

Table 29. *Normative Calculations from Appendix 4-A*

	(1)	(2)	(3)	(4)	(5)
Ilmenite	1.8	2.1	1.6	3.9	0.7
Orthoclase	41.8	10.5	3.2	12.5	50.2
Albite	1.5	14.4	14.8	22.3	18.5
Anorthite	22.3	27.3	31.2	21.2	9.1
Composition	$An_{93.1}$	$An_{65.6}$	$An_{67.8}$	$An_{48.7}$	$An_{32.9}$
Magnetite	8.0	9.6	2.6	5.2	0.8
Hematite	–	0.1	–	–	1.3
Diopside	0.3	18.2	20.3	22.9	5.2
Composition	$Wo_{52.5}En_{38.3}Fs_{9.8}$	$Wo_{53.7}En_{46.3}$	$Wo_{51.6}En_{32.1}Fs_{16.4}$	$Wo_{51.5}En_{31.5}Fs_{17}$	$Wo_{53.7}En_{46.3}$
Hypersthene	18.4	11.9	24.8	8.0	0.8
Composition	$En_{78.4}Fs_{21.6}$	En_{100}	$En_{66.2}Fs_{33.8}$	$En_{65}Fs_{35}$	En_{100}
Olivine	7.3	–	–	–	–
Composition	$Fo_{71.1}$	–	–	–	–
Quartz	–	5.9	1.5	4.1	13.5

(1) Diabase dike (1 sample); metasomatized (Lapham and Saylor, 1970)
(2) Top chilled margin (1 sample)
(3) Average normal diabase (10 samples vertical distribution)
(4) Average diabase pegmatite (2 samples)
(5) Average granophyre (2 samples)

Where sufficient Fe^{2} is present for pyroxene calculation, preservation of the same Mg/Fe ratio for diospide, hypersthene, and olivine assumes no Mg/Fe fractionation as crystallization proceeds. Actual olivine composition (if present, as near the sheet base) would be more magnesium rich and hypersthene composition more iron rich than in the norm.

The following comments on specific normative minerals further modify or emphasize the results of the norm calculations for the Cornwall samples:

Ilmenite:	The quantitative maximum in diabase pegmatite is a true reflection of its mineralogical occurrence.
Orthoclase:	The calculation for the dike and the chilled margin yield an excess partly because the solid solution of the Or molecule in plagioclase is not considered and partly because of potassium metasomatism during ore-stage mineralization; maximum occurrence in granophyre is a true reflection of the actual mineralogy.
Plagioclase:	Both the albite maximum and plagioclase composition in diabase pegmatite are accurate reflections of the mineralogy (excepting late alteration, veins, micropegmatite). Plagioclase composition generally is more calcic than observed.
Magnetite:	Maximum amount (i.e., most favorable Fe^{3}/Fe^{2} ratio) occurs in upper chilled margin and may be indicative of the oxidation conditions early in the crystallization sequence; a secondary maximum in diabase pegmatite agrees with its mineralogic occurrence. Note that the metasomatized dike has considerably more normative magnetite than the sheet.
Diopside:	Least accurate with respect to mode: it is present in the dike but not in the granophyre. In the dike, much of the calcium allotted to anorthite is in diopside and the resultant aluminum excess is in spinel or pyroxene. In granophyre, calcium is present in minor amounts in calcite and amphibole. Note the compositional similarity resulting from similar Ca-Mg-Fe ratios.
Hypersthene:	Abundant in diabase and diabase pegmatite as shown by norm.
Olivine:	Mineralogically present but rare in the chilled margin; normative distribution emphasizes the difference between dike and sheet diabase.

Quartz:	Emphasizes the difference between sheet and dike; there is less than 5% in the norm and hence the sill is not termed a quartz diabase.

Vertical Chemical Variation

Because of the general similarity between the Cornwall and Palisades sheets, the two are compared for selected elements in Figure 47 (the thickness of the Palisades sill was expanded to 1230′ for comparative purposes). Most of the oxides have similar depth trends, except near the sheet top at Cornwall where the more silicic differentiates are present and near the base and where there is an olivine layer in the Palisades sheet. There is significantly less total Fe throughout the Cornwall sheet. At Cornwall, Ni increases toward the base (Appendix 4-A) similar to MgO and total Fe. CaO and Na_2O exhibit a slight slope reversal at Cornwall in the middle of the sheet which was not noted in the Palisades sheet, indicating a fluctuation in plagioclase abundance and/or composition. Generally the trends illustrate incomplete mixing with slight, but consistent, chemical gradients that resulted from fractional crystallization. The trends clearly demonstrate that chemical analyses from any one part of the sheet will not accurately represent the whole pluton.

Just below 1000 feet (vertical depth), alkalies, Al_2O_3, and SiO_2 abruptly decrease, then increase again toward the base; MgO and Ni increase, and CaO decreases irregularly. Total Fe is greater below 1000 feet than in normal diabase above. These sharp chemical changes might have resulted from the injection of a separate lower sheet with an internal chilled contact just below 1000 feet. Analogously Walker 1969 has proposed two magma intrusions for the Palisades sill. However, the chemical changes also might result from a combination of basal contact effects (about 260 feet above the base), analogous to roof effects and from a crude cryptic gravitative layering, especially since the sialic constituents (Al, Si, Ca, Na, K) decrease concomitantly with an increase in the more mafic constituents (Mg, Fe, Ni). If the trends here were the result of an assimilated wedge of the underlying sediments, alkalies (from Mill Hill Slate) or calcium (from Buffalo Springs limestone) would be expected to increase markedly. Actually, not only do Na_2O and CaO decrease, but Al_2O_3 also decreases. These characteristics are not considered to be representative of a sedimentary element influx as inferred by Shannon (1924, p. 37-39) for the Goose Creek, Virginia diabase. Pearce (1970, p. 31) also concluded that for the Palisades sill, the assimilation of arkose to yield the sialic differentiates is an unsatisfactory explanation for the observed chemical variation. The vertical distribution of SiO_2, Al_2O_3, MgO, K_2O, and CaO also indicate that the upper chilled margin sample is not representative of total *in situ* diabase sheet magma (Figure 47 and Appendix 4-A).

Differentiation

General Differentiation Trends

The chemical analyses, on which discussion of differentiation is largely based, are listed in Appendices 4 (for Cornwall) and 5 (for other locations). These compilations include analyses for Triassic diabase sheets of eastern North America, diabase sheets other than North American, eastern North American diabase dikes, diabase pegmatites, and diabase granophyres (including some "aplite"). Averages for the Palisades and Karroo diabases (compiled from the original publications) are treated as a single diabase composition. The diabase analysis used for comparative purposes from the Gettysburg Pluton is that noted by Hotz (1953, p. 690-691) at Dillsburg. Previous data and those discussed below confirm that this sample most probably is not representative of the entire Dillsburg sheet. Generalizations based on comparisons with diabase dikes are tentative; however, there are minor differences in the analyses (Appendix 5; Lapham and Saylor, 1970; R. Smith II, written communication; P. Weigand, written communication). Geographic distribution of sheets, and perhaps of dikes, may be reflected in the chemical analyses (see Appendix 5 where analyses are arranged from east to west; also, Lapham and Saylor, 1970, and personal communication, R. Smith II).

The diabase dikes in Pennsylvania rarely show any sign of a differentiate other than a chilled margin and an occasional textural coarsening (also see Lapham and Saylor, 1970). The large sheets, on the other hand, always contain additional differentiates, diabase pegmatite being the most common. In general, the chemical changes from chilled margin to normal diabase, diabase pegmatite, and granophyre at Cornwall parallel differentiation trends of other Triassic and world-wide occurrences of diabase sheets (Figures 47-55). In all such sheets, there is only a small chemical fractionation from normal to pegmatitic diabase, but a very abrupt change from pegmatite to the final granophyric residuum. In Pennsylvania, the presence of volatiles (in addition to K_2O and Na_2O, H_2O is slightly more abundant in the differentiates than in normal diabase) in an otherwise viscous, silica-rich fluid must play the dominant role in volatile collection in upper levels of the sheet as discrete pods, schlieren, or veins. This is especially true for the rather low-temperature mineral suite of the granophyre (minimum probably less than 660°C, assuming an approach to H_2O saturation).

The small volume of late granophyric residuum differs considerably in composition from sheet to sheet (Figure 48). Its composition is quite sensitive to, and dependent upon, small differences in the compositional trend that preceded it during the crystallization of the majority of the magma as normal and pegmatitic diabase. The chilled margin, on the other hand, represents the most compositionally uniform facies, a consequence of its rapid crystallization at high temperature under a sharp cooling gradient controlled by the rather uniform bulk composition of the magma. However, for at least three Pennsylvania and New Jersey sheets (Cornwall, Palisades, Dillsburg), this margin does not represent the average composition of the whole *in situ* sheet (Figure 48). For example, SiO_2 and Na_2O increase in amount from the chilled margin through all succeeding crystallization stages (Figure 48). Pearce (1970) has discussed the more mafic character of the Palisades sill chilled margin as a possible function of the Soret effect. Thus, as suggested previously, the chilled margin may be unrepresentative of total sheet magma composition; i.e., some material may have been excluded from the magma that yielded in the *in situ* sheet, such as the ore fluid and perhaps the diabase dike like apophyses.

Data are compared for four similar Triassic differentiated sheets (Figure 48): the Cornwall diabase sheet, the Palisades diabase sill, the Dillsburg diabase sheet, and the Karroo dolerites of South Africa. Their differentiation trend is consistently similar for all oxides (the pigeonitic rock series trend of Kuno, 1968), and, for the most part, the compositional range for each rock type within the diabases is consistent within rather narrow quantitative limits. These two observations imply not only a uniform cyrstallization trend but also a rather uniform parent source material of world-wide distribution. Individual oxide variation for each sheet differentiate follows, based on Figure 48.

SiO_2: Increases during differentiation, but with very little increase from normal diabase to pegmatitic diabase. The Cornwall quantities are slightly lower than for the other sheets, except in granophyre. Differences in the chilled margin may be indicative of initial early magma differences. The Palisades "white vein" (plotted as granophyre) shows considerable silica enrichment, but this difference probably is not unusual for the highly varied granophyres.

TiO_2: Increases with differentiation from a narrow range in the chilled margin to a maximum in diabase pegmatite and a minimum in the granophyric stage; the Dillsburg sheet is a notable exception just as it is with total iron. Pennsylvania Triassic sheets show somewhat steeper differentiation slopes than the Palisades and Karroo sheets.

Al_2O_3: Is not consistent among the four sheets in late differentiates. The Palisades trend appears to be the most anomalous. The Cornwall sheet exhibits the most uniform distribution with perhaps a slight early suppression of Al_2O_3 indicative of a somewhat shallower origin and/or of high orthopyroxene content (see also Figure 49). The late enrichment at Cornwall appears to be unique (cf. Kuno, 1968); only Hawaiian alkali basalts show late Al_2O_3 enrichment, but it is much less pronounced.

MgO: Except at Dillsburg, attains a maximum in normal diabase and decreases through the remaining differentiates. The extremely low amount in the Dillsburg sheet for "normal" diabase (Hotz, 1953) probably is a good indication that this sample (119 feet below the top) is not really representative of normal diabase.

Fe_{total}: Usually increases after the crystallization of normal diabase, then decreases again similar to TiO_2. Maximum concentration is in the pegmatitic diabase or in rocks transitional between pegmatite and granophyre. The Palisades sill is an exception because of the maximum 60 feet above the base in the olivine layer. Total iron enrichment is least pronounced at Cornwall and does not exceed 12 percent $FeO+Fe_2O_3$ in normal diabase.

Na_2O: Generally increases from chilled margin to granophyre. Cornwall contains less in each rock type than the other sheets and shows less late enrichments. This lack may correlate with sodium addition into the hornfels or with later hydrothermal ore solutions. A metasomatized diabase dike at Cornwall (Table 25) and one west of Dillsburg (Lapham and Saylor, 1970) contains less Na_2O than the nearby sheets.

K_2O With the exception of the Cornwall chilled margin, generally increases to a maximum in the granophyre. The enrichment at Cornwall is exceptional. The differentiation trend slopes are steeper at Cornwall than elsewhere.

CaO: Except for the suspect "normal" Dillsburg sample, reaches a maximum in normal diabase, decreasing thereafter. Compositional difference is greatest in pegmatitic diabase.

The concentration of H_2O in each differentiate (and contemporary liquid) is less certain. Analyses show a wide range within each rock type. Comparison of analyses from Cornwall, Dillsburg (Hotz, 1953), the Karroo (Walker and Poldervaart, 1949), and the Palisades (Walker, 1940) show

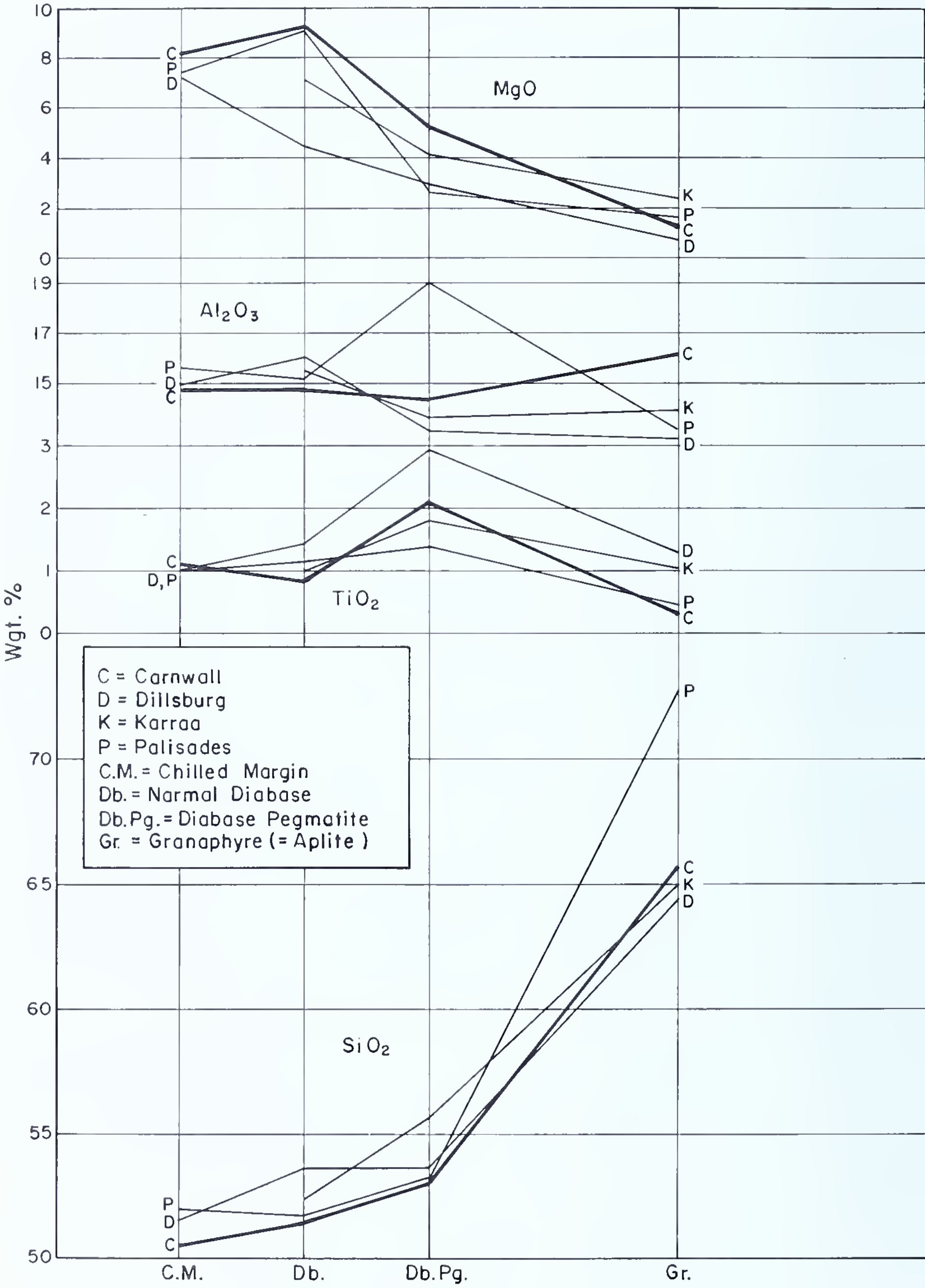

Figure 48. Comparative chemical differentiation trends by igneous rock type for the Cornwall, Dillsburg, Karroo, and Palisades diabase suites. The Cornwall chilled

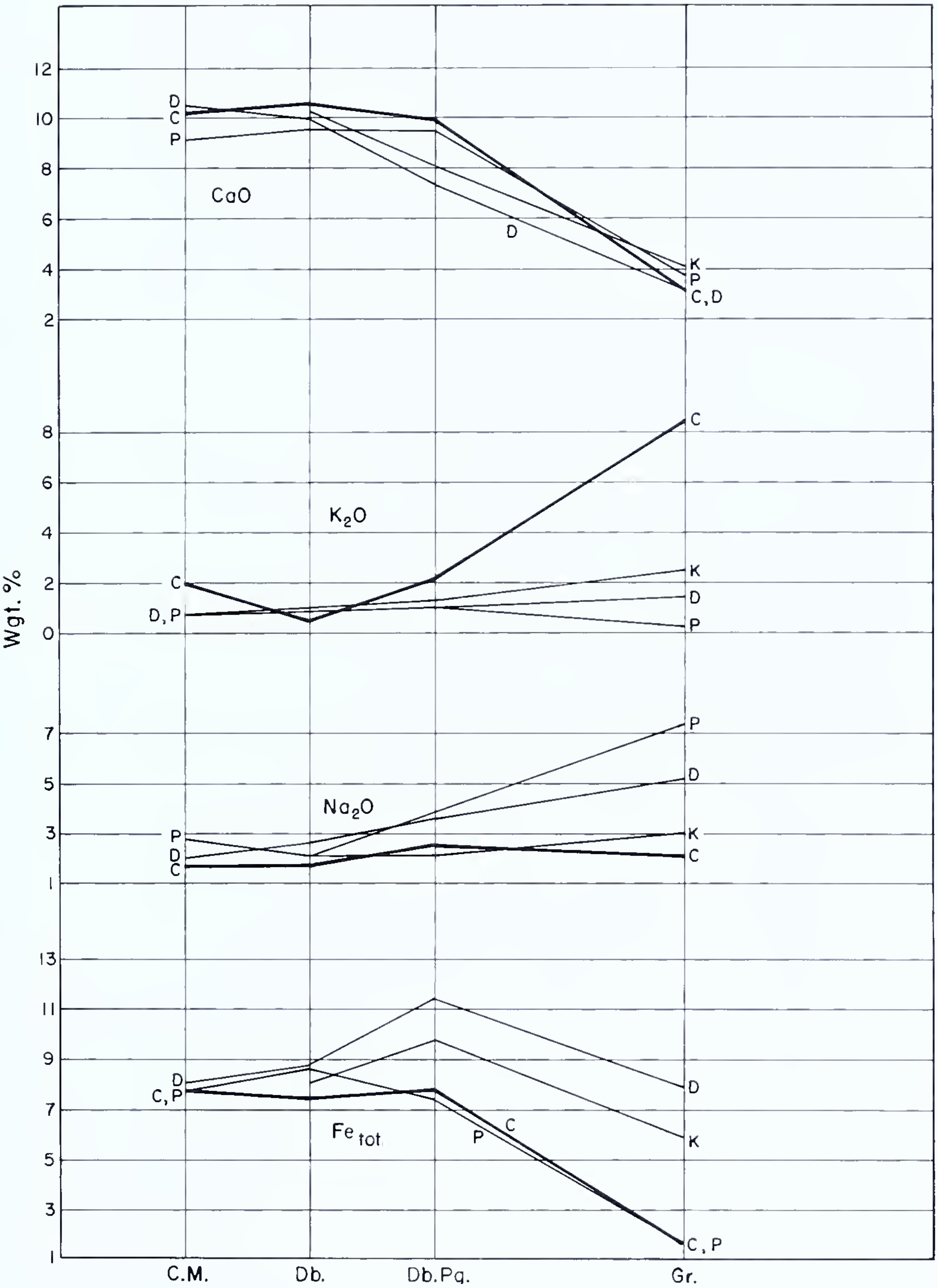

margin probably has been subjected to K-metasomatism from the overlying ore zone.

apparently consistent H_2O trends. From normal diabase to pegmatitic diabase, H_2O increases slightly and then decreases in granophyre. The H_2O content of the Cornwall chilled margin, based on one analysis, is anomalously high, probably a result of metasomatim with enrichment also of K_2O and Au.

Gottfried and others (1968) have shown that during differentiation at Dillsburg there is an increase in niobium, tantalum, zirconium, hafnium, thorium, and uranium. They further note that niobium and tantalum concentrations follow iron and titanium, a maximum occurring in the transitional granophyre rocks at Dillsburg. Although comparative data are not available for Cornwall, a similar increase during differentiation and a niobium-tantalum maximum in diabase pegmatite probably occurred. Distribution of gold in rocks of different differentiation stages at Cornwall and Dillsburg shows no clear-cut differences (written communication, David Gottfried), with the exception of a high 8.1 ppb in the Cornwall upper chilled margin adjacent to the ore zone (also rich in gold). The range of gold content at Cornwall (0.4-8.1 ppb) is considerably lower than at Dillsburg (9.5-22.6 ppb), the Dillsburg contents apparently being anomalous (written communication, David Gottfried).

The plot of rock type versus oxide percent (Figure 48) is very similar in differentiation trend to the solidification index (SI): MgO x 100/MgO + FeO + Fe_2O_3 + Na_2O +K_2O versus oxide percent (Figure 49). Kuno (1968) has used the SI to characterize basalt fractionation trends (approximately parallel to successive magma compositions) for the Skaergaard, Karroo, Dillsburg, and Palisades suites. The SI data for Cornwall illustrated in Figure 49 include the serpentinized and amphibolitized diabase at 1066 feet (SI=50) and the small diabase dike (SI=32). For most oxides, the dike composition point does not lie along sheet fractionation curves (Figure 49), supporting the field evidence that it is either a separate (later) intrusion or has been metasomatized (cf. Lapham and Saylor, 1970) or both.

In Figure 48, the chilled margin is assummed to be the first crystallization phase; in Figure 49 the chilled margin sample has an SI of 37 (top) similar to the 38.5 at 35 feet above the base, which is less than normal diabase and indicates that total composition (early phenocrysts plus later interstitial material) reflects some magmatic liquid younger than that of the earliest magma.

Several other features of the SI are noteworthy. Total iron enrichment attains a maximum at a lower SI than TiO_2, whereas at Dillsburg, the Palisades, and Karroo the maxima occur at the same solidification stage (Kuno, 1968). Although these maxima are largely the result of Fe-Ti oxide crystallization, it is evident that at Cornwall the spinel phase becomes progressively enriched in iron relative to titanium beginning at the diabase pegmatite stage. The Skaergaard SI curves exhibit a similarly later iron maximum (Kuno, 1968, Figure 4, p. 634).

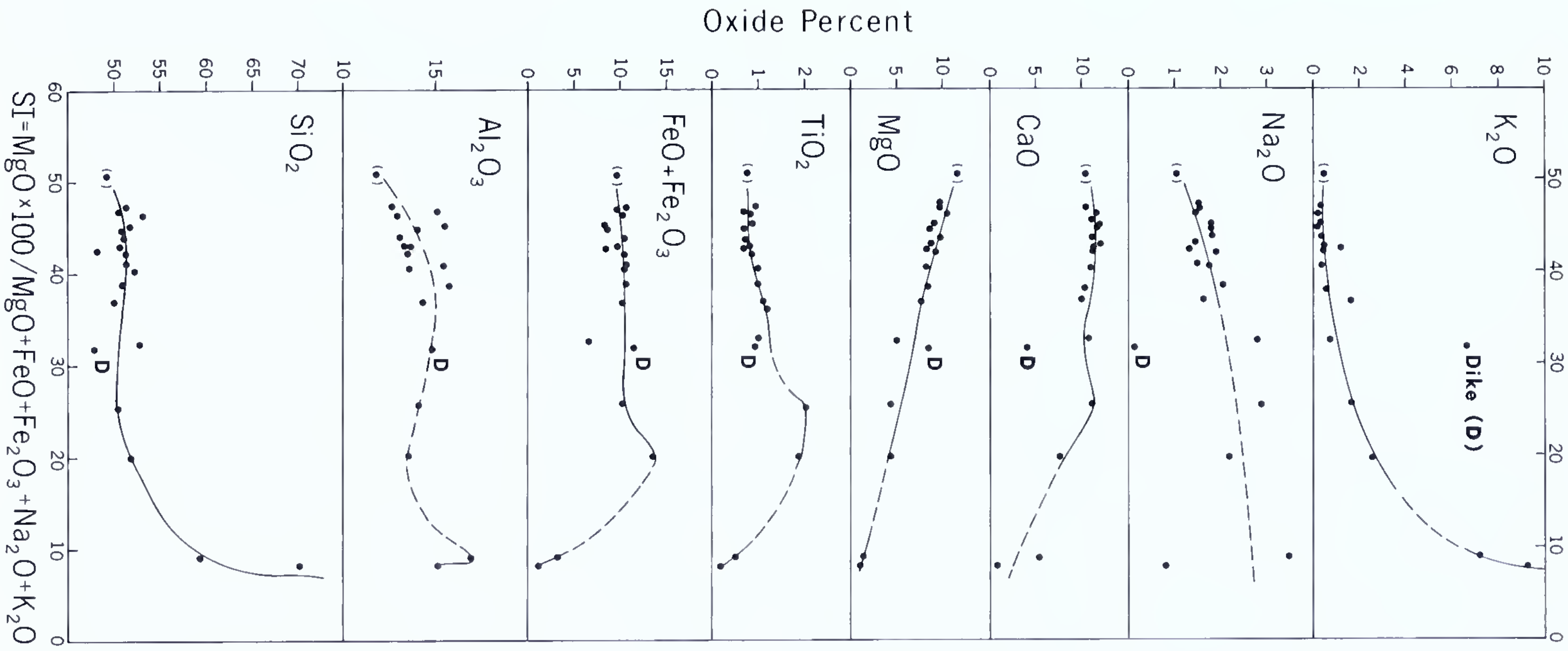

Figure 49. Solidification Index versus oxide percent for the Cornwall sheet and dike (D); point in parenthesis represents serpentinized diabase at 1066′ depth; the chilled margin sample plots at SI = 37 (top) and is similar to SI = 38.5 at 35 feet above the base; Al_2O_3 analyses above curve all are by R. Smith (Appendix 4-A); dike has been subjected to potassium metasomatism (Lapham and Saylor, 1970).

The SI range at Cornwall (8 to 50) is very similar to that of the Palisades (15 to 55), but is wider than for Dillsburg samples (3 to 35) and narrower than for Karroo samples (4 to 70) (see Kuno, 1968). The narrow range at Dillsburg probably results from a lack of samples from the basal portions of the sheet. At Cornwall, SI increases uniformly from the upper chilled margin (SI-37) to a maximum in normal diabase (SI-50) about 160 feet above the base. Kuno (1968, p. 633) suggests that rocks with an SI greater than 40 may be products of accumulation of olivine crystals. All of the Cornwall diabase samples from 433 feet to 1202 feet below the top have an SI greater than 40. Only from 1066 feet to the base is there any evidence of olivine, and it is very sparse (Table 23). The maximum SI of 50 at 1066 feet results from extensive serpentinization along microshears; olivine replacement textures do not exceed one percent by volume in this sample.

In Figure 50, the Palisades, Cornwall, and Dillsburg sheets have been included on the MFA differentiation diagram of Figure 34. The Cornwall trend (solid circles and line) follows almost exactly the compositions of the

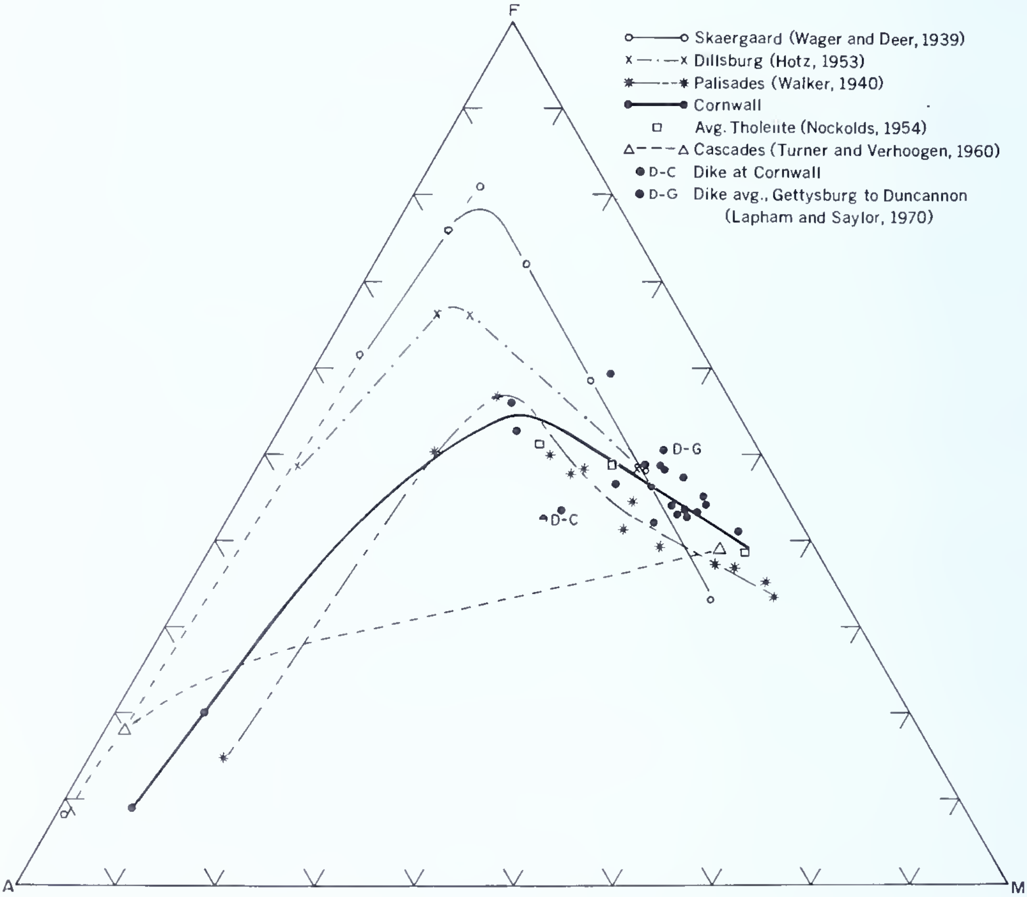

Figure 50. MFA differentiation diagram for Skaergaard, Dillsburg, Palisades, Cascades, Cornwall, average tholeiite, and Pennsylvania Triassic dike magmas.

average tholeiite series (boxes) up to the point of maximum total iron. Additional differentiation toward a magma rich in total alkalies is not exhibited by tholeiitic basalts but is characteristic of differentiated basalt suites (e.g., Skaergaard high-iron, high-alumina basalt curve) and diabase (or dolerite). The Palisades sill (dashed line) is most similar to the Cornwall and average tholeiitc throughout the differentiation series. Both the Dillsburg and Skaergaard trends exhibit greater total iron enrichment previous to alkali (and silica) enrichment. As Kuno (1968, p. 638) has noted, all of these curves exemplify the differentiation scheme characteristic of tholeiites and high-alumina basalt suites.

Although the MFA-plot is the standard method for comparing differentiated suites, a plot of total alkalies, CaO, and MgO (MCA, is in some ways more meaningful for these suites (Figure 51). The use of the MFA diagram is predicated upon the change in the Fe/Mg ratio in olivine, orthopyroxene, and clinopyroxene, followed by the crystallization of sodic and/or potassic feldspar. There are some drawbacks to the MFA diagram

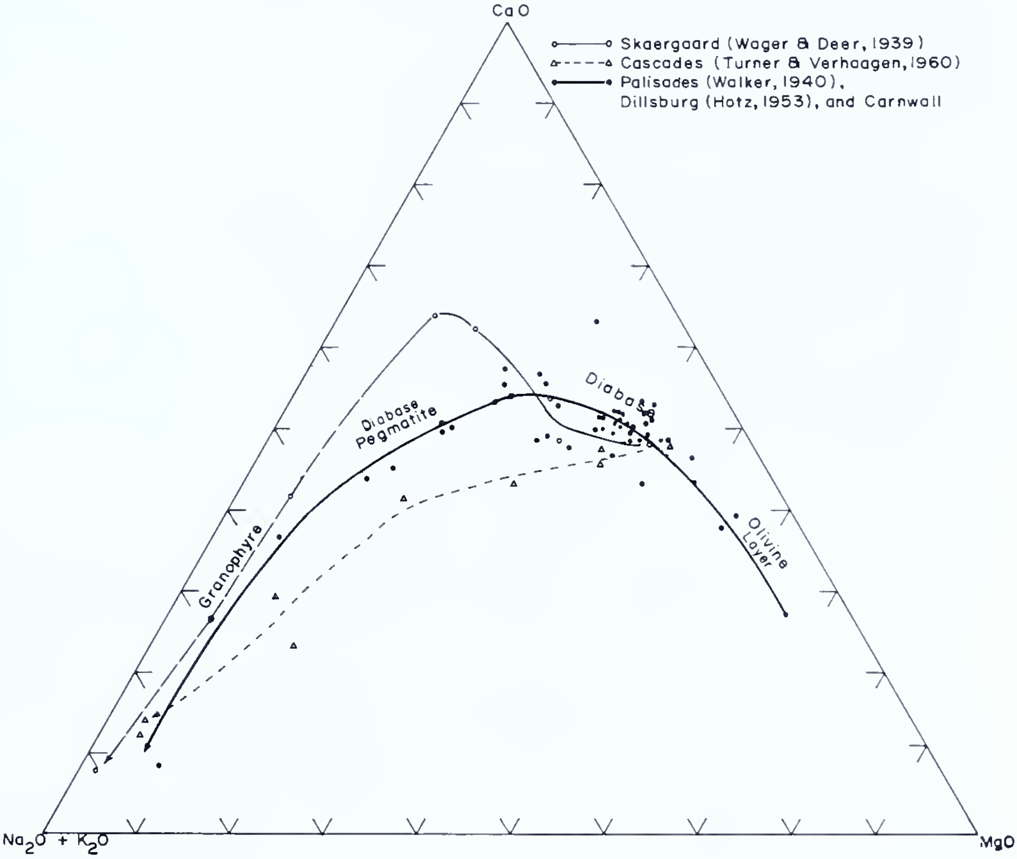

Figure 51. MCA differentiation trend plot of $(Na_2O + K_2O)$, CaO, and MgO for Skaergaard, Cascades, Palisades, Dillsburg, and Cornwall magmas; olivine layer includes chilled-margin plotted points.

with respect to Triassic diabase. Olivine usually is scarce or absent; thus, changes in its Fe/Mg ratio are insignificant with respect to the MFA diagram. Reliance on the Fe/Mg ratio to express early differentiation emphasizes changes in the pyroxenes and de-emphasizes plagioclase, which commonly is more abundant. Fe/Mg in silicates also is dependent upon oxidizing (P_{O_2}) conditions in the magma, since this will exert a control on iron substitution. Changes in oxidation could be expected to result in an erroneous picture of differentiation if based on the Fe/Mg ratio. The fact that the MFA curve at Cornwall exhibits some repression of total iron enrichment relative to that at Dillsburg may be a consequence of oxidation in the Cornwall magma.

To some extent, an MCA diagram obviates these objections. For example, the Palisades, Dillsburg, and Cornwall sheets belong to the same general magma type and exhibit the same general differentiation trends. On the MFA diagram, trend differences are exaggerated, whereas on the MCA diagram (Figure 51), these three diabase sheets yield the same differentiation curve. On the MCA curve, however, the CaO apex distinguishes normal and pegmatitic diabase better than does the FeO apex on the MFA diagram. As a consequence, it is more indicative of a particular rock type within the differentiation series than the MFA diagram. The MCA diagram does have some limitations, however. The separation between high-alumina basalt (Skaergaard), tholeiite (Dillsburg, Cornwall, Palisades), and the calc-alkali basalt suite (Cascades) is not so great, and the curves are less smooth. In general, the MCA diagram reflects the change in plagioclase composition from calcic to sodic types and the time-distribution of magnesium-rich and calcium-rich pyroxene crystallization. Normal diabase and chilled facies compositions, which plot in the same field, are somewhat more spread out on the MCA diagram because of the simultaneous crystallization of magnesium-rich pyroxene and calcium-rich plagioclase. As plagioclase becomes more sodic and pyroxene becomes less abundant, the differentiation curve moves diagonally toward and then along the A-C join. This is reflected more truly by an alkali-CaO tie line than an alkali-Fe tie line, especially at Cornwall where there is less iron enrichment in the pyroxenes than at Dillsburg.

Sulfur Isotope Fractionation

The study of isotope fractionation is another method that recently has been used to study magma fractionation (Taylor and Epstein, 1962; Smitheringale and Jensen, 1963). Table 30 presents results of a sulfur isotope study (Smitheringale and Jensen, 1963) on the Triassic igneous rocks of eastern North America. The δS^{34} refers to the enrichment of S^{34} relative to S^{32} measured with respect to a standard meteoritic composition. None of the samples analyzed was from the Cornwall sheet, but the Gettysburg, Morgantown, and Palisades plutons are represented. The range for normal sheet diabase is rather small and the δS^{34} mean, about 0.1 o/oo, is very close to that of meteoritic sulfur. This is taken to mean that there has been little change, such as by crustal contamination, in the isotopic sulfur content of the diabase plutons from that of a primary basaltic magma. From normal diabase through granophyre, there is a gradual enrichment of S^{34} (Table 30). This results from the preferential concentration of S^{32} in sulfide which, as crystallization proceeds, gradually impoverishes the remaining magma residuum in S^{32}. This isotopic enrichment sequence is taken as evidence of magmatic continuity from normal diabase through granophyre. It is interesting to note that there is a much greater range in the younger (?) diabase dikes than in diabase sheets.

The higher vapor pressure of H_2S relative to that of SO_2 also would tend to favor residual enrichment in S^{34} (Smitheringale and Jensen, 1963, p. 1202-1205) by enriching the vapor phase in S^{32}, providing that a vapor phase can form. Obviously the crystallization stage at which any vapor phase might separate would have a large effect on the isotopic sulfur composition of that phase, and perhaps also a noticeable effect on the remaining magma (see Part 6, "Sulfur Isotope Data").

Table 30. *Sulfur isotope ranges for S^{34} from Triassic diabase* (Smitheringale and Jensen, 1963)

	S^{34} (0/00)
Meteoritic	-1.9 to +0.5
Chilled Margin (sheet)	-0.2 to +0.4
Fine-grained Diabase (sheet)	-0.2
Normal Diabase (sheet)	-0.1 to +1.0
Coarse and Pegmatitic Diabase (sheet)	+0.2 to +8.7
Aplite-Granophyre	+3.0 to +8.4
Younger (?) Diabase Dikes	-3.6 to +7.2

Alkali Differentiation Trends

The preceding discussion has demonstrated, from gross chemical characteristics, the normality of the differentiation trend of the Cornwall sheet when compared with other sheets in the eastern North American Triassic Province, as well as with world-wide occurrences. The trend of alkali differentiation, however, is somewhat more sensitive to minor variations, a result of chemical fractionation to the small residuum volume.

In all of the sheets considered, enrichment of alkalies begins during the diabase-pegmatite stage (see Figures 48 and 49) at SI 19 and 25, increasing toward a maximum weight percentage concentration during late granophyre crystallization (Figures 50-52). It is assumed here that residual concentration of alkalies, particularly K_2O, in the granophyre was the result of the fractionation of other components, chiefly MgO, FeO, and CaO rather than the result of hydrothermal activity or volatile transfer. A good case for this assumption has been made by Pearce (1970, p. 29) for the Palisades sill. Because accurate volumes of the four major plutonic rock types (chilled margin, normal diabase, diabase pegmatite, and granophyre) and of a rock representative of the parent magma are not known, trends of absolute amounts (e.g., grams, tons, etc.) of the elements during differentiation are not known and may modify the extent of apparent alkali enrichment (see Chayes, 1970, for a discussion of the view that alkali enrichment has not been persuasively demonstrated for the Skaergaard basalt suite). In the ensuing discussions, "enrichment" is taken to mean "apparent enrichment" based on only a few chemical analyses of each major rock type, the average of which (plus later crystallizations) is assumed to be representative of the contemporary magma without taking into consideration rock-type volumes or a presumed parental magma composition. Cornwall diabase exhibits normal alkali enrichment within this restricted definition. The relative rate of increase of Na_2O from diabase to granophyre is usually greater than the increase in K_2O for diabase sheets and dikes (Turner and Verhoogen, 1960,

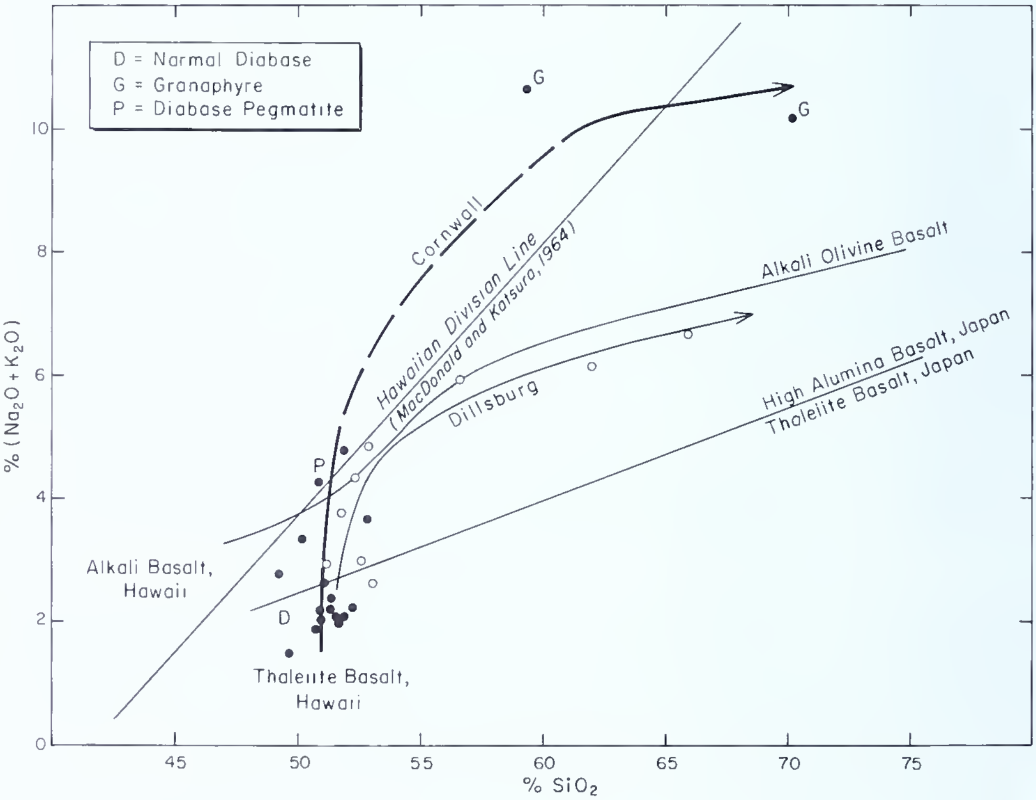

Figure 52. Silica variation diagram of percent (Na_2O + K_2O) versus SiO_2 comparing Cornwall (solid dots) and Dillsburg (open circles) differentiation trends with the Hawaiian Basalt line and the Japanese basalt types of Kuno (1968).

p. 217). The exceptions are ring dikes and large differentiated gabbros (Hotz, 1953, p. 697), dacitic residual glasses (Turner and Verhoogen, 1960, p. 216-217), and the monzonitic complex reported by Boesen (1964). Although Hotz (1953, p. 693) attempted to show a relationship between granophyre volume and K_2O/Na_2O, such comparisons are better restricted to sheet and dike diabase of the same magma and differentiation scheme. Within this framework, the sharply contrasting difference between pronounced K_2O enrichment at Cornwall and pronounced Na_2O enrichment in Dillsburg, Palisades, and to a lesser extent in the Karroo dolerites, requires explanation. The final alkali ratio should be a direct function of fractional differentiation routes within parental magma of any given composition.

At Cornwall, as at Dillsburg, both Na_2O and K_2O increase during fractionation (see Figures 48, 49, and 52). On a silica variation diagram of silica versus total alkalies (Figure 52), it can be seen that in normal diabase where silica is low, the alkali/silica ratio at Cornwall is similar to, and only slightly less than that at Dillsburg. However, as differentiation proceeds, the fractionation at Cornwall differs: at Cornwall the total alkali increase is greater and more rapid relative to silica. Most of this increase is the result of granophyric potassium enrichment such that at Cornwall $K_2O \gg Na_2O$. The reverse is true in the late differentiates at Dillsburg: $Na_2O > K_2O$. A part of this difference may be attributed to initial magma differences.

The rate of increase of total alkalies as silica increases has been used to characterize basalt type. In a study of Hawaiian basalts, MacDonald and Katsura (1964) suggested a Hawaiian basalt line dividing alkali and tholeiite basalts (Figure 52). From a study of Japanese basalts (Kuno, 1960 and 1968; Kuno, Yamasaki, Ida, and Nagashima, 1957), a three-fold division has been suggested with a field for high-alumina basalt lying between alkalic and tholeiitic types (Figure 52). The Skaergaard suite (Kuno, 1968, p. 655) alkali/silica fractionation essentially remains within the high-alumina basalt field throughout. The Karroo dolerites remain near the tholeiite high-alumina basalt boundary except for extreme fractionation at $SiO_2 > 65$ (Kuno, 1968, p. 640). The Dillsburg and Palisades diabase begin alkali-silica fractionation in the tholeiite field and move into the Japanese high-alumina basalt field at $SiO_2 < 55$. This fractionation at Cornwall is even more extreme, passing into the alkali (olivine) basalt field (Figure 52) of Kuno (1968, p. 640) at $SiO_2 = 51\text{-}52$ in diabase pegmatite rocks. In this respect, the Cornwall tholeiite suite somewhat resembles trends exhibited by alkali rock series (Kuno, 1968, p. 653 and 672). Such extreme enrichment of alkalies appears to be unusual for tholeiitic basalts, although some have been noted (see Jamieson and Clarke, 1970).

Bowen (1928, p. 104) cites the granophyres as evidence that magma fractionation occurred. However, the Cornwall and Dillsburg granophyres differ noticeably and this difference may be a function of the degree of fractionation. Bowen (1928, p. 96-124) has considered the differences between strong and weak fractional crystallization. In the system An-Ab-Or, the fractionation path of a liquid is not the same as the equilibrium path: i.e., the weaker the fractionation, the closer the liquid approaches an equilibrium path. With weak fractional crystallization in this system, the liquid path is strongly curved toward Or from the Ab-An field. Under strong fractionation, the Or-plagioclase boundary is reached at a lower Or/Ab ratio and the residual liquid is more sodium-rich and more abundant. Thus, strong feldspar fractionation, even in the presence of silica or pyroxenes, results in a smaller incremental rate of K_2O increase than crystallization under weak fractionation conditions. Although with sufficiently strong fractionation K_2O may tend to increase at a somewhat greater rate than Na_2O in the residual liquid, the two curves may not intersect and the Na_2O content may continue to exceed that of K_2O.

At Dillsburg, the abundant volume of sodium rich granophyre certainly is indicative of strong fractionation. At Cornwall, the granophyre is less abundant and is potassium-rich ($Or \gg Ab$). These are characteristics of weaker fractionation. Zoned plagioclase, a characteristic of strong fractionation, occurs in the Cornwall sheet, but is common only near the base and more sparingly near the top. From the description by Hotz (1953, p. 682-683), it apparently is more abundant at Dillsburg. Consequently, although fractionation was certainly operative in the Cornwall magma, it may have been "moderate," or less strong than at Dillsburg, unless all of the differences are attributed to initial magma composition.

Although the K_2O content in Cornwall granophyre is higher than at Dillsburg, its volume is considerably less. In addition, normal diabase at Cornwall contains less K_2O than at Dillsburg. Therefore, there probably was less total K_2O in the Cornwall magma. There also is less Na_2O throughout the Cornwall diabase (Figure 48). These and other chemical differences among sheets (Figure 48; in major elements, Appendices 4 and 5; in chilled margin trace element composition, written communication, R. Smith II) suggest that original magmas compositional differences in alkalies existed in Pennsylvania. Possibly, in addition to a somewhat weaker fractionation at Cornwall, the *in situ* magma differed compositionally because of a withdrawal of constituents before final emplacement by a separation of the magma chambers each having slightly different compositions, by separate tapping of a single source, or by differences in fractional melting.

Iron Differentiation And Oxidation Trends

The previous section has discussed fractional crystallization as functions of original magma composition and crystallization of the feldspar series. However, there also is significant fractionation in the pyroxene series and among iron oxides that bears directly on iron enrichment and on the relationship between diabase and magnetite ore introduction.

The extent of iron oxidation and the total iron content for world-wide occurrences of diabase and basalt vary. Of 23 analyses from eastern North America (all Triassic, Appendix 6), all except two show between 7 and 9 percent total iron, these two exceeding 9 percent. Thus, total iron in this magmatic province is rather uniform. Of the remaining samples (exclusive of eastern North America, Appendix 6), 50 percent lie between 7 and 9 percent, but the range still is rather narrow; nearly 90 percent lie between 6.5 and 9.5 percent total iron. The FeO/Fe_2O_3 ratio varies slightly. The lowest ratios are for Triassic diabases of eastern North America and, as noted by Kuno (1968, p. 622), for alkali-olivine basalt. Total iron in basalts and diabases appears to be related to this oxidation ratio. As noted by Walker and Poldervaart (1949) for Karroo dolerites, there is a tendency for greater total iron where the FeO/Fe_2O_3 ratio is greatest. This is to be expected because minerals crystallizing in the more mafic portions of these magmas (neglecting the silica-rich differentiates) can incorporate more Fe^2than Fe^3. As is true for basalt suites in general, at Cornwall and Dillsburg ferric iron increases relative to ferrous iron in diabase pegmatite and granophyre, indicating increasing oxidation during differentiation. In fact, in granophyre at Cornwall, hematite is the most stable iron-oxide phase, and it is also present, but perhaps less abundant, at Dillsburg.

The different behavior of iron during differentiation in the various types of basalts and diabase sheets can be portrayed in several ways. One is the variation of total iron with rock type (Figure 53). Because the genetically associated rock types within such different suites as the Cascades, the Skaergaard, and the Triassic diabases are not strictly comparable (for example, rhyolite and granophyre), these types only approximately represent the same stage of differentiation. In all suites, total iron attains a maximum before the final silica-rich residuum crystallizes. However, here the similarities end. The calc-alkali Cascades suite shows no progressive iron enrichment and total iron content of the magma apparently was less than for the tholeiite suites. The major enrichment of the Palisades diabase is in the olivine layer near the base, with a secondary and minor increase within normal diabase, decreasing steadily thereafter. Both the Cornwall diabase and the Skaergaard suite exhibit a later iron maximum, in diabase pegmatite and gabbro respectively, but of vastly different magnitudes. The maximum iron enrichment at Dillsburg is at a somewhat later stage, in rocks transitional between diabase pegmatite and granophyre. Enrichment here is greater than at Cornwall, neglecting rock-type volumes. With respect to total iron enrichment, it must be remembered that in most cases the total volume of the later differentiates is small compared to the volume of the whole intrusive. Thus, there may be little difference between the total iron in the Palisades sheet and that in the Dillsburg sheet when the volume of the Palisades olivine layer is taken into consideration. On the other hand, the Cornwall sheet appears to be iron-deficient. The slight enrichment may be

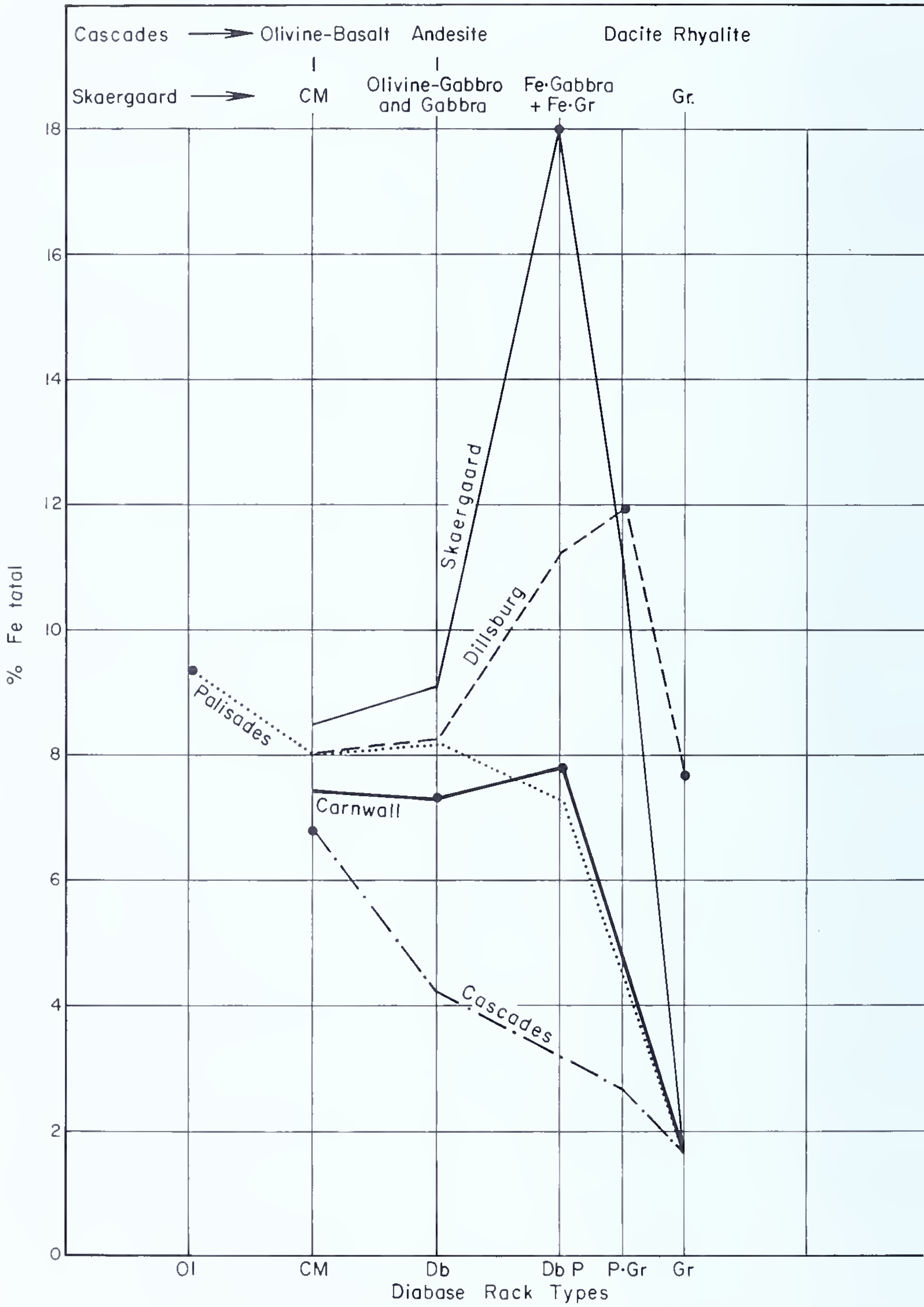

Figure 53. Comparison of differentiation trends for percent FeO (total iron) in Skaergaard, Cascades, Cornwall (heavy line), Dillsburg, and Palisades magmas. Rock-type correlations for Skaergaard and Cascades rocks are with approximate rock-type equivalents. Ol = olivine layer, CM = chilled margin (upper, at Cornwall), Db = normal diabase, DbP = diabase pegmatite, P-Gr = transitional between diabase pegmatite and granophyre, Gr = granophyre.

consequent upon this fact. In this regard it is more similar to alkali-olivine basalt than to tholeiite where $FeO+Fe_2O_3$ usually exceeds 15 percent (Kuno, 1968, p. 662).

The variation of total iron with "R", the silica/total alkali ratio (Figure 54), is another way of illustrating the variation in the behavior of iron during differentiation. Quite smooth curves result, in part because silica and alkalies change sympathetically, both increasing during differentiation, and in part because of the small silica range and low alkali content of normal diabase.

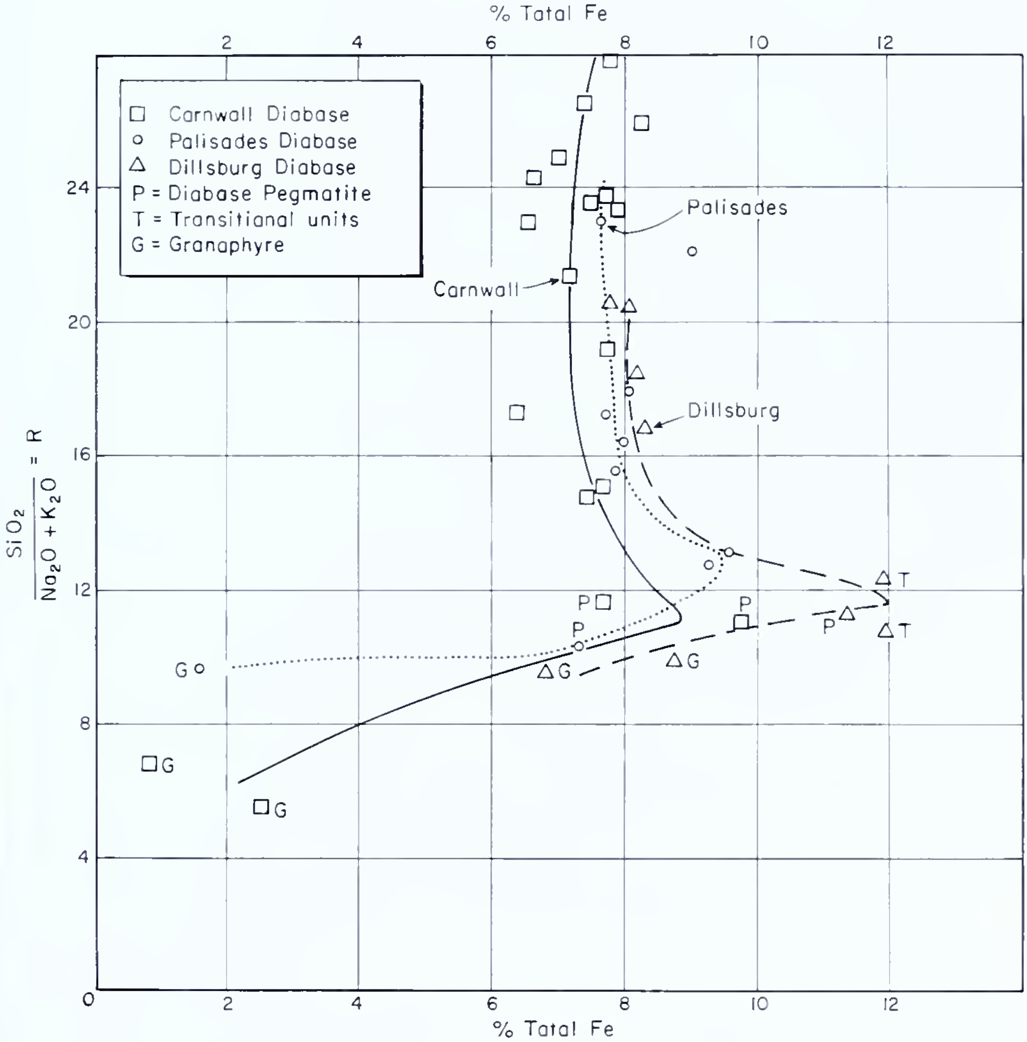

Figure 54. Plot of percent $SiO_2/(Na_2O + K_2O)$ versus percent total Fe comparing differentiation trends for Cornwall, Dillsburg, and Palisades magmas. Palisades point to right of curve represents the olivine layer. Some analyses of total Fe at Cornwall by Smith (Appendix 4; text) may be low and are to the left of the Cornwall curve.

The curves emphasize iron enrichment that is maximal at Dillsburg and minimal at Cornwall (the high iron content of the Palisades olivine layer does not lie along this Palisades differentiation curve). They also illustrate a different stage of differentiation at which the enrichment maximum occurs with respect to both rock type and the silica/alkali ratio (R). A secondary Palisades iron maximum occurs at R=12.8 near the top of the sill, the Dillsburg maximum occurs at approximately R=11.6 in transitional pegmatite-granophyre, and the Cornwall maximum occurs at approximately R=10.9 in diabase pegmatite. Thus, iron concentration is relatable to silica and alkali variation. Initially, in normal diabase of all three sheets, iron content is constant while R decreases as a result of nearly constant silica and increasing alkali, principally sodium. Following this, iron content increases at a nearly constant R (both silica and alkalies increase). The alkali enrichment coincident with iron enrichment is greater (a lower R value) at Cornwall but earlier in the sequence than at Dillsburg. After this, iron decreases sharply while R remains constant or decreases slightly. In all of the diabase suites, alkalies increase relative to silica toward the final differentiation product. The shape of these curves is similar for all three sheets, but their coordinate positions are a function of the competition between silica-alkali and iron enrichment trends. The curve with the least total iron enrichment (Cornwall) exhibits the earliest enrichment maximum at the lowest ratio of silica to alkalies. The curve with the greatest total iron enrichment (Dillsburg)exhibits the latest enrichment maximum at a slightly higher ratio of silica to alkalies. The curves indicate that total iron enrichment within the diabase sheet is favored by inhibition of alkali enrichment with respect to silica and that if this condition prevails, maximum iron enrichment may appear later in the differentiated residua system.

The oxidation of iron (assuming negligible deuteric oxidation) also affects the course of differentiation and reveals differences among basalts and diabases. In the ensuing discussion, as in previous discussions of trends, it will be assumed that each of the major rock types sampled is representative of that particular crystallization-differentiation stage. It also is assumed that the oxidation state of precipitating crystals maintained a nearly constant oxidation ratio with the magmatic liquid from which they were crystallizing at any one time (Yoder and Tilley, 1962, p. 429).

Changes in FeO/Fe_2O_3 with total iron reflect three distinct differentiation stages in the Karroo, Palisades, Cornwall, and Dillsburg magmas. In the first stage, total iron remained approximately constant in the solid phase (chilled margin and normal diabase) while Fe^3 increased in amount in the liquid relative to Fe^2, the latter being used up in the crystallizing minerals. This was followed by a period of nearly uniform oxidation as total iron increased in the solid phase after normal diabase had crystallized. At Cornwall, Fe^3 in the solid phase decreased slightly (cf. columes 3 and 4, Table 25), enriching the remaining liquid slightly in Fe^3. The last stage represents strongly decreasing total iron under conditions of nearly constant or slightly increasing oxidation. At Cornwall, this final iron crystallization and liquid enrichment in Fe^3 is represented by ferriferous and hematitic orthoclase with little or no magnetite. Thus, although there is a general trend of Fe^3 enrichment in the crystals of the differentiating magma, the curves are not simple depletion curves (Figure 55). Assuming a closed system, the controlling factors are 1) the degree of concentration of volatiles, 2) the initial magma oxygen fugacity that may be a function of H_2O content dissolved in the liquid (Hamilton and Anderson (1967, p. 475) believe it to be the controlling factor), and 3) the ability of the crystallizing minerals to accept iron in a particular oxidation state. The rate of crystallization and the rate of temperature lowering may play a subsidiary role in the control of oxidation. The small differences in the final crystallization stages of the various sheets with respect to iron oxidation must be the result of one or more of the first three factors, the second two being responsible, in part, for the similar shape (Figure 55) of all of the diabase iron-fractionation curves.

A similar family of curves illustrating oxidation during differentiation is illustrated in Figure 55, after Osborn (1959) and Yoder and Tilley (1962). The experimental curve at constant P_{O_2} is taken from Osborn (1959). The points from which the curves are drawn all lie quite close to the curves, with the exception of the Karroo granophyres and a few of the Cornwall samples with anomalously high SiO_2 that may be in error (see "Analytical Accuracy"). Yoder and Tilley (1962, p. 428-430) have discussed this type of curve in some detail. Basically they may be termed depletion curves for which available oxygen is successively used up and P_{O_2} decreases during mineral crystallization and falling temperature. The distribution (D) of a constituent, which may be approximated in terms of iron oxides, between magma and precipitating crystals can be expressed as follows (Neumann, Mead, and Vitiliano, 1954, p. 94):

$$\frac{(FeO/Fe_2O_3)\text{ crystals}}{(FeO/Fe_2O_3)\text{ magma}} = D_{T,\,p} \qquad (5-3)$$

where T=temperature and p=density at which D is constant. For high values of D, the precipitating crystals contain more FeO relative to Fe_2O_3 than the contemporary magma. This magma will then become enriched in Fe_2O_3. This is the general situation for tholeiitic (and diabasic) magmas (Figure 55) and the course of crystallization (measured against silica enrichment) represents increasing oxidation and perhaps also oxygen depletion. However, under extreme fractional crystallization, initial FeO/Fe_2O_3 ratios in the magma may not control the differentiation trend and a simple distribution coefficient may not be an accurate representation (Hamilton and Anderson,

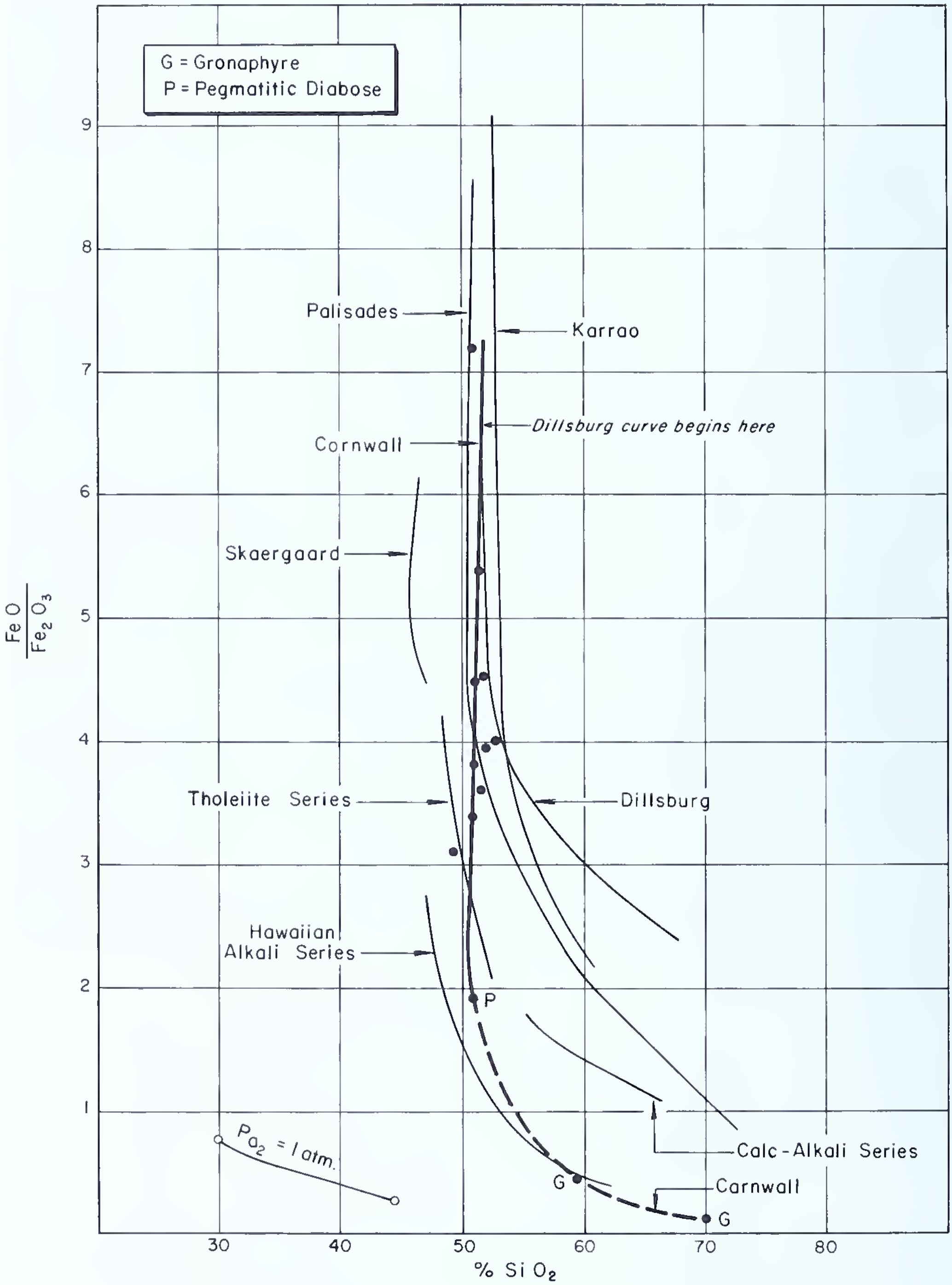

Figure 55. Plot of FeO/Fe_2O_3 versus percent SiO_2 comparing iron oxidation trends during differentiation of mafic magmas; solid circles and thick line represent Cornwall analyses. High Fe_2O_3 in Cornwall granophyre (dashed curve) may be incorrect although hematite is present (see text). Note upper parts of the Cornwall and Dillsburg curves are superimposed, but diverge at low FeO/Fe_2O_3 ratios.

1967, p. 475). Some control of FeO/Fe_2O_3 on enrichment (and a lack of extreme fractionation) at Cornwall has been noted.

The family of curves in Figure 55 is displaced, the nearly vertical part of each curve representing samples of normal diabase at nearly constant SiO_2. The iron-oxide ratio change indicates the incorporation of Fe^2 in crystals and the enrichment of Fe^3 relative to Fe^2 in the remaining magma. The flexion point of the curves occurs at various FeO/Fe_2O_3 ratios between the range of 50 to 54 percent SiO_2. This flexion point is represented by the crystallization of diabase pegmatite. The remainder of the curve for each suite tends to flatten out more nearly parallel to the constant PO_2 curve, moving toward the end point of granophyre crystallization. It is immediately noticeable that PO_2 must not have been constant throughout the sequence of crystallization. Hamilton and Anderson (1967, p. 477) similarly noted that the possibility of a constant (or increasing) PO_2 is small unless there is H_2 diffusion. The quite small scatter of points about the curves (Figure 55) may indicate small local differences in oxidation within a generally uniform framework of increasing oxidation of the crystalline phase. The flexion point results from the maximum period of titanium and iron-oxide crystallization (approximately at the typical diabase pegmatite stage). In this case, the crystallizing minerals and probably P_{H_2O} influenced the oxidation state of the remaining magma. A similar conclusion was reached by Yoder and Tilley (1962, p. 430). However, the initial oxidation state of the primary magma may control the kinds and composition of principal crystals and hence the subsequent trends, particularly the stage at which magnetite crystallizes relative to the silicates and the extent of late iron enrichment (depressed at Cornwall). The concentration of volatiles, decreasing temperature, temperature gradients, partial pressure of H_2O relative to total oxygen pressure, and magma composition will govern the minerals crystallizing with particular effectiveness during late crystallization stages when the volume of liquid is small. A line through the flexion points (approximately the diabase pegmatite stage) of the family of curves has a positive slope resulting from the displacement of these curves at higher silica values to higher FeO/Fe_2O_3 ratios. This could be interpreted to mean that there was a noticeable influence of the differentiated magma oxidation state on the course of late magma crystallization and on the oxidation state of resultant minerals.

There are small but significant differences in FeO/Fe_2O_3 among the diabases of Triassic magmas, expecially in the Cornwall sheet. Although the greatest range occurs previous to granophyre crystallization in the Karroo, Palisades, Dillsburg, and Cornwall sheets, the greatest range among these four is exhibited by Cornwall diabase (Figure 55). Except for some old analyses of Pennsylvania Triassic dikes (Appendix 5), the iron oxides in the Cornwall sheet are the most oxidized (FeO/Fe_2O_3 averages about 4/1) and those in the Dillsburg sheet are among the least oxidized. Furthermore, differentiation to diabase pegmatite and granophyre begins at the lowest

FeO/Fe_2O_3 at Cornwall and at the highest ratio at Dillsburg; that is, at Cornwall, oxidation proceeded farther (at approximately constant SiO_2) before differentiation to the residual liquids. These two observations, the earlier crystallization stage of increased oxidation of iron at Cornwall and the more oxidized character of most normal diabase samples at Cornwall, explain the earlier iron enrichment maximum (largely Fe^2) at Cornwall relative to the situation at Dillsburg.

It also is of interest that the Cornwall samples with the highest FeO/Fe_2O_3, 7.8 (not plotted on Figure 55 because of probably anomalously high SiO_2 at 53.3%) and 7.2, occur at 1040 and 1114 foot depths respectively, in the basal 200 feet of the sheet. This, together with the somewhat greater total iron here, may reflect a chemical cryptic layering or a lower-sheet injection. If the latter is the case, the difference in iron oxidation between the Cornwall and other Triassic sheets in Pennsylvania becomes more pronounced.

To summarize, oxidation and P_{O_2} in the diabase magma may have been rather high at Cornwall, but P_{O_2} probably decreased with falling temperature as oxidation of iron increased slightly. During crystallization of the later differentiates, increasing H_2O concentration in the remaining magma and the mineral phases crystallizing are suggested as governing factors. As P_{O_2} dropped with falling temperature (assuming a melt originally containing about one percent by weight H_2O), both iron and silica enrichment occurred at Cornwall (see discussion by Hamilton and Anderson 1967, particularly p. 477-479). An early, high FeO/Fe_2O_3 ratio as occurs in the Dillsburg and Palisades sheets results in abundant iron available for incorporation into olivine and pyroxene lattices. On the other hand, a somewhat higher Fe^3 and less total Fe content at Cornwall would have prevented significant incorporation of iron into the silicates and any significant enrichment. At Cornwall, the depletion of the sheet in total iron may indicate a physical separation of iron before sheet injection, since once a magma is emplaced within the crust its crystallization trend is essentially fixed (Yoder and Tilley, 1962, p. 520-521). Thus, the similar differentiation trend of the Cornwall, Dillsburg, Palisades, and Karroo sheets results despite differences in FeO/Fe_2O_3. These characteristics at Cornwall, together with the difference in solidification index for maximum concentrations between iron and titanium (Figure 49), the late enrichment of potassium relative to sodium, and the overall alkali deficiency, are believed to bear upon the origin of magnetite ore and associated metasomatism (see Part 6).

Summary of Cornwall Magma Differentiation Environment

The data and inferences presented in the previous sections can be applied to speculation concerning diabase differentiation at Cornwall; for example, the "competition" between the Bowen trend of alkali-silica enrichment and the Fenner trend of iron enrichment. To some degree, both are present at Cornwall resulting from moderate fractionation, total iron and alkali depletion, and oxidation effects. Another basic consideration is the influence of P_{O_2} and oxidation upon the differentiation trend and the associated problems of the role of H_2O and the more mobile elements such as sodium and potassium in a fluid environment. Study of the Cornwall sheet and comparison with Karroo, Palisades, and Dillsburg sheets yield information regarding the extent of fractionation and its effect upon final residuum composition. A few of the limiting conditions imposed on the early history of the magma at subcrustal or near subcrustal levels can be noted. The discussion of the relationship of these problems to ore deposition and to the Triassic magmatic province as a whole is deferred to later sections of this report (Part 6).

The composition of diabase magma on a world-wide basis is quite uniform and conforms to tholeiitic basalt composition. Estimates of equilibrium FO_2 at 1200 °C are in the range of $10^{-6.4}$ to $10^{-8.5}$ bars (Hamilton, Burnham, and Osborne, 1964, p. 37). Lowering the temperature will lower the equilbrium f_{O_2} necessary to maintain the FeO/Fe_2O_3 ratio by approximately one order of magnitude for every 100 °C (Kennedy, 1955). However, Fudali (1965) noted that experimentally determined values of f_{O_2} are apt to be higher than the actual value of a natural basalt system and concluded that 10^{-8} atm is reasonable for most basalts (Fudali, 1965, p. 1074). This is higher than the range 10^{-9} - 10^{-15} atm as estimated from the data of Lindsley (1962, 1963) for equilibrium pairs of ulvöspinel-magnetite and ilmenite-hematite at their probable compositions in the Cornwall sheet (see Part 6 "Titanium-Iron Geochemistry and Province Ore Origin"). The magma at depth responsible for the Cornwall sheet, however, may have had a slightly higher Fe_2O_3/FeO ratio than most basalts and possibly a higher f_{O_2} rather early in its magmatic history. Values in the range of $10^{-6.5}$ to 10^{-7} atm during crystal intrusion would seem reasonable. Excess H_2O could be a factor in raising P_{O_2}, although there is only slight amphibolitization (and serpentinization or chloritization) of the *in situ* diabase sheet at Cornwall, particularly of the olivine and pyroxene in the chilled margin. The petrographic evidence (see "Chilled Facies" discussion) does not clearly distinquish early from late amphibolitization (although magnetite nucleation on amphibole pseudomorphs raises the possiblity of early alteration). If the alteration is early, then the high H_2O content of the chilled margin (Appendix 4-A) could in part reflect a high H_2O content in the early magma, which in turn allows the possibility of oxidation of ferrous iron and early oxide mineral crystallization. (However, it must be remembered that the chilled margin is metasomatized). Above temperatures of about 1080° C, amphibolite, rather than basalt, is stable for water pressures of 1400 bars or more (Yoder and Tilley, 1962, p. 453). If these limits were attained, it could have been only briefly during initial crystallization, unless a high P_{H_2O} portion of the initial magma were isolated from that which yielded the main sheet after a high equilibrium f_{O_2} was established and before the onset of main stage crystallization. Nevertheless, a rather high P_{O_2} probably existed throughout crystallization (below the P_{O_2} conditions for complete amphibolitization) and was causal in leading to a dominantly silica-rich, rather than a dominantly iron-rich, residuum (Kennedy, 1955; Fudali, 1965).

It also is possible that the Cornwall portion of the York Haven diabase magma was a pocket of anomalously higher oxidation conditions such as has been recorded recently in Hawaiian lavas (Wright and Sata, 1966). Thus, it is not necessary to propose a generally high f_{O_2} for all of the York Haven Pluton from east of Cornwall west to the Susquehanna River. If separate feeder channels existed at depth, oxidation may have differed within the pluton from place to place. Oxidation at Cornwall also might tend to suppress the more mafic of Bowen's two reaction series that involve early olivines and pyroxenes relative to the plagioclase series. In this regard, it might be noted that the chilled margin at Cornwall is largely composed of plagioclase with only minor olivine and pyroxene.

Estimates of temperature at the beginning of crystallization are somewhat more reliable than estimates of oxygen pressure. If the pyroxene inversion curve is assumed to be valid at the total pressure of the magma, initial temperatures were at least 1050° C. However, Yoder and Tilley (1962, p.390-391) have suggested that it may not be strictly valid in the pressure environment of intitial crystallization. They pointed out that at high pressures (300 bars and below 1250° C) orthopyroxene is favored, and noted the possibility of the coexistence of ortho-and clinopyroxene above the inversion curve. They also noted (Yoder and Tilley, 1962, p. 383) that the melting of natural basalts occurs over a narrow range, between 1155°C and 1170° C. Hamilton, Burnham, and Obsorne (1964, p. 37) noted that at 1000 bars, plagioclase appears at 1012°C, the temperature increasing as pressure decreases about 1.5°C per 100 bars (although the linearity of the rate is not stated). Oxidizing conditions would tend to lower the liquidus temperature. Low total iron, or its removal, might have a similar, although small, effect (Yoder and Tilley, 1962, p. 381). Consequently, the initial temperature might be expected to lie at or near 1175°C (±50°C) before intrusion into upper crustal levels with clino-orthopyroxene inversion occurring slightly after crustal intrusion.

At temperatures greater than 1000 ° C, magnetite is stable in the presence of water (Yoder and Tilley, 1962, p. 438). At such a temperature, or somewhat higher, magnetite appears before the silicate liquidus is reached according to experimental data (Yoder and Tilley, 1962, p. 383). In corollary fashion, Kennedy (1955, p. 501) noted earlier that at a moderate to high P_{O2}, iron-rich spinel forms early in the crystallization sequence, as opposed to late in the sequence when the P_{O2} is low. These experimental data, combined with differences in P_{O2} (and/or P_{H_2O}) and alkali content, are believed to be indicative of slightly different courses of magma evolution at Cornwall and Dillsburg, especially with respect to *in situ* total iron, water, and alkali compositions that resulted from differences in magma composition and oxidation.

After crystallization, the main volume of diabasic magma was injected into the upper crust. Subsequent crystallization differentiation, probably with moderate fractionation, began and ultimately resulted in the sequence of moderate iron enrichment followed by silica and alkali residuum. This trend appears to be essentially normal; that is, it is the same trend evidenced in most other differentiated diabase sheets with less eventual total iron and alkali enrichment than in the western part of the province. At an early stage, P_{H_2O} was probably not equal to P total, and the discontinuous pyroxene-(hornblende)-biotite reaction series resulted. Although oxygen probably became depleted, oxidation of the precipitating crystals continued until the small volume of late differentiates formed after the crystallization of most iron-titanium oxides.

SPECULATION ON THE ABSENCE OF AN OLIVINE LAYER

In the one analyzed drill core through the sheet at Cornwall, there was no concentration of olivine. As noted previously, in the first 150 feet above the base there are a few serpentinized phenocrysts that originally may have been olivine, but they are not common. Here and elsewhere in the Pennsylvania Triassic Province, olivine or olivine relics are sparingly present in the chilled margins. Near Bermudian Springs, in the Dillsburg sheet, there may be a thin olivine-rich concentration near the base of a small offshoot sill. It is not comparable in size to the Palisades olivine layer and was not considered by Hotz (1953) to be similar. Near Middletown, in the western part of the York Haven Pluton, there appears to be a thin concentration of olivine just above the lower chilled margin. Note, however, that the presence of olivine has not been verified, and these concentrations may be orthopyroxene.

The absence of an olivine layer at Cornwall (assuming the drill core to be representative), and the scarcity of olivine in general in the Pennsylvania diabase plutons, is in sharp contrast to the Palisades diabase, which presumably belongs to the same magmatic province. This is especially true since the magnesium content of the Cornwall and other Pennsylvania sheets is as great, or greater, than that of the Palisades diabase (Figure 48). Three possibilities can be considered: 1) olivine was separated from the diabase magma before intrusion of the Pennsylvania diabase 2) an olivine concentration was originally present in Pennsylvania diabase but has been resorbed; or 3) little or no olivine crystallized from the Pennsylvania diabase magma(s).

There is no evidence supporting accumulation of residual olivine crystals from the York Haven magma. Although various sheet levels are exposed, no major concentration is anywhere evident. There is no noticeable depletion corresponding to olivine composition. If there is a separated olivine fraction, it remains at depth and down dip. Such a position of accumulation would favor magma intrusion during or after tilting had promoted gravitative settling.

Similarly, there is little evidence to support resorption, although if it were complete, no evidence would be expected. Any such process would have had to almost completely resorb olivine in the Pennsylvania sheets and yet not have affected the early olivine layer in the Palisades sheet. The small concentrations that do exist could be remnants of an incomplete resorption. They have not been studied petrographically. Available pore reaction space for resorption to occur in a concentrated olivine layer is small and the prospect of reestablishing equilibrium at a lower temperature with less mafic intercumulus liquid seems unlikely unless the layer was on the order of a few inches to a few feet in thickness. On the other hand, resorption by reaction of Mg-olivine and Ca-poor pyroxene to form orthopyroxene and pigeonite could have occurred before olivine crystals segregated or if convection was such that settling could not occur and equilibrium in the above reaction could be established. Resorption of olivine to orthopyroxene has been suggested for the Karroo dolerites (Poldervaat, 1944; Kuno, 1968, p. 695). Bronzite in Pennsylvania may have crystallized by this process. Another possibility, suggested by Kullerud and Yoder (1963, p. 216), is that a reaction may occur between sulfur and olivine, completely obliterating the olivine and yielding iron sulfide, magnetite, and magnesium silicate (see equations 6-1 and 6-2). However, sulfur distribution is unknown and this mechanism remains to be tested.

It may be equally problematical to propose that olivine never concentrated into a discrete horizon. At high pressures (>20 km), orthopyroxene rather than olivine is favored for the liquidus phase (Green, 1967, p. 426-429), but this mechanism would not apply to high temperature magmas within the crust. At Cornwall, the low total iron might tend to restrict olivine growth (Kennedy, 1948). However, in the Dillsburg sheet, total iron is higher and olivine still is scarce. An *in situ* crystallization at a high angle of sheet tilt, or an early, thorough mixing by convection also might prevent olivine settling. However, for at least part of the southern area of diabase sheets, the so-called sills, horizontal intrusion may have occurred (see Part 2, "Structure"). The chemico-mineralogical differences in the Cornwall sheet with depth, while small, indicate that any convection present probably was insufficient to thoroughly mix the crystallizing magma. However, it might have been more effective in preventing olivine settling when there was a low solid to liquid ratio early in the crystallization sequence. Multiple injection, a suggested possibility at Cornwall, also might have re-heated and disturbed the basal portions of the main overlying body, promoting both convection and olivine resorption. On the other hand, Walker (1969, p.144-164) believes that the olivine layer of the Palisades Pluton is a result of a second magma injection. Regional structural dislocations, if they occurred during or slightly after injection, also might have had some effect on convection.

DIABASE DIKES OF PENNSYLVANIA

Introduction

Numerous diabase dikes intrude the Precambrian, Palezoic, and Triassic sediments and metamorphic rocks of southeastern Pennsylvania. It often has been assumed that these dikes represent feeder necks that once were channels supplying magma for extrusive flows and intrusive sheets, but in part they might also have been the last phase of tholeiite magmatic activity that was preceded by flows and sheets. Accurate detailed data concerning the sheet-dike sequence are sparse. Some new petrographic, chemical, and structural data are summarized here that shed some light on these problems.

Evidence that dikes might be younger than sheets (and flows) is all indirect, except for the observation that a bronzite dolerite dike cuts the Palisades pluton (Walker, p. 26). In a general summary, Frankel (1967, p. 96) notes that in many areas flows are followed by sheet intrusion. In the similar Karroo dolerite province, dike injection followed that of the sill (Walker and Poldervaart, 1949, p. 686). By analogy with these and other magmatic provinces, the sequence of extrusive basalt to intrusive sheets to dikes in northeastern North America could be presumed. On the Pennsylvania State Geologic Map (Gray and others, 1960), the dikes appear to transect all igneous and sedimentary units of the Triassic basin. However, chilled margins of dikes against sheets rarely have been observed. As discussed subsequently, the dike fractures in any one area have a characteristic strike. At Cornwall, fractures with this orientation are: 1) post-sheet diabase but pre-ore, and 2) post-ore, indicating that they, and by analogy the dike fractures, are younger than sheet diabase. However, the one dike observed at Cornwall in the ore zone appears to be metasomatized (Lapham and Saylor, 1970) and hence may not be significantly different in time from the sheet. Another observation bearing on time is that the direction of maximum principal stress allowing lateral sheet injection would have differed considerably from that favoring vertical dike injection. Such different stress orientations imply a time difference. Justus and others (1970) refer to similar dikes in North Carolina as being of Jurassic age. As noted and discussed by de Boer (1967 and 1968), there is evidence from the remanent magnetization of dikes to the northeast that basaltic magma reached the upper crust at several different times from late Triassic to Jurassic time. Additional support for Triassic dike intrusion can be found in southeastern Maine where these dikes have intruded ring-dike structures assigned to the White Mountain magma series, dated at about 180 my (Hussey, 1962; Lyons and Faul, 1969, p. 312). Lastly, the geographic distribution of dike diabase is more widespread and is largely southeast of the locus of sheet intrusion. Such a distribution could be the result of a lack of contemporaneity of the two injections.

Evidence that dikes and sheets are essentially synchronous but of two time and magma-composition episodes has recently been offered (R. Smith II, personal communication). An eastern compositional type (both sheets and dikes) is suggested as having intruded earlier than a western compositional type (both sheets and dikes) based on some cross-cutting and chilled contact relationships. However, the time relationships observed so far permit sequences other than this simple, two-stage sequence. For example, the following sequence from oldest to youngest also is permitted by the present data: eastern-type flows, eastern-type sheets, western-type sheets, eastern-type dikes, and western-type dikes. Since the extensional fracture-and-dike system is not deformed or related to fold geometry, the dikes, at least in the eastern area, are believed to be post-basin deformation. Consequently, basin deformation may separate, in a time sense, compositionally equivalent sheets from dikes.

The most striking characteristic of these diabase dikes is their remarkable continuity, extending for miles at a width commonly less than a hundred feet. Throughout their length, they maintain a generally uniform strike trend, although in detail deviations exist (see strike data of Lapham and Saylor, 1970). Textural, compositional, mineralogical differences apparently are small (Lapham and Saylor, 1970), but may be significant. In Pennsylvania, the dikes rarely cut Precambrian units. One exception is in the area of Reading, Pennsylvania (personal communication, David B. MacLachlan). A few of the dikes extend north and northwest of the Triassic Province, but by far the majority are to the south and southeast in the crystalline Piedmont.

Mapping in the Lebanon Valley, particularly in the vicinity of Cornwall, revealed the possibility that fracture planes with a northeast strike characterized a Triassic, or later, deformation (personal communication, Alan Geyer) and opened the possibility of differentiating them from Paleozoic fractures. King (1961) plotted the major dike trends of the Applachian Mountain System and noted that their trend changes from northwest in the southern Appalachians, to northeast in the northern New England Appalachians. He also noted that this trend bears no consistent relationship to the trend of the Triassic Newark Gettysburg basin nor to that of the older rocks that the dikes transect. King (1961, p. B-95) concluded that the pattern of the dikes may be the result of deep-seated tensile stresses active during late Triassic time, in contrast to a surficial stress pattern. Wise and Nickelsen (Nickelsen, 1963, p. 14-16) suggested that the trend of the dikes in Pennsylvania approximately parallels the trend of the Appalachian culmination and the adjacent anthracite depression. They further suggested that this trend may indicate a late Triassic north-south arching with basement control similar to that which may have controlled the Paleozoic culmination.

Petrography

A total of 57 petrographic thin sections from diabase dike samples collected by the author, by Timothy Saylor (Lapham and Saylor, 1970), and by Arthur Socolow have been examined to obtain a general description of dike diabase. Detailed investigation undoubtedly will modify this summary.

Contacts with country rock commonly are sheared and sharp, although small apophyses of diabase extend into host rock. Country rock alteration within a few feet of the contact consists of recrystallization (where the host is a carbonate lithology), chloritization, serpentinization, and reduction of hematite to magnetite. Mineralogical composition and order of mineral crystallization are basically the same, although somewhat simpler, as for the diabase sheets. Textures range from aphanitic at chilled margins to coarsely holocrystalline and occassionally porphyritic. A flow-like texture has been observed (e.g.) the dike at Clark's Ferry, (written communication, Robert Smith), but nowhere else in Pennsylvania. Segregates of granophyre and diabase pegmatite have not been observed. Small schlieren of pegmatitic diabase are uncommon. Interstitial micropegmatite may be present, but often is absent.

Metallic oxides are present on the order of one to five percent in all dikes examined. Alteration to leucoxene is uncommon. Free quartz is rare but occurs in micrographic intergrowths with potassic feldspar (also rare). Other minerals usually present include Ca-rich and Ca-poor clinopyroxene, orthopyroxene, plagioclase (occasionally zoned), brown biotite, green hornblende, serpentine, olivine, and amphibolitized olivine in chilled margins and fine-grained portions. Pyroxene exsolution commonly is absent. Plagioclase near country rock contacts commonly is sericitized. Mineral abundance within the dikes seems to be at least as variable as that in the normal diabase of the sheets.

Because of the paucity of data, no conclusions can be drawn with respect to sheet-dike comparisons other than apparently more abundant olivine, a lack of granophyric differentiates, and a narrower textural range in the dikes. A search for evidence of fluid mobility, chemical and physical, might be interesting, since thin dikes are continuous over great distances under conditions of generally permissive intrusion. On the other hand, dikes can intrude at less than the lithostatic pressure (in contrast to sheets) and less mobility may be required.

Chemistry

Several chemical analyses of dikes from the eastern Appalachian belt are presented in Appendix 5-C. No attempt has been made to obtain an exhaustive list, although all of the reliable published analyses that could be found for Pennsylvania dikes have been included: a single dike analysis from Conshohocken, an analysis from Cornwall (Appendix 4-A and 5-C), and an average of 12 new analyses from five locations along the strike of the dike extending from Gettysburg to Duncannon (Appendix 5-C, #4; Lapham and Saylor, 1970). Most other dike analyses are old and suspect because of low total iron, a high ferric/ferrous ratio, low magnesia, high alumina, or other unexplained discrepancies from the expected composition. The analyses that have been listed (other than at Cornwall) indicate that, relative to sheets, some dikes exhibit a lower average K_2O and perhaps Na_2O, possibly a higher average Al_2O_3 and CaO, and wide divergences in total iron, which may be characteristic but the ranges are wide (see Lapham and Saylor, 1970). The Pennsylvania-Maryland dikes may be lower in total iron and higher in Al_2O_3 than dikes elsewhere (see Lapham and Saylor, 1970), but this may be an effect of unsystematic sampling or analytical error.

The dike analysis at Cornwall is somewhat higher in Al_2O_3 than the neighboring sheet but also higher in total iron. It also is lower in SiO_2, TiO_2, MgO, CaO, and Na_2O, and higher in K_2O and H_2O than the sheet. The rather anomalous anaylsis of the Cornwall dike (cf. analyses in Lapham and Saylor, 1970) suggests that the dike here has been metasomatized with introduction of K_2O; hence, it may be pre-ore and may not be appreciably younger than the sheet. Smith (personal communication) from his low TiO_2 analyses of this dike, believes that this composition may represent a magma younger than the adjacent Cornwall sheet. The Conshohocken dike is the only one listed with an Fe_2O_3/FeO ratio greater than one. This ratio also is high for the Cornwall dike. The Gettysburg-Duncannon dike, west of the ore deposits, has a normal Fe_2O_3/FeO ratio (Lapham and Saylor, 1970). This 50-mile long dike also shows no compositional differences between chilled margin and fine-grained interiors and no significant differences from north to south (Lapham and Saylor, 1970). Slight differences in the Fe_2O_3/FeO ratio might be expected if the dike magma originated from a single source magma that earlier yielded sheet diabase, suffered differential oxidation, and was the source of an ore fluid in some areas. There also are differences in Al_2O_3 (Lapham and Saylor, 1970) and in S, Cu, and TiO_2 (written communication, R. Smith 11, 1967). Thus, there is a possibility that more than one magma chamber or magma composition existed throughout the span of magmatic activity. Work in progress (R. Smith II, written communication) indicates that these differences occur approximately east and west of the Susquehanna River. Consequently, some of the apparent analytical differences between sheets and dikes may result from comparisons between different magma provinces, and may not be a time function of magma tapping.

Structural Deformation

The diabase dikes of Pennsylvania occupy steeply dipping, nearly vertical fractures that may extend for many miles through the Piedmont, Great Valley, and Triassic Lowlands provinces. Structural analysis of this dike-fracture system may be able to answer several important questions: Why did diabase intrude this apparently consistent system of fractures? Why are the dikes so uniform and so numerous? Why are they localized largely south and east of the Triassic basin? Why do the dike-filled fractures fan across Pennsylvania and what kind of crustal deformation caused this final episode of magmatism and fracturing in the Appalachian geosyncline?

A detailed strike-trend analysis of the Triassic dike-fracture system is a first step in finding answers to these questions. The dikes of Pennsylvania and northern Maryland can be treated separately from those to the south because the changing strike trend from Alabama to New England is locally irregular here. Projections of the strike of local Appalachian dike systems from Alabama to New England (King, 1961, p. B-96, Figure 41.1) show that several separate trend "foci" exist, indicating discrete areas of varied deformation resulting from differences in local stresses. This is particularly true of the dike-fracture system in Pennsylvania. To define this locally changing pattern, the Pennsylvania dikes were arbitrarily divided into five areas from west to east, each area containing one major dike trend, usually definable by a single, long dike (Figure 56). Using the dikes on the Geologic Map of Pennsylvania (Gray, and others, 1960) which yields more detail than Figure 56, each dike section of constant strike was numbered and the strike azimuth measured. In all, 253 measurements were made on Pennsylvania dikes. In addition, dikes were measured in Maryland from Washington and Frederick Counties southwest of the Pennsylvania subdivision. Each of these measurements was then plotted on a 180° histogram to examine strike constancy, pattern of strain, and east-west variation. A generalized summary of these data plotted at 5° azimuth intervals is presented in Figure 56, arranged approximately from west (Maryland) to east. By measurement of each change in dike strike, it was hoped that a crudely quantitative expression of the fracture orientations preferred by diabase intrusion would be obtained. More detailed analysis undoubtedly would reveal greater differences in strike trends, but azimuth maxima should remain about the same. The arrow above each diagram (Figure 56) represents the strike direction of the major dike in the arbitrary areal subdivision.

In the Cornwall area, N20° E-N30° E fractures, which are intruded by diabase dikes elsewhere (Figure 56 diagram III), are present in the ore zone but contain no diabase (Figure 23). One such fracture (a major fault) has been suggested as a possible ore-fluid channel (see Part 4, "Geology of the Cornwall Ores" and Plate 22). Another fracture system with the same strike orientation apparently offsets fractures that at places are ore veins (Figure 23). Hence, there may have been repeated movement and/or extension of the N20°-N30° E fracture trend: a first movement before or during ore emplacement and a second after ore emplacement (see Part 4, "Structures of the Eastern Ore Body").

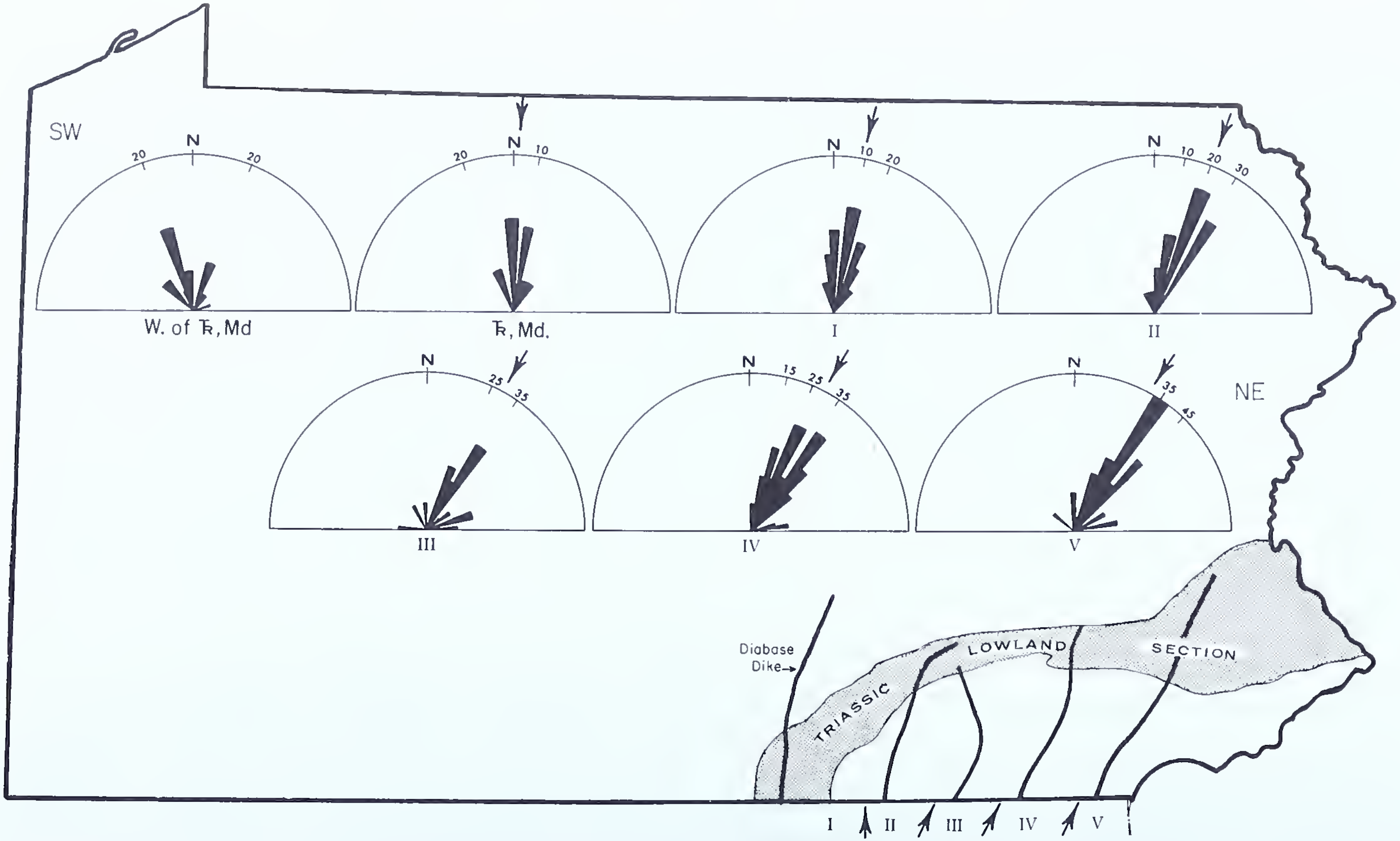

Figure 56. Rose diagrams of strike orientations of diabase dikes in Maryland and Pennsylvania, from southwest (top left) to northeast (bottom right). Roman numerals indicate arbitrary areal subdivisions between arrows and each such area includes one major dike system as illustrated. Arrows on rose diagram represent the average strike of the major dike system in that subdivision.

Each of the areas from Maryland through eastern Pennsylvania shows a distinct strike maximum. Scatter increases somewhat eastward. A clear change in strike from northwest on the southwest and west to northeast on the east is evident. This strike maximum does not maintain a constant angle with respect to the present margin of the Triassic basin nor does it maintain a constant angle with respect to Appalachian curvature (the Appalachian culmination noted by Nickelsen, 1963), because the extent of fanning of the dikes is less than the change in strike of the nearby Paleozoic sediments. Although there may be some small-scale refraction evident as a dike passes from one rock type to another, this refraction is not measurable on the scale of measurement used; hence, the changes are a response to regional or local stress-field differences, rather than to competency effects.

From these data, it seems clear that the dike-filled fractures formed a radial pattern in respone to either a single, varied, vertically-induced stress field, or in response to local basement-initiated rotational extension during fracture-plane formation. Since the maximum change in strike directions occurs in Pennsylvania where the Triassic basin makes an abrupt change in strike from northeast to nearly east-west, it seems logical to suppose that a rotational movement by deep-seated east-west translation, resulting in new surficial extension directions, was responsible for at least part of the strike fanning. That some stress reorientation did occur is clear from offsets of several of the dikes (Geologic Map of Pennsylvania, Gray and others, 1960). These offsets are commonly right lateral. However, they are not faults because the adjacent country rock is not offset.

These data indicate that, while there is a general strike fanning from the southern to the northern Appalachians, there has been an additional superimposed rotational effect along the locus of Appalachian curvature in Pennsylvania, and that some of this fanning could have resulted from local basement translation. The locus of projections of the dike fans in Maryland and Pennsylvania is near Baltimore, Maryland, which is approximately the same focus as for the symmetry axis of Appalachian curvature and hence supports the possibility that at least part of the surface expression of this curvature is related to east-west extension approximately along the axis of the Pennsylvania Triassic basin. However, bacause the fanning also occurs on a regional scale throughout the Appalachians, there also was a deep-seated stress related to basement arching parallel to the Appalachian geosynclinal trough (a likely site for tholeiitic magma generation). King (1961, p. B-95) previously noted the probability of basement involvement.

Some additional structural implications of the above analysis invite interesting speculation. Presumably, the fracture system intruded by diabase was formed before magma ascension but in response to structural dislocation that involved the basement. Vertical fractures (or fracture zones) are likely avenues of magma crustal ingress, and this is reflected in the steep-dipping attitudes of the dikes. Earlier fractures that could have served as channels already may have been sealed or were too shallow. Dike-fracture orientations, or the stress fields that produced them have been rotated with an increasingly eastward trend under a general deformational environment that allowed diabase magma to intrude the crust. Consequently, a lateral, east-west, subcrustal displacement might have occured penecontemporaneously with Appalachian arching.

It is also noteworthy that the majority of dikes lie south and east of the Pennsylvania Triassic basin as if the magma source lay in this direction (approximately toward the fracture focus) at subcrustal depths. This could imply that any *basement* movement associated with translational crustal dislocation lay southeast of the Triassic belt, even though its Triassic surface expression is to the north or northwest. Perhaps uplift and translation are a single, basement-related process. Drake and Woodward (1963) have postulated a major fault in this area.

Beginning with the early suggestion of Walker and Poldervaart (1949, p. 687-690) that the diabase dikes of the Karroo are associated with the early disruption of Gondwanaland in Triassic-Jurassic time, there has been considerable recent research in support of a genetic relationship (e.g., Siedner and Miller, 1968; Behrendt and Wotorson, 1970; Justin and others, 1970; Smith and Hollam, 1970). Triassic dikes in both the South American and African plates appear to have been emplaced just previous to Gondwanaland disruption. Crustal stress created between continental segments and mantle may have induced extensional crustal release and tholeiite intrusion as a precursor to the major rifting of continental plates in Jurassic and Cretaceous time. By analogy with the South-African (-Tasmanian-Australian) situation, the late Triassic dike tectonics of the Appalachians may have a similar tectonic origin.

PLATE 1. METAMORPHOSED LIMESTONE

Limestone (Buffalo Springs Formation) above western ore body replaced by diopside (high relief); plane-polarized light.

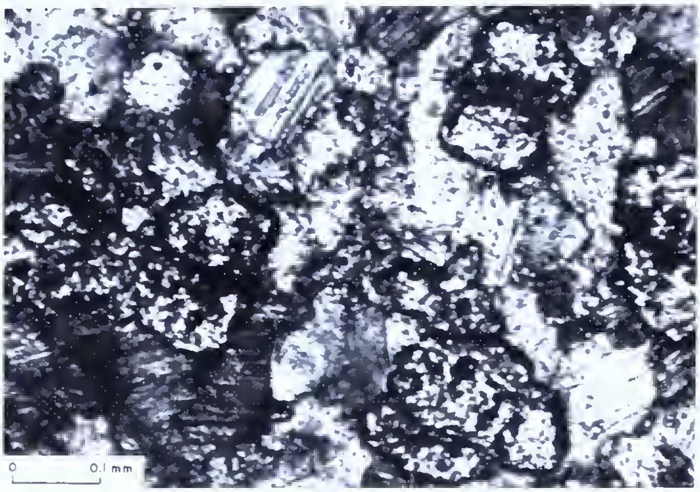

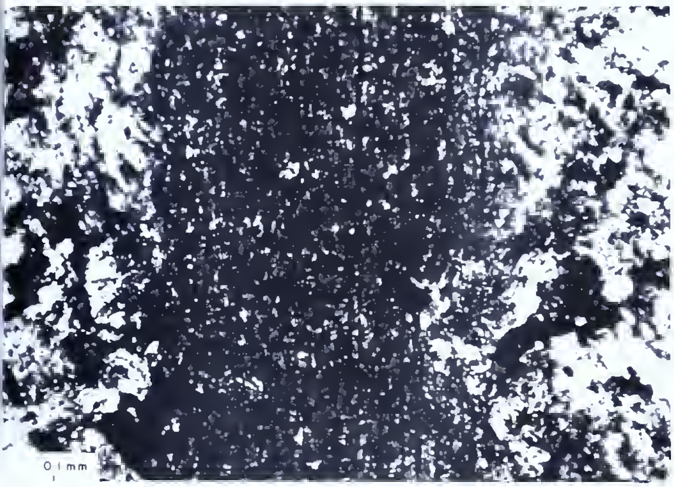

B. Contact metamorphic phlogopite crystal (dark), originally in host limestone, now replaced by diopside; crossed nicols.

Contact metamorphic phlogopite (white) replaced by calcite (black) in turn replaced by serpentine (gray); crossed nicols.

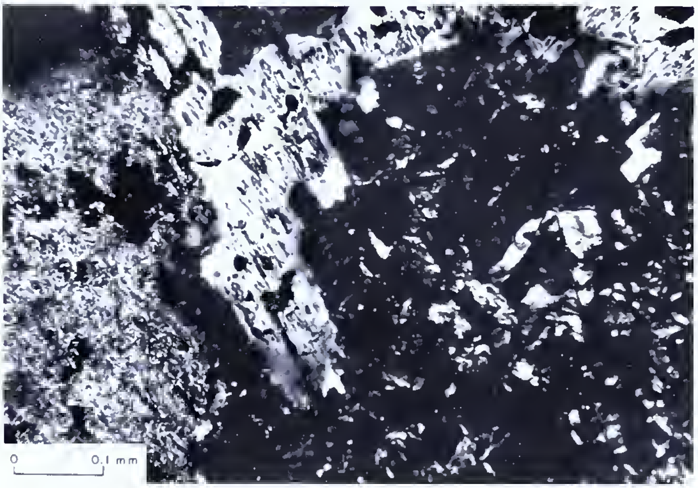

PLATE 2. THE BLUE CONGLOMERATE

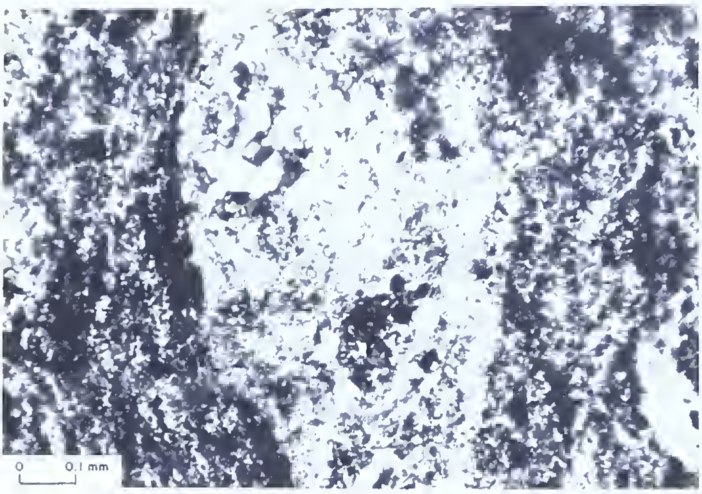

A. Quartz and mica pebble fragmen (pelitic) in quartz-free matrix crossed nicols. Pebbles are commonly much larger than illustrated here

B. Mixture of angular quartz and large pelitic fragment in quartz-free matrix; plane-polarized light.

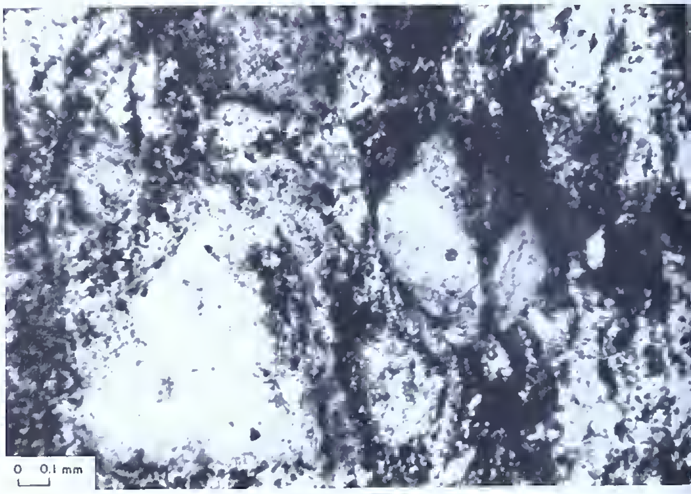

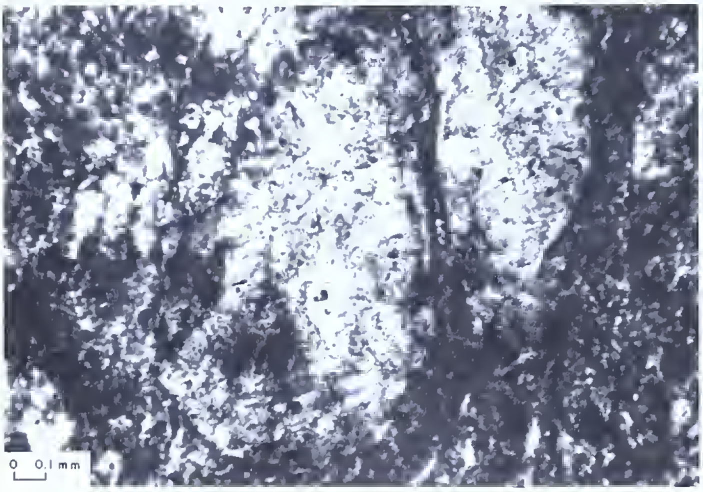

C. Quartz fragments, brecciated and partly replaced by matrix; plane-polarized light.

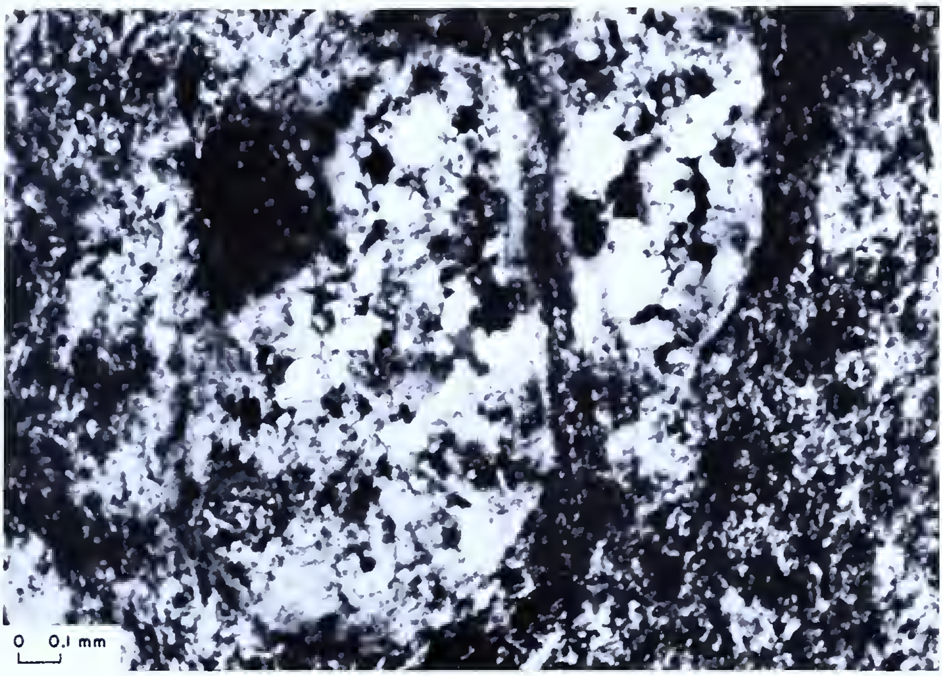

D. Same as C; crossed nicols, illustrating equilibration between pebble fragments and matrix after contact metamorphism and metasomatism.

PLATE 3. MILL HILL SLATE: PETROGRAPHIC COMPOSITION

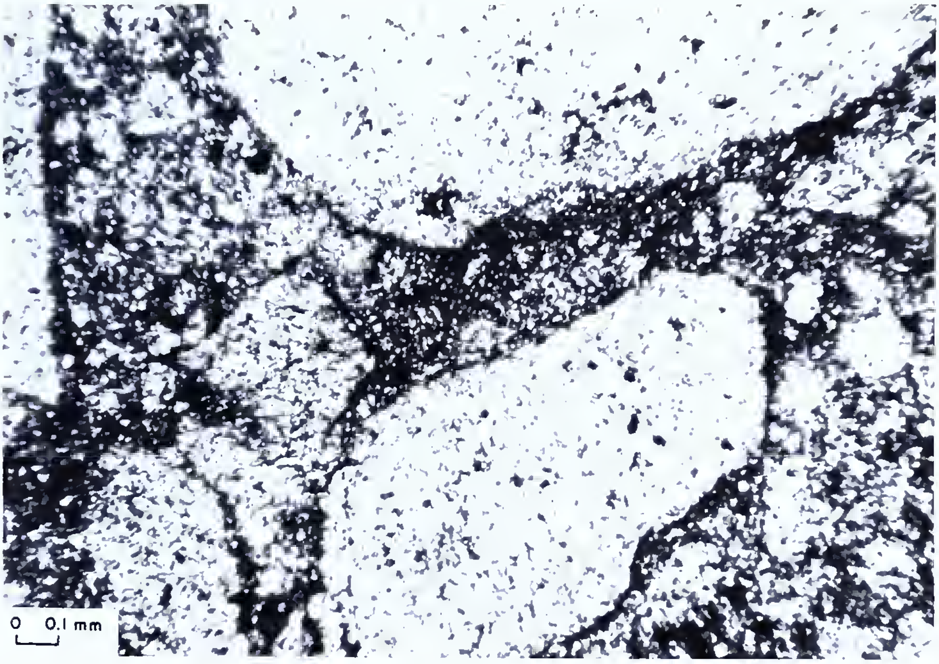

A. Pelitic fragments of mica, clay, and minor quartz and/or feldspar (see text) in somewhat brecciated matrix rich in plagioclase; rather atypical of this lithology; plane-polarized light.

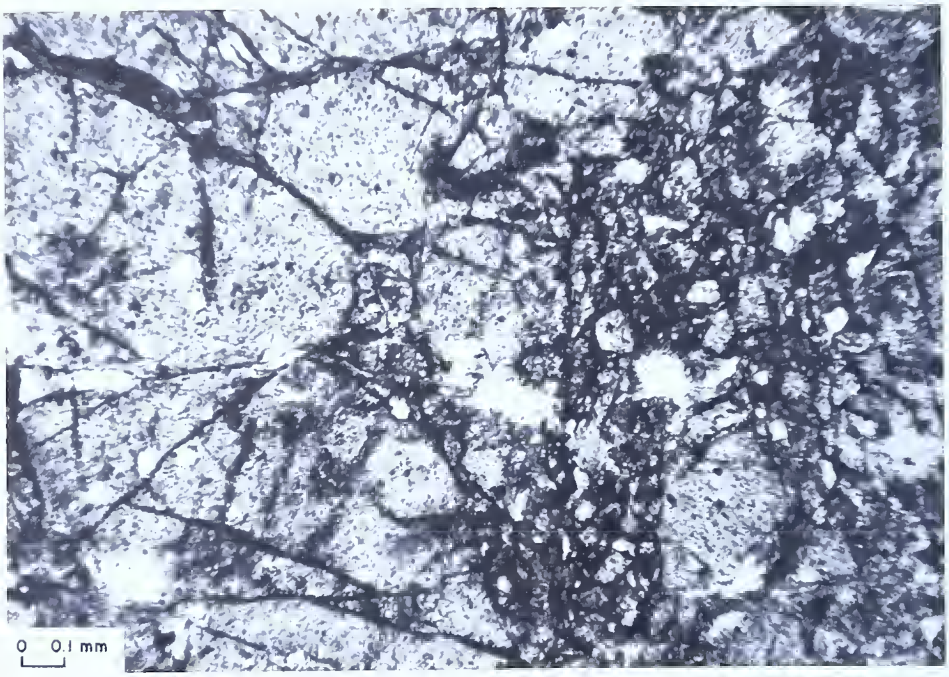

B. Brecciated pelitic fragments, composition as above; plane-polarized light.

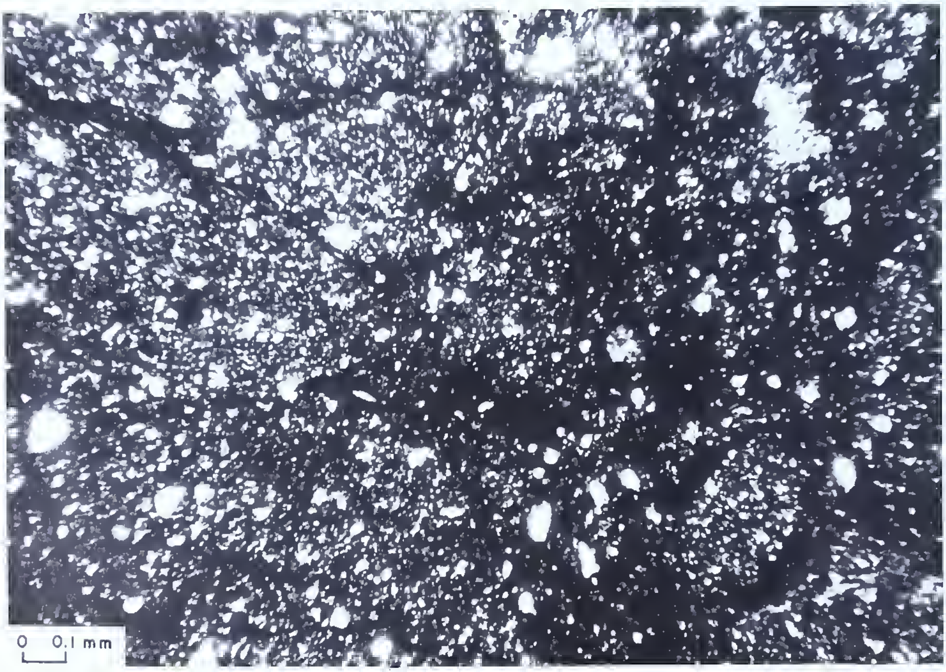

C. Same photograph as B. but with crossed nicols. Metamorphism largely has destroyed original compositional differences of fragments.

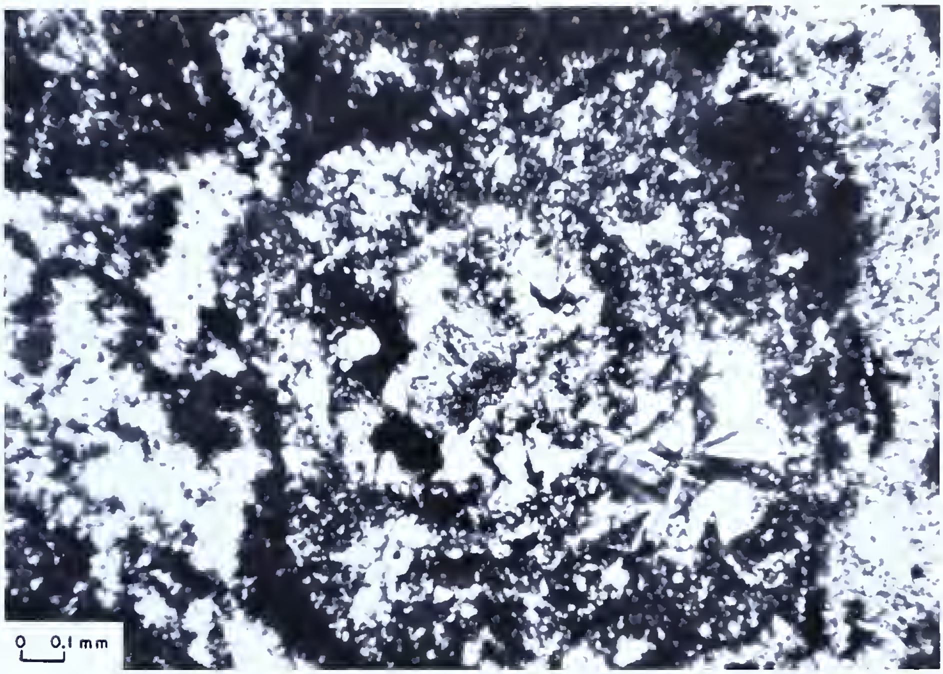

D. Limy Mill Hill Slate matrix with metamorphic knot of plagioclase (albite) and diopside. Laminae that bend around granoblastic growth centers are typical of metamorphic Mill Hill Slate with a slight amount of superimposed metasomatism but lacking pink Fe-orthoclase; crossed nicols.

PLATE 4. MILL HILL SLATE TEXTURE AND COMPOSITION

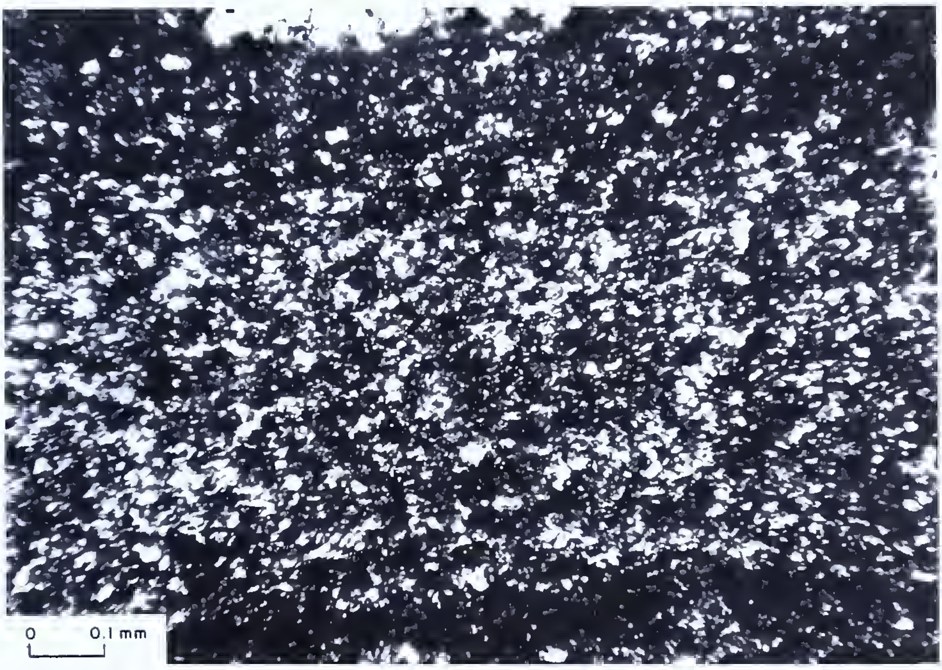

A. Textural banding, or lamination, typical of the Mill Hill Slate, Plagioclase is a major component (see text); crossed nicols.

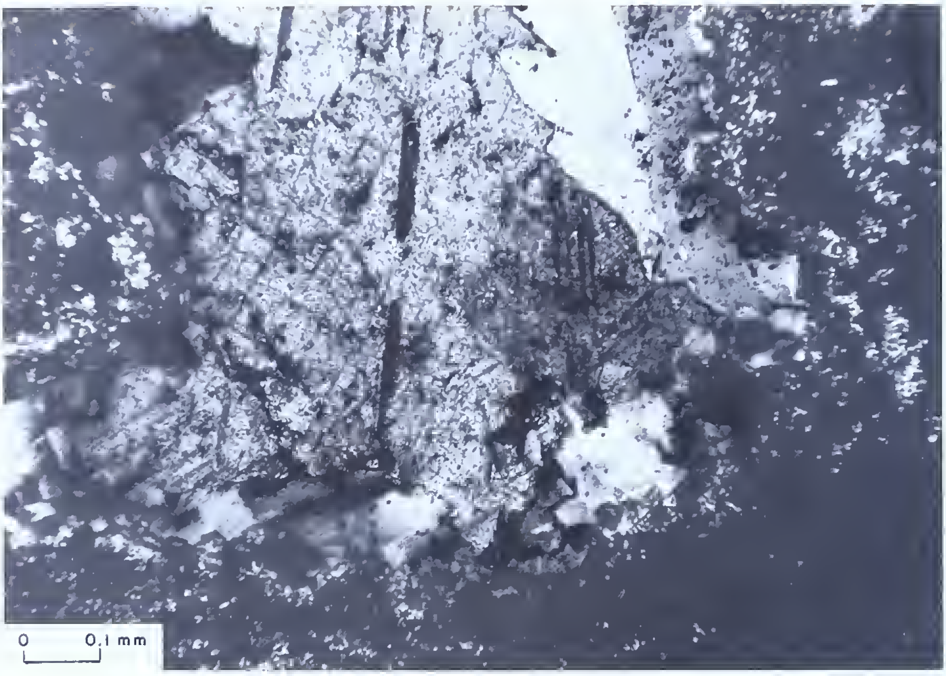

B. Vein of quartz, calcite, plagioclase (untwinned) and minor diopside (twinned) and tremolite partly transverse and partly aprallel to banding. Banding (or foliation) is parallel to long dimension of photograph; crossed nicols.

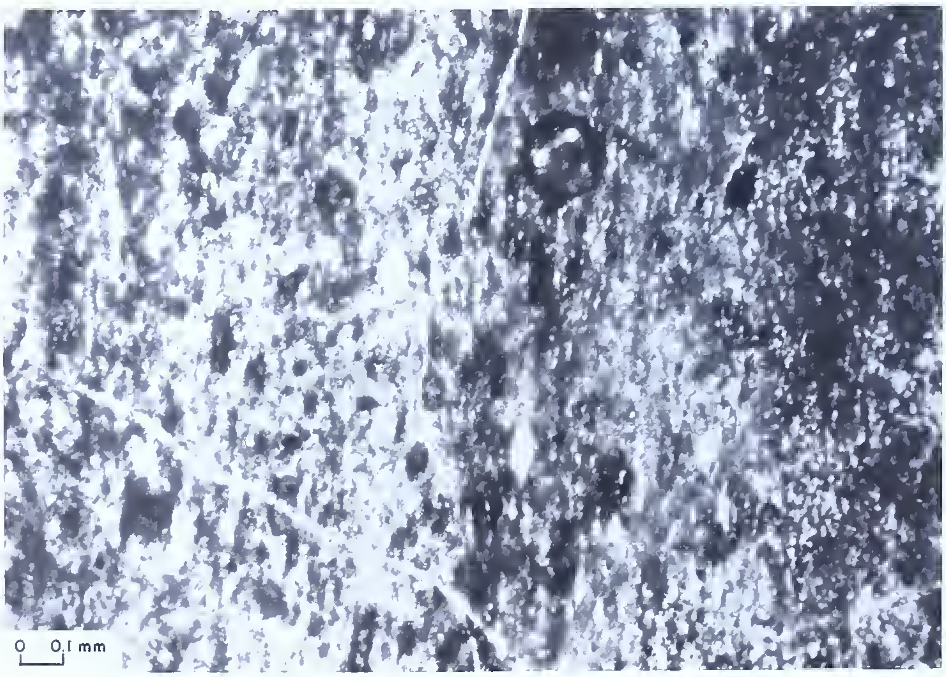

C. Typically banded limy Mill Hill Slate with coarse-grained diopside and fine-grained plagioclase; crossed nicols.

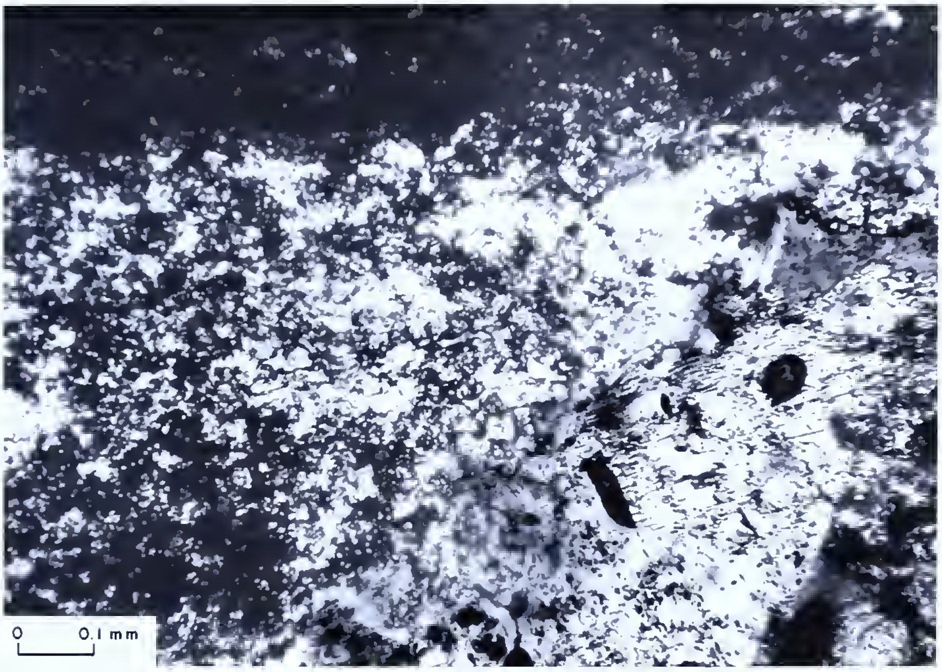

D. Banded limy Mill Hill Slate with low temperature metasomatic knot of calcite and zeolites (for discussion of matrix, see text); crossed nicols.

PLATE 5. INCLUSIONS IN DIABASE

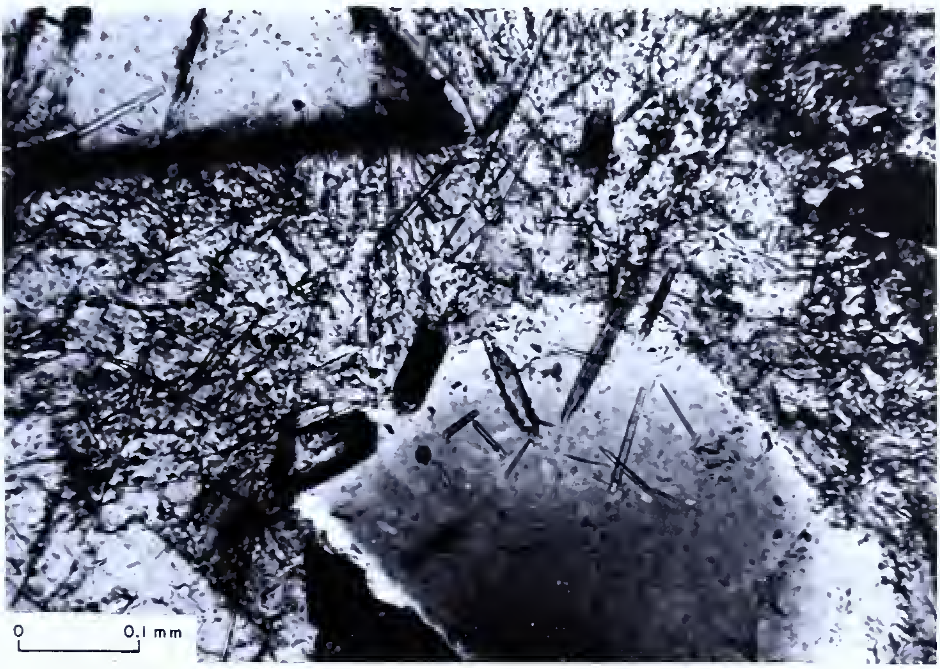

A. Partly assimilated and metamorphosed limestone inclusion with tremolite needles, potassic feldspar, micropegmatite (upper right); plane-polarized light.

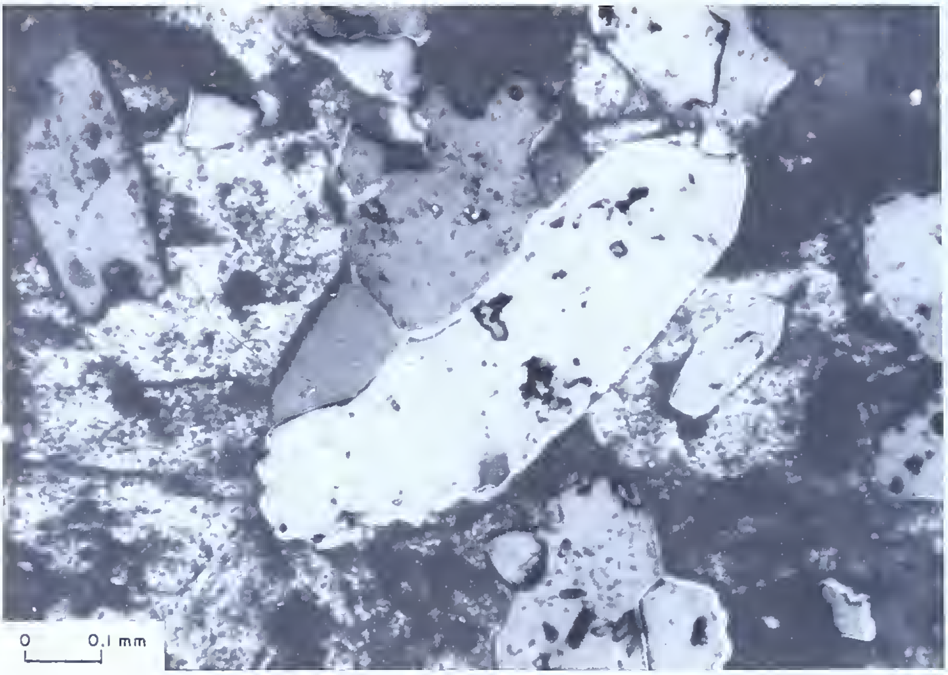

B. Contact of Blue Conglomerate inclusion with diabase illustrating recrystallized quartz (white) with microcline (dark gray) and altered plagioclase; crossed nicols.

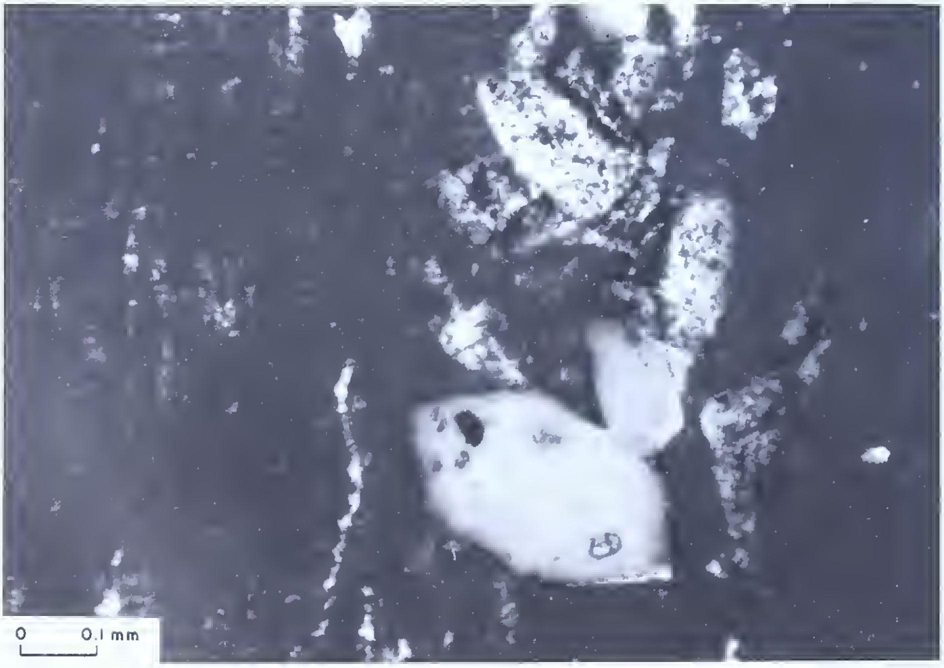

C. Same contact as above, illustrating recrystallization of quartz in microcline (dark); crossed nicols.

PLATE 6. LATE DEFORMATION IN THE ORE ZONE

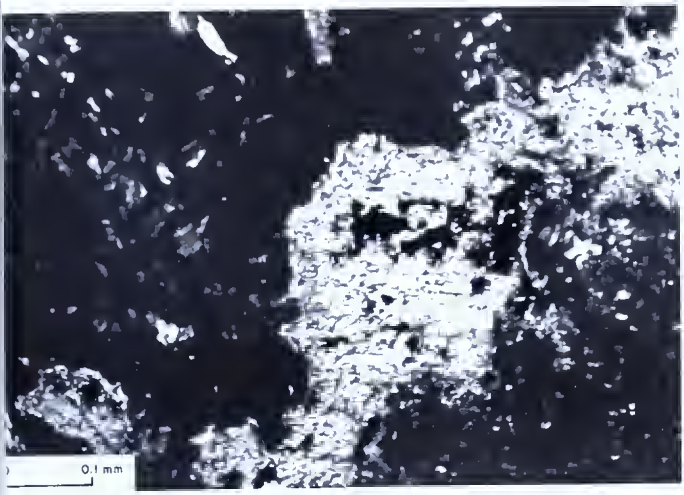

A. Vein of phlogopite replaced by late calcite in original host limestone. Deformation occurred after replacement; crossed nicols.

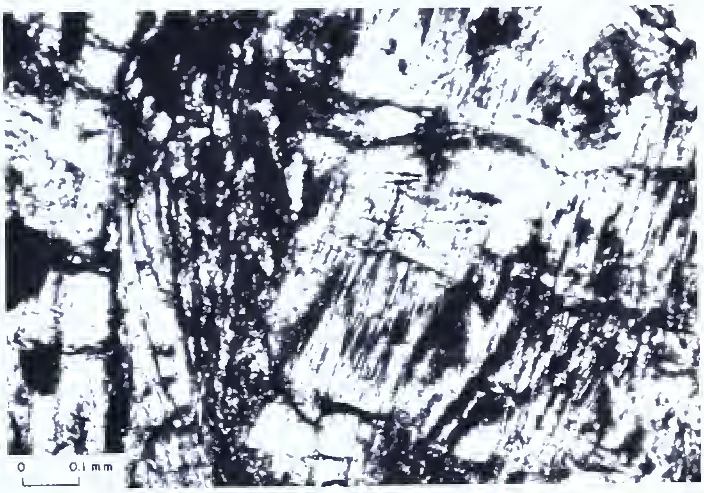

B. Magnetite (black) replacement of tremolite (light) followed by deformation of the tremolite cyrstals; plane-polarized light.

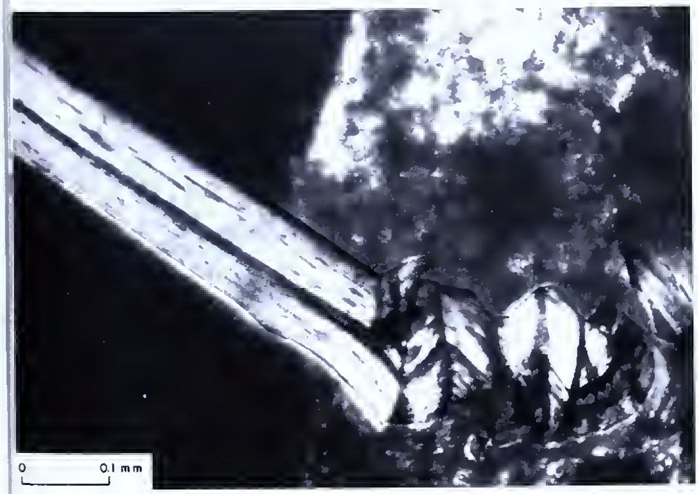

C. Muscovite crystal enveloped by pyrite (black). The envelopment protected the muscovite from late deformation in an actinolitic matrix; crossed nicols.

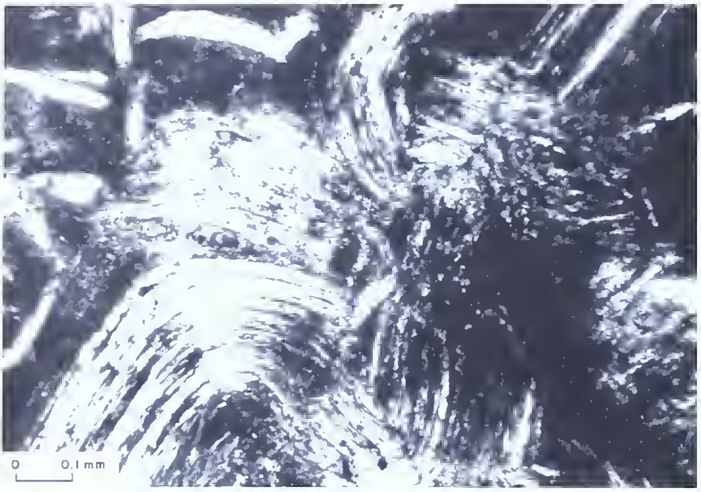

D. Deformation of actinolite after actinolite-magnetite ore stage deposition. Sample taken from part of eastern ore body near fa shown on diabase contour map (Pl 22); crossed nicols.

PLATE 7. POLISHED SECTION PETROGRAPHY: PARAGENESIS

A. Magnetite (gray) replaces early, fractured pyrite (white).

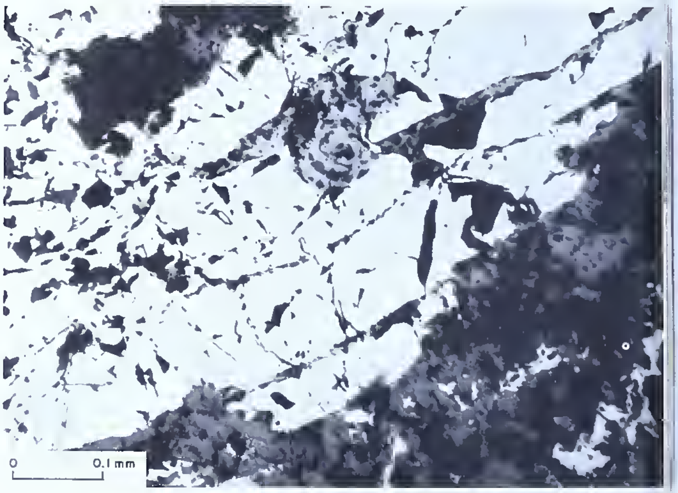

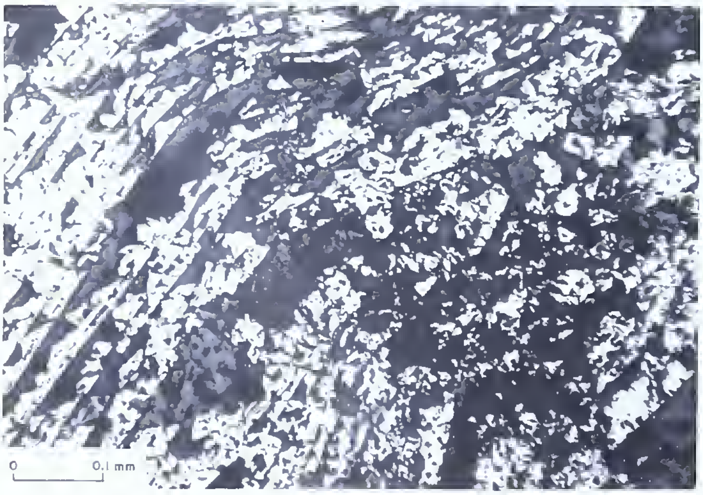

B. Platy magnetite replacement original hematite, later folded ar faulted. Gangue of actinolite (blac replaced magnetite before foldin Sample from ore hanging wall.

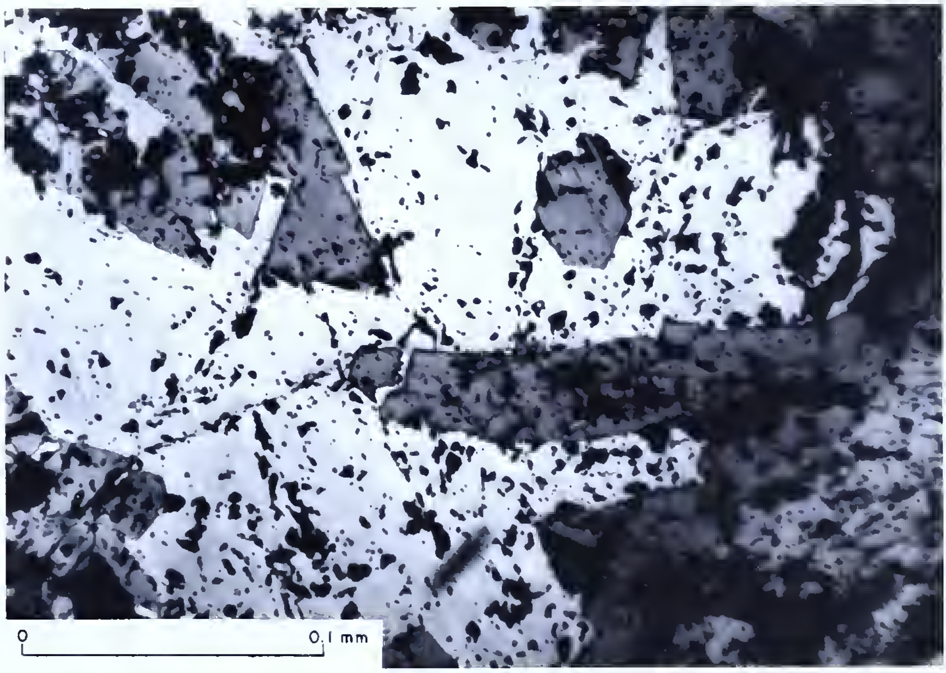

C. Chalcopyrite (gray) replacing magnetite (white) along (111) crystal planes of magnetite.

PLATE 8. POLISHED SECTION PETROGRAPHY: PARAGENESIS

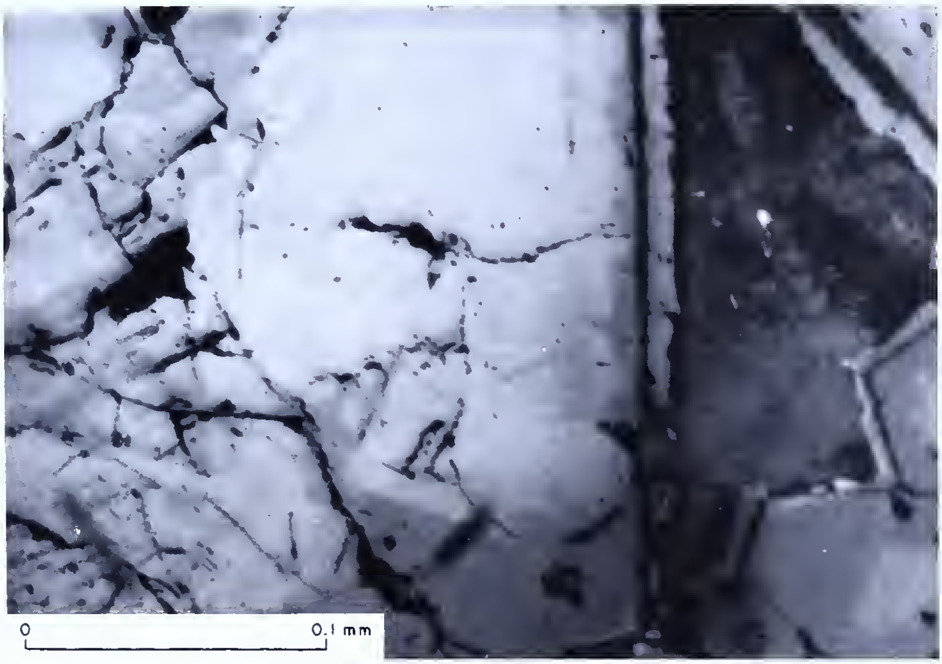

A. Illustration of two generations of magnetite. Darker gray, younger magnetite in lower right-to-left with core of lighter gray, older magnetite (see Davidson and Wyllie, 1965). Darkest gray is mixed gangue and magnetite.

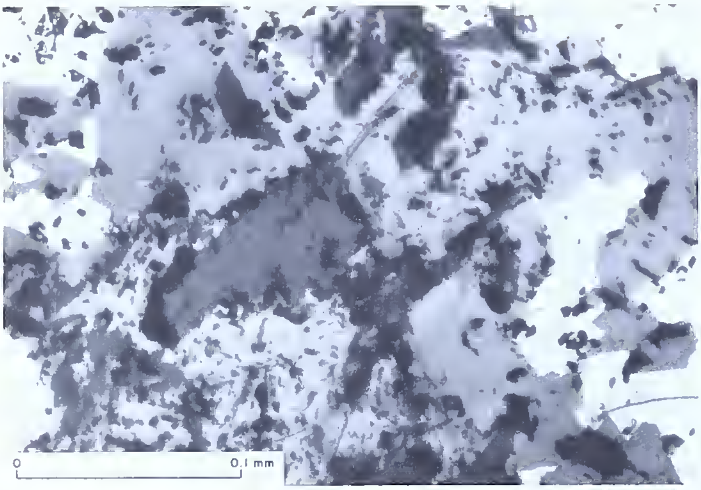

B. Sphalerite (light gray) replac chalcopyrite. Gangue is dark gra and black.

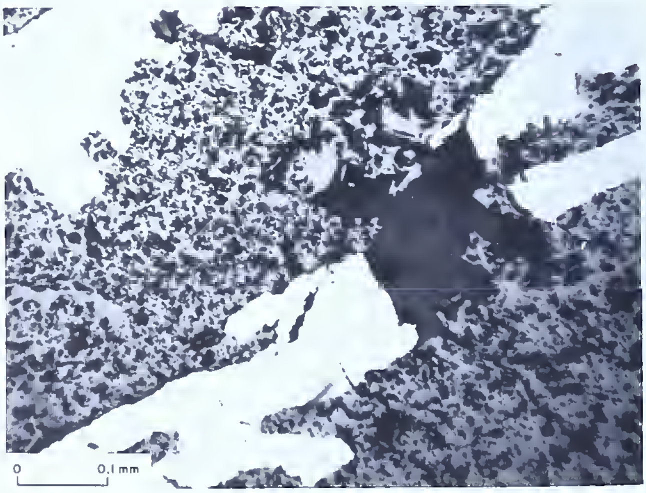

C. Pyrite vein (gray) replaces magnetite (white). Pyrite cuts magnetite vein and transects foliation. Sample is from the southwestern footwall of the eastern ore body. Compare with Plate 7-A where magnetite replaces pyrite.

PLATE 9. ORE REPLACEMENT, OF DIFFERENT ROCK TYPES

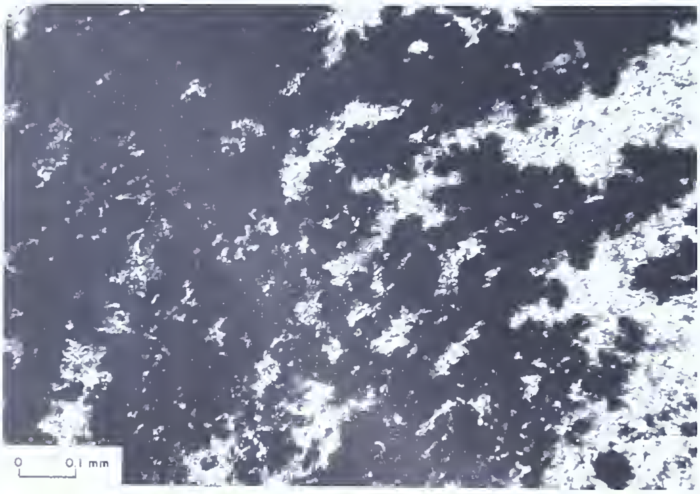

A. Magnetite (black) replacement o folded, limy Mill Hill Slate; plane polarized light.

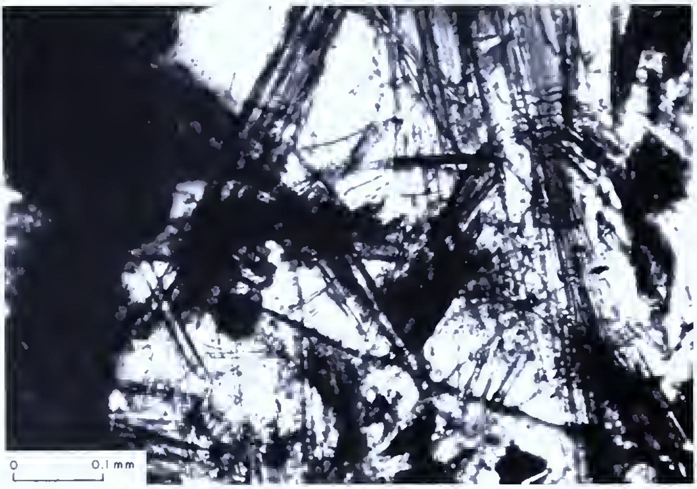

. Magnetite (black) replacement of metamorphosed Blue Conglomerate (from eastern ore body) containing actinolite blades with quartz and potassic feldspar; plane-polarized light.

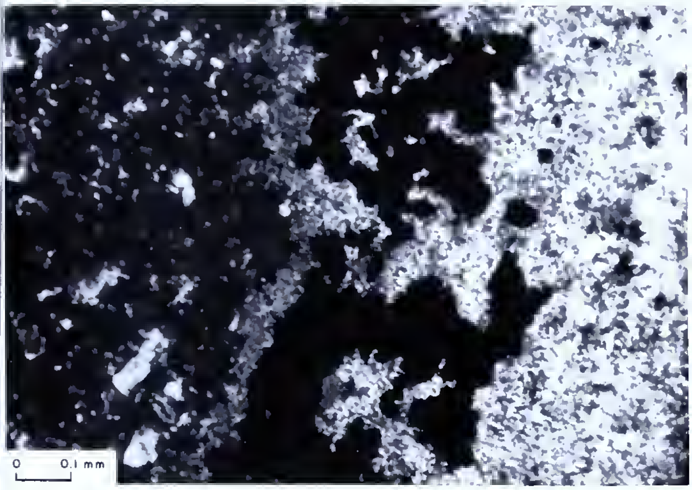

C. Magnetite replacement of foliated dolomitic limestone (Buffalo Springs Formation) from hanging wall of western ore body. Massive magnetite in center is replacing calcite. To left, small grains of magnetite with calc-silicates have replaced dolomite. Photograph illustrates compositional control upon replacement; plane-polarized light.

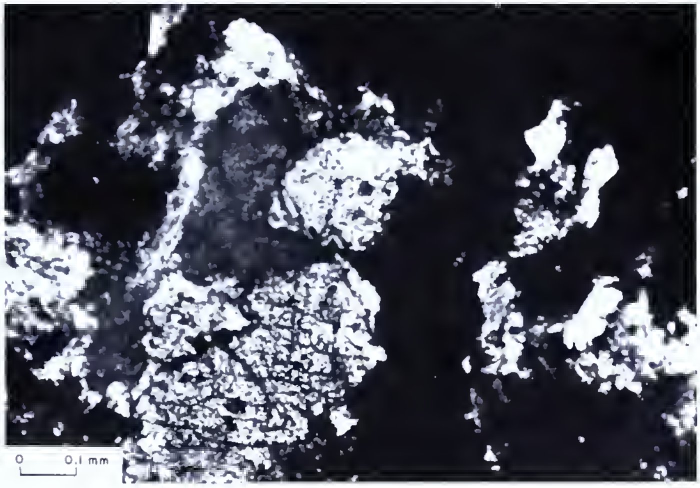

D. Magnetite replacement of amphibolitized (gray) clinopyroxene in diabase near southwestern footwall of eastern ore body; plane-polarized light.

PLATE 10. MAGNETITE REPLACEMENT TEXTURES

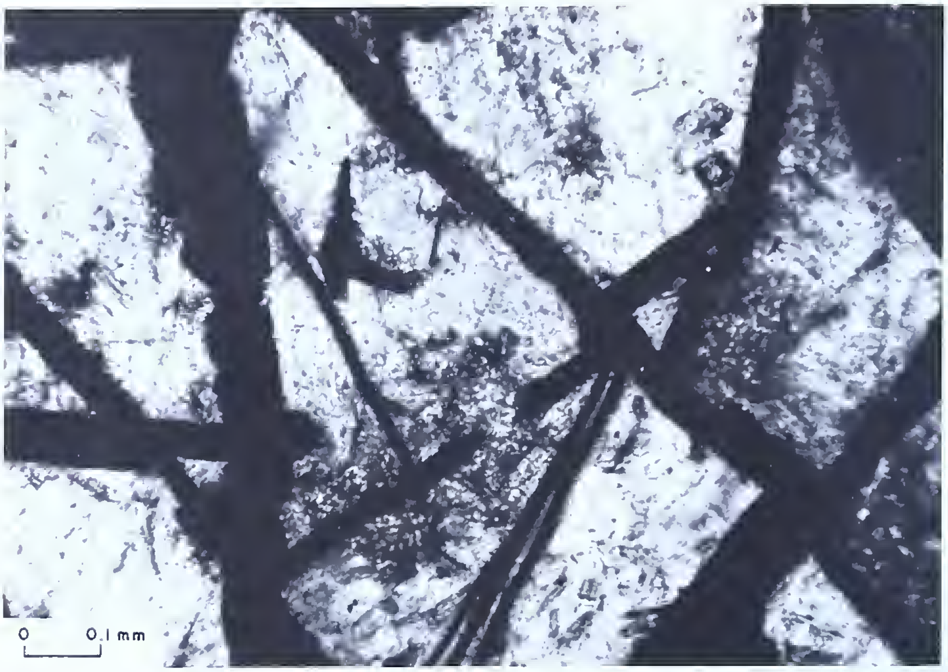

A. Hematite blades, now partially to completely altered to magnetite, in recrystallized calcite of host limestone; hanging wall of eastern ore body; plane-polarized light.

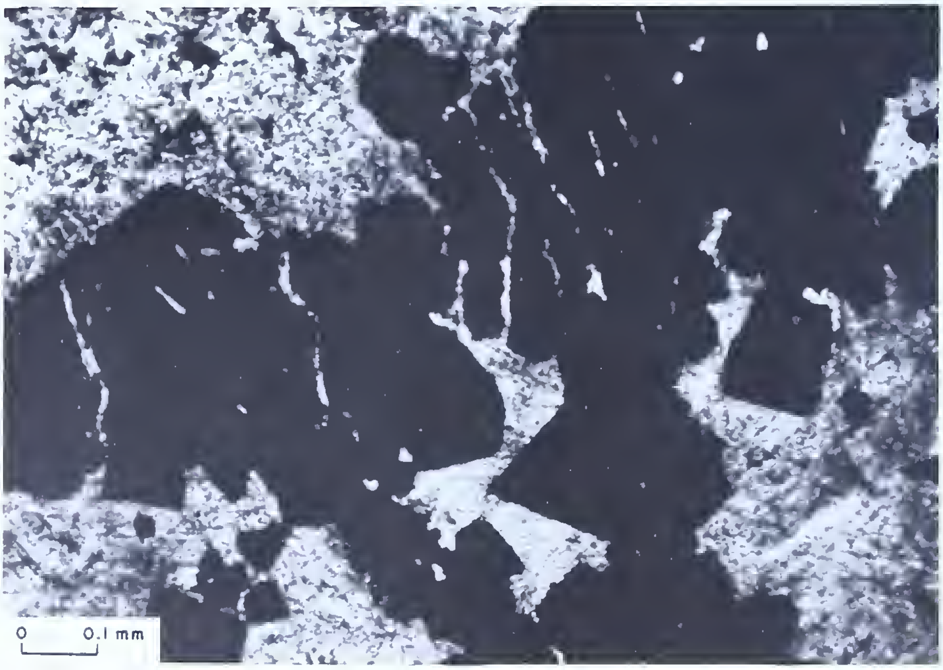

B. Calcite (grayish-white) partly enveloped by magnetite (black) in a groundmass of actinolite (fine-grained; gray). Magnetite is euhedral toward calcite and anhedral toward actinolite, both of which it replaces; from near footwall of south-central eastern ore body; plane-polarized light.

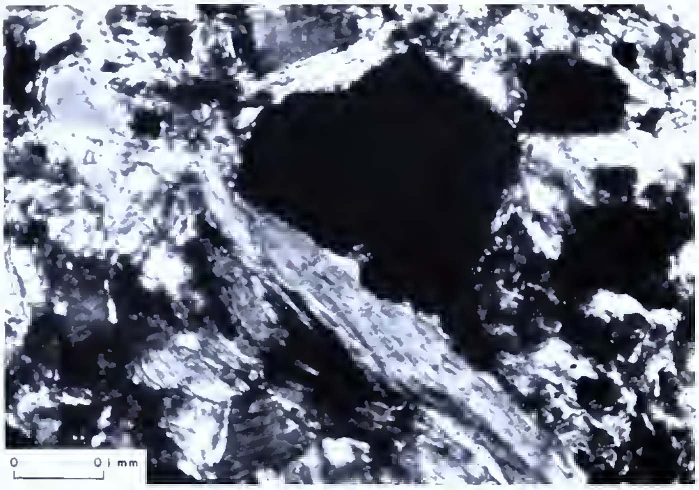

C. Magnetite (black) showing only slight replacement across the cleavage of a large muscovite lath. More replacement occurs parallel to (001) cleavage and where mica grains are smaller. Black squares are pyrite crystals; crossed nicols.

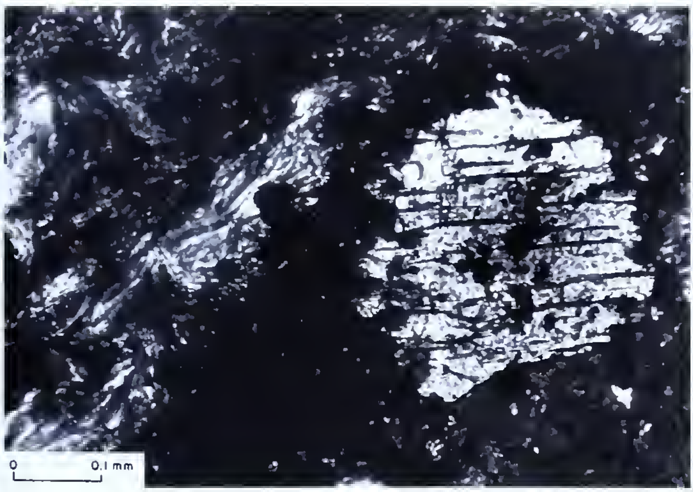

D. Magnetite penecontemporaneous with actinolite and chlorite groundmass; large diopside crystal illustrates difficulty of magnetite replacement of diopside; crossed nicols.

PLATE 11. MAGNETITE-GANGUE PARAGENETIC RELATIONSHIPS

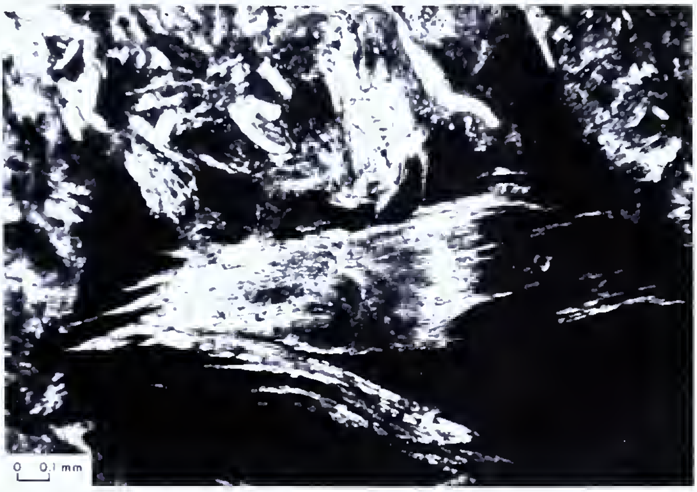

A. Magnetite has replaced coarse actinolite preferentially parallel to amphibole cleavage. Groundmass of finer actinolite is younger than magnetite; from southwestern footwall of eastern ore body; compare paragenesis with Plate 10-B and 10-D; plane-polarized light.

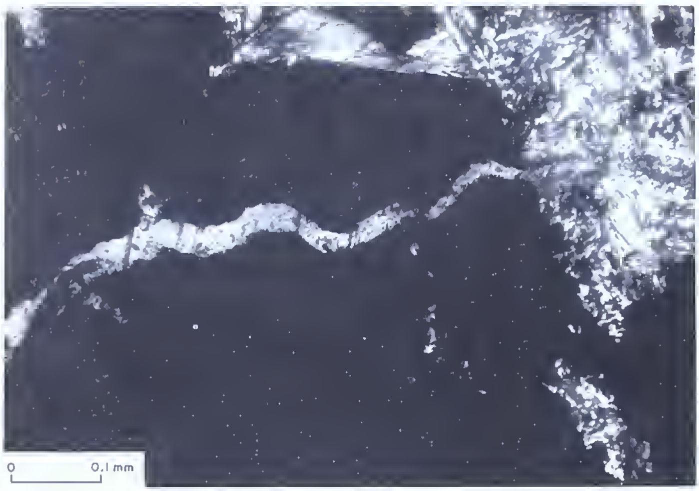

B. Magnetite pull-apart fracture fill by secondary calcite. Calcite fractu filling has been cut off by replac ment of late, fine-grained actinoli groundmass. Compare paragenes of magnetite-actinolite with Pla 10-B, 10-D, and 11-A. Note lack disturbance of the fractured ma netite and that deformation stresses, on a local scale, accom panied ore stage mineralizatio crossed nicols.

C. Metasomatic plagioclase in Blue Conglomerate deformed during (?) growth and then replaced by magnetite preferentially along twin plane boundaries. Plagioclase is slightly sericitized; crossed nicols.

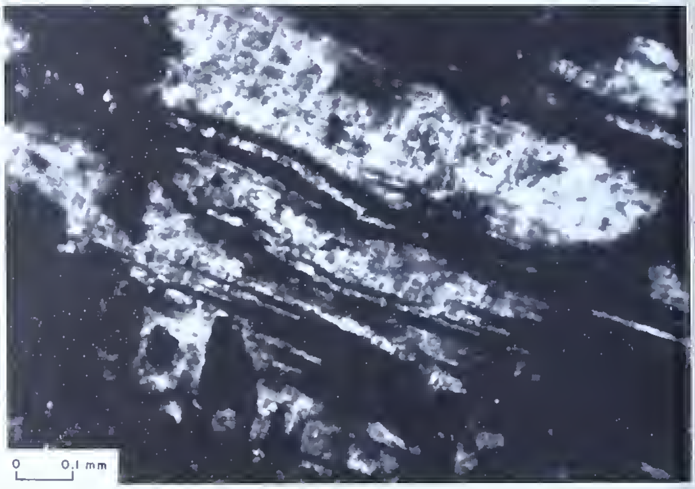

PLATE 12. PHENOCRYSTS AND CHILLED MARGIN TEXTURES OF DIABASE

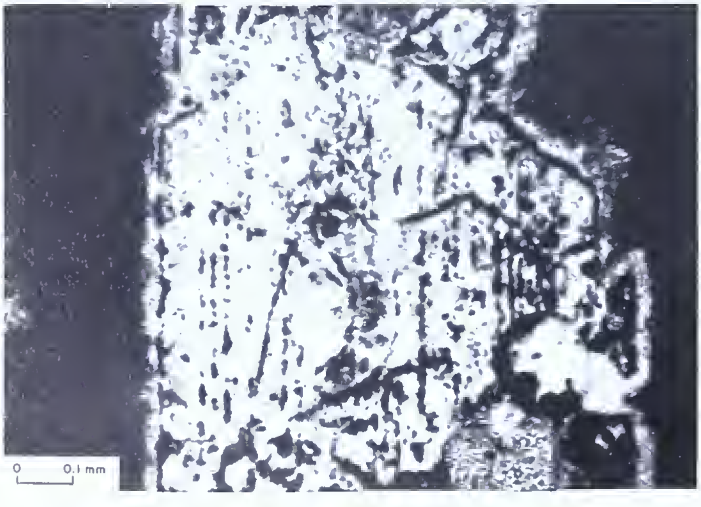

A. Orthopyroxene phenocryst now partially amphibolitized. Magnetite exsolution appears to have occurred as a result of the alteration process, crystallographically controlled. Groundmass contains a heavy concentration of a "dusted" opaque mineral, probably magnetite. Pyroxenes are rare in the Cornwall chilled margin; plane-polarized light.

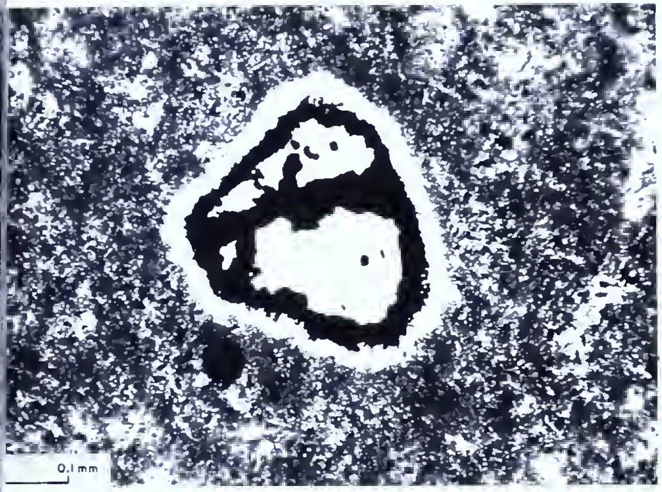

B. Amphibolitized olivine phenocryst. Groundmass is dusted with magnetite but the dusting has been cleared around the phenocryst, probably during amphibolitization. The magnetite rim here may be the result of at least two processes: exsolved Fe induced by amphibolitization and groundmass clearing; however, it is not a universal characteristic of the chilled margin (see text); plane-polarized light.

Amphibolitized olivine phenocryst with rim of magnetite. The volume of magnetite and lack of "dust" clearing of groundmass opaques suggest either variable Fe composition of original olivine or Fe introduction (see text and Plates 12-B,1) and 13-B). Plagioclase laths (white) do not contain magnetite. This is a typical margin texture; plane-polarized light.

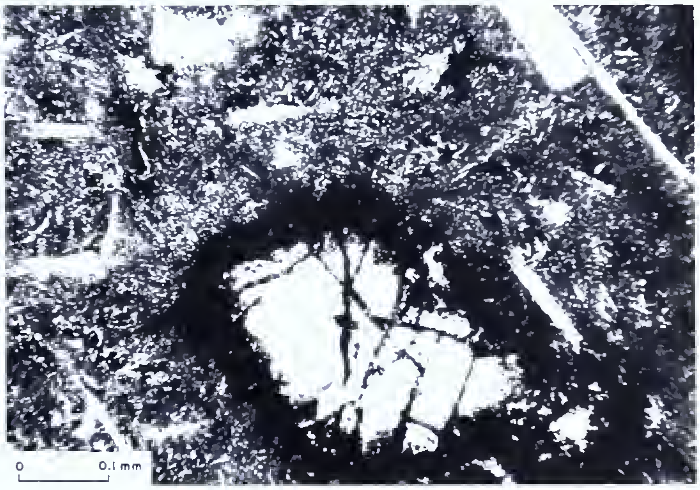

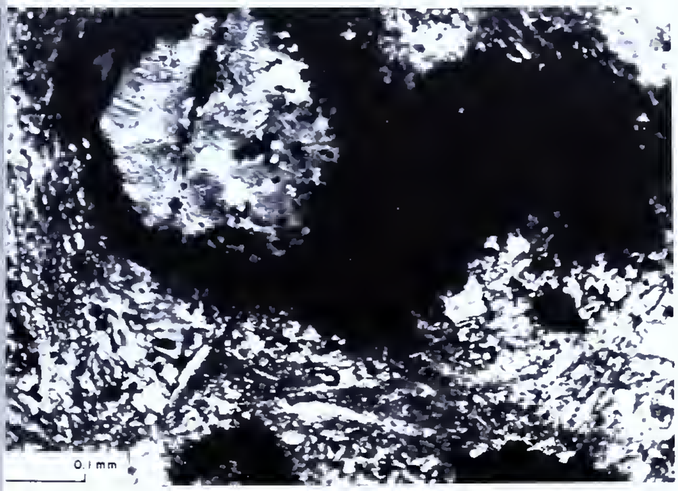

D. Amphibolitized olivine phenocryst with introduced magnetite preferentially crystallized around the coarse phenocryst (see text). Sample taken from south-western footwall of eastern ore body and is from the same thin section as Plate 12-B; plane-polarized light.

PLATE 13. TEXTURES AND REPLACEMENT OF DIABASE CHILLED MARGIN

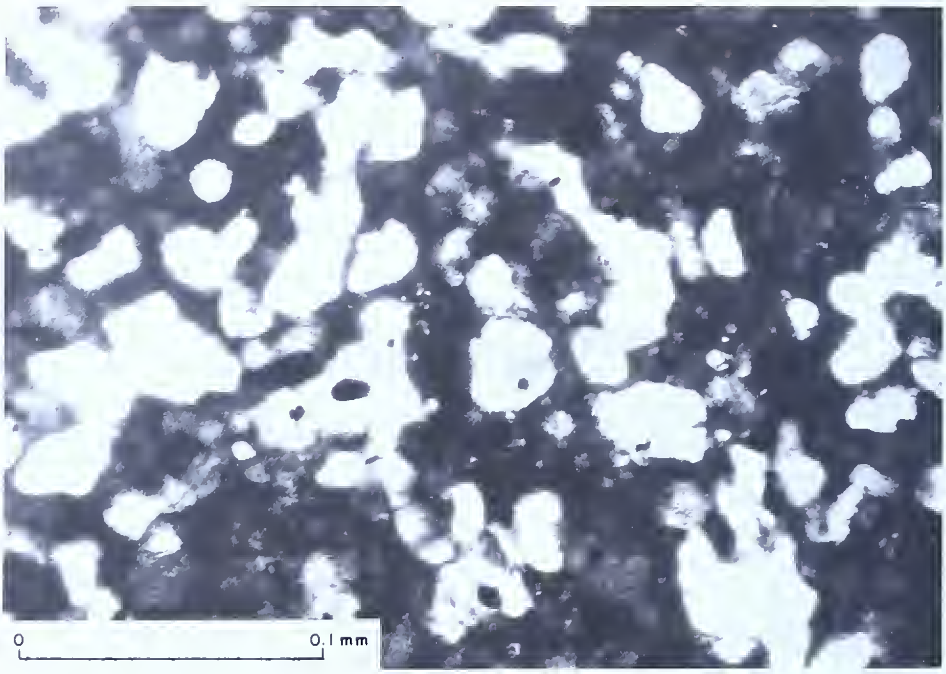

A. Top of chilled margin sketched in detail in Figure 35. Black areas are nearly all isotropic glass. White areas are pigeonite with minor untwinned plagioclase. Texture is micro-porphyritic. Such interstitial glass is rare in the chilled diabase below the eastern ore body and does not extend beyond a few millimeters from the top; crossed nicols.

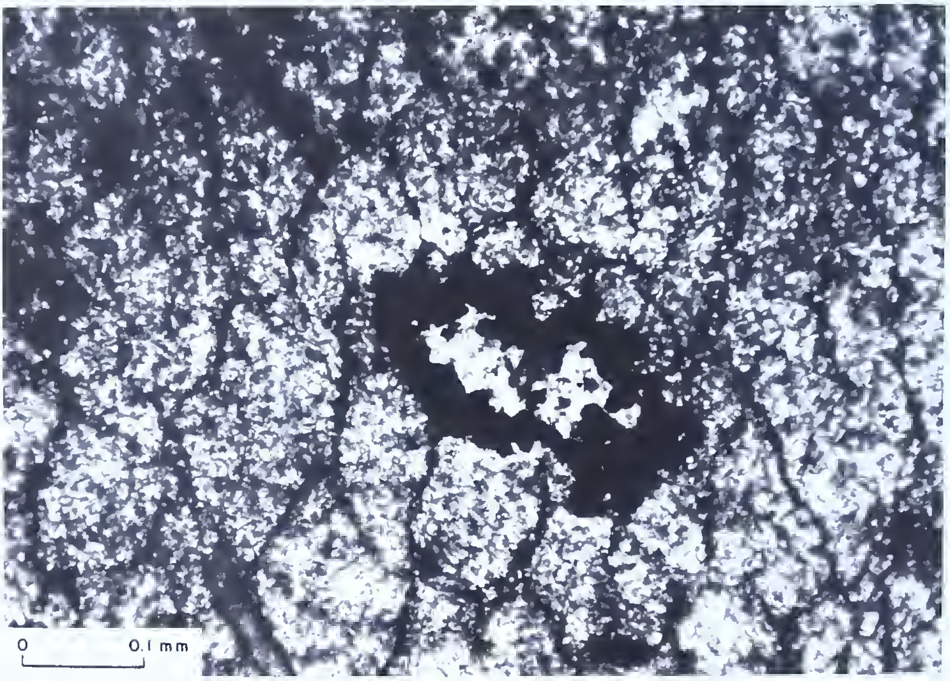

B. Polygonal contraction cracks along top surface of diabase sheet; amphibolitized olivine phenocryst with secondary magnetite in center (see text and Plate 12); plane-polarized light.

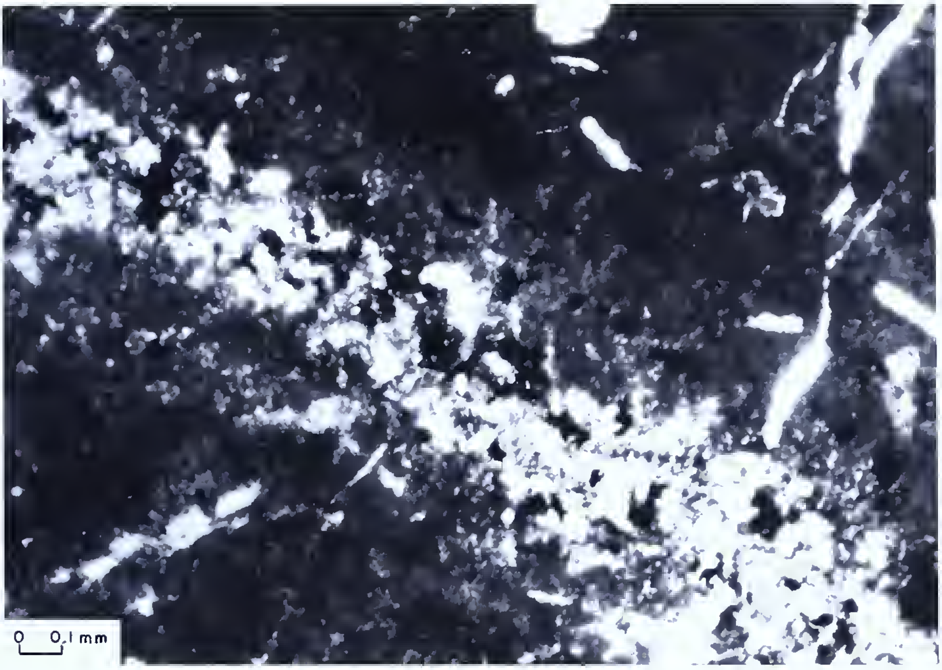

C. Contraction crack approximately perpendicular to top of diabase and filled with metamorphic diopside, some magnetite, and chlorite. Note heavy clouding of groundmass which is characteristic near contraction fracture fillings. Clear laths in groundmass are plagioclase, usually untwinned (see text); plane-polarized light.

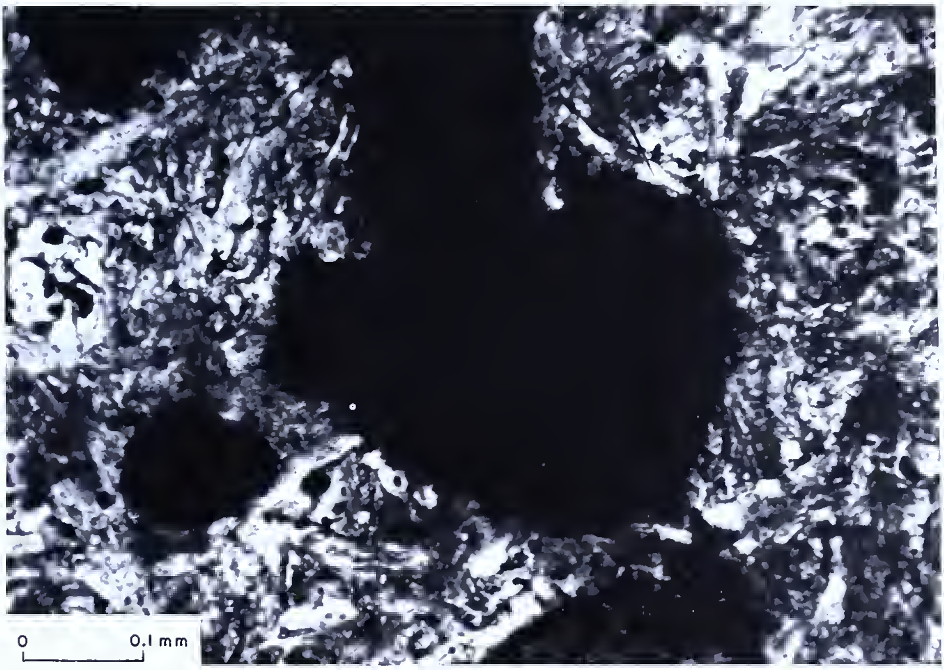

D. Chilled margin of diabase replaced by massive ore magnetite. Sample is from southwestern area of eastern ore body. White laths are plagioclase; less rectangular grains are pigeonite. Plane-polarized light. Same section as Plate 12-B and D where magnetite introduction associated with phenocrysts has been suggested.

PLATE 14. PLAGIOCLASE PARAGENESIS AND ZONING IN DIABASE

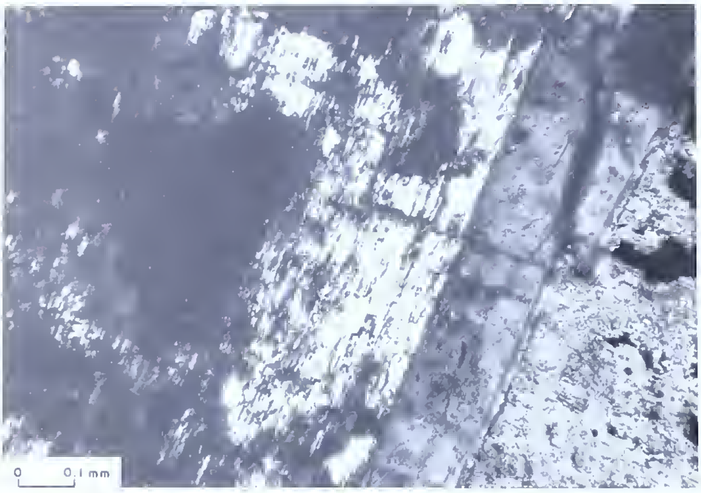

A. Two generations of plagioclase
diabase pegmatite. Earlier, m
clacic plagioclase is highly alte
(sericitized) whereas later rim plag
clase, more sodic, is unaltered (gr
Multiple generations of plagiocl
in diabase pegmatite are comm
(see Figure 45); crossed nicols.

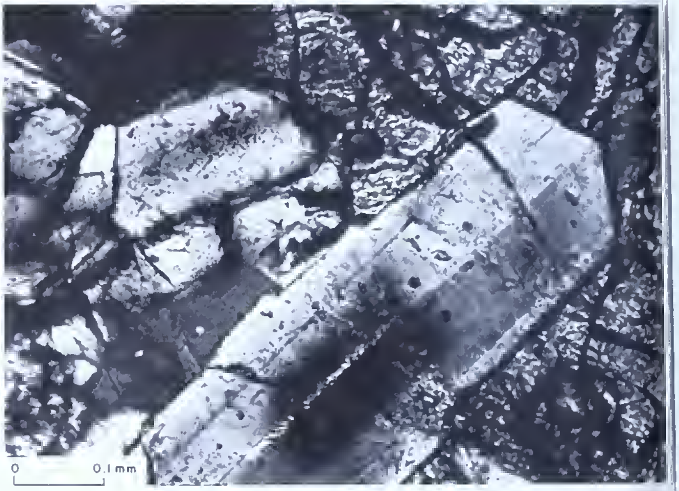

B. Zoned plagioclase with continuous Carlsbad plus abite twins; pyroxenes (pigeonite, hypersthene) in this section also show considerable exsolution (see Plate 16-D); crossed nicols.

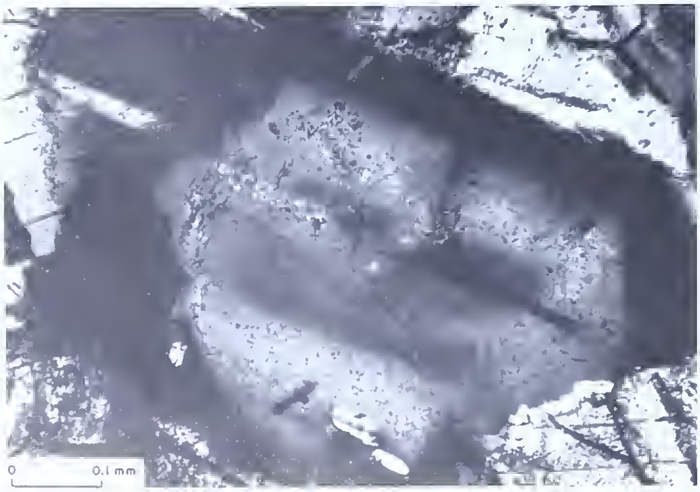

C. Zoned plagioclase with variabl
high-calcic core and sodic (at extin
tion) rim. Section also contains clin
hypersthene and is from basal thi
of sheet (see Table 23); crosse
nicols.

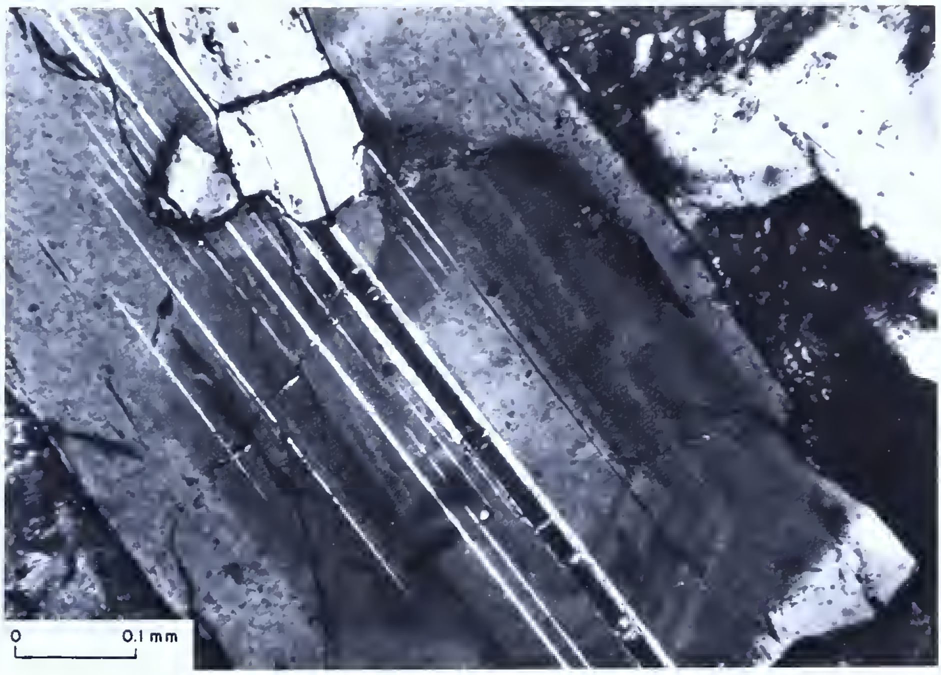

D. Oscillatory zoned plagioclase; from same section as above; crossed nicols.

PLATE 15. ORTHOPYROXENE AND ORTHOPYROXENE-CLINOPYROXENE RELATIONSHIPS IN DIABASE

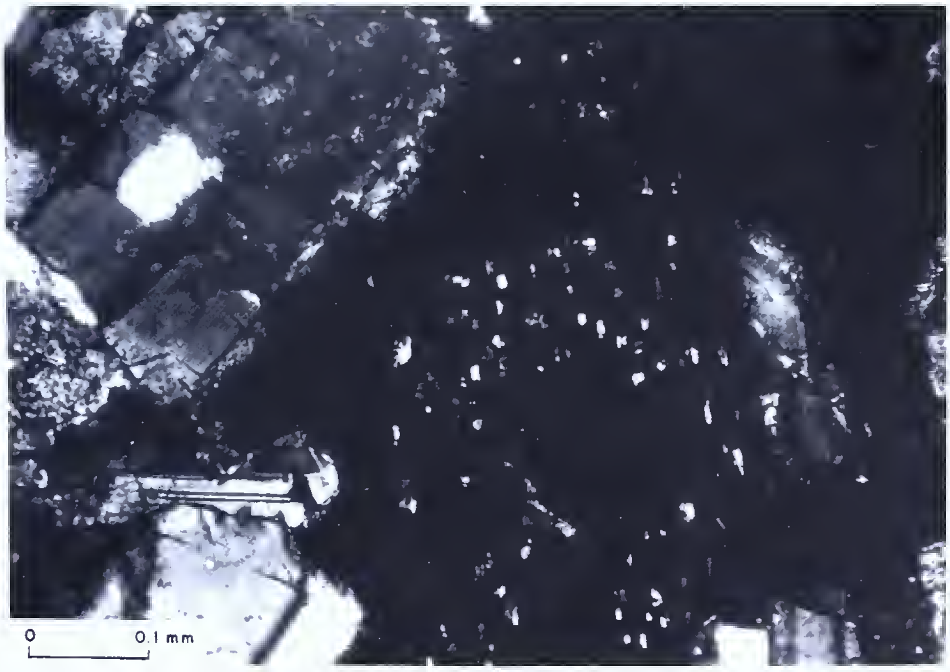

A. Hypersthene at extinction (black) with small clinopyroxene exsoltuion rods (white spots). The exsolution distribution suggests a core of different composition; crossed nicols.

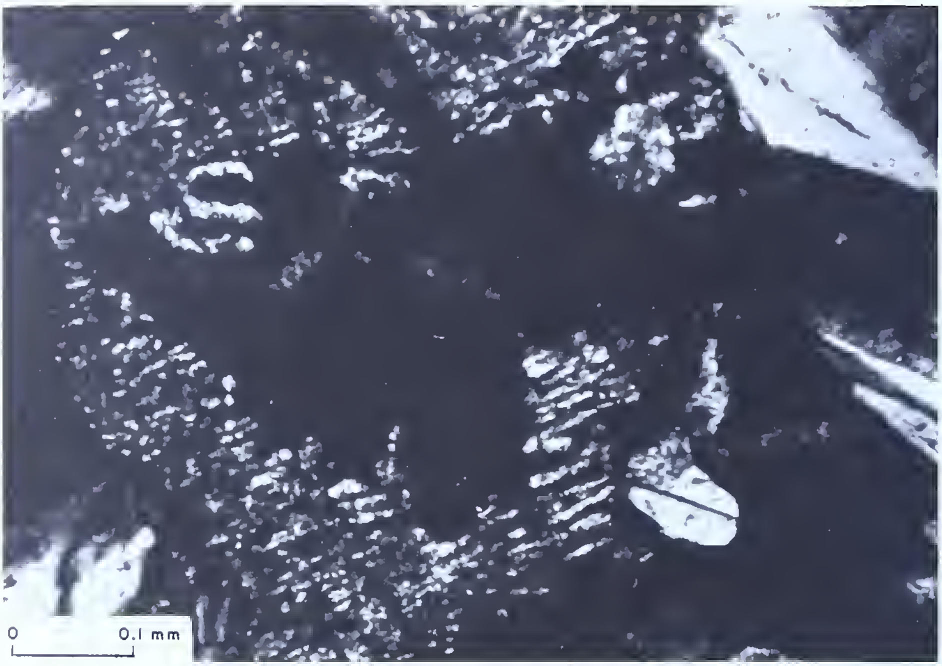

B. Hypersthene at extinction (black) with rod-like oriented inclusions around grain periphery. This section contains alteration by sericitization and amphibolitization. Such rim exsolution appears to be more common where these later effects are notable. Exsolved material is highly birefringent under high magnification so that the clinopyroxene probably is augite. Augite (gray-black) is present in contact with the hypersthene (lower right); crossed nicols.

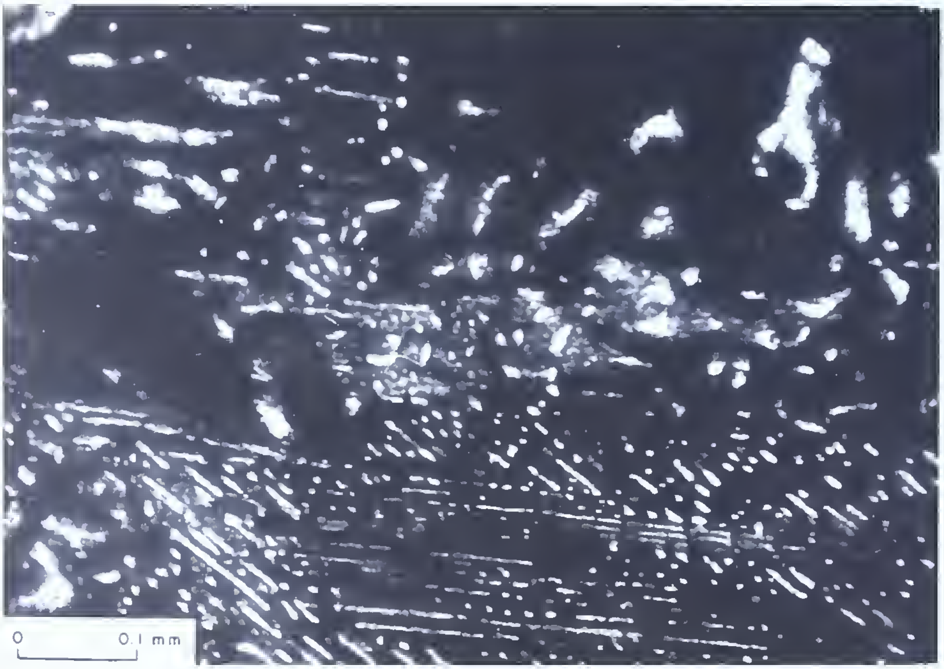

C. Amphibole at extinction with oriented rods of augite exsolution. The original orthopyroxene (?) has been altered completely but the more resistant augite exsolution has remained unaltered. Note excellent crystallographic control on exsolution orientation; crossed nicols.

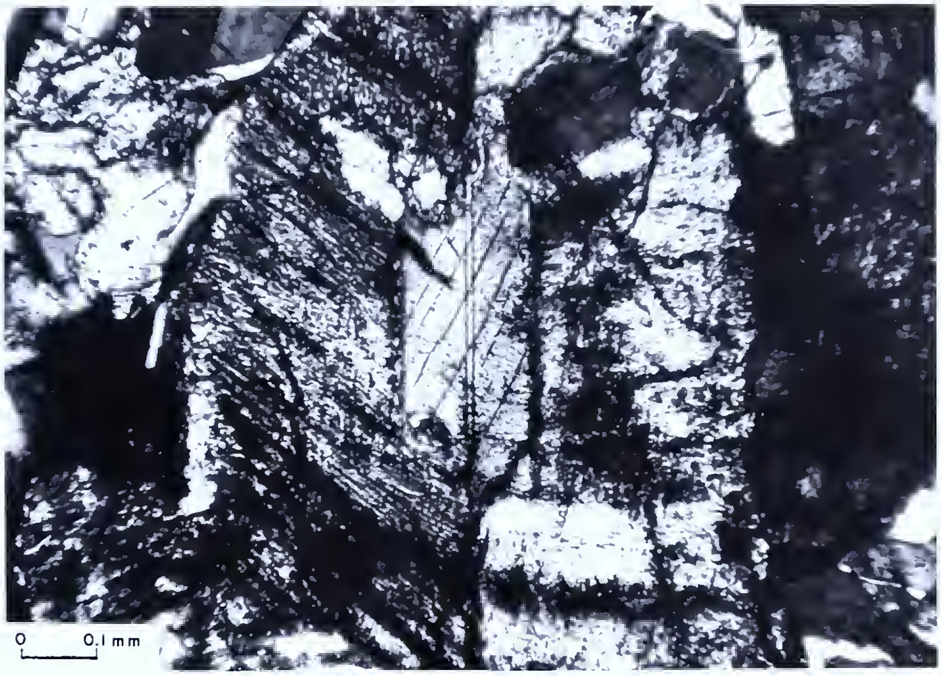

D. Twinned hypersthene (late) with pigeonite core. There is no direct evidence of inversion (see text). The diabase here is transitional between normal and pegmatitic diabase (where large hypersthene crystals are common); crossed nicols.

PLATE 16. CLINOPYROXENE-CLINOHYPERSTHENE HYTERSTHENE RELATIONSHIPS IN DIABASE

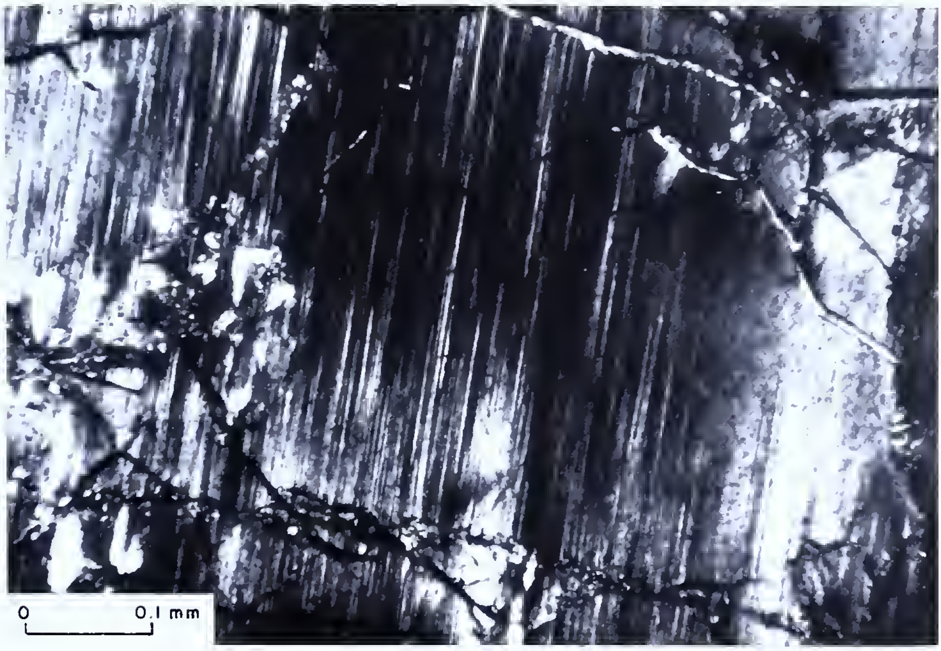

A. Clinohypersthene with an extinction angle of 9° (see text) at extinction in hypersthene (inverted pigeonite?). Although patchy areas of clinohypersthene in hypersthene are common, the lamellar development of clinohypersthene shows that this transition is crystallographically oriented as well as petrologically controlled (see Table 22, text, and Boyd and Brown, 1969, p. 212). Section illustrated is the same as Plate 15-D; crossed nicols.

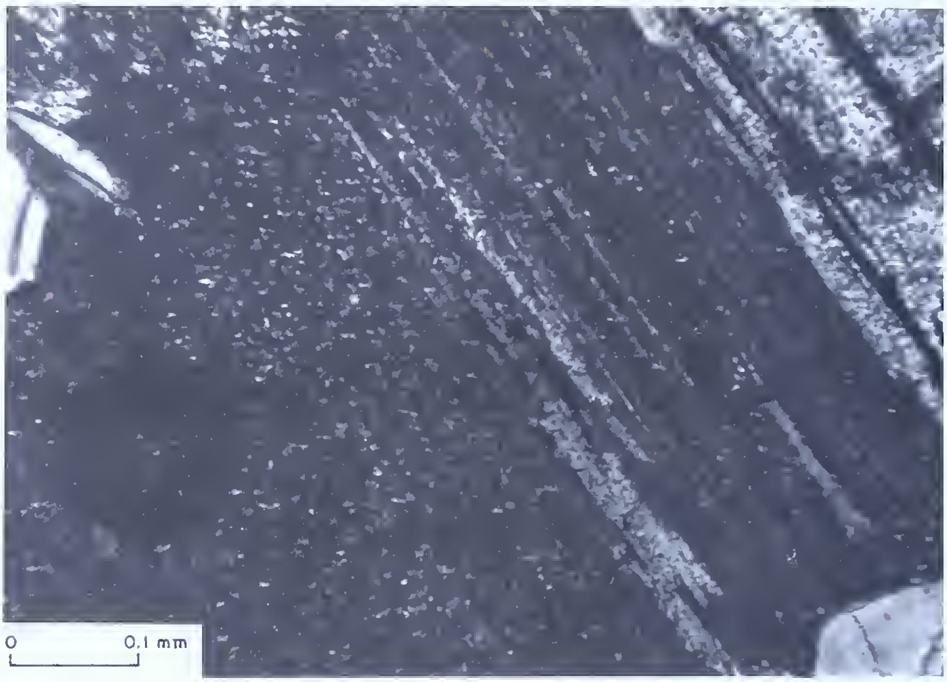

B. Further development of clinohypersthene with 15 extinction angle (dark at extinction; i.e., camera rotated about 20 ; in hypersthene (inverted pigeonite?) which is somewhat more typical than in Plate 16-A. Both pyroxenes are slightly altered (augite is distinguished, among other characteristics, by a lack of alteration). Photograph is from a section containing zoned plagioclase (Plate 14-C); crossed nicols.

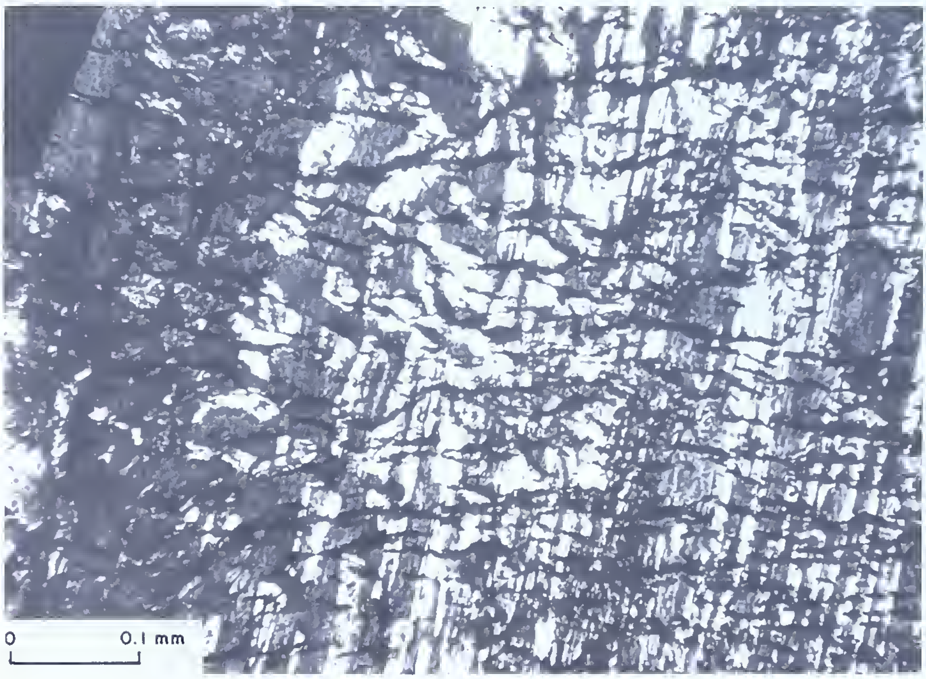

C. Irregular, deformed coarse exsolution lamellae in hypersthene. This feature is rare in the Cornwall diabse. From top third sheet in section containing zoned plagioclase (see Table 23); crossed nicols.

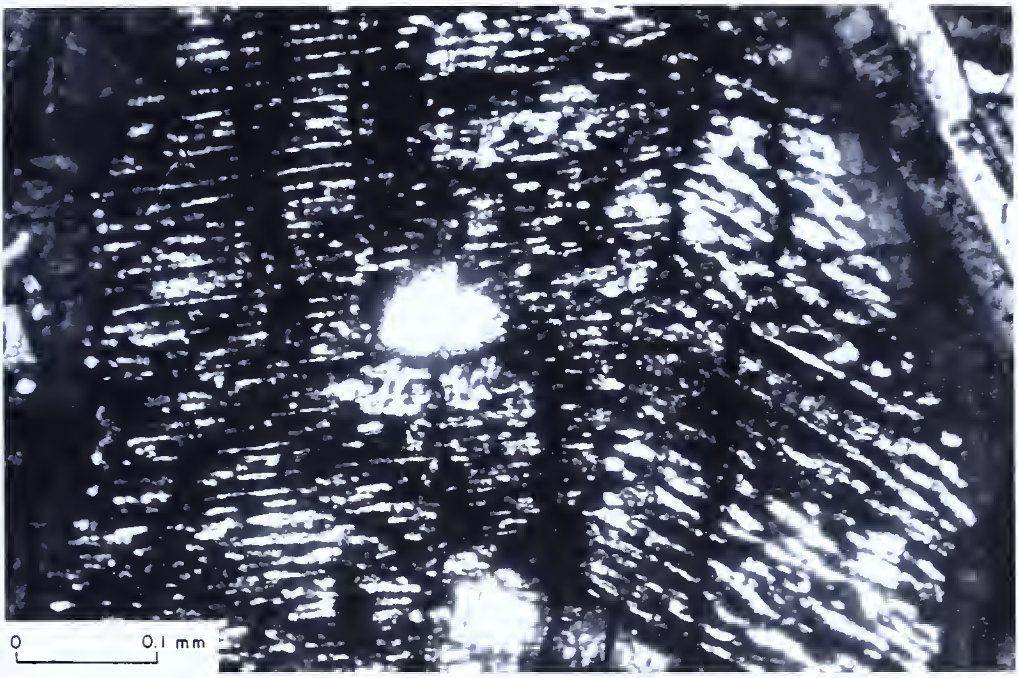

D. Herringbone twin in hypersthene (inverted?) with pigeonite cores along twin boundary. Coarse exsolution rods are augite. Hypersthene (ferriferous?) has been altered, partly to an iron oxide, and is not optically identifiable. Section is transitional between normal and pegmatitic diabase and is from the section illustrated in Plates 14-B and 17-C; crossed nicols.

PLATE 17. EXSOLUTION AND ALTERATION TEXTURES OF CLINOPYROXENES IN DIABASE

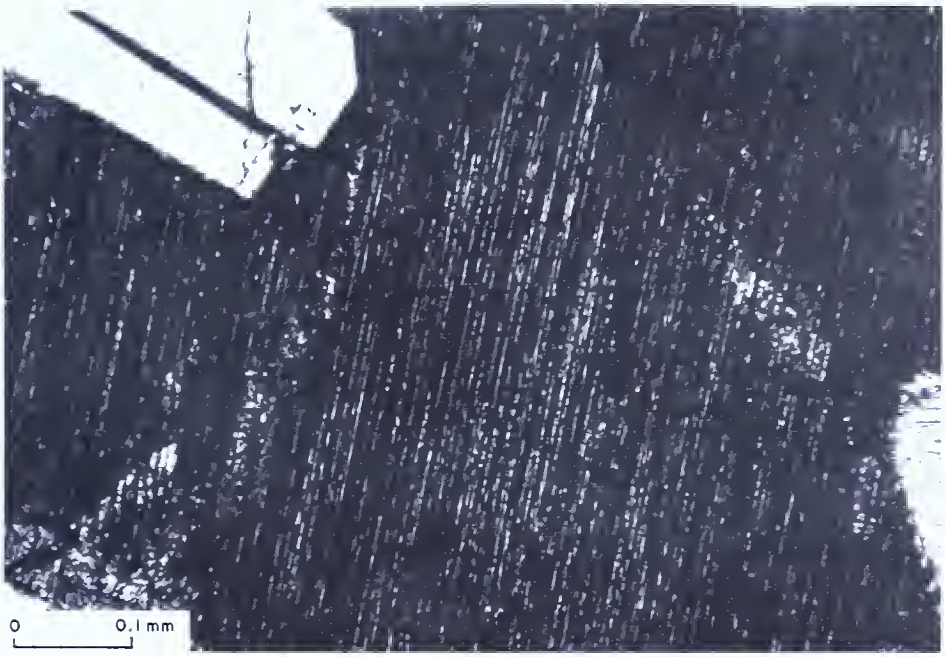

A. Very fine augite exsolution lamellae in pigeonite intergrown with augite crystal (light gray). Camera turned so that parallel extinction is not top to bottom of photograph; crossed nicols.

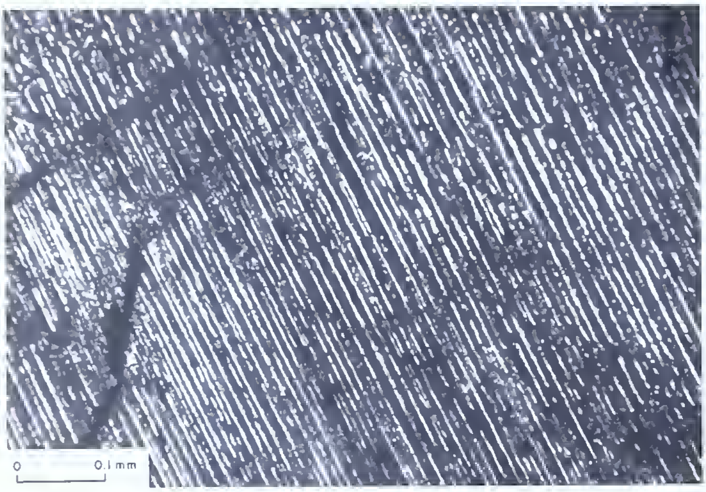

B. Fine augite exsolution lamellae i
pigeonite, slightly coarser than i
Plate 17-A. Small spots may b
exsolution rods or lamellae at
high angle to the plane of th
photograph; crossed nicols.

C. Coarse augite exsolution only near rim of pigeonite (core is black). Distribution of exsolution suggests different pigeonite compositions, as the Ca/Mg ratio increased during crystallization. There is a lack of good crystallographic control on exsolution. Same section at Plates 14-B and 16-C and 20-B, all of which exhibit a changing and oscillatory local environment; crossed nicols.

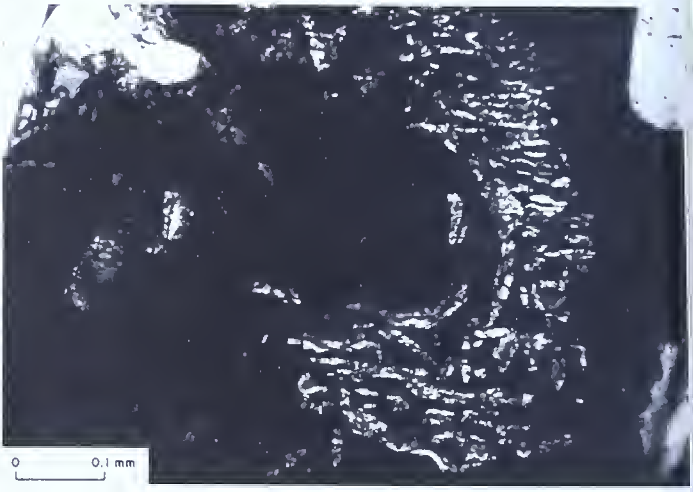

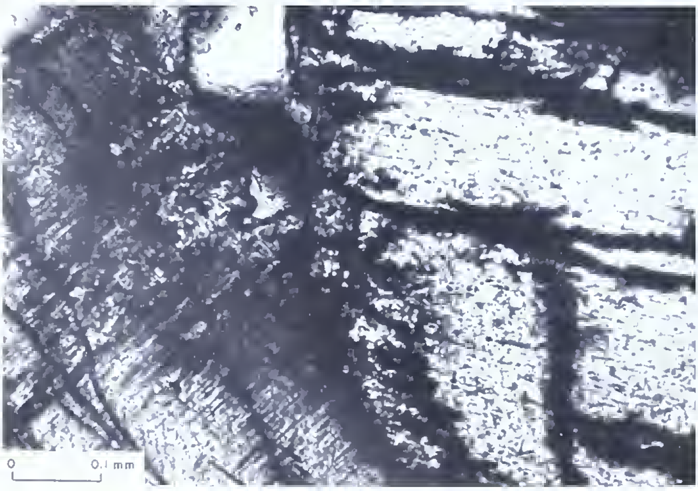

D. Preferential alteration of hypersthene (on left) by amphibole proceeding inward from boundary (with augite on right) along cleavage. Augite (lighter) exhibits only secondary iron oxidation along fractures and no alteration. The hypersthene probably preceeded augite and its alteration reflects the greater occurrence of amphibolitization of orthopyroxene in a late, more hydrous environment; crossed nicols.

PLATE 18. PETROGRAPHY OF DIABASE PEGMATITE AND GRANOPHYRE

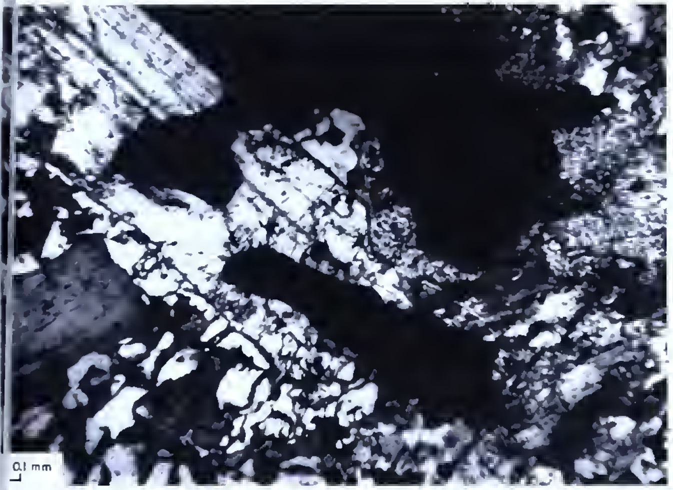

A. Typical diabase pegmatite with ilmenite (black) invading a moderately-sodic plagioclase. Some interstitial micropegmatite (upper right corner) is more characteristic of pegmatitic than normal diabase; crossed nicols.

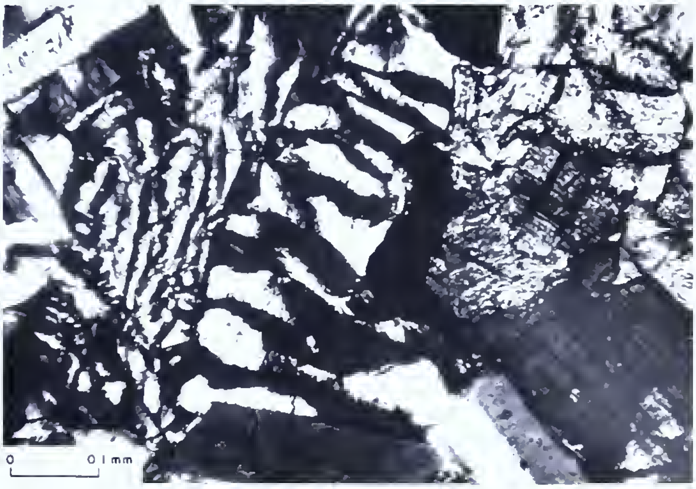

Zebra-like texture of micropegmatite in transitional pegmatite and normal diabase. Gray crystal in upper right is augite. Same section as Plates 14-B, 16-C, and 17-C, all of which show exsolution characteristic of diabase of this rather coarse grain size; crossed nicols.

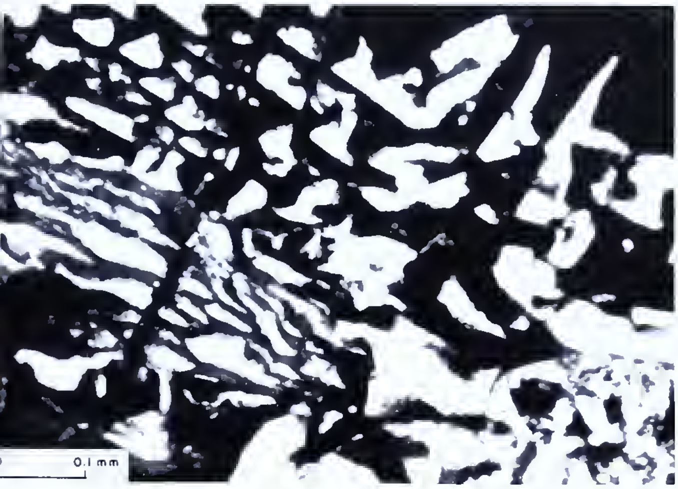

C. Micropegmatitic intergrowth of quartz and microcline (dark) illustrating crystallographic control on quartz orientation; crossed nicols.

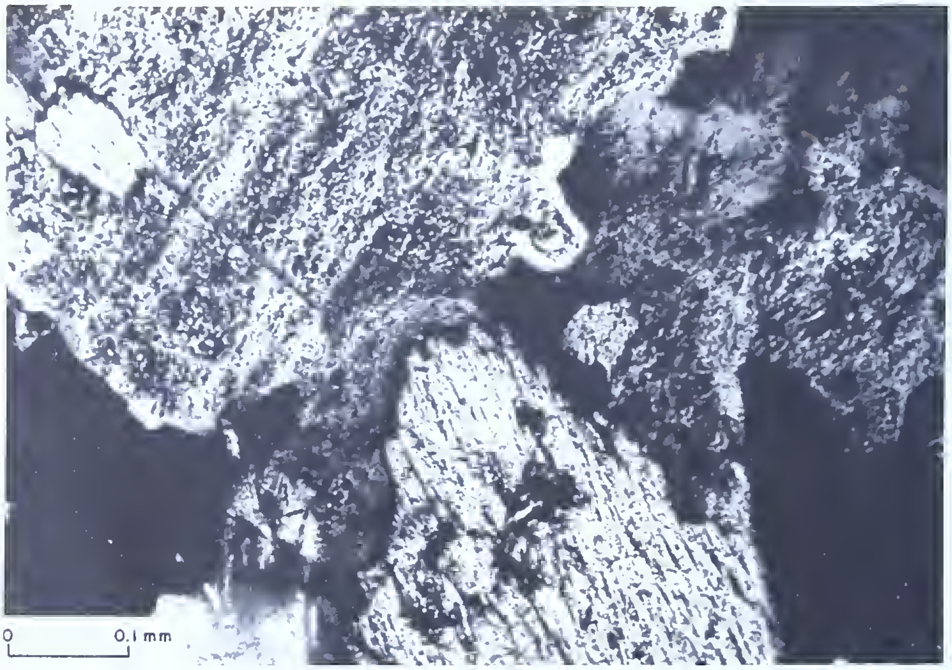

D. Ferriferous orthoclase (gray-spotted, white crystals) with green hornblende (lighter-spotted, at base of photograph) with ilmenite (black at lower right) and quartz (at extinction at left). This section is from the granophyre analyzed in Appendix 4-A and in Table 4, sample No. C4-150; crossed nicols.

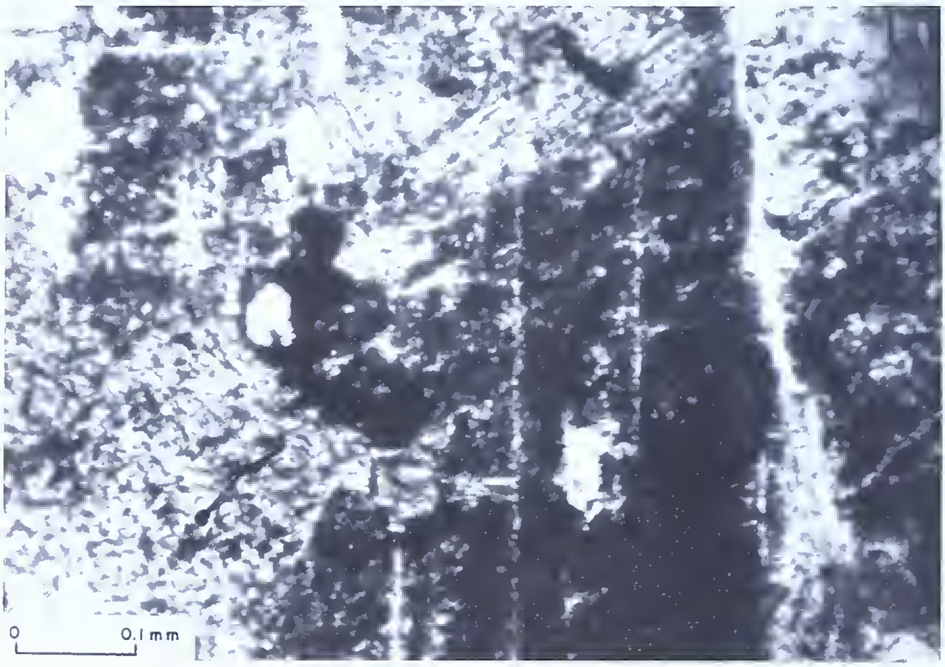

E. Sericitized albite (at extinction) in a matrix of quartz and sericite, illustrating that much of the K_2O in the potassium-rich granophyre at Cornwall is in sericite. Section is same chemically analyzed granophyre as in Plate 18-D (No. C4-150); crossed nicols.

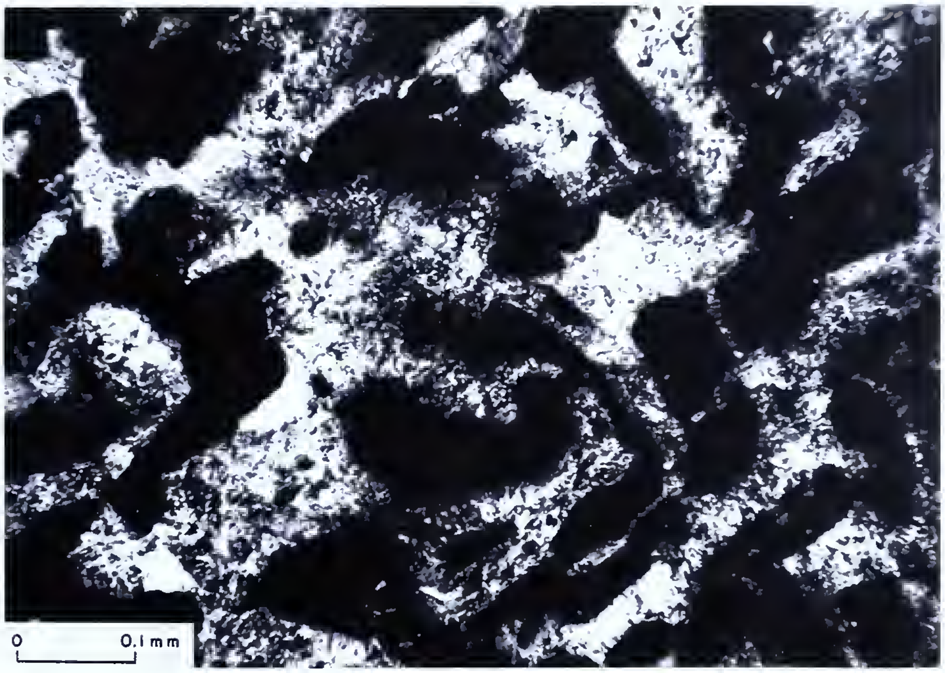

F. Quartz rods (black) in hematitic orthoclase, a common texture in granophyre at Cornwall. Note lack of good crystallographic control in comparison with quartz-microcline intergrowths (Plate 18-C); crossed nicols.

PLATE 19. PARAGENESIS AND TEXTURES OF DIABASE FELDSPARS

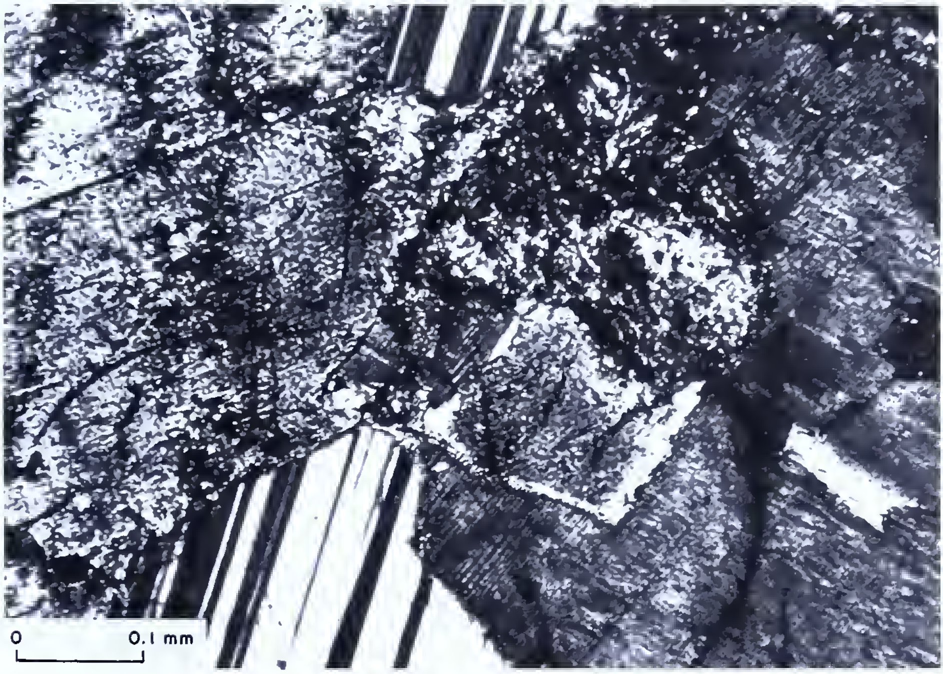

A. Calcic plagioclase ($<An_{55}$) transected by late (less Mg) pigeonite poikilitically enclosed by a (ferriferous?) augite containing opaque iron (-titanium?) oxide inclusions (center of photograph); in diabase pegmatite; crossed nicols.

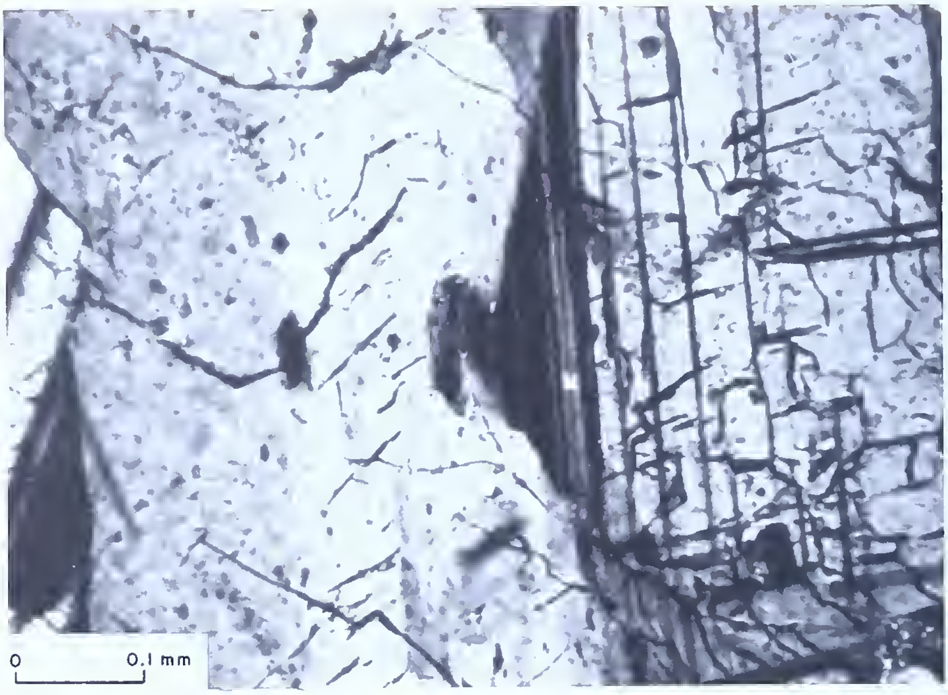

B. Zoned plagioclase (on left) poikilitically enclosing older, composite-twinned, relatively homogeneous plagioclase; crossed nicols.

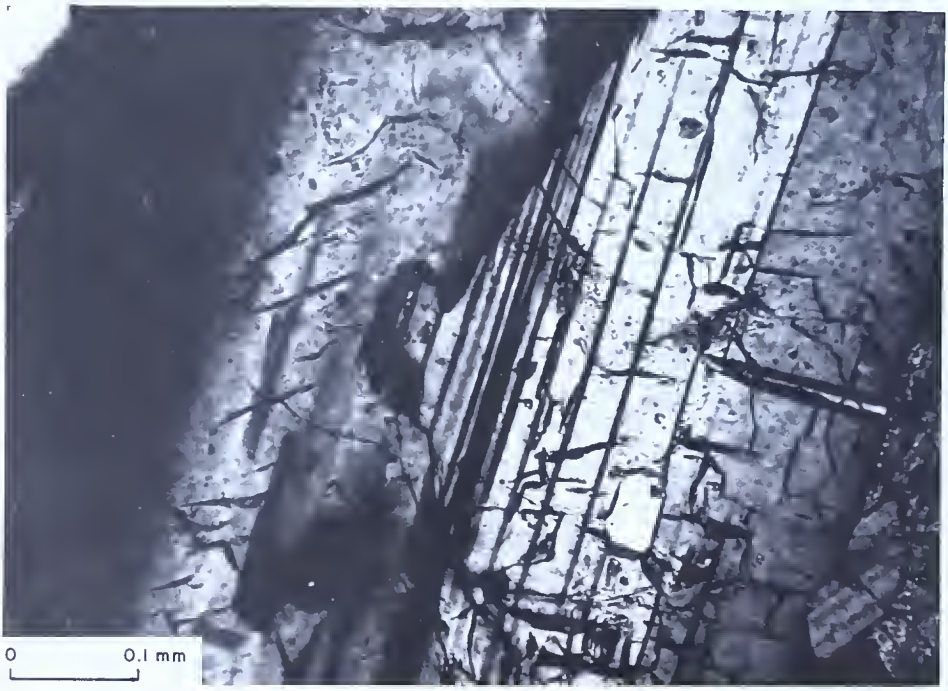

C. Same photograph as Plate 18-C, illustrating sequence and oriented to emphasize zoning; crossed nicols.

PLATE 20. PARAGENESIS AND TEXTURES OF DIABASE PYROXENE AND AMPHIBOLE

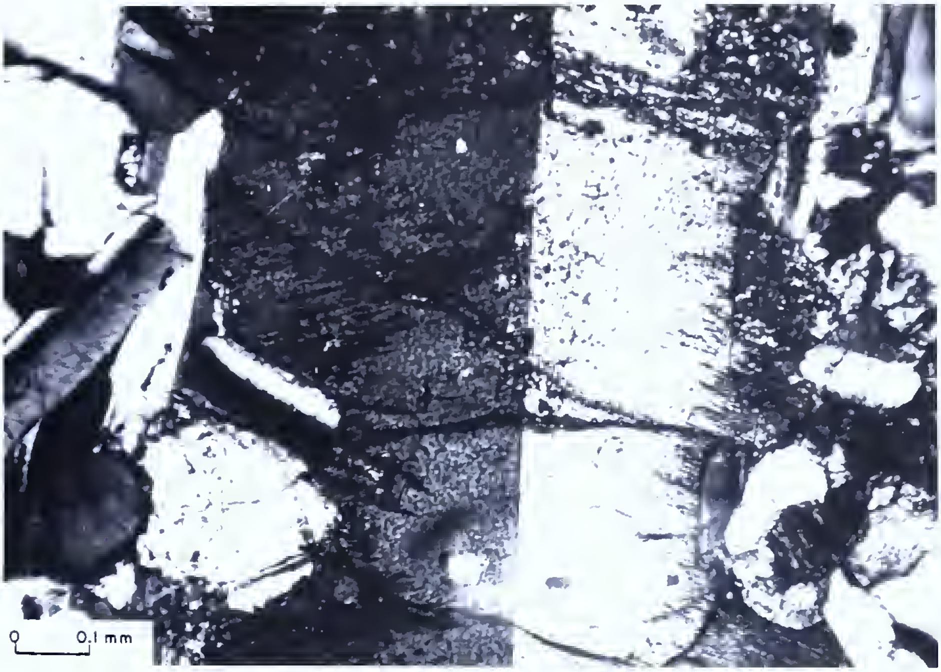

A. Twinned pigeonite with included clinopyroxene (augite) and plagioclase (calcic). Fracture alteration is limonite (±hematite). Section also contains clinohypersthene-hypersthene mixed crystals. Same section as in Plates 5-C and 15-A; crossed nicols.

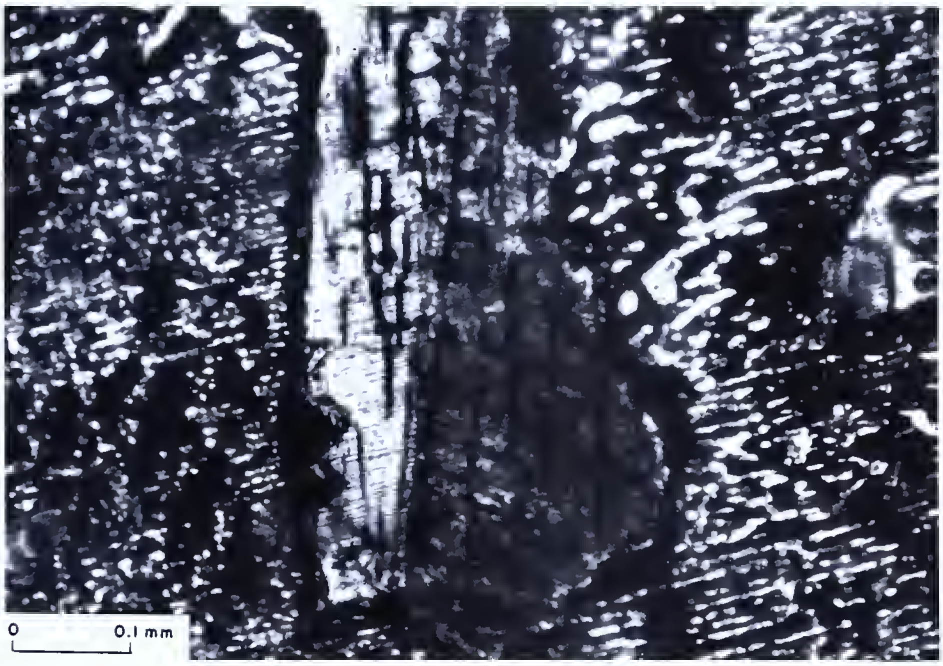

B. Hypersthene host grain at extinction with twinned pigeonite core and coarse plates of lamellar exsolution of augite (?) in orthopyroxene. This is relatively common in coarse (not pegmatitic) diabase. Note patchy extinction (exsolution?) of pigeonite core; crossed nicols.

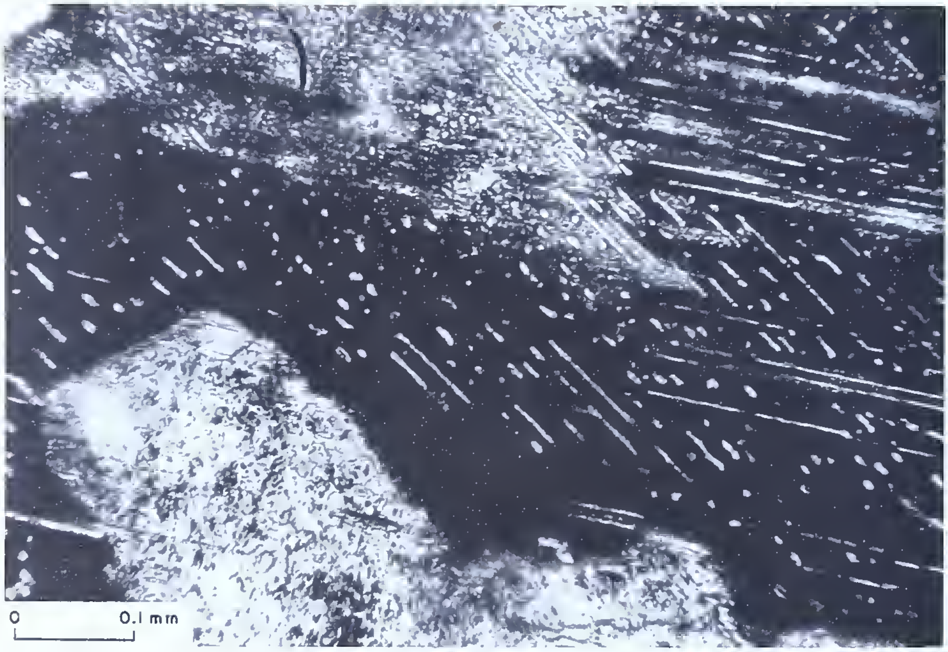

C. Amphibolitized orthopyroxene (dark) with augite exsolution crystallographically controlled. Augite (light) is younger than the orthopyroxene; from same section as in Plate 19-B; crossed nicols.

PART 6 GENESIS OF THE MAGNETITE ORES OF CORNWALL AND OF THE PENNSYLVANIA TRIASSIC METALLOGENIC PROVINCE

INTRODUCTION

The magnetite deposits associated with Triassic diabase belong to a single metallogenic province. Each ore occurrence has been referred to as "magnetite of the Cornwall type" as a result of the excellent work of Spencer (1908). In accepting these generalizations, it has been assumed that the similarities among the ore deposits require an identity of genesis. In the search for this identity, apparent contradictions arose among the researchers who have examined the major deposits at Boyertown, French Creek, Morgantown, Cornwall, and Dillsburg. In recent years all have agreed, as the data in this report demonstrate, that in some fashion magnetite ores are related to igneous diabase, but here the agreement has ceased. Two fundamentally different hypotheses have been pursued with vigor, each with its own body of supporting evidence, neither completely satisfactory for the province as a whole. These hypotheses can be posed in the form of two questions: did the magnetite originate from within the immediately adjacent diabase by some process of ejection, or was the magnetite a separate, probably hydrothermal, phase that originated from a common tholeiitic magma source not directly related to the adjacent sheet? Thus, the question has been phrased as an either-or proposition with very little straddling of the genetic fence. One of the purposes of this discussion of genesis is to show that these viewpoints may be too restrictive, that the theory that best fits the available evidence actually may be a combination of the two hypotheses, depending on which ore body is under consideration, and that, in detail, the mechanism of ore introduction need not be exactly the same for every magnetite deposit in the metallogenic province. From the present detailed study of diabase, contact rocks, and ore, it is possible to define the sequence of events from diabase magma injection to ore deposition, some aspects of the process of ore transport, the nature of the responsible solutions, and the factors that controlled ore deposition. Although the importance of most of these processes can be evaluated from the available data, many of their underlying causes remain a matter of speculation. If this discussion stimulates further field and experimental research on the Triassic magnetite ores, a major goal will have been accomplished. It seems unlikely that all of the ideas presented here will withstand the test of future, more sophisticated research. What is more important is that a new approach be demonstrated that leads away from the narrow confines of one or another rigid school of genetic thought.

The ensuing discussion will proceed from a consideration of the Cornwall area to that of the Triassic magmatic province. Throughout, one of the purposes of this examination is to look for interrelationships among the various forms of diabase magma, magnetite ore deposits, and the major structures of the Triassic basin. It is interesting to speculate that there may be a causal connection between the unique association of magnetite with diabase in Pennsylvania and the unique structural environment of the Pennsylvania Triassic belt. Broader based studies than the present one, if aimed in this direction, may provide an answer to genetic source relationships.

MAGNETITE ORE DEPOSIT COMPARISONS

The Pennsylvania magnetite deposits are the only major occurrences known to the authors where the associated igneous rock is diabase. Because of this fact, no extended comparison will be made with other magnetite deposits, although problems of ore transport and replacement may be the same, especially where the host rock is limestone.

Examples of magnetite deposits associated with igneous rocks are listed in Table 31. This comparison of ore and igneous rock is not meant to imply that the source of the magnetite for all of the listed deposits is the igneous rock with which it is spatially associated. However, in each case, a magmatic origin has been suggested. In general, the most commonly associated igneous rock is granitic, such as a quartz monzonite or syenite. A few magnetite deposits are associated with diorite or quartz diorite. The titaniferous magnetite-ilmenite deposits associated with anorthosite (Adirondack area, New York State) are considered to be distinct and not directly comparable. The Vancouver Island occurrence presents similar problems to those at Cornwall (Eastwood, 1965). Here the ore is a limestone replacement deposit, so that problems of transport and deposition are similar to those in Pennsylvania, but the source of the ore, structural situation, skarn mineralogy, and ore textures differ significantly.

A small magnetite-sulfide-hematite limestone replacement west of Sudbury, Ontario is most similar to the Cornwall ore deposit (Osborne, 1929). Here the ore mineralization is associated with amphibolite that is believed to be an alteration product of quartz-diabase of post-Huronian age. With the exception of wollastonite present in the Sudbury area, the contact metamorphic assemblage is similar: garnet, diopside, biotite, chlorite, and calcite. With the exception of galena and a cobalt mineral at Sudbury, the ore minerals also are similar: hematite (specularite), magnetite, pyrite, chalcopyrite, and sphalerite. Furthermore, a similar bladed magnetite occurs near the altered diabase in calcite in the Sudbury district and is believed to have been reduced from specularite. Osborne (1929) ascribes the origin of these deposits to alkali-ore emanations from diabase, although no alkali-mineral enrichment was observed. The source of the alkalies is presumed to have been a diabase residuum associated with micropegmatitic granophyre in diabase. Reduction of Fe^3 by CO is suggested as the mechanism of magnetite limestone replacement.

Table 31. *Types of Igneous Rocks Associated with Magnetite Ore Deposits*

Location	Associated Igneous Rock
Adirondacks, N. Y.	augite syenite and diorite gneiss
Banat Province, Hungary	diorite-syenite
Cranberry, N. C.	alkaline magmas
Eagle Mountain, Calif.	quartz monzonite
Elba, Italy	granite
El Laco, Chile	intermediate to basic volcanics
Fierro, N. M.	quartz monzonite porphyry
Hanover, N. M.	granodiorite
Heroult, Calif.	diorite
Iron Springs, Utah	quartz syenite porphyry
Kiruna District, Sweden	syenite or quartz porphyry
Lahn Sipreline, Germany	diabasic flows
Vancouver Is., B. C., Canada	diorite or quartz monzonite
West of Sudbury, Ont., Canada	amphibolite (meta-diabase)
Wyssokaia Gora, Urals, U. S. S. R.	augite syenite

The Quaternary Chilean El Laco deposit of magnetite, hematite, and martite is believed by Rogers (1969) to have originated as an ore magma directly derived from a mafic volcanic magmatic source. It is possible that the processes of mafic magmatic iron concentration here are similar to the processes that operated in the Cornwall tholeiite, but a detailed analysis of the Chilean magmas and ore is not yet available. The author makes no mention of any late stage alkali-rich or silica-rich extrusives that would be comparable in composition to the intrusive diabase pegmatites and granophyres proposed as the iron-ore source in Pennsylvania (cf. Hotz, 1953; Davidson and Wyllie, 1968).

HYPOTHESES CONCERNING THE ORIGIN OF MAGNETITE

Note has been made of the several major theories put forward to explain the origin of "Cornwall type" magnetite deposits. Summarized, they are 1) remobilization of iron from the adjacent sedimentary units by diabase intrusion (Rogers, 1858; Lesley and d'Invilliers, 1886); 2) expulsion of iron from the adjacent diabase, with an emphasis on the later stages of diabase crystallization as the immediate source (Spencer, 1908; Hickok, 1933; Hotz, 1950 and 1953; Davidson and Wyllie, 1965 and 1968); and 3) hydrothermal iron introduction from the same source that produced the diabase plutons (Gray and Lapham, 1961; Lapham, 1962 and 1968; Sims, 1968). In recent years, several different ore derivations have been proposed. Although these have not been directly applied to the Pennsylvania magnetites, they may be applicable and deserve brief consideration.

A possible diabase source of titanium-free magnetite leading to the formation of ore might be extrapolated from the discussion of Buddington and others (1955, p. 526-527). They note that magnetite in igneous rocks usually contains less titanium than the associated ore concentrations. The smaller amounts of titanium in the magnetite of igneous rocks, they suggest, may be the result of deuteric or hydrothermal reworking by late-stage igneous fluids. Such a low-titanium magnetite exists in the Pennsylvania diabases (Davidson and Wyllie, 1968) and this diabase has been suggested by them as a possible source of the essentially titanium-free Pennsylvania magnetite ores (Davidson and Wyllie, 1968). On the other hand, it should be pointed out that the Pennsylvania diabase-ore association represents a reverse titanium distribution between igneous rocks and ore from that noted by Buddington and others (1955).

Ridge (1956a) related the magnetite ores of the Kiruna, Sweden district to differing magma conditions that resulted in two end-member types of iron ores: the Kirunavaara and the Rektor, with an intermediate type at Gallivare. The Kirunavaara type is characterized by a relatively higher ratio of magnetite to hematite and less wall-rock alteration than at Rektor. Although both are believed to be products of an acid parent magma (quartz or syenite porphyry), he attributed their difference to oxidation in the parent magma or in the separated ore-magmas. Thus the Kirunavaara represents a magma that was lower in water (or total volatiles), or a magma from which a greater amount of volatiles had escaped previous to the formation of the ore fluid, perhaps under less partial pressure, or a combination of both. Ridge also noted that the rate of oxygen escape from the ore melt may be significant, the Kirunavaara representing a more rapid escape, and Rektor-Gallivare a slower escape. The ores are apparently believed to have come from the same source at depth as the associated acidic plutons. The situation is similar to that of the Pennsylvania diabases and ores, although the relative amounts of magnetite and hematite and the extent of wall-rock alteration have not been quantitatively compared for the various Pennsylvania deposits. Keeping to the Ridge analogy for the Kiruna district, the possibly more ferric diabase at Cornwall might be analogous to the more oxidized Rektor-Gallivare ore-melt type and the slightly more ferrous diabase at Dillsburg to the less oxidized Kirunavaara ore-melt type. However, the analogy here is between Pennsylvania diabase (a magma system) and Kiruna ores (an ore-fluid and melt system); that is, the Pennsylvania ores were not crystallized directly from a magmatic melt. Other differences also exist, such as the oxidation sequence (magnetite to hematite in Kiruna ores, and the reverse at Cornwall and Dillsburg). Nevertheless, a basic reliance on changes in magma oxidation and in oxidation state of crystallizing mineral components represents a similar approach to the two, otherwise different, magnetite districts.

Another possible mechanism for the early separation of iron ore is suggested by Kullerud and Yoder (1963). Sulfur reacts with rock-forming silicates, particularly with the olivine series, releasing oxygen for the formation of magnetite or hematite. Such a reaction illustrates that the addition of oxygen is not necessary for oxidation to occur. They note that the addition of only a few percent sulfur can bring about the formation of typical sulfide-ore assemblages. Typical examples of such a reaction are as follows (Fa=fayalite; Mag=magnetite; Qtz=Quartz; Hem=hematite):

$$2\mathrm{Fa} + 1\mathrm{S} = 1\mathrm{FeS} + 1\mathrm{Mag} + 2\ \mathrm{Qtz}, \text{ and} \qquad (6\text{-}1)$$
$$3\mathrm{Fa} + 2\mathrm{S} = 2\mathrm{FeS} + 2\ \mathrm{Hem} + 3\ \mathrm{Qtz}. \qquad (6\text{-}2)$$

It can be seen that as the amount of sulfur increases, magnetite is replaced by hematite. In a troctolite used as an example (50 percent olivine with a 1/1 ratio of Fe/Mg and 50 percent plagioclase), the addition of 2.3 percent sulfur completely broke down all of the olivine into iron sulfide, magnetite, and magnesium silicate. Such a process could account for an early concentration of iron sulfide and magnetite and for a lack of olivine in the main body of diabase sheets. However, normal Cornwall diabase appears to contain less than 0.03 percent sulfur (Appendix 4-A), less than would appear to be necessary for the breakdown of significant amounts of olivine. For other Triassic sheets in Pennsylvania, data are too scanty or unreliable to draw conclusions. Essentially, this mechanism is one that remains to be tested.

All of the above ideas are at least in part compatible with available data concerning the Pennsylvania Triassic metallogenic province. None are by themselves wholly satisfactory for explaining the details of ore fluid source, transport, or deposition. They should, however, be kept in mind as possible avenues for future, more detailed, investigation. Possibly oxidation of the magma and certainly the crystallization history of iron-titanium oxides in diabase are important at Cornwall. In this regard, two observations from Cornwall are of importance in understanding the genesis of the Cornwall ores: throughout the vertical extent of the diabase sheet, total iron content is usually low and the Fe_20_3/FeO ratio may be slightly high.

ORIGIN AND MAGMATIC HISTORY OF THE CORNWALL MAGNETITE

Introduction

The Cornwall deposit is a replacement of limestone immediately above Triassic diabase. In this respect, it is similar to most other magnetite deposits of the province. However, the basic similarities do not require that the introduction mechanism or immediate source of the ore fluid be exactly the same in detail at each location. As a consequence, the genesis of Cornwall magnetite can be treated separately from other Triassic occurrences in Pennsylvania.

The possible sources of iron which have been most prominently discussed in the literature are 1) the country rock, 2) the adjacent diabase sheet, and 3) a common magma other than the *in situ* sheet. In addition, the possibility of a compound sheet injection raises the further possibility that a lower part of the Cornwall sheet may have served as the ore source. Each of these hypotheses will be examined.

The Country Rock as a Source of Iron

The host rock is essentially a limestone, dolomitic and argillaceous in part. There is no field evidence of local residual, limonitic deposits that could have been remobilized by heat from cooling diabase. Chemical analyses of host limestone, Mill Hill Slate, and Blue Conglomerate, contact metamorphic and metasomatized rocks, and bleached Triassic sediments do not show any noticeable depletion in iron (Tables 1, 2, 4, 8, 10, and 16). Iron has been remobilized within these units but apparently has not left the system. Bleaching of the contact units and the formation of specular hematite in the Triassic sediments can be used only as evidence of changes in oxidation state and local iron mobility. Magnetite ore bears no spatial, textural, or temporal relation to these units. As discussed in Part 3, "Genesis of Potassium Metasomatism," it is unlikely that the iron originated from host rock alteration, because there probably was insufficient iron available, its required long-distance mobility seems improbable, confirmatory host rock textures are absent, and demonstrated ore solution movement toward diabase and toward a particular area above diabase is highly improbable. The country rock merely has provided a suitable host with local structural and stratigraphic conditions controlling such features as mineral replacement limits and textures.

The hypothesis of a country rock source does not seem to have been seriously entertained since the late 1800's and will not be considered further here.

The Adjacent Diabase as a Source of Iron

The major reasons for postulating an expulsion of iron from diabase immediately adjacent to the ore zones are 1) the constancy of the diabase-ore association in the metallogenic province, 2) the occurrence of ore almost universally above diabase in accordance with theoretical upward release of mobile constituents under temperature, pressure, and crystallization gradients, 3) depletion in the Cornwall diabase of total iron, 4) the enrichment of iron in differentiates at Cornwall (and Dillsburg), reinforced by the fact that the locus of these differentiates is largely near the top of the diabase sheet, 5) the occurrence of sulfides in pegmatitic diabase schlieren (Appendix 3), 6) the presence of late, titanium-free magnetite in the sheet (Davidson and Wyllie, 1968), and 7) the presence at Cornwall of ferriferous and hematitic orthoclase in both the granophyre and the eastern ore zone, appearing to represent a continuous process. Throughout the discussion it is assumed that any ore expulsion from diabase would have left behind some direct evidence of the process, although S. Anthony Morse (written communication) suggests this is not a necessary requirement for formulating an expulsion model.

The first point (diabase—ore association) certainly demonstrates a significant relationship. However, it does not define the time, or sequential, relationship between ore and diabase, but only a spatial and an ultimately genetic one. The second point (ore above diabase) is more an apparent relationship than a real one. In most cases an easily replaceable limestone host is necessary and this lies above the known ore bodies. In addition, there are several magnetite concentrations below diabase (e.g., the Doner Mine north of Cornwall, the Esterly mine in the Jacksonwald syncline, and perhaps the Carper Mine west of Cornwall). The actual amount of magnetite that might be below the sheets is essentially unexplored. At Cornwall, there is an ore body well below the top of the sheet (below most late differentiates) and magnetite-filled veins extend well into, and probably through, the sheet. These and other data previously discussed show that this spatial association is not directly indicative of the source of the iron.

Late stage iron enrichment in diabase is discussed more fully in the discussion of "Titanium-Iron Geochemistry and Province Ore Origin." There is no observational evidence for escape of iron from Cornwall diabase, although separation of titanium-rich and titanium-poor magnetite did occur within the York Haven pluton. However, late iron enrichment and oxidation of a mixed spinel are normal features of diabase and diabase differentiates whether or not there is any associated ore. Throughout the diabase-ore province, there appears to be no spatial relationship between distribution of granophyre (and diabase pegmatite) within a particular sheet and ore deposit location or ore-zoning. Textures at Cornwall do not show evidence of filter pressing or ore solution escape, and the differentiates do not lie along fractures or channelways, nor are they known to cut the upper chilled margin. Thus, although late titanium-deficient magnetite occurs in diabase, there is no evidence of its removal from the sheet coincident with residual fluids. In addition, the volume of the Cornwall granophyre is quite small and its iron content quite low, a typical characteristic of all diabase granophyres. Maximum enrichment of iron occurred in the differentiation sequence previous to granophyre crystallization; thus, there would seem to be no obvious temporal relationship between magnetite and an ore solution associated with the granophyric residuum. Furthermore, the orthoclase in the ore zone appears to have preceded the ore and to be replaced by it. On the other hand, orthoclase in diabase post-dates the maximum iron enrichment in diabase (diabase pegmatite). Consequently, neither the presence of ferriferous orthoclase in ore and granophyre nor Ti-free magnetite in diabase is particularly convincing evidence for a diabase ore source.

An additional question should be asked with regard to the hypothesis that iron could have come from the Cornwall diabase. As was noted previously, chemical analyses of the Cornwall sheet indicate that it is depleted in total iron on the order of 0.5 to 1.0 percent Fe total (Tables 26 and 32; Figure 53). Calculations show that this is easily sufficient to account for the magnetite ore bodies at Cornwall. Assuming 100 million tons of magnetite ore (a conservative figure, since this is nearly the amount mined to date), a sheet 0.2 mile thick, and a density of average diabase (between 2.7 and 2.9), a 1 percent total iron deficiency would require a diabase sheet about 1200 feet x 0.4 mile x 0.4 mile. A 0.5 percent total iron deficiency in diabase would require a sheet 1200 feet x 0.55 mile x 0.55 mile. Both of these volumes are reasonable and the volume is much less than that of the Cornwall sheet (plate 21). If a maximum of 200 million tons of ore is assumed (includes the unmined portions of the operated ore bodies and the untouched footwall ore), the volume still will be well within the limits of the Cornwall sheet, about 1200 feet x 0.8 mile x 0.8 mile at 0.5 percent total iron. Regardless of the source of the iron for the magnetite ore deposits, these calculations show that the diabase magma would not have to have been unusually rich in total iron compared to non-ore-associated diabase (Table 32). An average, normal value appears to be about 8.0 percent total iron (Table 32). Like the diabase depletion in total iron and the consistent association of ore and diabase, this calculation shows only that the ore could be genetically realted to diabase magma, but not necessarily to *in situ* sheet crystallization.

Table 32. *Average Percent Fe total in Diabase and Basalt*

	% Fe
1. Tasmania dolerite (Edwards, 1942)	6.7
2. Cornwall diabase, Pennsylvania (R. Smith, written communication)	7.2
3. Cornwall diabase, Pennsylvania (this report)	7.4
4. Downes Mountain dolerite (Walker and Poldervaart, 1941)	7.8
5. Triassic diabase dikes, eastern North Am. (Appendix 5-C)	7.9
6. Triassic diabase sheets, non-ore (Appendix 5-A,B)	8.0
7. Dillsburg diabase, Pennsylvania (Hotz, 1953)	8.0
8. Karroo dolerites, South Afr. (Walker and Poldervaart, 1949)	8.1
9. Palisades sill, N.J. (Walker, 1940)	8.3
10. Average tholeiite (Poldervarrt, 1955)	8.4
11. Average basalt (Daly, 1933)	8.8
12. Average tholeiite (Nockolds, 1954)	9.1
13. Whin Sill (Holmes and Harwood, 1928)	9.3

There are many cogent arguments against the hypothesis of iron (and sulfide) introduction from the adjacent diabase sheet. They can be summarized as follows:

1. The Cornwall diabase essentially is mineralogically and chemically normal when compared with other diabase plutons (except for a slightly lower total iron content, perhaps a high Fe_20_3/FeO ratio, and possibly low Na_20+K_20). This being so, why should there be an anachronous, iron-rich, hydrothermal phase associated with it when iron ore introduction did not occur as a result of the crystallization differentiation of other, similar diabase sheets in Pennsylvania and elsewhere? In other words, diabase is ubiquitous, but diabase and magnetite ore are unique to the Pennsylvania provine. These analogies lead to the suggestion that it is not the diabase itself, but some other and more fundamental geological phenomenon that is the direct cause and source of the ore.

2. As noted, ore is not always above diabase, and the amount of ore which may exist below the diabase has not been adequately determined. The observed occurrence of ore within the diabase sheet (footwall ore body beneath the eastern end of the open pit) and beneath it (Doner Mine near Cornwall) is incompatible with expulsion of iron from the top of the diabase sheet. This results from the fact that the source fluids, whether from the top or the center of a sheet, would either move upward or remain within the diabase. If all of the Cornwall area ores had the same source, then the main ore bodies above the diabase also could not have formed from a fluid derived from the top of the sheet.

3. Studies of mineral paragenesis and the sequence of faulting indicate that there was a time lapse, of unknown extent, between solidification of the chilled upper margin and the deposition of ore in the host limestone. Post-diabase faults are both pre- and post-ore (probably true at the Carper mine also, Geyer, 1970). To what extent faulting may have occurred during the final stages of diabase solidification is unknown, but some plagioclase crystals are sheared near a major fault (Plate 21). Contact metamorphic and metasomatic minerals also had crystallized before the ore stage began. The chilled margin, where observed, is continuous. Contraction cracks within this margin are filled with contact metamorphic diopside that, in turn, is replaced by magnetite. Introduction and nucleation of iron in the chilled margin over the eastern ore body has occurred, probably accompanied by some contact metamorphism by ore of the chilled margin. Thus, both mineral parageneses and the character of the chilled margin are inconsistent with ore derived by ejection from or through the top of the sheet. However, if the time lapse between the solidification of the margin and that of the crystallization of late differentiates is sufficient for the various metamorphic and replacement processes to have occurred, then time alone is not a viable criterion. Alternatively, ore fluids might have escaped through a lower, separate diabase sheet

that has no surface expression (unlikely in view of the dips) or through an unexposed portion of the Cornwall sheet. For the latter, a very narrow zone of segregation of volatiles would be required to yield the observed ore zonation. Collection to such a zone seems unlikely.

4. Diabase expulsion of iron fails to explain adequately the chemical and mineralogical zoning of the eastern ore body (Figures 26-32). This is especially significant, since the zoning is related not to the locus of any differentiates within the sheet, but to a major fault transecting it and to ore veins, mineralized shears, and the footwall ore body within diabase. These structures and zonation are strategically located, as far as the distribution of magnetite is concerned, approximately between the two major ore occurrences.

5. Although diabase pegmatite is enriched in iron with sparse pyrite and chalcopyrite, and thus could be a possible ore source, its major concentrations occur well below the top of the sheet, and only in small schlieren or pockets near the top. Most occurrences of magnetite, sulfides and chlorite are on joints or in shears. The vertical core log (Appendix 3) shows that these minerals occur throughout the sheet (to within 100 feet of the base). They are believed to be related to the steep fault and shear zone that penetrates the sheet (Parts 2 and 4) and that is on strike with the footwall ore body. All diabase pegmatite and granophyre are of small volume and show no textural evidence of migration. They are not confined to areas below the ore zone, both being present elsewhere in diabase sheets whether or not there is associated ore.

6. A method of removing titanium-free magnetite from differentiates rich in iron-titanium oxides is required for *in situ* sheet expulsion of magnetite. The amount of low-titanium magnetite present in these stages as an oxidation or unmixing product, apparently is very nearly the exact amount to be expected from the oxidation of original mixed spinel (see "Titanium-Iron Geochemistry and Province Ore Origin"). Based on textural evidence, the low-titanium magnetite in the diabase differentiates does not appear to have been particularly mobile, occuring largely as rims on mixed spinel (also see Davidson and Wyllie, 1968).

7. There is no textural evidence of an ore feeder channel (other than a mineralized fault) or of expulsion of interprecipitate liquid from the diabase in any of its differentiates. The general composition of the sheet, except perhaps near the base, is quite uniform. An originally high concentration of iron in one part of the pluton, or its depletion migration to one part, seems unlikely in view of the chemical analyses of a vertical core (Table 33). However, the basal 100 to 200 feet may contain more total iron (Table 33, analyses by R. Smith II), resulting either from slight accumulation or a separate injection such that iron depletion of diabase may be uniform only through

the upper 1000 to 1100 feet. On the other hand, these differences are less than the differences among different analytical laboratories (Table 33) and sampling errors may be large.

8. The ore is spatially related to a metasomatic aureole, principally of chlorite and actinolite with minor muscovite and potassic feldspar. That residual concentrations of silica, alumina, potassium, iron, sulfur, and minor metallic cations (copper, nickel, cobalt, gold, and silver) all were concentrated together in the diabase differentiates and expelled together seems somewhat unlikely. Furthermore, these trace elements are enriched in the ore zone, but the diabase contains apparently normal amounts. For example, gold is of normal concentration throughout the Cornwall diabase; that is, the diabase contains the same amount of gold as other Triassic Appalachian non-ore-associated diabases (written communication, David Gottfried). Since the gold occurs with chalcopyrite in a chalcopyrite-magnetite ore association it was a component of the ore solution. The same situation is true for nickel and cobalt, which range between 10 and 30 ppm (Appendix 4-A), an amount apparently normal for Triassic diabase of this province (cf. Lapham and Saylor, 1970) regardless of the presence of ore.

Table 33. *Variation in Total Fe with Depth of Normal Cornwall Diabase*

	Total Fe	(in %)
Vertical Core Depth	This Report	R. Smith*
Upper Chilled Margin	7.34	
433′	7.29, 7.54, 8.31**	7.44
493′		6.33
550′		7.38
649′	7.20	
750′	7.32	
937′		6.61
1021′		6.57
1040′		7.80
1066′	7.11	
1114′	7.11	6.92
1159′		8.19
1202′		7.76
1202′	7.58	7.76
1227′		

*Written communication, 1970; see Appendix 4-A.

**Analyses of same sample by three different commercial laboratories.

Certainly not all of these arguments are of equal weight, but together they sum up a body of evidence that is difficult to reconcile with the diabase-expulsion theory. Any proposal of origin must satisfy these objections.

Multiple Diabase Injection as a Source of Iron

From the interpretation of data in the foregoing sections, there is some indication that the Cornwall sheet may be a compound sheet with an internal, partially chilled contact about 1060 feet vertically below the upper chilled margin. It could be proposed that this basal part of the pluton was a separate injection which provided ore-solution access through a pre-existing fracture in the upper sheet. An analagous case could be made for ore in the Dillsburg district that lies between diabase sheets or for the Boyertown core described by Hawkes and others (1953) that shows replaced diabase above a fresh, unaltered diabase sheet; that is, that the lower of two sheets was the immediate ore source. However, ore does occur below diabase where there is no known underlying sheet (Esterly and Carper mines). At Cornwall, this requires some rigidity of the upper sheet, a time interval in which a stress can be applied, and sufficient mobility of an iron-rich fluid in the lower sheet to move into an ore channel. These seem unlikely. If such had been the case, a well-defined, aphanitic, internal chilled contact might be expected, but this is absent (Appendix 3). (A postulated lower sheet that yielded an ore fluid could not have intruded first because ore rests upon the upper sheet.) To some extent this hypothesis probably is tenable only because of our lack of petrologic and geochemical information about this lower part of the diabase. However, with the exception of more porphyritic textures (commonly hypersthene), more olivine, and more zoned plagioclase, it is very much the same as the upper part of the diabase. There may be more total iron in the lower portion of the sheet but the difference does not appear to be significant (Table 33). The objections to an *in situ* diabase origin cited previously also apply here. Considerably more data will have to become available before this hypothesis can be given serious consideration.

A "Primary Magma" as the Source of Iron and Diabase

The use of the term "primary magma" refers, in this context, to a magma that gave rise both to diabase plutons and ore solutions, as distinguished from the *in situ* magma from which the diabase sheet at Cornwall crystallized and differentiated. It is not meant to imply a primary magma in the sense of a possible ultimate parent magma from which tholeiite might be derived.

The hypothesis presented and examined here postulates the existence of a magma at depth before intrusion of diabase into upper crustal levels and a separate, later ore fluid. An early fractionation and/or magma separation process is envisioned that allowed the tapping, or escape, of different fractions at different times (and temperatures?), resulting in basaltic volcanism, diabase sheet intrusion, ore solution introduction, and diabase dike intrustion. A time lapse between sheet and ore introduction probably existed but is of unknown duration. The ore mineralization at Cornwall is believed to represent a separate, mobile, fluid phase, emanating directly from a source magma, but not necessarily at the same subcrustal level for the time of ore-fluid tapping as for the tapping of the diabase sheet magma. Ore fluid introduction followed along planes of structural weakness previously utilized by the intrusion of the major volume of diabase magma. Deposition of this ore fluid occurred where a favorable lithology was encountered.

Summaries of the evidence for a primary magma origin, for the development and composition of an ore phase at depth before its upper crustal introduction, for mode of transport, and for environmental controls upon ore deposition will be considered before attempting to synthesize a genetic history of the Cornwall magma and its relation to the Triassic magmatic province.

The hypothesis of a common magma source for both diabase and ore seems clearly indicated by analysis of the available data. The observations and interpretations pertinent to delineating this origin, as opposed to *in situ* ore derivation, are summarized in Table 34. The observations (column 1) and interpretations (column 2) have been discussed in the preceding sections or will be dealt with more thoroughly in a discussion of the magnetite ores of the metallogenic province. Many interpretations are interdependent, so that one may eliminate the possibility of another.

The diabase-magnetite association (observation 1) is indiscriminate with regard to a distant source or an *in situ* ore origin, but is considered to be evidence of a genetic interrelationship between tholeiitic magma and ore.

The conclusion of observation 2 assumes that the introduction of sulfides and various metallic cations belongs, genetically and temporally, to the ore stage. The late-stage differentiates at Cornwall are similar to other differentiated diabase rocks. It does not seem probable that ore fluid of this composition was simultaneously concentrated in and expelled from this particular diabase pegmatite or granophyre, and certainly not from the normal *in situ* diabase magma, before differentiation. Such compositional concentrations in diabase would be highly atypical.

The conclusions of points 3 and 9 assume that magnetite-rich ore fluids would not be expelled both through the base and the top of a sheet and that the magnetite that forms footwall ore bodies could not have migrated from above the sheet at one point to below the sheet (i.e., through the sheet) some distance away, a problem raised by the footwall Doner mine occurrence near Cornwall.

Although the time lapse between initial diabase intrusion and ore deposition is unknown, considerable mineralization occurred between

Table 34. *Summary of Observations and Conclusions Pertinent to Ore Genesis at Cornwall*

Observations	Conclusions Inferred
1. Association of diabase and magnetite is common in Pennsylvania.	Diabase and ore are genetically related, but time and process are unspecified.
2. There is a close spatial association of chlorite, actinolite, sulfides, trace cations (Ag, Au, Ni, Co) and low-Ti-magnetite.	The ore fluid was of variable composition, rich in iron, trace metals, and sulfides, low in Ti, and hydrous to some extent.
3. Ore is generally, but not always, above diabase.	The locus of ore deposition was controlled by available structures, favorable host, and upward ore fluid movement under T-P-X, gradients; ore genetically unrelated to top of diabase sheet.
4. Mineralization occurred in the sequence contact metamorphism to metamorphism to ore; the latter two intimately and paragenetically related and the former ubiquitous near diabase; faulting of diabase is both pre- and post-ore.	A time lapse that included faulting and metasomatism existed between diabase intrusion and ore deposition; metasomatism is a unique, ore-related process, unrelated to *normal* diabase injection (place and time of metasomatism and metamorphism differ).
5. The upper chilled margin was metasomatized; magnetite was introduced with nucleation on altered phenocrysts; contraction cracks were filled with metamorphic diopside and replaced by magnetite.	The upper chilled margin crystallized and cooled before ore deposition began, indicating a considerable loss of intrusive heat and a time lapse before ore deposition.
6. The upper chilled margin is unbroken over the western ore body and where observed over the eastern body except by faults, contraction cracks, and mineralized veins extending into, and probably through, diabase. These structures are not spatially associated with late diabase differentiates.	No material escaped *in situ* diabase after solidification of upper chilled margin unless through mineralized faults in immediate area of Cornwall ore bodies or through some other, unobserved, channel as at the Elizabethtown open pit.

Table 34. *(Continued)*

Observations	Conclusions Inferred
7. Metasomatic mineralization, sulfide cations, total iron, and ore-actinolite parageneses are zoned, focusing near the ore footwall of southwest side of eastern ore body.	Movement of metasomatic and ore fluid was up and out from the southwest of the eastern ore body and toward the western ore body.
8. A major NE-striking fault offsets diabase and is on strike with ore veins in diabase and an ore body within diabase; except for bleaching, diabase textures are normal adjacent to fault; zoning (point 7) is focused approximately above this fault.	This fault system probably extends through the pluton as an ore channel access to host limestone; ore solutions migrated along the basal limestone-diabase contact and/or up the fault zone.
9. Ore lies below diabase to E of fault (Doner Mine) but does not lie below diabase (drill core into lower limestone) W of fault.	Ore solutions entered the fault system from north or east side, or along the fault from NE or SW.
10a. With the exception of Na_2O, K_2O, and total iron, the chemical composition of diabase is normal, including Au, Ni, and Co. b. The differentiation trend of the diabase is normal. c. Textures are diabasic, pegmatitic, and micro-pegmatitic with no observed evidence of unusual local internal stress except at 1066 feet below the top.	The Cornwall diabase is similar to non-ore-associated diabase with respect to major and trace-element compositions and crystallization differentiation or fractionation trend; iron and some alkali withdrawal from the magma probably occurred before *in situ* crystallization.
11. The total Fe content of diabase is low by 0.5 to 1.0%; maximum concentration of Fe (-Ti) oxides occurs in diabase pegmatite and was later oxidized, in part, to largely *in situ*, low-Ti-magnetite that does not show textural evidence of migration and concentration in the sheet.	Low total Fe reflects a diabase magma depleted in Fe, but maximum Fe in the small volume of pegmatitic diabase and oxidation trend are normal; the magnetite ore probably was not generated from Fe-Ti oxides in diabase unless late, Ti-poor magnetite mobilization in diabase occurred in samples not studied or unless its effects are unobservable.
12. Oxidized Fe-Ti oxides in diabase differentiates occur commonly where there is no magnetite ore.	There is no necessary relationship between oxidation to Ti-poor magnetite in diabase and the formation of a Ti-poor magnetite ore fluid.

Table 34. *(Continued)*

Observations	Conclusions Inferred
13. Granophyre is low in total iron; volumes of pegmatitic and granophyric phases are small; both occur below the top of the sheet, and pegmatitic diabase also in basal part; textures largely show enclosed, unstressed, crystallization segregates.	Known distributions of late differentiates are spatially unrelated to loci of ore bodies or ore channels; expulsion of any significant volume of volatiles from the examined occurrences of differentiates is extremely unlikely.
14. S^{34} (o/oo) increases from normal diabase through granophyre; S^{34} is higher in ore than in diabase or in other Pennsylvania Triassic ores (French Creek, Morgantown).	A small fractionation of S occurred during differentiation; enrichment in ore of S^{34} at Cornwall resulted from a late sulfide phase with high S^{34} and/or crustal contamination.
15. Aeromagnetic gamma distributions show that the whole Cornwall and Middletown sheets (York Haven Pluton) have a lower magnetic intensity level than other sheets.	The York Haven Pluton is depleted in iron oxide minerals, but this depletion is unrelated to loci of ore deposits (Note: magnetic low over Cornwall ore area may be due to reverse direction of magnetization).

the two processes. A large contact-metamorphic halo developed, and metasomatism, now observed principally as potassium-bearing silicates above the eastern ore zone, was well under way before magnetite appeared (conclusions 4, 5, and 6). By this time, the chilled margin and at least some of the diabase magma had solidified. Both effectively sealed off the diabase pluton from the possibility of fluid escape through fractures in a solidified, or largely solidified, magma.

Traces of movement of the ore fluid from a focus at the western footwall of the eastern ore body toward the western ore body are evidenced by chemical and mineralogical zonation (point 7). However, the idea of a separate channel through diabase in the vicinity of the western ore body cannot be eliminated. This area is now completely mined out and unavailable for study, although Hickok makes no mention of such a channel here. In this regard, it is perhaps significant that replacement of limestone by ore in the western ore body did not always extend to the hanging wall limit of available replaceable limestone. A few small areas of limestone near the footwall also were not replaced. The focus of the zoning indicates a point source. The diabase in this area is not noticeably depleted in opaque oxides and there is no evidence that an ore fluid concentrated or passed through the diabase here.

The major fault that offsets diabase (point 8) cannot be traced into the ore zone because of microfaulting and brecciation of the host rock and ore textures. The fault is best seen up dip, above the postulated focus of ore-solution migration. Thus, there is no direct evidence of a clear time or genetic relationship between faulting of the host rock and ore deposition. There is also no apparent textural change in the ore that is relatable to this fault except for shear zones extending eastward (Figure 23). Therefore, the up dip portion of the fault in the ore hanging wall apparently was not utilized as an ore channel. A source other than the adjacent sheet is indicated by the spatial coincidence of faulting, mineralized ore veins, and ore below the top of the diabase.

The compatibility of normal diabase crystallization with either an *in situ* ore expulsion or a distant ore source really is not known (Table 34, point 10). An unusual product of diabase differentiation such as an ore deposit might be expected to have an unusual diabase magma for a parent. Except for Na_20, K_20, and total iron content, this does not appear to have been true, and when the entire province is considered, neither total iron in diabase nor its extent of oxidation can be directly correlated with the presence (or absence) of an iron-ore deposit. Any relationship that exists is more subtle. Differences in Fe(total), Na/K, and Au between Cornwall and Dillsburg diabases suggest that some chemical fractionation, with or without minor compositional differences in the two original magmas, may have been influential in ore fluid generation.

Davidson and Wyllie (1969) have suggested that the titanium-poor, oxidized magnetite in the diabase differentiates may have been mobilized to form the titanium-poor ore magnetite. However, oxidized mixed spinels are characteristic of most diabase differentiates whether or not there is any known associated ore (Table 34, point 12). Although data concerning quantity and location of magnetite in diabase relative to ore and non-ore situations are not known, from the available information there does not seem to be a direct relationship between the two magnetite occurrences. The mechanism of Davidson and Wyllie (1968) also requires the presence of a mobilizing fluid to collect and expel the ore solution from the diabase. The rapid, anhydrous crystallization of granophyre might leave a metasomatically active residual hydrous vapor phase capable of acting as an ore-fluid medium (Barker, 1970). There is no textural evidence that this occurred, although it would be difficult to detect. Because of the small volume of granophyre and its lack of spatial relationship in diabase to the movement of ore solutions above, filter-pressing of an interprecipitate liquid through a largely crystallized solid sheet would be required, with the collection of this fluid in a localized area below the southwestern portion of the eastern ore body. These fluids also would have to extract most of their iron from the oxides in the previously crystallized diabase pegmatite, the iron-rich phase of the diabase, whose volume at Cornwall (and elsewhere) is small and bears no spatial relationship to ore zonation. As a consequence of these observations, this mechanism presently seems unlikely.

Because there is no known spatial relationship between diabase differentiates and ore occurrences, and because the volume of these differentiates is small at Cornwall (Table 34, point 13), it might be suggested that this restriction favors expulsion from the immediately adjacent diabase. It could be proposed that there are few such differentiates because a mobile phase escaped the sheet boundaries, thus depleting the diabase in fluids of diabase pegmatite and/or granophyre composition, However, granophyre is present where there is no ore (e.g., Gettysburg, Quakertown, Palisades, and Karroo sheets) and at Dillsburg where ore occurs. Furthermore, such a suggestion would necessitate 1) removal from the diabase of a rather large volume of localized material, and 2) removal after crystallization of the chilled margin and after crystallization of the main body of the pluton, i.e., after iron enrichment had begun. The direct evidence for such a removal is scanty. The sodium and potassium metasomatism of hornfels units, particularly ferriferous orthoclase crystallization, might be related to the granophyric residuum in diabase, but such is not believed to be the case at Cornwall (see "Genesis of Potassium Metasomatism"). A "granophyre" outside the confines of diabase has been described from a core (A. Davidson, written communication) in the Triassic basin probably near Warwick (Morgantown Pluton), although its exact location has been lost. The core log alternates between "hornfels" and "granophyre." However, the granophyre, if such it is, is atypical; it is composed of layered or gradational mineral segregates, exhibits anastomosing apophyses, and is interlayered with hornfels units. Because of uncertainties about its location, its spatial relation to diabase, its identification as Triassic granophyre, and the identification of the hornfels units, this core information does not provide reliable evidence that *in situ* magmatic fluids have overcome the lithostatic pressure and penetrated the dense, crystallized diabase margin into overlying country rock. Elsewhere, (e.g., Hotz, 1950, 1953; this report), granophyre is entirely within diabase. Furthermore, there is no textural evidence that an intergranular liquid has been locally squeezed out of normal diabase and no evidence that large concentrations were removed from any area below ore (see points 5 and 6).

With the scant available data, it is difficult to find a clear indication of origin of the Cornwall, or province, ores from published sulfur isotope studies (Table 34, point 14). Enrichment in S^{34} is noticeably greater in Cornwall ores than in other ores of the province, and, consequently, the difference in S^{34} amounts between ore and diabase is probably also greater, although the critical data for Cornwall diabase are lacking (Smitheringale and Jensen, 1963). Closer correspondence in sulfur isotope composition between late diabase differentiates and ore might be expected where a volatile phase was directly expelled from diabase, with a short crustal transfer distance and hence little chance of crustal contamination. It can, therefore, be reasoned that the sulfur isotope data indicate a slight preference for a separate magmatic introduction of ore in a hydrothermal phase that migrated through a longer crustal distance, assimilating more crustal sulfur.

Within the qualifications and limits posed above, the authors believe the interpretations placed on the available data indicate that the iron ores at Cornwall resulted from a separate hydrothermal introduction after the injection of diabasic magma but from the same ultimate magmatic source area from which the *in situ* diabase sheet was derived. It seems logical that the younger (?) diabase dikes are a part of this magmatic system.

Early Magmatic History of the Cornwall Ores

The early history of the Cornwall tholeiite magma and ore-fluid phase is clouded with uncertainty. Chief among the problems is the necessity to extrapolate from the observed phases that crystallized in the upper crust back to compositions and geochemical environments that existed at higher temperatures and greater depths. For example, estimates of P_{O_2} (approximately the equivalent of f_{O_2} at high temperatures) must be based on extrapolations from laboratory measurements on synthetic systems, from compositions approaching that of basalt, from measurements with natural-rock basalt melts and lava flows, and from $Fe0/Fe_2 0_3$ and TiO_2 compositions chiefly in late-crystallizing opaque oxides. Deductions from the latter are dependent upon the time of spinel crystallization relative to magma stage, a temporal position not always easily determined. As Hamilton and Anderson (1967, p. 468) have pointed out, there is no known direct relationship among composition, temperature, and P_{O_2} (or P_{H_2O}). Fudali (1965) noted that P_{O_2} ranging from $10^{-6.4}$ to $10^{-8.5}$ atm did not noticeably alter the oxidation state of a basalt. However, P_{O_2} and P_{H_2O} can be expected to influence the direction of fractionation, particularly iron enrichment and depletion trends (Hamilton and Anderson, 1967; Taylor and Epstein, 1963; Yoder and Tilley, 1962; Osborne, 1959 and 1962; Kennedy, 1948 and 1955). Based on experimental data and observations from the Cornwall area, some speculations can be advanced about the Cornwall magma that are pertinent to our understanding of the formation of an ore fluid.

The Cornwall diabase differentiation trend departs only slightly from that of other diabases (e.g., Karroo) and from tholeiite basalts, none of which have associated ore deposits. The Cornwall granophyric differentiates are unusually rich in $K_2 0$, with $K_2 0/Na_2 0 \gg 1.0$. Normal Cornwall diabase contains somewhat less $K_2 0$ and probably less $Na_2 0$ than most other sheets in this province (Appendix 5-A), and less than most average tholeiites (Appendix 5-B), indicating late relative alkali enrichment and an overall sheet deficiency because the granophyre is volumetrically small. (The gradient for $K_2 0$ increase versus $Si0_2$ during differentiation is unusually steep for a tholeiite, resembling some alkali basalt trends (Kuno, 1968, Figure 39)). Total iron throughout normal diabase is noticeably lower than in most diabases and tholeiites (Table 32). The amount of iron in the chilled margins also is low (Figure 56 and Appendix 4-A), so that any removal of iron from the sheet magma may have been completed by the time of early olivine and pyroxene crystallization. (Late iron enrichment in Cornwall diabase is volumetrically small and normal in trend for diabase differentiation suites.) Some Cornwall diabase mineralogy is also pertinent: less ferriferous augite than at Dillsburg, the presence of free quartz, the scant amount of olivine, and replacement of chilled-margin olivine by the hydrous phases, serpentine and hornblende. These data are believed to indicate that the sheet magma was depleted in total iron, perhaps resulting from oxidation with a greater than normal P_{O_2} in the early magma, influencing somewhat the subsequent chemical and mineralogical differentiation.

Experimental data also apply to these observations. Kennedy (1948) suggested that early oxidation of a magma can result from reaction with a volatile phase at high temperatures and that such a reaction will prevent olivine from forming, resulting in free quartz and magnetite. Kennedy (1955, p. 50) also noted that at moderate to high partial pressures of oxygen a spinel will crystallize before silicates. Hill and Roeder (1967) concurred, but noted that if f_{O_2} is low, high chromium contents are required; otherwise, at high f_{O_2}, spinel crystallizes early in normal tholeiites. In a summary discussion, Hamilton and Anderson (1967, p. 461-463) concluded that a high initial P_{O_2} favors early depletion of iron in the magma, presumably by spinel crystallization, but noted also that P_{O_2} declines as crystallization proceeds, even though P_{O_2} increases. They calculated (Hamilton and Anderson, 1967, p. 472) that in a melt with two percent H_20, 15 percent Fe0 would oxidize to Fe_20_3. The early oxidation of iron and the crystallization of spinel would inhibit the incorporation of iron into early silicates, i.e., into olivine and pyroxene. An iron-rich fraction would thus accumulate, the spinel (iron-bearing) as crystal accumulates and the liquid as magma following an iron (-titanium) enrichment trend. A high H_2O content early in the Cornwall magma may have caused amphibolitization of early olivine (see Part 5) and perhaps a high P_{O_2}, in the neighborhood of 10^{-6} to 10^{-7}atm (see "Titanium-Iron Distribution, P_{O_2}, and Ore Origin"), that would have a small effect on the diabase oxidation state. Taylor and Epstein (1963, p. 55) also suggest such a role for H_20 in a discussion of the Skaergaard magma. Magmas in this diabase–ore province not depleted in iron (and not associated with ore) may not have suffered early spinel withdrawal and hence a primary magma, if a single one existed, may have undergone variable oxidation (see Wright and Weiblen, 1967). Alternatively, separate magma sources or unusual structural conditions at Cornwall may have existed near the base of the crust that caused differences in oxidation. Another, or contributory, process may have been the separation of an iron-rich fraction from the silicate melt as a result of the assimilation of limestone at some point during upward magma transport. Ovchinnikov (1959) has shown that this may occur with resultant metallic iron, magnetite, or hematite separation, depending upon the partial pressure of oxygen. He also notes (Ovchinnikov, 1960) that in a basaltic melt, the resultant iron-rich mineral component is titanium-poor, although the basalt contained a significant amount of titanium. Thus, a method exists for the early separation (i.e., before differentiation) of iron and titanium.

The next conjectural step is to examine the possibility that an iron-rich (spinel) magma fraction withdrawn at an early magmatic stage (before final diabase emplacement) could have been the source of the Cornwall deposit. Certainly it seems necessary that the low total iron content through all sheet differentiation stages must be genetically related to some mechanism for early withdrawal of iron from the magma. Differences in diabase gold content between Cornwall (0.4-8.1 ppb) and Dillsburg (8.5-22.6 ppb) also support an early chemical fractionation. Considerable structural, textural, and zonation data have been discussed that favor a source more distant than the adjacent sheet (also see Table 34). Sulfur isotope ratios support, but do not prove, a longer crustal path at Cornwall than at Dillsburg (where Hotz (1953) advocated diabase expulsion of ore). However, production of a mobile hydrothermal ore phase from the Cornwall tholeiite magma at depth is not an easy process to envision, even though there could have been an iron-rich fractional accumulation of spinel. A high water content (and probably alkalies) is required. Any such low density phase in the magma chamber would have had to be tapped together with the higher-density, more iron-rich, phase after withdrawal and after emplacement of the diabase tholeiite sheet magma. One or more of several conditions may have obtained. Initial crystallization of anhydrous minerals (olivine, plagioclase, and pyroxene) would have enriched the liquid in dissolved water. Although withdrawal of a high-temperature diabasic magma also might have left a more fluid residuum, it is difficult to conceive of a situation whereby this residuum would be left behind. However, if magma-chamber stopping, especially selective melting of low-melting-temperature fractions, continued after diabase magma withdrawal, and/or if the temperature at which subcrustal fractional melting was taking place decreased after sheet-magma tapping, there would be an increase in the ratio of hydrous fractions and of "incompatible elements" to major elements added to the magma. Potassium, the major metasomatic component, is one of these incompatible elements (Green and Ringwood, 1969). Somewhat similarly, reaction between ore fluid and hydrous crustal wall rocks during ascent may have contributed to ore-mobility (not supported by the meager sulfur isotope data). Mafic cation and halogen or alkali complexes may have been important in uniting and mobilizing the two fractions of the hydrothermal ore fluid, but data supporting such a process are lacking.

Regardless of the difficulties of such a distant magmatic source, and they are many, the authors feel compelled to support such a suggestion on the basis of observational data. Because other diabase provinces do not have any associated potassium metasomatism or magnetite-sulfide ore, the history of the Cornwall (and Dillsburg?) magma is believed to have been unique, perhaps along the lines outlined here.

Environment of Ore Transport and Deposition

Discussions of the character of ore solutions during transport and deposition have waged a long battle in the geologic literature, and this is as true of magnetite ores as of base-metal sulfides. The principal discussions, still in progress, have concerned the alkalinity or acidity of the ore solution, the redox characteristics of the ore fluid, whether ore is transported in gaseous or liquid solution, and whether the ore metal has been carried as a cation, a colloidal suspension, or a complex ion. Although the answers to these questions are important to a complete understanding of the ore process at Cornwall, they cannot be answered satisfactorily by field observations and will have to await additional ore-solution experimentation. A few observations, however, are pertinent. In the light of recent sulfide and magnetite ore studies, it is felt that brief mention of their possible applicability to Cornwall is deserved. No attempt has been made to make a comprehensive survey of all of the available experimental data.

In discussing magma fractionation, an ore-phase separation has been referred to as a hydrothermal solution containing mobile cations that may have considerable amounts of dissociated ions and complexes. The term pneumatolytic has not been used because it implies a gas phase in equilibrium with a magma. Once the ore-bearing fluid moves away from its source such equilibrium no longer obtains. The general term "ore fluid" is used here to include the hydration and dissociation of at least some of its components, particularly near the site of deposition. As Holser and Schneer (1961, p. 377, 382) have demonstrated for iron in the $HC1\text{-}H_20$ system, solvent action, not volatility, has the greater influence upon iron concentration and transfer.

Holser and Schneer (1961) found that iron concentration in HC1 solution increased with increasing acidity, probably carried as the ferrous ion by reaction with the hydrogen ion (Holser and Schneer, 1961, p. 380):

$$2FeFe_20_4\ (c) + 12H^{+} = 6Fe^{+2}(aq) = 6H_20(l) = 0_2(g) \tag{6-3}$$

They conclude that "geologically significant concentrations of iron can be mobilized at temperatures and pressures similar to those at which hydrothermal deposits were formed and in solutions two orders of magnitude more dilute in HC1 than these natural fluids" (Holser and Schneer, 1961, p. 382) and, again, that they "can suggest no mechanism by which it (iron solubility) will increase in basic solutions" (Holser and Schneer, 1961) despite the recognition that many geologists have favored alkaline transport from a magma residuum (e.g., Kennedy, 1955; Ridge, 1965B; Turner, and Verhoogen, 1958, p. 143-144). Holser and Schneer further note that acid transport simplifies deposition in carbonate host rocks by neutralization. At Cornwall, carbonate rocks are the favored lithology for magnetite replacement and this is perhaps the strongest argument in favor of acid transport. A similar conclusion for magnetite metasomatic replacement was reached by Sangster (1969) from a study of deposits near Vancouver and from a review of the literature.

On the other hand, metasomatism just previous to ore deposition shows enrichment in K_2O in the eastern ore body (although less is known from the western ore body, it is believed to be farther from the area of ore solution introduction). Normal Cornwall diabase is slightly deficient in Na_2O and K_2O, raising the possibility that one or both may have been part of the ore-transport fluid. Chlorite is one of the minerals most closely associated with magnetite deposition. Subsequent to the ore stage, zeolites predominate. Each of these observations suggest that by the time the ore fluid was depositing most of the magnetite and sulfides, conditions were alkaline.

In an experimental study of the iron sulfide-oxide system, Barnes and Kullerud (1960) note that at about 250° C, neutral pH is about 5.6 and that magnetite probably is stable only in alkaline solution (Barnes and Kullerud, 1960, p. 137). Increases in total sulfur concentration will increase the alkalinity, at constant P_{O_2} and temperature (Barnes and Kullerud, 1960). They note that at a total sulfur concentration of 10^{-3} moles, simultaneous deposition of pyrite, pyrrhotite, and magnetite can occur. The pH may, however, become more acidic if P_{O_2} decreases as crystallization passes from magnetite to pyrite, a paragenetic situation common at Cornwall (assuming no change in total sulfur concentration). Thus, in the system magnetite-sulfides, which is typical at Cornwall, an alkaline pH at or near the site of deposition seems reasonable.

The paragenetic sequence of metallic minerals at Cornwall shows that pyrite both precedes and follows magnetite crystallization, with pyrrhotite probably following magnetite. Siderite is not present. These observations, which place certain limits on the concentrations and partial pressures of oxygen, sulfur, and carbon dioxide, can be compared with experimental results. Because of the sequential shift from pyrite to magnetite and back to pyrite, a change in P_{S_2} might be expected. However, Salotti (1964) has discussed this problem and concludes that the sequence from magnetite to pyrite to pyrrhotite can be explained essentially as a decrease in the partial pressure of oxygen with nearly constant P_{S_2} at a constant temperature of about 600° C and 1000 atm total pressure. Thus, the final crystallization of pyrite may indicate only a slight increase in P_{S_2}.

In the system $Fe\text{-}S\text{-}H_2O$ at 1 atm and 25°C, Garrels and Christ (1965, p. 159) have demonstrated that the sequence hematite, magnetite-pyrite, and pyrrhotite-pyrite or pyrite is possible by decreasing P_{O_2} without necessarily increasing P_{S_2} (see Figure 57). Although partial pressures will change considerably at the elevated temperatures of Cornwall ore deposition (for example, a constant P_{O_2} can be expected to become less oxidizing as temperature increases (Barnes and Kullerud, 1961, p. 664), similar phase relationships between P_{O_2} and P_{S_2} are possible. Three sequential crystallization paths are illustrated (Figure 57) that range from a maximum P_{S_2} fluctuation (path 1) to a minimum fluctuation (path 3). The sequence at Cornwall fits well into a scheme of generally decreasing P_{O_2} : hematite followed by pyrite, pyrite-magnetite, pyrrhotite or pyrrhotite-magnetite, and pyrite (Figure 57, path 2). The association chalcopyrite-pyrite also limits P_{O_2} and P_{S_2} (Barnes and Kullerud, 1961, p. 169) and is compatible with this trend. The final crystallization of pyrite and zeolites (± calcite) probably represents slightly increasing P_{S_2}, particularly since it is a lower temperature assemblage in which P_{O_2} will oxidize more effectively. However, the applicability of this scheme depends greatly on initial temperature and temperature changes during the crystallization sequence, factors that would modify the trend path but probably still under a generally decreasing P_{O_2}.

Most methods of estimation of the temperatures of Cornwall ore deposition are in the neighborhood of 500° C or less. The transformation of pyrite and magnetite to pyrrhotite and hematite occurs at 675° C at P-total $= 10^{-2}$ atm (Barnes and Kullerud, 1961, p. 671), and is certainly above the temperature of magnetite crystallization throughout most of the deposit (the pyrrhotite-hematite assemblage is not present). A somewhat lower maximum of 650° C was proposed by Tsusue (1964) for the similar Morgantown deposit on the basis of subsolidus temperatures derived from X-ray study of calcite-dolomite veins. He also estimated the temperature of the Morgantown ores as not greater than 500° C on the basis of the magnetite-serpentine association (also present at Cornwall) and the amount of $MgCO_3$ is solid solution in calcite associated with magnetite. Below 560° C, Barnes and Kullerud (1961) note that the assemblages pyrite-megnetite-pyrrhotite and hematite-magnetite-pyrite are stable, although experimentally, reactions became sluggish below 500°C. From the small amount of titanium in the Cornwall magnetite ore, utilizing the data of Buddington and others (1955), ore-forming temperatures would not have exceeded 500° C, although the applicability of their diagram is uncertain for this association at such low titanium concentrations. Sangster (1969) concluded that magnetite replacement of limestone in southwestern British Columbia occurred between 500° C and 600° C, a conclusion that also seems reasonable for the Cornwall deposit.

Conclusions On The Origin Of Cornwall Ore

Field and laboratory evidence point to an origin for the Cornwall magnetite that is not directly related to the adjacent diabase sheet. Rather, the evidence indicates that both are related to a common magmatic source. One possible

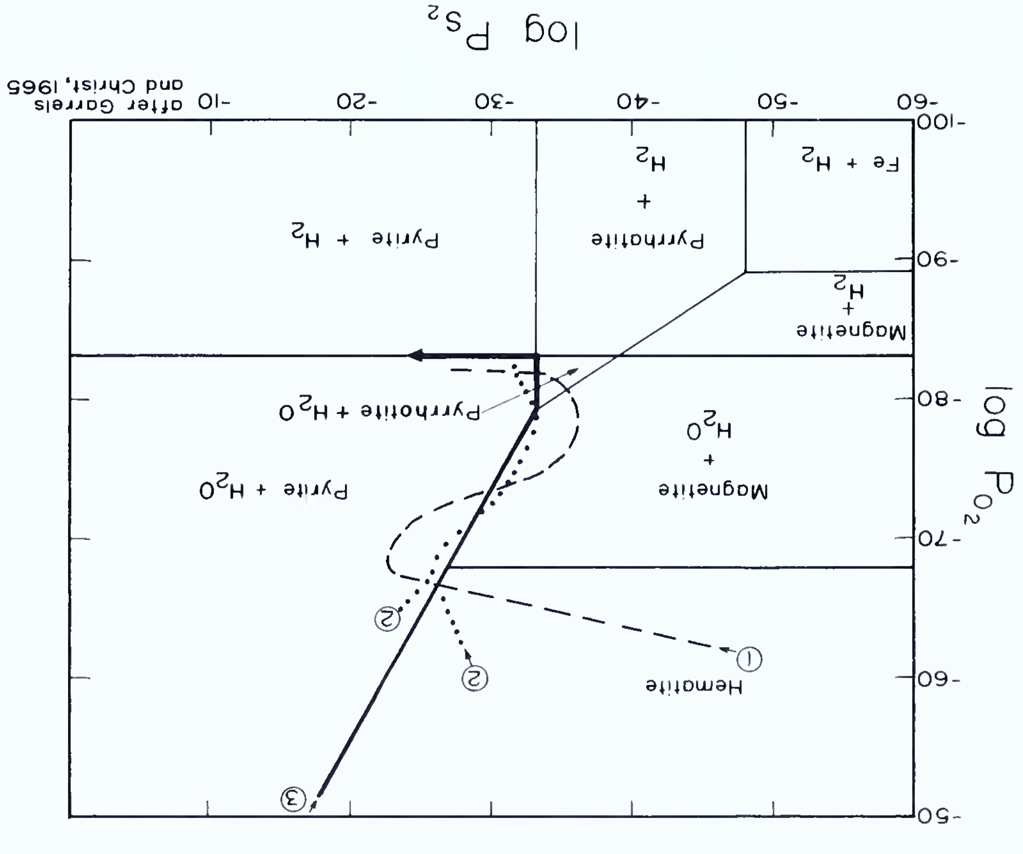

Figure 57. Phase diagram of sulfide-oxide stabilities as a function of P_{O_2} and P_{S_2} at one atm. total pressure and 25°C. Trends 1., 2., and 3. might have existed at Cornwall at higher temperatures (see text); after Garrels and Christ (1965).

mechanism has been proposed as an explanation for this unique association in a unique structural environment; it is that a primary magma, or magmas, of tholeiitic composition was the source for an early volcanism, followed by later injections of sheet diabase and metasomatic and hydrothemal ore fluids. The proposed mechanism for this series is based partly on early spinel crystallization fractionation followed by anhydrous silicate mineral crystallization, and partly on temperature fluctuations at the site of magma generation with tapping of the different melt fractions. As a consequence of sheet magma withdrawal, early crystallization, and continued but lower temperature fractional melting of the subcrust, the remaining magma would become more fluid and could have combined with an iron-rich spinel residumm to form a hydrothermal ore fluid. Other, or more refined, mechanisms eventually may prove more satisfactory, but will not necessarily vitiate the fundamental requirement for a separate, more distant source of iron than can be provided by the adjacent Cornwall diabase sheet. The ore fluid contained iron, sulfur, copper, nickel, gold, silver, alkalies, and perhaps boron and halogens. Late stage mineralization indicates alkaline conditions of crystallization which could have been modified from acid transport by host rock reaction. Crystallization of ore occurred near 500° C and under a decreasing P_{O_2} environment, perhaps at a nearly constant P_{S_2}, until late stage ore deposition, when P_{S_2} increased slightly.

SUMMARY OF POST-PALEOZOIC GEOLOGIC EVENTS AT CORNWALL

From the foregoing discussions of structural deformation, ore deposition, metamorphism, and magma generation, it is possible to reconstruct an abbreviated sequence of the major geologic events in the Cornwall area bearing upon the genesis of the Triassic magma and magnetite ore. For the sake of clarity, details are omitted, minor events not summarized, and generalizations made that only approximate the conditions as they are believed to have existed.

1. Basement-controlled Triassic downwarp and/or faulting was initiated and red-bed sedimentation from a southerly source was followed by a north source influx. A few basaltic flows extruded near the end of sedimentation along the north margin.

2. Deformation of the basin which included rotational tilting and high-angle faulting (particularly along basin margins; see Faill, 1969), and probably overthrusting against the north margin shelf. In part, these events may be genetically and temporally related to magma generation and movement at depth before sheet emplacement.

3. Magma generation (by fractional melting?) occurred, perhaps locally under conditions of differing P_{O_2} and/or P_{H_2O}. before and/or during

magma ascent. It is suggested that fractional crystallization and separation of an early (Fe) spinel-rich component somewhat depleted the presently emplaced Cornwall diabase magma in total iron and that this fraction was not tapped at the time of sheet emplacement.

4. Emplacement of the Cornwall north limb diabase followed along structural discontinuities and rafted Cambrian limestone, and occurred during or after south limb emplacement, rotational tilting, and domain folding. Magma engulfed blocks of Cambrian limestone, Blue Conglomerate, and Mill Hill Slate of Ordovician age, but did not appreciably assimilate them. An upper chilled facies, cooling with the local development of contraction cracks, effectively sealed the pluton from the possible escape of mobile constituents.

5. A second magma injection may have occurred below the main sheet and before its solidification. The sheet exhibits alternate chemical and mineralogical cryptic layering of the basal 200 feet.

6. Contact metamorphism of the adjacent host rocks extended into the hornblende-hornfels facies and was accompanied by migration of constituents such as potassium, sodium, and calcium, and probably silica along with H_2O and CO_2. Mineral reactions reduced the oxidation state of pre-existing sediments, except locally at formational and lithofacies contacts where hematite crystallized. A maximum temperature of 600-700° C is estimated.

7. *In situ* crystallization of diabase began at the top of the sheet, and then took place in the basal and central portions. Normal differentiation trends yielded enrichment in iron and titanium (diabase pegmatite), followed by silica, sodium, and potassium (granophyre). The solidification index for the rocks of these stages indicates that maximum titanium enrichment may have slightly preceded that of iron. A rather rapid increase in Fe^3/Fe^2 at constant SiO_2 may have inhibited total iron enrichment. The crystallization sequence is similar to that for an oxygen depletion scheme. Late stage rocks exhibit deuteric oxidation and hydration of earlier-formed minerals.

8. It is suggested that a potassium-rich ore fluid was tapped from a lower-temperature magma chamber after jointing and faulting of the diabase sheet had provided a channel to host rock above diabase. It is assumed to have moved along the path of ascent of the previous diabasic magma. Metasomatism preceded and was continuous with the hydrothermal ore solution. During alteration and chemical exchange processes, the chilled margin was retrograded and partly replaced by metasomatic orthoclase, diopside, and then by ore minerals. Oxides and sulfides of metallic cations followed during the ore stage, probably with decreasing P_{O_2} at the site of deposition. The ore fluid spread out and upward from a fault focal lineament on the western side of the eastern ore body. Some ore replaced limestone

below diabase on the east side of the fault. Late-stage chloritization and zeolitization followed as pH increased slightly. Ore deposition was accompanied by small scale deformation, including post-ore faulting.

9. The last tapping of the magma chamber at a higher temperature produced dikes that are more ubiquitously distributed than the sheets. The extensional stress that yielded the intruded fractures is believed to result from extension that encompassed the entire length of the Appalachians. Local fanning of the fractures may be an indication of the superposition of local stress fields. These events are believed to be related to continental rifting.

10. Erosion of several thousand feet of Triassic sediments and diabase.

THE TRIASSIC METALLOGENIC PROVINCE

Structural Environment and Diabase Sheet Terminology

The Triassic metallogenic province extends from the magnetite deposits of the Dillsburg district on the southwest to magnetite deposits of the Boyertown district more than 100 miles to the northeast (Figure 58). The Gettysburg "sill" (southeast limb of the Gettysburg Pluton) south of the Dillsburg district is associated with some magnetite ore. The belt of magnetite occurrences is not only restricted to associated sheets of diabase, in contrast to narrow, barren dikes, but also to that part of the province that strikes nearly east-west. The two major deposits, Cornwall and Morgantown, are located near a major flexure in the regional strike.

Local structural relationships between ore and diabase are important in understanding the mode of ore introduction and the sequence of events. Although most ore bodies lie above diabase, ore at the Doner mine northeast of Cornwall and at the Esterly mine (Spencer, 1908) in the Jacksonwald syncline to the east is below diabase. Ore at the Carper mine west of Cornwall lies in a normal fault north of south-dipping sheet diabase (Spencer, 1908) and therefore, depending on the amount of fault displacement, also may be below diabase (Geyer, 1970). As discussed previously, these occurrences are inconsistent with the hypothesis that the ore fluid was expelled upward out of the adjacent diabase sheet. Fault relationships at the Carper mine (Geyer, 1970) as at Cornwall, give evidence of at least one episode of faulting after diabase sheet injection and before ore introduction. At the Carper mine, the ore lies in a fault parallel to, and at, the present north Triassic sediment margin. This fault appears to transect sheet diabase and is in turn offset by a north-south tear fault. Consequently, ore was introduced after one, or both, episodes of faulting.

Based on their outcrop pattern, gravity data (Hersey, 1944), and aeromagnetic patterns (Bromery and Griscom, 1967; R.W. Bromery, written communication), the diabase plutons can be divided into four major plutonic units (Figure 58). Three of these major diabase plutons can be further subdivided into individual, although connected, sheets, each with its own ring-shaped closure, or partial closure. Minor offshoots and subsidiary sheets probably belong to the main pluton (see Hotz, 1952). In the past, various parts of the major plutons have been given individual names, such as Gettysburg Sill for the southeastern edge of the pluton near Gettysburg (Stose and Bascom, 1929) or Shelly Intrusive for the northern part of the eastern sheet in the Quakertown Pluton (McLaughlin, 1959). Other authors have extended some of these more specific names to a larger part of the diabase (e.g., Hotz, 1952; Beck, 1965; De Boer, 1968). Hotz (1952) recognized that many of these individually named sills are actually part of a single, connected sheet, in part stripped by erosion. Recognition that four major closures exist allows convenient reference to them as well as to specific sheets within the major plutons. Accordingly, the following teminology is used in this report until more formal names have been applied, keeping in mind that separate sheet names are not meant to imply separate sheet intrusions.

The Gettysburg Pluton encompasses an entire diabase outcrop and ring closure from the Maryland border to Bowmansdale and Lewisberry, northeast of Dillsburg and southwest of the Susquehanna River (Figure 58). Discordant diabase divides this pluton approximately in the center. The southwestern portion of the pluton is referred to as the Cashtown sheet and the northeastern portion as the Dillsburg sheet. The southeast limb is largely concordant. According to Hotz (1950), an upper, eroded sheet near Dillsburg is discordant at the north border.

The York Haven Pluton (equivalent to Yorkhaven, a site name that now is spelled York Haven) encompasses diabase closures from just southwest of the Susquehanna River to just east of Cornwall (Figure 58). The name "York Haven" was used by Stose and Jonas (1933 and 1939) for the south limb of the pluton. Beck (1965) evidently extended the term Yorkhaven Sill of the former authors to include the whole diabase pluton. The western ring-shaped outcrop area of this pluton is referred to as the Middletown sheet, the middle closure as the Bachmanville sheet, and the eastern part as the Cornwall sheet.

The Morgantown Pluton encompasses the Birdsboro-French Creek-Morgantown mining areas and appears to be a single sheet closure. Although the southern part of this pluton has been referred to as the St. Peters Sill (Stose and Jonas, 1939) and the entire pluton as the Birdsboro body by Beck (1965), the name Morgantown Pluton is preferred. The diabase at Birdsboro appears to be somewhat atypical in terms of texture and the sill terminology is not applicable to all the diabase.

The Quakertown Pluton encompasses a series of four major diabase outcrop rings from Boyertown on the west to Coffman Hill on the east (Figure

58). Locally, near Boyertown, some granophyre is present (Hotz, 1952, p. 384). The eastern and western parts of this pluton have been referred to as the Haycock Sill (including the Shelly Intrusive) and the Ziegler Sill (equivalent to Zieglersville?) respectively (Stose and Jonas, 1939, p. 125 and Fig. 7). In this report, the eastern sheet closure is called the Haycock sheet, the central ring the East Greenville sheet, and the western ring the Ziegler sheet, recognizing that these are probably a single major pluton (Hersey; 1944) stripped by erosion to the present outcrop pattern, as suggested by Hotz (1952). At Coffman Hill, east of the Haycock sheet, there is another diabase erosional remnant that was probably part of the Quakertown Pluton. A joining anticline of diabase is common to each adjacent pair of diabase sheets, excluding the deeply eroded Coffman Hill sheet.

In addition, a small syncline (Jacksonwald) containing a diabase sill and an overlying basalt flow is present between the Morgantown and Quakertown plutons (McLaughlin, 1959). For reference, these are termed the Jacksonwald sheet and the Jacksonwald flow respectively.

Each of the four main plutons is separated from its neighbors by intervening Triassic sediments unbridged by diabase. As noted previously, the east and west margins of major plutons where diabase is discordant may, in part, represent faults along which emplacement of diabase magma occurred. The use of separate names for these saucer-shaped sheets is not meant to imply a separate feeder for each; a single channel to magma at depth may have supplied the magma for each major pluton. Feeders for individual sheets would then be offshoots from the main channel and would be controlled by local structure. Other small sheets undoubtedly exist (Stose and Bascom 1929); some probably eroded away.

It has been suggested here that the saucer shape of all major plutons may be geometrically similar to that at Cornwall. Such a suggestion implies that the saucer shape results from lithologic and structural boundary controls. Thus, on the south, east-west striking portions of sheets are essentially (but not wholly) concordant with Triassic lithofacies boundaries. On the north, east-west striking portions are controlled by south-dipping, overlapped erosional surfaces but, in places, appear to transect Triassic sediments (Hotz, 1952, Figure 3). Faults may have played an important role in this transection. The change in dip of the sheet, i.e., at the center of the saucer, could have been determined by pre-existing lithologic or structural discontinuities; e.g., by a thrust-slice fault plane in Cambro-Ordovician rocks that steepens at depth, by a buried erosional fault scarp (either of major or minor displacement) that was active at least through part of Hammer Creek time, by a down-warped Paleozoic erosional shelf, or by roof-collapse faulting resulting from magma movement northward and upward.

The presently exposed shape may be in part, the result of erosion that exposed different sheets at different levels. Nevertheless, controls must have acted on the rising magma that limited the stratigraphic horizon to which it rose. The weight of lithologic overburden of youngest preserved Triassic sediments is among the most important of these. Chilled margins, diabase textures, and contact metamorphism indicate that nowhere is there exposed a surface flow directly associated with a major diabase pluton (the surface volcanics at Bendersville and Jacksonwald are not parts of major plutons as far as is known). If such occurred, the record of it has been lost by erosion. Other factors were also important in controlling the level of the sheets. Upward or lateral magmatic force was a function of volatile content, fluid viscosity, extent of cyrstallization at depth and during ascent, channel-wall friction, and differences in density. If, for example, the ascending magma at Dillsburg had a greater proportion of volatiles, and more, less dense material than at Cornwall or Morgantown, it might have risen to a higher sedimentary level. If erosional stripping is a constant, then we could be viewing deeper levels of these sheets to the west (and the extreme east) than in central basin areas. In spite of this conjecture, however, the localization of all sheets in the Hammer Creek and its equivalents (except for a part of the Morgantown Pluton) suggests that ease of intrusion into these upper stratigraphic levels exerted a noticeable control on their present position along the present north basin margin.

Detailed study of all of the diabase sheets and associated magnetite deposits has not been made, although some detail is available for all of them, particularly the Dillsburg, Cornwall, and Morgantown districts. If the conditions hypothesized for the Cornwall magma and ores are correct, two distinct processes could have been responsible for the formation of the magnetite ores of the province. Ore expelled from diabase could be represented by the Dillsburg district and hydrothermal ore from a magma at depth by the Cornwall and Morgantown districts (see Sims, 1968, for a discussion of ore origin at Morgantown). In the light of these possibilities, the entire metallogenic province has to be reexamined.

Aeromagnetic Data

The Triassic igneous province is well defined by magnetic highs and associated lows (Bromery and Griscom, 1967). Closure of magnetic contours verifies the outcrop form of the major plutons and individual sheets within the plutons as representing the actual three-dimensional closure of sheet-like bodies. It is partly on this basis that a valid geometry for naming them has been proposed here. Within the closure of the highs that represent diabase outcrop, a typical birds-eye-maple contour pattern is present, reflecting the presence of small plutons and sheet irregularities at depth, some metamorphic and ore effects in the overlying Triassic sediments, and probably the character of the underlying Paleozoic shelf along the north margin. Each of the pluton and sheet closure areas is characterized by a distinct magnitude and pattern of gamma relief and is listed below in order of decreasing magnitude of magnetic relief:

1. Dillsburg sheet in the Gettysburg Pluton (probably a shallow sheet with some effects from underlying Precambrian basement).

2. All three sheets of the Quakertown Pluton (with more steeply dipping limbs than is characteristic of most other sheet limbs).

3. Morgantown Pluton.

4. Cashtown sheet of the Gettysburg Pluton (also perhaps a rather shallow sheet).

5. Middletown and Bachmanville sheets of the York Haven Pluton.

6. Cornwall sheet of the York Haven Pluton.

It may be significant that the greatest gamma contrast is between the area over the York Haven Pluton, and more specifically the Cornwall sheet, and the area over the Dillsburg sheet. At least in part, this difference may be the result of the varied quantity of magnetic oxides present in the respective diabases (and the adjacent overlying sedimentary units), and perhaps can be approximated by total iron content in the sheets (assuming the effects of Paleozoic sediments to be a constant, or negligible). Relationship between aeromagnetic relief and total iron of diabase might prove a fruitful tool for determining general levels of iron distribution though the province diabase where sheet depths and thicknesses are known. However, the distribution and quantity of magnetic oxides in diabase differentiates also must be considered (Beck, 1966), as well as the direction of remanent magnetization. At Cornwall, the latter is in opposition to the present field direction, tending

Table 35. *Sulfur Fractionation in Triassic Diabase and Ores (from Smitheringale and Jensen, 1963)*

	δS^{34} (0/00)
A. Diabase (from SW to NE)	
Goose Creek, Va. (stock)	+0.4
Gettysburg, Pa. (sill)	+0.1 to +1.0
Birdsboro, Pa. (sheet)	-0.1
Palisades, N.J. (sill)	-0.2 to 0.0
B. Diabase Differentiates (from SW to NE)	
Goose Creek, Va.	+1.4 to +5.4
Birdsboro, Pa.	+1.6 to +8.7
Palisades, N.J.	+0.2 to +4.9
C. Diabase Dikes	
North Carolina	-3.6 to +3.7
Conshohocken, Pa.	+1.5
D. Ores and Sulfide Veins (Pyrite) (from W to NE)	
Dillsburg, Pa.	+5.2 avg.
Cornwall, Pa.	+12.4 avg.
French Creek, Pa.	+5.4 avg.
Palisades, top of sill, N.J.	+7.2

to decrease the overall gamma level. Some individual highs, not directly over surface diabase, probably are related to magnetite concentrations. In the Dillsburg and Middletown sheets, there are small highs where local olivine or bronzite concentrations have been noted, although any actual correspondence with amount of iron (-titanium) oxides is not known. Highs may also be evidence of a locally shallow depth to the pre-Triassic basement or of feeder channels for the diabase sheets.

Magnetic lows, especially in the Cornwall sheet and the Quakertown Pluton, are most noticeable along the north outcrop belt of diabase and much less pronounced along the south. This is true along both the upper and lower sedimentary contacts. At least in part, these lows probably are related to magnetic contrasts resulting from diabase contact metamorphism and the attitudes of diabase and country rock (Beck, 1966, p. 115).

Sulfur Isotope Data

A summary of the sulfur isotope data of Smitheringale and Jensen (1963) for the Triassic rocks of eastern North America is presented in Table 35. For diabase samples, they reported no evidence of contamination of diabase magma by crustal sulfur, derived from the observation that the values cluster around meteoritic and mantle sulfur abundances (Smitheringale and Jensen, 1963, p. 1195). A gradual enrichment in S^{34} from normal diabase through the late differentiates (Table 35) is found throughout the diabase province. Although their sampling distribution is erratic, there is some indication of greater variation within dikes than within sheets (cf. Table 35-A and C). From the available chemical and petrographic data on the dikes (see previous discussion of "Diabase Dikes of Pennsylvania") as well as the sulfur isotope data, it is evident that the two diabase forms should not be equated; the possibilities of crustal contamination and igneous differentiation should be thoroughly investigated for the dike magma. Similarly, until results from ores and sheets are compared for the same sheet-ore association, any conclusions drawn must be tentative. For example, data on the ore at Cornwall cannot be directly compared with diabase data from the Gettysburg sill, especially if metallic ore mineralization at the two locations was introduced along different transport paths.

Sulfur-isotopes in pyrite of the Dillsburg and French Creek ore zones are less enriched in S^{34} than at Cornwall, and are also within the range of the results for late-diabase differentiates (Table 35). Although each location is represented by only three or four samples (Smitheringale and Jensen, 1961, p. 1201), the large difference between isotopic enrichment in the Cornwall and Dillsburg ores is suggestive of a different genetic mechanism or transport path for the ore-forming fluid. Enrichment in S^{34} may occur during differentiation, presumably as a function of oxidation, fractionation, contamination, or by formation of sulfate from a sulfide. For Dillsburg pyrite, sulfur-isotope abundances (low S^{34} enrichment) are consistent with a residual diabase fluid that escaped from the adjacent diabase if sulfur isotope abundances of the Dillsburg sheet are the same as those in the adjacent sheet of the same pluton at Gettysburg (Table 35); however, no data have been reported from the Dillsburg sheet adjacent to ore. The general uniformity of Pennsylvania Triassic sheet diabase sulfur-isotope analyses makes this assumption seem probable and is consistent with the ore expulsion theory of Hotz (1953) for the Dillsburg district. The Cornwall isotopic abundances, on the other hand, show a much greater S^{34} enrichment than later differentiates from other sheets. Again, data on diabase-differentiate sulfur abundances at Cornwall are lacking, so that comparisons may be misleading. Assuming, however, that the high S^{34} Cornwall ore characterizes a wide divergence from isotopic sulfur abundances in late differentiates, then an ore mechanism different from that at Dillsburg is implied for Cornwall.

If a vapor phase were formed at some time in the history of the Cornwall magma, and it is probably possible only at a low confining pressure, H_2S would be favored over SO_2. Consequently, the vapor phase would become impoverished in S^{34} relative to the remaining *in situ* diabase magma from which the vapor phase separated. Because this phase separation would have occurred after differentiation crystallization had begun, some enrichment in S^{34} already would have taken place. The vapor phase then would be sulfide and S^{32} enriched relative to the remaining magma. Cornwall ore is not enriched S^{32} relative to any of the diabase differentiates analysed.

To obtain S^{34} enrichment of an ore solution by crustal contamination, probably the only remaining feasible process, the path that the ore solution traveled, would have to have been longer at Cornwall than at Dillsburg because of the greater S^{34} enrichment at Cornwall (assuming the same original sulfur isotope composition for both magmas). If anything, the reverse is true; the ore deposits are concentrated at Cornwall and scattered at Dillsburg. Because of this, and because there is a greater discrepancy between sulfur isotope composition of Cornwall ore and diabase differentiates than elsewhere in the province (Table 35), these data tend to support an ore derivation at Cornwall that is not directly related to the adjacent diabase.

Titanium-Iron Geochemistry and Province Ore Origin

One of the most notable characteristics of the Cornwall ore body, and in fact of the whole Triassic magnetite metallogenic province, is the lack of titanium in the ore zone magnetite. On the other hand, the opaque minerals in the diabase, especially in the later pegmatite and granophyre differentiates, contain considerable quantities of titanium. At first glance, this would appear to rule out the diabase differentiates as a source for the ore. A high-titanium magnetite in diabase hardly could be the same magnetite that escaped in hydrothermal solution to form ore. However, the situation is not quite so simple. As noted by Davidson and Wyllie (1968), titanium-poor magnetite also occurs in diabase. Observational and experimentally derived theoretical data on the Fe-Ti-O system reveal several possible mechanisms that must be explored. More pertinent but unavailable, would be data on the Fe-Ti -O-H_2O system.

Experimental crystallization studies in the Fe-Ti-O system at elevated temperatures (Muan, 1958; MacChesney and Muan, 1959; MacChesney and Muan, 1960; Phillips and Muan, 1962; Lindsley, 1962, and Lindsley, 1963) reveal changes in liquid composition and structure of the solid phase with decreasing temperature, varying P_{O_2}, and amount of available titanium. In the region O-12 wgt. percent TiO_2 , as more TiO_2 is added to the system, the liquidus temperature decreases from a maximum of 1594° C for pure iron oxide to 1524° C for 12 wgt. percent TiO_2 and the liquid becomes progressively enriched in TiO_2 (MacChesney and Muan, 1959, p. 937-938). According to these authors, magnetite is the primary crystalline phase in this region. At greater weight percentages of TiO_2 up to 27 wgt. percent TiO_2 , and in the temperature range 1524° C to 1493° C, hematite is the stable primary phase. Thus, although these absolute temperatures are not applicable to a diabase magma system, it should remain true that the hexagonal alpha-R_2O_3 phase will be stable at lower temperatures and higher TiO_2 contents than the spinel phase. Between the two is a two-phase region of both magnetite and hematite stability. In general, increasing TiO_2 and increasing P_{O_2} raises the minimum equilibrium temperature of magnetite stability. By extrapolation of their data, MacChesney and Muan (1959, p. 941) have graphically illustrated a similar theoretical relationship for a lower oxygen pressure (10^{-2} atm.) than that at which experiments were conducted. Crystallization in the Pennsylvania magmatic province thus is believed to have begun in the single phase magnetite region and concluded with granophyre in the two-phase hematite and magnetite field.

Lindsley (1963, p. 64) has presented equilibrium curves for equilibrium pairs of magnetite-ulvöspinel and ilmenite-hematite as a function of changing composition, temperature, and oxygen fugacity. Assuming these pairs to be in equilibrium and knowing the composition of each pair, it is possible to determine equibrium crystallization temperatures and oxygen partial pressures for the simple oxide system (approximately applicable to silicate magmas). In most cases, however, exact compositions of these pairs is not known. Furthermore, equilibrium crystallization between the ulvöspinel-magnetite pair and the hematite-ilmenite pair has not been demonstrated in Pennsylvania diabases; in fact, lower temperature re-equilibration with partial oxidation of ulvöspinel certainly occurred. However, assuming equilibrium, from the qualitative electron probe analyses and point-counting of opaque oxides by Davidson and Wyllie (1968), probable ranges of temperatures and oxygen fugacities from Lindsley's curves are as follows:

	Temperature °C	fO_2 in atm
normal diabase:	970 to 1150	$10^{-10.5}$ to 10^{-12}
diabase pegmatite:	840 to 1040	$10^{-10.5}$ to 10^{-15}
diabase granophyre:	770 to 840	about 10^{-15}

Mt_{20} Usp_{80} with Hem_5 Il_{95} at an f_{O_2} of 10^{-10} atm,
Mt_{30} Usp_{70} with Hem_{10} Il_{90} at an f_{O_2} of 10^{-10} atm,
Mt_{40} Usp_{60} with Hem_{15} Il_{85} at an f_{O_2} of $10^{-9.7}$ atm.

Assuming an initial maximum granophyre crystallization temperature for the oxides of about 800 C, the following are stable in granophyre:

Mt_{15} Usp_{85} with Hem_1 Il_{99} at an f_{O_2} of $10^{-17.5}$ atm,
Mt_{40} Usp_{60} with Hem_3 Il_{97} at an f_{O_2} of 10^{-16} atm,
Mt_{70} Usp_{30} with Hem_{10} Il_{90} at an f_{O_2} of 10^{-14} atm.

Neglecting the absolute oxygen, this would imply a decreasing P_{O_2} with falling temperature during the differentiation sequence as oxygen is depleted by crystallization of the metallic oxides (also see Hamilton and Anderson, 1967, Figure 13, p. 469).d

Calculations by Buddington and Lindsley (1964, p. 318-322) of equilibrium P_{H_2O}/P_{H_2} show that this ratio remains essentially constant during cooling, and the resultant f_{O_2} will decrease by several orders of magnitude for a several hundred degree temperature drop. In such a situation, oxidation of a magnetite-ulvöspinel mixture to a ferrous ilmenite and a titaniferous magnetite will occur because of the slope of the T-f_{O_2} curves for these oxides (Buddington and Lindsley, 1964, p. 315) and/or because of H_2 diffusion (Hamilton and Anderson, 1967, p. 472). In addition, this oxidation can take place in the presence of quite small amounts of water: 1 weight percent water with 2 weight percent Mt_{50} Usp_{50} and a trace of ilmenite in a crystallizing magma (Buddington and Lindsley, 1964, p. 321). They also note that "to form hematite upon cooling to 500° C, (from a magma initially at or above 1000° C,) would require a thousand-fold decrease in f_{H_2}/P_{H_2O}" (Buddington and Lindsley, 1954, p. 321). As a consequence, ultimate oxidation to hematite would not commonly occur. At Cornwall, hematite is present throughout granophyre and is less abundant at Dillsburg. From the estimates of crystallization temperature of f_{O_2} for Pennsylvania diabases, it is likely that as f_{O_2} decreased, the environment became more oxidizing during progressive differentiation (cf. Fig. 4, p. 315 in Buddington and Lindsley, 1964).

Table 36. *FeO (Total)/TiO_2 Ratios In Diabase*

	Normal Diabase	Diabase Pegmatite	Diabase Granophyre
Cornwall:	92/8	83/17	86/14
Dillsburg:	89/11	85/15	83/17

A crude compositional approximation of the FeO-Fe_2O_3-TiO_2 system for the smaller volumes of late differentiates can be obtained from the bulk rock chemical analyses (Appendix 4 and 5), recalculated to 100 percent Utlizing the previously cited data of MacChesney and Muan (1959), it can be seen from Table 36 that the Cornwall and Dillsburg diabase pegmatites and granophyres have a sufficiently high TiO_2 to exceed the 12 percent stability limit of magnetite; hence, an R_2O_3 phase might have been stable. Because some of the iron is withdrawn from this limited opaque-oxide system as part of the silicate crystallization sequence, the proportion of TiO_2 for oxide crystallization becomes greater and the oxides might be expected to be in the two-phase region, or totally within the stability field of the R_2O_3 structure if f_{O_2} were sufficiently high at the temperature of crystallization, a situation that might have existed only after normal diabase crystallization.

Another method of compositional estimation in the FeO-Fe_2O_3-TiO_2 system can be made from petrographic observation of the oxides. The opaque oxides in the diabase sheets consist of mixed spinel (at Cornwall and in the Quakertown and Gettysburg diabase plutons, Davidson and Wyllie, 1968) with ilmenite and skeletal ilmenite in a silicate matrix. At Cornwall, late, probably low-titanium, magnetite and hematite are also present in diabase pegmatite and rarely in granophyre. Ilmenite is also nonexistent in Cornwall granophyre. According to Davidson and Wyllie (1968, electron probe data), the early magnetite mixed with ulvöspinel contains noticeable titanium in contrast to the later magnetite, but the distribution of these two magnetites among the various diabase sheets has not been determined. In the Dillsburg diabase, ilmenite increases in the late phases (Table 36 and Figure 49), apparently at the expense of mixed spinel. At Cornwall, particularly in diabase pegmatite, late magnetite, hematite, secondary titanium-oxides (leucoxene and sphene), and perhaps some ilmenite are secondary to, ore replacements of, earlier mixed spinel. There is no evidence that clearly indicates an equilibrium between the ulvöspinel-magnetite and the hematite-ilmenite pairs. Thus, although data are not available to quantify temperature, composition, or f_{O_2} in the diabase system, directions of change should be valid and the late differentiates appear to have crystallized in, or near, the two-phase region.

As noted (also see Davidson and Wyllie, 1968), the present association of opaque oxides may represent a sequence of processes that can be approximated by an oxidation reaction (omitting solid solution relationships):

$$3Fe_2TiO_2 + O = Fe_3O_4 + 3FeTiO_3 , \qquad (6\text{-}4)$$

the subsolidus oxidation of ulvöspinel (or ulvöspinel-magnetite solid solution) to magnetite and ilmenite. Since oxidation has been shown to be characteristic of the later stages of diabase differentiation and was suggested by Buddington and others (1955, p. 526-527) to be characteristic of residual differentiation fluids, this is not an unreasonable approximate representation. Under decreasing temperature, such an oxidation has been experimentally verified (Buddington and Lindsley, 1965). In Cornwall diabase pegmatite, microscopic observation indicates that the proportions of original mixed spinel, now oxidized and exsolved to ulvöspinel, (Usp) magnetite (Mt), and ilmenite (Il), may have been approximately as follows:

$$(0.6\ \mathrm{Usp} + 0.3\ \mathrm{Mt}) + 0.1\ \mathrm{oxygen} = 0.4\ \mathrm{Usp} + 0.2\ \mathrm{Il}, \qquad (6\text{-}5)$$

assuming that unmixing, rather than simultaneous crystallization, was the dominant process (i.e., that ilmenite did not invert from the high-temperature $FeTiO_3$ form).

Thus, it could be postulated that the low-titanium magnetite in diabase is the same magnetite as that of the ore zone and that purging of titanium from mixed spinel by oxidation was the ultimate ore source. This theory, advanced by Davidson and Wyllie (1968), contains several implicit assumptions: (1) that all of the low-titanium magnetite in diabase results from a separation, with ilmenite, from an original mixed spinel (eq. 6-5); (2) that a residual magmatic fluid existed and transported titantium-poor magnetite into the ore zone; (3) that neither the original titaniferous mixed spinel relicts nor the ilmenite was transported by this ore fluid (the ore is titanium-poor); (4) that ore-associated diabase now contains less low-titanium magnetite than should be present from unmixing and oxidation processes; (5) that there is a volumetric correspondence for ore-associated diabase occurrences and non-ore-associated diabase between amount of low-titanium magnetite remaining in the late differentiates and that now external to diabase (assuming that iron ± titanium contents in the original magmas were not vastly different from place to place).

Examination of these assumptions reveals that some are unlikely and that for others evaluation will have to await the acquisition of additional information. Davidson and Wyllie (1968) present some quantitative data showing that the observed amount of low-titanium magnetite presently within diabase is consistent with unmixing and oxidation of an original mixed spinel (assumption 1). However, quantitative data are lacking for specific sheets, especially for non-ore versus ore associations and their respective diabases. Additionally, a direct spatial relationship between low-titanium magnetite and mixed spinel commonly is not visible. The latter admits of the possiblity, not previously considered, of late, direct crystallization of some low-titanium magnetite in diabase (see discussion of solidification index) where titanium is deficient and iron in excess.

There is no textural evidence that late, low-titanium magnetite has been mobilized or concentrated in diabase (opaque oxides in diabase pegmatite are rather uniformly distributed) toward the focal area beneath the eastern ore zone, no evidence of a residual transporting solution, and no evidence of egress (assumption 2). (The "low-titanium" pegmatitic vein of magnetite described by Tomlinson (1945, p. 534-536) at Cornwall is considerably more titantium-rich than ore magnetite and hence not pertinent to ore derivation mechanisms.) However, it might be postulated that no trace of these processes would remain, or at least none that could be readily observed. To postulate such a source model would be to rely on an unprovable hypothesis, and hence this argument is rejected on the basis of the available information.

Although it is conceivable that a hydrothermal fluid could transport low-titanium magnetite from diabase without also including ilmenite in the process (assumption 3), it seems less probable that the original titaniferous mixed spinel would remain behind, unaffected. If such a process could, and did, operate it would have to have operated subsequent to mixed spinel oxidation. Because mixed spinel appears to be among the youngest minerals to crystallize in diabase pegmatite and because it is absent in granophyre at Cornwall, this fluid would have to have concentrated after the crystallization of most of the late differentiates.

As noted, there does not appear to be any significant deficiency in low-titanium magnetite at Cornwall (specific data have not been published for other specific localities); that is, for the amount of mixed spinel relicts there is about the requisite amount of ilmenite and magnetite for an initial ratio of Usp to Mt of 2:1 (eq. 6-5), an amount assumed reasonable by Nickel (1958) and Davidson and Wyllie (1968) (assumption 4). Large amounts of magnetite do not appear to have been removed to form ore. However, sufficiently accurate quantitative data are lacking.

Similarly, data are lacking concerning the mixed spinel to ilmenite + magnetite ratio in ore-associated versus non-ore-associated diabase (assumption 5). However, unmixing and oxidation with consequent production of a low-titanium magnetite occurs in diabases whether or not there is associated ore; that is, the formation of low-titanium magnetite in diabase is a common occurrence, whereas the formation of ore is unique to certain sheet associations and is found only in the Pennsylvania magmatic province. In this connection, it also is noteworthy that at Cornwall the volume of diabase pegmatite is small. Because it was at this stage that most of the opaque oxides crystallized, this stage also is the only one likely to have been a potential ore source. Furthermore, diabase pegmatite rock types are discontinuous and scattered throughout the sheet. Thus, from the viewpoints both of volume and distribution, they are an unlikely ore parent, at least at Cornwall.

A second hypothesis of magnetite origin could be advanced based on the possibility that low-titanium magnetite crystallized directly from the contemporary magma, rather than as a product of mixed spinel, and that this was mobilized to form an ore fluid. All stages of diabase crystallization at Cornwall from the chilled facies through normal diabase to diabase pegmatite and granophyre are slightly deficient in total iron. If this iron had been withheld until the crystallization of diabase pegmatite or granophyre, rocks representing these stages would have been unually rich in opaque oxides. Because neither differentiate is unusually enriched in the titaniferous mixed spinel (see Figure 48 and Table 29) and because almost all of the low-titanium magnetite now in these differentiates can be accounted for by essentially *in situ* oxidation of mixed spinel, this iron would have to have crystallized directly as titanium-poor magnetite and now be removed as ore. Direct evidence of low-titanium magnetite crystallization and its removal are lacking. Many of the objections cited previously still pertain. In addition, most of the late low-titanium magnetite, if not all, originated during oxidation of ulvöspinel, and thus its direct crystallization would require the late comtemporary magma to have been of greater volume and considerably richer in iron than present data show.

In summary, the objections to ore formation from late, titanium-poor magnetite in diabase, taken together with previously discussed field, geochemical, mineralogical, and petrographic data, are believed not to be compatible with an *in situ* diabase source for the Cornwall ore, and perhaps not for the entire province, although the situation at Dillsburg seems somewhat more favorable for a diabase source. Sims (1968, p. 123), in a study of the Morgantown deposit, reached a similar conclusion to that for Cornwall: "The source of the ore fluids probably was from the primary magma source of the diabase... which escaped after the crystallization of the diabase..."

COMPARISON AND GENESIS OF TRIASSIC MAGNETITE DEPOSITS

Comparative Data from the Dillsburg, Morgantown and Boyertown Districts

All of the Triassic magnetite deposits in Pennsylvania are spatially associated with diabase sheets and most of them with replaceable carbonate host rocks. The two major deposits, Cornwall and Morgantown (Figure 58)

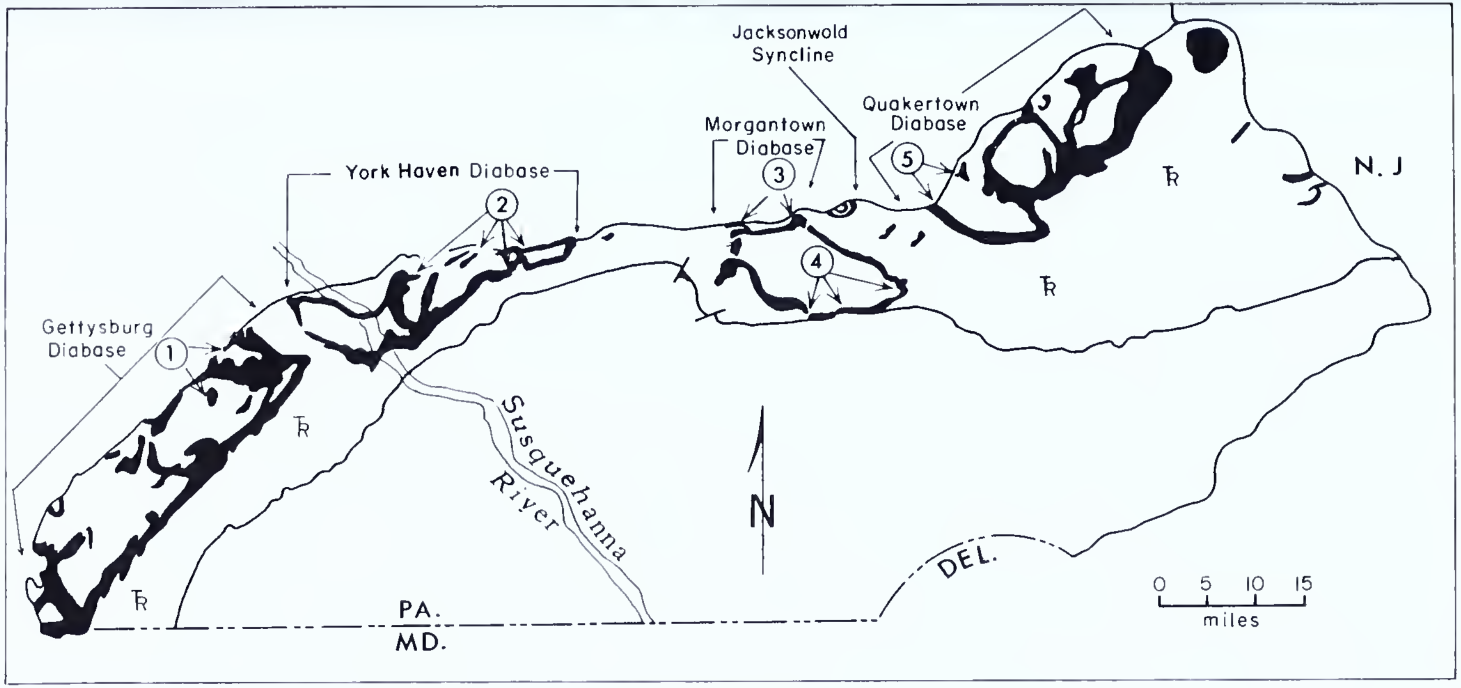

EXPLANATION

① DILLSBURG : inactive group

② CORNWALL : including, from west to east, Hummelstown, Carper, Cornwall (active), and Doner mines.

③ WHEATFIELD : including, from west to east, Wheatfield and Ruth mines, Fritz Island and Esterly (in Jacksonwald Syncline); all inactive.

④ MORGANTOWN-FRENCH CREEK : including, from west to east, Morgantown (active), and the Jones, Hopewell and French Creek inactive mines.

⑤ BOYERTOWN : inactive group.

Figure 58. Map of Diabase-Magnetite Ore Districts in the Pennsylvania Triassic Belt (see text)

are replacements of limestone, dolomitic limestone, and dolomite. Smaller concentrations of ore in the Dillsburg and Boyertown districts (Figure 58) also replace, to a limited extent, limy shale, limestone conglomerate, and siltstone. These two controls on ore locus were first demonstrated by Spencer (1908) and remain the two most important factors that are common to the ores of the entire metallogenic province. Other factors relating to the relative times of deformation, diabase emplacement and ore-zone mineralization, and to ore deposit genesis, are less uniform or less well-known for districts other than Cornwall. However, ore deposit descriptions in the literature, particularly those by Hotz (1950, 1953), Spencer (1908), Hawkes and others (1953), and Sims (1968), contain important data that can be compared with information from the Cornwall districts and that relate to these fundamental problems.

The mode and time of deformation of the Triassic basin is still not clearly understood. Data at Cornwall have been presented that show that faulting, particularly normal faulting, occurred over a measurable time span from before ore introduction to post-ore deformation before, or near the beginning of diabase sheet emplacement. At both Morgantown (Sims, 1968) and Boyertown (Spencer, 1908), faulting on a small scale has occurred after ore emplacement. These, together with the fractures filled by diabase dikes, indicate widespread upper Triassic (to early Jurassic?) deformation. Evidence for faulting during sedimentation is largely inferred from the hypothesis of a half-graben Triassic basin model. At Morgantown (south Triassic margin), Sims (1968) notes the presence of normal faults which he assumes to be related to half-graben development. At Boyertown, Hawkes and others (1953) state that a core revealed fault movement along the Triassic-Paleozoic contact at the north margin. However, elsewhere along the north margin, faulting can be demonstrated only as a post-sedimentation event (e.g., Geyer, 1970, vicinity of the Carper mine and observations at Highspire and Lemoyne) or as nonexistent, such as near Boyertown (Spencer, 1908) and at Cornwall. From the available evidence, it is only clear that faulting along the north margin occurred after basin filling and is unrelated temporarily to initial basin downwarp. Any earlier movement along these faults is unknown.

The hypothesis of expulsion of ore fluids from adjacent diabase would be expected to require an upward movement of the fluid out of diabase. Although many ore deposits are above the adjacent sheet, some are not. Those of the Carper and Doner mines below diabase in the Cornwall district and of the Esterly mine in the Jacksonwald syncline (between the Morgantown and Quakertown plutons, Figure 58) have been noted previously. In the Dillsburg district, ore lay below diabase at the Bell mine, the Altman mine, the Underwood mine, and probably at the McCormick open pit (Spencer, 1908). Some ore in the Dillsburg district (Spencer, 1908; Hotz, 1952) and near Boyertown (Hawkes and others, 1953, core-B) also occurred between diabase sheets. In addition, the "Black Vein" of ore in the Boyertown district was separated from diabase several hundred feet of barren sediments (Spencer, 1908). Clearly, the ore fluid moved both above and below diabase and did not originate from the immediately adjacent sheet by upward expulsion. From more detailed considerations similar to those at Cornwall, Sims (1968) also concluded that the Morgantown ore fluid was not generated from the adjacent diabase (e.g., granophyre is absent, diabase pegmatite is scarce, diabase composition and textures are uniform, etc.).

A prime indicator of ore gensis is the time relationship among diabase emplacement, diabase solidification, and the introduction of the ore fluid. Any fluid emanating from diabase, presumable near the stage of pegmatitic or granophyric differentiate crystallization, would have to originate and migrate before complete solidification of diabase. On the other hand, a measurable time lapse between diabase and ore crystallization indicates an ore-fluid source other than the adjacent diabase. The establishment of a time lapse can be made only inferentially. Considerable data from the Cornwall district have been presented that favor a measurable time separation. Based on a study of the Morgantown ore body, Sims (1968, p. 122) reached a similar conclusion: "Because ore minerals replace silicate minerals and occur in fractures in the diabase, and because the ore is essentially free of titanium, it is concluded that mineralization took place after diabase intrusion and crystallization." Sims (1968) also presents evidence that the top of the diabase is hydrothermally altered and that small veinlets that pinch out at depth contain contact metasomatic and ore minerals filled in from above. At the Jones mine in the Morgantown district, ore also has been observed to fill cracks in the top of the diabase (Spencer, 1908). At Boyertown, Hawkes and others (1953, core B) note an ore occurence between diabase sheets, the upper one of which is almost completely replaced by ore mineralization. On the other hand, they interpret the fresh nature of the lower sheet to mean that it is younger than ore deposition, although this certainly need not be the case (alteration by thermal solutions is always greatest upward and a core sample is too small to bear the weight of such a broad generalization). At the Warwick mine in the Morgantown district, Spencer, (1908) reports a dike of trap rock (diabase) that "cuts the ore." However, the field description is the same as for the Cornwall dike (sample C2-1, Appendix 4-A) for which the chemical composition clearly indicates an alteration by ore metasomatism and a pre-ore emplacement (Lapham and Saylor, 1970). It is quite possible that this Warwick dike is a sheet apophysis that transected laminated host-rock textures previous to ore introduction, thus giving the appearance of a post-ore dike.

These observations from other districts confirm those at Cornwall and indicate that, throughout the province, ore post-dates both the upper portions of the diabase sheet (Table 37) and an earlier metasomatic mineral assemblage. Although time relationships between ore and the diabase differentiates are not known, these differentiates are scarce or absent throughout much of the ore province. Their distribution is summarized subsequently.

The points of similarity with the Cornwall deposits, summarized here (also see Table 37) and given in greater detail by Spencer (1908), are evidence of a general chemical and structural uniformity and consistent spatial and mineralogical association. Origin of these deposits is believed to be related to unique geologic conditions that existed early in the history of a compositionally normal tholeiitic magma. These conditions apparently have not been duplicated elsewhere, because similar magmas, some even of the same age (the sheets of New Jersey, the Goose Creek, Virginia sill, and the Karroo dolerites), do not have magnetite deposits associated with them.

Systematic Variables

To some extent the differences among the various sheets and ore deposits are more diagnostic of genetic mechanism than are the obvious similarities. As has been pointed out previously, a common ultimate origin does not necessitate a common mode of ore emplacement, although such actually may be the case. Several significant variables exhibit a more-or-less systematic variation from west to east within the Triassic Province, and these can be empirically related to type of associated diabase and character of ore occurence. The more important variables, some of them non-systematic, are summarized in Table 37 and Part 7.

The scattered Dillsburg deposits are located just west of the western flexural bend in strike of the Triassic outcrop belt; those of the Boyertown area in the Quakertown Pluton, also small but in vein-like bed replacements, are located near the eastern change in basin trend (Figure 58). The two major ore districts, Cornwall and Morgantown, lie between these geographical and structural extremes, are more concentrated, and contain greater total ore tonnages than the Dillsburg and Boyertown deposits. The tonnage figures given (Table 37), while not representing the total amount of iron introduction, do give a good comparison of relative magnitude. To the tonnage quantity at Morgantown should be added an unknown quantity of ore removed from the French Creek, Warwick, and Jones mines. In terms of total ore, the Morgantown district probably represents the greatest amount of iron introduction and concentration (although the amount eroded at Cornwall is unknown and could have been larger).

The general composition of the ore zone is similar in all deposits but differences do exist (Table 37). There is noticeably less sulfide (and consequently less silver, gold, cobalt and copper) mineralization at Morgantown than at Cornwall. Comparative data for the Dillsburg district are not available. The French Creek mine in the Morgantown district, judging by the accessible dump material, contained considerable sulfide mineralization,

Table 37. *Selected Significant Differences Among Triassic Ore Deposits and Diabase Sheets in Pennsylvania, SW to NE*

Variable	Dillsburg Dist.	Cornwall Dist.	Morgantown Dist.
1. Ore deposit character			
concentration:	Many small deposits, scattered	A few concentrated deposits	Several concentrated deposits
total ore volume:	1.5×10^6 tons mined	1×10^8 tons mined	1×10^8 tons or more
chemistry:	sulfides common; some trace metals	abundant sulfides and trace metals; Co in pyrite to above 2.0%	less sulfides and trace metals than Cornwall; Co in pyrite to at least 0.5%
2. Granophyre			
volume:	large	small	small (?)
orthoclase:	uncommonly ferric or hematitic	commonly ferric or hematitic	?
Na: K ratio:	Na: K > 1	K: Na > 1	?
3. Diabase mineralogy			
olivine:	chilled facies and rarely at base	chilled facies and rarely near base	chilled facies
late pyroxene:	Fe-rich and Px abundant	Fe-rich uncommon and Px less abundant	?
mineral deformation:	none noted	none	none
ore veins:	none noted	magnetite-chlorite-actinolite in fault	small Cu-Fe veins in upper diabase

Table 37. *(Continued)*

4. Diabase chilled margin fractures:	small fractures pinching out downward	small contraction cracks with diopside and magnetite	small (0.5 mm thick) fractures pinching out with depth
replacement:	?	occasionally replaced by ore and ore-gangue	locally epidotized and hydrothermally altered
5. Diabase chemistry (see Fig. 48)			
Fe	somewhat low to normal	less than normal	unknown
Au	anomalously high	normal	unknown
K, Na	probably normal	probably slightly deficient	unknown
Mg	apparently low	apparently high	unknown
Ti	apparently high	apparently normal	unknown
6. Iron in diabase			
total Fe:	moderate (8.0%)	low (7.5%)	low (?)
max. enrichment stage:	transitional pegmatite-granophyre	pegmatite	?
oxide abundance:	high	low	?

with cobaltiferous pyrite commonly present as at Cornwall. The significance of this, and probably other differences, in the composition of the ore districts, particularly those asociated with a single sheet or pluton, remains to be analyzed on a quantitatively comparable basis (see item 5, Table 37).

Differences in composition and character of the diabase plutons across the province are noticeable (items 2-6, Table 37). Whereas general mineralogy is similar, variations in plagioclase composition apparently exist, Cornwall diabase perhaps being less calcic than the Dillsburg (and Palisades) sheet. Olivine maybe present near the base of the sheets in the Gettysburg and York Haven plutons along the south sheet edges, although sparsely, and to the east in the New Jersey-New York Palisades sill. It is essentially absent near the north diabase limb base at Cornwall. Late crystallizing pyroxene is more iron-rich at Dillsburg on the west than at Cornwall and Morgantown (Sims, 1968) in the central part of the province. Late differentiates, especially granophyre, decrease eastward from the Dillsburg sheet, probably to the Morgantown Pluton. Sims (1968) did not observe any in the Grace Mine at Morgantown, but the author observed one small schlieren near Hopewell in the Morgantown Pluton and granophyre has been reported at Warwick by Anthony Davidson (personal communication; see "A Primary Magma as the Source of Iron and Diabase"). Eastward from Morgantown, its quantitative proportion in diabase is not known, but some is present in the Boyertown area of the Ziegler sheet (reported as a pink felspar-hornblende syenite by d'Invilliers, 1883) and in the New Jersey sills. Orthoclase in granophyre is slightly iron-rich (hematitic) at Dillsburg but more iron-rich at Cornwall. The concentration of sodium in Dillsburg granophyre exceeds that of potassium, but the reverse is true at Cornwall. Both appear to be somewhat deficient in the Cornwall sheet as a whole (see Fig. 48 and 54). Iron variation in diabase is even more distinct across the province, although pertinent data are lacking for the Morgantown Pluton. Total iron in diabase (based on averages for normal diabase) is lowest in the east-west striking portion of the Pennsylvania Triassic belt and increases both southwest and northeast (Table 38 and Appendix 4-A and 5). The Cornwall sheet appears to represent a minimal total iron value in this province (also see Lapham and Saylor, 1970), although the Middletown sheet and the diabase in the vicinity of Morgantown should be analyzed for comparison. Similarly, more analyses of the Cashtown sheet of the Gettysburg Pluton and of the Quakertown Pluton (particularly the Ziegler sheet) are needed to detail this variation in total iron. Aeromagnetic patterns, even though complicated by other interpretive factors, are consistent with these generalizations for total iron distribution. Thus, there is an approximate inverse correspondence between total iron in diabase and amount of introduced iron ore.

The abundance of iron(-titanium) oxides in late diabase differentiates (diabase pegmatite and granophyre) attains a maximum in the Dillsburg sheet and is less elsewhere. Furthermore, this oxide concentration crystallized earlier in the diabase differentiation sequence at Cornwall than at Dillsburg, so that maximum iron (-titanium) oxide crystallization at Dillsburg coincides more nearly with the time of maximum alkali and volatile residuum enrichment than at Cornwall.

Ore Genesis Generalizations and Speculations

From the above semi-quantitative observations, a few generalized conclusions can be drawn pertinent to the genetic process of ore formation. Four parallels exist: 1) the amount of late volatile and mobile constituents in diabase, represented by the silica-alkali rich differentiates, decreases from Dillsburg though Cornwall probably to Morgantown (and if it increases again at Boyertown, yields a translated mirror image symmetry with the Dillsburg deposits); 2) total amount of iron in diabase, and particularly in late phases of diabase crystallization, decreases from Dillsburg on the west to Cornwall, and perhaps Morgantown, on the east; 3) the volume of iron ore associated with these diabase plutons increases from the Dillsburg deposits to the Cornwall and Morgantown districts, before again decreasing eastward in Pennsylvania and into New Jersey; and 4) the major deposits occur at flexural nodes where the trend of the Triassic basin curves markedly. One interpretation that may be put upon these generalizations in the light of a proposed primary magma source for the Cornwall ore is that the amount of late volatiles or more mobile cations and the total iron in the *in situ* diabase sheets are a direct measure of the amounts that have been withheld from the diabase sheets before their intrusion into Triassic sediments. It is also a measure of the composition of a separate magma fraction poor in titanium and rich in iron, metallic cations, sulfide, alkali ions, and probably water that later was tapped as an ore fluid. Either there were sufficiently large amounts of some of these constituents retained in the primary magma at depth at the time of tapping of the diabase magma or they collected subsequently at a lower temperature of fluid generation. A late residuum in diabase may crystallize as an *in situ* diabase pegmatite or granophyre. There also is the possibility that at some localities a portion of this late liquid may escape (after mixed spinel oxidation) from the injected *in situ* diabase sheet to form an ore phase, as suggested by Davidson and Wyllie (1968). Some Dillsburg district deposits could represent such a case (principally those above diabase). The scattered nature of the Dillsburg deposits, the large amount of granophyre there, the quantity of iron enrichment, and the late differentiation stage of the enrichment maximum just before granophyre crystallization could be indicative of such a process at Dillsburg, as suggested by Hotz (1950, 1953). The Cornwall deposit, on the other hand, and perhaps Morgantown as well, is believed to typify an introduction as a hydrothermal solution from a primary magma source after the diabase sheet had been emplaced and solidified.

At least in superficial aspects, the Boyertown district ore deposits in the western part of the Quakertown Pluton (Zeigler sheet) more closely resemble the Dillsburg deposits than do the Cornwall or Morgantown districts. It is of speculative interest to note that the character of the ore deposits and the granophyre abundance of the two east-west ends of the metallogenic province might be translated mirror images of each other, of interest particularly with respect to the arcuate shape of the Triassic basin. This presents a problem that as yet has no answer, but one implication may be that a change in the mechanism of ore introduction from Dillsburg eastward to Cornwall and perhaps also from Boyertown westward to Morgantown, is the result of a subcrustal deformation that influenced the early oxidation and/or composition of primary magmas at depth. If this east-west portion of the Triassic belt is the result of basement translation and if this deformational zone extends into basement mantle material where a tholeiite magma could be tapped, a zone of weakness could have existed that may have been related, in Triassic time, to the offshore fault at this latitude, as noted by Drake and Woodward (1963). Note, however, that Triassic sheets occur elsewhere (e.g., Virginia), although they are less extensive and are not saucer-shaped. It is therefore apparent, that a transcurrent rupture zone is not necessary to the generation of sheet magma, but perhaps is related to the generation of an ore fluid. Speculative as this suggestion is, it seems logical that diabase and ore must be related in some temporal and genetic fashon to major structural elements, even if only to the extent of facilitating the formation of a large volume of mantle material of slightly differing compositions into a melt and permitting more easily the introduction of basaltic flows, diabase plutons, ores, and diabases dikes into the crust. At the extreme of speculation lies the possible relevance of these events to plate tectonics and to the Mesozoic divergence of large crustal segments.

PART 7. ECONOMIC POTENTIAL OF PENNSYLVANIA MAGNETITE

by D.M. Lapham

INTRODUCTION

To date (1972), more than 140 million tons of magnetite ore have been mined from Triassic magnetite deposits in Pennsylvania. The scattered deposits of the Dillsburg and Boyertown districts are not at present being mined, but large concentrations of ore at Cornwall and Morgantown are in operation. Other mines in the French Creek area of the Morgantown Pluton have been mined in the past. Thus the magnetite province of Pennsylvania has been a major source of iron as well as other trace metals and a notable contributor to Pennsylvania's industrial wealth. Unless new, economically mineable ore bodies are discovered at Cornwall, the mines here are expected to close in a few years. After this, only the extensive Morgantown deposit will be in operation. It is thus important that any possible extension of present mining sites be discovered while the facilities for mining and processing still exist in the area. It is just as important to the development of Pennsylvania's mineral wealth that any new ore districts or ore deposits be explored and opened as a counterbalance toward the time when the Cornwall deposit is no longer a producer. Eventually, it may become economical to mine deposits of lesser concentration, those which are more scattered, or those which are presently at too great a depth to be ecomonically utilized. For these objectives, the source and method of ore introduction and the criteria by which ore deposits can be recognized must be as fully understood as possible.

There are certain general geological requirements which must be fulfilled for a magnetite ore deposit to exist in the Triassic metallogenic province of Pennsylvania. All of the deposits are associated with large diabase sheets, and their presence indicates that the necessary conditions for an ore fluid may exist. Related to this is the location of the sheets and ore within the Triassic belt. It is believed that the unusual structural conditions represented by the east-west striking part of the Triassic belt were instrumental in allowing the generation at depth of a large volume of diabase magma, its surficial intrusion, and the possibility of associated ore introduction.

Futhermore, it is suggested that major ore concentrations will occur only near the structural flexure points; that is, near the areas of strike change within this east-west striking portion of the Triassic belt. Other criteria relate to the composition of the magma. For example, there must have been a sufficient concentration of volatiles to form an ore fluid and to transport the metallic cations into the surrounding country rocks. Thus, either an original tholeiite magma must have had a portion of its original composition withheld for later introduction as an ore fluid, or a later, lower-temperature magma formed and was tapped after sheet intrusion, or the diabasic magma that intruded as a diabase sheet must have been able to concentrate and expel residual, ore-rich fluids. Examination of the diabase sheets has shown that the amount of granophyre present in a particular diabase sheet may be a direct measure of this fluid concentration withheld, and inversely proportional to ore quantity. Other, more local, factors are also important. Replaceable rock units must exist for ore to be deposited. In the magnetite ores of Pennsylvania, this essentially requires the presence of carbonate units. Shales, sandstones, and other sedimentary rock types seldom show any significant magnetite enrichment. Finally, large, high-grade concentrations are more likely to result from the presence of suitable structural channels for the introduction of ore, from sufficient permeability of the host rocks to allow ore fluid mobility and replacement, and, in some cases, from an impermeable cap above the replaceable horizon to confine the ore solution into a deposit of high concentration.

Exploration below diabase for ore is difficult because there are so few criteria available for site selection and drilling. The general controls cited above can be helpful. Analysis of diabase for total iron deficiency and lack of large volumes of granophyre are also general indicators. However, the location of a drilling site is best based upon a knowledge of the local structure and stratigraphy. Replaceable carbonate beds must be known or suspected below diabase. Lack of a structural channel through diabase to overlying sediments must be substantiated, because an ore fluid would tend to have moved upward along such a channel where erosion becomes significant. Another factor, in areas of known deposits, must be considered. The larger the known concentration above diabase, the less chance there is for a large ore body below diabase; nevertheless, ore above diabase is the best concrete evidence that ore fluids have been active in a specific area and that ore may exist below a diabase sheet. The Cornwall deposit can be used as an example. If there is any ore below the sheet, then it should lie either along or east-southeast of the major fault that is believed to have served as an ore channel. At present, such detailed knowledge is the only good clue to potential ore below diabase.

One futher generalization should be considered. There is the possibility that, in spite of the general similarity of all of the magnetite ore districts, there were two different modes of origin: ore from adjacent diabase and ore from depth. In this regard, a factor that does not appear to be critical is whether or not there has been oxidation of a mixed spinel to ilmenite and low-titanium magnetite in diabase differentiates; that is, the oxidation appears to be ubiquitous in diabase. However, volumes of opaque oxides, particularly any late, low-titanuim magnetite, and their distribution (quantitative) throughout the province are unknown and may be significant. This will be particularly important in any areas where expulsion of ore directly from the sheet diabase is believed to have occurred. The Dillsburg district could represent such a case. Also, in several respects the lesser tonnage concentrations of the Dillsburg and Boyertown districts differ in kind from the greater tonnages of the Cornwall and Morgantown districts. Since it would be valuable to know whether a potential magnetite ore deposit is likely to be highly concentrated with large tonnages or rather scattered with lesser tonnages, a comparison between the districts may be important. For details of these deposits, the reader is referred to foregoing sections of this report and to the other reports that have been cited.

Exploration in Known Magnetite Districts

Perhaps the most important fact that can be learned from known magnetite districts is the direction in which the ore fluids moved. This direction allows geologists to determine where the ore fluid came from, the path it took through crustal rock units, and the outer limits to which the ore fluid extended. At any place along this path where proper conditions existed for replacement by magnetite and associated ore minerals (e.g., a carbonate horizon), a potential ore body should be sought. Determination of this path can best be accomplished by zoning studies. For the Pennsylvania magnetite deposits, the best indicators of zonation are: 1) variations in trace metal concentrations, at Cornwall particularly copper, nickel, and sulfur; 2) variations in the sequence of crystallization of the minerals, particularly magnetite and actinolite; 3) relationships between thickness of ore or ore composition and structural channels along which the ore fluid could have moved; 4) zoning of metasomatic minerals with respect to their temperatures of crystallization, and the distinction between these metasomatic minerals (such as chlorite and actinolite) and contact metamorphic minerals (such as diopside and tremolite); 5) trace element or oxidation state variation in ore minerals, particularly cobalt in pyrite, and the variation of unit cell size of magnetite (as shown at Cornwall); 6) the relative ability, or ease, with which the ore minerals (magnetite, etc.) are able to replace the previously crystallized gangue minerals (diopside, etc.) such that ore distribution becomes partially dependent upon the distribution and ease of replacement of earlier minerals; and 7) the general shape of the ore deposits or ore mineralization which may reveal a directional orientation. Once the path of ore fluid movement has been established by measuring one or more of the above variables, the search for new ore concentrations in known districts becomes largely a matter of judicious drilling. For example, if the source direction has been established, exploration of replaceable units in the direction from which the ore came may reveal additional concentrations. Where the ore is believed to have cut through diabase by means of fault channels, ore could exist below diabase in the direction of the source and/or down dip where appropriate replaceable limestone, or dolomitic limestone, exists. By exploring in a lateral direction, extensions of ore bodies may be found by determining the directions in which the ore fluid spread out, keeping in mind that ore bridges from one body to another may have been removed by subsequent erosion. Such has apparently been the case at Cornwall between the eastern and western ore bodies. The method also might apply to the bedded replacement deposits in the Boyertown district.

A rough idea of the amount of introduced iron ore that should be present in a diabase-associated ore deposit neglecting eroded differentiates rich in iron can be obtained by calculating the amount of known introduced ore and comparing this amount with the deficiency of iron in the diabase. The approximate composition of gangue minerals, the iron content of unreplaced host rocks, and the total volume of ore plus gangue minerals should be included in the iron calculation.This means that for a determination of total introduced iron, the amount of iron included in the calculation will have to include estimates for areas beyond the economic limits of mineable ore. To determine the amount of iron deficiency in diabase, chemical analyses of the entire sheet are most accurate. From the shape of the sheet, its volume can be calculated. By comparing the average value of iron in normal diabases (8.2 to 8.5 percent) with the average for a particular sheet in question, the deficiency in iron will be known and total iron deficiency can be calculated from the sheet volume. If the total introduced iron outside the sheet is considerably less than the amount of total iron by which the diabase is deficient, then there is the possibility of the existence of another ore body, or of loss of ore by erosion. A simpler, but still less accurate method for this kind of calculation is to compare two known districts with respect to total known ore and total average diabase iron composition. If, for example, one ore body contains less iron than another, and the diabase associated with it also contains less iron, then there is a possibility that not all of the ore has been found. However, to some extent, usually unknown, these types of calculations depend on diabase feeder distribution and the uniformity of the parent magma composition.

Another such indicator may be the extent of enrichment of sulfide minerals in isotopic S^{34}. The greater this enrichment is in country rock sulfides relative to the enrichment in diabase sulfides, the longer the ore transport path may have been. Thus, a low to moderate enrichment suggests the possibility of a long ore-transport path and/or considerable wall-rock stoping by the ore fluid. Such a case may also enhance the possibility of a large, concentrated ore deposit as it appears to have done at Cornwall. As an exploration tool indicative of type and quantity of ore deposit, this method is yet untested, but is one that shows promise for future research and exploration in areas of known sulfide introduction into country rock. Here again, the Boyertown district where ore is both close to and far removed from diabase might provide a good test area.

The application of the known details at Cornwall leads to some suggestions for methods of further exploration in this district. From the nature of the imperable Mill Hill Slate and Blue Conglomerate on the east, it is unlikely that there is an eastern extension of ore above diabase. To the west of the eastern ore body, an unknown amount of ore apparently has been stripped by erosion where an ore fluid is believed to have migrated from the east into the present western ore body. A few small ore remnants of this ore bridge remain only at the east end of the open pit and at the Elizabeth mine. Consequently, the only ore which could remain would be along the hypothesized ore channel through diabase where limestone blocks may have been engulfed, or beneath the diabase sheet where there is available limestone. As noted previously, the Doner mine (below diabase on the east side of the proposed main Cornwall fault channel, Plate 21), is evidence that ore solution movement occurred below diabase either along the fault plane, or east and southeast of the fault. This location would then be the most likely area for exploration drilling if ore below diabase becomes economical. Drill holes through the sheet west of the fault have already revealed the absence of ore. This absence is as would be expected from the zoning and structural studies presented here. It is not likely that further drilling on this western side of the fault will be of any value, unless perhaps to the south or southwest at considerable depth down the dip of the sheet.

Exploration for New Magnetite Deposits

Comparisons of the Dillsburg and Cornwall deposits can be instructive. Since the Dillsburg deposits are more scattered and contain smaller concentrations of ore, any significant differences between the two may be indicative of the size and concentration of an ore body elsewhere in the district. Of primary interest is the fact that the Cornwall sheet is more depleted in iron than the Dillsburg sheet, even though the geographical extent of this depletion has not been studied. Assuming that the tholeiitic diabase magma that yielded the intrusive sheets was originally uniform in total iron content, this depletion in the sheets is of an expectable magnitude for the relative sizes of the ore deposits. Another interesting difference in diabase iron content is that the maximum total amount of iron is greatest at an earlier diabase crystallization stage at Cornwall in the diabase pegmatite, and at a later diabase crystallization stage at Dillsburg in rock transitional between diabase pegmatite and granophyre. Related to this correlation is the greater amount of late stage residual fluid concentrates preserved at Dillsburg, evidenced by a large volume of granophyre. This correlation raises the possibility that expulsion of iron from diabase occurred where there were large concentrations of residual fluids that might have acted as a medium for ore fluid transport. This in turn would lead to a scattered type of low concentration deposits, their location dependent upon the locus of late fluids that could transport iron, leaving titanium behind, and then break through the diabase chilled margins. Their concentration would be dependent upon the volume of fluid which was able to be collected from intergranular pore fluid at different points near the top of the sheet. Since this collection would be expected to vary in amount considerably from place to place, the size and distribution of ore bodies would be expected to vary in similar fashion. Also with regard to these volatiles in late diabase differentiates, it may be important to note that in the granophyre of the Dillsburg area sodium exceeds potassium, while the reverse is true at Cornwall. It may be that this variation influenced the formation of the two ore deposit types and is the result of the composition of the withdrawn ore fluid and the magma crystallization stage at which this fluid was expelled. An hypothesis has been advanced for the origin of Cornwall ore that depends upon early iron withdrawal from a primary magma at depth, perhaps influenced by structural location. As a consequence, this early withdrawal of iron may correlate with a more concentrated and more extensive deposit. This hypothesis needs further testing. The Morgantown Diabase Pluton and the Quakertown Diabase Pluton offer another pair similar, respectively, to the Cornwall and Dillsburg district pair, where this suggestion can be tested.

Table 38. *Average Percent Total Average Fe in Diabase Sheets* from SW to NE (see Appendix 4) compared with Triassic Dikes*

Sheets:	% Fe (total)
Virigina (1)	9.47
Gettysburg Diabase (6)	8.29
Cornwall Sheet, York Haven Diabase (Table 25)	7.4
Cornwall Sheet, York Haven Diabase (10, R. Smith)	7.2
Quakertown Diabase (5)	7.73
New Jersey (2)	9.53
Triassic Dikes ** (19)	8.08

* Excludes low-Fe analyses at Birdsboro (Morgantown Diabase), Goat Hill, Pennsylvania (Gettysburg Diabase), and Culpepper, Virginia, which are probably in error. Numbers in parentheses indicate number of samples averaged. Also see Table 32.

** Data from Appendix 5-F and Table 3 in Lapham and Saylor (1970) for eastern North America.

Another tool that may be useful for the exploration for new magnetite deposits is an analysis of the aeromagnetic highs that may result from magnetite concentrations. The Morgantown ore deposit was discovered by a magnetometer survey (ore began about 500 feet below the surface); other deposits may also turn up from a study of magnetic patterns. Hawkes and others (1953) have discussed two magnetic highs in the Boyertown district that represent potential ore concentrations. They also noted that a low-altitude aeromagnetic survey may not resolve an ore body that can be distinguished from higher altitude flights. Bromery and Griscom (1967) have suggested the investigation of three aeromagnetic anomalies that could represent magnetite concentrations: 1) south of Hopewell associated with the Morgantown Pluton; 2) two miles south of Heidlersburg in the Cashtown sheet, and 3) just south-southeast of Gettysburg, also in the Cashtown sheet (Gettysburg Pluton). However, these anomalies are not sufficient to define an ore body, as noted previously (see "Aeromagnetic Data" discussion). Some of the anomalously high magnetic intensities may be the result of diabase at, or near, the surface. They could be particularly misleading in the Gettysburg Pluton if transitional diabase pegmatite-granophyre were the rock type at the location of the anomaly (the volume of this rock type is apparently greater in the Gettysburg Pluton than in other Pennsylvania plutons). Elsewhere, aeromagnetic anomalies may result from the configuration and composition of the underlying sub-Triassic basement. Furthermore, it is in the late diabase differentiates that the greatest concentration of iron oxides occurs. Opposed direction of remanent field magnetization, extent and kind of country rock metamorphism, and local dip variation of the Triassic sediments are some of the other factors that contribute to magnetic highs. As a consequence, this tool is most useful in conjunction with accurate geologic knowledge of the specific area under consideration, particularly the factors discussed in this section of the report.

In conclusion, the exploration for new deposits in Pennsylvania would perhaps best be carried out by analyses of sheets, or parts of sheets, abnormally low in total iron, by determining where potassium and sodium are deficient in diabase sheets or are not wholly contained within the sheet, by determining where potassium exceeds sodium in the granophyre, by examining areas where replaceable limestone is available above and below sheets, and by aeromagnetic and chemical testing procedures within a likely area. Potentially productive areas, including oxidized magnetite and copper-rich sulfides low in magnetite, in which to apply these exploration techniques probably should be confined to that part of the Triassic belt which lies in, or east of, the Dillsburg sheet of the Gettysburg Pluton and west of the Haycock sheet of the Quakertown Pluton. Within this area more attention might be paid to the Middletown and Bachmanville sheets of the York Haven Pluton, west of Cornwall, and to known areas of magnetite concentrations where limestone may be replaced below diabase sheets. However, exploration below diabase will be wasteful and largely hit-or-miss unless data on ore fluid movement and diabase composition are available from geological research studies to guide geophysical, geochemical, and drilling exploration programs. At present, such footwall deposits are not economically feasible, but research is important now for the future requirements.

REFERENCES

Ault, W. U. and Kulp, J. L. (1959), *Isotope geochemistry of sulfur*, Geochim. et Cosmochim Acta. v. 16, p. 201-235.

Barker, D.S. (1970), *Composition of granophyre, myrmekite, and graphic granite*, Geol. Soc. America Bull., v. 81, p. 3339-3350.

Barnes, H. L. and Killerud, G. (1960), *Equilibrium between pyrite, pyrrhotite, magnetite, and aqueous solutions*, Ann. Rept. Dir. Geophys. Lab., Carnegie Inst., Washington, Year Book 59, p. 135-137.

__________(1961), *Equilibria in sulfur-containing aqueous solutions in the system Fe-S-O, and their correlation during ore deposition*, Econ. Geology, v. 56, p. 648-688.

Bascom, F., Wherry, E. T., Stose, G. W., and Jonas, A. I. and others (1931), *Geology and mineral resources of the Quakertown-Doylestown district, Pennsylvania and New Jersey*, U. S. Geol. Survey Bull. 828, 38 p.

Beck, M. E., Jr. (1965), *Paleomagnetic and geological implications of measured magnetic properties of diabase sheets of south-eastern Pennsylvania*. Jour. Geophys. Research, v. 70, p. 2845-2856.

__________(1966), *The effect of magmatic differentiation on the magnetic properties of diabase sheets of southeastern Pennsylvania*. U. S. Geol. Survey Prof. Paper 550-D, p. 109-116.

Brehrendt, J. C. and Woterson, C. S. (1970), *Aeromagnetic and gravity investigations of the coastal area and continental shelf of Liberia, West Africa, and their relation to continental drift*. Geol. Soc. America Bull. v. 81, p. 3563-3574.

Boesen, R. S. (1964), *The clinopyroxenes of a monzonitic complex at Mount Dromedary, New South Wales.* Am. Mineralogist, v. 49, p. 1435-1457.

Bowen, N. L. (1928), *The evolution of the igneous rocks.* Princeton Univ. Press, 322 p.

__________and Tuttle, O. F. (1950), *The system* $NaAlSi_3O_8$-$KAlSi_3O_8$-H_2O.

Boyd, F. R. and Brown, G. M. (1969), *Electron-probe study of pyroxene exsolution,* in *Pyroxenes and amphiboles: crystal chemistry and phase petrology.* Miner. Soc. Amer. Spec. Paper 2, p. 211-216.

Brindley, G. W. and Gillery, F. H. (1956), *X-ray identification of chlorite species.* Am. Mineralogist v. 41, p. 169-186.

Bromery, R. W. (1967), *Earthquake epicenters,* in *engineering geology of the Northeast Corridor, Washington, D. C. to Boston, Massachusetts.* U. S. Geol. Survey Misc. Inv. Map 1-514C.

__________and Griscom, A. (1967), *Aeromagnetic and generalized geologic map of southeastern Pennsylvania.* U. S. Geol. Survey Geophys. Inv., Map GP 577.

Bromery, R. W. and others (1961), *Aeromagnetic maps of the Manheim quadrangle, Lancaster and Lebanon Counties, Pennsylvania.* U. S. Geol. Survey Geophys. Inv. Map GP 256.

__________(1961), *Aeromagnetic map of the Lititz quadrangle, Lancaster and Lebanon Counties, Pennsylvania.* U. S. Geol. Survey Geophys. Inv. Map GP 257.

__________(1961), *Aeromagnetic map of the Lebanon quadrangle, Lebanon County, Pennsylvania.* U. S. Geol. Survey Geophys. Inv. Map GP 254.

__________(1961), *Aeromagnetic map of the Richland quadrangle, Lebanon and Lancaster Counties, Pennsylvania.* U. S. Geol. Survey Geophys. Inv. Map GP 255.

Brown, G. M. (1957), *Pyroxenes from the early and middle stages of fractionation of the Skaergaard intrusion, East Greenland.* Mineralog. Mag., v. 31, p. 511-543.

__________(1967), *Mineralogy of basaltic rocks* in *Basalts - The Poldervaart treatise on rocks of basaltic composition.* ed. H. H. Hess and A. Poldervaart. New York and London, Interscience Publishers, v. 1., p. 103-162.

Buddington, A. F., Fahey, J. and Vlisidis, A. (1955), *Thermometric and petrogenetic significance of titaniferous magnetite.* Am. Jour. Sci., v. 253, p. 497-532.

__________and Lindsley, D. H. (1964), *Iron-titanium oxide minerals and synthetic equivalents.* Jour. Petrology, v. 5, p. 310-357.

Chayes, F. (1955), *Potash feldspar as a by-product of the biotite-chlorite transformation.* Jour. Geol., v. 63 p. 75-82.

__________(1970), *On estimating the magnitude of the Hidden Zone and the compositions of the residual liquids of the Skaergaard Layered Series.* Jour. Petrology, v. 11, p. 1-4.

__________and Velde, D. (1965), *On distinguishing basaltic lavas of circumoceanic and oceanic-island type by means of discriminant functions.* Jour. Sci., v. 263, p. 206-222.

Clarke, F. W. (1924), *The data of geochemistry.* U. S. Geol. Survey Bull. 770, 841 p.

Coombs, D. S. (1954), *Ferriferous orthoclases from Madagascar.* Mineralog, Mag., v. 30, p. 409-427.

Callahan, W. H. and Newhouse, W. H. (1929), *A study of the magnetite orebody of Cornwall, Pennsylvania.* Econ. Geology, v. 24, p. 403-411.

Crowley, M. S. and Roy, R. (1964), *Crystalline solubility in the muscovite and phlogopite groups.* Am. Mineralogist, v. 49, p. 348-362.

Daly, R. A. (1933), *Igneous rocks and the depth of the earth.* McGraw-Hill Book Co., N. Y., 508 p.

Davidson, Anthony and Wyllie, P. J. (1965), *Zoned magnetite and platy magnetite in Cornwall type ore deposits,* Econ. Geology, v. 60, p. 766-771.

__________(1968). *Opaque oxide minerals of some diabase-granophyre associations in Pennsylvania.* Econ. Geology v. 63, p. 950-960.

de Boer, J. (1967), *Paleomagnetic-tectonic study of Mesozoic dike swarms in the Appalachians.* Jour. Geology. Research, v. 72, p. 2237-2250.

__________(1968), *Paleomagnetic differentiation and correlation of the late Triassic volcanic rocks in the central Appalachians.* Geol. Soc. America Bull., v. 79, p. 609-626.

d'Invilliers, E. V. (1883), *The Geology of Berks County.* 2nd Pa. Geol. Survey Report D 3, p. 314-316.

Donnay, J. D. H. and Donnay, C. (1963), *Crystal data determinative tables,* 2nd edition, Brooklyn, N. Y., Polcrystal Book Service (Am. Crystallographic Assoc. Mon. 5), 1302 p.

Drake, A. A., Jr. (1969), *Precambrian and lower Paleozoic geology of the Delaware Valley, New Jersey-Pennsylvania.* Geol. Soc. America Guidebook, Field Trip 1-A, p. 51-131.

Drake, C. L., Heirtzler, J., and Hirshman, J. (1963), *Magnetic anomalies off eastern North America.* Jour. Geophys. Research, v. 68, p. 5259-5275.

Drake, C. L. and Woodward, H. P. (1963), *Appalachian curvature wrench faulting and offshore structures.* New York Acad. Sci. Trans., ser. 2, v. 26, p. 48-63.

DuToit, A. L. (1939), *The Geology of South Africa.* 2nd edition, Edinburgh, 512 p.

Eastwood, G. E. P. (1965), *Replacement magnetite on Vancouver Island, British Columbia.* Econ. Geology, v. 60, p. 124-148.

Edwards, A. B. (1942), *Differentiation of the dolerites of Tasmania.* Part 1, Jour. Geology, v. 50, p. 451-480.

Engle, A. E. J. and Engel, C. G. (1964a), *Composition of basalts from the Mid-Atlantic Ridge.* Science, v. 144, p. 1330-1333.

__________(1964 b), *Igneous rocks of the East Pacific rise.* Science, v. 146, p. 477-485.

__________and Havens, R. G. (1965), *Chemical characteristics of oceanic basalts and the upper mantle.* Geol. Soc. America Bull., v. 76, p. 719-734.

Erickson, G. P. and Kulp, J. L. (1961), *Potassium-argon dates on basaltic rocks* in *Geochronology of rock systems.* New York Acad. Sci. Annals. v. 91 p. 321-323.

Eskola, P. (1915), *On the relation between chemical and mineralogical composition in the metamorphic rocks of the Orijarvi region.* Comm. Geol., Finlande Bull. 44.

__________(1939), *Die Entstehung der Gesteine.* Springer, Berlin, p. 347.

Evans, B. W. (1967), *Mineralogy of tholeiite basalt as a function of cooling rate and sub-solidus history.* (abs.). Geol. Soc. America Bull. p. 61.

Faill, R. (1969), *Tectonic development of the Triassic basin in Pennsylvania.* Geol. Soc. American Abstracts, VI, no. 7, p. 273-274.

Fanale, F. P. and Kulp. J. L. (1962), *The helium method and the age of the Cornwall, Pennsylvania magnetite ore,* Econ. Geology, v. 57, p. 735-746.

Faust, G. T. (1963), *Mineralogic studies and crystal chemistry.* U. S. Geol. Survey, Prof. Paper 475-A, p. A142.

Frankel, J. J. (1967), *Forms and structures of intrusive basaltic rocks* in *Basalts-The Poldervaart treatise on rocks of basaltic composition.* ed. by H H. Hess, and A. Poldervaart, Interscience publishers, New York and London, v. 1, p. 63-102.

Frazer, P., Jr. (1880), *The geology of Lancaster County.* 2nd Pa. Geol. Survey Report CCC, 350 p.

Fudali, R. F. (1965), *Oxygen fugacities of basaltic and andesitic magmas.* Geochim, et Cosmochim. Acta., v. 29, p. 1063-1075.

Fyfe, W.S., Turner, F.V., and Verhoogen, J. (1958), *Metamorphic reactions and metamorphic facies*. Geol. Soc. America, Mem. 73, 260 p.

Garrels, R.M. and Christ, C.L. (1965), *Solutions, minerals, and equilibria*. Harper and Row, N.Y., 450 p.

Geyer, A.R., (1970), *Geology and mineral resources, and environmental geology of the Palmyra Quadrangle, Lebanon and Dauphin Counties*. Pa. Geol. Survey Atlas 157D, 46 p.

Geyer, A.R., Buckwalter, T.V., McLaughlin, D.B., and Gray, C. (1963), *Geology and Mineral Resources of the Womelsdorf Quadrangle*, Pa. Geol. Survey Atlas 177C, 96 p.

_________(1963), *Geology of the Womelsdorf quadrangle*. Pa. Geol. Survey, Atlas 177C, 96 p.

Glaeser, J.D. (1963), *Lithostratigraphic nomenclature of the Triassic Newark-Gettysburg Basin*. Pa. Acad. Sci., Proc. v. 37, p. 179-188.

_________(1964), *Provenance, dispersal, and depositional environments of Triassic sediments in the Gettysburg-Newark Basin*. Ph.D. dissertation, Northwestern Univ., 298 p.

_________(1966), *Provenance, dispersal, and depositional environments of Triassic sediments in the Newark-Gettysburg basin*. Pa. Geol. Survey, Bull, G43, 168 p.

Goldschmidt, V.M. (1922), *On the metasomatic processes in silicate rocks*. Econ. Geology, V. 17, p. 105-123.

Gottfried, D., Greenland, P.L., and Campbell, E.Y. (1968), *Variations of Nb-Ta, Ar-Hf, Th-U, and K-Cs in two diabase-granophyre suites*. Geochim. at Cosmochim. Acta, v. 32, p. 925-948.

Gray, Carlyle, (1956), *Diabase at Cornwall, Pennsylvania*. Pa. Acad. Sci., Proc. v.30, p. 182-185.

Gray, C., Geyer, A.R., and McLaughlin, D.B. (1958), *Geology of the Richland (7-1/2) quandrangle*, Pa. Geol. Survey Atlas A167D.

Gray, C. and Lapham, D.M. (1961), *Guide to the geology of Cornwall, Pennsylvania*. Pa. Geol. Survey Bull. G35, p. 1-18.

Gray, C. and others (1960), *Geologic map of Pennsylvania*. Pa. Geol. Survey, Map No. 1.

Green, D.H. (1967), *Effect of high pressure on basaltic rock* in *Basalts, The Poldervaart treative on rocks of basaltic composition*, ed. H.H. Hess, and A. Poldervaart, New York and London, Interscience publishers, vol. 1., p. 402-443.

_________and Ringwood, A.E. (1969), *The origin of basalt magmas*, in *The Earth's Crust and Upper Mantle*. Am. Geophys. Union Geophys. Mon. 13, p. 489-495.

Hagner, A.F., Collins, L.G., Clemency, C.V. (1963), *Host rock as a source of magnetite ore, Scott mine, Sterling Lake, N.J.*, Econ. Geology, v. 58, p. 730-768.

Hall, C.E. (1881), *Geology of Philadelphia County*, 2nd Pa. Geol. Survey Report C6, p. 96-99, 134.

Hamilton, D.L., Burnham, C. Wayne, and Osborn, E.F. (1964), *The solubility of water and effects of oxygen fugacity and water content of crystallization in mafic magmas*. Jour. Petrology, v. 5, p. 21-39.

Hamilton, E.I. (1963), *Isotopic composition of strontium in the Skaergaard intrusion. East Greenland*. Jour. Petrol. v. 4, p. 383-391.

Hawkes, H.E., Wedow, H., and Balsley, J.R. (1953), *Geologic investigations of the Boyertown magnetite deposits in Pennsylvania*. U.S. Geol. Survey Bull. 995D, p. 135-148.

Helgeson, H.C. (1964), *Complexing and hydrothermal ore deposition*. Pergamon Press, MacMillan Co., 128 p.

Hermes, O.D. (1964), *A quantitative petrographic study of dolerite in the Deep River Basin, N.C.*. Am. Mineralogist, v. 49, p. 1718-1729.

Hersey, J.B. (1944), *Gravity investigation of central-eastern Pennsylvania*. Geol. Soc. America Bull., v. 55, p. 417-444.

Hey, M.H. (1954), *A new review of the chlorites*. Mineralog. Mag., v. 30, p. 277-292.

Hickok, W.O. (1932), *The Cornwall ore deposits, Pennsylvania.* Unpub. PhD Thesis, Yale Univ.

__________(1933), *The iron ore deposits at Cornwall, Pennsylvania.* Econ. Geology, v. 28, p. 193-255.

Hill, Robin and Roeder, Peter (1967), *Solubility of spinel in basaltic melts (abs).* Geol. Soc. America Spec. Paper 115 (1968) p. 96-97.

Holmes, Arthur and Harwood, H.F. (1928), *The age and composition of the Whin Sill and the related dikes of North of England.* Minerolog. Mag., v. 21, p. 493-542.

Holser, W.T. and Schneer, C.J. (1961), *Hydrothermal magnetite.* Geol. Soc. America Bull., v. 72, p. 369-386.

Hoover, K.V., Saylor, T.E., Lapham, D.M. and Tyrell, M.E. (1972) *Properties and uses of shales and clays of southeastern Pennsylvania.* Pa. Geol. Survey Bull. M63, 329p.

Hotz, P.E. (1950), *Diamond-drill exploration of the Dillsburg magnetite deposits, York County, Pennsylvania.* U.S. Geol. Survey Bull. 969A, p. 1-25.

__________(1952), *Form of diabase sheets in southeastern Pennsylvania.* Am. Jour, Sci., v. 250, p. 375-388.

__________(1953), *Petrology of granophyre in diabase near Dillsburg, Pennsylvania.* Geol. Soc. America Bull., v. 64, p. 675-704.

Hussey, A.M. 2nd (1962), *The geology of southern York County, Maine.* Maine Geol. Survey Spec. Studies Ser., No. 4, 67 p.

Jaeger, J.C. (1957), *The temperature in the neighborhood of a cooling intrusive sheet.* Am. Jour. Sci., v. 255, p. 306-318.

Jahns, R.H. Martin, R.F., and Tuttle, O.F. (1969), *Origin of granophyre in dikes and sills of tholeiitic diabase (abs).* Am. Geophys. Union Trans., v. 50, p. 337.

Jamieson, B.G. and Clarke, D.B. (1970), *Potassium and associated elements in tholeiitic basalts.* Jour. Petrology v. 11, p. 183-204.

Johannsen, Albert (1937), *A descriptive petrography of the igneous rocks.* v. 3, The Intermediate Rocks, Univ. Chicago Press, 360 p.

Jonas, A.I. and Stose, G.W. (1930), *Geology and mineral resources of the Lancaster quadrangle.* Pa. Geol. Survey, Atlas 160, 106 p.

Justus, P. S., Thayer, P. A., and Weigand, P. W. (1970), *Comparative geochemistry and petrology of diabase dikes in North Carolina Triassic basin.* Geol. Soc. America v. 2 No. 3 p. 223.

Kennedy, G.C. (1948), *Equilibrium between volatiles and iron oxides in igneous rocks.* Am. Jour. Sci., v. 246, p. 529-549.

__________(1955), *Some aspects of the roles of water in rock melts.* Geol. Soc. America, Spec. Paper 62, p. 489-533.

Kerr, P.F. (1959), *Optical Mineralogy.* McGraw-Hill Co. New York 3rd edition, 442 p.

King, P.B. (1961), *Sytematic pattern of Triassic dikes in the Applachian region.* U.S. Geol. Survey, Prof. Paper 424B, p. B93-B95.

Knopf, E.B. and Jonas, A.I. (1929), *Geology of the crystalline rocks of Balitmore County, Maryland.* Md. Geol. Survey, 181 p.

Kroll, R.L. (1971) *The Barndoor diabase intrusions, north central Connecticut.* Geol. Soc. America Abs v. 3, no. 1, p. 40-41.

Kullerud, Gunnar and Donnay, G. (1967), *Sulfide-oxide relations* Carnegie Inst. Wash. Yearbook, v. 65, 1965-1966, p. 356-357.

Kullerud, Gunnar, and Yoder, H.S., Jr. (1963), *Sulfide-silicate relations.* Carnegie Inst. Wash. Yearbook v. 62, 1962-1963 p. 215-218.

Kuno, Hisashi (1959), *Origin of Cenozoic petrograhic provinces of Japan and surrounding areas.* Bull. Volvanol. Ser. 2, v. 20, p. 37-76.

_________(1960), *High-alumina basalt.* Jour. Petrology, v. 1., p. 121-135.

_________(1968), *Differentiation of basalt magmas,* in *Basalts--The Poldervaart treatise on rocks of basaltic composition* Hess and A. Poldervaart, New York and London, Publishers, Interscience and others, v. 2, p. 623-688.

Kuno, H., Yamasaki, K. Ida, C. and Nagashima, R. (1957), *Differentiation of Hawaiian magmas.* Japanese Jour. Geol. Geography, v.28, p. 179-8.

Lapham, D.M. (1960), *Photomicrography of the Cornwall ore body, Cornwall, Pennsylvania (abs).* Geol. Soc. America Bull., v. 71, pt. 2, p. 1913.

_________(1962), *Magnetite mine, Cornwall, Pennsylvania,* in *Northern field excursion guidebook.* Internat. Mineralog. Assoc. 3rd Cong. Washington, D.C., p. 36-40.

_________(1968), *Triassic magnetite and diabase at Cornwall, Pa.* in *Ore Deposits of The United States: 1933-1967* (Graton-Sales Volume), v. 1, New York, Am. Inst. Mining, Metall. and Petroleum Engineers, p. 72-94.

_________and Geyer, A. R. (1969), *Mineral collecting in Pennsylvania.* Pa. Geol. Survey Bull. G33, 3rd edition, 164 p.

Lapham, D.M. and Faill, R. (p. 71) *230 Million Years of Rock Missing,* Pa. Geol. Survey, Pa. Geol., v. 2, p. 5.

Lapham, D.M. and Saylor, T.E. (1970), *Chemical analyses of three Triassic (?) diabase dikes in Pennsylvania.* Pa. Geol. Survey I.C. 68, 16 p.

Lesley, J.P. and d'Invilliers, E.V. (1886), *Report on the Cornwall iron ore mines, Lebanon County.* 2nd Geol. Survey of Pa., Ann. Rept. 1885, p. 491-570.

Lindgren, Waldemar (1933), *Mineral deposits.* McGraw-Hill Co., New York, 4th edition, 930 p.

Lindsley, D.H. (1962), *Investigation in the system FeO-*Fe_2O_3*-*TiO_2. Carnegie Inst. Washington Yearbook, v. 61, p. 100-106.

_________(1963), *Fe-Ti oxides in rocks as thermometers and oxygen barometers.* Carnegie Inst., Washington Yearbook, v. 62, p. 60-66.

Lodochnikow, W. (1936), *Serpentine and serpentinite der Iltschir-lagerstatte,* U.S.S.R. Central Geol. Prosp. Inst. Trans. fasc. 38, p. 743.

Lyons, J.B. and Faul, H. (1969), *Isotopic geochronology of the northern Appalachians. in Studies of Appalachian geology: Northern and Maritime,* ed. Zen, E-an, and others, Interscience Publishers, P. 305-318.

MacChesney, J.B. and Muan, A. (1959), *Studies in the system iron oxide-titanium oxide.* Am. Mineralogist, v. 44, p. 926-945.

_________(1960), *The system iron oxide* TiO_2*-*SiO_2 *in air.* Ceramic Soc. Jour., v. 43, p. 586-591.

MacDonald, G.A. and Katsura, T., Jr. (1964), *Chemical composition of Hawaiian lavas.* Jour. Petrology, v. 5, p. 82-133.

MacLaughlan, D.B. (1966), *Structural geology of the Lebanon Valley allochthon.* p. 32-49 in MacLaughlan, D.B. and Root, S.I. (1966), *Comparative tectonics and stratigraphy of the Cumberland and Lebanon valleys,* Pa. Geol. Field Conference Guidebook 31, 90 p.

_________(1967), *Geology of the carbonate rocks of Dauphin County, Pennsylvania.* Pa. Geol. Survey, Bull. G44, 168 p.

McDougall, Ian (1961), *Optical and chemical studies of pyroxenes in a differentiated Tasmanian dolerite.* Am. Mineralogist, v. 46, p. 661-687.

McLaughlin, D.B. (1959), *Triassic igneous and contact metamorphic rocks in Geology and mineral resources of Bucks County, Pa.* Pa. Geol. Survey Bull. C9, p. 141-153.

_________(1963), *Newly recognized folding in the Triassic of Pennsylvania.* Pa. Aca. Sci. Proc., v. 37, p. 156-159.

_________and Gerhard, R. C. (1953), *Stratigraphy and origin of the Triassic fluvatile sediment, Lebanon and Lancaster Counties.* Pa. Acad. Sci. Proc., v. 27, p. 136-142.

Montgomery, Arthur, (1956), *Thermal metamorphism of redbeds by diabase at Ringing Rocks near Kintnersville, Pa.* Pa. Acad. Sci. Prov., v. 30, p. 176-181.

Muan, Arnulf, (1958), *Phase equilibria at high temperatures in oxide systems involving changes in oxidation states.* Am. Jour. Sci., v. 256, p. 171-207.

__________and Osborne, E. F. (1956), *Phase equilibria at liquidus temperatures in the system* $MgO\text{-}Fe_2O_3\text{-}SiO_2$. Am. Ceramic Soc. Jour., v. 39, p. 121-140.

Mudge, M.R. (1968), *Depth control of some concordant intrusions.* Geol. Soc. America Bull., v. 79, p. 315-332.

Neumann, Henrich, Mead, J., and Vitaliano, C.J. (1954), *Trace element variation during fractional crystallization as calculated from the distribution law.* Geochim. et. Cosmochim. Acta, v. 6, p. 90-99.

Newhouse, W.H. and Callahan, W.H. (1927), *Two kinds of magnetite.* Econ. Geology, v. 22, p. 629-632.

Nickel, E.H. (1958), *The composition and microtexture of ulvöspinel-magnetite intergrowth.* Canadian Mineralogist, v. 6, p. 191-199.

Nickelsen, R.P. (1963), *Fold patterns and continuous deformation mechanisms of the central Pennsylvania folded Appalachians.* Pittsburgh Geol. Soc. Field Conference Guidebook, p. 13-29.

Nockolds, S.R. (1954), *Average chemical compositions of some igneous rocks.* Geol. Soc. America Bull., v. 65, p. 1007-1032.

O'Neill, B.J. (1964), *Atlas of Pennsylvania's mineral resources, Pt I: Limestone and Dolomites of Pennsylvania.* Pa. Geol. Survey Bull. M 50, p. 40.

O'Neill, B.J., Lapham, D.M., Jaron, M.C., Socolow, A.A., Hamlin, H.P. and Thompson, R.D. (1965), *Properties and uses of Pennsylvania shales and clays.* Pa. Geol. Survey Bull. M 51, p. 234-249.

Osborne, E.F. (1959), *Role of oxygen pressure in the crystallization and differentiation of basaltic magma.* Am. Jour. Sci., v. 257, p. 609-647.

__________(1962), *Reaction series for subalkaline igneous rocks based on different oxygen pressure conditions.* Am. Mineralogist, v. 47, p. 211-226.

Osborne, F.F. (1929), *A diabase contact metamorphic deposit in Ontario.* Econ. Geology, v. 24, p. 722-732.

Ovchinnikov, L.N. (1959), *Experimental study of the processes of ore genesis.* Acta. Geol. Acad. Sci. Hungary, Tomus V.

__________(1960), *Some regular phenomena in the magmatogene ore genesis.* Geol. Congr. 21st., Norden, pt. 16, p. 7-16.

Pearce, T.H. (1970), *Chemical variations in the Palisades sill.* Jour. Petrology, v. 11, p. 15-32.

Peets, R. B. (1957), *Mining history of Cornwall, Pennsylvania.* Mining Engineering, v. 9, p. 741-746.

Pettijohn, F.J. (1949), *Sedimentary rocks.* Harper and Brothers, New York, N.Y., 526 p.

Phillips, Bert and Muan, A. (1962), *Phase equilibria in the system* $MgO\text{-}FeO\text{-}Fe_2O_3$ *in temperature range 1400° to 1800° C.*, Amer. Ceramic Soc. Jour., v. 45, p. 588-591.

Pierce, K.L. and Armstrong R.L. (1966), *Tuscarora fault, and Acadian (?) bedding plane fault in central Appalachian valley and ridge province.* Amer. Assoc. Petroleum, Geologists Bull., v. 50, p. 385-390.

Poldervaart, Arie (1944), *The petrology of the Elephant's Head dike and New Amalfi sheet.* Royal Soc. South Africa Trans., v. 30, p. 85-120.

__________(1947), *The relationship of orthopyroxene to pigeonite.* Mineralog. Mag., v. 28, p. 164.

__________(1955), *Chemistry of the earth's crust.* Geol. Soc. America Spec. Paper 62, p. 119-144.

__________and Hess, H. H. (1951), *Pryoxenes in the crystallization of basaltic magma.* Jour. Geology, v. 59, p. 472.

Poldervaart, Arie and Parker, A.B. (1964), *The crystallization index as a parameter of igneous differentiation in binary variation diagrams.* Am. Jour. Sci., v. 262, p. 281-289.

Poldervaart, Arie and Walker, K.R. (1962), *The Palisade sill*, in *Northern field excursion guidebook.* Internat Mineralog. Assoc. 3rd Cong., Washington, D.C. p. 5-7.

Popovich, D.E. (1965), *Distribution of certain elements in the major rock units of the Cornwall and Morgantown mines, Pennsylvania.* M.A. Thesis Pa. State Univ., 77 p.

Ridge, J.O. (1956a), *The geology of the iron ore of Kiruna and Gallivare Sweden.* Pa. State Univ. Min. Industries Bull., v. 25, p. 1-6.

__________(1956b), *Transportation and deposition of hydrothermal minerals.* Int. Geol. Cong. 20th Sess., Resumes, p. 100.

Roger, H.D. (1858), *The geology of Pennsylvania.* First Pa. Geol. Survey, v. 2, pt. 2, 1046p.

Rogers, D.P. (1969), *The extrusive iron oxide deposits, "El, Laco", Chile, (abs).* Geol. Soc. America Spec. Paper 121, p. 252-253.

Root, S.I. (1970), *Structure of the northern terminus of the Blue Ridge in Pennsylvania.* Geol. Soc. America Bull., v. 81, p. 815-830.

Salotti, C.A. (1964), *The possible role of oxygen in the anomalous pyrite-pyrrhotite relation.* Econ. Geology, v. 59, p. 1588-1595.

Sanders, J.E. (1963), *Late Triassic tectonic history of northeastern United States.* Am. Jour. Sci., v. 261, p. 501-524.

Sangster, D.F. (1969), *The contact metasomatic magnetite deposits of south-western British Columbia.* Canada Geol. Survey Bull. 172, 85 p.

Sarbadhikari, T.R. (1965), *On the difference in twinning between phenocryst and ground mass plagioclase of basalts.* Am. Mineralogist, v. 50, p. 1466-1469.

Schwartz, G.M. and Sandberg, A.E. (1940), *Rock slides in diabase sills at Duluth, Minnesota.* Geol. Soc. America Bull., v. 51, p. 1135-1171.

Seifert, K.E. (1964), *The genesis of plagioclase twinning in the Nonewaug granite.* Am Mineralogist, v. 49, p. 297-320.

Shale, S.J. (1953), *After two centuries of mining Cornwall keeps its methods up-to-date.* Mining Engineering, v. 5, p. 670-675.

Shannon, E.V. (1924), *The mineralogy and petrology of intrusive Triassic diabase at Goose Creek, London Country, Va.,* U.S. Nat. Mus. Proc., v. 66, 86 p.

Shepherd, E.S. (1938), *The gases in rocks and some related problems.* Am. Jour. Sci., v. 35 A p. 311-351.

Shirozu, H. (1958), *X-ray powder patterns and cell dimensions of some chlorites in Japan with a note on their interference colors.* Min. Jour. Japan, v. 2, p. 209.

Siedner, G. and Miller, J.A. (1968), *K-Ar age determinations on basaltic rocks from south-west Africa and their bearing on continental drift.* Earth and Planetary Sci. Letters, Northland Pub. Comp., Amsterdam, p. 451-458.

Simpson, Dale R. (1969), *Hornfels associated with Triassic diabase.* Geol. Soc. America Abs. v. 1, No. 1, p. 55-56.

Sims, S.J. (1968), *The Grace Mine magnetite deposit, Berks County, Pennsylvania* in *Ore Deposits of the United States: 1933-1967.* New York, Am. Inst. Mining, Metall. and Petroleum Engineers, v. 1, p. 108-124.

Smith, J.V. and Gay, P. (1958), *The powder patterns and lattice parameters of plagioclase feldspars, II.* Mineralog. Mag., v. 31, p. 744.

Smith, A.G. and Hallam, A. (1970), *The fit of the southern continents.* Nature, v. 225, p. 139-144.

Smith, J.R. and Yoder, H.S., Jr. (1956), *Variations in X-ray powder diffraction patterns of plagioclase feldspars.* Am. Mineralogist, v. 41, p. 632.

Smitheringale, W.G. and Jensen, M.L. (1963), *Sulfur isotopic composition of the Triassic igneous rocks of eastern United States.* Geochim. et Cosmochim. Acta, v. 27, p. 1183-1207.

Socolow, A.A. (1961), *Geologic interpretation of certain aeromagnetic maps of Lancaster, Berks and Lebanon Counties.* Pa. Geol. Survey, IC 41, 19 p.

Spencer, A.C. (1908), *Magnetite deposits of the Cornwall type in Pennsylvania.* U.S. Geol. Survey, Bull., v. 359, 102 p.

Stose, G.W. (1932), *Geology and mineral resources of Adams County, Pennsylvania.* Pa. Geol. Survey, Bull. C1, 153 p.

__________and Bascom, F. (1929), *Description of the Fairfield and Gettysburg quadrangles.* U. S. Geol. Survey, Atlas 225, Fairfield-Gettysburg folio, Pa.

__________and Jonas A. I. (1927), *Ordovician shale and associated lava in southeastern Pennsylvania.* Geol. Soc. America Bull., v. 38, p. 505-536.

__________and Jonas, A. I. (1933), *Geology and mineral resources of the Middletown quadrangle, Pennsylvania.* U. S. Geol. Survey, Bull, 840, 86 p.

__________and Jonas, A. I. (1939), *The geology and mineral resources of York County, Pennsylvania.* Pa. Geol. Survey, Bull. C67, 199 p.

Taylor, H.P. and Epstein, S. (1962), *Relationships between* O^{18}/O^{16} *ratios in coexisting minerals of igneous and metamorphic rocks,* Part I, *Principles and experimental results.* Geol. Soc. America Bull., v. 73, p. 461-480.

__________and Epstein, S. (1963), O^{18}/O^{16} *ratios in rocks and coexisting minerals of the Skaergaard intrusion, East Greenland.* Jour. Petrology, v. 4, p. 51-74.

Thompson, J.B., Jr. (1957), *The graphical analysis of mineral assemblages in pelitic schists.* Am. Mineralogist, v. 42, p. 842-858.

__________(1959), *Local equilibrium in metasomatic processes,* in *Researches in Geochemistry.* Wiley and Sons Inc., N.Y., p. 427-457.

Thornton, C.P. and Tuttle, O.F. (1960), *Chemistry of igneous rocks, I. Differentiation index.* Am. Jour. Sci., v. 258, p. 664-684.

Tomkieff, S. I. (1929), *A contribution on the petrology of the Whin sill,* Mineralog. Mag., v. 22, p. 100-120.

Tomlinson, W. H. (1945), *Notes on the derivatives of the Triassic diabases of Pennsylvania.* Econ. Geology, v. 40, p. 526-536.

Turnock, A.C. and Eugster, H.P. (1962), *Fe-Al oxides: phase relationships below 1000°C.,* Jour. Petrology, v. 3, p. 533-565.

Tsusue, Akio (1964), *Mineral aspects of the Grace Mine magnetite deposits.* Pa. Geol. Survey, Min. Res. Rept. M49, 10 p.

Turner, F.J. and Verhoogan, J. (1960), *Igneous and metamorhpic petrology.* McGraw-Hill, N.Y., 694 p.

Tuttle, O.F. and Bowen, N.L. (1958), *Origin of granite in the light of experimental studies in the system* $NaAlSi_3O_8$ *-* SiO_2 *-* H_2O. Geol. Soc. America Mem. 74, p. 10-13.

Vogel, T. A. (1964), *Optical-crystallographic scatter in plagioclase.* Am. Mineralogist, v. 49, p. 614-633.

Wager, L.R. (1960), *The major element variation of the layered series of the Skaergaard intrusion and a re-estimation of the average composition of the hidden layered series and of the successive residual magmas.* Jour. Petrology, v. 1, p. 364-398.

__________(1963), *The mechanism of adcumulus growth in the layered series of the Skaergaard intrusion,* in *Symposium on layered intrusions.* Mineralog. Soc. America, Spec. Paper 1, p. 1-9.

Wager, L.R. Brown, G.M., and Wadsworth, W.J. (1960), *Types of igneous cumulates.* Jour. Petrology, v. 1, p. 73-85.

__________and Deer, W. A. (1939), *The petrology of the Skaergaard intrusion, Kangerdlugssuaq, East Greenland,* in Geol. Inv. in East Greenland, Mdd. on Gronland, Bd. 105, n. 4, pt. 3, p. 1-335.

Walker, F. (1940), *Differentiation of the Palisade diabase, New Jersey*. Geol. Soc. America Bull., v. 51, p. 1059-1106.

__________(1941), *The Hangnest dolerite sill, South Africa*. Geol. Mag., v. 78, p. 429-450.

__________(1949), *Karroo dolerites of the Union of South Africa*. Geol. Soc. America Bull., v. 60, p. 591-706.

__________and Poldervaart, A. (1940), *The petrology of the dolerite sill of Downes Mountain, Calvinia*. Geol. Soc. South Africa Trans., v. 43, p. 159-173.

Walker, K.R. (1969), *The Palisades sill, New Jersey: A reinvestigation*. Geol. Soc. America Special Paper 111, 178 p.

Washington, H.S. (1922), *Deccan traps and other plateau basalts*. Jour. Geology, v. 32, p. 797.

Wilkinson, J.F.G. (1967), *The petrography of basaltic rocks, in Basalts: The Poldervaart treatise on rocks of basaltic composition*, ed. H.H. Hess and A. Poldervaart. New York and London, Interscience publishers v. 1., p. 163-214.

Witthoft, John, (1964), *Alleged Phoenician inscriptions from York County, Pa.*, Pennsylvania Acta., v. 13, p. 42-69.

Witthoft, John (1964), *Alleged Phoenician inscriptions from York County, Pa.*, Pennsylvania Archeologist, p. 93-94

Wones, D.R. (1963), *Phase equilibria of "ferriannite"*, KFe_3^2, $Fe^3Si_3O_{10}(OH)_2$. Am. Jour. Sci. v. 261, p. 581-596.

__________and Appleman, D. E. (1961), *X-ray crystallography and optical properties of synthetic monoclinic* $KFeSi_3O_8$ *iron-sanidine; in Short papers in the geologic and hydrologic sciences*. U.S. Geol. Survey Prof. Paper 424-C, p. C309-C310.

__________and Appleman, D. E. (1963a), *Properties of synthetic triclinic* $KFeSi_3O_8$, *iron-microcline with some observations on the iron-microcline, iron-sanidine transition*. Jour. Petrology, v. 4, No. 1, p. 131-137.

__________and Appleman, D. E. (1963b), *Iron-feldspar polymorphs in the system* K_2O-FeO-Fe_2O_3-SiO_2H_2O *(abs)*. Min. Soc. America, Spec. Paper No., p. 314.

__________and Eugster, H. P. (1956), *Stability of biotite; experiment, theory, and application*. Am. Mineralogist, v. 50, p. 1228-1272.

Woollard, G.P. (1969), *Tectonic activity in North America as indicated by Earthquakes*, in *The Earth's crust and upper mantle*. Am. Geophys. Union Geophys. Mon. 13, p. 125-133.

Wright, T.L. (1964), *The alkali feldspars of the Tatoosh pluton, Mount Rainier National Park*. Am. Mineralogist, v. 49, p. 715-735.

__________(1968), *X-ray and optical study of alkali feldspar: II. An X-ray method for determining the composition and structural state from measurement of* 2θ *values for three reflections*. Am. Mineralogist, v. 53, p. 88-104.

__________and Sato, M. (1966), *Oxygen fugacities of magmatic gases from crystallizing Hawaiian tholeiite (abs)*. Am. Geophys. Union Trans., v. 47, p. 209.

__________and Weiblen, W. (1967), *Mineral composition and paragenesis in tholeiite basalt from Maukaopuhi lava lake, Hawaii (abs)*. Geol. Soc. America Spec. Paper 115, p. 242-243.

Yoder, H.S. and Eugster, H.P. (1955), *Synthetic and natural muscovites*. Geochim. et Cosmochim. Acta, v. 8, p. 225-280.

__________and Tilley, C.E. (1962), *Origin of basalt magmas: an experimental study of natural and synthetic rock systems*. Jour. Petrology, v. 3, p. 342-532.

__________Tilley, C. E., and Schairer, J. F. (1963), *Pyroxenes and associated minerals in the crust and mantle*. Carnegie Inst., Washington Yearbook, v. 62, p. 84-95.

Zen, E-an (1963), *Components, phases, and criteria of chemical equilibrium in rocks*. Am. Jour. Sci., v. 261, p. 929-042.

Zietz, Isidore and Gray, Carlyle (1960), *Geophysical and geological interpretation of a Triassic structure in eastern Pennsylvania*. U.S. Geol. Survey Prof. Paper 400-B, p. B174-B178.

APPENDIX 1

MINERALS AT CORNWALL, PENNSYLVANIA

* Actinolite (byssolite)
* Adularia
Aegirine-augite
Albite
* Analcime
Andalusite(?)
Andesine
* Andradite
Anorthoclase
* Antigorite
Apatite
* Apophyllite
* Aragonite
Augite
* Azurite
Bieberite(?)
* Biotite
* Bornite
* Brochantite
* Brucite
* Calcite
* Chabazite
* Chalcanthite
* Chalcocite
* Chlorite
* Chrysotile
* Chrysocolla
Clinohypersthene
Clinozoisite
* Copper (native)
Cordierite(?)
* Covellite
Crednerite(?)
* Cuprite
* Datolite
* Diopside
* Dolomite
Enstatite
* Epidote
* Erythrite
Ferrohedenbergite(?)
Fluorite
Galena
Gmelinite(?)
* Grossular
* Gypsum
Harmotome(?)
Hedenbergite
* Heulandite
Hornblende
* Hyalite Opal
Hypersthene
* Idocrase
Ilmenite
* Kaolinite
Labradorite
* Laumontite
* Leonhardite
* Limonite
* Magnetite
* Malachite
* Marcasite
Mesolite(?)
* Microcline
* Millerite
* Muscovite
* Mn-Na (pink) muscovite
* Natrolite
Olivine
* Orthoclase
* Fe-Orthoclase
* Pectolite
Pigeonite
* Prehnite
* Pyrite (cobaltian)
* Pyroaurite
* Pyrrhotite
* Quartz
Rhodochrosite(?)
Rutile
Scheelite
* Sphalerite
Sphene
* Stilbite
* Talc
Thomsonite(?)
* Tourmaline (elbaite and schorl
* Tremolite
Ulvöspinel
* Wurtzite, 4H or 6H
Zircon
* Zoisite(?)

* Chalcopyrite * Hematite * Phlogopite

* If permission for collecting is obtained,
these minerals may be collected on waste dumps.

APPENDIX 2

GARNET X-RAY DATA

(1)		(2)		(3)	
dÅ	$1/1_o$	dÅ	$1/1_o$	dÅ	$1/I_o$
4.239	12	4.226	15	4.226	12
3.009	15	3.011	15	~3.01	~10
2.996	60	2.998	60	2.993	50
2.692	20	2.693	18	~2.69	~15
2.679	85	2.680	~100	2.680	90
2.557	8	2.564	8	2.555	6
2.460	15	2.458	10	~2.46	~10
2.449	55	2.452	55	2.446	55
2.354	12	2.356	15	2.352	15
2.194	12	2.195	15	2.190	15
1.947	20	1.949	28	1.947	25
1.899	15	1.902	18	1.899	12
1.733	5	1.736	8	1.733	5
1.667	30	1.666	35	1.664	30
1.605	100	1.607	100	1.605	100
1.502	15	1.503	18	1.504	15
1.345	20	1.344	25	1.343	25
1.313	20	1.316	28	1.313	27
1.282	15	1.283	20	1.282	22

*Cu K_α radiation; Debye-Scherrer Camera; visual intensity estimate

(1) Garnet in recrystallized host limestone
(2) Garnet at limestone-Mill Hill Slate contact
(3) Garnet in bleached Triassic conglomerate

APPENDIX 3

LOG OF VERTICAL CORE THROUGH DIABASE: D.D.H. #155 (SEE PLATE 21)

(Logged by C. Gray)

Depth from Surface (ft.)	Remarks
0-44	No core
44-45	Fine-grained diabase

Depth from Surface (ft.)	Remarks
45-55	Fine- to medium-grained diabase
55-59	Medium-grained diabase; ½" pegmatitic schlieren; actinolite on joints.
59-63	Medium-grained diabase
63-69	Medium-grained diabase; 3" pegmatitic schlieren
69-73	Medium-grained diabase; pegmatitic with sulfides
73-78	Medium- to coarse-grained diabase; vuggy pegmatitic schlieren with chalcopyrite, pyrrhotite (?)
78-85	Medium-grained diabase
85-98	Normal diabase (N.D.), coarse pegmatitic pods and patches
98-106	N.D.; chalcopyrite, pyrrhotite actinolite on joint; 6-8" pegmatitic schlieren
106-108	N.D.; actinolite on joint
108-116	N.D.; diabase-pegmatite pod
116-123	N.D.
123-132	N.D.; 3" pegmatitic schlieren
132-145	N.D.; zeolites in vug; actinolite, chlorite, chalcopyrite on joints; 2" pegmatitic patch
145-208	N.D.
208-235	N.D.; chalcopyrite, chlorite on joint; jointing intense
235-256	N.D.; biotite veinlet
256-270	N.D.; white vein (sericitized plagioclase, carbonate)
270-274	Diabase-granophyre transitional rock

Depth from Surface (ft.)	Remarks
274-297	N.D.; zeolite veinlets; intensely jointed
297-320	N.D.; zeolites, sulfides
320-328	N.D.; patches of pegmatitic diabase and transitional granophyre
328-329	Coarse-grained diabase; magnetite-ilmenite in pegmatitic diabase; jointed
329-330	N.D.
330-332	Pegmatitic diabase and granophyre; sulfides and actinolite on joint
332-367	N.D. with patches of pegmatitic schlieren and pods
367-434	N.D.; intense jointing with actinolite
434-480	N.D.; jointed
480-504	N.D.; vertical vein of magnetite, chlorite, actinolite
504-509	Medium-grained to normal diabase
509-511	Normal to coarse-grained diabase
511-527	N.D.
527-547	N.D.; seam with natrolite
547-551	N.D.; actinolite and zeolite in vein
551-565	N.D.; patches of coarse-grained diabase
565-566	Pegmatitic diabase
566-595	N.D.; patches of coarse-grained diabase
595-650	N.D.

Depth from Surface (ft.)	Remarks
650-686	N.D.; intense vertical jointing; small patches of coarse diabase
686-690	N.D.; 4" vein of magnetite, actinolite; zeolite veinlet (apophyllite)
690-718	N.D.
718-743	N.D.; zeolite veinlet
743-835	N.D.; occasional thin zeolite seams
835-847	N.D.; magnetite, actinolite in seam
847-860	N.D.; magnetite, zeolite in seam
860-875	N.D.; brecciated; small faults and joints; zeolite seam
875-883	N.D.
883-895	N.D.; sheared
895-935	N.D.
935-954	N.D.; larger pyroxene crystals
954-1045	N.D.
1045-1047	N.D.; sheared with chlorite
1047-1064	N.D.
1064-1068	Brecciated; steep dipping veinlets of magnetite-actinolite with crustification textures; sharp vein-diabase contact; some altered diabase
1068-1119	N.D. to medium-grained diabase; some shearing; a few magnetite-actinolite veinlets; asbestiform veinlet
1119-1136	N.D.; actinolite vein; some altered diabase

Depth from Surface (ft.)	Remarks
1136-1137	N.D. to coarse-grained diabase; transitional granophyre with pyrite, iron oxide and pegmatitic diabase
1137-1144	N.D. to pegmatitic diabase with magnetite, ilmenite; sheared
1144-1197	N.D. to medium-grained diabase
1197-1207	Medium-grained diabase; porphyritic pyroxenes; sheared
1207-1245	Medium-grained diabase; some shearing
1245-1258	Medium-grained diabase; chlorite; brecciated
1258-1265	Fine-grained chilled facies; serpentinized; brecciated
1265-1315	Limestone; serpentinized near diabase; brecciated; interbanded dolomite and limestone; folded

N.D. = Normal diabase texture

Note: Total pegmatitic diabase constitutes 3 per cent of total core by volume; amount of granophyre encountered is less

APPENDIX 4

CHEMICAL ANALYSES AT CORNWALL (in %)

Part A. Diabase and Related Igneous Rocks

Sample Oxide	C2-1 "Dike," Lapham, and Saylor, 1970 (by Sp.)	C4-308 Upper Chilled Margin (by Sp.)	C4-150 Granophyre (by Mc.)	38-G Granophyre (by Sp.)	38-P Diabase Pegmatite (by Sp.)	C-17 Diabase at 270′ (by Sm.)	C-18 Diabase Pegmatite at 330′		
							(by Mc.)	(by Sm.)	Average
SiO_2	48.00	50.10	59.46	70.10	51.90	52.90	50.54	51.10	50.82
TiO_2	0.90	1.09	0.53	0.18	1.86	1.03	2.35	1.79	2.07
Al_2O_3	14.80	14.20	16.88	15.00	13.60	19.45*	14.04	14.40	14.22
Fe_2O_3	5.25	6.50	2.57	0.97	10.69	1.39	7.44	3.46	3.46
FeO	6.11	3.63	0.91	0.12	2.97	5.54	3.68	6.65	6.65
MnO	0.27	0.24	0.06	0.02	0.15	0.133	0.21	0.212	0.211
MgO	8.53	7.90	1.43	1.02	4.62	5.15	4.75	5.10	4.93
CaO	4.06	9.92	5.24	0.98	7.90	11.10	11.02	11.55	11.29
Na_2O	0.17	1.65	3.50	0.79	2.23	2.83	2.86	2.87	2.87
K_2O	6.70	1.72	7.23	9.42	2.62	0.86	1.72	1.22	1.47
CO_2	0.22	0.16	0.16	0.22	0.16	N.A.	0.24	N.A.	0.24
H_2O comb.	4.05	2.18	1.72	0.22	0.92	N.A.	0.88	N.A.	0.88
NiO%, Ni ppm	0.003%*	0.006%*	N.A.	0.001%*	0.002%*	72 ppm	N.A.	52 ppm	52 ppm
CoO%, Co ppm	0.003%*	0.001%*	N.A.	0.003%*	0.001%*	35 ppm	N.A.	32 ppm	32 ppm
F	0.23	0.22	0.216	0.13	0.16	N.A.	0.034	N.A.	0.034
S	0.060	0.043	0.036	0.045	0.065	0.0195	0.023	0.016	0.020
SrO	N.A.	N.A.	N.A.	N.A.	N.A.	0.026	N.A.	0.019	0.019
Li_2O	N.A.	N.A.	N.A.	N.A.	N.A.	N.A.	N.A.	N.A.	N.A.
P_2O_5	N.A.	N.A.	N.A.	N.A.	N.A.	0.100	N.A.	0.210	0.210

Sample	C-19 Diabase at 433′					C-20 Diabase at 493′ (by Sm.)	C-21 Altered Diabase at 550′ (by Sm.)		C-22 Diabase at 649′ (by Sp.)	C-24 Diabase at 750′ (by Sp.)
Oxide	(by Mc.)	(by Sp.)	(by Sm.)	by C.	Average		A	B		
SiO_2	51.94	51.36	53.30*		52.20	49.20	50.40	51.00	51.30	51.30
TiO_2	0.98	0.85	0.83		0.89	0.71	0.78	0.90	0.84	0.70
Al_2O_3	13.52	13.37	14.50		13.80	17.60*	11.25	15.85	13.50	13.10
Fe_2O_3	7.78	8.52	1.89	2.29	2.09	2.03	2.19	2.25	9.27	9.63
FeO	2.70	1.72	8.02	8.63	8.31	6.32	7.93	7.11	0.93	0.76
MnO	0.19	0.16	0.167		0.17	0.178	0.178	0.145	0.16	0.17
MgO	8.57	8.71	8.35		8.54	8.25	9.10	8.45	9.15	9.80
CaO	10.68	11.18	11.45		11.10	11.55	13.30	10.70	11.40	11.30
Na_2O	1.78	1.58	1.86		1.74	1.74	0.94	1.89	1.88	1.80
K_2O	0.43	0.61	0.51		0.52	1.07	0.43	0.56	0.52	0.40
CO_2	0.13	0.40	N.A.		0.27	N.A.	N.A.		0.32	0.32
H_2O comb.	0.93	1.34	N.A.		1.14	N.A.	N.A.		0.60	0.31
NiO%, Ni ppm	0.10%	N.A.	109 ppm		0.056%	93 ppm	103 ppm	117 ppm	0.007%*	0.008*
CoO%, Co ppm	N.A.	N.A.	44 ppm		0.0044%	34 ppm	45 ppm	43 ppm	$<$0.001%	$<$0.001%
F	0.004	0.08	N.A.		0.042	N.A.	N.A.		0.32	0.33
S	0.015	0.020	0.0095		0.0148	0.010	0.0170	0.0120	0.020	0.022
SrO	N.A.	N.A.	0.018		0.018	0.018	0.007	0.016	N.A.	N.A.
Li_2O	0.12	N.A.	N.A.		0.12	N.A.	N.A.		N.A.	N.A.
P_2O_5	N.A.	N.A.	0.095		0.095	0.100	0.115	0.110	N.A.	N.A.
Total	99.869	99.900	101.0148		101.1202	98.7887	96.6518	99.009	100.218	99.951

APPENDIX 4. *(continued)*

Oxide / Sample	C-26 Porphyritic Diabase at 937′ (by Sm.)	C-27 Diabase at 1021′ (by Sm.)	C-28 Altered Diabase at 1040′ (by Sm.)	C-30 Sheared Diabase at 1066′ (by Sp.)	C-31 Diabase at 1114′			C-32 Diabase at 1159′ (by Sm.)	C-33 Porphyritic Diabase at 1202′ (by Sm.)
					(by Sp.)	(by Sm.)	Average		
SiO_2	51.80	51.00	53.30*	49.70	51.10	50.50	50.80	51.70	51.70
TiO_2	0.78	0.70	0.87	0.75	0.71	0.79	0.75	i.02	1.02
Al_2O_3	15.60	14.10	13.00	11.80	13.60	16.90*	15.25	12.70	15.40
Fe_2O_3	1.36	1.80	1.56	5.94	9.29	1.10	1.10	1.93	2.19
FeO	7.28	6.84	8.63	3.84	0.80	7.92	7.92	8.80	8.02
MnO	0.156	0.167	0.178	0.25	0.17	0.174	0.172	0.182	0.170
MgO	8.90	8.80	10.35	11.48	10.20	9.15	9.68	11.30	8.45
CaO	12.00	12.05	11.50	10.48	11.08	10.96	11.02	10.55	11.00
Na_2O	1.71	1.85	1.50	1.04	1.65	1.50	1.58	1.53	1.54
K_2O	0.43	0.37	0.33	0.50	0.50	0.41	0.46	0.44	0.55
CO_2	N.A.	N.A.	N.A.	0.29	0.16	N.A.	0.16	N.A.	N.A.
H_2O comb.	N.A.	N.A.	N.A.	3.42	0.57	N.A.	0.57	N.A.	N.A.
NiO%, Ni ppm	121 ppm	117 ppm	131 ppm	0.008%*	0.010%	133 ppm	0.012%	150 ppm	121 ppm
CoO%, Co ppm	42 ppm	39 ppm	47 ppm	<0.001%	0.001%	44 ppm	0.0027%	51 ppm	45 ppm
F	N.A.	N.A.	N.A.	0.17	0.18	N.A.	0.18	N.A.	N.A.
S	0.0105	0.0145	0.0130	0.022	0.020	0.010	0.015	0.0235	0.0210
SrO	0.020	0.016	0.017	N.A.	N.A.	0.016	0.016	0.016	0.015
Li_2O	N.A.	N.A.	N.A.	N.A.	N.A.	N.A.	N.A.	N.A.	N.A.
P_2O_5	0.110	0.130	0.100	N.A.	N.A.	0.095	0.095	0.130	0.120
Total	100.1728	97.8531	101.3658	99.691	100.041	99.5427	99.7827	100.3416	100.2126

APPENDIX 4. (continued)

Oxide / Sample	C-34 Diabase at 1227′, 35′ above base (by Sp.)	(by Sm.)	Average	G-1 (by Sp.)	G-1 Accepted Range	W-1 (by Sp.)	W-1 Accepted Range	BCR-1 Split 74 (by C.)
SiO_2	51.20	51.00	51 10					54.02
TiO_2	0.93	1.19	1.06					2.25
Al_2O_3	13.70	18.05*	15.88					13.99
Fe_2O_3	9.38	1.84	1.84	0.82	0.65-1.25	1.49	0.91-2.33	3.57
FeO	1.32	8.33	8.33	0.95	0.89-1.10	8.80	8.22-9.04	8.78
MnO	0.16	0.170	0.165					0.20
MgO	8.43	7.60	8.02					3.48
CaO	10.66	10.45	10.56					6.95
Na_2O	2.42	1.72	2.07					2.78
K_2O	0.63	0.54	0.59					1.45
CO_2	0.16	N.A.	0.16					0.01
H_2O comb.	0.65	N.A.	0.65					1.76
NiO%, Ni ppm	0.007%	98 ppm	0.008%					15 ppm
CoO%, Ni ppm	0.001%	41 ppm	0.0026%					60 ppm
F	0.20	N.A.	0.20					N.A.
S	0.033	0.0210	0.027					N.A.
SrO%, Sr ppm	N.A.	0.014	0.014					335 ppm
Li_2O%	N.A.	N.A.	N.A.					N.A.
P_2O_5	N.A.	0.120	0.120					0.35
Total	99.881	101.0589	100.7966					99.6310

APPENDIX 4. *(Continued)*

Explanation

C = Analysis by E.L. Conwell Co., Philadelphia, Pa.; 50 grams minimum sample

Mc = Analysis by A.S. McCreath Co.; 60 grams minimum sample

Sm = Analysis by R. Smith, Pennsylvania State University, University Park, Pa.; 5-20 gram sample, written communication, 1971

Sp = Analysis by Spectrochemical Laboratories, Inc., Pittsburgh, Pa.; 60 grams minimum sample

N.A. = No analysis determined

330′ = Depth; from vertical core through diabase, D.D.H. #155

C-21 A = Less altered sample at 550′ depth

C-21 B = More altered sample at 550′ depth

Note: See "Analytical Accuracy" in text for discussion; averages exclude Fe_2O_3 and FeO by Mc. and Sp.
Analyses marked by an * may be in error (see text).

APPENDIX 4. *(continued)*

Part B. Bulk Rock Analyses of Gangue and Hornfels

	1*	2*	3*	4*	5+	6+
SiO_2	58.55	59.38	52.09	54.71	39.48	45.60
TiO_2	0.90	0.88	NA	NA	0.53	0.74
Al_2O_3	14.67	16.36	23.16	23.74	14.24	7.20
Fe_2O_3	3.47	2.44	3.66	3.56	6.34	5.23
FeO	3.45	1.45	5.90	3.27	5.06	2.93
MnO	0.20	0.15	NA	NA	0.127	0.137
MgO	1.85	0.90	2.72	2.05	17.75	22.31
CaO	5.80	4.95	2.54	0.48	7.92	5.66
Na_2O	3.64	2.88	3.97	3.70	0.24	0.30
K_2O	3.65	7.95	2.40	6.05	5.40	5.40
CO_2	0.15	0.74	0.66	0.29	0.32	0.42
H_2O comb.	3.05	1.41	2.27	1.50	1.53	3.34
P_2O_5	NA	NA	NA	NA	0.048	0.206
SrO	0.004	0.003	NA	NA	NA	NA
NiO	0.05	0.01	NA	NA	NA	NA
ZnO	< .001	0.10	NA	NA	NA	NA
CoO	0.002	0.01	NA	NA	NA	NA
CuO	0.01	0.05	NA	NA	NA	NA
Cr_2O_3	0.005	0.005	NA	NA	NA	NA
BaO	0.01	0.03	NA	NA	NA	NA
F	0.32	0.23	NA	0.09	0.168	0.156
S	NA	NA	NA	NA	0.013	0.013

* Spectrochemical Laboratories, Pittsburgh, Pa.
+ McCreath and Son, Inc., Harrisburg, Pa.
NA No analysis determined

1. Mill Hill Slate hornfels (C-5)
2. Mill Hill Slate, metasomatized (C4-10)
3. Blue Conglomerate hornfels (C4-304)
4. Blue Conglomerate, metasomatized (C-M)
5. Gangue from footwall (C4-196)
6. Gangue from hanging wall, eastern ore body

APPENDIX 5

CHEMICAL ANALYSES

Part A. Diabase Sheets: Triassic of North America

Oxide	1. Avg. Palisades, N.J. (Walker, 1940)	2. Rocky Hill, N.J. (Shannon, 1924)	3. Goat Hill, Pa. (Hall, 1881)	4. Jericho Hill, Pa. (Hall, 1881)	5. Mt. Pleasant, Pa. (Hall, 1881)	6. Haycock Hill, Pa. (Hall, 1881)	7. Haycock Hill, Pa. (Hall, 1881)	8. Rock Hill, Pa. (Hall, 1881)
SiO_2	51.12	50.34	53.92	52.82	52.91	52.73	52.54	53.16
TiO_2	1.14	1.56	0.43*	0.26*	1.03	1.02	0.63	0.86
Al_2O_3	14.09	15.23	18.72*	16.18	14.45	11.77	14.79	13.90
Fe_2O_3	1.80	2.82	4.89	5.45	6.42*	3.50	4.38	4.40
FeO	9.19	11.17	4.37	5.72	4.38	6.45	6.34	5.10
MnO	0.09	0.14	Tr	N.A.	N.A.	N.A.	N.A.	N.A.
MgO	8.94	5.81	3.86	5.88	8.34	9.33	7.95	10.63
CaO	9.38	9.61	10.42	8.38	9.92	10.96	11.21	9.75
Na_2O	2.14	2.93	3.08	2.56	1.80	1.55	2.00	1.16
K_2O	0.77	1.02	0.81	0.82	0.57	0.48	0.67	0.48
K_2O comb.	1.18	0.26	0.41	0.93	0.29	0.48	0.34	0.49
P_2O_5	0.12	0.14	0.19	0.19	0.12	0.16	0.23	0.15
Totals	99.96	101.03	101.10	99.19	100.23	98.43*	101.08	100.08
Fe_{total}	8.40	10.66	6.83*	8.25	7.89	7.46	7.99	7.04

*Analysis of questionable accuracy or unusual quantity.

APPENDIX 5. *(continued)*

	9.*	10.	11.	12.	13.	14.	15.	16.	17.
Oxide	Birdsboro Pa. (Stose & Bascom, 1919)	Rossville, Pa. (Frazer, 1880)	Dillsburg, Pa. (Frazer, 1880)	Dillsburg, Pa. (Frazer, 1880)	Dillsburg, Pa. (Frazer, 1880)	Dillsburg, Pa. (Frazer, 1880)	Dillsburg, Pa. (Hotz, 1953)	Culpepper Co., Va. (Stose & Bascom 1929)	Goose Creek, Va. (Shannon, 1924)
SiO_2	46.87*	52.48	53.32	52.14	56.13	51.88	52.89	51.31	51.56
TiO_2	1.98	1.15	1.00	1.04	1.98	1.01	1.44	Tr*	1.48
Al_2O_3	13.36	15.27	13.87	17.41*	12.32	13.73	15.79	13.64	13.81
Fe_2O_3	9.79*	2.39	3.12	4.94	5.86	2.79	1.71	0.52	0.96
FeO	2.71	8.22	7.17	6.42	6.15	8.05	9.19	8.49	11.32
MnO	N.A.	N.A.	0.47	N.A.	0.49	0.42	0.18	Tr	0.19
MgO	4.35	7.35	7.57	3.72*	1.54*	7.86	4.33	12.73*	7.40
CaO	14.70*	10.28	10.42	9.21	5.52	10.68	9.78	12.41*	10.08
Na_2O	4.64	2.05	2.05	2.95	5.88*	2.32	2.49	1.40	2.08
K_2O	2.01*	0.45	0.73	0.85	0.17	0.61	0.64	N.A.	0.96
H_2O comb.	N.A.	0.38	0.69	1.59	3.78*	1.10	1.30	N.A.	N.A.
P_2O_5	N.A.	0.15	0.22	0.04	0.44	0.21	0.18	N.A.	0.16
Totals	100.41	100.17	100.63	100.31	100.26	100.66	99.92	100.50	100.00
Fe_{total}	8.95	8.06	7.75	8.44	8.88	8.30	8.34	6.96*	9.47

*Analysis of questionable accuracy or unusual quantity.

APPENDIX 5. *(continued)*

Part B. Diabase Sheets: Other than North America

Oxide	1. Whin Sill (Holmes and Harwood, 1928)	2. Karroo Avg. (Walker and Poldervaart, 1949)	3. Downes Mtn. (Walker and Poldervaart, 1949)	4. Tasmania (Edwards, 1942)	5. Avg. Victoria Falls (DuToit 1939)	6. Avg. Antarctica Dolerite (Walker and Poldervaart, 1949)	7. Avg. Tholeiite (Nockolds, 1954)	8. Avg. Tholeiite (Poldervaart, 1955)	9. Quartz Dolerite (Manson, 1967)
SiO_2	50.52	52.5	53.21	52.65	50.5	54.0	51.3	51.0	51.6
TiO_2	2.39	1.0	1.73	0.58	3.0*	0.7	2.0	1.4	1.5
Al_2O_3	13.76	15.4	13.95	16.23	14.0	16.1	14.2	15.6	15.1
Fe_2O_3	3.87	1.2	1.24	0.51	3.3	0.8	2.9	1.1	2.3
FeO	8.50	9.3	8.93	8.21	9.3	7.4	9.1	9.8	8.9
MnO	0.16	0.2	0.23	0.15	0.2	0.1	0.2	0.2	0.2
MgO	5.42	7.1	7.19	6.64	5.4	7.0	6.4	7.0	6.1
CaO	9.09	10.3	8.95	11.34	10.9	11.1	10.5	10.5	10.1
Na_2O	2.42	2.1	2.65	1.58	2.0	1.8	2.3	2.2	2.2
K_2O	0.96	0.8	1.13	0.90	0.8	1.0	0.9	1.0	0.9
H_2O comb.	2.27	N.A.	0.71	1.33	N.A.	N.A.	N.A.	N.A. H_2O^+:	0.9
P_2O_5	0.26	0.1	0.21	0.01	0.1	N.A.	0.2	0.2	0.2
Total	99.62	100.0	100.13	100.13	99.5	100.0	100.0	100.0	99.99
Fe_{total}	9.31	8.07	7.81	6.74*	9.54	6.31*	9.10	8.38	8.40

* Analysis of questionable accuracy or unusual quantity.

APPENDIX 5. *(continued)*

Part C. Diabase Dikes: Triassic of North America (excluding Cornwall)

Oxide	1. Conn. (Shannon, 1924)	2. Mt. Holyoke, Mass. (Shannon, 1924)	3. Conshohocken, Pa. (Hall, 1881)	4. Gettysburg-Duncannon, Pa., Avg. of 12 (Lapham and Saylor, 1970)	5. Rocky Ridge, Md. (Bascom et al., 1931)	6. New Market, Md. (Shepherd, 1938)	7. Baltimore Co., Md. (Knopf and Jonas, 1929)
SiO_2	51.78	52.68	51.56	50.84	51.68	51.28	52.12
TiO_2	1.41	N.A.	1.63	0.73	0.72	0.78	0.32
Al_2O_3	14.20	14.14	17.38*	15.14	15.87	14.35	14.33
Fe_2O_3	3.59	1.95	6.57*	2.35	1.46	1.12	5.93
FeO	8.25	9.75	3.85*	8.42	8.43	9.31	5.45
MnO	0.43	0.44	N.A.	0.18	0.15	0.16	N.A.
MgO	7.64	6.38	3.42*	8.19	7.84	7.97	7.49
CaO	10.70	9.38	10.19	11.29	11.08	11.42	10.27
Na_2O	2.14	2.56	2.19	1.68	1.86	2.03	1.87
K_2O	0.39	0.88	1.46*	0.42	0.34	0.27	0.92
H_2O comb.	0.63	1.60	2.15*	1.32	0.31	0.48	1.23
P_2O_5	0.14	N.A.	0.13	0.11	0.12	0.13	0.15
Total	101.30	99.76	100.53	100.67	99.86	99.30	100.08
Fe_{total}	8.92	8.94	7.58	8.06	7.53	8.01	8.38

* Analysis of questionable accuracy or unusual quantity.

APPENDIX 5. *(continued)*

Part D. Diabase Pegmatite

Oxide	1. Palisades, N.J. (Walker, 1940)	2. "Syenite" Dillsburg, Pa. (Frazer, 1880)	3. Dillsburg, Pa. (Hotz, 1953)	4. Goose Creek, Va. (Shannon, 1924)	5. Avg. Karroo (Walker and Poldervaart, 1949)
SiO_2	52.50	49.28*	52.56	52.94	54.44
TiO_2	1.36	2.59	2.91	2.32	1.77
Al_2O_3	18.28*	13.01	12.77	14.80	13.18
Fe_2O_3	1.97	6.50	4.78	0.16	1.97
FeO	7.61	10.94	10.18	12.00	10.48
MnO	0.09	0.29	0.20	N.A.	0.27
MgO	2.58*	6.15	2.69*	5.42	4.10
CaO	9.34	4.88*	7.21	8.32	7.87
Na_2O	3.78	2.76	3.65	1.98	2.22
K_2O	1.03	0.83	1.03	N.A.	1.23
H_2O comb.	1.56	1.80	1.52	N.A.	1.63
P_2O_5	0.06	0.17	0.27	0.28	0.29
Total	100.16	99.20	99.77	98.22*	99.45
Fe_{total}	7.29	13.04*	11.25	9.43	9.52

* Analysis of questionable accuracy or unusual quantity.

APPENDIX 5. *(continued)*

Part E. Diabase Granophyre

Oxide	1. Palisades, N.J. (Walker, 1940)	2. Dillsburg, Pa. (Hotz, 1953)	3. Dillsburg, Pa. (Hotz, 1953)	4. Goose Creek, Va. (Stose and Bascom, 1929)	5. Whin Sill (Tomkieff, 1929)	6. Skaergaard (Wager and Deer, 1939)	7. Northland Sill, Duluth (Schwartz and Sandberg, 1940)	8. Avg. Karroo (Walker and Poldervaart, 1949)
SiO_2	72.52	61.69	66.04	71.60	65.20	58.81*	63.33	63.45
TiO_2	0.42	1.46	1.03	0.34	0.39	1.26	1.55	1.02
Al_2O_3	11.84	12.61	12.72	13.16	13.72	12.02	12.99	13.65
Fe_2O_3	1.23	2.98	2.48	1.28	3.63	5.77	2.87	1.61
FeO	0.87	8.32	6.55	0.38	3.72	9.38	5.12	5.77
MnO	0.06	0.15	0.11	0.03	N.A.	0.21	0.16	0.10
MgO	1.48	0.77	0.54	2.12	1.01	0.72	2.21	2.34
CaO	2.54	4.04	2.65	3.76	2.79	5.02*	2.05	4.01
Na_2O	7.12	5.71	4.62	5.92	5.22	3.91	3.97	3.06
K_2O	0.36	0.57	2.26	0.70	2.17	2.39	3.52	2.52
H_2O comb.	0.82	0.98	1.03	N.A.	1.99	0.40	1.83	1.03
P_2O_5	0.14	0.50	0.22	N.A.	0.38	0.71	0.37	0.15
Total	99.40	99.78	100.25	99.29	100.22	100.61	99.97	98.71
Fe_{total}	1.54	8.54	6.82	1.19	5.43	11.32*	5.99	5.62

* Analysis of questionable accuracy or unusual quantity.

APPENDIX 5. *(continued)*

Part F. Comparative Averages of Appendix 5, A-E
(excluding Cornwall, Pa.)

Oxide	Avg. Tr. sheets eastern North America A., 1-17	Avg. diabase sheets not North America B., 1-6	Avg. Tr. dikes eastern North America C., 1-7	Avg. Diabase Pegmatite D., 1-5	Avg. Diabase Granophyre E., 1-8
SiO_2	52.24	52.23	51.71	52.34	65.33
TiO_2	1.13	1.57	0.93	2.19	0.93
Al_2O_3	14.61	14.91	15.06	14.41	12.84
Fe_2O_3	3.87	1.82	3.28	3.08	2.73
FeO	7.08	8.61	7.64	10.24	5.01
MnO	0.28	0.17	0.27	0.21	0.12
MgO	6.92	6.46	6.99	4.19	1.40
CaO	10.16	10.28	10.62	7.52	3.36
Na_2O	2.53	2.09	2.05	2.88	4.94
K_2O	0.75	0.93	0.67	1.03	1.81
H_2O comb.	0.94	1.44	1.10	1.63	1.15
P_2O_5	0.18	0.14	0.13	0.21	0.35
Total	100.69	100.45	100.45	99.33	99.97
Fe_{total}	8.22	7.96	8.12	10.11	5.81

APPENDIX 6

Reference sources for total Fe and FeO/Fe_2O_3 (see Text)

1. Goose Creek, Va. diabase (Shannon, 1924)
2. Average tholeiite (Poldervaart, 1955)
3. Average Karroo dolerite (Walker and Poldervaart, 1949)
4. Average Dillsburg diabase (Hotz, 1953)
5. Average Palisades diabase (Walker, 1940)
6. Downes Mountain dolerite (Walker and Poldervaart, 1949)
7. Virginia diabase (Stose and Bascom, 1929)
8. Tasmania dolerite (Edwards, 1942)
9. Antarctica dolerite (Walker and Poldervaart, 1949)
10. Indian Ocean basalt (Engel and Engel, 1964b)
11. Rocky Hill, N.J. diabase (Shannon, 1924)
12. Average Deccan basalt (Washington, 1922)
13. Victoria Falls dolerite (DuTiot, 1939)
14. Average tholeiite (Nockolds, 1954)
15. Average alkali basalt (Nockolds, 1954)
16. Average Whin sill (Holmes and Harwood, 1928)
17. Average Hawaiian tholeiite (MacDonald and Katsura, 1964)
18. Rossville, Pa. diabase (Frazer, 1880)
19. Dillsburg, Pa. diabase (Frazer, 1880)
20. Average Mid-Atlantic Ridge tholeiite (Engel and Engel, 1964a)
21. Average Pacific tholeiite (Engel and Engel, 1946b)
22. Dillsburg, Pa. diabase (Frazer, 1880)
23. Average North American Triassic sheet diabase (Appendix 5F)
24. Average alkali basalt, Mid-Atlantic Ridge (Engel and Engel, 1964a)
25. Average of 4 North American diabase dikes (Appendix 5C)
26. Haycock Hill, Pa. diabase (Hall, 1881)
27. Carlsberg Ridge, Indian Ocean tholeiite (Engel and Engel, 1964b)
28. Haycock Hill, Pa. diabase (Hall, 1881)
29. Dillsburg, Pa. diabase (Frazer, 1880)
30. Dike, Cornwall, Pa. (Appendix 4A)
31. Dillsburg, Pa. diabase (Frazer, 1880)
32. Jericho Hill, Pa. diabase (Hall, 1881)
33. Rock Hill, Pa. diabase (Hall, 1881)
34. Goat Hill, Pa. diabase (Hall, 1881)
35. Mt. Pleasant, Pa. diabase (Hall, 1881)
36. Cornwall, Pa. diabase (Appendix 4A)
37. Cornwall, Pa. diabase pegmatite (Appendix 4A)
38. Birdsboro, Pa. diabase (Stose and Bascom, 1929)

39,44. Cornwall, Pa. granophyre (Appendix 4A)

SUBJECT INDEX

A

Adinoles, 43, 73, 81, 94
Aeromagnetic data, 28, 256, 268, 271-273, 287, 295, 296
Age determination, 20
Aggregate, 104
Algal structures (also see Cryptozoans), 10, 11, 12
Alkali feldspar fixation potential, 3, 76, 84, 85, 86, 93, 99, 102, 103
Amphibole
  actinolite, 4, 5, 14, 40, 41, 42, 44, 48, 54, 56, 59, 62, 64, 66, 68, 77, 78, 83, 109, 113, 114, 120, 121, 122, 123, 124, 125, 127, 133, 134, 135, 136, 137, 138, 154, 155, 156, 167, 168, 171, 187, 188, 193, 251, 254, 255, 285, 292
  general occurence, 45, 61, 64, 73, 76, 79, 84, 127, 135, 163, 164, 165, 167, 169, 190
  hornblende, 38, 56, 57, 66, 67, 70, 77, 78, 79, 90, 168, 171, 187, 193, 235, 260, 267, 287
  tremolite, 39, 41, 42, 48, 62, 67, 76, 87, 120, 123, 135, 171, 292
Amphibolitization, 113, 135, 161, 162, 163, 164, 168, 183, 191, 212, 229, 230, 235, 242, 260
Analcime, 87, 128, 135, 171
Andalusite, 57, 58
Andesite, 159
Andradite, 127
Anorthosite, 242
Apatite, 67, 129, 168, 170, 190, 191, 193
Aplite, aplitic ore, 67, 98, 101, 102, 122, 124, 137, 191, 207, 217
Aplitic diabase pegmatite, 188, 201
Apophyllite, 128, 135, 169, 171, 187
Appalachian arching, 234, 239, 240
Appalachian curvature, 21, 234, 239
Appalachian geosyncline, 237, 239
Arkose, 38, 194, 206
Arsenic, 125, 131
Azurite, 127

B

Barium 64, 86
Basalt (also see Diabase, Tholeiite)
  alkali enrichment trend, 158, 219
  alkali olivine, 2, 158, 159, 199, 209, 219, 221, 223, 259
  alumina, 158, 159, 208-209, 215, 216, 219
  calc-alkali, 158, 216, 221
  chemical composition, 97, 157, 158, 159, 261
  crustal contamination, 260
  depth of intrusion, 29, 31, 160
  differentiation, 158, 159, 215, 219, 220, 221, 261
  equilibrium, 220
  fractional crystallization, fractionation, 2, 97, 158, 212, 216, 219, 220
  iron content, 158, 159, 215, 221, 223, 248, 260
  iron enrichment trend, 158, 259
  mantle source, 160
  metasomatism, 94
  mineralogy, 157, 167
  oxidation, 221, 224, 259-260
  oxygen partial pressure, fugacity (also see under Diabase sheet and Tholeiite), 229, 259, 260, 261
  temperatures (also see Diabase sheet–temperatures), 230
  texture, 157
  tholeiite (also see Tholeiite), 158, 159, 160, 219, 223, 229, 259
  volatiles (also see water content), 260
  water content (also see Tholeiite magma and Diabase sheet–water content), 260
Bismuth, 125
Boron (also see Metasomatism – boron), 129-130, 266
Bornite, 123, 127
Breccia, brecciation (also see Blue Conglomerate – breccia), 3, 14, 15-16, 22, 24, 26, 29, 33, 41, 44, 46, 47, 48, 58, 83, 109, 113, 114, 115, 116, 117, 121, 122, 123, 136, 156, 160, 183, 187, 256
Brucite, 67, 128
Byssolite (also see Amphibole – actinolite), 127, 128, 133, 135

C

Calcite, 24, 39, 41, 42, 44, 45, 48, 49, 54, 59, 61, 62, 63, 64, 67, 68, 70, 73, 75, 76, 77, 79, 83, 84, 86, 87, 122, 123, 124, 125, 128, 133, 135, 168, 171, 194, 242, 264
Chalcocite, 123
Chalcopyrite, 103, 109, 113, 114, 123, 125, 133, 136, 138, 142, 152, 168, 170, 171, 242, 250, 251, 264
Chemical composition
  Buffalo Springs Formation (see LITHO-

LOGIC INDEX)
  diabase (see Diabase dikes and Diabase sheet)
  host limestone (see LITHOLOGIC INDEX)
  magnetite (see Magnetite – composition and Magnetite – trace elements)
  pyrite (see Pyrite – composition)
Chevron folds, 24
Chlorite, chloritization, 4, 14, 38, 41, 42, 44, 45, 47, 48, 49, 54, 56, 59, 60, 61, 62, 64, 65, 67, 68, 73, 75, 76, 78, 81, 82, 83, 84, 85, 90, 99, 109, 113, 121, 122, 124, 125, 127, 133, 135, 137, 155, 162, 163, 164, 165, 167, 168, 169, 171, 177, 183, 184, 187, 190, 191, 193, 194, 229, 235, 242, 250, 251, 254, 263, 268, 285, 292
Chromium, 260
Clinozoisite, 168
Cobalt, 64, 86, 101, 103, 104, 105, 125, 128, 129, 130, 131, 242, 251, 254, 255, 284, 285, 287, 292
Conglomerate, 19, 38, 43, 48, 71, 114, 282
Continental drift, rifting, 2, 5, 240, 268, 289
Copper, 4, 5, 64, 86, 103, 104, 105, 123, 124, 125, 130, 138, 142, 146-148, 251, 266, 284, 285, 292, 296
Cordierite, 38, 56, 57, 58, 78, 79, 84
Covellite, 123, 127
Cross–bedding, 3, 14, 24, 69
Cryptozoans (also see Algal structures), 12
Cuprite, 127

D

Dacite, 219
Datolite, 39, 87, 128, 137, 157, 168, 169, 171
Desilication (also see Metamorphism – desilication), 83
Diabase
  definition (also see Basalt, Tholeiite), 157
  genesis (also see Basalt, Diabase sheet and Tholeiite), 157, 160
  quartz–diabase, 157, 206, 242
  weathering (also see Weathering, Diabase sheet – alteration), 157
Diabase Dike
  age relationships, 20, 21, 233-34, 236, 253, 259, 268, 283
  apophyses, 235
  chemical composition, 198, 199, 202, 207, 218, 233, 234, 235-236, 295, 312, 321, 324
  chilled margin, 233, 234, 235, 236
  contacts, 235
  contact metamorphism, 235
  Cornwall area, 27, 31, 198, 233, 236, 237, 312
  differentiates, 235
  differentiation, 207, 214, 218, 236
  distribution, 27, 233-234, 237, 240, 268
  feeders, 233
  fractures, 120, 233, 236-237, 238, 239, 240, 282
  iron content, 295
  magnetization (remanent), 233
  metasomatism, 198, 209, 212, 213, 233, 236, 283
  mineralogy, 202, 205, 206, 234, 235
  ore relationships, 155, 236, 268, 283
  solidification index, 212-213
  structural relationships, 2, 5, 20, 38, 120, 233, 234, 235, 236-240, 268, 289
  sulfur isotopes, 217, 272, 273
  textures, 207, 234, 235, 236
  thickness, 31
Diabase sheet
  aeromagnetic data, 28, 256, 268, 271-273, 287
  age (relative) of intrusion, 20, 31, 32, 34-35, 232, 233-234, 253, 254, 261, 282
  alkali content, enrichment, metasomatism, 1, 2, 94, 96, 100, 193, 195, 209, 215, 216, 217-220, 223, 224, 228, 229, 230, 231, 259, 285, 286, 287, 288, 294, 296
  alteration, 66, 109, 113, 136, 157, 162, 163, 164, 167, 168, 169, 170, 171, 183, 184, 191, 193, 195, 205, 212, 214, 229, 230, 242, 252, 283, 286, 313
  apophyses, 109, 208, 258, 271, 283
  bleaching (also see Triassic basin–bleached sediments), 109, 122
  brecciation (also see Breccia, Brecciation), 33, 113, 160, 184, 187
  cataclasis, 170
  chemical composition, 1, 4, 31, 86, 99, 100, 101, 103, 157, 158-159, 174, 179, 188, 195, 197-203, 205, 206, 207-208, 209-212, 213, 214, 215, 216, 217, 219, 220, 224, 229, 231, 234, 248, 249, 250, 251, 255, 257, 259-260, 261, 263, 267, 272, 274, 277, 278, 280, 283, 285, 286, 287, 292, 296, 312-316, 318-320, 322-324
  chilled margin, 1, 2, 12, 20, 31, 79, 98, 99, 101, 122, 123, 135, 157, 160-69, 173, 175, 180, 183, 188, 194, 195, 198, 199, 202, 203,

204, 205, 206, 207, 208, 209, 212, 213, 215, 216, 217, 218, 220, 222, 224, 229, 230, 231, 234, 247, 249, 252, 254, 256, 260, 267, 271, 280, 285, 286, 294
contacts, 26, 60, 66, 67, 70, 77, 83, 93, 101, 103, 108, 122, 128, 129, 160, 161, 174, 186, 193, 241, 255, 270, 273
contamination, 192, 194, 217, 261, 273
contraction cracks, 32, 122, 133, 156, 161, 162, 164, 165, 198, 249, 254, 267, 286
convection, 3, 194, 198, 232
cooling rate, 181, 182, 208
cryptic layering, 2, 3, 31, 157, 194, 206, 228, 267
crystal accumulation, settling (also see layering, Olivine), 160, 186, 187, 198, 214, 231-232, 260, 261
cumulates, 157, 214
depth of intrusion, of origin, 5, 20, 27, 29, 31 209, 259
differentiates, 1, 31, 50, 91, 96, 99, 101, 102, 131, 132, 157, 170, 183, 184, 191, 192, 197, 198, 202, 206, 207, 209, 228, 231, 247, 249, 250, 251, 253, 254, 255, 256, 257, 258, 259, 261, 272, 273, 274, 275, 277, 278, 279, 280, 284, 287, 288, 291, 292, 294, 295
differentiation, 2, 7, 68, 94, 96, 100, 102, 132, 157, 158, 159, 160, 178, 180, 182, 187, 188, 194-197, 199, 207-233, 247, 249, 252, 253, 255, 256, 257, 259, 260, 261, 267, 273, 274, 276, 278
faults, fractures, 4, 25, 28, 33, 37, 102, 109, 114, 117, 120, 137, 150, 161, 163, 164, 247, 249, 250, 252, 254, 255, 256, 267, 268, 270, 283, 285, 286, 292
feeder, 27, 28, 30, 34, 230, 233, 270, 273, 293
filter pressing, 257
flow texture, 157, 162
form (also see structures), 1, 26, 27-29, 30, 34, 109, 269-272, 292
fractional crystallization, fractionation, 2, 7, 155, 157, 160, 177, 179, 194, 201, 205, 206, 207, 212, 219-228, 229, 231, 252, 255, 257, 259, 261, 262, 266, 267, 273
glass, 161, 162, 163, 164, 165, 168
grain size, 160, 162, 163, 168, 169, 170, 174, 175, 184
granophyre, 1, 2, 3, 4, 5, 7, 41, 49, 50, 51, 52, 53, 56, 63, 64, 65, 67, 68, 74, 90, 94, 95, 96, 97, 98, 99, 100, 101, 102, 103, 111, 137, 157, 158, 162, 166, 168, 169, 170, 171, 172, 173, 175, 179, 183, 184, 187, 188, 189, 190, 191-194, 195, 198, 199, 200, 202, 203, 204, 205, 207, 208, 209, 212, 217, 218, 219, 220, 221, 222, 224, 225, 226, 227, 243, 247, 248, 250, 253, 256, 257, 258, 259, 267, 270, 274, 275, 276, 277, 279, 280, 283, 285, 286, 287, 288, 289, 290, 291, 294, 295, 296, 308-311, 312, 323, 324
gravitative settling (also see Diabase sheet – crystal accumulation and cumulates), 232
gravity, 268
hydration (also see volatiles and water content), 20, 169, 267
hydrogen diffusion, pressure, 227, 276
incompatible elements, 261
intercumulous or interprecipitate liquid, 164, 168, 169, 187, 232, 250, 257
internal chilled contact, multiple injection, 184, 206, 228, 232-233, 246, 250, 252, 267
intrusion mechanism, 28-29, 30, 31, 34, 37, 199, 240, 261, 267, 270, 271
iron content, 1, 2, 3, 5, 158, 159, 188, 197, 198, 199, 201, 203, 206, 208, 209, 212, 216, 221, 222, 223, 224, 225, 226, 227, 229, 230, 231, 232, 245, 246-247, 248, 249, 250-251, 252, 255, 256, 257, 259-260, 272, 277, 278, 286, 287-288, 292, 293, 294, 295, 296
iron depletion, deficiency, 2, 209, 221, 225-227, 228, 246, 248, 250, 255, 256, 260, 261, 267, 280, 291, 292, 293, 294, 296
iron diffusion, 163, 164
iron enrichment trend, 2, 3, 100, 179, 192, 195, 209, 212, 215, 216, 220, 221, 223, 224, 226-229, 230, 231, 247, 248, 250, 260, 267, 280, 286
joints 29, 37, 102, 108, 161, 164, 165, 188, 198, 250, 267
layering (also see convection, cryptic layering, Olivine), 31, 157, 160, 162, 169, 184, 206, 215, 258
magma composition, 220, 229-230, 259, 260, 261
magma generation (also see Tholeiite–magma generation), 103, 160, 220, 229, 231, 236, 252, 259-261, 266, 274, 289, 290
magnetization (also see Paleomagnetism), 272-273, 295
metamorphism, 163
metasomatism (also see Metasomatism), 82, 90, 91, 160, 163, 212, 229, 254, 261
micropegmatite, 1, 157, 167, 168, 169, 170, 172, 173, 174, 175, 176, 181, 184, 187, 188,

189, 195, 197, 205, 243, 255
mineralogy, 136, 157, 161, 162-169, 170-183, 184-197, 198, 199, 205-206, 214, 215, 216, 227, 230, 231, 232, 249, 250, 256, 260, 261, 267, 272, 274-275, 276, 277, 278, 279, 283, 285, 287, 306
normative composition, 202-206
ore in, (also see Diabase sheet–veins), 113-114, 117, 122, 127, 137, 138, 156, 160, 164, 168, 250, 252, 254, 257, 283, 285, 286
ore solutions, relationships, 7, 96, 99, 209, 220, 241, 242, 244, 245, 246-252, 254, 261, 268, 271, 273, 278-280, 282, 283, 284, 288, 290, 291, 292
oxidation, 2, 193, 197, 205, 216, 221, 224-228, 229-231, 244, 245, 247, 249, 250, 257, 259, 260, 267, 273, 275, 276, 278, 279, 280, 288, 291
oxygen depletion, 2, 225-226, 231, 267, 276
oxygen fugacity, 2, 225, 229-230, 259, 276, 277
oxygen isotopes, 194
oxygen pressure, 2, 216, 225, 227, 228, 229-230, 244, 259, 260, 266, 275-276
paleomagnetism (also see Paleomagnetism), 32
paragenesis, minerals, 163, 168, 191, 194-196, 224, 225, 227, 230, 232
paragenesis, rock types, 168, 192, 194, 195, 224, 227, 231, 249, 267
pegmatite, pegmatitic, 3, 7, 41, 66-67, 102, 111, 162, 166, 169, 170, 171, 172, 173, 174, 175, 179, 181, 182, 183, 184, 188-189, 190-191, 192, 193, 194, 195, 199, 201-202, 204, 205, 207, 208, 209, 212, 216, 217, 218, 219, 221, 222, 224, 227, 243, 247, 248, 250, 253, 255, 256, 257, 258, 267, 274, 276, 277, 278, 279, 280, 283, 286, 287, 288, 294, 295, 308-311, 312, 322, 324
porphyritic, 160, 162, 163, 165, 169, 170, 183, 252
potassium, 91, 94, 97, 98, 99, 100, 101, 102, 103, 192, 193, 199, 209, 212, 218, 219, 220, 228, 251, 257, 259, 261
residua (also see granophyre, differentiates, differentiation), 1, 2, 4, 68, 94, 100, 102, 158, 191, 193, 202, 207, 217, 220, 221, 224, 228, 229, 230, 231, 243, 247, 248, 251, 258, 261, 262, 266, 274, 278, 279, 288, 290, 294
shearing, 113, 136, 156, 164, 170, 184, 187, 214, 249, 250
silica content, 40, 208, 218, 219, 223, 224, 225, 227, 251
silica enrichment trend, 2, 96, 193, 195, 208, 215, 218, 219, 221, 223, 224, 225, 228, 230, 231, 259, 288
sodium enrichment (also see Metasomatism –sodium), 2, 81, 91, 94, 102, 192, 208, 209, 218, 219, 220, 224, 228, 251, 257, 259
solidification index, 2, 194-195, 212-214, 228, 267
strontium isotopes, 194
structure, deformation, 1, 4, 5, 21, 26-29, 31, 34, 37, 108, 109, 154, 183, 233, 270, 272, 282
sulfur isotopes, 131, 216-217, 256, 258, 261, 272-274, 293
temperatures of crystallization, 2, 79, 207, 225, 227, 228, 229, 230, 231, 232, 259, 261, 275, 276, 277, 278, 290
texture, 31, 157, 160, 161, 162, 163, 164, 165, 168, 169-170, 174, 183, 184, 187, 188, 190, 191-192, 196, 207, 214, 217, 247, 250, 252, 255, 256, 271, 283, 307-311
thickness, 27, 28, 31, 79, 116, 183, 195, 200, 272
titanium content (also see Titanium), 2, 3, 184, 188, 195, 201, 202, 208, 209, 212, 227, 228, 245, 248, 250, 259, 267, 274-275, 277, 278, 279, 286, 288, 291
topography, surface, 27, 29, 108, 109, 136, 154, 156, 161
trace elements, 198, 212, 220, 251, 255, 261, 286
vapor phase, 217, 257, 274
veins in (also see Ore–veins in diabase), 67, 108, 109, 113, 122, 127, 137, 138, 163, 164, 168, 170, 171, 183, 187, 188, 193, 194, 205, 247, 250, 254, 255, 257, 283, 285, 308-311
volatiles, 20, 189, 194, 198, 207, 218, 225, 227, 246, 250, 256, 258, 271, 288, 290, 294
water content, 2, 20, 163, 168, 169, 184, 207, 209, 212, 225, 228, 229, 231, 260, 261, 276
water pressure (also see water content), 227, 229, 230, 231, 259, 266, 276
xenoliths in, 30, 37, 66-68, 86
Diorite, 242
Dolerite, 157, 170, 180, 188, 189, 191, 194, 195, 199, 201, 208, 215, 219, 221, 232, 233, 248, 284
Dolomite, dolomitization, 10, 11, 12, 21, 39, 41, 69, 99, 108, 246, 264, 282

E

Earthquake activity, 38
Epidote, epidotization, 38, 39, 46, 55, 56, 59, 61, 62, 64, 65, 66, 68, 70, 76, 78, 168, 171, 188, 286
Erosion, 5, 20, 26, 29, 30, 31, 33, 34, 36, 37, 38, 108, 109, 114, 116, 127, 154, 268, 269, 270, 271, 291, 292, 293

F

Fanglomerates (also see Triassic sediments), 31
Faulting (see Diabase sheet, Paleozoic structure and Triassic basin)
Fayalite (also see Olivine), 163, 164, 167, 245
Feldspar
  adularia, 46, 49, 54
  alkali, 3, 42, 43, 45, 46, 48, 53, 59, 60, 76, 79, 83, 85, 86, 88
  anorthoclase, 46
  cryptoperthite, 60
  distribution, quantity (also see Plagioclase distribution, quantity), 165-166, 167
  Fe, 57
  Fe–microcline, 52, 53, 54, 57, 83, 89
  Fe–orthoclase, 3, 43, 44, 45, 51-54, 56, 60, 61, 62, 64, 67, 68, 76, 79, 80, 81, 83, 84, 85, 86, 88, 89, 90, 93, 94, 100, 101, 122, 124, 133, 187, 190, 191, 192, 195, 225, 247, 248, 258, 285
  Fe–sanidine, 52, 53, 57, 83, 89
  graphic intergrowth, 191, 192
  microcline, 3, 39, 44, 45, 46, 53, 54, 57, 59, 61, 64, 67, 68, 70, 75-76, 77, 79, 81, 82, 83, 86, 89, 90, 94, 168, 190, 192
  microperthite, 46, 54, 168, 169
  myrmekite, 192, 193
  obliquity, 45, 46, 51, 60, 61, 70, 76
  occurrence, general, 24, 38, 39, 41, 46, 75, 86, 87, 93, 102, 122, 129, 135, 161, 163, 165, 197, 215, 220, 287
  optical–crystallographic scatter, 172, 175
  orthoclase, 3, 14, 41, 42, 43, 44, 45, 46, 47, 48, 51, 52, 53, 54, 59, 61, 62, 64, 67, 68, 76, 77, 78, 79, 80, 81, 84, 85, 86, 87, 89, 94, 98, 99, 101, 122, 124, 133, 135, 137, 183, 188, 192, 193, 195, 204, 205, 220, 225, 247, 248, 267, 285, 287
  perthite, 45, 60, 66, 189, 192
  plagioclase–albite, 46, 48, 53, 54, 55, 56, 59, 61, 67, 68, 70, 73, 78, 81, 83, 85, 86, 87, 168, 204, 205
  plagioclase alteration, 166, 168, 171, 175, 183, 191, 194, 235
  plagioclase–andesine, 46, 48
  plagioclase–anorthite, 56, 60, 166, 167, 174, 175, 203, 204, 205
  plagioclase – bytownite, 167
  plagioclase clouding, 164-165, 167
  plagioclase composition, 1, 3, 44, 45, 46, 51, 54, 56, 59, 60, 61, 63, 64, 66, 70, 75, 76, 81, 84, 87, 122, 166-167, 169, 171-177, 184-187, 188, 189, 190, 192, 193, 195, 196-197, 203, 204, 205, 206, 215, 216, 220, 287
  plagioclase corrosion, 167
  plagioclase crystal growth, diffusion, 166, 175, 177, 184, 188, 195, 196
  plagioclase distribution, quantity (also see occurrence), 165, 172, 174, 184-187, 188, 206, 252
  plagioclase fractionation, differentiation, 177, 216, 220
  plagioclase – interprecipitate, 167
  plagioclase – labradorite, 46, 48, 78, 128
  plagioclase occurrence, quantity, 1, 41, 44, 49, 54, 56, 58, 59, 60, 62, 64, 66, 67, 68, 70, 73, 75, 77, 79, 80, 81, 82, 84, 86, 87, 99, 122, 123, 128, 136, 157, 161, 164, 165, 168, 169, 187, 188, 191, 192, 193, 235, 245, 249, 261
  plagioclase – oligoclase, 46, 47, 48, 87, 128, 168
  plagioclase paragenesis, 46, 54, 57, 166, 167, 168, 174, 175, 195, 216, 230, 261
  plagioclase reaction, 84, 87, 177, 193-194, 245
  plagioclase structure, 166, 172, 184, 249
  plagioclase temperature, 230
  plagioclase texture, 165, 167, 168, 170, 172, 177, 189
  plagioclase twinning, 46, 47, 66, 163, 165-166, 167, 169, 170, 171-172, 174-175, 177
  plagioclase zoning, 3, 46, 167, 169, 170, 175, 177, 187, 188, 189, 220, 235, 252
  potassium, potassic (also see alkali feldspar), 46, 48, 51, 54, 56, 58, 59, 60, 61, 66, 70, 79, 81, 83, 87, 89, 91, 92, 93, 96, 99, 100, 128, 167, 168, 169, 170, 191, 192, 193, 215, 235, 251, 256
  sanidine, 3, 53, 57, 79, 89, 90

Feldspathization potential (also see Alkali feldspar fixation potential), 75, 76, 85, 86, 102
Fluorite, 54, 67, 68, 83, 86, 137, 157

G

Gabbro, 219, 221
Galena, 124, 242
Garnet, 38, 39, 41, 42, 45, 56, 59, 67, 68, 71, 76, 109, 127, 133, 135, 137, 168, 171, 242, 307
Gettysburg basin, 20
Gettysburg sill, 268, 269, 273
Glass (also see Diabase sheet – glass), 89, 219
Gold, 103, 212, 251, 254, 255, 257, 261, 266, 284, 286
Graphite, 14
Graywacke, 49, 50
Grubb, Peter, 9

H

Halogens, 90, 157, 266
Hawaiian basalt (line), 199, 209, 218, 219, 230
Haycock sill, 270
Hematite, 38, 39, 41, 42, 43, 48, 49, 52, 56, 57, 60, 67, 68, 71, 79, 83, 85, 88, 89, 94, 99, 101, 122, 123, 124, 125, 127, 129, 132, 133, 135, 136, 141, 156, 165, 167, 168, 171, 183, 191, 192, 193, 198, 204, 221, 225, 226, 229, 235, 242, 243, 244, 245, 246, 247, 261, 263, 264, 267, 275-276, 277, 278, 285, 287
Heulandite, 128, 171
History
  genetic theories, 6-8, 241, 246
  mining, 5, 9-10, 103, 104, 105, 108
Hornfels (see Metamorphism)
Hornstone, 38
Hydrothermal alteration, 43

I

Iddingsite, 161
Idocrase, 157
Ilmenite, v, 4, 168, 170, 171, 179, 182, 183, 187, 188, 190, 191, 193, 204, 205, 229, 242, 275-276, 277, 278, 279, 291
Iron
  basalts, tholeiites (also see Diabase sheet), 158, 159, 209, 211, 215, 216, 259
  mobility, mobilization (also see Diabase sheet, Hematite, Magnetite, Ore), 5, 71-72, 84, 262
  ore distribution (also see Ore – distribution), 138, 142-145, 152
  oxidation, reduction (also see Magnetite–oxidation–reduction), 2, 3, 7, 71, 73, 88, 125, 183, 191, 197, 216, 221, 224, 225, 226, 228, 235, 275, 279, 280
Ironstone, v, 157

J

Jacksonwald syncline, 247, 268, 270, 282
Japanese basalts, 218, 219

K

Kaolinite, 44, 45, 47, 48, 49, 54, 56, 57, 60, 63, 73, 76, 77, 85

L

Lead, 125
Leucoxene, 171, 191, 235, 277
Limestone (also see LITHOLOGIC INDEX: Host limestone), 156, 242, 243, 245, 247, 264, 282, 292, 293, 296
Limonite, 125, 157

M

Magnetism (see Aeromagnetic data, Paleomagnetism)
Magnetite (also see Ore and Ore zone)
  composition, 3, 4, 71, 124, 129, 130, 131,

140, 141, 142, 171, 182, 244, 247, 248, 250, 254, 257, 264, 274-275, 278, 279, 291
  crystal growth, forms, 121, 122, 124, 125, 133, 135, 137, 161, 162, 169, 182-183, 191, 230, 242, 275, 277
  crystal structure, 125, 139, 140, 142
  diabase replacement (also see Diabase sheet – ore in, veins), 113, 156, 160, 164, 165, 168
  distribution, abundance (also see Ore – distribution), v, 27, 40, 54, 108, 109-111, 120, 122, 137, 142, 154, 204, 205, 247, 250, 253, 255, 257, 279, 281, 291
  equilibrium, 229, 275, 276, 277
  genetic theories (also see Ore – genesis), 6-8, 94, 164, 167, 183, 230, 232, 241, 242, 243-266, 280
  hydrothermal (also see Ore – hydrothermal), 73, 100, 184, 241
  iron content, 124, 140-142, 275, 277
  mineral associations, 4, 5, 41, 42, 45, 54, 57, 67, 68, 100, 113, 121, 122, 124, 125, 127, 129, 133, 135, 136, 137, 138, 156, 171, 188, 190, 191, 193, 251, 263, 264, 277
  mining methods (also see History), 9, 10, 103, 104, 105-108
  occurrence, 1, 41, 42, 45, 48, 49, 54, 59, 61, 62, 67, 68, 71, 76, 83, 88, 96, 113, 114, 121, 122, 123, 124, 125, 133, 136, 161, 162, 163, 164, 165, 167, 169, 170, 171, 182, 183, 188, 190, 191, 193, 197, 203, 204, 205, 225, 242, 247, 250, 254, 268, 273, 281, 285, 286
  ore–fluid migration (also see Ore–solution migration), 7, 114, 120
  oxidation, reduction (also see Ore–Oxidation–reduction), 131, 135, 141, 183, 205, 242, 243, 244, 245, 257, 275, 276, 278, 279, 296
  paragenesis (also see Ore zone – paragenesis), 5, 54, 88, 100, 120, 125, 127, 133-135, 138, 142, 152, 156, 168, 171, 191, 205, 227, 230, 231, 249, 256, 259, 263, 264, 279, 292
  phenocrystic diabase nucleation (also see Nucleation), 133
  reactions 57, 89, 141, 259, 262, 263, 278
  replacement (also see Ore – replacement), 49, 54, 67, 83, 88, 108, 111, 113, 120, 121, 122, 123, 124, 125, 127, 129, 133, 135, 136, 137, 138, 141, 142, 152, 154, 156, 160, 165, 168, 243, 249, 254, 263, 264
  temperature of formation, 100, 230, 275, 276
  texture (also see Magnetite – crystal growth), 54, 120, 121, 122, 123, 124, 125, 138, 139, 156, 162, 163, 164, 165
  titaniferous, 3, 4, 191, 242, 247, 255, 274-275, 276, 277, 279
  titanium content (also see Titanium; Magnetite – composition; Diabase sheet – titanium), 3, 4, 7, 182, 197, 291
  trace elements (also see Magnetite – composition), 129-130, 140
  unit cell measurements, 129-131, 138-142, 154, 292
  veins (also see Diabase –veins, Ore – veins in diabase), 183, 184, 188, 285, 286
  zoning, 5, 122, 124, 127, 131
Malachite, 127
Manganese, 104, 129
Marble, 39
Marcasite, 124, 127
Martite, 243
Metamorphism
  contact, aureole, dike diabase, 38, 235
  contact aureole, sheet diabase, 20, 31, 38, 39, 41, 132, 136, 154, 160, 256, 267, 271, 273
  desilication, 76
  dynamic, 11, 48
  equilibrium, 55-56, 64-66, 67, 76-79
  grade, facies, 42, 55-57, 64-66, 70, 76, 77, 78, 267
  hornfels geochemistry, chemistry, 39, 42, 49-50, 51, 56, 66, 69, 70, 71-76, 77, 80, 81, 82, 86, 88, 90-94, 96, 97, 98, 103, 129, 246, 267, 317
  hornfels mineralogy, 14, 15, 38, 42, 51, 54, 55, 56, 59, 60, 61, 62, 64, 65, 66, 69, 71, 74, 75, 76, 77, 80, 84, 88, 93, 94, 103, 120, 123, 126, 132, 135, 136, 156, 242, 246, 249, 292
  hornfels occurrence, distribution, 1, 14, 15, 18, 23, 29-30, 31, 38-39, 42-43, 58, 70, 71, 73, 91, 103, 114
  limestone, 12, 29-30, 39-42, 67-68, 73, 75
  oxidation, reduction, 38, 63, 71-72, 267
  paragenesis, 41, 42, 44, 47, 48, 62, 67-68, 73, 77, 79, 81, 100, 123, 126, 133, 135, 168, 249, 254
  permeability of hornfels, 70, 103, 290
  temperature, 3, 57, 70, 77, 78, 79, 89, 91, 93, 103, 156, 267
  texture, 42, 43, 44, 48, 60, 66, 69, 70, 71, 75, 77, 103
  thermal, 55, 66-68, 69-70, 71-79, 81-82, 89, 91, 92, 102, 103, 123

  water content, volatiles, 71, 75, 77, 79, 87, 91, 92
Metasomatism
  alkali (also see potassium, sodium, 90, 96, 97
  aluminum, 64, 80, 82, 88, 89, 94, 96, 97, 98, 133, 138
  boron, 67, 68, 80, 86, 87, 90, 94
  fluorine, 67, 68, 80, 86, 90, 94
  general, distribution, occurrence, 3, 42, 43, 62, 69, 82-83, 86, 94, 102, 123
  genesis, 3, 49-50, 51, 56, 64, 67, 68, 69, 70, 81, 82, 83, 85, 86, 90-103, 169, 228
  geochemistry, chemistry, 3, 39, 49, 50, 51, 54, 56, 64, 68, 70, 72, 80-82, 83, 84-87, 88, 89, 93-96, 97, 98, 103, 129, 246, 317
  grade, facies, equilibrium, 56, 57, 64-66, 82, 87, 89
  halogen, 100
  iron, 64, 65, 80, 86, 87, 88, 89
  mineralogy, 39, 51, 54, 55, 56, 59, 60, 61, 62, 64, 65, 67-68, 69, 76, 79-80, 83-88, 89, 90, 91, 93, 126, 132, 136, 154, 155, 156, 171, 192, 194, 198, 249, 251, 255, 256, 267, 283, 292
  oxidation, 87-88, 93
  paragenesis, 54, 62, 67-68, 73, 81, 82, 83, 87, 91, 93, 103, 126, 133, 194, 249, 254, 263, 267
  permeability, 83, 103, 109
  pH, 83, 89-90, 103, 156
  potassium, 3, 37, 42, 43, 49, 50, 51, 56, 57, 58, 64, 65, 66, 68, 69, 73, 77, 80, 81, 82, 84, 86, 87, 88-89, 90-103, 129, 133, 137, 205, 211, 236, 256, 258, 263, 267
  potential for, 70, 85, 86
  silica, 3, 40, 48, 50, 64, 80, 81, 82, 87, 88, 89, 95, 96, 97, 133, 138, 267
  sodium, 3, 43, 50, 51, 62, 65, 66, 68, 73, 80, 81, 86, 87, 89, 91, 93, 94, 95, 96, 97, 98, 99, 102, 133, 258, 267
  temperature, 3, 69, 83, 87, 89-90, 91, 93, 103, 137, 292
  texture, 54, 58-59, 60, 69, 79-80, 83, 84
  trace elements, 64, 86
  volatiles, water, 3, 54, 64, 67, 83, 87, 88, 91, 92, 94
Mica
  annite, ferriannite, 57, 89
  biotite, 41, 45, 47, 48, 49, 51, 54, 56, 58, 59, 60, 64, 65, 70, 78, 79, 80, 89, 168, 170, 171, 187, 188, 190, 191, 193, 235, 242
  general, occurrence, 4, 14, 40, 44, 45, 47, 48, 51, 61, 62, 63, 70, 73, 76, 77, 79, 83, 84, 86, 87, 89, 92, 122, 127, 129, 134, 135, 137, 198
  illite, 44, 75, 80, 85, 94
  muscovite, 38, 41, 44, 45, 47, 48, 54, 57, 59, 60, 62, 64, 65, 66, 67, 68, 70, 75, 78, 79, 80, 81, 82, 84, 85, 87, 120, 127, 133, 135, 155, 171, 187, 193, 251
  paragonite, 87, 127
  phlogopite, 39, 41, 42, 67, 68, 76, 81, 120, 121, 127, 133, 135, 168
  sericite, sericitization (also see Sericitization), 46, 48, 49, 58, 66, 68, 123, 168, 171, 190, 193
Millerite, 124, 127
Mill Hill thrust, 4, 23, 30, 37
Mines
  Altman, 282
  Bell, 282
  Carper, 4, 113, 156, 247, 249, 252, 268, 282
  Doner, 15, 25, 27, 28, 108, 113, 247, 249, 253, 255, 268, 282, 293
  East End open pit, Cornwall, iii, 10, 12, 15, 16, 29, 105, 108, 110-111, 124, 127, 142, 154
  eastern ore body, Cornwall, 4, 9, 10, 14, 15, 16, 17, 22, 23, 25, 27, 28, 32, 40, 41, 43, 44, 49, 51, 54, 58, 66, 67, 68, 70, 73, 83, 85, 86, 88, 93, 94. 98, 99, 100, 102, 104, 105, 108, 109, 111, 113, 114-120, 121, 122, 123-128, 130, 132-135, 136-154, 155, 156, 169, 174, 183, 192, 197, 237, 247, 249, 250, 254, 255, 256, 257, 263, 267, 279, 293
  Elizabeth open pit, 10, 28, 58, 108, 109, 114, 154, 254, 293
  Esterly, 247, 252, 268, 282
  Footwall ore body, Cornwall, 30, 67, 68, 108, 111-113, 114, 156, 247, 249, 250, 253, 255
  French Creek (also see French Creek), 284, 287
  Grace (also see Morgantown), 287
  Jones, 283, 284
  McCormick, 282
  open pit, Cornwall, iii, 9, 12, 15, 22, 27, 39-40, 44, 104, 105, 108, 110, 111, 113, 124, 249, 293
  Underwood, 282
  Warwick, 283, 284
  western ore body, Cornwall, iii, 4, 9, 17, 26, 27, 28, 40, 41, 44, 58, 98, 101, 104, 105, 108, 109, 111, 113, 114, 120, 124, 128, 132, 135, 136, 137, 139, 142, 154, 156, 162, 169, 174, 183, 197, 199, 254, 255, 256, 263, 293

Miogeosyncline, 36
Mohorovicic Discontinuity, 38
Montmorillonite, 59, 60, 61
Monzonite, 219
Mylonite, mylonitization, 16, 123, 136

N

Natrolite, 87, 128, 135, 171
Nepheline, 158
Nickel, 4, 5, 104, 125, 128, 129, 130, 131, 142, 152-154, 206, 251, 254, 255, 261, 292
Niobium, 212
Nucleation, 163, 164, 167, 168, 169, 229, 249, 254

O

Olivine, 1, 2, 3, 31, 34, 135, 136, 157, 158, 160, 161, 162, 163, 164, 167, 168, 170, 184, 187, 194-195, 203, 204, 205, 206, 209, 214, 215-216, 221, 222, 223, 224, 228, 229, 230, 231-233, 235, 245, 252, 260, 261, 273, 285, 287
Oolites, 11, 12, 21
Ore
  below diabase, 113, 247, 249, 252, 255, 268, 282, 283, 290, 291, 292, 293, 296
  channel, feeder, 4, 5, 28, 37, 102, 113, 120, 154, 237, 250, 252, 254, 255, 256, 257, 267, 290, 291, 292, 293
  comparisions (also see genesis), 103, 242, 243, 268, 271, 273, 280-289, 291, 293, 294
  diabase replacement (also see Diabase sheet – ore in; Magnetite – diabase replacement), 113, 156, 160, 164, 283
  distribution (also see Magnetite distribution), 108, 109, 120, 136, 137, 155, 246, 247, 249, 254, 256, 258, 281, 285-288, 293-294
  economics, exploration, 6, 289-296
  flow, 29, 120, 123, 154, 156
  fluid, 262-263, 266, 267, 279, 280, 282, 283, 288, 289, 290, 291, 292, 293, 294, 296
  footwall, 10, 40, 109, 111, 117, 122, 123, 125, 127, 129, 130, 133, 134, 135, 137, 138, 139, 140, 142, 143, 146, 149, 152, 154, 256, 296
  form (also see Magnetite – form), 292, 294
  gangue 40, 120, 121, 122, 123, 124, 125, 126, 127, 128, 129, 130, 132, 133, 135, 136, 137, 138, 142, 154, 156, 251, 286, 292
  genesis, 1, 2, 3, 4, 5, 6, 7, 43, 56, 58, 82, 96, 99, 100, 103, 132, 135, 137, 154, 155-157, 160, 228, 241-266, 267, 268, 271, 273, 274-275, 278-280, 282, 283, 284, 288-290, 291, 294
  grade, 4, 104, 105, 142
  hanging wall, 40, 43, 44, 47, 49, 54, 63, 94, 108, 109, 111, 114, 121, 122, 123, 125, 127, 128, 129, 130, 133, 134, 135, 136, 137, 138, 139, 140, 141, 142, 144, 147, 150, 152, 154, 257
  hdrothermal (also see Magnetite), 4, 39, 41, 73, 81, 90, 101, 102, 126, 154, 155, 156, 241, 243, 249, 259, 261, 262, 266, 267, 271, 275, 279, 288
  mineralogy, 103, 109, 120-128, 132-135, 136, 137, 138, 171, 205, 242, 248, 253, 255, 267, 306
  occurrence, abundance, 43, 83, 96, 100, 113, 114, 183, 242, 243, 246, 247, 258, 281-282, 284, 285, 289, 290, 293, 294
  oxidation, reduction, 125, 129, 156, 242, 244-245, 255, 262, 264, 292
  oxygen partial pressure, fugacity, 56, 244, 263-264, 265, 266, 267, 275
  permeability, 109, 136, 290, 293
  pH of deposition, 100, 156-157, 262-263, 266, 268
  potassium metasomatism (also see Metasomatism – potassium), 99, 100, 102, 267
  replacement, 4, 5, 6, 10, 12, 21, 39, 43, 54, 60, 73-74, 86, 242, 245, 246, 248, 256, 267, 280, 282, 284, 286, 290, 291, 292, 296
  solution migration (also see Magnetite – ore fluid migration), 5, 7, 37, 58, 114, 129, 132-133, 138, 139, 140, 141, 142, 154, 156, 246, 253, 255, 256-257, 262, 291-292, 293, 296
  structures (also see Ore zone – structures), 120, 121, 125, 133, 137, 154, 242, 249, 253, 256, 257, 261, 268, 292
  sulfur isotopes, 256, 258, 272-274, 293
  sulfur partial pressure, 263-266

supergene enrichment, 103
temperature of deposition, formation, 56-57, 100, 132, 138, 141, 157, 263, 264, 266, 275
texture, veins (also see Ore – veins), 22, 23, 109, 113, 114, 117, 120-123, 125, 136, 139, 154, 156, 242, 246, 256, 257, 261, 284
thickness, 108, 109, 292
titanium (also see Titanium), 100, 101, 105, 129, 255, 274-275, 278, 283, 294
tonnage, production, 104, 248, 284, 285, 287, 288, 289, 291
transport, 100, 132, 155, 156-157, 241, 242, 253, 260-261, 262-264, 266, 273, 278, 279, 290, 293, 294
veins in diabase (also see Diabase sheet – veins in), 108, 109, 113-114, 117, 120, 122, 127, 137, 138, 168, 171, 183, 247, 254, 255, 257, 283, 285
water, volatiles content, 262, 284, 290
xenoliths in diabase, 113, 293
zoning (also see Magnetite – zoning), 120, 247, 250, 255, 256, 257, 261, 292, 293
Ore zone
  chemistry, 4, 64, 86, 88, 92, 94, 99, 101, 102, 120, 124, 128-132, 139, 142-154, 156, 251, 253, 254, 284, 285, 292
  mineralogy, mineralization, 58, 73, 88, 99, 102, 109, 120-128, 132, 135-142, 152, 154, 155, 156, 157, 192, 244, 251, 254, 255, 267, 268, 282, 285
  paragenesis, 100, 121, 122, 123, 124-126, 127, 132-135, 136, 137, 138, 152, 154, 233, 237, 248, 249, 254, 255, 263, 267, 292
  structure deformation (also see Ore – structures), 3, 4, 28, 108-121, 123, 125, 136, 139, 156, 237, 249, 254, 256, 257, 268, 293-294
  telescoping, 136
  temperature (also see Ore – temperature), 120
Orogeny
  Acadian, 23, 36
  Alleghanian, 36
  Taconic, 18, 23, 36
Orthoclase (see Feldspar)
Oxidation (see Basalt, Diabase sheet, Iron, Metamorphism, Ore, Tholeiite)

P

Paleomagnetism, 32, 34, 35, 272-273, 295
Paleozoic structure
  boudinage, 21, 22
  cleavage, 12, 22
  faults, fractures, 4, 12, 13, 15, 16, 17-18, 21-25, 30, 33, 36, 92, 116, 121, 156, 234
  folds, 2, 4, 11, 12, 14, 17, 21-24, 36, 108, 156
  wildflysch, 16
Penn, William, 9
Phoenician writing, 157
Phosphorus, 104, 105
Plagioclase (see Feldspar)
Plate tectonics, 5, 289
Prehnite, 39, 45, 59, 61, 76, 77, 87, 128, 135, 168
Pycnochlorite, 47
Pyrite
  composition (also see Pyrite – in ore), 64, 125, 131, 132, 292
  in Blue Conglomerate, 14, 45, 48-49, 76
  in diabase, 164, 168, 170, 193, 232, 250
  in limestone, 39, 41, 42, 68
  in Mill Hill Slate, 14, 59, 61, 64, 76, 109, 125
  in ore, 103, 104, 105, 120, 121, 123, 124, 125, 127, 131-132, 133, 136, 141, 152, 156, 242, 245, 263, 285, 287, 292
  mineral associations, occurrence, 41, 45, 48, 113, 114, 120, 125, 128, 133, 138, 168
  paragenesis, 120, 125, 133, 264
  sulfur isotopes, 272-274
  trace elements, 125, 131, 287
Pyrometasomatism, 4, 6, 7
Pyroxene
  abundance (also see distribution, general), 180
  aegirine – augite, 179, 191
  alteration, 165, 171, 177, 178, 183, 191, 229
  augite, 113, 177, 178, 180, 181, 184, 187, 188, 189, 195
  bronzite, 157, 180, 232, 233, 273
  clinoenstatite, 180
  clinohypersthene, 3, 4, 178, 180, 181, 187, 188, 195
  clinopyroxene, 123, 157, 161, 162, 163, 164, 165, 168, 170, 171, 177, 178, 179, 180, 181, 182, 189, 203, 215, 230, 235
  composition, 178, 179, 180, 181, 182, 184, 188, 195, 203, 204, 205, 216, 228, 232, 260, 285, 287
  crystal growth, diffusion, 179, 180, 181, 182, 196
  differentiation, fractionation (also see pyroxene species), 216, 220
  diopside, 4, 24, 40, 41, 42, 44, 45, 48, 54, 56,

59, 61, 62, 67, 68, 70, 75, 76, 77, 78, 79, 80, 81, 87, 109, 122, 123, 133, 134, 135, 136, 137, 138, 154, 155, 156, 163, 164, 165, 168, 177, 204, 205, 242, 249, 254, 267, 286, 292
  distribution (also see general occurrence), 179, 180, 183, 184, 188
  enstatite, 163, 167, 171, 177, 179, 180, 187
  exsolution, 163, 165, 167, 169, 170, 177, 178, 179, 180-182, 189, 191, 235
  ferroaugite, 178, 187, 188, 189, 260
  ferrohedenbergite, 178, 179
  ferrohypersthene, 178, 182, 187, 189
  general occurrence (also see distribution), 1, 4, 38, 73, 79, 135, 165, 170, 171, 190, 192, 193, 197, 216, 220, 232, 285, 291
  hedenbergite, 165, 178, 182, 188, 203
  herringbone structure, 177, 181, 182, 187, 188
  hypersthene, 3, 158, 177, 178, 179, 180, 181, 182, 187, 188, 189, 193, 195, 203, 204, 205, 252
  inversion, 113, 177, 178, 179, 180, 181, 182, 188, 189, 195, 230
  nomenclature, definitions, 177-178
  orthopyroxene, 113, 157, 165, 167, 168, 171, 177, 179, 180, 181, 182, 189, 195, 209, 215, 230, 231, 232, 235
  paragenesis, 165, 179, 180, 182, 189, 195, 216, 230, 232, 260, 261, 267, 285, 287
  pigeonite, 3, 165, 171, 177, 178, 179, 180, 181, 182, 187, 188, 189, 195, 208, 232
  resorption, 170
  Schiller, 167
  subcalcic augite, 165
  temperature, 179, 181, 182
  texture, 180, 182, 183, 189
  titaniferous, 178, 179, 182
  twinning, 165, 167, 169, 170, 181, 189
  zoning, 3, 170, 179, 181, 187, 188, 191
Pyrrhotite, 124, 125, 156, 263, 264

Q

Quartz
  igneous, 157, 158, 167, 168, 169, 170, 187, 190, 191, 192, 193, 195, 204, 206, 235, 260
  metamorphic, metasomatic, 3, 39, 42, 45, 47, 48, 54, 171
  occurrence, 14, 15, 16, 24, 39, 41, 42, 43, 44, 45, 46, 47, 48, 49, 51, 54, 56, 57, 58, 59, 60, 61, 62, 66, 69, 70, 73, 75, 76, 77, 79, 80, 81, 84, 85, 87, 122, 129, 135, 245
Quartz diorite, 242
Quartzite, 58
Quartz monzonite, 242

R

Rafting, 1, 4, 22, 23, 29, 37, 54, 267
Revolutionary War, 5, 9
Rheomorphism, 68
Rhyolite, 221
Ripidolite, 47
Rutile, 191, 193

S

St. Peters sill, 269
Sandstone, 11, 19, 38, 48, 290
Saussuritization, 164, 165, 167
Scapolite, 86
Selenium, 128
Sericitization (also see Mica – sericite), 46, 66, 123, 135, 164, 171, 175, 183, 191, 235
Serpentine
  chrysotile, 164, 168, 171
  general occurrence, 38, 41, 67, 127, 163, 164, 167, 168, 169, 177, 187, 235, 260, 264
  trace elements, 128
Serpentinization, 111, 125, 127, 161, 162, 165, 183, 184, 187, 212, 213, 214, 229, 231, 235
Shale, 3, 10, 11, 12, 17, 18, 19, 36, 38, 39, 43, 47, 48, 49, 50, 51, 62, 63, 65, 66, 69, 71, 72, 73, 74, 75, 81, 82, 85, 88, 90, 91, 92, 93, 94, 96, 184, 282, 290
Shelly intrusive, 269, 270
Siderite, 263
Silication (also see specific silicates), 3, 40, 41, 44, 48, 67, 73, 74, 75, 84, 87, 123, 126, 136
Silicification, 3, 7, 39, 40-41, 51, 75, 84, 99, 100
Siltstone, 19, 71, 75, 114, 282
Silver, 103, 125, 251, 254, 266, 284
Sodium (also see Metasomatism – sodium), 39, 129, 130, 133
South Lebanon thrust, 23
Sphalerite, 124, 125, 171, 242
Sphene, 168, 171, 188, 193, 277
Spilitization, 94
Spinel (also see ulvöspinel), 2, 140, 163, 182, 183, 188, 191, 193, 205, 212, 230, 247, 250, 257, 259, 260, 261, 266, 267, 275, 277, 278, 279, 280, 288, 291
Steatization (also see Talc), 125, 127
Stilbite, 87, 125, 128, 135, 171

Stilpnomelane, 171
Stromatolites, 21
Stylolites, 11
Sulfide, 1, 135, 141, 155, 156, 164, 188, 217, 232, 242, 245, 247, 249, 250, 253, 254, 255, 256, 262, 263, 265, 267, 274, 284, 293, 296
Sulfur
  isotopes, 4, 5, 131-132, 256, 258-259, 261, 272-274, 293
  ore magma, 5, 245
  ore – zone distribution, grade, 4, 5, 104, 105, 138, 142, 149-151, 152, 263, 292
Syenite, 242, 243, 287

T

Taconic orogeny (see Orogeny)
Tactite, 43
Talc [Steatite] (also see Steatization), 127
Tantalum, 212
Tholeiite (also see Basalt, Diabase)
  alkali enrichment, 100, 103, 219
  chemical composition, 158, 159, 214-215, 229, 248, 259-260, 284, 289, 290, 320
  differentiation (also see Basalt – differentiation), 214-215
  feldspars, 172
  fractionation, 2, 100
  high iron, 158
  iron enrichment, content, 100, 214-215, 221, 225, 248, 260, 294
  magma generation, 34, 35, 103, 160, 239, 240, 252, 259-260, 289
  olivine–rich, 159, 163, 199
  ore relationship (also see Diabase sheet – ore), 243, 253, 259, 266, 284, 289, 290
  oxidation (also see Diabase sheet – oxidation), 4, 260, 289
  potassium (also see Diabase sheet – potassium), 103
  residuum, 68
Titanium, 1, 3, 4, 64, 100, 101, 105, 124, 129, 130, 131, 158, 182, 183, 188, 191, 193, 195, 201, 202, 208, 209, 212, 227, 228, 231, 236, 243, 245, 247, 250, 254, 255, 257, 259, 260, 261, 264, 267, 273, 274-280, 287, 288, 294
Topaz, 86
Tourmaline, 45, 54, 67, 68, 76, 83, 86
Transcurrent faulting, 289
Transfusion, 192, 194, 202
Traprock (also see Diabase), v, 157
Triassic basin
  aeromagnetic data, 35, 271-273
  age determinations, 30, 34-38
  bleached sediments, 19, 31, 38, 39, 71, 246, 255
  conglomerates, fanglomerates (also see Conglomerate), 48
  domains, 25
  erosional surface (also see Erosion), 19, 30, 32, 38, 270
  faults, margin faults, 4, 5, 25, 26, 28, 31, 33, 37, 114, 117, 123, 156, 249, 260, 270, 282, 289
  folding, 4, 25, 26, 31, 233
  marginal shelf, 19, 30, 33, 37, 266, 270, 271
  origin, 19, 20, 24, 35-36, 37
  paleomagnetism (also see Paleomagnetism), 32, 34
  shape, depth, 27, 35-36, 284, 288, 289
  structure, deformation, 1, 2, 4, 5, 6, 16-17, 19, 21, 25-38, 48, 114, 120, 123, 135, 233, 234, 239, 240, 242, 260, 266, 268, 270, 282, 284, 288, 289, 290
Triassic border (margin)
  faults, 4, 5, 21, 26, 29, 30, 31, 36, 114, 266, 268, 282
  north margin, 11, 12, 15, 21, 23, 26, 27, 30, 31, 33, 34, 36, 48, 114, 266, 269, 271, 282
Triassic sediments
  distribution, contacts, 15, 19, 114
  lithologies, mineralogy, 11, 19-20, 31, 38, 71
  metamorphism (also see Metamorphism), 11, 19, 31, 70, 71
  source, 19-20, 35, 37, 266
  structure, 1, 2, 16, 21, 25-26, 27-28, 30, 31, 33, 35, 114, 295
  thickness, 35
Triassic volcanics, extrusives, 2, 20, 37, 157, 233, 234, 252-253, 266, 271, 289
Troctolite, 245

U

Ulvöspinel, 4, 7, 171, 182, 191, 197, 229, 275-276, 277, 278, 279, 280
Uralitization, 164, 165, 191

V

Vanadium, 124, 129, 131
Vermiculite, 59, 60, 61, 62

W

Weathering, 48, 49, 62, 63, 71, 73, 132, 157
Whin sill (also see LOCALITY INDEX), 188
White Mountain magma series, 233
Wollastonite, 242
Wurtzite, 124, 127

X

Xenoliths (see Blue Conglomerate, Diabase sheet)

Y

Yellow Breeches thrust, 23, 34, 116
York Haven sill, 28, 269

Z

Zeolites, zeolitization, 39, 41, 45, 49, 54, 59, 61, 62, 67, 73, 76, 77, 83, 87, 90, 92, 100, 124, 125, 126, 127, 128, 135, 157, 161, 164, 168, 171, 183, 184, 188, 190, 193, 194, 263, 264, 268
Ziegler sill (also see LOCALITY INDEX and LITHOLOGIC INDEX), 270
Zinc, 64, 86, 101, 125
Zircon, 127, 170
Zoisite, 133

B

Bachmanville sheet, 269, 272, 296
Blue Conglomerate
  age (also see Blue Conglomerate – stratigraphy), 7, 14
  breccia, 14, 29, 41, 43, 44, 46, 47, 48, 50, 55, 70, 75, 76, 80, 83, 87, 109, 156
  chemical composition, 49-50, 51, 55, 62, 65-66, 70, 71, 72, 73, 74, 76, 77, 79, 84, 85, 88, 97, 98, 127, 128, 246, 317
  distribution, quantity, 70, 73, 86, 92, 94, 109, 114-118, 136
  equilibrium, facies, 55-57, 77, 88-89
  faulting, brecciation of, 14, 15, 16, 23, 29, 43, 48
  metamorphism, 11, 14, 39, 41, 42, 43-57, 58, 69, 70, 72, 75, 76, 77, 85, 86, 92
  metasomatism, 3, 14, 41, 43-57, 58, 64, 67, 69, 70, 72, 81, 82, 83, 84, 85, 86, 91, 94, 99, 102
  mineralogy, 14, 15, 16, 24, 25, 39, 43-49, 51, 52, 53, 54, 55, 56, 60, 67, 70, 75, 76, 77, 79, 80, 81, 83, 84, 85, 87, 88, 89, 94, 109, 127, 129, 133
  ore contact, 109, 111
  ore replacement, 122, 136, 156
  permeability, 83, 109, 136, 156, 293
  stratigraphy and correlation, structures, 11, 13, 14, 15, 16, 17, 23, 27, 29, 30, 34, 43-44, 48, 49, 54, 56, 58, 60, 108, 110-111, 114, 115, 117, 267
  texture, 14, 16, 24, 42, 44, 46, 47, 48, 54, 60, 66, 71, 75, 83
  thickness, 16, 114, 116, 117, 118
  weathering, alteration, 48, 49
  xenoliths, 14, 16, 66-67
Brunswick Formation, 19
Buffalo Springs Formation, 1, 10, 11, 12, 13, 14, 17, 18, 19, 21, 22, 23, 26, 27, 29, 30, 36, 39-40, 41, 110-111, 128, 129, 206

C

Cashtown Sheet, 269, 272, 287, 295
Cocalico Formation, 18, 92
Coffman Hill Pluton (Sheet), 20, 270
Conococheague Group, 11
Cornwall Sheet (also see Diabase Sheet), 1, 100, 201, 216, 217, 227, 256, 269, 272, 273, 294, 295

D

Dillsburg Sheet (also see Dillsburg), 1, 2, 158, 163, 189, 192, 194, 201, 207, 208, 214, 216, 227, 231, 232, 269, 272, 273, 274, 277, 294, 296

E

East Greenville Sheet, 270
Epler Formation, 18

G

Gettysburg Formation, 19
Gettysburg Pluton, 34, 207, 216, 258, 268, 269, 272, 277, 287, 295, 296

H

Hammer Creek Formation, 19, 25, 26, 27, 31, 33, 34, 35, 37, 270, 271
Haycock Sheet, 270, 296
Holyoke volcanics, 20
Host limestone (also see Buffalo Springs Formation), 1, 11, 12, 13, 14, 15, 16, 17, 21, 22, 23, 29, 39-40, 41, 43, 44, 47, 58, 67-68, 73, 75, 82, 87, 92, 93, 94, 100, 103-104, 108, 109, 111, 114, 115, 121, 122, 123, 127, 128, 129, 133, 135, 136, 142, 152, 155, 156, 245, 246, 249, 255, 256, 257, 263, 266, 267
  xenoliths, 67-68, 109, 110-111, 113

J

Jacksonwald flow, 270, 271
Jacksonwald sheet, 1, 270

M

Martinsburg Formation
  chemical composition, geochemistry, 49, 50, 56, 62, 63, 71, 72, 73, 74, 81, 82, 85, 88, 90, 91, 92, 93, 95
  mineralogy, 56, 64, 65, 69, 92, 94
  stratigraphy, 3, 4, 17-19, 23, 43, 56, 58, 69, 116
Middletown sheet, 256, 269, 272, 273, 287, 296
Millbach Formation, 10, 11-12, 23
Mill Hill Slate
  age (also see Mill Hill Slate – stratigraphy), 14, 17, 23, 58
  brecciation, 14, 16, 58, 121, 156
  chemical composition, 14, 25, 51, 62-64, 69, 70, 71, 72, 73, 74, 75, 77, 78, 79, 84, 86, 90, 97, 98, 132, 206, 246, 317
  distribution, quantity, 70, 73, 77, 86, 92, 93, 94, 109, 114-118, 136, 155
  equilibrium, facies, 64-66, 76, 77, 88-89
  hornfels, 14
  laminations, banding, 14, 15, 24, 25, 55, 58, 59, 60, 61, 62, 63, 69, 77, 83, 121, 122
  metamorphism, 11, 14, 18, 43, 58, 60-61, 63, 64, 65, 69, 70, 72, 75, 76, 77, 85, 89, 92, 96
  metasomatism, 3, 18, 43, 51, 53, 58, 60-61, 62-64, 65, 68, 69, 70, 72, 81, 82, 83, 84, 85, 86, 91, 94, 99, 100, 102
  mineralogy, 14, 15, 25, 46, 52, 53, 56, 58-62, 64-66, 70, 75, 76, 77, 78, 79, 80, 81, 83, 84, 85, 86, 87, 88, 89, 93, 94, 109, 125, 127, 128, 137
  nomenclature, 58
  ore contact, 109, 155
  ore replacement, 122, 136, 156
  permeability, 83, 109, 136, 156, 293
  stratigraphy and correlation, 11, 14, 15, 17-19, 23, 24, 26, 27, 43, 44, 47, 48, 114
  structure, structural features, 13, 14, 15, 17-18, 23, 24, 27, 29, 30, 34, 36, 58, 60, 102, 114, 115, 117, 121, 267
  texture, 14, 47, 48, 58-59, 60, 69, 71, 77, 83
  thickness, thinning, 109, 114, 116, 117, 118
Morgantown Pluton, 1, 32, 217, 258, 269, 270, 271, 272, 282, 287, 294, 295

N

Newark Group, 19, 26
New Oxford Formation, 26, 35
Northland Sill, 323

P

Precambrian "basement", 19, 272

Q

Quakertown Pluton, 25, 258, 269, 270, 272, 273, 277, 282, 284, 287, 289, 294, 295, 296

R

Richland Formation, 10, 23

S

Schaefferstown Formation, 10, 12, 23
Snitz Creek Formation, 10, 11, 12, 22, 23
Stockton Formation, 35
Stonehenge Formation, 23

Y

York Haven Pluton, 1, 27, 32, 34, 170, 230, 231, 247, 256, 269, 272, 287, 295, 296

Z

Ziegler sheet, 1, 270, 287, 289

LOCALITY INDEX

A

Adirondacks, N.Y., 242, 243
Antarctica, 201, 320
Appalachian Mountain System, 234, 268
Australia, 240

B

Baltimore, Md., 239
Baltimore Co., Md., 321
Banat, Hungary, 243
Bendersville, Pa., 271
Bermudian Springs, Pa., 231
Big Hill, Cornwall, Pa., 9, 108, 114, 127
Birdsboro, Pa., 32, 269, 272, 295, 319
Blue Ridge province, Pa., 21
Bowmansdale, Pa., 269
Boyertown, Pa., 4, 19, 26, 33, 34, 114, 241, 252, 268, 269, 270, 280, 282, 283, 284, 287, 288, 291, 292, 293, 295
Brazil, 20
Brickerville, Pa., 18
British Columbia, Canada, 264
Buckingham Mountain, Pa., 36
Bushveld, South Africa, 178, 181

C

Cascades, Washington, 158, 159, 214, 215, 216, 221, 222
Clark's Ferry, Pa., 235
Coffman Hill, Pa., 20, 269, 270
Connecticut basin, 20, 321
Conshohocken, Pa., 235, 236, 272
Cornwall Center, Pa., 12
Cornwall, England, 9
Cornwall Furnace, Pa., 9
Cornwall Station, Pa., 22
Cranberry, N.C., 243
Culpepper Co., Va., 295, 319

D

Deep River Basin, N.C., 172
Dillsburg, Pa., 3, 4, 7, 38, 39, 96, 97, 101, 103, 131, 132, 158, 172, 173, 180, 183, 189, 192, 194, 201, 202, 203, 207, 208, 209, 210-211, 212, 214, 215, 216, 219, 220, 221, 222, 223, 224, 226, 227, 228, 229, 231, 241, 244, 247, 248, 252, 257, 258, 260, 261, 262, 268, 269, 271, 272, 273, 274, 276, 277, 280, 282, 284, 285-286, 287, 288, 289, 291, 294, 319, 322, 323
Downes Mountain, So. Africa, 188, 201, 248, 320
Duluth, Minn., 323
Duncannon, Pa., 235, 321

E

Eagle Mountain, Calif., 243
Elba, Italy, 243
El Laco, Chile, 243

F

Fierro, N.M., 243
French Creek, Pa., 38, 101, 125, 131, 132, 241, 256, 269, 272, 273, 284, 287, 289

G

Gettysburg, Pa., 236, 258, 269, 272, 274, 295, 321
Gifford Pinchot State Park, Pa., 157
Goat Hill, Pa., 295, 318
Gondwanaland, 240
Goose Creek, Va., 172, 184, 188, 202, 206, 272, 284, 319, 322, 323
Governor Dick Hill, Pa., 28
Grassy Hill, Cornwall, Pa., 9
Great Valley, Pa., 10, 17, 19, 21, 22, 23, 30-31, 236

H

Hammer Creek, Pa., 9, 11, 19
Hangnest, Karroo, So. Africa, 191, 192, 201
Hanover, N.M., 243
Harrisburg, Pa., 23
Haycock Hill, Pa., 318
Heidlersburg, Pa., 295
Heroult, Calif., 243
Highspire, Pa., 4, 18, 19, 24, 26, 33, 34, 282
Hopewell, Pa., 287, 295

I

Iron Springs, Utah, 243

J

Jacksonwald, Pa., 271
Jericho Hill, Pa., 318

K

Karroo, So. Africa, 68, 158, 179, 180, 184, 189, 191, 192, 195, 202, 207, 208, 209, 210-211, 212, 214, 219, 221, 224, 225, 227, 228, 229, 232, 233, 240, 248, 258, 259, 284, 320, 322, 323
Kleinfeltersville, Pa., 18
Kiruna District, Sweden, 243, 244

L

Lahn Sipreline, Germany, 243
Lancaster Valley, Pa., 22
Lebanon, Pa., 9, 23
Lebanon County, Pa., 49, 50, 51, 56, 62, 64, 72, 82, 85, 90, 91, 92
Lebanon Valley, Pa., 22, 23, 234
Lemoyne, Pa., 4, 282
Lewisberry, Pa., 269

M

Madagascar, 52, 53, 90
Maine, 233
Middle Hill, Cornwall, Pa., 9, 27, 132
Middletown, Pa., 231
Mill Hill, Pa., 14, 58
Miners Village, Pa., iii, 9, 15
Mineville, N.Y., 129, 130, 138
Morgantown, Pa., 1, 7, 38, 40, 101, 124, 127, 216, 241, 256, 264, 268, 269, 271, 280, 282, 283, 284, 285-286, 287, 288, 289, 291, 295
Mt. Holyoke, Mass., 321
Mount Pleasant, Pa., 15, 318

N

New Market, Md., 321
North Carolina, 233, 272

P

Palisades, N.J., 31, 94, 158, 163, 167, 170, 178, 180, 184, 186, 188, 189, 194, 199, 200, 201, 202, 203, 206, 207, 208, 209, 210-211, 212, 214, 215, 216, 217, 219, 221, 222, 223, 224, 227, 228, 229, 231, 233, 248, 258, 272, 284, 287, 318, 322, 323
Piedmont, 19, 21, 35, 234, 236

Q

Quakertown, Pa., 258, 269
Quentin, Pa., 15, 24, 58, 81, 82, 93

R

Reading, Pa., 11, 234
Reading Prong, 19, 21
Rexmont, Pa., 24, 25, 27, 28
Rock Hill, Pa., 318
Rocky Hill, N.J., 318
Rocky Ridge, Md., 321
Rossville, Pa., 319

S

Schaefferstown, Pa., 18
Schuylkill River, Pa., 19
Skaergaard, Greenland, 158, 159, 194, 203, 212, 214, 215, 216, 218, 219, 221, 222, 260, 323
South Africa, 20, 240
South America, 240
Sterling Lake, N.Y., 129, 130
Sudbury, Ontario, 242, 243
Susquehanna River, Pa., 19, 230, 236, 269

T

Tasmania, 240, 248, 320
Triassic Lowlands, Pa., 236

V

Valley and Ridge, Pa., 19, 21
Vancouver Island, Wash., 242, 243, 263
Victoria Falls, Africa, 201, 320

W

Warwick, Pa., 258, 283, 284, 287
Wheatfield, Pa., 38
Whin, 188, 201, 248, 320, 323
Wyssokaia Gora, U.S.S.R., 243

Y

York Haven, Pa., 269

Z

Zieglersville, Pa., 270

TOPOGRAPHIC AND GEOLOGIC SURVEY
Arthur A. Socolow, State Geologist

COMMONWEALTH OF PENNSYLVANIA
DEPARTMENT OF ENVIRONMENTAL RESOURCES

MINERAL RESOURCES REPORT 56, PLATE 22

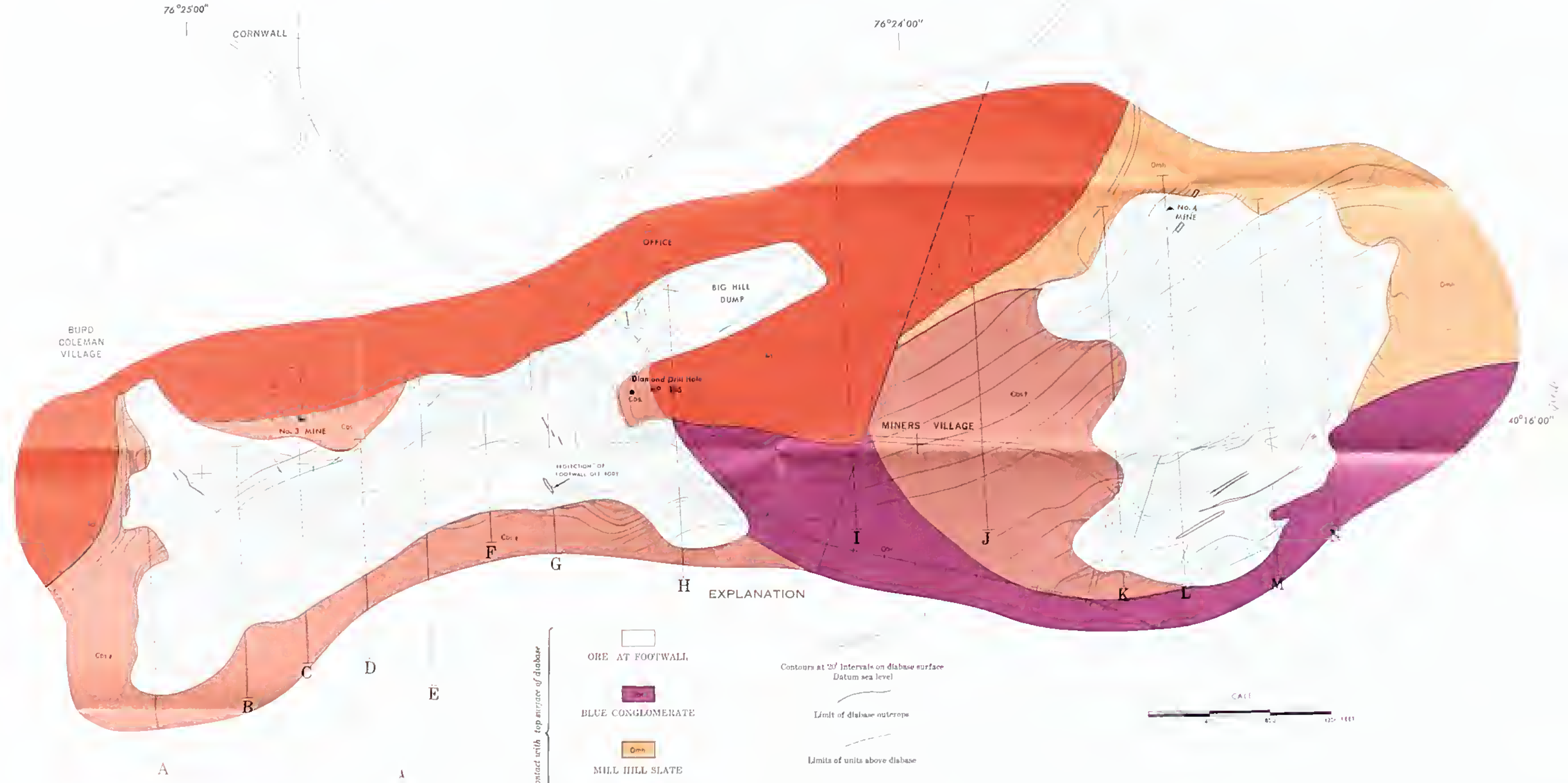

EXPLANATION

Units in contact with top surface of diabase

ORE AT FOOTWALL

Cbc BLUE CONGLOMERATE

Omh MILL HILL SLATE

Cbs BUFFALO SPRINGS FORMATION

Trd DIABASE OUTCROP
(Overlying Formations
Removed by Erosion
Before Mining)

Contours at 20' intervals on diabase surface
Datum sea level

Limit of diabase outcrops

Limits of units above diabase

Approximate limits of ore before mining

Trace of non-mineralized (or inferred) faults
on diabase surface showing dip

Trace of major mineralized fractures or faults
on diabase surface

GEOLOGY OF THE TOP OF THE DIABASE SHEET AT CORNWALL, PENNSYLVANIA

Carlyle Gray and Davis M. Lapham

1973

TOPOGRAPHIC AND GEOLOGIC SURVEY
Arthur A. Socolow, State Geologist

COMMONWEALTH OF PENNSYLVANIA
DEPARTMENT OF ENVIRONMENTAL RESOURCES

1973

GEOLOGIC SECTIONS ACROSS THE CORNWALL ORE BODIES, CORNWALL, PENNSYLVANIA

Geology Compiled by C. Gray 1952-1964

MINERAL RESOURCES REPORT 56, PLATE 23

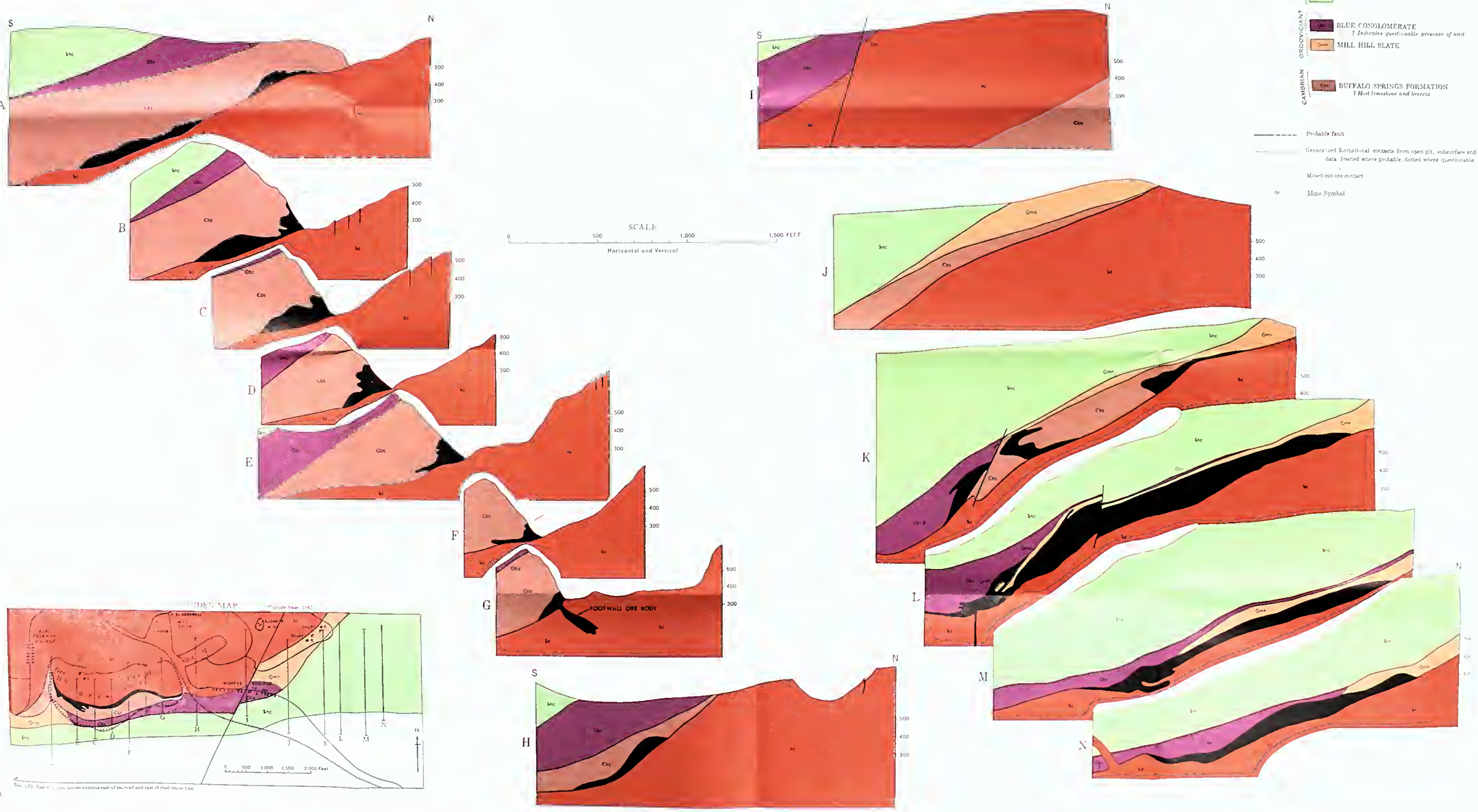

EXPLANATION

TRIASSIC

■	ORE
Ŧd	DIABASE *? diabase dikes*
Ŧhc	HAMMER CREEK FORMATION

ORDOVICIAN?

Obc	BLUE CONGLOMERATE *? Indicates questionable presence of unit*
Omh	MILL HILL SLATE

CAMBRIAN

Cbs	BUFFALO SPRINGS FORMATION *? Host limestone and breccia*

Probable fault

Generalized formational contacts from open pit, subsurface and drilling data. Dashed where probable, dotted where questionable

Mined out ore contact

Mine Symbol

TOPOGRAPHIC AND GEOLOGIC SURVEY
Arthur A. Socolow, *State Geologist*

COMMONWEALTH OF PENNSYLVANIA
DEPARTMENT OF ENVIRONMENTAL RESOURCES

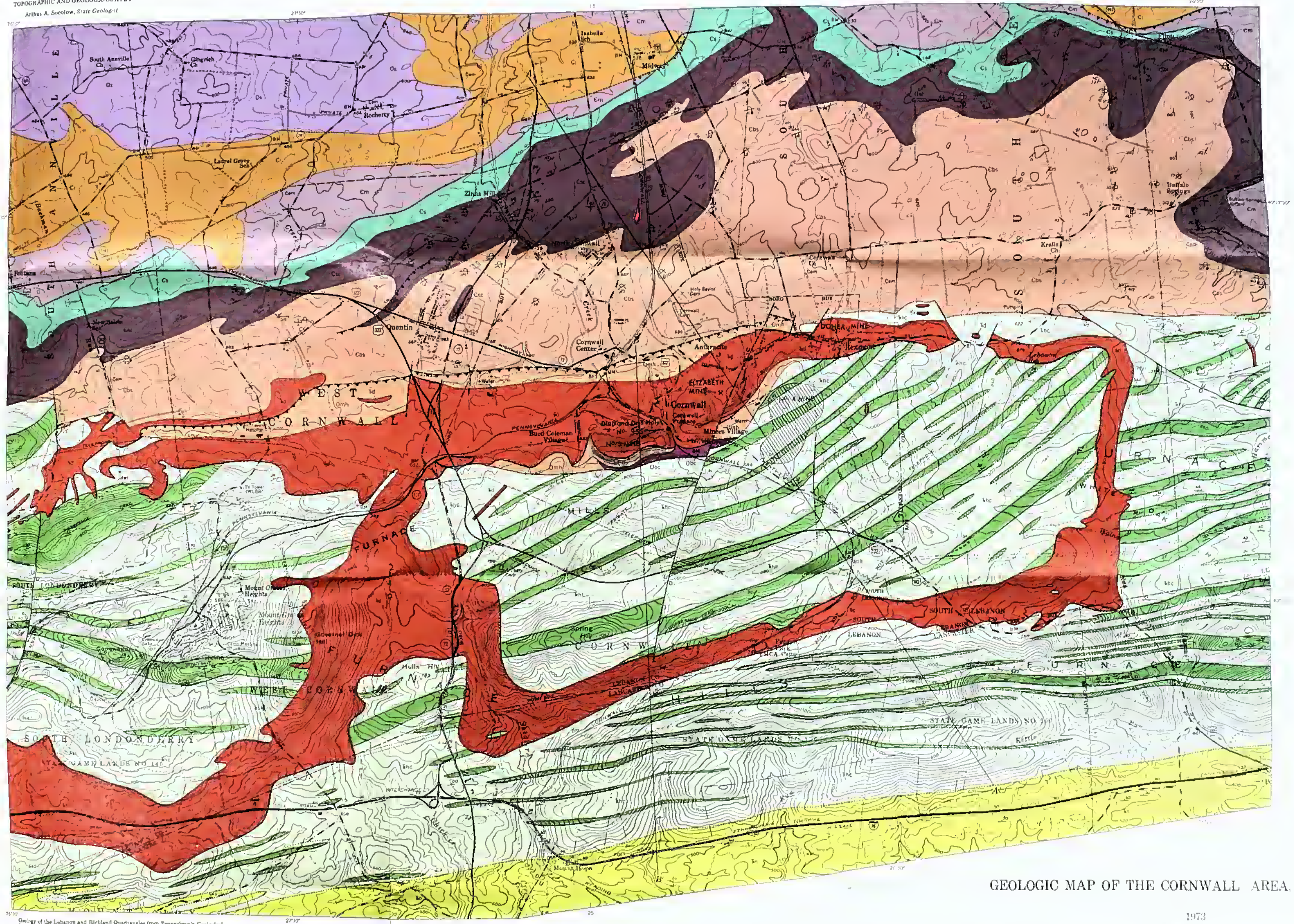

Geology of the Lebanon and Richland Quadrangles from Pennsylvania Geological Survey Atlases 167c (Geyer and others 1958) and 167d (Gray and others 1958) with modifications by C. Gray and D. Lapham; of the Manheim and Lititz Quadrangles from unpublished maps of D. B. McLaughlin. U.S. Geological Survey topographic map base, portions of Lebanon 7½ minute and Manheim 7½ minute quadrangles, 1967.

EXPLANATION

TRIASSIC

DIABASE
Trd
Quartz Normative tholeiitic sheets and vertical Triassic or post-Triassic ? dikes

HAMMER CREEK FORMATION
Trhc
Red sandstone with shale (light green) and conglomerate lenses (dark green)

NEW OXFORD FORMATION
Trn
Interbedded red sandstone and shale.

? ORDOVICIAN

MILL HILL SLATE
Omh
Fine grained, limy and shaly hornfels, structurally below the "Blue Conglomerate"; may be equivalent to the Martinsburg Formation; west of Cornwall, combined with Obc.

BLUE CONGLOMERATE
Obc
Hornfelsed quartz and shale pebble breccia, may be equivalent to the Martinsburg Formation, may be older than Omh.

LOWER ORDOVICIAN

STONEHENGE FORMATION
Os
Medium to medium light gray limestone; medium to finely crystalline, cherty, thin shaly beds and laminations, edgewise conglomerate.

MIDDLE AND LATE CAMBRIAN

RICHLAND FORMATION
Cr
Medium gray dolomite, cherty, oolitic, sandy, some edgewise conglomerate.

MILLBACH FORMATION
Cm
Pale red purple to light gray limestone; finely laminated, oolitic, numerous cryptozoon reefs, medium to finely crystalline, several dolomite beds.

SCHAEFFERSTOWN FORMATION
Cs
Medium light to medium gray limestone; finely crystalline, laminated, medium bedded

SNITZ CREEK
Csc
Medium gray dolomite, sandy, laminated, cherty, finely crystalline

BUFFALO SPRINGS FORMATION
Cbs
Light to pinkish gray limestone, cryptozoon beds near top, sandy in part, fine to coarsely crystalline, interbedded dolomite, laminated in part

SYMBOLS

Contact, dashed where probable, dotted where inferred
High angle fault, dashed where probable
Thrust fault, dotted where inferred
Possible contact within diabase at internal chilled contact
Approximate area of underground eastern ore body
Strike and dip
Strike of vertical beds
Overturned strike and dip
Strike and dip of beds rotated more than 90°
Strike and dip of overturned beds where upper bed can be distinguished
Strike and dip of cleavage
Horizontal cleavage
Plunge of minor anticline, showing degree of plunge
Mine
Diamond drill hole

GEOLOGIC MAP OF THE CORNWALL AREA, PENNSYLVANIA

1973

CONTOUR INTERVAL 20 FEET

GEOLOGIC SECTIONS

Scale same as map; no vertical exaggeration

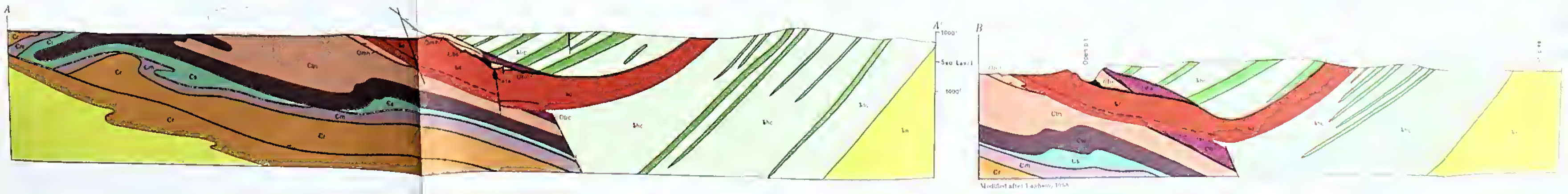

Modified after Lapham, 1968